BIOGENIC REEFS AT RISK: FACING GLOBALLY WIDESPREAD LOCAL THREATS AND THEIR INTERACTION WITH CLIMATE CHANGE

EDITED BY: Massimo Ponti, Riccardo Rodolfo-Metalpa, Bert W. Hoeksema, Cristina Linares and Carlo Cerrano

PUBLISHED IN: Frontiers in Marine Science

frontiers Research Topics

ISSN 1664-8714
ISBN 978-2-88974-003-1
DOI 10.3389/978-2-88974-003-1

About Frontiers

Frontiers is more than just an open-access publisher of scholarly articles: it is a pioneering approach to the world of academia, radically improving the way scholarly research is managed. The grand vision of Frontiers is a world where all people have an equal opportunity to seek, share and generate knowledge. Frontiers provides immediate and permanent online open access to all its publications, but this alone is not enough to realize our grand goals.

Frontiers Journal Series

The Frontiers Journal Series is a multi-tier and interdisciplinary set of open-access, online journals, promising a paradigm shift from the current review, selection and dissemination processes in academic publishing. All Frontiers journals are driven by researchers for researchers; therefore, they constitute a service to the scholarly community. At the same time, the Frontiers Journal Series operates on a revolutionary invention, the tiered publishing system, initially addressing specific communities of scholars, and gradually climbing up to broader public understanding, thus serving the interests of the lay society, too.

Dedication to Quality

Each Frontiers article is a landmark of the highest quality, thanks to genuinely collaborative interactions between authors and review editors, who include some of the world's best academicians. Research must be certified by peers before entering a stream of knowledge that may eventually reach the public - and shape society; therefore, Frontiers only applies the most rigorous and unbiased reviews.
Frontiers revolutionizes research publishing by freely delivering the most outstanding research, evaluated with no bias from both the academic and social point of view. By applying the most advanced information technologies, Frontiers is catapulting scholarly publishing into a new generation.

What are Frontiers Research Topics?

Frontiers Research Topics are very popular trademarks of the Frontiers Journals Series: they are collections of at least ten articles, all centered on a particular subject. With their unique mix of varied contributions from Original Research to Review Articles, Frontiers Research Topics unify the most influential researchers, the latest key findings and historical advances in a hot research area! Find out more on how to host your own Frontiers Research Topic or contribute to one as an author by contacting the Frontiers Editorial Office: frontiersin.org/about/contact

BIOGENIC REEFS AT RISK: FACING GLOBALLY WIDESPREAD LOCAL THREATS AND THEIR INTERACTION WITH CLIMATE CHANGE

Topic Editors:
Massimo Ponti, University of Bologna, Italy
Riccardo Rodolfo-Metalpa, UMR ENTROPIE, New Caledonia
Bert W. Hoeksema, Naturalis Biodiversity Center, Netherlands
Cristina Linares, University of Barcelona, Spain
Carlo Cerrano, Marche Polytechnic University, Italy

Citation: Ponti, M., Rodolfo-Metalpa, R., Hoeksema, B. W., Linares, C., Cerrano, C., eds. (2021). Biogenic Reefs at Risk: Facing Globally Widespread Local Threats and Their Interaction With Climate Change. Lausanne: Frontiers Media SA.
doi: 10.3389/978-2-88974-003-1

Table of Contents

frontiers in Marine Science

EDITORIAL
published: 16 November 2021
doi: 10.3389/fmars.2021.793038

Editorial: Biogenic Reefs at Risk: Facing Globally Widespread Local Threats and Their Interaction With Climate Change

Massimo Ponti[1,2*†], *Cristina Linares*[3†], *Carlo Cerrano*[2,4,5,6†], *Riccardo Rodolfo-Metalpa*[7†] *and Bert W. Hoeksema*[8,9†]

[1] Dipartimento di Scienze Biologiche, Geologiche e Ambientali, University of Bologna, Ravenna, Italy, [2] Consorzio Nazionale Interuniversitario per le Scienze del Mare (CoNISMa), Rome, Italy, [3] Departament de Biologia Evolutiva, Ecologia i Ciències Ambientals, Institut de Recerca de la Biodiversitat, Universitat de Barcelona, Barcelona, Spain, [4] Dipartimento di Scienze della Vita e dell'Ambiente, Polytechnic University of Marche, Ancona, Italy, [5] Stazione Zoologica Anton Dohrn, Naples, Italy, [6] Fano Marine Center, Fano, Italy, [7] ENTROPIE, Institut de Recherche pour le Développement (IRD), Université de la Réunion, Centre National de la Recherche Scientifique (CNRS), Institut Français de Recherche pour l'Exploitation de la Mer (IFREMER), Université de Nouvelle-Calédonie, Nouméa, New Caledonia, [8] Taxonomy, Systematics and Geodiversity Group, Naturalis Biodiversity Center, Leiden, Netherlands, [9] Groningen Institute for Evolutionary Life Sciences, University of Groningen, Groningen, Netherlands

Keywords: bioconstruction, biodiversity, human impact, disturbance, ecological shift, marine conservation, resilience, citizen science

OPEN ACCESS

Edited and reviewed by:
Angel Borja,
Technological Center Expert in Marine and Food Innovation (AZTI), Spain

***Correspondence:**
Massimo Ponti
massimo.ponti@unibo.it

†ORCID:
Massimo Ponti
orcid.org/0000-0002-6521-1330
Cristina Linares
orcid.org/0000-0003-3855-2743
Carlo Cerrano
orcid.org/0000-0001-9580-5546
Riccardo Rodolfo-Metalpa
orcid.org/0000-0001-7054-1361
Bert W. Hoeksema
orcid.org/0000-0001-8259-3783

Specialty section:
This article was submitted to Marine Ecosystem Ecology, a section of the journal Frontiers in Marine Science

Received: *11 October 2021*
Accepted: *23 October 2021*
Published: *16 November 2021*

Citation:
Ponti M, Linares C, Cerrano C, Rodolfo-Metalpa R and Hoeksema BW (2021) Editorial: Biogenic Reefs at Risk: Facing Globally Widespread Local Threats and Their Interaction With Climate Change. Front. Mar. Sci. 8:793038. doi: 10.3389/fmars.2021.793038

Editorial on the Research Topic

Biogenic Reefs at Risk: Facing Globally Widespread Local Threats and Their Interaction With Climate Change

INTRODUCTION

Biogenic reefs are secondary marine substrates, also referred to as bioconstructions or bioherms, made by autogenic ecosystem engineers (*sensu*, Jones et al., 1994) that provide habitats for various species. Their ecological role goes far beyond simple physical effects because they can modulate many resources and interactions between species inhabiting the reefs. Marine bioconstructions involve a variety of fragile three-dimensional habitats, from shallow water coral reefs to mesophotic coralligenous concretions, hosting rich, and diverse benthic assemblages (Cocito, 2004; Ingrosso et al., 2018; Cerrano et al., 2019). Biogenic reefs can be found from the intertidal to the deep sea; some are ephemeral and last a few years, while others remain active for millennia. The main framework builders are able to form bioconstructions at different latitudes, from tropical to polar zones, and include films of cyanobacteria and diatoms, calcareous rhodophytes, sponges, hermatypic symbiotic and aposymbiotic corals, polychaetes as serpulids and sabellariids, mollusks like vermetids, oysters and mussels, and bryozoans.

Biogenic reefs have an inestimable value for the biodiversity they host and the countless ecosystem goods and services they provide, which are only partially quantifiable in their economical values. Considering the time required for their formation, their destruction can often be considered almost irreversible, so bioconstructions require the utmost attention in any conservation measure. Indeed, both tropical and temperate biogenic reefs are increasingly threatened by multiple stressors resulting in the decline of reef communities worldwide (e.g., Harborne et al., 2017; Ellis et al., 2019; Maher et al., 2019; Bevilacqua et al., 2021). Natural and anthropogenic stressors include decline in water quality, overexploitation of resources, habitat destruction, and global climate change among others, which have all been linked in tropical and temperate areas with the occurrence of mass coral

bleaching and a variety of diseases and mass mortality events (e.g., Carpenter et al., 2008; Garrabou et al., 2009; Ban et al., 2014; Burge et al., 2014; Thompson et al., 2014; Ponti et al., 2016; Gómez-Gras et al., 2021).

Many environmental stressors and anthropogenic disturbances are thought to favor the onset of infectious disease, either on their own or more commonly synergistically (Harvell et al., 2007). For example, anomalously high sea surface temperatures and their increasing frequency have been shown to raise coral susceptibility and pathogen virulence, influencing the severity, and rate of spread of infections (Randall et al., 2014; Wooldridge, 2014). Furthermore, disease susceptibility and the increase of corallivores has also been linked to stressing conditions as high sedimentation rates, water turbidity, eutrophication, and the development of diving tourism (e.g., Fabricius, 2005; Lamb et al., 2014; Pollock et al., 2014; Nicolet et al., 2018).

Nowadays, many studies focus on possible ecological effects of global climate change, which has resulted in massive worldwide coral bleaching in the tropics (e.g., Baker et al., 2008; Hughes et al., 2018), and in massive mortality events in the Mediterranean Sea (Ponti et al., 2014; Turicchia et al., 2018a; Garrabou et al., 2019; Gómez-Gras et al., 2021). Although it is not easy to categorize and disentangle the synergic effects of different threats, a simple literature review based on identified keywords related to the major threats highlighted how studies have mainly focused on climate change related issues and secondarily on pollution (**Figure 1**). Apparently, we are losing sight of the impacts on biogenic reefs associated with more "localized" disturbances, such as decline in water quality, overexploitation of resources, destructive fisheries, spread of non-indigenous species, recreational activities, and urbanization. Such stressors are increasing in intensity and frequency on a global scale and will therefore undoubtedly be playing a pivotal role in the health and functionality of biogenic reefs, especially about disease outbreaks, resilience to ecological shifts, and loss of ecological goods and services. This Frontiers Research Topic (RT) entitled "*Biogenic Reefs at Risk: Facing Globally Widespread Local Threats and their Interaction with Climate Change*," aims to fill the gaps by collecting new insights on worldwide biogenic reefs threats, advancing in monitoring technologies, and providing innovative perspectives on conservation and restorations strategies.

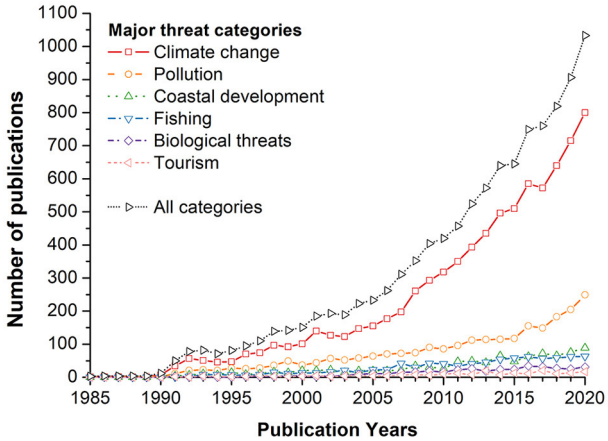

FIGURE 1 | Time series of publications registered in Web of Science Core Collection, including in the title or abstract or keywords at least one the following habitat descriptors: "biogenic reef*" or bioconstruction* or bioherm* or "coral reef*" or "Sabellaria reef*" or "sabellariid reef*" or "serpulid reef*" or "oyster reef*" or "vermetid reef*" or "mussel bed*" or "oyster bed*" or "rhodolith bed*" or "maerl bed*" or coralligenous or "algal bank*"; and one of the following terms related to the major threat categories: **Climate change** ("climate change*" OR "heat wave*" OR "ocean warming" OR acidification OR "sea level rise" OR storm* OR hurricane* OR cyclone* OR typhoon* OR bleaching OR disease* OR mortalit*); **Pollution** (pollution OR oil spills OR plastic OR litter OR dumping OR eutrophication OR hypoxia OR anoxia OR waste OR "agricultural runoff" OR "heavy metal*" OR "trace element*" OR mining OR pah* OR sunscreen* OR pharmaceutical* OR herbicide OR fungicide* OR pesticide* OR "organic enrichment"); **Coastal development** ("coastal development*" OR urbanization OR dredging OR siltation OR debris OR "habitat fragmentation" OR "habitat loss" OR "genetic erosion"); **Fishing** ("destructive fishing" OR "blast fishing" OR overexploitation OR overfishing OR trawling OR bycatch); **Biological threat** ("alien species" OR "non-indigenous species" OR mucilage* OR invasion*); **Tourism** ("tourism impact*" OR anchoring OR "diving impact*" OR trampling) (Retrieved on 28/09/2021).

EMERGING ISSUES

Among the most relevant emerging issues that are not directly linked to climate change but are threatening biogenic reefs worldwide, there are newly discovered diseases, like the stony coral tissue loss disease which outbreaks are spreading fast in the Caribbean (Estrada-Saldívar et al., 2021; Heres et al., 2021; Meiling et al., 2021). Since we know very little about the origin of pathogens in corals, there is also a need for a better understanding of the etiology, the evolution, and biogeography of coral diseases (Montano et al., 2020).

Possible ecological cascading effects on biogenic reefs due to the spread of non-indigenous species are poorly known, among them those related to the invasion of lionfishes in the Caribbean (*Pterois volitans*; McCard et al., 2021) and the Mediterranean Sea (*Pterois miles*; Poursanidis et al., 2020), the rapid spread of invasive sun corals (*Tubastraea* spp.) in the (sub)tropical Atlantic because of shipping (Creed et al., 2017), and the increasing occurrence of various species of coral killing sponges in the Indo-Pacific ocean (e.g., Turicchia et al., 2018b; Fromont et al., 2019; Ashok et al., 2020), as well as the spreading of invasive macroalgae in Mediterranean temperate biogenic reefs (Kersting et al., 2013). A contribution to the understanding of trophic cascade effects in the conservation of temperate biogenic reefs was provided by the article published in this RT by Christie et al., whose experiments indicate that mesopredators such as the green crab (*Carcinus maenas*) and the goldsinny wrasse (*Ctenolabrus rupestris*) may be co-responsible for the decrease in blue mussel (*Mytilus edulis*) beds in northern Europe.

The pollution issues are very pronounced, especially in Southeast Asia (e.g., Heery et al., 2018; Adyasari et al., 2021; Reichert et al., 2021), and should not be underestimated also in other regions, especially concerning plastics and emerging pollutants in general, as highlighted in this RT by Angiolillo and Fortibuoni. Likewise, the negative impact

of fishing activities is still underestimated in many regions, including developed countries, and especially regarding the deep biogenic reefs. Two manuscripts in this RT stressed the urgency to fill the knowledge gap on the current and predicted distribution, according to climate change scenarios, of the deep bioconstructions to protect them from fishing threats and maintain a pocket of pristine-like biodiversity (Dias et al.; Fragkopoulou et al.). Moreover, there is an increasing impact of land reclamation triggering devastating local dredging activities (e.g., Topçu et al., 2018; Pancrazi et al., 2020). In addition to the direct habitat removal, one of the main effects of land reclamation and coastal development, is the increase in water turbidity that can undermine the resilience of surrounding biogenic reefs, especially those with a strong dependence on light, as in the study carried out on Singapore' coral reefs and presented in this RT by Morgan et al.

Another threat to biogenic reefs that has received much attention is that of massive outbreaks of corallivores. Well-known examples are outbreaks of crown-of-thorns starfish (*Acanthaster* spp.) and gastropod snails of the genus *Drupella*, which may cause serious coral mortality (Turner, 1994; Pratchett et al., 2017). Whether there is a direct relation with climate change is not clear, but it is striking that such outbreaks can occur directly after massive coral bleaching event and may affect coral populations that have survived the bleaching (e.g., Hoeksema et al., 2013; Saponari et al., 2021).

CONSERVATION MEASURES AND FUTURE PERSPECTIVES

Information on many local, but globally spread, threats to biogenic reefs is still limited. Therefore, it is urgent to draw the most complete picture on these impacts including the multiple stressors acting in synergy with climate change effects. In this RT, Ford et al. and Montefalcone et al., although working in different geographical areas and with different approaches, similarly concluded that local human impacts can deeply alter the resilience of tropical coral reefs toward repeated climate change related disturbance events, jeopardizing the future of these ecosystems. To this end, field and manipulative experiments simulating effects of ecological shifts due to both pulse and press disturbances affecting biogenic reefs and modeling approaches that can provide insights into future trends should be strongly encouraged.

A widespread and standardized approach to analyzing the health of biogenic reefs in relation to local disturbances could help mitigate their effects and improve solutions. However, since climate change acts on a global scale, and many anthropogenic disturbances, although local, have a global spread, the conservation and restoration of our planet's biogenic reefs must be addressed with at least international approaches and policies (e.g., the European Green Deal and the European Biodiversity Strategy, the Coral Triangle Initiative). In this perspective, individual Marine Protected Areas can do little for the conservation of these habitats if they do not act synergistically as functional wide-area networks (Giakoumi et al., 2018). In this respect, Gazulla et al. contributed to the RT by providing a case study on the conservation and restoration of the red coral *Corallium rubrum* populations based on the connectivity network obtained by a demo-genetic approach. Similarly, citizen science initiatives are proving able to provide effective community-based monitoring at the regional or global level supplementing institutional actions (Sully et al., 2019; Turicchia et al., 2021).

Coastal development and coastal defense around the world are undergoing to a profound paradigm shift, passing from large concrete structures to nature-based solutions, including the application of new eco-friendly materials and shapes (Airoldi et al., 2021; Sella et al., 2021) that can favor the settlement of local species and, over time, the restoration of coastal biogenic reefs, such as coral reef and oyster beds. A better understanding of the effectiveness of such manmade structures would require more long-term research comparing the development of their communities with that of adjacent biogenic reefs (Perkol-Finkel et al., 2006; Hill et al., 2021; Monchanin et al., 2021).

Finally, from a technological perspective, three papers published within this RT highlighted that new measuring and monitoring tools, based both on underwater (Dellisanti et al.; Rossi et al.) and aerial platforms (Bajjouk et al.), can be developed, especially for the mapping and conservation of relatively shallow waters biogenic reefs.

The widespread and continuous alteration of biogenic reef ecosystems is affecting mainly ecosystem engineers, rapidly fragmenting their complex, and delicate trophic web, weakening the whole bioconstructions' architecture. This increasing fragility open the door to pathogens and non-indigenous species deeply compromising natural recovery and restoration strategies (Ponti et al., 2018; Verdura et al., 2019). Without an effective and rapid reduction of anthropogenic pressures on temperate and tropical bioconstructions we will not have any possibility to reverse the present rate of biodiversity loss.

Overall, the topic addressed here is very broad, embracing very different fragile marine ecosystems from tropical to temperate seas and the relationship humans have with their conservation and restoration. The diversity of the contributions collected in this RT focusing on different stressors and using different approaches and technologies to study biogenic reefs around the world reflects this complexity well. They provide new insights not only on the cumulative and synergic effects of multiple threats and their interaction with climate change in different systems but also stress on needs and gaps to advance in biogenic reefs monitoring, conservation, and restoration. These papers are aimed at a very wide audience, from scientists to managers and policymakers, as well as stakeholders involved in biogenic reefs goods and services. We believe they will support future advances to improve understanding of biogenic reefs conservation ecology, ultimately leading to a healthier ocean. We thank all contributing authors and are confident that readers will enjoy reading these papers on threats to biogenic reefs.

AUTHOR CONTRIBUTIONS

All authors contributed to writing and editing this editorial. **Figure 1** was prepared by MP. All authors contributed to the article and approved the submitted version.

REFERENCES

Adyasari, D., Pratama, M. A., Teguh, N. A., Sabdaningsih, A., Kusumaningtyas, M. A., and Dimova, N. (2021). Anthropogenic impact on Indonesian coastal water and ecosystems: current status and future opportunities. *Mar. Pollut. Bull.* 171, 112689. doi: 10.1016/j.marpolbul.2021.112689

Airoldi, L., Beck, M. W., Firth, L. B., Bugnot, A. B., Steinberg, P. D., and Dafforn, K. A. (2021). Emerging solutions to return nature to the urban ocean. *Ann. Rev. Mar. Sci.* 13, 445–477. doi: 10.1146/annurev-marine-032020-020015

Ashok, A. M., Calcinai, B., and Edward, J. K. P. (2020). The coral-killing red sponge *Clathria* (*Microciona*) *aceratoobtusa* (Porifera: Demosponigiae) invades various coral communities of Gulf of Mannar Marine National Park, southeast India. *Eur. Zool. J.* 87, 1–11. doi: 10.1080/24750263.2019.1708486

Baker, A. C., Glynn, P. W., and Riegl, B. (2008). Climate change and coral reef bleaching: an ecological assessment of long-term impacts, recovery trends and future outlook. *Estuar. Coast. Shelf Sci.* 80, 435–471. doi: 10.1016/j.ecss.2008.09.003

Ban, S. S., Graham, N. A. J., and Connolly, S. R. (2014). Evidence for multiple stressor interactions and effects on coral reefs. *Glob. Change Biol.* 20, 681–697. doi: 10.1111/gcb.12453

Bevilacqua, S., Airoldi, L., Ballesteros, E., Benedetti-Cecchi, L., Boero, F., Bulleri, F., et al. (2021). Mediterranean rocky reefs in the anthropocene: present status and future concerns. *Adv. Mar. Biol.* 89, 1–51. doi: 10.1016/bs.amb.2021.08.001

Burge, C. A., Mark Eakin, C., Friedman, C. S., Froelich, B., Hershberger, P. K., Hofmann, E. E., et al. (2014). Climate change influences on marine infectious diseases: implications for management and society. *Ann. Rev. Mar. Sci.* 6, 249–277. doi: 10.1146/annurev-marine-010213-135029

Carpenter, K. E., Abrar, M., Aeby, G., Aronson, R. B., Banks, S., Bruckner, A., et al. (2008). One-third of reef-building corals face elevated extinction risk from climate change and local impacts. *Science.* 321, 560–563. doi: 10.1126/science.1159196

Cerrano, C., Bastari, A., Calcinai, B., Di Camillo, C., Pica, D., Puce, S., et al. (2019). Temperate mesophotic ecosystems: gaps and perspectives of an emerging conservation challenge for the Mediterranean Sea. *Eur. Zool. J.* 86, 370–388. doi: 10.1080/24750263.2019.1677790

Cocito, S. (2004). Bioconstruction and biodiversity: their mutual influence. *Sci. Mar.* 68, 137–144. doi: 10.3989/SCIMAR.2004.68S1137

Creed, J. C., Fenner, D., Sammarco, P., Cairns, S., Capel, K., Junqueira, A. O. R., et al. (2017). The invasion of the azooxanthellate coral *Tubastraea* (Scleractinia: Dendrophylliidae) throughout the world: history, pathways and vectors. *Biol. Invasions* 19, 283–305. doi: 10.1007/s10530-016-1279-y

Ellis, J. I., Jamil, T., Anlauf, H., Coker, D. J., Curdia, J., Hewitt, J., et al. (2019). Multiple stressor effects on coral reef ecosystems. *Glob. Change Biol.* 25, 4131–4146. doi: 10.1111/gcb.14819

Estrada-Saldívar, N., Quiroga-García, B. A., Pérez-Cervantes, E., Rivera-Garibay, O. O., and Alvarez-Filip, L. (2021). Effects of the stony coral tissue loss disease outbreak on coral communities and the benthic composition of cozumel reefs. *Front. Mar. Sci.* 8:632777. doi: 10.3389/fmars.2021.632777

Fabricius, K. E. (2005). Effects of terrestrial runoff on the ecology of corals and coral reefs: review and synthesis. *Mar. Pollut. Bull.* 50, 125–146. doi: 10.1016/j.marpolbul.2004.11.028

Fromont, J., Richards, Z. T., and Wilson, N. G. (2019). First report of the coral-killing sponge *Terpios hoshinota* Rützler and Muzik, 1993 in Western Australia: a new threat to Kimberley coral reefs? *Diversity*. 11:184. doi: 10.3390/d11100184

Garrabou, J., Coma, R., Bensoussan, N., Bally, M., Chevaldonne, P., Cigliano, M., et al. (2009). Mass mortality in Northwestern Mediterranean rocky benthic communities: effects of the 2003 heat wave. *Glob. Change Biol.* 15, 1090–1103. doi: 10.1111/j.1365-2486.2008.01823.x

Garrabou, J., Gómez-Gras, D., Ledoux, J.-B., Linares, C., Bensoussan, N., López-Sendino, P., et al. (2019). Collaborative database to track mass mortality events in the Mediterranean Sea. *Front. Mar. Sci.* 6:707. doi: 10.3389/fmars.2019.00707

Giakoumi, S., McGowan, J., Mills, M., Beger, M., Bustamante, R. H., Charles, A., et al. (2018). Revisiting "success" and "failure" of marine protected areas: a conservation scientist perspective. *Front. Mar. Sci.* 5:223. doi: 10.3389/fmars.2018.00223

Gómez-Gras, D., Linares, C., Dornelas, M., Madin, J. S., Brambilla, V., Ledoux, J.-B., et al. (2021). Climate change transforms the functional identity of Mediterranean coralligenous assemblages. *Ecol. Lett.* 24, 1038–1051. doi: 10.1111/ele.13718

Harborne, A. R., Rogers, A., Bozec, Y. M., Mumby, P. J., and Annual, R. (2017). Multiple stressors and the functioning of coral reefs. *Ann. Rev. Mar. Sci.* 9, 445–468. doi: 10.1146/annurev-marine-010816-060551

Harvell, D., Jordan-Dahlgren, E., Merkel, S., Rosenberg, E., Raymundo, L., Smith, G., et al. (2007). Coral disease, environmental drivers, and the balance between coral and microbial associates. *Oceanography*. 20, 172–195. doi: 10.5670/oceanog.2007.91

Heery, E. C., Hoeksema, B. W., Browne, N. K., Reimer, J. D., Ang, P. O., Huang, D., et al. (2018). Urban coral reefs: degradation and resilience of hard coral assemblages in coastal cities of East and Southeast Asia. *Mar. Pollut. Bull.* 135, 654–681. doi: 10.1016/j.marpolbul.2018.07.041

Heres, M. M., Farmer, B. H., Elmer, F., and Hertler, H. (2021). Ecological consequences of stony coral tissue loss disease in the Turks and Caicos islands. *Coral Reefs* 40, 609–624. doi: 10.1007/s00338-021-02071-4

Hill, C. E. L., Lymperaki, M. M., and Hoeksema, B. W. (2021). A centuries-old manmade reef in the Caribbean does not substitute natural reefs in terms of species assemblages and interspecific competition. *Mar. Pollut. Bull.* 169, 112576. doi: 10.1016/j.marpolbul.2021.112576

Hoeksema, B. W., Scott, C., and True, J. D. (2013). Dietary shift in corallivorous *Drupella* snails following a major bleaching event at Koh Tao, Gulf of Thailand. *Coral Reefs* 32, 423–428. doi: 10.1007/s00338-012-1005-x

Hughes, T. P., Anderson, K. D., Connolly, S. R., Heron, S. F., Kerry, J. T., Lough, J. M., et al. (2018). Spatial and temporal patterns of mass bleaching of corals in the anthropocene. *Science* 359, 80–83. doi: 10.1126/science.aan8048

Ingrosso, G., Abbiati, M., Badalamenti, F., Bavestrello, G., Belmonte, G., Cannas, R., et al. (2018). Mediterranean bioconstructions along the Italian coast. *Adv. Mar. Biol.* 79, 61–136. doi: 10.1016/bs.amb.2018.05.001

Jones, C. G., Lawton, J. H., and Shachak, M. (1994). Organisms as ecosystem engineers. *Oikos* 69, 373–386. doi: 10.2307/3545850

Kersting, D. K., Ballesteros, E., De Caralt, S., and Linares, C. (2013). Invasive macrophytes in a marine reserve (Columbretes Islands, NW Mediterranean): spread dynamics and interactions with the endemic scleractinian coral *Cladocora caespitosa*. *Biol. Invasions* 16, 1599–1610. doi: 10.1007/s10530-013-0594-9

Lamb, J. B., True, J. D., Piromvaragorn, S., and Willis, B. L. (2014). Scuba diving damage and intensity of tourist activities increases coral disease prevalence. *Biol. Conserv.* 178, 88–96. doi: 10.1016/j.biocon.2014.06.027

Maher, R. L., Rice, M. M., McMinds, R., Burkepile, D. E., and Thurber, R. V. (2019). Multiple stressors interact primarily through antagonism to drive changes in the coral microbiome. *Sci. Rep.* 9:6834. doi: 10.1038/s41598-019-43274-8

McCard, M., South, J., Cuthbert, R. N., Dickey, J. W. E., McCard, N., and Dick, J. T. A. (2021). Pushing the switch: functional responses and prey switching by invasive lionfish may mediate their ecological impact. *Biol. Invasions* 23, 2019–2032. doi: 10.1007/s10530-021-02487-7

Meiling, S. S., Muller, E. M., Lasseigne, D., Rossin, A., Veglia, A. J., MacKnight, N., et al. (2021). Variable species responses to experimental Stony Coral Tissue Loss Disease (SCTLD) exposure. *Front. Mar. Sci.* 8:670829. doi: 10.3389/fmars.2021.670829

Monchanin, C., Mehrotra, R., Haskin, E., Scott, C. M., Plaza, P. U., Allchurch, A., et al. (2021). Contrasting coral community structures between natural and artificial substrates at Koh Tao, Gulf of Thailand. *Mar. Environ. Res.* 172:105505. doi: 10.1016/j.marenvres.2021.105505

Montano, S., Maggioni, D., Liguori, G., Arrigoni, R., Berumen, M. L., Seveso, D., et al. (2020). Morpho-molecular traits of Indo-Pacific and Caribbean *Halofolliculina* ciliate infections. *Coral Reefs* 39, 375–386. doi: 10.1007/s00338-020-01899-6

Nicolet, K. J., Chong-Seng, K. M., Pratchett, M. S., Willis, B. L., and Hoogenboom, M. O. (2018). Predation scars may influence host susceptibility to pathogens: evaluating the role of corallivores as vectors of coral disease. *Sci. Rep.* 8, 5258–5258. doi: 10.1038/s41598-018-23361-y

Pancrazi, I., Ahmed, H., Cerrano, C., and Montefalcone, M. (2020). Synergic effect of global thermal anomalies and local dredging activities on coral reefs of the Maldives. *Mar. Pollut. Bull.* 160:111585. doi: 10.1016/j.marpolbul.2020.111585

Perkol-Finkel, S., Shashar, N., and Benayahu, Y. (2006). Can artificial reefs mimic natural reef communities? The roles of structural features and age. *Mar. Environ. Res.* 61, 121–135. doi: 10.1016/j.marenvres.2005.08.001

Pollock, F. J., Lamb, J. B., Field, S. N., Heron, S. F., Schaffelke, B., Shedrawi, G., et al. (2014). Sediment and turbidity associated with offshore dredging increase coral disease prevalence on nearby reefs. *PLoS ONE* 9:e102498. doi: 10.1371/journal.pone.0102498

Ponti, M., Fratangeli, F., Dondi, N., Segre Reinach, M., Serra, C., and Sweet, M. J. (2016). Baseline reef health surveys at Bangka Island (North Sulawesi, Indonesia) reveal new threats. *PeerJ* 4:e2614. doi: 10.7717/peerj.2614

Ponti, M., Perlini, R. A., Ventra, V., Grech, D., Abbiati, M., and Cerrano, C. (2014). Ecological shifts in Mediterranean coralligenous assemblages related to gorgonian forest loss. *PLoS ONE* 9, e102782. doi: 10.1371/journal.pone.0102782

Ponti, M., Turicchia, E., Ferro, F., Cerrano, C., and Abbiati, M. (2018). The understorey of gorgonian forests in mesophotic temperate reefs. *Aquat. Conserv.* 28, 1153–1166. doi: 10.1002/aqc.2928

Poursanidis, D., Kalogirou, S., Azzurro, E., Parravicini, V., Bariche, M., and Dohna, H. Z. (2020). Habitat suitability, niche unfilling and the potential spread of *Pterois miles* in the Mediterranean Sea. *Mar. Pollut. Bull.* 154:111054. doi: 10.1016/j.marpolbul.2020.111054

Pratchett, M., Caballes, C., Wilmes, J., Matthews, S., Mellin, C., Sweatman, H., et al. (2017). Thirty years of research on crown-of-thorns starfish (1986–2016): scientific advances and emerging opportunities. *Diversity* 9:41. doi: 10.3390/d9040041

Randall, C. J., Jordan-Garza, A. G., Muller, E. M., and Van Woesik, R. (2014). Relationships between the history of thermal stress and the relative risk of diseases of Caribbean corals. *Ecology* 95, 1981–1994. doi: 10.1890/13-0774.1

Reichert, J., Tirpitz, V., Anand, R., Bach, K., Knopp, J., Schubert, P., et al. (2021). Interactive effects of microplastic pollution and heat stress on reef-building corals. *Environ. Pollut.* 290:118010. doi: 10.1016/j.envpol.2021.118010

Saponari, L., Dehnert, I., Galli, P., and Montano, S. (2021). Assessing population collapse of *Drupella* spp. (Mollusca: Gastropoda) 2 years after a coral bleaching event in the Republic of Maldives. *Hydrobiologia* 848, 2653–2666. doi: 10.1007/s10750-021-04546-5

Sella, I., Hadary, T., Rella, A., Riegl, B., Swack, D., and Perkol-Finkel, S. (2021). Design, production and validation of the biological and structural performance of an ecologically engineered concrete block mattress: A Nature Inclusive Design for shoreline and offshore construction. *Integr. Environ. Assess. Manag.* doi: 10.1002/ieam.4523

Sully, S., Burkepile, D. E., Donovan, M. K., Hodgson, G., and van Woesik, R. (2019). A global analysis of coral bleaching over the past two decades. *Nat. Commun.* 10:1264. doi: 10.1038/s41467-019-09238-2

Thompson, A., Schroeder, T., Brando, V. E., and Schaffelke, B. (2014). Coral community responses to declining water quality: Whitsunday Islands, Great Barrier Reef, Australia. *Coral Reefs* 33, 923–938. doi: 10.1007/s00338-014-1201-y

Topçu, N. E., Turgay, E., Yardimci, R. E., Topaloglu, B., Yüksek, A., Steinum, T. M., et al. (2018). Impact of excessive sedimentation caused by anthropogenic activities on benthic suspension feeders in the Sea of Marmara. *J. Mar. Biol. Assoc. UK* 99, 1075–1086. doi: 10.1017/S0025315418001066

Turicchia, E., Abbiati, M., Sweet, M., and Ponti, M. (2018a). Mass mortality hits gorgonian forests at Montecristo Island. *Dis. Aquat. Org.* 131, 79–85. doi: 10.3354/dao03284

Turicchia, E., Cerrano, C., Ghetta, M., Abbiati, M., and Ponti, M. (2021). *MedSens* index: the bridge between marine citizen science and coastal management. *Ecol. Indic.* 122:107296. doi: 10.1016/j.ecolind.2020.107296

Turicchia, E., Hoeksema, B. W., and Ponti, M. (2018b). The coral-killing sponge *Chalinula nematifera* as a common substrate generalist in Komodo National Park, Indonesia. *Mar. Biol. Res.* 14, 827–833. doi: 10.1080/17451000.2018.1544420

Turner, S. J. (1994). The biology and population outbreaks of the corallivorous gastropod *Drupella* on Indo-Pacific reefs. *Oceanogr. Mar. Biol. Annu. Rev.* 32, 461–530.

Verdura, J., Linares, C., Ballesteros, E., Coma, R., Uriz, M. J., Bensoussan, N., et al. (2019). Biodiversity loss in a Mediterranean ecosystem due to an extreme warming event unveils the role of an engineering gorgonian species. *Sci. Rep.* 9:5911. doi: 10.1038/s41598-019-41929-0

Wooldridge, S. A. (2014). Differential thermal bleaching susceptibilities amongst coral taxa: re-posing the role of the host. *Coral Reefs* 33, 15–27. doi: 10.1007/s00338-013-1111-4

Conflict of Interest: The authors declare that the research was conducted in the absence of any commercial or financial relationships that could be construed as a potential conflict of interest.

Publisher's Note: All claims expressed in this article are solely those of the authors and do not necessarily represent those of their affiliated organizations, or those of the publisher, the editors and the reviewers. Any product that may be evaluated in this article, or claim that may be made by its manufacturer, is not guaranteed or endorsed by the publisher.

frontiers in Marine Science

ORIGINAL RESEARCH
published: 07 July 2020
doi: 10.3389/fmars.2020.00550

Disappearing Blue Mussels – Can Mesopredators Be Blamed?

Hartvig Christie[1], Patrik Kraufvelin[2†], Lucinda Kraufvelin[3], Niklas Niemi[3] and Eli Rinde[1]*

[1] Norwegian Institute for Water Research (NIVA), Oslo, Norway, [2] Department of Aquatic Resources, Institute of Coastal Research, Swedish University of Agricultural Sciences, Öregrund, Sweden, [3] Department of Environmental and Marine Biology, Åbo Akademi University, Turku, Finland

Despite many theories, the recent evident decreases in blue mussel (*Mytilus edulis*) abundance in southern Norway and western Sweden (eastern North Sea) have not yet been explained. To test the possible role of increased predation, an ongoing mesocosm experiment exploring general effects of two mesopredators on the structure of littoral macroalgal and macrofaunal communities was used. These mesopredators were the green crab (*Carcinus maenas*) and the goldsinny wrasse (*Ctenolabrus rupestris*) which were distributed in a crossed manner to 12 large mesocosms containing diverse rocky shore communities. For the purposes of this study, boulders covered with recently recruited blue mussels and barnacles (*Balanus improvisus*) from a natural shore were brought in to the mesocosms during two seasons (August and October), and the coverage of the animals (just blue mussels in summer, both mussels and barnacles in autumn) was registered repeatedly over 24 h. The mussels were rapidly consumed by crabs and wrasses, whereas high survival was recorded on boulders in the controls without predators. The barnacles were only eaten by the crabs and not before most of the mussels had been consumed. As both the green crab and the goldsinny wrasse have been reported to increase in abundance, probably related to overfishing of top predators, the resulting higher predation pressure on especially small blue mussels (recruits) may contribute to the mussel decline along these temperate rocky shores.

Keywords: blue mussel disappearance, predation, mesopredator release, green crabs, wrasses

OPEN ACCESS

Edited by:
Massimo Ponti,
University of Bologna, Italy

Reviewed by:
Britas Klemens Eriksson,
University of Groningen, Netherlands
Kjell Larsson,
Linnaeus University, Sweden
Christian Buschbaum,
Alfred Wegener Institute, Helmholtz Centre for Polar and Marine Research (AWI), Germany

****Correspondence:***
Hartvig Christie
hartvig.christie@niva.no

†ORCID:
Patrik Kraufvelin
orcid.org/0000-0003-3224-8388

Specialty section:
This article was submitted to Marine Ecosystem Ecology, a section of the journal Frontiers in Marine Science

Received: *25 February 2020*
Accepted: *16 June 2020*
Published: *07 July 2020*

Citation:
Christie H, Kraufvelin P, Kraufvelin L, Niemi N and Rinde E (2020) Disappearing Blue Mussels – Can Mesopredators Be Blamed? Front. Mar. Sci. 7:550. doi: 10.3389/fmars.2020.00550

INTRODUCTION

During the last years, there has been a concern about decreasing abundances of the blue mussel *Mytilus edulis* in coastal waters of southern Norway and western Sweden (Skagerrak and eastern North Sea) that has been reported by both scientists and people collecting mussels for recreational purposes (Andersen et al., 2016; Frigstad et al., 2018; Lundström, 2020). The blue mussel has also become much harder to locate at long-term monitoring stations for contaminants in southern Norway (Green et al., 2018). Increased *Mytilus* spp. mortality have in other countries been linked to diseases, climate change, habitat disruption, and predation (e.g., Rilov and Schiel, 2006; van der Heide et al., 2014; Eggermont et al., 2017; Seuront et al., 2019), but so far the causes for the reduction of *Mytilus* abundance in Skagerrak have not been clarified. The same factors mentioned above in international studies, including hybridisation between the three occurring *Mytilus* species, have been suggested as potential causes of *M. edulis* losses in South Norway. At the southeast coast of Norway, Brooks and Farmen (2013) found *M. edulis* to be the only species, whereas the rarer

Mytilus trossulus and *Mytilus galloprovincialis* were found at other parts (and downstream) along the Norwegian coast, which contradicts the hybridisation theory at least for the south-eastern part of the coast. Observations of high mussel abundance on ropes in harbors and normal recruitment and growth in mussel farms do not support the disease/parasite theory, nor a negative role of higher water temperatures. However, the ropes can serve as refuges from some sort of predation, in particular from mobile benthic species. Thus, the observations of high mussel abundances on ropes support an increased predation pressure as being a potential cause of reduced *M. edulis* populations.

The general efficiency of predators in reducing mussel abundance is well known since the study by Paine (1966) in his highly cited paper. The efficiency of sea stars as blue mussel predators has been documented in southern Norway (Christie, 1983). Further, Elner (1978) showed the role of crabs and Peteiro et al. (2010) the role of fish predation for reducing blue mussel abundance, while Rilov and Schiel (2006) found increasing populations of both labrid fish and crabs to reduce mussel abundance.

During the last decades, the coastal ecosystems in Skagerrak have undergone dramatic changes (Weijerman et al., 2005; Moy and Christie, 2012; Östman et al., 2016). As a response to the drastic reduction in abundance of the top predator coastal cod, *Gadus morhua* (Cardinale and Svedäng, 2004; Baden et al., 2012), several mesopredators have increased considerably in abundance (mesopredator release *sensu* Prugh et al., 2009) posing an increased predation risk. Small fish and crustacean predators have been reported to increase in rocky shore ecosystems; typical examples of species that have become more common is the goldsinny wrasse (*Ctenolabrus rupestris*) (Gjøseter and Paulsen, 2004; Bergström et al., 2016 and references therein) and the green crab (*Carcinus maenas*) (Eriksson et al., 2011; Infantes et al., 2016). To test possible effects of increasing densities of these two mesopredators on mussels, a sudden intense recruitment of blue mussels in July–August 2019, in both the inner and outer Oslofjord, were used by taking advantage of an ongoing large mesocosm experiment. This was a long-term experiment running from June to October, and the mussel experiments were initiated as short-term add-on experiments in these mesocosms. To test how these two mesopredators directly affect blue mussels, boulders with attached mussels were simply transplanted into the 12 controlled mesocosms. A new, less intense recruitment event in October 2019 allowed repetition of the summer experiment in autumn and testing the mesopredator impact on both mussels and barnacles.

MATERIALS AND METHODS

At NIVA's research station Solbergstrand by the Oslofjord in southeastern Norway, rocky shore mesocosm experiments have been carried out in 12 large outdoor concrete basins, each containing 12 m^3 of seawater (see **Figure 1A**). The mesocosms are 4.75 × 3.65 m at surface level and 1.3 m deep at high tide. Diverse shore ecosystems based on seaweeds and associated macrofauna have been established over several years. These mesocosms are supplied with a continuous flow of 4 m^3h^{-1} of seawater from 1 m depth in the fjord and they are equipped with wave machines and tidal regulation. For further description of the mesocosms, see Bokn et al. (2003) and Kraufvelin et al. (2006a,b, 2010, 2020). In 2019, the project CRABFISH started in early June and ended in mid-October, being set up for testing predatory top-down effects by the goldsinny wrasse (*C. rupestris*) and the green crab (*C. maenas*) on the entire seaweed ecosystem. The mesocosms were distributed among four treatments; three mesocosms did not receive any predators ("Control"), three mesocosms were allocated 50 green crabs each ("Crabs," i.e., ca 4 crabs per m^2 bottom area or m^3 of water), three mesocosms were assigned 50 wrasses each ("Fish," i.e., the same fish density as for crabs), and the three remaining mesocosms received 50 green crabs and 50 wrasses each ("CrabFish," i.e., ca 4 crabs and 4 fishes per m^2 bottom area or m^3 of water). Population densities of *C. maenas* (Moksnes, 2002) and wrasse (Gjøsæter, 2002; Skiftesvik et al., 2014) are hardly quantified in the field, but found to vary over short distances. However, Sayer et al. (1993) reported a density of 4 individuals per m^2 of goldsinny wrasse to be high. The density of crabs and fishes remained at the initial level throughout the study (own recordings), but some crabs were observed to climb out of the mesocosms at night and migrated randomly to neighboring mesocosms (extending the meaning of the word walkover). To maintain the three control mesocosms and the three fish-only mesocosms without crabs, the mesopredators occurring in wrong mesocosms had to be caught regularly using baited traps and put back into the nearest Crab or CrabFish mesocosms. Despite these efforts, an effect of crabs on blue mussel cover was observed in the "Control" mesocosms in the August experiment (one crab attacking mussels in each of two control mesocosms).

In late July, high abundance of small *M. edulis* (shell length 2–3 mm) was observed in the shallow coastal areas outside the research station at Solbergstrand, covering cobblestones, boulders, seaweeds and seagrass blades. Twelve stones (cobbles/boulders, see Wentworth scale), with a flat top surface area of about 25 × 30 cm were collected from the fjord and one boulder was transplanted into each of the mesocosms in early August. The initial blue mussel cover (i.e., percent cover at the top surface of the boulder) and cover of mussels at short (h) time intervals up to 24 h, were estimated to the nearest 5% by snorkeling in the mesocosms (trying not to disturb the predators). Pictures were taken along with the snorkeling for controlling the cover estimates (see **Figure 1B**). Ahead of each cover estimate, the amount of mesopredatory crabs and wrasses on and adjacent to each blue mussel boulder was counted.

Later in August, the fjord population of the blue mussels had disappeared (own observations by snorkeling), but a new recruitment event was observed in early October, although less intense with a resulting lower blue mussel density/cover than in August. Hence, it was possible to repeat the experiment in October. This time, 72 stones, each with a top surface area of ca. 10 × 15 cm were collected from the same site at Solbergstrand as in August, and six stones were transplanted into each mesocosm.

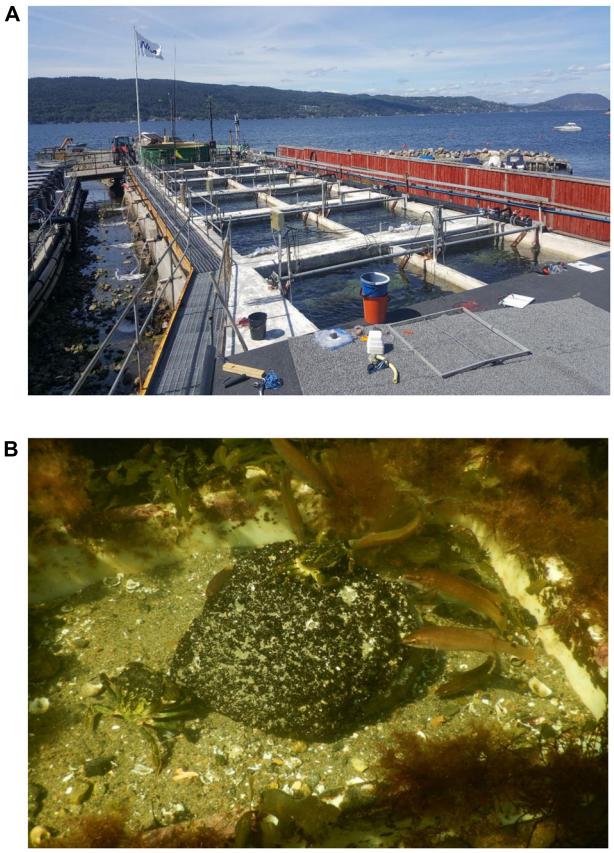

FIGURE 1 | Images showing an overview of the 12 mesocosms at NIVAs Research Station at the Oslofjord **(A)**, and an example of green crabs and goldsinny wrasses attacking a stone with juvenile mussels **(B)**.

The initial cover and the cover of mussels at short time intervals up to 24 h were estimated as above. The blue mussels in October 2019 were of the same size as those in August 2019. Because crabs were observed eating barnacles (*Balanus improvisus*) attached to the lower parts of the stones, after they had eaten the mussels in August, the percent cover of barnacles on the stones was also estimated in the October experiment. Unfortunately, there were no resources available for taking action to perform well-designed field experiments using e.g., cages for those two settlement occasions, as the settlements came unexpected.

The differences in the development of mussel and barnacle cover between treatments were analyzed with generalized additive models (GAM, Wood, 2011). Cover was used as response variable and time and treatment as explanatory variables. The model included interaction between the two explanatory variables (time and treatment), and allowed a different smooth for each treatment level, using treatment as the "by" variable in the R-package *mgcv* (Wood, 2011). The analysis was done in R (version 3.5.2, R Core Team, 2019). Wald tests of the significance of each parametric and smooth term of the models (i.e., one GAM was created for each species per experimental month; i.e., *Mytilus*-August, *Mytilus*-October, and *Balanus*-October) were done. This is a type III ANOVA, rather than a sequential type I ANOVA test (Wood, 2011). The figures are produced using *ggplot2* (Wickham, 2016) and *tidyverse* (Wickham et al., 2019). GAM was chosen to be able to identify any non-linear (curvilinear or asymptotical) trends in cover over time (Hastie and Tibshirani, 1990).

Seawater temperature and salinity were registered both in August and in October.

RESULTS

The temperature was 20–21°C and 12°C in August and October, respectively, whereas salinity was 20 psu in August and 25 psu in October.

In the August study, the initial coverage of small blue mussels was 100% on all boulders, while it was around 40–50% in October. Both predators were observed to be feeding on the mussels within short time. In both experiments, the cover of mussels was reduced to almost zero within 24 h in all mesocosms that received either crabs, fish or both predators (**Figure 2**). The cover of blue mussels declined most rapidly in the mesocosms with both predator species present, followed by the mesocosms with crabs and then the ones with fish alone. With both predator species present, the cover was reduced to zero within 5 h in both August and October. The Wald tests revealed a significant effect of treatment and of the interaction between treatment and time, for each of the three GAMs (**Table 1**). All smooth terms of the treatment levels vs. time showed a significant decline in cover over time for each GAM, except for the controls in October (both species) and for *B. improvisus* in the fish treatment. There was a small, but significant predation effect in the control mesocosms in August due to the walkover by one crab in each of the two Controls (the smooth term of the treatment level Control vs. time was significantly different from zero in the *Mytilus*-August GAM; $F = 8.1$, $p = 0.005$, **Table 1**). However, no predation effect was observed in the control mesocosms in October (i.e., the smooth term of the treatment level Control vs. time was not significant in the *Mytilus*-October GAM).

The barnacles were observed to be eaten only by the crabs (**Figure 3**); this is confirmed by the fact that the smooth term of the treatment level Fish vs. time was not significantly different from zero in the *Balanus*-October GAM (**Table 1**). The consumption of barnacles took mainly place after an initial decline in mussels (mainly after 5 h). As for the mussels, the crabs were able to reduce/consume the provided barnacles within 24 h.

All models performed well and explained a substantial part of the variation in cover over time and between treatments. The explained deviance was above 70% for all GAMs (**Table 1**).

Only a smaller fraction of the total mesopredator individuals present in each mesocosm was observed to attack the blue mussels on the boulders. Only rarely, more than 5 crabs or 10 fish individuals were observed to be actively feeding on the mussels at a single occasion. Our own observations of the development of the blue mussel recruitment events in the fjord outside the

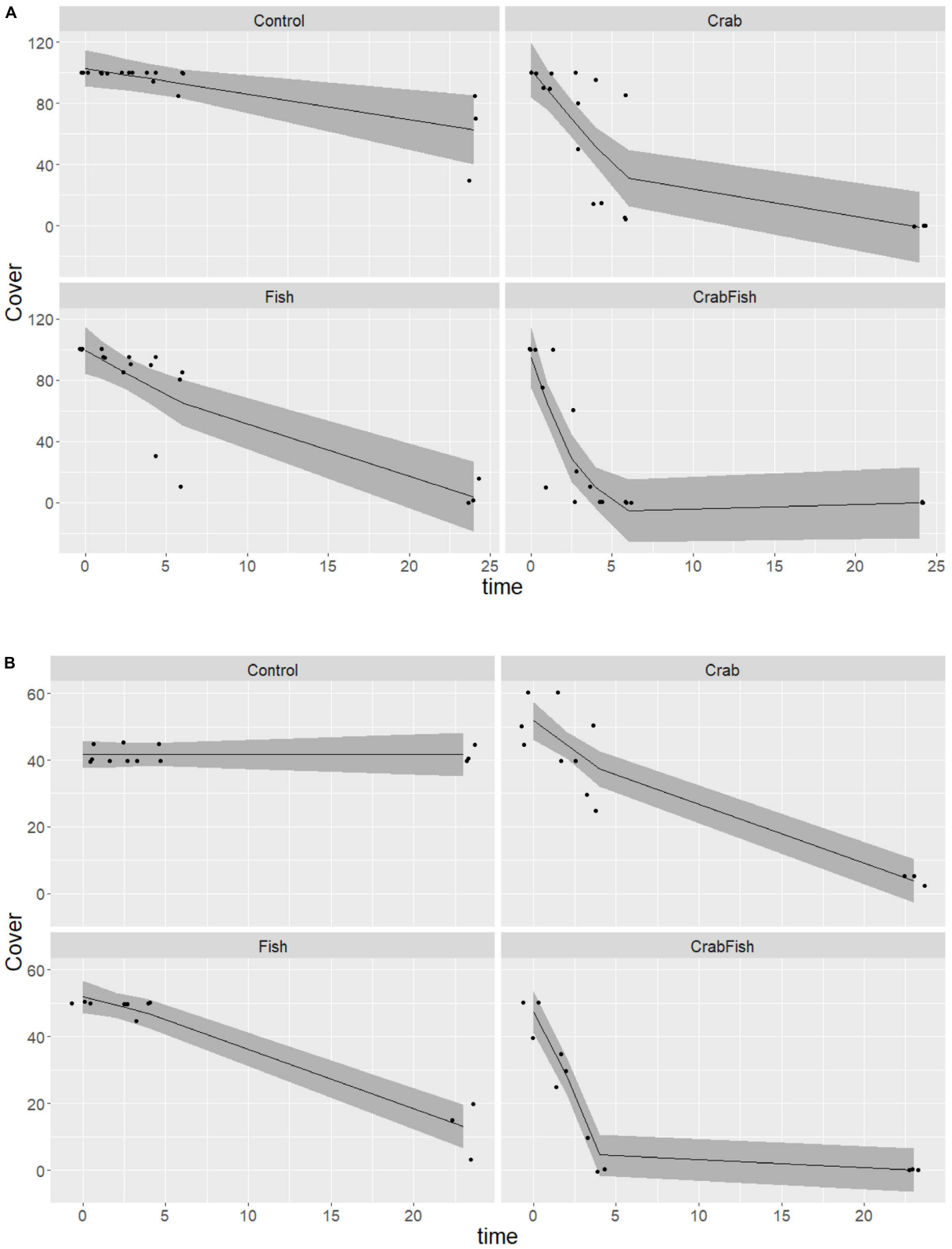

FIGURE 2 | Predicted and observed development in *M. edulis* cover over time in a 24 h experiment in August **(A)** and in October **(B)** 2019, given four different treatments (Control: no predators added, Crab: only crabs added as predator, Fish: only fish added as predator, CrabFish: i.e., both crabs and fish added as predator species to the mesocosms). The shaded area shows the 95% confidence levels of the predicted GAM values (i.e., cover as a function of treatment + time × treatment) and the points represent the observed cover at different times. There were always three replicates, and some overlapping points are not visible.

TABLE 1 | Summary of the three GAMs performance; i.e., R-square adjusted and explained deviance, and the results of the Wald test of each model.

Mytilus August model (R-sq. adj = 0.77, dev. explained = 80.3%, *n* = 72)				
Parametric terms		**df**	**F**	***p*-value**
Treatment		3	27.47	2.4E-11
Approximate significance of smooth terms	**edf**	**Ref.df**	**F**	***p*-value**
s(time):TreatmentControl	1	1.001	8.125	0.00591
s(time):TreatmentCrab	2.106	2.327	22.769	6.27E-09
s(time):TreatmentCrabFish	2.631	2.871	18.302	5.92E-09
s(time):TreatmentFish	1.561	1.831	25.862	8.79E-08
Mytilus October model (R-sq adj = 0.91, dev. explained = 92.5%, *n* = 48)				
Parametric Terms		**df**	**F**	***p*-value**
Treatment		3	35.84	4.52E-11
Approximate significance of smooth terms	**edf**	**Ref.df**	**F**	***p*-value**
s(time):TreatmentControl	1	1	0	1
s(time):TreatmentCrab	1.809	2.038	60.77	<2e-16
s(time):TreatmentCrabFish	2.582	2.835	45.53	<2e-16
s(time):TreatmentFish	1.355	1.59	60.58	2.03E-12
Balanus October model (R-sq. adj = 0.67, dev. explained = 71.8%, *n* = 48)				
Parametric Terms		**df**	**F**	***p*-value**
Treatment		3	7.83	0.000316
Approximate significance of smooth terms	**edf**	**Ref.df**	**F**	***p*-value**
s(time):TreatmentControl	1	1	0	1
s(time):TreatmentCrab	1	1	29.94	1.84E-06
s(time):TreatmentCrabFish	1	1	48.63	5.53E-09
s(time):TreatmentFish	1	1	0	1

One GAM each was created for blue mussel M. edulis cover for August and October 2019, respectively, and one GAM for the barnacle B. improvisus cover in October 2019, all on boulders deployed to mesocosms. The treatments were the presence of two predator species; Crab alone, Fish alone, both species together (CrabFish), and both species absent (i.e., the Control). The GAMs included treatment and the interaction between time and treatment (The R-formula of the models was on this form: Cover ∼s(time, bs = "cr," by = Treatment, k = 4, m = 1) + Treatment + 1).

research station, indicated a total disappearance of small mussels during a few weeks in August 2019. One month after the second recruitment in October, only a few small blue mussels were observed to remain in the uppermost parts of the intertidal zone, while the rest of the mussels was gone.

DISCUSSION

This pilot experiment shows the predation efficiency of two common mesopredator species, the goldsinny wrasse and the green crab, and their ability to reduce high and intermediate cover of small blue mussels to local extinction during a very short time period (within hours). The green crabs were most efficient in removing the blue mussels (as well as the barnacles), while the wrasses only predated on the mussels. Both species introduced together was the most efficient predator combination on blue mussel abundance. Hence, the presence of the other predator did not hamper the predation activity of either of the two predator species. On the contrary, when the crabs started to crush the mussels in the "CrabFish" treatments, this activity attracted the wrasses, probably due to some chemical cues. Thus, there was a co-consumption by the two species making the mussel reduction more efficient on the boulders than what was possible by consumption by either crabs or fish alone. The crabs preferred the small mussels, and they started to eat the barnacles first after most mussels were consumed. The low interest in barnacles among the wrasses are in accordance with gut content analysis by Kraufvelin et al. (2020), revealing small blue mussels to be their preferred prey organisms.

The two experiments (in August and October 2019) were performed in large littoral mesocosms with diverse natural seaweed ecosystems, where the predators had sufficient access to alternative prey items such as gastropods, amphipods, isopods, polychaetes and other invertebrates (Kraufvelin et al., 2002, 2006a,b, 2010, 2020; Bokn et al., 2003; Díaz et al., 2012). The rapid attraction to and predation on mussels by the two predator species within these mesocosms, indicate a high preference of juvenile blue mussels as prey. However, only between 5 and 20%

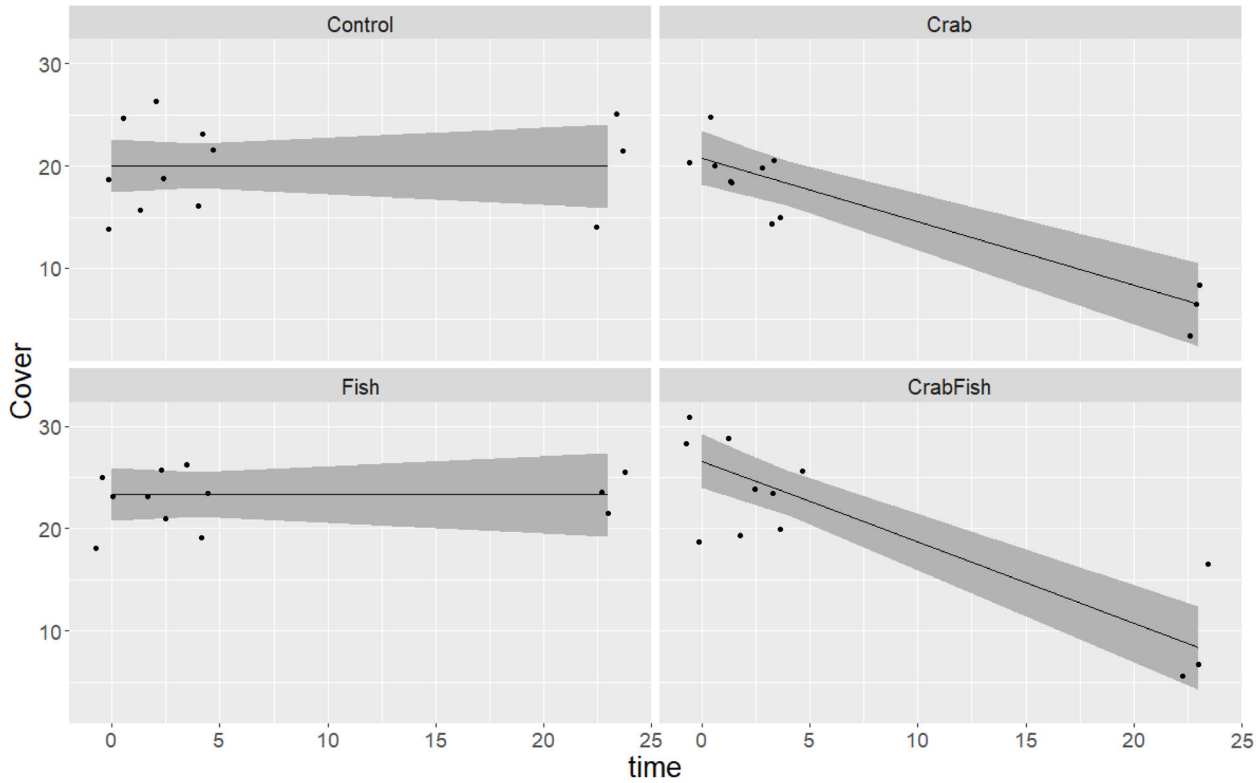

FIGURE 3 | Predicted and observed development of *B. improvisus* cover over time in a 24 h experiment in October 2019, given four different treatments (Control: no predators added, Crab: only crabs added as predator, Fish: only fish added as predator, CrabFish: i.e., both crabs and fish added as predator species to the mesocosms). The shaded area shows the 95% confidence levels of the predicted GAM values (i.e., cover as a function of treatment + time × treatment) and the points represent the observed cover at different times.

of the predators present in the mesocosms were observed in close proximity to the stones with mussels.

Many different predators are known to prey on blue mussels. The common starfish (*Asterias rubens*) is an important predator on adults and recruits of blue mussels in the NE Atlantic (see Hiscock et al., 2019) and also the eider duck, *Somateria mollissima* (Bustnes and Erikstad, 1990; Westerbom et al., 2002) is an important predator. Our experiment suggests that increasing populations of other small predators such as the green crab and the goldsinny wrasse may cause a severe threat to blue mussel beds/reefs and especially to mussel recruitment. This is primarily because of their preference of juvenile blue mussels as prey and their efficiency as predators preventing recruitment to larger size groups. In particular, the co-consumptive effect of the two predators might increase this threat. Recent observations of high mortality of hundreds of starved eider ducks in south Norway in winter/spring 2020, reported through media, has been suggested to be caused by a lack of larger blue mussels. This highlights the need to understand the role of these mesopredators for the structure and function of coastal ecosystems.

Top-down cascade effects favoring small mesopredators, such as small fish and crabs, are likely initiated because of reduced number and size of top predators and may cause significant community changes. Moksnes et al. (2008) and Östman et al. (2016) reported similar effects of small fish in natural environments, and Kraufvelin et al. (2020) in mesocosms. Furthermore, this study supports the wide attention on increasing top down control by different crab species due to reductions of other populations of top predators (Hughes et al., 2013; Fagerli et al., 2014; Infantes et al., 2016; Christie et al., 2019). As our study indicates, increasing predator abundance is expected to lead to increased predation that affects particularly preferred prey organism as mussels. Rilov and Schiel (2006) describe a similar scenario where increased densities of crabs and wrasses caused increasing decline in juvenile mussels. As higher mesopredator population densities are expected to cause increased predation effects, the level of mesopredator increase in an area may be crucial for continued existence or extinction of mussel beds/reefs. As blue mussel beds create habitats for diverse communities (Norling and Kautsky, 2007; Díaz et al., 2015; Norling et al., 2015; Westerbom et al., 2019), changes in predator population levels may lead to large structural and functional changes in shallow reef ecosystems.

The field observations indicate that *M. edulis* can settle and recruit during several seasons (see also Bayne, 1964), with the potential of avoiding predation pressure at least during some of the recruitment events. However, our experiment showed high mesopredator activity in both summer and autumn by two

predators that quickly can change from other prey organisms to small mussels. Also, our field observations indicate efficient predation on mussel recruits in the natural environment within a few weeks. In addition to green crabs and the goldsinny wrasse that both have become more abundant in this area (Gjøseter and Paulsen, 2004; Eriksson et al., 2011; Bergström et al., 2016; Infantes et al., 2016), other species of small fish, hermit crabs (*Pagurus sp.*), sea stars (*A. rubens*), and eider ducks (*S. mollissima,* although on larger size classes) are relevant blue mussel predators in the area, further increasing the predator pressure. Our experiment highlights the importance and efficiency of boosted mesopredator density on blue mussel mortality, but it cannot exclude the contribution from other predators and factors for the recent decreases in blue mussel abundance on rocky shores of the eastern North Sea.

DATA AVAILABILITY STATEMENT

The datasets generated for this study are available on request to the corresponding author.

ETHICS STATEMENT

The experiments fully comply with ethical standards and the experiments have received permission from the Norwegian Food Safety Authorities / Food and Animal authorities in Norway. All applicable international, national (Norwegian Food Safety Authorities) and institutional guidelines for the care and use of animals were followed.

AUTHOR CONTRIBUTIONS

All authors were involved in field activities, in contributing to the manuscript, and giving approval for publication of this manuscript. HC had the lead in writing and ER the lead of the statistical analysis and figures.

FUNDING

The mesocosm part of this work was funded by internal money from the Norwegian Institute for Water Research (NIVA) and by the EU network of mesocosm facilities AQUACOSM (https://www.aquacosm.eu/). PK also received financial support from Svenska Litteratursällskapet i Finland r.f. (Ingrid, Margit och Henrik Höijers Donationsfond II).

ACKNOWLEDGMENTS

We are grateful to Oddbjørn Pettersen, Per Ivar Johannessen, and Per Kristian Ekern for excellent regular maintenance of the Solbergstrand mesocosms.

REFERENCES

Andersen, S., Grefsrud, E. S., Mortensen, S., Naustvoll, L. J., Strand, Ø, Strohmeier, T., et al. (2016). *Reports on Disappearing Blue Mussels – Summing up for 2016*. Norwegian: Institute of Marine Research.

Baden, S., Emanuelsson, A., Pihl, L., Svensson, C. J., and Åberg, P. (2012). Shift in seagrass food web structure over decades is linked to overfishing. *Mar. Ecol. Prog. Ser.* 451, 61–73. doi: 10.3354/meps09585

Bayne, B. (1964). Primary and secondary settlement in *Mytilus edulis* L. (Mollusca). *J. Anim. Ecol.* 33, 513–523.

Bergström, L., Karlsson, M., Bergström, U., Pihl, L., and Kraufvelin, P. (2016). Distribution of mesopredatory fish determined by habitat variables in a predator-depleted coastal system. *Mar. Biol.* 163: 201. doi: 10.1007/s00227-016-2977-9

Bokn, T. L., Duarte, C. M., Pedersen, M. F., Marbá, N., Moy, F. E., Barrón, C., et al. (2003). The response of experimental rocky shore communities to nutrient additions. *Ecosystems* 6, 577–594. doi: 10.1007/s10021-002-0108-6

Brooks, S. J., and Farmen, E. (2013). The distribution of the mussel *Mytilus* species along the Norwegian coast. *J. Shellfish Res.* 32, 265–270.

Bustnes, J. O., and Erikstad, K. E. (1990). Size selection of common mussels, *Mytilus edulis*, by common eiders, *Somateria mollissima*: energy maximization or shell weight minimization? *Can. J. Zool.* 68, 2280–2283. doi: 10.1139/z90-318

Cardinale, M., and Svedäng, H. (2004). Modelling recruitment and abundance of Atlantic cod, *Gadus morhua*, in the eastern SkagerrakKattegat (North Sea): evidence of severe depletion due to a prolonged period of high fishing pressure. *Fish. Res.* 69, 263–282. doi: 10.1016/j.fishres.2004.04.001

Christie, H. (1983). Use of video in remote studies of rocky subtidal community interactions. *Sarsia* 68, 191–194. doi: 10.1080/00364827.1983.10420571

Christie, H., Gundersen, H., Rinde, E., Filbee-Dexter, K., Norderhaug, K. M., Pedersen, T., et al. (2019). Can multitrophic interactions and ocean warming influence large scale kelp recovery? *Ecol. Evol.* 9, 2847–2862. doi: 10.1002/ece3.4963

Díaz, E. R., Erlandsson, J., Westerbom, M., and Kraufvelin, P. (2015). Depth-related spatial patterns of sublittoral blue mussel beds and their associated macrofauna diversity revealed by geostatistical analyses. *Mar. Ecol. Prog. Ser.* 540, 121–134. doi: 10.1002/ecs2.2883

Díaz, E. R., Kraufvelin, P., and Erlandsson, J. (2012). Combining gut fluorescence technique and spatial analysis to determine *Littorina littorea* grazing dynamics in nutrient-enriched and nutrient-unenriched littoral mesocosms. *Mar. Biol.* 159, 837–852. doi: 10.1007/s00227-011-1860-y

Eggermont, M., Bossier, P., Pande, G. S. J., Delahaut, V., Rayhan, A. M., Gupta, N., et al. (2017). Isolation of Vibrionaceae from wild blue mussel (*Mytilus edulis*) adults and their impact on blue mussel larviculture. *FEMS Microbiol. Ecol.* 93: fix039. doi: 10.1093/femsec/fix039

Elner, R. W. (1978). The mechanics of predation by the shore crab, *Carcinus maenas* (L.), on the edible mussel, *Mytilus edulis* L. *Oecologia* 36, 333–344. doi: 10.1007/bf00348059

Eriksson, B. K., van Sluis, C., Sieben, K., Kautsky, L., and Råberg, S. (2011). Omnivory and grazer functional composition moderate cascading trophic effects in experimental *Fucus vesiculosus* habitats. *Mar. Biol.* 158, 747–756. doi: 10.1007/s00227-010-1602-6

Fagerli, C. W., Norderhaug, K. M., Christie, H., Pedersen, M. F., and Fredriksen, S. (2014). Predators of the destructive sea urchin grazer (*Strongylocentrotus droebachiensis*) on the Norwegian coast. *Mar. Ecol. Prog. Ser.* 502, 207–218. doi: 10.3354/meps10701

Frigstad, H., Andersen, G. S., Trannum, H. C., Naustvoll, L.-J., Kaste, Ø, and Hjermann, D. Ø (2018). *Synthesis of Climate Relevant Results From Selected Monitoring Programs in the Coastal Zone. Part 2: Quantitative analyses*. Norwegian: Norwegian Environment Agency.

Gjøseter, J., and Paulsen, Ø (2004). *Strandnotundersøkelser på Skagerrakkysten 2003*. Bergen: Institute of Marine Research.

Gjøsæter, J. (2002). Fishery for goldsinny wrasse (*Ctenolabrus rupestris*) (Labridae) with pots along the Norwegian Skagerrak coast. *Sarsia* 87, 83–90. doi: 10.1080/00364820275363176

Green, N. W., Schøyen, M., Hjermann, D. Ø, Øxnevad, S., Ruus, A., Lusher, A., et al. (2018). *Contaminants in Coastal Waters of Norway 2017*. Bergen: Institute of Marine Research.

Hastie, T., and Tibshirani, R. (1990) . *Generalized Additive Models*. London: Chapman and Hall, 352.

Hastie, T., Tibshirani, R., and Friedman, J. (2009). *The Elements of Statistical Learning: Data Mining, Inference and Prediction*. Berlin: Springer.

Hiscock, K., Christie, H., and Bekkby, T. (2019). "The ecology of the rocky subtidal habitats of the Northeast Atlantic," in *Interactions in the Marine Benthos: Global Patterns and Processes*, eds S. J. Hawkins, K. Bohn, L. B. Firth, and G. A. Williams (Cambridge: Cambridge University Press).

Hughes, B. B., Eby, R., VanDyke, E., Tinker, M. T., Marks, C. I., and Johnson, K. S. (2013). Recovery of a top predator mediates negative eutrophic effects on seagrass. *PNAS* 110, 15313–15318. doi: 10.1073/pnas.1302805110

Infantes, E., Crouzy, C., and Moksnes, P.-O. (2016). Seed predation by the shore crab *Carcinus maenas*: a positive feedback preventing eelgrass recovery? *PLoS One* 11:e0168128. doi: 10.1371/journal.pone.0168128

Kraufvelin, P., Christie, H., and Gitmark, J. K. (2020). Top-down release of mesopredatory fish is a weaker structuring driver of temperate rocky shore communities than bottom-up nutrient enrichment. *Mar. Biol.* 167: 49.

Kraufvelin, P., Christie, H., and Olsen, M. (2002). Littoral macrofauna (secondary) responses to experimental nutrient addition to rocky shore mesocosms and a coastal lagoon. *Hydrobiologia* 484, 149–166. doi: 10.1007/978-94-017-3190-4_13

Kraufvelin, P., Lindholm, A., Pedersen, M. F., Kirkerud, L. A., and Bonsdorff, E. (2010). Biomass, diversity and production of rocky shore macroalgae at two nutrient enrichment and wave action levels. *Mar. Biol.* 157, 29–47. doi: 10.1007/s00227-009-1293-z

Kraufvelin, P., Salovius, S., Christie, H., Moy, F. E., Karez, R., and Pedersen, M. F. (2006b). Eutrophication-induced changes in benthic algae affect the behaviour and fitness of the marine amphipod *Gammarus locusta*. *Aquat. Bot.* 84, 199–209. doi: 10.1016/j.aquabot.2005.08.008

Kraufvelin, P., Moy, F. E., Christie, H., and Bokn, T. L. (2006a). Nutrient addition to experimental rocky shore communities revisited: delayed responses, rapid recovery. *Ecosystems* 9, 1076–1093. doi: 10.1007/s10021-005-0188-1

Lundström, K. (2020). "Blåmussla *Mytilus edulis*," in *Fisk- Och Skaldjursbestånd I Hav Och Sötvatten 2019. Resursöversikt*. (Göteborg: Havs- Och Vattenmyndighetens Rapport 2020:3), 34–37.

Moksnes, P.-O. (2002). The relative importance of habitat-specific settlement, predation and juvenile dispersal for distribution and abundance of young juvenile shore crabs *Carcinus maenas* L. *J. Exp. Mar. Biol. Ecol.* 271, 41–73. doi: 10.1016/s0022-0981(02)00041-2

Moksnes, P. O., Gullström, M., Tryman, K., and Baden, S. (2008). Trophic cascades in a temperate seagrass community. *Oikos* 117, 763–777. doi: 10.1111/j.0030-1299.2008.16521.x

Moy, F. E., and Christie, H. (2012). Large-scale shift from sugar kelp (*Saccharina latissima*) to ephemeral algae along the south and west coast of Norway. *Mar. Biol. Res.* 8, 309–321. doi: 10.1080/17451000.2011.637561

Norling, P., and Kautsky, N. (2007). Structural and functional effects of *Mytilus edulis* on diversity of associated species and ecosystem functioning. *Mar. Ecol. Prog. Ser.* 351, 163–175. doi: 10.3354/meps07033

Norling, P., Lindegarth, M., Lindegarth, S., and Strand, Å (2015). Effects of live and post-mortem shell structures of invasive Pacific oysters and native blue mussels on macrofauna and fish. *Mar. Ecol. Prog. Ser.* 518, 123–138. doi: 10.3354/meps11044

Östman, Ö, Eklöf, J., Eriksson, B. K., Olsson, J., Moksnes, P.-O., and Bergström, U. (2016). Top-down control as important as nutrient enrichment for eutrophication effects in North Atlantic coastal ecosystems. *J. Appl. Ecol.* 53, 1138–1147. doi: 10.1111/1365-2664.12654

Paine, R. T. (1966). Food web complexity and species diversity. *Am. Nat.* 100, 65–75. doi: 10.1086/282400

Peteiro, L. G., Filgueira, R., Labarta, U., and Fernandez-Reiris, M. J. (2010). The role of fish predation on recruitment of *Mytilus galloprovincialis* on different artificial mussel collectors. *Aquacult. Eng.* 42, 25–30. doi: 10.1016/j.aquaeng.2009.09.003

Prugh, L. R., Stoner, C. J., Epps, C. W., Bean, W. T., Ripple, W. J., Laliberte, A. S., et al. (2009). The rise of the mesopredator. *BioScience* 59, 779–791. doi: 10.1525/bio.2009.59.9.9

R Core Team (2019). *R: A Language and Environment for Statistical Computing*. Vienna: R Foundation for Statistical Computing.

Rilov, G., and Schiel, D. R. (2006). Trophic linkages across seascapes: subtidal predators limit effective mussel recruitment in rocky intertidal communities. *Mar. Ecol. Prog. Ser.* 327, 83—-93.

Sayer, M. D. J., Gibson, R. N., and Atkinson, R. J. A. (1993). Distribution and density of populations of goldsinny wrasse (*Ctenolabrus rupestris*) on the west coast of Scotland. *J. Fish Biol.* 43, 157–167. doi: 10.1111/j.1095-8649.1993.tb01185.x

Seuront, L., Nicastro, K. R., Zardi, G. I., and Goberville, E. (2019). Decreased thermal tolerance under recurrent heat stress conditions explains summer mass mortality of the blue mussel *Mytilus edulis*. *Sci Rep* 9: 17498. doi: 10.1038/s41598-019-53580-w

Skiftesvik, A. B., Blom, G., Agnalt, A. L., Durif, C. M., Browman, H. I., Bjelland, R. M., et al. (2014). Wrasse (Labridae) as cleaner fish in salmonid aquaculture – The Hardangerfjord as a case study. *Mar. Biol. Res.* 10, 289–300. doi: 10.1080/17451000.2013.810760

van der Heide, T., Tielens, E., van der Zee, E. M., Weerman, E. J., Holthuisen, S., Eriksson, B. K., et al. (2014). Predation and habitat modification synergistically interact to control bivalve recruitment on intertidal mudflats. *Biol. Conserv.* 172, 163–169. doi: 10.1016/j.biocon.2014.02.036

Weijerman, M., Lindeboom, H., and Zuur, A. (2005). Regime shifts in marine ecosystems of the North Sea and Wadden Sea. *Mar. Ecol. Prog. Ser.* 298, 21–39. doi: 10.3354/meps298021

Westerbom, M., Kilpi, M., and Mustonen, O. (2002). Blue mussels, *Mytilus edulis*, at the edge of the range: population structure, growth and biomass along a salinity gradient in the north-eastern Baltic Sea. *Mar. Biol.* 140, 991–999. doi: 10.1007/s00227-001-0765-6

Westerbom, M., Kraufvelin, P., Erlandsson, J., Korpinen, S., Mustonen, O., and Díaz, E. (2019). Wave stress and biotic facilitation drive community composition in a marginal hard bottom ecosystem. *Ecosphere* 10: e02883.

Wickham, H. (2016). *ggplot2: Elegant Graphics for Data Analysis*. New York, NY: Springer-Verlag.

Wickham, H., Averick, M., Bryan, J., Chang, W., D'Agostino McGowan, L., François, R., et al. (2019). Welcome to the tidyverse. *J. Open. Sourc. Softw.* 4: 1686. doi: 10.21105/joss.01686

Wood, S. N. (2011). Fast stable restricted maximum likelihood and marginal likelihood estimation of semiparametric generalized linear models. *J. R. Stat. Soc. B* 73, 3–36. doi: 10.1111/j.1467-9868.2010.00749.x

Conflict of Interest: The authors declare that the research was conducted in the absence of any commercial or financial relationships that could be construed as a potential conflict of interest.

frontiers in Marine Science

ORIGINAL RESEARCH
published: 24 July 2020
doi: 10.3389/fmars.2020.00587

Influence of Local Pressures on Maldivian Coral Reef Resilience Following Repeated Bleaching Events, and Recovery Perspectives

Monica Montefalcone, Carla Morri and Carlo Nike Bianchi*

DiSTAV, Department of Earth, Environment and Life Sciences, University of Genoa, Genoa, Italy

Two severe heat waves triggered coral bleaching and mass mortality in the Maldives in 1998 and 2016. Analysis of live coral cover data from 1997 to 2019 in shallow (5 m depth) reefs of the Maldives showed that the 1998 heat wave caused more than 90% of coral mortality leaving only 6.8 ± 0.3% of survived corals in all the shallow reefs investigated. No significant difference in coral mortality was observed among atolls with different levels of human pressure. Maldivian reefs needed 16 years to recover to the pre-bleaching hard coral cover values. The 2016 heat wave affected all reefs investigated, but reefs in atolls with higher human pressure showed greater coral mortality than reefs in atolls with lower human pressure. Additionally, exposed (ocean) reefs showed lower coral mortality than those in sheltered (lagoon) reefs. The reduced coral mortality in 2016 as compared to 1998 may provide some support to the Adaptive Bleaching Hypothesis (ABH) in shallow Maldivian reefs, but intensity and duration of the two heat waves were different. Analysis of coral cover data collected along depth profiles on the ocean sides of atolls, from 10 to 50 m, allowed the comparison of coral mortality at different depths to discuss the Deep Refuge Hypothesis (DRH). In the upper mesophotic zone (i.e., between 30 and 50 m), coral mortality after bleaching was negligible. However, live coral cover did not exceed 15%, a value lower than coral survival in shallow reefs. Low cover values of corals surviving in the mesophotic reefs suggest that their role as refuge or seed banks for the future recovery of some species in shallow-water reefs of the Maldives may be small. The repeatedly high coral mortality after bleaching events and the long recovery period, especially in sites with human pressure, suggest that the foreseen increased frequency of bleaching events would jeopardize the future of Maldivian reefs, and ask for reducing local pressures to improve their resilience.

Keywords: coral reefs, local human pressure, sea water warming, adaptive bleaching hypothesis, mesophotic reefs, deep refuge hypothesis, Maldives

OPEN ACCESS

Edited by:
Massimo Ponti, University of Bologna, Italy

Reviewed by:
Paolo Galli, University of Milano-Bicocca, Italy
Lorenzo Bramanti, UMR8222 Laboratoire d'Ecogéochimie des Environnements Benthiques (LECOB), France

****Correspondence:***
Monica Montefalcone
monica.montefalcone@unige.it

Specialty section:
This article was submitted to Marine Ecosystem Ecology, a section of the journal Frontiers in Marine Science

Received: *03 March 2020*
Accepted: *25 June 2020*
Published: *24 July 2020*

Citation:
Montefalcone M, Morri C and Bianchi CN (2020) Influence of Local Pressures on Maldivian Coral Reef Resilience Following Repeated Bleaching Events, and Recovery Perspectives. Front. Mar. Sci. 7:587. doi: 10.3389/fmars.2020.00587

INTRODUCTION

Coral reefs throughout the world are facing the consequences of changing Earth's climate. The ENSO phenomenon, which is a natural periodic fluctuation in sea surface temperature (El Niño) and air pressure of the overlying atmosphere (Southern Oscillation) across the equatorial Pacific Ocean (Dijkstra, 2006), has important consequences for the climate around the globe. Ocean

warming worldwide and particularly intense ENSO episodes are leading to an increase in the severity, duration and frequency of coral bleaching events, which threatens the long-term stability of coral reefs, hampering their resilience to local human pressure (Hughes et al., 2018a). Reefs in the world have recently been affected by three major global bleaching events, in 1998, 2010, and 2016. The U.S. National Oceanic and Atmospheric Administration (NOAA) declared that the last bleaching event can be considered as the longest, the most widespread, and probably the most damaging on record (Hughes et al., 2017). More than 70% of coral reefs around the world bleached and experienced catastrophic levels of coral mortality (Eakin et al., 2016).

Corals suffer thermal stress when sea surface temperatures exceed the seasonal means and protract for extended periods to cause the disruption of the mutualistic symbiosis between corals and their dinoflagellate endosymbionts (zooxanthellae), resulting in the expulsion of zooxanthellae and consequent coral mortality (LaJeunesse et al., 2018). The relationship among heat exposure, bleaching, and consequent mortality of different taxa is still not well understood (Hughes et al., 2018b). However, a protracted value of 1°C above the maximum summer mean has been often described as high enough to cause coral bleaching (Kayanne, 2017), depending also upon sea and whether conditions. Current projections foresee the collapse of coral reefs by the end of this century due to the increased frequency and severity of coral bleaching events worldwide (Hoegh-Guldberg, 1999; Hoegh-Guldberg et al., 2007; Veron et al., 2009; Bay et al., 2017; Heron et al., 2017). However, these projections do not consider the potential of corals to survive a changing climate by adapting and/or developing responses apt to increase their resilience to climate-driven stressors. In this regard, two hypotheses have been proposed: (i) the adaptive bleaching hypothesis (hereafter ABH); and (ii) the deep refuge hypothesis (hereafter DRH).

Although coral reefs are confined to stable habitats and narrow environmental conditions, the ABH postulates that the loss of one or more zooxanthellae strains, rapidly replaced by different ones with the formation of a new symbiotic consortium, has the potential to create new and more tolerant organisms, capable of surviving a variety of extreme conditions (Buddemeier and Fautin, 1993). Capacity to adapt ensured coral reef communities to persist over geological time scales through significant climate and sea-level fluctuations (Buddemeier et al., 2004); however, oceans are presently warming at a faster rate with respect to the geological past and decadal evolutionary responses to warming may drive the selection of the most adequate species able to adapt rapidly to environmental change (Padfield et al., 2015). Genetic adaptation to sea warming has been predicted (Matz et al., 2018), and reduced bleaching and mortality by some corals exposed to previous bleaching events has been often reported (Coles et al., 2018, and references therein). Adaptive bleaching mechanisms are not common in all corals (McClanahan and Muthiga, 2014; McClanahan, 2017), and shifts in species composition and decline in coral diversity are predicted to occur as temperature increases (Bahr et al., 2016; Richardson et al., 2018).

According to the DRH, marine organisms in deeper habitats are buffered from high surface temperatures and increased temperature variability (Bongaerts et al., 2010; Morri et al., 2017; Bianchi et al., 2019, and references therein). Mesophotic coral ecosystems are light-dependent communities developing at tropical and subtropical latitudes that extend from 30 m depth to as deep as about 165 m (Kahng et al., 2010), at the lower limit of the photic zone (Hinderstein et al., 2010; Loya et al., 2016; Laverick et al., 2017). Although working at mesophotic depths is constrained by traditional scuba limits, investigations on mesophotic coral reefs have grown exponentially in recent years due to advances in technology and because of the increasing recognition of their potential role as refuge for shallow-water reefs (Hoegh-Guldberg and Bruno, 2010; Loya et al., 2016; Muir et al., 2017, 2018). Corals show bleaching and mortality especially in shallow waters (Jokiel, 2004) whilst the occurrence of bleaching events and consequent mortality is normally lower at greater depths (Baird et al., 2018). DRH therefore suggests that mesophotic coral ecosystems may provide refuge and a source of recruits to facilitate recovery of shallow-water reefs damaged after a disturbance (Glynn, 1996; Riegl and Piller, 2003; Holstein et al., 2015; Thomas et al., 2015; Prasetia et al., 2017; Baird et al., 2018). Mesophotic reefs may display an important degree of overlap in species composition, and maintain connectivity with shallow reefs (Lesser et al., 2018; Muir et al., 2018), thus contributing to the local persistence of heat sensitive species despite periods of elevated seawater temperatures during strong ENSO episodes (Gatti et al., 2017; Shlesinger et al., 2018). Most families of scleractinian corals have been shown to be represented in the mesophotic zone of the Great Barrier Reef, with many also extending to greater depths, thus giving each evolutionary lineage some potential for being safeguarded in the case of shallow-reef degradation (Muir et al., 2018).

Repeated heat waves in the Maldives during the last decades provided the opportunity to better understand the impact of bleaching and mass mortality on coral communities. The general trend of coral recovery after the severe bleaching event of 1998 has already been investigated in previous papers (Bianchi et al., 2003, 2006, 2017; Lasagna et al., 2008), while the bleaching event of 2010 was comparatively milder and did not cause widespread mortality (Morri et al., 2015). The consequences of the further severe bleaching event of 2016 have been analyzed by Montefalcone et al. (2018a), especially with respect to the constructional potential of Maldivian reefs. The availability of a twenty-three year series of data on coral cover in the Maldives, encompassing the two most important bleaching events of 1998 and 2016 allowed comparing their impact and exploring the following hypotheses: (1) coral mortality after the 2016 bleaching event should be lower than after the 1998 event, according to the ABH; (2) coral mortality in deep waters should be lower than in shallow waters, meaning that mesophotic reefs can offer refuge to thermal stress as postulated by the DRH. Clearly, we did not analyze the ecophysiological mechanisms of ABH and DRH but simply concentrated on their manifest consequence: increased coral survival.

This study aims at: (i) reconstructing the thermal regime in the Maldives to identify the heat waves that caused severe bleaching and mass coral mortality in the last two decades; (ii) reconstructing the trend of human pressure (tourism and

resident population) in the Maldives to be compared with coral mortality rates in coincidence with the bleaching events; (iii) evaluating the trajectories of change and recovery patterns in shallow reef communities after the two mass mortality events; (iv) investigating geographical patterns of hard coral survival during the last bleaching event according to location (i.e., atolls with high or low human pressure) and reef exposure (i.e., lagoon- or ocean-facing reefs); (v) discussing the ABH using our long-term series of coral cover data collected on shallow reefs at about 5 m depth; (vi) discussing the DRH by analyzing coral cover reduction and mortality along depth profiles, from 10 to 50 m, surveyed in years with and without coral mortality.

MATERIALS AND METHODS

Study Area and Field Activities

The Maldives Archipelago consists of 27 atolls with ca. 1190 small coral islands stretched over an area of 860 km long from about 7°070 N to 0°400 S in latitude and 72°330 E to 73°450 E in longitude, with more than 99% of its territory covered by water. Coral reefs of the Maldives are considered as the seventh largest coral reef system on Earth, representing 3.14% of the World's reef area (Dhunya et al., 2017).

Scientific cruises took place annually in late April – early May between 1997 and 2019. Every year, eight to eleven sites were chosen randomly and surveyed across the atolls of Ari, Felidhoo, Gaafu Alifu (Suvadiva), North Malé, South Malé, Rasdhoo, and Thoddoo (**Supplementary Table S1**). Based on the occurrence of inhabited islands and infrastructures, the atolls of North Malé and South Malé were considered to be subjected to higher human pressure with respect to the remaining atolls (Godfrey, 2006). Data (see below for detail) were collected by scuba diving at reef sites located either on the ocean-exposed reefs or in lagoon sites (lagoon-facing sides of the atoll rim or patch reefs).

To evaluate the overall reef status of the Maldives (with a main focus on the central atolls because of logistic constraints), our sampling design implied a completely randomly selection of the study sites each year, to assure data independency. Monitoring the history of a specific reef site was indeed not within the scope of this long series of cruises. Each year an equal number of ocean reefs and lagoon reefs has been sampled, always distinguishing between atolls with high or low human pressure. Although the cruise route differed from year to year, some reefs (31%) were casually revisited in different years (**Supplementary Table S1**). In total, 168 sites were surveyed; their geographical position was recorded using a portable GPS.

Climate and Local Human Pressure Regimes

Sea surface temperature data was used as a proxy for climate change (Montefalcone et al., 2018b). A twenty-three year trend (1997–2019) of monthly maximum sea surface temperature (SST) was plotted from data provided by the U.S. National Oceanic and Atmosphere Administration (NOAA) (available at http://coralreefwatch.noaa.gov/vs/gauges/maldives.php) for the area of the Maldives Archipelago. Satellite data were calibrated by the usual process of linear regression with discontinuous field data on sea surface temperature from our own archives, collected contemporaneously with the biological data. Maximum SSTs were compared to the two regional bleaching thresholds defined for the Maldives, corresponding to: (i) 30.9°C for severe bleaching events that are likely to cause widespread coral mortality and live coral cover reduction (NOAA, 2016); and (ii) 30.5°C for moderate bleaching events that usually have no wide-scale impacts on Maldivian coral reefs (Montefalcone et al., 2018a).

Since both the intensity and the duration of thermal stress are key factors in bleaching response, the Coral Bleaching Degree Heating Week (DHW) has been developed by NOAA (Kayanne, 2017) as an index of thermal stress, which measures the amount of heat stress accumulated in an area over the past 12 weeks. Intensity and duration of thermal stress are combined into the DHW single number, which is thus expressed as "degree C-weeks". DHW values >4.0 are likely to induce some bleaching, whilst DHW values >8.0 result in widespread bleaching and mass coral mortality (Kayanne, 2017). To estimate DHW for the Maldives we counted the number of weeks per year when the monthly mean SST was higher than the temperatures triggering moderate (30.5°C) or severe (30.9°C) bleaching events in the Maldives, and we added up all temperatures exceeding the regional bleaching thresholds during that time period. The estimated values of DHW for the Maldives were then compared with DHW values available from the NOAA coral reef watch database[1] considering the region of the "northern-eastern hemisphere centre" (i.e., the central Indian Ocean) over an area of 60 degrees $\times$ 40 degrees. A linear regression was performed on a total of 19 observations to test relationships between estimated values of DHW for the Maldives and DHW values available from NOAA coral reef watch.

As regards human pressure, the twenty-three year trends (1997–2019) of the resident population (number of inhabitants) and of the number of tourist arrivals in the Maldives were plotted from data provided by the United Nations (Department of Economic and Social Affairs Population Division), by the National Bureau of Statistics in the Maldives (Department of National Registration), and by the Ministry of Tourism data (compiled from annual reports, available at https://www.tourism.gov.mv/downloads/stats). For the four main central atolls investigated in this study (North and South Malé, Felidhoo, and Ari), the resident population (number of inhabitants) obtained from the national census carried out in 1995, 2000, 2006, and 2014 (available at http://statisticsmaldives.gov.mv/yearbook/statisticalarchive) and the twenty-three year trends (1997–2019) of the number of beds in the resorts were also provided.

Data Collection

Shallow reefs at 5±1m depth were surveyed each year. Composition and status of reef communities were described using live hard coral, bleached (but still alive) coral, and recently dead coral. The latter has been defined as coral deprived of living polyps but with the whole colony still in place and with

[1]https://coralreefwatch.noaa.gov/product/5km/index_5km_composite.php

a well-defined shape of the corallites (meaning that the main erosive processes have not started yet, i.e., usually within 1 year from coral death). The percent substratum cover for each of the three categories was visually estimated by the plain view technique of Wilson et al. (2007). Divers hovered 1–2 m above the bottom observing an area of 20 m^2, in three replicate spots (tens of meters apart) at each reef site and at each sampling time. To reduce bias in visual estimations, the same observers collected data during the surveys from 1997 to 2013, while new observers trained by the former estimated cover values from 2014 to 2019.

In a limited number of years (i.e., 1997, 1998, 1999, 2007, 2012, 2013, 2015, 2016, 2017, 2018, and 2019) the same surveying method (making sure to maintain a constant depth during each data collection) has also been used to visually estimate the percent substratum cover of live hard coral, bleached coral, and recently dead coral down depth profiles in each of the surveyed reefs (**Supplementary Table S1**), at depths corresponding to the lower photic reef (i.e., 10 and 20 m) and at depths corresponding to the upper mesophotic reef (i.e., 30, 40, and 50 m) (Loya et al., 2016, and references therein).

Data Management and Analysis

Twenty-three year (1997–2019) trends of the mean (± standard error) percent cover of live hard coral and recently dead coral in shallow reefs were obtained. While the severe bleaching event of 1998 had been already described in detail in previous papers (Bianchi et al., 2003, 2006, 2017; Lasagna et al., 2008; Morri et al., 2015), here we analyzed with greater detail the bleaching event of 2016, exploring patterns of live hard coral cover in the pre-bleaching year (2015), during the event (2016), in the post-bleaching year (2017), and in the following early recovery years (i.e., 2018 and 2019), contrasting atolls with high or low human pressure.

To compare the two bleaching events of 1998 and 2016, two subsets were extrapolated from the whole dataset (Montefalcone et al., 2018a): the pre-bleaching years (1997 vs. 2015), the years of the bleaching (1998 vs. 2016), and the 2 years after (1999 and 2000 vs. 2017 and 2018).

The mean (± standard error) coral mortality (in %) was computed as the ratio of recently dead coral to live coral in the two subsets (i.e., 1997–2000 and 2015–2018), using the following formula:

$$\text{coral mortality} = [\text{RDC}/(\text{HC} + \text{BC} + \text{RDC})] \times 100$$

where RDC is the cover of recently dead coral, HC the cover of live hard coral, and BC the cover of bleached coral.

The mean (± standard error) of the coral mortality and of the percent cover of HC and RDC was computed down the depth profile (10 m to 50 m) in two periods: i) years without coral mortality (i.e., 1997, 1998, 2012, 2013, 2015, and 2019), and ii) years with coral mortality during or short after either the moderate or severe bleaching events (i.e., 1999, 2007, 2016, 2017, and 2018).

Non-parametric permutational analysis of variance (one-way PERMANOVA, PRIMER6 + PERMANOVA; Anderson, 2001), run on untransformed data using the Euclidean distance, was used to test for differences in:

(i) live hard coral cover in shallow reefs (5 m depth) between atolls with high human pressure (North Malé and South Malé) and atolls with low local human pressure (2 levels) after the bleaching event of 2016;

(ii) live hard coral cover in shallow reefs (5 m depth) between lagoon reefs and ocean reefs (2 levels) after the bleaching event of 2016;

(iii) coral mortality in shallow reefs (5 m depth) among the years when coral mortality occurred (4 levels: 1999, 2016, 2017, and 2018);

(iv) coral mortality across depths (5 levels: 10, 20, 30, 40, and 50 m) when coral mortality occurred (pooling data from 1999, 2007, 2016, 2017, and 2018).

To test for differences in the percent cover of live hard corals, a two-way PERMANOVA was also performed with the factor "Mortality occurrence" (2 fixed levels: years without coral mortality and years with coral mortality during or short after bleaching events) and the factor Depth (5 levels: 10, 20, 30, 40, and 50 m) fixed and orthogonal.

The pair-wise test was used to discriminate among levels of significant factors.

RESULTS

Climate and Human Pressure Regimes in the Maldives

Peaks in maximum SST exceeded the moderate regional bleaching threshold in various years of the investigated period, but only the heat waves of 1998 and 2016 surpassed the severe regional bleaching threshold of 30.9°C (**Figure 1**). The heat wave of 1998 lasted from April to June and reached an estimated DHW value of 11.2, distinctly higher than the value of 8.2 reported in the NOAA database (**Table 1**). In 2016, we estimated a DHW value of 8.8, comparable to that of 8.9 provided by NOAA (**Table 1**), which was reached between mid-April and mid-June 2016. Notwithstanding occasional discrepancies due to the different size of the cells investigated, the DHW values we estimated for the Maldives proper were positively correlated ($r = 0.96$, $n = 19$) with those contained in the NOAA database for the whole central Indian Ocean.

Resident population in the Maldives increased slowly but steadily in the last decades (**Figure 2A**), passing from 244,814 people in the census of the year 1995 to 298,968 in 2006 and to 344,023 in 2014; the trend has been linear, leading to an estimated growth rate of 1.8% yearly. The same constant increase of the resident population was observed for the atolls of North and South Malé (**Figure 2B**), which have seen their population doubled in the last 20 years with an estimated growth rate of 4.2% yearly. On the contrary, the atoll of Ari passed from 11,955 people in the census of the year 1995 to 14,050 in 2014 and that of Felidhoo reduced from 1,678 people to 1,601 in the same period.

Tourist arrivals in the country grew exponentially, passing from around 366 thousands in 1997 to one million and half in 2019, with an increase rate of over 400%; a reduction in

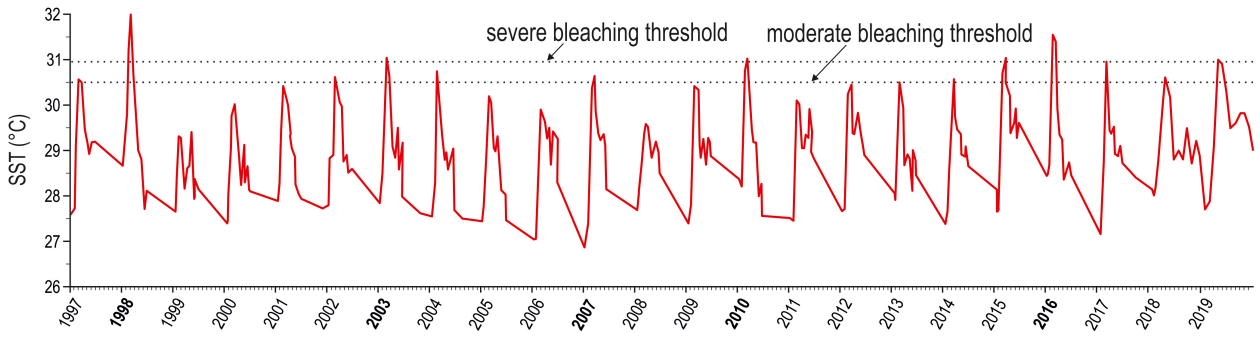

FIGURE 1 | Twenty-three year trend (1997–2019) of maximum monthly sea surface temperature (SST, red solid line). Bold values on the *x* axis correspond to years when bleaching events have been reported for the Maldives (from Morri et al., 2015, and references therein; NOAA, 2016). The threshold temperatures triggering moderate and severe bleaching events are also indicated (according to NOAA, 2016 and Montefalcone et al., 2018a).

2005 - possibly a consequence of the December 2004 tsunami – was rapidly recovered in 2006 (**Figure 2C**). The number of beds in the resorts increased exponentially in the atolls of Ari and Felidhoo, and more than exponentially in North and South Malé, where an impressive increase occurred especially after 2013 (**Figure 2D**); the number of beds in North and South Malé was twice than in Ari and one order of magnitude higher than that in Felidhoo.

TABLE 1 | Number of weeks (W) per year when the monthly mean sea surface temperature (SST) was higher than the temperatures triggering moderate (30.5°C) and severe (30.9°C) bleaching; degree heating weeks (DHW) above the moderate (30.5°C) and severe (30.9°C) bleaching thresholds per year as estimated from the monthly SST for the Maldives and DHW values reported in the NOAA coral reef watch database from the region "northern-eastern hemisphere centre" (i.e., central Indian Ocean) over an area of 60 degrees × 40 degrees (available at https://coralreefwatch.noaa.gov/product/5km/index_5km_composite.php).

	W > 30.5°C	W > 30.9°C	DHW > 30.5°C	DHW > 30.9°C	DHW NOAA
1997	4		0.8		0.7
1998	5	8	1.0	**11.2**	**8.2**
1999					
2000					0.1
2001					
2002	4		0.8		0.2
2003	4	3	2	0.3	2.8
2004	4		0.8		0.7
2005					0.4
2006					0.2
2007	4		0.8		0.9
2008					
2009					0.3
2010	4	2	1.6	0.2	2.3
2011					0.1
2012					0.3
2013					0.6
2014	3		0.3		0.1
2015	4	4	0.8	0.4	1.3
2016		8		**8.8**	**8.9**
2017	6		2.4		0.3
2018	6		0.6		0.5
2019		8		0.7	0.9

DHW values >8.0, which are expected to induce widespread bleaching and mass mortality, are in bold.

Impact of Bleaching on Shallow Reefs

Live hard coral cover on shallow reefs of the Maldives dropped from values around 70% to a value lower than 8% after the 1998 bleaching event, and gradually returned to a value comparable to the pre-bleaching one only by 2014 (**Figure 3**). In 2015, recovery was apparently complete, with live hard coral cover reaching over 70% in several reefs. However, in reefs of North Malé atoll subjected to high human pressure live hard coral cover hardly exceeded 40% (**Figure 4** and **Supplementary Table S2**). In 2016, many hard corals died following the new mass bleaching and dropped to a mean live cover value of around 20% (**Figure 3**). Bleaching affected indistinctly all sites (**Supplementary Table S2**) in both lagoon and ocean reefs. However, coral mortality after the bleaching event showed high spatial variability (**Figure 4** and **Supplementary Table S2**), with reefs in atolls affected by comparatively lower human pressure exhibiting higher values of live hard coral cover compared to reefs in the two atolls of North Malé and South Malé, where human pressure is high on average (**Table 2**). Reefs started to recover already in 2017, and reached a mean live hard coral cover value of over 30% (**Figure 3**). Recovery, however, was distinctly lower in the atolls of North and South Malé (**Figure 4**) than in atolls with lower human pressure. Pattern of recovery was also different according to reef type: ocean reefs had suffered lower mortality with respect to lagoon reefs (**Figure 5**), and were therefore able to show live hard coral cover values higher than lagoon reefs in the immediate aftermath of the bleaching event (**Table 3**). Between 2018 and 2019 live hard coral in reefs subjected to low human pressure exhibited cover values up to 50–70%, whilst most reefs in atolls with high human pressure hardly reached 40% (**Figure 4** and **Supplementary Table S2**).

After the two bleaching events of 1998 and 2016, at 5 m depth, cover of recently dead corals was higher in 1999 than in 2017 (**Figure 3**). Accordingly, coral mortality was significantly higher

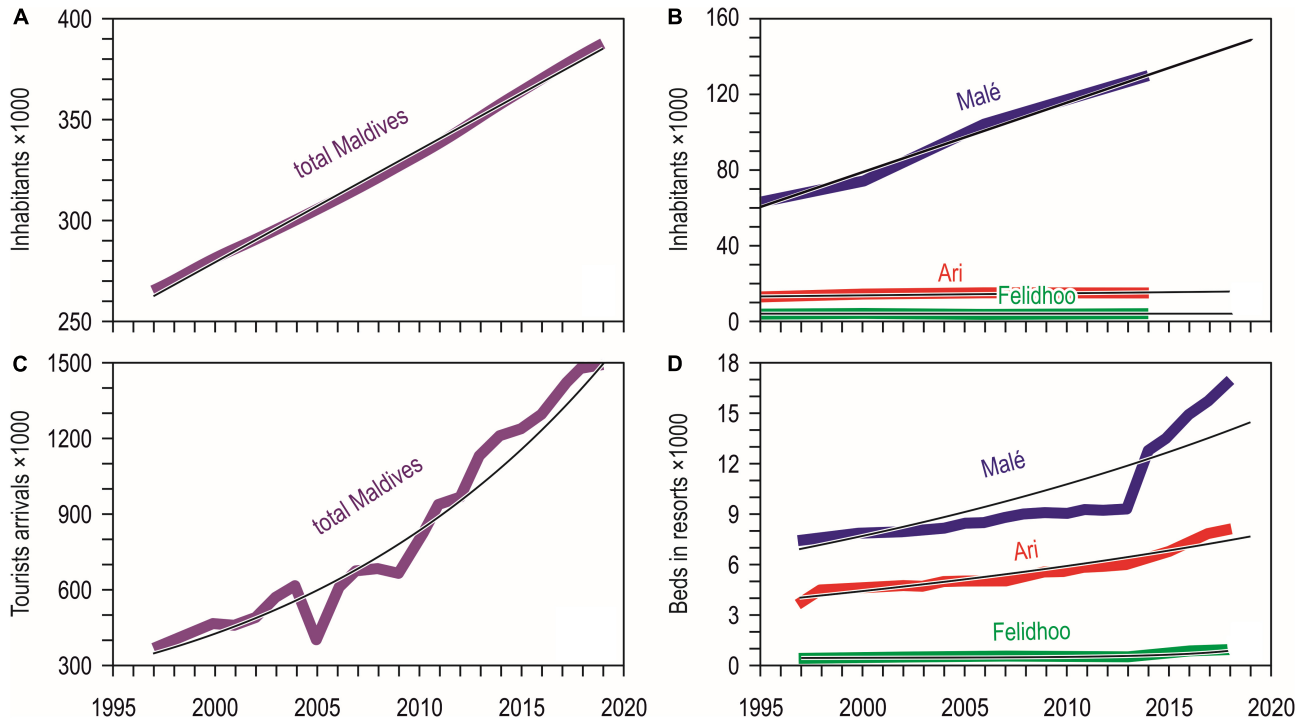

FIGURE 2 | (A) Twenty-three year trend (1997–2019) of the total number of inhabitants of the Maldives (number of inhabitants = 5.584 year-10889; R^2 = 0.997) (from United Nations, Department of Economic and Social Affairs, Population Division; National Bureau of Statistics in Maldives, Department of National Registration); **(B)** Number of inhabitants according to the national census of 1995, 2000, 2006, and 2014 (available at http://statisticsmaldives.gov.mv/yearbook/statisticalarchive) for the four main atolls compared in this study: North and South Malé (number of inhabitants = 3.659 year-7240; R^2 = 0.987), Ari (number of inhabitants = 0.106 year-199.2; R^2 = 0.733), and Felidhoo (number of inhabitants = –0.006 year-1396; R^2 = 0.492); **(C)** Twenty-three year trend (1997–2019) of tourists arrivals in the Maldives (tourists arrivals = 2E-56·$e^{0.067 \cdot year}$; R^2 = 0.943) (from Ministry of Tourism data, compiled from annual reports and available at https://www.tourism.gov.mv/downloads/stats); **(D)** Twenty-three year trends (1997–2019) of the number of beds in the resorts of the four main atolls compared in this study: North and South Malé (number of beds = 9E-27·$e^{0.034 \cdot year}$; R^2 = 0.779), Ari (number of beds = 3E-22·$e^{0.029 \cdot year}$; R^2 = 0.920), and Felidhoo (number of beds = 3E-36·$e^{0.043 \cdot year}$; R^2 = 0.821) (from Ministry of Tourism data, compiled from annual reports and available at https://www.tourism.gov.mv/downloads/stats).

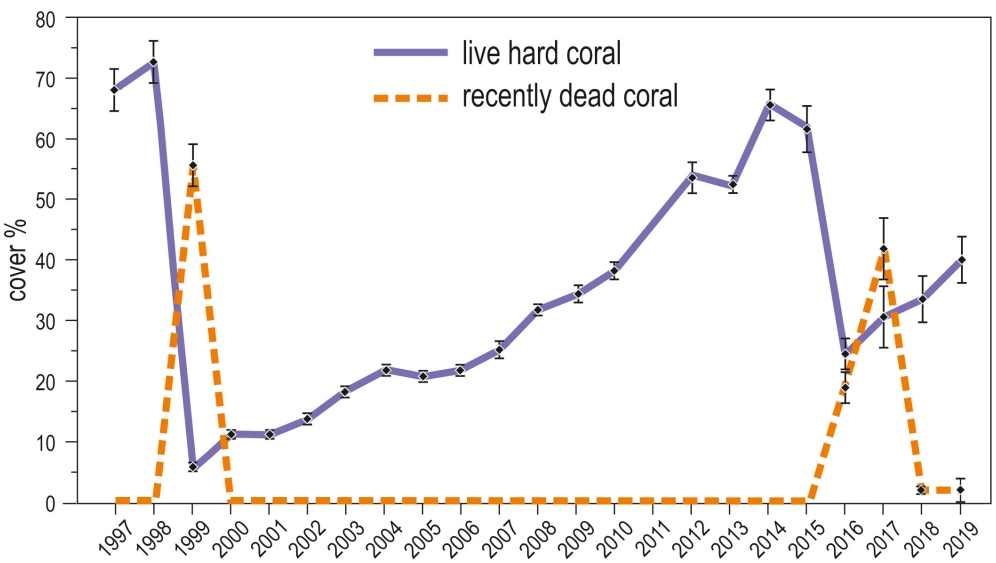

FIGURE 3 | Twenty-three year trends (1997–2019) of the mean (± standard error) percent cover of live hard coral (violet solid line) and recently dead coral (orange dashed line) in shallow reefs (about 5 m depth) of the Maldives.

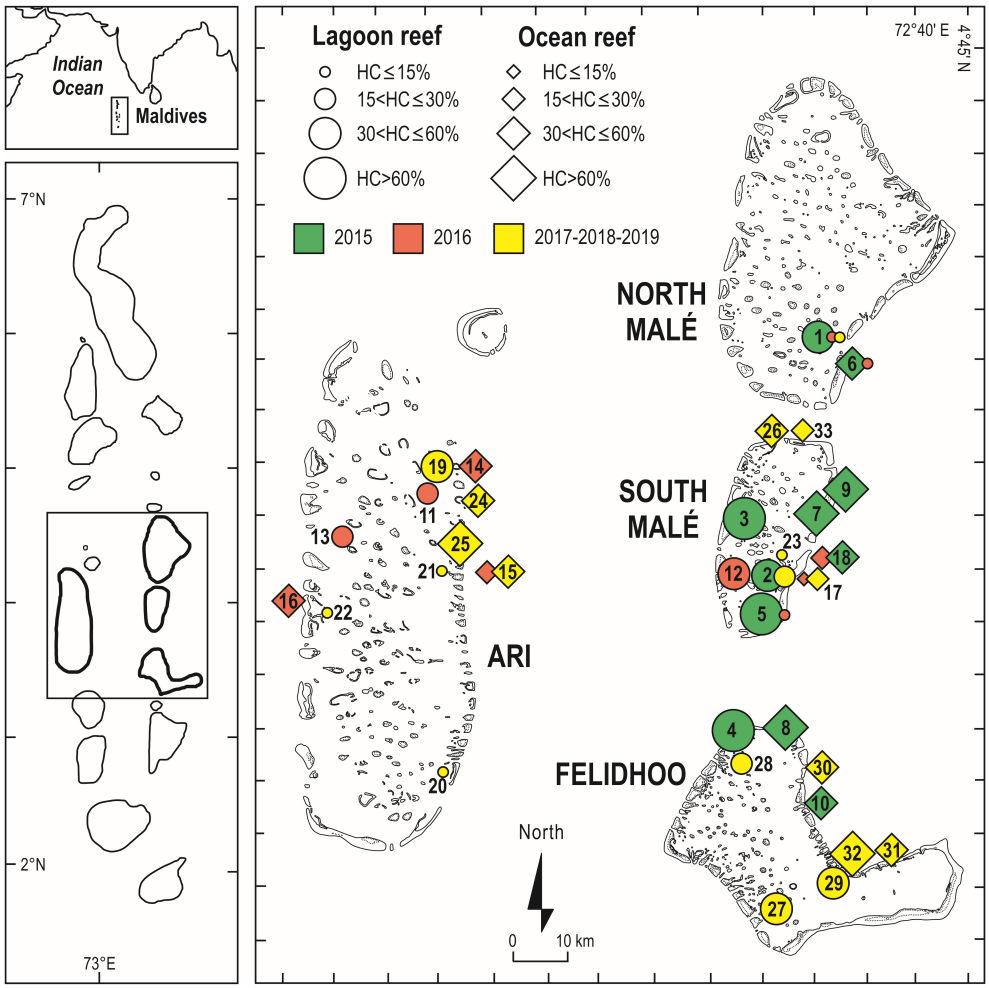

FIGURE 4 | Geographical setting of the Maldives Archipelago and of the central atolls surveyed in recent years, with the mean percent cover of live hard corals at shallow reefs (5 m depth) in the 51 reefs surveyed during the 2015, 2016, 2017, 2018, and 2019 scientific cruises. Each reef is labeled according to the codes reported in **Supplementary Table S2**. In green are the reefs surveyed before the 2016 mass bleaching event (i.e., the pre-bleaching year in 2015), in red are the reefs surveyed during the bleaching event (in 2016), and in yellow are the sites surveyed after the bleaching event. For a safe of clarity the post-bleaching year (in 2017) and the years of early recovery (2018 and 2019) are grouped in this figure. North Malé and South Malé are atolls affected by high human pressure, whilst Ari and Felidhoo atolls by low human pressure.

in 1999 than in the remaining years with mortality (**Figure 6** and **Table 4**). However, differently from the 1998 bleaching event, bleached and recently dead corals were observed also in the 3 years following the 2016 bleaching event (**Figure 3** and **Supplementary Table S2**). Mortality was always higher in high human pressure atolls than in low pressure atolls (**Figure 6**).

TABLE 2 | Results of one-way PERMANOVA on live hard coral cover in shallow reefs (5 m depth) between atolls with high human pressure (North Malé and South Malé) and atolls with low local human pressure after the bleaching event of 2016.

	Live hard coral cover				
	df	**MS**	**Pseudo-F**	**P (perm)**	**Unique permutations**
Condition	1	5867	16.55	**0.001**	397
Residual	121	355			
Total	122				

Significant values are in bold.

Impact of Bleaching With Depth

Hard corals bleached from shallow water down to about 30 m depth. Consistently, bleaching-induced coral mortality was high at 10 m and 20 m, low at 30 m and negligible at 40 m and 50 m depth (**Figure 7A** and **Table 5**). The cover of live hard corals decreased gradually with depth (**Figure 7B**). At the lower photic depths (10 and 20 m), live coral cover decreased after the mass mortality episodes, whilst at the upper mesophotic depths (i.e., 30, 40, and 50 m) live hard coral cover showed no significant decline (**Figure 7B**). Only at lower photic depths (10 and 20 m) differences in live hard coral cover between years with or without mortality were significant (**Table 6**).

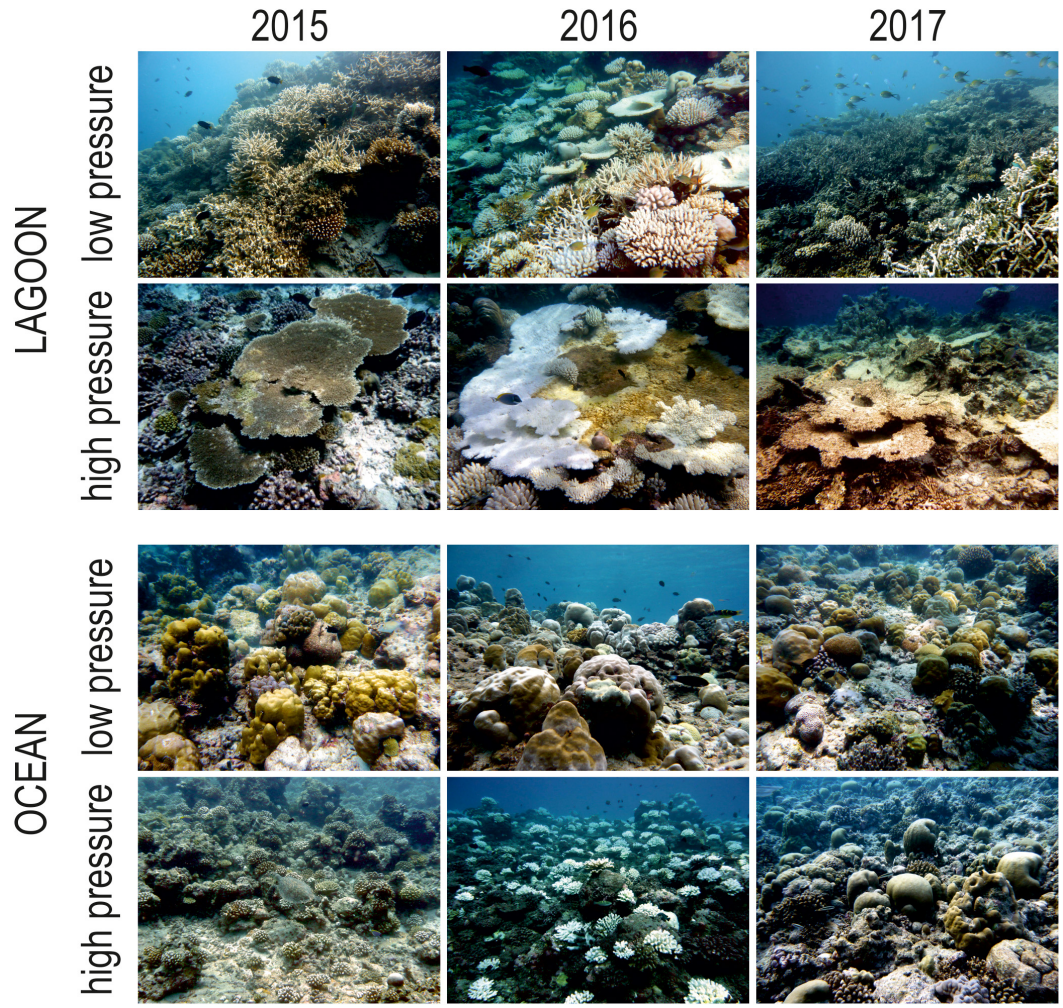

FIGURE 5 | Representative pictures of Maldivian lagoon and ocean reefs subjected to low and high human pressure in 2015, 2016, and 2017 (i.e., before, during, and after the 2016 mass bleaching event, respectively) at 5 m depth.

TABLE 3 | Results of one-way PERMANOVA on live hard coral cover in shallow reefs (5 m depth) between lagoon reefs and ocean reefs after the bleaching event of 2016.

Live hard coral cover					
	df	**MS**	**Pseudo-F**	**P (perm)**	**Unique permutations**
Condition	1	7190.3	20.896	**0.001**	410
Residual	121	344.1			
Total	122				

Significant values are in bold.

DISCUSSION

Maldivian coral reefs experienced two severe bleaching events in 1998 and in 2016. After the 1998 bleaching event, more than 90% of hard corals died (Bianchi et al., 2003, 2006), and it took 16 years for reefs to recover the pre-bleaching values of live hard coral cover (Morri et al., 2015). Such a recovery was consistent with that observed in the eastern tropical Pacific Ocean (Romero-Torres et al., 2020), but was surprisingly slow as compared to the fast coral cover recovery observed in the neighboring Chagos Archipelago (Sheppard et al., 2008) and in other remote Indian Ocean locations with similar oceanographic conditions (Gilmour et al., 2013). All these latter studies concerned nearly uninhabited islands; on the contrary, the Maldives are experiencing a still moderate but nevertheless continuously increasing level of human pressure because of population increase, coastal development, and tourism intensification (Jaleel, 2013; Nepote et al., 2016). In addition, starting from 2016, the atolls of North and South Malé have been subject to important land reclamation engineering works with consequent increase of sediments in the lagoons (Pancrazi et al., 2020).

Visual estimation of substratum cover is among the most universally used metric to quantify sessile benthic organisms (Bianchi et al., 2004), but might be an insufficient descriptor of recovery when considered alone (Johns et al., 2014). In the Maldives, coral species richness was recovered after 4 years

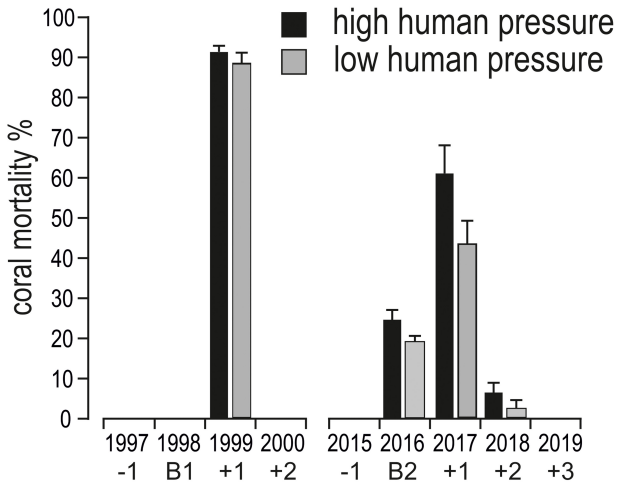

FIGURE 6 | Mean (+ standard error) coral mortality (in %) in shallow reefs (5 m depth) of the Maldives in the years before (–1, i.e., 1997, 2015), during (B1, i.e., 1998, and B2, i.e., 2016), in the 2 years after (+1 and +2, i.e., 1999 and 2000) the mass bleaching event of 1998, and in the 3 years after (+1, +2, and +3, i.e., 2017, 2018, and 2019) the mass bleaching event of 2016.

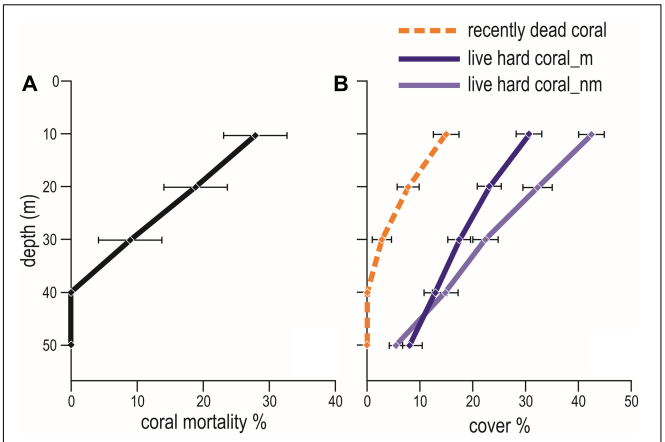

FIGURE 7 | Mean (± standard error) values of: **(A)** coral mortality down a depth profile (from 10 m to 50 m); and **(B)** percent cover of live hard coral in years with coral mortality (i.e., 1999, 2007, 2016, 2017, and 2018) (live coral_m, dark violet solid line) and in years without coral mortality (i.e., 1997, 1998, 2012, 2013, 2015, and 2019) (live coral_nm, violet solid line), and of recently dead coral (orange dashed line) in the Maldives.

(Benzoni and Pichon, 2007) and *Acropora* colonies density and size after 6 years (Lasagna et al., 2010b). However, recover of all descriptors at ecosystem level (community structure, seascape, trophic organization, and structural complexity) took 14 to more than 16 years and was rarely complete (Bianchi et al., 2017). While previous papers already investigated the general trend of coral recovery in the Maldives after the mass bleaching event in 1998 (Lasagna et al., 2008; Morri et al., 2015; Bianchi et al., 2017), this study showed that during the 2016 bleaching event, 60% of hard corals in the Maldives bleached and died when the accumulated heat exposure exceeded the critical regional bleaching threshold of degree heating weeks (DHW = 8.0) for 2 months. Hard corals bleached in almost all reefs surveyed during 2016, although differences in coral mortality were observed among the reefs investigated in the subsequent years. Local ecological and environmental differences influenced the severity of coral bleaching in the various areas (McClanahan et al., 2018). Reefs in remote areas or affected by a comparatively lower degree of human pressure, such as in Felidhoo and Ari atolls, kept a higher value of live hard coral cover than reefs in more developed and urbanized areas, such as in North and South Malé atolls (Dhunya et al., 2017; Stevens and Froman, 2019). Reefs affected by local human pressure have already been shown to be more vulnerable to climate disturbance (Montefalcone et al., 2011; Nepote et al., 2016).

Corals in ocean reefs proved more resistant to the 2016 bleaching event than those in lagoon reefs. Ocean reefs are close to deep cooler waters, have higher water movement and waves that may attenuate light intensity and ensure mixing of water, and are generally unaffected by nutrients coming from land: all factors that can potentially reduce bleaching and mortality (Muir et al., 2017). Differences between ocean and lagoon reefs are expressed not only in morphology, topography and exposure (Lasagna et al., 2008, 2010a; Rovere et al., 2018), but also in the species composition of the coral communities. Maldivian lagoon reefs are typically dominated by tabular and branching *Acropora* corals (Bianchi et al., 1997; Lasagna et al., 2010b).

TABLE 4 | Results of one-way PERMANOVA on coral mortality in shallow reefs (5 m depth) among the years when coral mortality occurred (i.e., 1999, 2016, 2017, and 2018).

	Coral mortality				
	df	**MS**	**Pseudo-F**	**P (perm)**	**Unique permutations**
Year	3	33606	99.91	**0.001**	999
Residual	92	336			
Total	95				

Pair-wise test: 1999 > 2016**; 1999 > 2017**; 1999 > 2018**; 2016 < 2017**; 2016 > 2018**; 2017 > 2018**

*Significant values are in bold; **p < 0.001.*

TABLE 5 | Results of one-way PERMANOVA on coral mortality across depths (10, 20, 30, 40, and 50 m) when coral mortality occurred in the Maldives (pooling data from 1999, 2007, 2016, 2017, and 2018).

	Coral mortality				
	df	**MS**	**Pseudo-F**	**P (perm)**	**Unique permutations**
Depth	4	1869.1	6.93	**0.001**	999
Residual	63	269.3			
Total	67				

Pair-wise test: 10 m > 30 m*; 10 m > 40 m*; 10 m > 50 m*; 20 m > 40 m*; 30 m > 50 m*

*Significant values are in bold; *p < 0.05.*

TABLE 6 | Results of two-way PERMANOVA on the percentage cover (in %) of live hard coral in the years without coral mortality (years nm) and years with coral mortality (years m), across a depth profile (10, 20, 30, 40, and 50 m) in the Maldives.

	Live hard coral cover				
	df	**MS**	**Pseudo-F**	**P (perm)**	**Unique permutations**
Mortality occurrence (Mo)	1	2064	14.06	**0.001**	997
Depth (D)	4	5927	40.37	**0.001**	999
Mo × D	4	328	2.23	0.072	999
Residual	200	146			
Total	209				

Pair-wise test. Mo: years nm > years m*; D: 10 m > 20 m*; 10 m > 30 m**; 10 m > 40 m**; 10 m > 50 m**; 20 m > 30 m*; 20 m > 40 m**; 20 m > 50 m**; 30 m > 40 m*; 30 m > 50 m**; 40 m > 50 m*

*Significant values are in bold. *p < 0.05; **p < 0.001.*

Susceptibility to thermal stress of *Acropora* corals is known to be widely variable (Muir et al., 2018), but in the Maldives they suffered a catastrophic die-off in both 1998 (Tkachenko, 2014) and 2016 (Pisapia et al., 2019), as already reported by studies in other localities (Loya et al., 2001; Pratchett et al., 2013). On the contrary, ocean reefs are dominated by massive corals (Bianchi et al., 1997), which experienced only partial colony mortality after the two bleaching events (Bianchi et al., 2006; Perry and Morgan, 2017; Pisapia et al., 2019). Higher resistance of ocean reefs is also likely linked to higher propagule exchanges due to stronger currents and water movements in comparison to lagoon reefs (Kinlan and Gaines, 2003).

Although the 2016 heat wave has been declared as the most damaging on record (Eakin et al., 2016; Hughes et al., 2017), corals in the Maldives survived to a larger extent with respect to 1998. According to our calculation for the Maldives, the thermal anomaly of 1998 was distinctly higher than that of 2016 in terms of DHW, but the two were comparable according to the NOAA coral reef watch database (which, however, considered an area wider than the Maldives). In any case, the 1998 heat wave was a relatively longer event, whilst the 2016 heat wave was less prolonged. The lower coral mortality in 2016 might give some support for the ABH in some species of shallow Maldivian coral reefs, as already hypothesized by McClanahan and Muthiga (2014). However, differences in duration and intensity between the two heat waves hamper a definite answer. Coral adaptability might be not the only explanation for a lower coral mortality in 2016: processes of acclimatization, ecological reorganization, and an effective coral heterotrophy (Houlbrèque and Ferrier-Pagès, 2009; Grottoli et al., 2014; McClanahan, 2017; Coles et al., 2018) have also been evoked.

In the Maldives (as elsewhere in the world) shallow reefs in the upper photic zone, within 10 m depth, are usually the target of most coral-reef monitoring programs (Jimenez et al., 2012; Tkachenko, 2012). Due to scuba diving constrains, comparatively fewer explorations have been conducted in the lower photic zone, below 10 m depth, where coral reefs can still be constructional (Morri et al., 1995; Bianchi et al., 1997) and even exhibit high coral cover in some cases (Sheppard, 1980). Although mesophotic reefs are rarely included in reef assessments (Pyle et al., 2016; Garavelli et al., 2018; Studivan and Voss, 2018a), there is a growing interest to investigate the upper mesophotic coral-reef ecosystems, 30 m to 50 m depth, for their potential to serve as thermal refuge (Semmler et al., 2016). Nevertheless, ecological information on mesophotic reefs in the Maldives is poor compared to that on shallow reefs (Morri et al., 1995, 2010; Bianchi et al., 1997).

Our results showed significantly reduced bleaching in the upper mesophotic reefs and a negligible coral mortality after the two bleaching events at depths between 30 and 50 m, thus providing some support to DRH. In many coral reefs of the world, the upper mesophotic reef community represents an extension of the shallow-water community (Pyle et al., 2016; Lesser et al., 2018), as many coral species are shared across these depths (Kahng et al., 2017; Studivan and Voss, 2018b; Zlatarski, 2018). However, our results also indicated that coral cover reduced drastically with depth from shallow to deep waters, with cover values always <20% in the latter. These values are lower than that of the survivors on shallow reefs. Even assuming a great fecundity for mesophotic coral species, there is no reason to think that their potential for contributing to reef recovery after severe events surpasses that of the survivors in photic reefs.

Although widely used as indicator of reef health (Montefalcone et al., 2018a), coral cover does not account for differences in susceptibility between species. Susceptibility of the different species to bleaching over depth has never been widely quantified, and available information on deep reefs during severe bleaching events is limited (Muir et al., 2017; Morais and Santos, 2018). Except for the ultrasensitive fire corals of the genus *Millepora* (Smith et al., 2014; Morri et al., 2017), some recent studies suggest that the applicability of the DRH may be only site- and species-specific (Semmler et al., 2016), and should not be considered as a general phenomenon (Smith et al., 2016; Bongaerts et al., 2017). Some controversy occurs regarding the hypothesis that deep reefs can provide a refuge from bleaching. An important role of mesophotic habitats has been demonstrated in the Indo-Pacific Ocean due to the high species richness of scleractinian corals, particularly at 30–45 m depths, able to preserve evolutionary lineages (Muir et al., 2018). During the 2016 bleaching event, 73% of the Maldivian coral species at 24–30 m depth have been not affected by bleaching (Muir et al., 2017). Deep areas of the ocean-side reefs on the Great Barrier Reef provided a refuge from the 2016 bleaching event for some colonies of the most abundant and ecologically important coral genera, e.g., *Acropora*, *Pocillopora*, and *Porites* (Baird et al., 2018). The survivors at depth may well be species that have been severely depleted in shallow reefs, thus making their contribution potentially critical. Shallow-reef assemblages in the Maldives share species with reefs at 30 m depth, but there are species that are not depth generalists (Benzoni and Pichon, 2007; Bigot and Amir, 2012): contrasting results might reflect local variations in both species composition and depth distribution of individual species down the reef slope (Laverick et al., 2018; Rocha et al., 2018). More data on recovery through time and at different

depths would be necessary to further test this hypothesis and to understand to which extent mesophotic Maldivian reefs may act as refuge to safeguard shallow reefs.

Similarly, to investigate the ABH, estimates on coral cover can only provide a first picture on the effects of thermal stress. Further investigations on community taxonomic composition and on the relative sensitivity of species to thermal stress should be envisaged to prove both the ABH and the DRH in the Maldivian coral reefs. Ecophysiology, molecular biology, and genetics would be fundamental approaches to prove resistance and adaptability of corals to ocean warming.

Periods of unusually high sea surface temperatures have already become long-lasting and frequent (Frölicher et al., 2018), and this trend is predicted to accelerate under future global warming scenarios (Hughes et al., 2018a). Coral tolerance limits are expected to be frequently exceeded due to the incessant increase in sea surface temperature (Heron et al., 2017) and predictions indicate that the majority of coral reefs will not survive the most pessimistic scenarios of global warming (Perry et al., 2018). Even trusting in coral adaptation to ocean warming, this process would probably be slower than the rate at which sea temperatures are currently rising - therefore it will not prevent the extinction of many stenothermal coral species (Frieler et al., 2013; Bay et al., 2017). Up to 16 years had been necessary for Maldivian coral reefs to recover from the severe bleaching event of 1998 (Morri et al., 2015; Pisapia et al., 2016; Perry and Morgan, 2017), and the predicted frequency of two severe bleaching events per decade (Hughes et al., 2018a) would thus jeopardize future recovery of Maldivian reefs (Montefalcone et al., 2018a). In addition to climatic effects, the increase in local human pressure in the last decades is cause of concern (Nepote et al., 2016; Pancrazi et al., 2020). Resident population in the Maldives, and especially in the highly anthropized atolls (such as those of Malé), is continuously growing, but this is not the case for the most remote and less developed atolls (such as Ari and Felidhoo). Tourism, in particular, has become the main component of Maldivian economy (Bertaud, 2002) and may be expected to keep growing exponentially in the near future. The only flexion in tourism growth has been in 2005, as a consequence of the tsunami of December 2004 (Morri et al., 2015), whilst in the atolls of Malé tourism has been showing a huge rise since 2013. Our study showed that the impact of 2016 bleaching and mortality was significantly greater on coral communities in atolls with higher human pressure. The observed 16 years required to Maldivian coral reefs to recovery from a severe bleaching event are likely to be not enough for recovering from the last mass bleaching event of 2016, especially for those reefs where the disturbance regime has growth exponentially. While containing climate stress requires international actions, regional management practices may prove successful in reducing local human pressure (Lasagna et al., 2014; Dhunya et al., 2017), thus making Maldivian coral reef ecosystems more resilient to climate change (Brown et al., 2013; Shaver et al., 2018). Keeping local impacts under control may represent a better conservation strategy than relying upon coral adaptive responses and depth refuge efficacy.

DATA AVAILABILITY STATEMENT

All datasets generated for this study are included in the article/**Supplementary Material**.

AUTHOR CONTRIBUTIONS

All authors listed have made a substantial, direct and intellectual contribution to the work, and approved it for publication.

FUNDING

Part of this work received economic support from University of Genoa internal funds (FRA, Fondi Ricerca d'Ateneo).

ACKNOWLEDGMENTS

Albatros Top Boat (Verbania, Milan and Malé) organized our scientific cruises in the Maldives: we especially thank Donatella 'Dodi' Telli, Massimo Sandrini, and Herbert Fontana for their support, and all the staff of Conte Max and Duke of York boats for assistance during field work. We also thank Save the Beach Maldives, especially Beybe (Assan Hamed), Sara Montagnani (University of Genoa), and all participants in field activities, who helped collecting data. The advice of Luigi Piazzi (University of Sassari) on statistical analyses is greatly acknowledged.

SUPPLEMENTARY MATERIAL

The Supplementary Material for this article can be found online at: https://www.frontiersin.org/articles/10.3389/fmars.2020.00587/full#supplementary-material

TABLE S1 | Sites surveyed during scientific cruises at the Maldives from 1997 to 2019.

TABLE S2 | Percentage cover (in %, mean ± s.e.) of live hard coral (HC), bleached coral (B), and recently dead coral (RDC) in the shallow reefs (5 m depth) surveyed in the Maldives during 2015, 2016, 2017, 2018, and 2019.

REFERENCES

Anderson, M. J. (2001). A new method for non-parametric multivariate analysis of variance. *Austral. Ecol.* 26, 32–46. doi: 10.1111/j.1442-9993.2001.01070.pp.x

Bahr, K. D., Jokiel, P. L., and Rodgers, K. S. (2016). Relative sensitivity of five Hawaiian coral species to high temperature under high-pCO_2 conditions. *Coral Reefs* 2, 1–10.

Baird, A. H., Madin, J. S., Álvarez-Noriega, M., Fontoura, L., Kerry, J. T., Kuo, C.-Y., et al. (2018). A decline in bleaching suggests that depth can provide a refuge

from global warming in most coral taxa. *Mar. Ecol. Progr. Ser.* 603, 257–264. doi: 10.3354/meps12732

Bay, R. A., Rose, N. H., Logan, C. A., and Palumbi, S. R. (2017). Genomic models predict successful coral adaptation if future ocean warming rates are reduced. *Sci. Adv.* 3:e1701413. doi: 10.1126/sciadv.1701413

Benzoni, F., and Pichon, M. (2007). Taxonomic re-appraisal of zooxanthellate scleractinian corals in the Maldive Archipelago. *Zootaxa* 1441, 21–33. doi: 10.11646/zootaxa.1441.1.2

Bertaud, A. (2002). *A Rare Case of Land Scarcity: The Issue of Urban Land in the Maldives*. New York, NY: Mimeo, 1–9.

Bianchi, C. N., Azzola, A., Bertolino, M., Betti, F., Bo, M., Cattaneo-Vietti, R., et al. (2019). Consequences of the marine climate and ecosystem shift of the 1980-90s on the Ligurian Sea biodiversity (NW Mediterranean). *Eur. Zool. J.* 86, 458–487. doi: 10.1080/24750263.2019.1687765

Bianchi, C. N., Colantoni, P., Geister, J., and Morri, C. (1997). "Reef geomorphology, sediments and ecological zonation at Felidu Atoll, Maldive Islands (Indian Ocean)," in *Proceedings of the 8th international coral reef symposium*, eds H. A. Lessios and I. G. MacIntyre (Panamá: Smithsonian Tropical Research Institute), 431–436.

Bianchi, C. N., Morri, C., Lasagna, R., Montefalcone, M., Gatti, G., Parravicini, V., et al. (2017). "Resilience of the marine animal forest: lessons from Maldivian coral reefs after the mass mortality of 1998," in *Marine Animal Forests: The Ecology of Benthic Biodiversity Hotspots*, eds S. Rossi, L. Bramanti, A. Gori, and C. Orejas (Cham: Springer International), 1241–1269. doi: 10.1007/978-3-319-21012-4_35

Bianchi, C. N., Morri, C., Pichon, M., Benzoni, F., Colantoni, P., Baldelli, G., et al. (2006). "Dynamics and pattern of coral recolonization following the 1998 bleaching event in the reefs of the Maldives," in *Proceedings of the 10th International Coral Reef Symposium*, eds Y. Suzuki, T. Nakamori, M. Hidaka, H. Kayanne, B. E. Casareto, K. Nadaoka, et al. (Tokyo: Japanese Coral Reef Society), 30–37.

Bianchi, C. N., Pichon, M., Morri, C., Colantoni, P., Benzoni, F., Baldelli, G., et al. (2003). Le suivi du blanchissement des coraux aux Maldives: leçons à tirer et nouvelles hypothèses. *Océanis* 29, 325–354.

Bianchi, C. N., Pronzato, R., Cattaneo-Vietti, R., Benedetti-Cecchi, L., Morri, C., Pansini, M., et al. (2004). Hard bottoms. *Biol. Mar. Medit.* 11(Suppl. 1), 185–215.

Bigot, L., and Amir, H. (2012). Scleractinia corals of Baa Atoll (Maldives): first checklist and overview of stony corals community structure. *Atoll Res. Bull.* 590, 67–83.

Bongaerts, P., Ridgway, T., Sampayo, E., and Hoegh-Guldberg, O. (2010). Assessing the 'deep reef refugia' hypothesis: focus on Caribbean reefs. *Coral Reefs* 29, 309–327. doi: 10.1007/s00338-009-0581-x

Bongaerts, P., Riginos, C., Brunner, R., Englebert, N., Smith, S. R., and Hoegh-Guldberg, O. (2017). Deep reefs are not universal refuges: reseeding potential varies among coral species. *Sci. Adv.* 3:e1602373. doi: 10.1126/sciadv.1602373

Brown, C. J., Sauders, M. I., Possingham, H. P., and Richardson, A. J. (2013). Managing for interactions between local and global stressors of ecosystems. *PLoS One* 8:e65765. doi: 10.1371/journal.pone.0065765

Buddemeier, R. W., Baker, A. C., Fautin, D. G., and Jacobs, J. R. (2004). "The adaptive hypothesis of bleaching," in *Coral Health and Disease*, eds E. Rosenberg and Y. Loya (Berlin: Springer), 427–444. doi: 10.1007/978-3-662-06414-6_24

Buddemeier, R. W., and Fautin, D. G. (1993). Coral bleaching as an adaptive mechanism. A testable hypothesis. *BioScience* 43, 320–326. doi: 10.2307/1312064

Coles, S. L., Bahr, K. D., Rodgers, K. S., May, S. L., McGowan, A. E., Tsang, A., et al. (2018). Evidence of acclimatization or adaptation in Hawaiian corals to higher ocean temperatures. *PeerJ* 6:e5347. doi: 10.7717/peerj.5347

Dhunya, A., Huang, Q., and Aslam, A. (2017). Coastal habitats of Maldives: status, trends, threats, and potential conservation strategies. *Int. J. Sci. Engineer. Res.* 8, 47–62.

Dijkstra, H. A. (2006). The ENSO phenomenon: theory and mechanisms. *Adv. Geosci.* 6, 3–15. doi: 10.5194/adgeo-6-3-2006

Eakin, M., Liu, G., Gomez, A., De la Cour, J., Heron, S., and Skirving, W. (2016). Global coral bleaching 2014-2017: status and an appeal for observations. *Reef Encount.* 31, 20–26.

Frieler, K., Meinshausen, M., Golly, A., Mengel, M., Lebek, K., Donner, S. D., et al. (2013). Limiting global warming to 2°C is unlikely to save most coral reefs. *Nat. Clim. Change* 3, 165–170. doi: 10.1038/nclimate1674

Frölicher, T. L., Fischer, E. M., and Gruber, N. (2018). Marine heatwaves under global warming. *Nature* 560, 360–366.

Garavelli, L., Studivan, M. S., Voss, J. D., Kuba, A., Figueiredo, J., and Chérubin, L. M. (2018). Assessment of mesophotic coral ecosystem connectivity for proposed expansion of a marine sanctuary in the northwest Gulf of Mexico: larval dynamics. *Front. Mar. Sci.* 5:174.

Gatti, G., Bianchi, C. N., Montefalcone, M., Venturini, S., Diviacco, G., and Morri, C. (2017). Observational information on a temperate reef community helps understanding the marine climate and ecosystem shift of the 1980-90s. *Mar. Poll. Bull.* 114, 528–538. doi: 10.1016/j.marpolbul.2016.10.022

Gilmour, J. P., Smith, L. D., Heyward, A. J., Baird, A. H., and Pratchett, M. S. (2013). Recovery of an isolated coral reef system following severe disturbance. *Science* 340, 69–71. doi: 10.1126/science.1232310

Glynn, P. W. (1996). Coral reef bleaching: facts, hypotheses and implications. *Glob. Change Biol.* 2, 495–509. doi: 10.1111/j.1365-2486.1996.tb00063.x

Godfrey, T. (2006). *Dive Maldives: A Guide to the Maldives Archipelago*, 3rd Edn. Washington, DC: Atoll Press.

Grottoli, A. G., Warner, M. E., Levas, S. J., Aschaffenburg, M. D., Schoepf, V., McGinley, M., et al. (2014). The cumulative impact of annual coral bleaching can turn some coral species winners into losers. *Glob. Change Biol.* 20, 3823–3833. doi: 10.1111/gcb.12658

Heron, S. F., Eakin, C. M., and Douvere, F. (2017). *Impacts of Climate Change on World Heritage Coral Reefs: A First Global Scientific Assessment*. Paris: UNESCO World Heritage Centre.

Hinderstein, L. M., Marr, J. C. A., Martinez, F. A., Dowgiallo, M. J., Puglise, K. A., Pyle, R. L., et al. (2010). Mesophotic coral ecosystems: characterization, ecology, and management. *Cor. Reefs* 29, 247–251. doi: 10.1007/s00338-010-0614-5

Hoegh-Guldberg, O. (1999). Climate change, coral bleaching and the future of the world's coral reefs. *Mar. Fresh. Res.* 50, 839–866.

Hoegh-Guldberg, O., and Bruno, J. F. (2010). The impact of climate change on the world's marine ecosystems. *Science* 328, 1523–1528. doi: 10.1126/science.1189930

Hoegh-Guldberg, O., Mumby, P. J., Hooten, A. J., Steneck, R. S., Greenfield, P., Gomez, E., et al. (2007). Coral reefs under rapid climate change and ocean acidification. *Science* 318, 1737–1742.

Holstein, D. M., Smith, T. B., Gyory, J., and Paris, C. B. (2015). Fertile fathoms: deep reproductive refugia for threatened shallow corals. *Sci. Rep.* 5:12407.

Houlbrèque, F., and Ferrier-Pagès, C. (2009). Heterotrophy in tropical scleractinian corals. *Biol. Rev.* 84, 1–17. doi: 10.1111/j.1469-185x.2008.00058.x

Hughes, T. P., Kerry, J. T., Álvarez Noriega, M., Álvarez Romero, J. G., Anderson, K. D., Baird, A. H., et al. (2017). Global warming and recurrent mass bleaching of corals. *Nature* 543, 373–377.

Hughes, T. P., Kerry, J. T., Baird, A. H., Sean, R., Connolly, S. R., Dietzel, A., et al. (2018a). Global warming transforms coral reef assemblages. *Nature* 556, 492–506.

Hughes, T. P., Anderson, K. D., Connolly, S. R., Heron, S. F., Kerry, J. T., Lough, J. M., et al. (2018b). Spatial and temporal patterns of mass bleaching of corals in the Anthropocene. *Science* 359, 80–83. doi: 10.1126/science.aan8048

Jaleel, A. (2013). The status of the coral reefs and the management approaches: the case of the Maldives. *Ocean Coast. Manag.* 82, 104–118. doi: 10.1016/j.ocecoaman.2013.05.009

Jimenez, H., Bigot, L., Bourmaud, C., Chabanet, P., Gravier-Bonnet, N., Hamel, M. A., et al. (2012). Multi-taxa coral reef community structure in relation to habitats in the Baa Atoll Man and Biosphere UNESCO Reserve (Maldives), and implications for its conservation. *J. Sea Res.* 72, 77–86. doi: 10.1016/j.seares.2012.04.011

Johns, K. A., Osborne, K. O., and Logan, M. (2014). Contrasting rates of coral recovery and reassembly in coral communities on the Great Barrier Reef. *Cor. Reefs* 33, 553–563. doi: 10.1007/s00338-014-1148-z

Jokiel, P. L. (2004). "Temperature stress and coral bleaching," in *Coral Health and Disease*, eds E. Rosenberg and Y. Loya (Berlin: Springer), 401–425. doi: 10.1007/978-3-662-06414-6_23

Kahng, S. E., Copus, J. M., and Wagner, D. (2017). "Mesophotic coral ecosystems," in *Marine Animal Forests: The Ecology of Benthic Biodiversity Hotspots*, eds

S. Rossi, L. Bramanti, A. Gori, and C. Orejas (Cham: Springer International), 185–206. doi: 10.1007/978-3-319-21012-4_4

Kahng, S. E., Garcia-Sais, J. R., Spalding, H. L., Brokovich, E., Wagner, D., Weil, E., et al. (2010). Community ecology of mesophotic coral reef ecosystems. *Cor. Reefs* 29, 255–275. doi: 10.1007/s00338-010-0593-6

Kayanne, H. (2017). Validation of degree heating weeks as a coral bleaching index in the northwestern Pacific. *Cor. Reefs* 36, 63–70. doi: 10.1007/s00338-016-1524-y

Kinlan, B. P., and Gaines, S. D. (2003). Propagule dispersal in marine and terrestrial environments: a community perspective. *Ecology* 84, 2007–2020. doi: 10.1890/01-0622

LaJeunesse, T. C., Parkinson, J. E., Gabrielson, P. W., Jeong, H. J., Reimer, J. D., Voolstra, C. R., et al. (2018). Systematic revision of Symbiodiniaceae highlights the antiquity and diversity of coral endosymbionts. *Cur. Biol.* 28, 2570–2580.

Lasagna, R., Albertelli, G., Colantoni, P., Morri, C., and Bianchi, C. N. (2010a). Ecological stages of Maldivian reefs after the coral mass mortality of 1998. *Facies* 56, 1–11. doi: 10.1007/s10347-009-0193-5

Lasagna, R., Albertelli, G., Morri, C., and Bianchi, C. N. (2010b). *Acropora* abundance and size in the Maldives six years after the 1998 mass mortality: patterns across reef typologies and depths. *J. Mar. Biol. Ass. U. K.* 90, 919–922. doi: 10.1017/s0025315410000020

Lasagna, R., Albertelli, G., Giovannetti, E., Grondona, M., Milani, A., Morri, C., et al. (2008). Status of Maldivian reefs eight years after the 1998 coral mass mortality. *Chem. Ecol.* 24(Suppl. 1), 155–160.

Lasagna, R., Gnone, G., Taruffi, M., Morri, C., Bianchi, C. N., Parravicini, V., et al. (2014). A new synthetic index to evaluate reef coral condition. *Ecol. Ind.* 40, 1–9. doi: 10.1016/j.ecolind.2013.12.020

Laverick, J. H., Andradi-Brown, D. A., and Rogers, A. D. (2017). Using light-dependent Scleractinia to define the upper boundary of mesophotic coral ecosystems on the reefs of Utila, Honduras. *PLoS One* 12:e0183075. doi: 10.1371/journal.pone.0183075

Laverick, J. H., Piango, S., Andradi-Brown, D. A., Exton, D. A., Bongaerts, P., Bridge, T. C. L., et al. (2018). To what extent do mesophotic coral ecosystems and shallow reefs share species of conservation interest? A systematic review. *Environ. Evid.* 7:15.

Lesser, M. P., Slattery, M., Laverick, J. H., Macartney, K. J., and Bridge, T. C. (2018). Global community breaks at 60 m on mesophotic coral reefs. *Glob. Ecol. Biogeogr.* 28, 1403–1416. doi: 10.1111/geb.12940

Loya, Y., Eyal, G., Treibitz, T., Lesser, M. P., and Appeldoorn, R. (2016). Theme section on mesophotic coral ecosystems: advances in knowledge and future perspectives. *Cor. Reefs* 35, 1–9. doi: 10.1007/s00338-016-1410-7

Loya, Y., Sakai, K., Yamazato, K., Nakano, Y., Sambali, H., and Van Woesik, R. (2001). Coral bleaching: the winners and the losers. *Ecol. Lett.* 4, 122–131. doi: 10.1046/j.1461-0248.2001.00203.x

Matz, M. V., Treml, E. A., Agayamova, G. V., and Bay, L. K. (2018). Potential and limits for rapid genetic adaptation to warming a Great Barrier Reef coral. *PLoS Gen.* 14:e1007220. doi: 10.1371/journal.pgen.1007220

McClanahan, T. R. (2017). Changes in coral sensitivity to thermal anomalies. *Mar. Ecol. Progr. Ser.* 70, 71–85. doi: 10.3354/meps12150

McClanahan, T. R., and Muthiga, N. A. (2014). Community change and evidence for variable warm-water temperature adaptation of corals in Northern Male Atoll, Maldives. *Mar. Poll. Bull.* 80, 107–113. doi: 10.1016/j.marpolbul.2014.01.035

McClanahan, T. R., Weil, E., and Baird, A. H. (2018). "Consequences of coral bleaching," in *Ecological Studies. Coral Bleaching: Patterns, Processes, Causes and Consequences*, eds M. J. H. van Oppen and J. M. Lough (Cham: Springer International), 231–263. doi: 10.1007/978-3-319-75393-5_10

Montefalcone, M., Morri, C., and Bianchi, C. N. (2018a). Long term change in bioconstruction potential of Maldivian coral reefs following extreme climate anomalies. *Glob. Change Biol.* 24, 5629–5641. doi: 10.1111/gcb.14439

Montefalcone, M., De Falco, G., Nepote, E., Canessa, M., Bertolino, M., Bavestrello, G., et al. (2018b). Thirty year ecosystem trajectories in a submerged marine cave under changing pressure regime. *Mar. Environ. Res.* 137, 98–110. doi: 10.1016/j.marenvres.2018.02.022

Montefalcone, M., Parravicini, V., and Bianchi, C. N. (2011). "Quantification of coastal ecosystem resilience," in *Treatise on Estuarine and Coastal Science*, eds E. Wolanski and D. S. McLusky (Waltham, MA: Academic Press), 49–70. doi: 10.1016/b978-0-12-374711-2.01003-2

Morais, J., and Santos, B. A. (2018). Limited potential of deep reefs to serve as refuges for tropical Southwestern Atlantic corals. *Ecosphere* 9:e02281. doi: 10.1002/ecs2.2281

Morri, C., Aliani, S., and Bianchi, C. N. (2010). Reef status in the Rasfari region (North Malé Atoll, Maldives) five years before the mass mortality event of 1998. *Est. Coast. Shelf Sci.* 86, 258–264. doi: 10.1016/j.ecss.2009.11.021

Morri, C., Bianchi, C. N., and Aliani, S. (1995). Coral reefs at Gangehi (North Ari Atoll, Maldive Islands). *Publ. Serv. Géol. Luxembourg* 29, 3–12.

Morri, C., Bianchi, C. N., Di Camillo, C. G., Ducarme, F., Allison, W. R., and Bavestrello, G. (2017). Global climate change and regional biotic responses: two hydrozoan tales. *Mar. Biol. Res.* 13, 573–586. doi: 10.1080/17451000.2017.1283419

Morri, C., Montefalcone, M., Lasagna, R., Gatti, G., Rovere, A., Parravicini, V., et al. (2015). Through bleaching and tsunami: coral reef recovery in the Maldives. *Mar. Poll. Bull.* 98, 188–200. doi: 10.1016/j.marpolbul.2015.06.050

Muir, P. R., Marshall, P. A., Abdulla, A., and Aguirre, J. D. (2017). Species identity and depth predict bleaching severity in reef-building corals: shall the deep inherit the reef? *Proc. Royal Soc. B* 284:20171551. doi: 10.1098/rspb.2017.1551

Muir, P. R., Wallace, C. C., Pichon, M., and Bongaerts, P. (2018). High species richness and lineage diversity of reef corals in the mesophotic zone. *Proc. Royal Soc. B* 285:20181987. doi: 10.1098/rspb.2018.1987

Nepote, E., Bianchi, C. N., Chiantore, M., Morri, C., and Montefalcone, M. (2016). Pattern and intensity of human impact on coral reefs depend on depth along the reef profile and on the descriptor adopted. *Est. Coast. Shelf Sci.* 178, 86–91. doi: 10.1016/j.ecss.2016.05.021

NOAA (2016). *Data From: Coral Reef Watch, updated daily. NOAA Coral Reef Watch Daily Global 5-km Satellite Virtual Station Time Series. Data for the Maldives, 1/1/16 to 1/4/17*. College Park, MA: NOAA.

Padfield, D., Yvon-Durocher, G., Buckling, A., Jennings, S., and Yvon-Durocher, G. (2015). Rapid evolution of metabolic traits explains thermal adaptation in phytoplankton. *Ecol. Lett.* 19, 133–142. doi: 10.1111/ele.12545

Pancrazi, I., Ahmed, H., Cerrano, C., and Montefalcone, M. (2020). Synergic effect of global thermal anomalies and local dredging activities on coral reefs of the Maldives. *Mar. Pollut. Bull.* (in press).

Perry, C. T., Alvarez-Filip, L., Graham, N. A. J., Mumby, P. J., Wilson, S. K., Kench, P. S., et al. (2018). Loss of coral reef growth capacity to track future increases in sea level. *Nature* 558, 396–400. doi: 10.1038/s41586-018-0194-z

Perry, C. T., and Morgan, K. M. (2017). Post-bleaching coral community change on southern Maldivian reefs: is there potential for rapid recovery? *Cor. Reefs* 36, 1189–1194. doi: 10.1007/s00338-017-1610-9

Pisapia, C., Burn, D., and Pratchett, M. S. (2019). Changes in the population and community structure of corals during recent disturbances (February 2016-October 2017) on Maldivian coral reefs. *Sci. Rep.* 9:8402.

Pisapia, C., Burn, D., Yoosuf, R., Najeeb, A., Anderson, K. D., and Pratchett, M. S. (2016). Coral recovery in the central Maldives archipelago since the last major mass-bleaching in 1998. *Sci. Rep.* 6:34720.

Prasetia, R., Sinniger, F., Hashizume, K., and Harii, S. (2017). Reproductive biology of the deep brooding coral *Seriatopora hystrix*: implications for shallow reef recovery. *PLoS One* 12:e0177034. doi: 10.1371/journal.pone.0177034

Pratchett, M. S., McCowan, D., Maynard, J. A., and Heron, S. F. (2013). Changes in bleaching susceptibility among corals subject to ocean warming and recurrent bleaching in Moorea, French Polynesia. *PLoS One* 8:e70443. doi: 10.1371/journal.pone.0070443

Pyle, R. L., Boland, R., Bolick, H., Bowen, B. W., Bradley, C. J., Kane, C., et al. (2016). A comprehensive investigation of mesophotic coral ecosystems in the Hawaiian Archipelago. *PeerJ* 4:e2475. doi: 10.7717/peerj.2475

Richardson, L. E., Graham, N. A. J., Pratchett, M. S., Eurich, J. G., and Hoey, A. S. (2018). Mass coral bleaching causes biotic homogenization of reef fish assemblages. *Glob. Change Biol.* 24, 3117–3129. doi: 10.1111/gcb.14119

Riegl, B., and Piller, W. E. (2003). Possible refugia for reefs in times of environmental stress. *Int. J. Earth Sci.* 92, 520–531. doi: 10.1007/s00531-003-0328-9

Rocha, L. A., Pinheiro, H. T., Shepherd, B., Papastamatiou, Y. P., Luiz, O. J., Pyle, R. L., et al. (2018). Mesophotic coral ecosystems are threatened and ecologically distinct from shallow water reefs. *Science* 361, 281–284. doi: 10.1126/science.aaq1614

Romero-Torres, M., Acosta, A., Palacio-Castro, A. M., Trem, E. A., Zapata, F. A., Paz-García, D. A., et al. (2020). Coral reef resilience to thermal stress in the eastern tropical Pacific. *Glob. Change Biol.* 26, 3880–3890. doi: 10.1111/GCB.15126

Rovere, A., Khanna, P., Bianchi, C. N., Droxler, A. W., Morri, C., and Naar, D. F. (2018). Submerged reef terraces in the Maldivian Archipelago (Indian Ocean). *Geomorphology* 317, 218–232. doi: 10.1016/j.geomorph.2018.05.026

Semmler, R. F., Hoot, W. C., and Reaka, M. L. (2016). Are mesophotic coral ecosystems distinct communities and can they serve as refugia for shallow reefs? *Cor. Reefs* 27, 1–12.

Shaver, E. C., Burkepile, D. E., and Silliman, B. R. (2018). Local management actions can increase coral resilience to thermally-induced bleaching. *Nat. Ecol. Evol.* 2:1075. doi: 10.1038/s41559-018-0589-0

Sheppard, C. R. C. (1980). Coral cover, zonation and diversity on reef slopes of Chagos atolls, and population structures of the major species. *Mar. Ecol. Progr. Ser.* 2, 193–205. doi: 10.3354/meps002193

Sheppard, C. R. C., Harris, A., and Sheppard, S. L. A. (2008). Archipelago-wide coral recovery patterns since 1998 in the Chagos Archipelago, central Indian Ocean. *Mar. Ecol. Progr. Ser.* 362, 109–117. doi: 10.3354/meps07436

Shlesinger, T., Grinblat, M., Rapuano, H., Amit, T., and Loya, Y. (2018). Can mesophotic reefs replenish shallow reefs? Reduced coral reproductive performance casts a doubt. *Ecology* 99, 421–437. doi: 10.1002/ecy.2098

Smith, T. B., Glynn, P. W., Maté, J. L., Toth, L. T., and Gyory, J. (2014). A depth refugium from catastrophic coral bleaching prevents regional extinction. *Ecology* 95, 1663–1673. doi: 10.1890/13-0468.1

Smith, T. B., Gyory, J., Brandt, M. E., Miller, W. J., Jossart, J., and Nemeth, R. S. (2016). Caribbean mesophotic coral ecosystems are unlikely climate change refugia. *Glob. Change Biol.* 22, 2756–2765. doi: 10.1111/gcb.13175

Stevens, G. M. W., and Froman, N. (2019). "The Maldives archipelago," in *World Seas: An Environmental Evaluation*, ed. C. Sheppard (Cambridge, MA: Academic Press), 211–236. doi: 10.1016/b978-0-08-100853-9.00010-5

Studivan, M. S., and Voss, J. D. (2018a). Assessment of mesophotic coral ecosystem connectivity for proposed expansion of a marine sanctuary in the northwest Gulf of Mexico: population genetics. *Front. Mar. Sci.* 5:152.

Studivan, M. S., and Voss, J. D. (2018b). Population connectivity among shallow and mesophotic *Montastraea cavernosa* corals in the Gulf of Mexico identifies potential for refugia. *Cor. Reefs* 37, 1183–1196. doi: 10.1007/s00338-018-1733-7

Thomas, C. J., Bridge, T. C. L., Figueiredo, J., Deleersnijder, E., and Hanert, E. (2015). Connectivity between submerged and near-sea-surface coral reefs: can submerged reef populations act as refuges? *Div. Distrib.* 21, 1254–1266. doi: 10.1111/ddi.12360

Tkachenko, K. S. (2012). The northernmost coral frontier of the Maldives: the coral reefs of Ihavandippolu Atoll under long-term environmental change. *Mar. Environ. Res.* 82, 40–48. doi: 10.1016/j.marenvres.2012.09.004

Tkachenko, K. S. (2014). The influence of repetitive thermal stresses on the dominance of reef-building *Acropora* spp. (Scleractinia) on coral reefs of the Maldive Islands. *Russ. J. Mar. Biol.* 40, 286–294. doi: 10.1134/s1063074014040105

Veron, J. E., Hoegh-Guldberg, O., Lenton, T., Lough, J. M., Obura, D. O., Pearce-Kelly, P., et al. (2009). The coral reef crisis: the critical importance of < 350 ppm CO_2. *Mar. Poll. Bull.* 58, 1428–1436.

Wilson, S. K., Graham, N. A. J., and Polunin, N. V. C. (2007). Appraisal of visual assessments of habitat complexity and benthic composition on coral reefs. *Mar. Biol.* 15, 1069–1076. doi: 10.1007/s00227-006-0538-3

Zlatarski, V. N. (2018). Investigations on mesophotic coral ecosystems in Cuba (1970-1973) and Mexico (1983-1984). *CICIMAR Oceánides* 33, 27–43.

Conflict of Interest: The authors declare that the research was conducted in the absence of any commercial or financial relationships that could be construed as a potential conflict of interest.

frontiers in Marine Science

REVIEW
published: 29 September 2020
doi: 10.3389/fmars.2020.581966

Impacts of Marine Litter on Mediterranean Reef Systems: From Shallow to Deep Waters

Michela Angiolillo[1,2]* *and Tomaso Fortibuoni*[3,4]

[1] *Istituto Superiore per la Protezione e la Ricerca Ambientale (ISPRA), Rome, Italy,* [2] *Stazione Zoologica Anton Dohrn (SZN), Napoli, Italy,* [3] *Istituto Superiore per la Protezione e la Ricerca Ambientale (ISPRA), Ozzano dell'Emilia, Italy,* [4] *Istituto Nazionale di Oceanografia e Geofisica Sperimentale (OGS), Trieste, Italy*

Biogenic reefs are known worldwide to play a key role in benthic ecosystems, enhancing biodiversity and ecosystem functioning at every level, from shallow to deeper waters. Unfortunately, several stressors threaten these vulnerable systems. The widespread presence of marine litter represents one of these. The harmful effects of marine litter on several organisms are known so far. However, only in the last decade, there was increasingly scientific and public attention on the impacts on reef organisms and habitats caused by litter accumulating on the seafloor. This review aims to synthesize literature and discuss the state of current knowledge on the interactions between marine litter and reef organisms in a strongly polluted basin, the Mediterranean Sea. The multiple impacts (e.g., entanglement, ghost-fishing, coverage, etc.) of litter on reef systems, the list of species impacted, and the main litter categories were identified, and a map of the knowledge available so far on this topic was provided. Seventy-eight taxa resulted impacted by marine litter on Mediterranean reefs, and the majority belonged to the phylum Cnidaria (41%), including endangered species like the red coral (*Corallium rubrum*) and the madrepora coral (*Madrepora oculata*). Entanglement, caused mainly by abandoned, lost, or otherwise discarded fishing gear (ALDFG), was the most frequent impact, playing a detrimental effect mainly on coralligenous arborescent species and cold-water corals (CWCs). The information was spatially heterogeneous, with some areas almost uncovered by scientific studies (e.g., the Aegean-Levantine Sea and the Southern Mediterranean Sea). Although many legal and policy frameworks have been established to tackle this issue [e.g., marine strategy framework directive (MSFD) and the Barcelona Convention], several gaps still exist concerning the assessment of the impact of marine litter on marine organisms, and in particular on reefs. There is a need for harmonized and standardized monitoring protocols for the collection of quantitative data to assess the impact of litter on reefs and animal forests. At the same time, urgent management measures limiting, for instance, the impact of ALDFG and other marine litter are needed to preserve these valuable and vulnerable marine ecosystems.

Keywords: marine litter, biogenic reefs, Mediterranean Sea, human activities, fishing impacts, vulnerable habitats, threatened species, entanglement

OPEN ACCESS

Edited by:
Carlo Cerrano,
Marche Polytechnic University, Italy

Reviewed by:
Sara Canensi,
Polytechnic University of Marche, Italy
Lars Gutow,
Alfred Wegener Institute, Helmholtz Centre for Polar and Marine Research (AWI), Germany

***Correspondence:**
Michela Angiolillo
michela.angiolillo@isprambiente.it

Specialty section:
This article was submitted to Marine Ecosystem Ecology, a section of the journal Frontiers in Marine Science

Received: *10 July 2020*
Accepted: *09 September 2020*
Published: *29 September 2020*

Citation:
Angiolillo M and Fortibuoni T (2020) Impacts of Marine Litter on Mediterranean Reef Systems: From Shallow to Deep Waters. Front. Mar. Sci. 7:581966. doi: 10.3389/fmars.2020.581966

INTRODUCTION

Biogenic reefs or marine bioconstructions are three-dimensional biogenic structures regulating ecological functions of benthic ecosystems from shallow to deeper waters (Ingrosso et al., 2018). They are shaped by one or few engineer species (benthic bioconstructors) that cause morphological and chemical–physical changes in the primary (abiotic) substrates and provide secondary (biotic) structures to generate biogenic new habitat suitable for a highly diverse associated fauna (Ingrosso et al., 2018).

Bioconstructor frameworks can provide a complex network of ecological niches for a large variety of organisms, including endangered and protected species, as well as species of high commercial value (Chimienti et al., 2020), functioning as habitat for shelter and feeding, spawning and nursery areas, substrata for both larval settlement and juvenile growth (e.g., Tursi et al., 2004; D'Onghia et al., 2010, 2015; Rosso et al., 2010). Since bioconstructions increase spatial complexity and settlement opportunities at every level, they are known worldwide to play a pivotal ecological role in enhancing and maintaining high marine biodiversity. Therefore, they contribute to ecosystems' goods and services, and to regulate natural resource dynamics (Lo Iacono et al., 2018).

The equilibrium between building and bioerosion processes determines bioconstruction development (Garrabou and Ballesteros, 2000) and can take centuries or even millennia of biological activities. However, some bioconstructions are ephemeral and can rapidly degrade. Bioconstructions can have various shapes and sizes, and they are distributed worldwide along depth gradients. The most known bioconstructions are the popular tropical reefs, noted for their beauty, high-diversity (polytypic), and complexity (Ingrosso et al., 2018). Much less attention has received other similar types of bioconstructions (mono- or oligotypic), found in other seas, included in temperate areas, such as the Mediterranean Sea.

The Mediterranean is a semi-closed basin considered one of the world's biodiversity hotspots, hosting 7.5% of global biodiversity (Bianchi and Morri, 2000) with a high percentage of endemism (Boudouresque, 2004; Coll et al., 2010), species of conservation concern (such as several cetaceans, sea turtles, monk seal) and endangered and protected habitats [i.e., meadows of the endemic *Posidonia oceanica*, coralligenous assemblages, animal forests *sensu lato* (Rossi et al., 2017) and deep-sea cold-water corals (CWCs; Davies et al., 2017)]. Some of these endangered habitats are biogenic reefs that provide structural complexity to seafloor habitats and support unique species and ecosystems (Orejas et al., 2009; Rossi, 2013; Bo et al., 2015; Davies et al., 2017; Rossi et al., 2017). For example, the coralligenous is a key ecosystem recognized as a natural habitat of community interest and Zone of Special Conservation at the European level (92/43/EEC Habitats Directive). From shallow to deeper waters, the Mediterranean Sea hosts a large variety of bioconstructions.

Ingrosso et al. (2018) identified a list of the main biogenic reefs in the Mediterranean Sea: vermetid reefs, which are biogenic formations that border rocky shores at the tide level; *Lithophyllum byssoides* trottoirs, common in the western and central Mediterranean, forming thick algae concretions that cover the rock surface; coral banks created by the shallow-water corals *Cladocora caespitosa* or *Astroides calycularis* formations/reefs, hosting a rich invertebrate fauna and that can cover up to 90% of some rocky areas (Goffredo et al., 2011); coralligenous assemblage, dwelled in rocky bottoms from 15 to 130 m depth (Ballesteros, 2006) developing extraordinary habitats with high biodiversity level; CWCs, that change the structural heterogeneity of the environment, forming large (monospecific or mixed) aggregations, the so-called animal forests, from 200 to 1000 m depth (Freiwald et al., 2009; Chimienti et al., 2018); and sabellariid or serpulid worm reefs, made of calcareous tube, where polychaetes live (Bianchi, 1981) that encrust any hard substrate. Other important and peculiar structures are recorded in the northern Adriatic Sea, and they are called "Tegnùe" or "Trezze" (Melli et al., 2017), subtypes of coralligenous habitats (Falace et al., 2015; Tosi et al., 2017). All these types of biogenic reefs are common throughout the whole Mediterranean Sea. Still, there are several knowledge gaps about their distribution, and knowledge on their biology and ecology is, in some cases, still fragmentary (Ingrosso et al., 2018).

Several direct and indirect anthropogenic pressures (industrial, urban and agricultural pollution, coastal development, marine litter, fishery, increase in sedimentation, organic enrichment, coastal development, deep-sea mineral mining and oil exploration, submarine cable, etc.) threaten these vulnerable bioconstruction systems, as well as climate change and the spread of alien species (Ballesteros, 2006; Coll et al., 2010; Piazzi et al., 2012). In particular, the widespread presence of marine litter represents one of the most important threats to biogenic reefs, which leads to a degradation of these habitats (de Carvalho-Souza et al., 2018) and the associated organisms (Galgani et al., 2018).

The Mediterranean is a densely populated sea with intense use of coasts, and it is notable for its contributions to the global economy and trade. It attracts 25% of international tourism (tens of millions of people descend each year), and about 220,000 vessels of more than 100 tons are estimated cross the Mediterranean annually, carrying 30% of the international maritime traffic (Ramirez-Llodra et al., 2013). Historical and current pressures in many ways have brought irreversible changes in the ecology of the Mediterranean Sea (Micheli et al., 2013). Mediterranean ecosystems are altered and threatened at an increasingly fast rate, and this basin is one of the most affected and polluted areas in the world (Barnes et al., 2009; Costello et al., 2010; Deudero and Alomar, 2015; Jambeck et al., 2015; Ramírez et al., 2018).

Due to its wide distribution, durability, and low biodegradability, marine litter is nowadays a remarkable and persistent threat to ecosystems and wildlife globally (Avio et al., 2017). Litter items, including micro-plastics, contaminate habitats from shallow water to the deep sea and from the poles to the equator (Worm et al., 2017). The most visible effect of marine litter is probably the entanglement of animals, which are hindered in their ability to move, feed, breathe, and reproduce (Li et al., 2016). This phenomenon is typically associated with abandoned, lost, or otherwise discarded fishing gear (ALDFG)

entangling marine mammals, sea turtles, seabirds, and fish (ghost-fishing; Galgani et al., 2018; Richardson et al., 2019). However, also many sessile erected species are deeply damaged by entanglement that may cause tissue abrasion, branch breaking, by-catches, etc. (e.g., Yoshikawa and Asoh, 2004; Angiolillo, 2019). These impacts may cause progressive and extended habitat degradation and a reduction in the coverage by biota on the seafloor (Laist, 1997; Fosså et al., 2002; Brown and Macfadyen, 2007). On the seabed, litter objects alter the surrounding habitat, interfering with life, and providing a previously absent hard substrate (UNEP, 2009).

Additionally, litter items can be used as a means of transport by alien invasive species traveling over long distances, both horizontally or vertically (Kühn et al., 2015). Moreover, microparticles of plastic (also known as microplastics when their size is < 5 mm in their largest dimension), specifically realized for various applications (primary microplastics) or deriving from the flaking of larger pieces (secondary microplastics), can be ingested by marine organisms and enter the trophic web (Corcoran et al., 2014; Gall and Thompson, 2015). Litter can be mistaken for food by several marine organisms, and indigestible debris may affect individual fitness, with negative consequences on survival (Kühn et al., 2015). The degradation of plastic, metals, and other litter material can also result in the release of toxic chemicals substances with chronic and sub-lethal consequences, which could likely compromise populations and communities and have long-term effects. Some xenobiotics, including persistent organic pollutants, toxic metals, pesticides, herbicides, pharmaceuticals as well as plastics and microplastics, are resistant to degradation, and deep waters and sediments have been suggested as their final accumulation site (Ramirez-Llodra et al., 2011; Ma et al., 2015). In the Mediterranean Sea, a recent review found that 116 species have ingested plastic, 44 species were found entangled in marine litter, and 178 taxa were found rafting on floating objects or using marine litter as a substratum (Anastasopoulou and Fortibuoni, 2019).

The presence of marine litter and its effects has stimulated increasingly global interest in this issue due to its ubiquity and its potential impact on human health (Hess et al., 1999; UNEP, 2009; Miyake et al., 2011). For several decades, the majority of studies had focused on the distribution of beach and floating litter and its impact by entanglement on charismatic organisms as marine birds, turtles, and mammals, and ingestion, in particular by fishes. Only in the last few years, increasing interest is also focusing on the distribution and injuries to benthic habitats and invertebrates caused by anthropogenic litter accumulating on the seafloor. Increasing awareness on this issue is stimulating scientific research, monitoring programs, NGO activities (Consoli et al., 2019), and it is initiating political action to tackle this environmental problem (Galgani et al., 2013; Galgani et al., 2019; Ronchi et al., 2019).

In 2008, the European Union issued the marine strategy framework directive (MSFD, 2008/56/CE), which is the leading European legal instrument to protect the marine environment in the Baltic Sea, North-east Atlantic Ocean, Mediterranean Sea, and Black Sea. The MSFD foresees 11 Descriptors, and Descriptor 10 states, "properties and quantities of marine litter do not cause harm to the coastal and marine environment." Four criteria were established to assess the achievement of the good environmental status (GES) of European seas considering Descriptor 10, one of which (D10C4) consists in "the number of individuals of each species which are adversely affected due to litter, such as by entanglement, other types of injury or mortality, or health effects." In 2016, the 19th Meeting of Contracting Parties agreed on the integrated monitoring and assessment program (IMAP) of the Mediterranean Sea and Coast and Related Assessment Criteria in its Decision IG. 22/7, which laid down the principles for integrated monitoring, including pollution and marine litter. IMAP Ecological Objective (EO) 10 (Marine Litter: "Marine and coastal litter do not adversely affect coastal and marine environment") includes Candidate Indicator 24: "Trends in the amount of litter ingested by or entangling marine organisms focusing on selected mammals, marine birds, and marine turtles."

Moreover, the Ecosystem Approach (EcAp), defined as "a strategy for the integrated management of land, water and living resources that promotes conservation and sustainable use in an equitable way" (Morand and Lajaunie, 2018), is now fully integrated into the mediterranean action plan (MAP) – Barcelona Convention System dedicated to the protection of the Mediterranean Sea against pollution and is in line with the MSFD and the decisions of the convention on biological diversity (CBD) and the Aichi targets. Nevertheless, to date, limited and fragmented knowledge is available on the effect of litter on the benthic realm, in particular for reef systems (de Carvalho-Souza et al., 2018) and the Mediterranean Sea (UNEP/MAP and SPA/RAC, 2018). Thus, this review aims to put together, synthesize and discuss the state of the current knowledge about the interactions of macro litter and the Mediterranean reef systems, from shallow to deep waters, investigating: (i) the spatial distribution and qualitative composition of litter causing impact; (ii) the different typologies of interaction and the species involved; (iii) the methods used to trace and identify marine litter on the bottom and its impact on reef species and; (iv) the knowledge gaps to help to find solutions to mitigate marine litter effects. Information provided here may contribute to the crafting of new indicators of entanglement to populate criteria D10C4 of the MSFD and IMAP Indicator 24 and identify main knowledge gaps (e.g., main species and habitats likely to be impacted) and areas where more scientific effort is needed.

BIBLIOGRAPHIC RESEARCH

Information was collected by consulting scientific databases on marine litter impacts on biota (Litterbase[1] and MedBioLitter[2]) and the search engines Web of Science, Scopus, Google Scholar, and ResearchGate. A list of keywords linked with marine litter and reefs was used, i.e., "marine litter," "deep marine debris," "submerged marine litter," "anthropogenic debris," "seafloor litter," "marine pollution," "garbage," "derelict fishing

[1]https://litterbase.awi.de

[2]http://panaceaweb.adabyron.uma.es/marine-litter/

gear," "ADLFG," "CWCs," "Mediterranean Sea," "entanglement," "ghost-fishing," "animal forest," "abrasion," "marine litter interaction," "coralligenous," "bioconstruction," and "fishing impact."

Sixty-seven publications reporting evidence of the impact of marine litter on Mediterranean reef systems were found, the first one published in 1994. However, the bulk of papers were published in the last decade (**Figure 1**). In the majority of publications, the impact of marine litter on animal forests and reefs was not the focus of the study. In this review, we selected only those cases where it was clearly defined that the impact was caused by marine litter, i.e., "any persistent, manufactured or processed solid material that is discarded, disposed of or abandoned in the marine or coastal environment" (UNEP, 2009). Thus, we excluded cases in which it was not clear if the impact was related to fishing activities or active fishing gear.

The information gathered from the publications included: the place where the study was conducted (coordinates and depth), the taxa involved, the type of reef impacted, the type of interaction, the type of litter, and the effect on impacted species. Species names were updated using the World Register of Marine Species (WoRMS) database,[3] and their conservation status was defined according to the International Union for Conservation of Nature (IUCN) Red List database,[4] referring to the Mediterranean subpopulation when specific information was available. Otherwise, we referred to the global assessment or, in some case studies in Italian waters, to the assessment performed by the Italian committee.[5] Case studies were subdivided into benthic environments as follows: 0–200 m (littoral), 200–1000 m (archibenthic), and 1000–4000 m (bathybenthic).

A SUMMARY OF THE IMPACTS ON REEF SPECIES

Study areas were not homogeneously distributed across Mediterranean subregions, and sampling effort was mainly concentrated in the Western Mediterranean Sea (51 papers), followed by the Adriatic Sea and the Ionian and Central Mediterranean Sea (seven papers each), and lastly, the Aegean-Levantine Sea (four papers; **Figure 2**). Moreover, almost the totality of studies was conducted in the Northern Mediterranean Sea: Italy ($n = 39$), Spain ($n = 9$), France ($n = 7$), Croatia ($n = 3$), Greece ($n = 3$), Malta ($n = 2$), Cyprus ($n = 1$) and Montenegro ($n = 1$). One study was conducted close to the Moroccan coast in the Chafarinas Islands (Spain; **Figure 2**). Case studies included evidence of marine litter impact on reefs from a few meters below the surface down to 1,208 m. Most case studies ($n = 40$) were focused in the littoral zone, followed by the archibenthic zone ($n = 27$) and bathybenthic zone ($n = 2$). The major part of studies was carried out on coralligenous (33%) and CWCs (50%) assemblages, or both coral aggregations (13%). Only two studies were conducted on the "tegnùe" (Melli et al., 2017; Moschino et al., 2019) and one on *Astroides calycularis* reefs (Terrón-Sigler, 2015). No data were available on the impact of marine litter on other types of Mediterranean biogenic reefs.

Seventy-eight taxa resulted impacted by marine litter on Mediterranean reefs (**Table 1**). The large majority belonged to the phylum Cnidaria (41%), followed by Chordata (22%), Arthropoda (13%), Porifera (9%), and Echinodermata (8%). The remaining taxa represented less than 5% (**Figure 3**). The list of impacted species included eight endangered (EN) species: the red coral (*Corallium rubrum*), the stony cup coral (*Dendrophyllia cornigera*), the cockscomb cup coral (*Desmophyllum dianthus*), the white coral (*Desmophyllum pertusum*), the smooth black coral (*Leiopathes glaberrima*), the madrepora coral (*Madrepora oculata*), the sea-sponge *Geodia cydonium,* and the giant devil ray (*Mobula mobular*). This provides evidence for the potential hazard represented by marine litter for threatened reef species. Seven vulnerable (VU) species were also found to be impacted by marine litter in the Mediterranean (**Table 1**), while the large majority ($n = 17$) of species were not evaluated (NE) or data deficient (DD; $n = 3$).

METHODS USED TO DETECT IMPACTS

In the Mediterranean Sea, the first scientific evidence of seafloor litter interaction with reefs and biota dates back to the end of the 1990s with visual investigations through SCUBA divers in shallow coastal environments (Harmelin and Marinopoulos, 1994; Bavestrello et al., 1997). The first studies using a remotely operated vehicle (ROV) were published in 2009 (Freiwald et al., 2009; Orejas et al., 2009; Salomidi et al., 2009), and later on, ROV was the method most used both in shallow and deep waters. We also found one case study where a fixed camera was used in the Ionian Sea (D'Onghia et al., 2017), and a paper where ROV and Agassiz trawl were used complementarily for *in situ* observation and to sample corals in the Blanes Canyon (France), respectively (Aymà et al., 2019).

Seafloor imagery is increasingly being used to study the abundance and distribution of species on the seafloor (Valisano et al., 2019). The advance and availability of exploration technologies, such as ROV-imaging, applied to previously unexplored hard bottoms, have provided a lot of *in vivo* information for the deep sea and reef systems, that in the last decades have revolutionized and rapidly increased the knowledge on these habitats and its threats. The increasing interest in deep-sea exploration had also caused the copious number of studies on litter compared to shallower waters (references herein).

In the last years, these methods have also been applied to the study of seafloor litter (Spengler and Costa, 2008), and they have allowed to describe and quantify litter interactions with marine organisms. Visual methods can be applied to all sea bottom types from the continental shelf to the bathyal environment, including complex reef habitats (Watters et al., 2010; Angiolillo et al., 2015). Visual data obtained by SCUBA divers, towed systems, ROVs or submersibles, and other camera platforms, equipped with specific scientific tools (HD video and camera, laser points, and geolocalization), have allowed

[3] www.marinespecies.org

[4] www.iucnredlist.org

[5] www.iucn.it

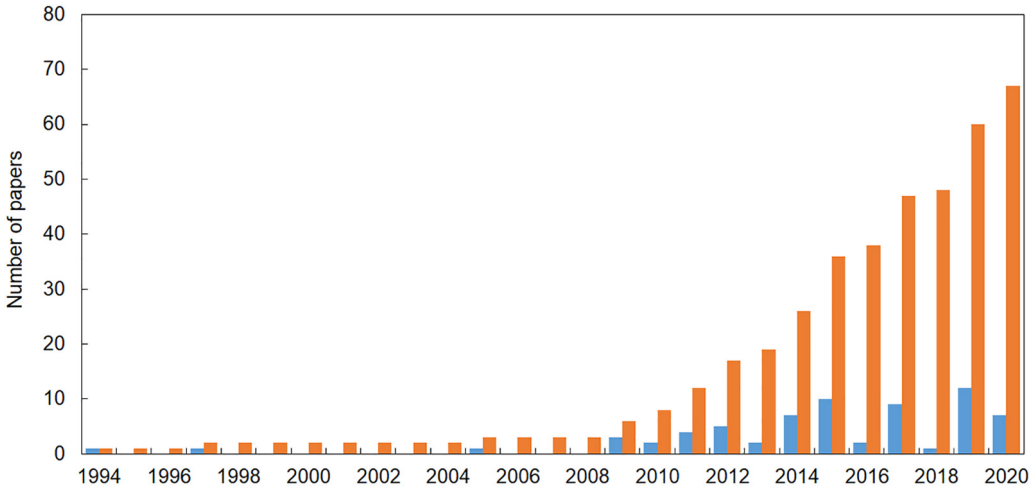

FIGURE 1 | The number of papers reporting evidence of the impact of marine litter on reef systems in the Mediterranean Sea (updated at the end of May 2020). Blue = number of papers published each year; orange = cumulative number of papers published since 1994.

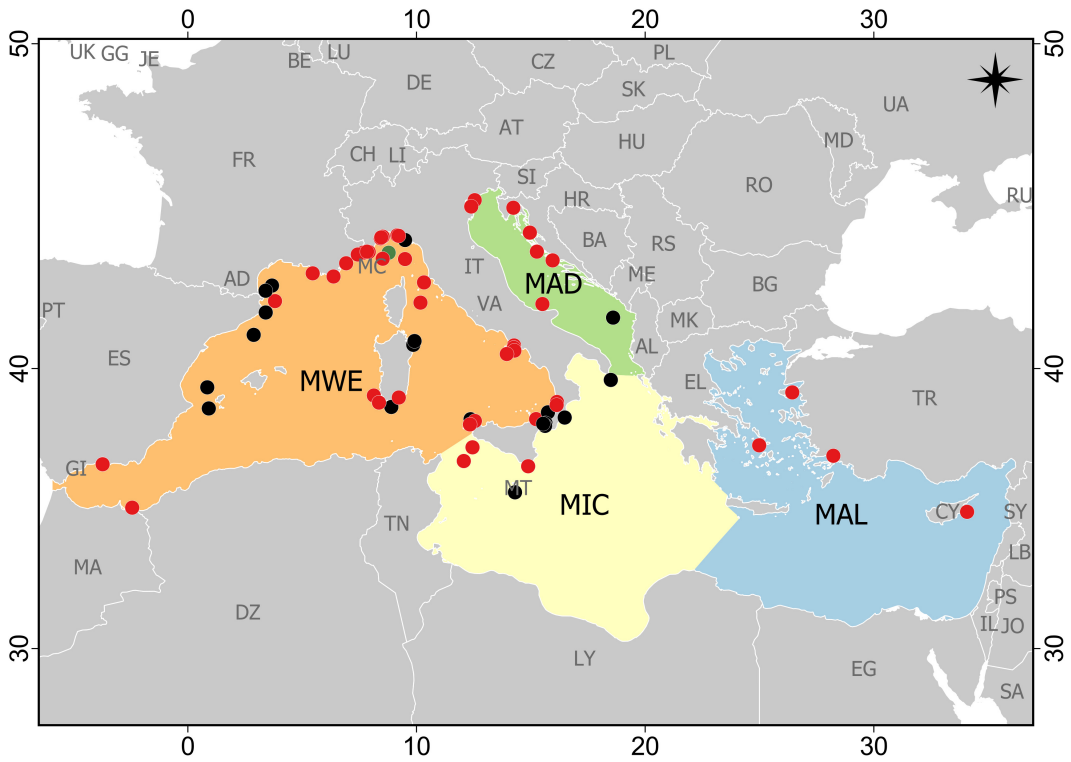

FIGURE 2 | Distribution of the case studies reporting the impact of marine litter on reef systems in the Mediterranean Sea (updated at the end of May 2020). Case studies are reported with different colors according to their benthic environment: littoral (0–200 m) – red dots; archibenthic (200–1000 m) – black dots; bathybenthic (1000–4000 m) – green dots (two case studies were referred to this environment, but one did not report the exact place and thus it was not possible to include it in the map). MWE, Western Mediterranean Sea; MIC, Ionian Sea and the Central Mediterranean Sea; MAD, Adriatic Sea; MAL, Aegean-Levantine Sea.

highlighting as marine litter represents one of the major pollution problems harming benthic organisms and habitats (Gilman, 2015). These methods do not cause any impact to the marine environment and are thus applicable in protected and sensitive areas such as marine protected areas (MPAs) and coral reefs (e.g., Betti et al., 2019, 2020; Chimienti et al., 2020). From videos and frame/photo, it is possible to obtain high-resolution quantitative data (depending on optical device), precise geolocalization, and provides *in situ* information at various depths.

However, the most common method to study seafloor litter is still through trawling hauls (i.e., otter, beam, Agassiz trawl),

TABLE 1 | List of the reef species impacted by marine litter in the Mediterranean.

Phylum and Taxa	IUCN category	Phylum and Taxa	IUCN category
Porifera		**Annelida**	
Aplysina cavernicola	LC (Italy)	*Sabella pavonina*	NE
Geodia cydonium	EN (Italy)	*Vermiliopsis* spp.	
Haliclona (Reniera) spp.		*Filograna implexa*	NE
Leiodermatium pfeifferae	NE	**Arthropoda**	
Pachastrella monilifera	VU (Italy)	*Geryon longipes*	NE
Poecillastra compressa	VU (Italy)	*Geryon trispinosus*	NE
Raspailia (Raspailia) viminalis	NE	*Maja squinado*	NE
Cnidaria		*Munida* spp.	
Acanthogorgia hirsuta	LC (Med)	*Munida rugosa*	NE
Alcyonacea		*Munida tenuimana*	NE
Alcyonium acaule	LC (Med)	*Pachylasma giganteum*	NE
Alcyonium coralloides	LC (Med)	*Palinurus elephas*	VU
Alcyonium palmatum	LC (Med)	*Paromola cuvieri*	NE
Antipathella subpinnata	NT (Med)	*Plesionika* spp.	
Antipathes dichotoma	NT (Med)	**Bryozoa**	
Astroides calycularis	LC (Med)	**Echinodermata**	
Bebryce mollis	DD (Med)	*Astrospartus mediterraneus*	NE
Callogorgia verticillata	NT (Med)	Cidaridae	
Ceriantharia		*Cidaris cidaris*	NE
Chironephthya mediterranea	NE	*Gracilechinus acutus*	NE
Corallium rubrum	EN (Med)	*Gracilechinus alexandri*	NE
Dendrophyllia cornigera	EN (Med)	*Ophiothrix* spp.	
Dendrophyllia ramea	VU (Med)	**Chordata**	
Desmophyllum dianthus	EN (Med)	*Anthias anthias*	LC
Desmophyllum pertusum	EN (Med)	*Callanthias ruber*	LC (Med)
Ellisella paraplexauroides	VU (Med)	*Coelorinchus caelorhincus*	LC
Eunicella cavolini	NT (Med)	*Conger conger*	LC
Eunicella singularis	NT (Med)	*Epinephelus aeneus*	NT (Med)
Eunicella verrucosa	NT (Med)	*Helicolenus dactylopterus*	LC (Med)
Leiopathes glaberrima	EN (Med)	*Mobula mobular*	EN
Leptogorgia sarmentosa	LC (Med)	*Mola mola*	VU
Madrepora oculata	EN (Med)	*Muraena helena*	LC (Med)
Paramuricea clavata	VU (Med)	*Scorpaena elongata*	LC (Med)
Paramuricea macrospina	DD	*Scorpaena notata*	LC (Med)
Parantipathes spp.		*Scorpaena porcus*	LC
Parantipathes larix	NT (Med)	*Scorpaena scrofa*	LC (Med)
Savalia savaglia	NT (Med)	*Scyliorhinus* spp.	
Swiftia dubia	DD (Italy)	*Serranus scriba*	LC (Med)
Viminella flagellum	NT (Med)	*Symphodus roissali*	LC (Med)
Mollusca		*Trachurus mediterraneus*	LC
Neopycnodonte cochlear	NE		
Sepia officinalis	LC		

The conservation status, according to the Red List of Threatened Species (IUCN), is reported. IUCN, International Union for Conservation of Nature; NE, not evaluated; VU, vulnerable; LC, least concern; EN, endangered; NT, near threatened; DD, data deficient. The bold terms refer to the "phylum".

mainly for its lower costs of operation in comparison with other methods and large scale evaluation (e.g., Galgani et al., 1996, 2000; Stefatos et al., 1999; Moore and Allen, 2000; Lee et al., 2006; Koutsodendris et al., 2008; Keller et al., 2010; Sánchez et al., 2013; Neves et al., 2015; Pasquini et al., 2016; Fortibuoni et al., 2019; Spedicato et al., 2019). In trawl surveys, litter is taken onboard and thus can be directly inspected, measured, counted, and weighed, allowing to obtain quantitative data. Nevertheless, the use of trawls should be avoided/limited on hard substrates such as reefs or in areas protected from fishery activity, since it is a destructive method. Besides, trawling does not enable to directly observe and assess the effects of litter on habitats and species nor the precise localization of litter and impacted organisms.

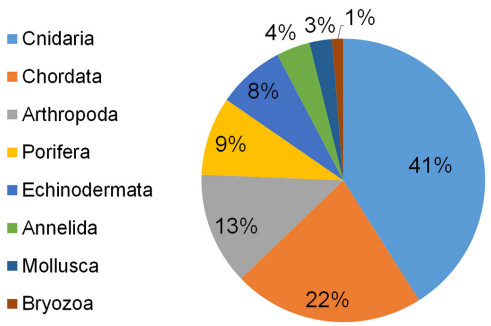

FIGURE 3 | Percentage of reef species impacted by marine litter in the Mediterranean Sea subdivided by phylum.

TYPES OF INTERACTION

The types of litter interactions were coded into six categories, i.e., entanglement, ghost-fishing, coverage, behavioral, substratum, and incorporation. Marine macrolitter were subdivided according to the MSFD Commission Decision 2017/848, into the following categories: artificial polymer materials, rubber, cloth/textile, paper/cardboard, processed/worked wood, metal, glass/ceramics, chemicals, undefined, and food waste. However, "ALDFG" (including longlines, trammel nets, gillnets, set nets, ropes, FADs, pots, etc.) were considered separately, considering the documented wide presence in biogenic reefs (Galgani et al., 2018). The effects on biota were not always described, and when the information was available, it was classified into nine groups: abrasion, behavioral, colonization, damage, death, detachment, entrapment, epibiosis, and necrosis.

Entanglement

Entanglement resulted in being the major impact of marine litter affecting marine organisms on Mediterranean reefs (**Supplementary Table S1**). We found evidence of entanglement for thirty-four taxa, most of which were cnidarians. Fishing gears were by large the most common litter type causing entanglement mainly through snagging and catches on reef organisms (**Figure 4**). Artisanal gears (trammel nets, gillnets, and long and fishing line, ropes, etc.) or lost fishing gear, under the pressure of bottom currents, can indeed easily become entangled in rocks and in all taxa that elevate on the substrate due to their massive or arborescent morphologies (**Figures 5A–C**). The abrasive action due to the continuous mechanical friction caused by entangled gear can cause breakage of ramifications of all erect biotic structures or a progressive removal of their tissues (Macfadyen et al., 2009; de Carvalho-Souza et al., 2018), making them more vulnerable to parasites or bacterial infections (Bo et al., 2014).

Abrasion/coenenchyme loss was the most common effect of entanglement by ALDFG reported for animal forests on Mediterranean reefs, and it was observed in all subregions. Eleven cnidarian species resulted impacted, including the endangered *Corallium rubrum*, as well as the sea-sponge *Leiodermatium pfeifferae*. Because of abrasion, a naked coral skeleton can be quickly covered by fast-growing epibionts (such as an encrusting sponges, zoanthids, or some alcyonaceans; Bo et al., 2014; Angiolillo et al., 2015; Angiolillo and Canese, 2018) and this phenomenon could cause colony loss (Bavestrello et al., 1997). The high frequency of these opportunistic organisms may suggest a general state of stress of the community (Bo et al., 2014) also due to marine litter impacts.

Necrosis and epibiosis linked to the impacts of marine litter on reefs were, for instance, widely reported by Giusti et al. (2019) in the Ligurian and Western Mediterranean Seas. Direct damages (e.g., broken branches) to coral colonies due to entangling marine litter were also observed on Mediterranean reefs (e.g., Madurell et al., 2012; Maldonado et al., 2013; Angiolillo et al., 2015; Consoli et al., 2018; Moccia et al., 2019). Fishing gear entangled on coral colonies was also shown to cause their detachment from the seafloor (Houard et al., 2012; Tsounis et al., 2012; Angiolillo et al., 2015; Kipson et al., 2015; Maldonado et al., 2015; Cattaneo-Vietti

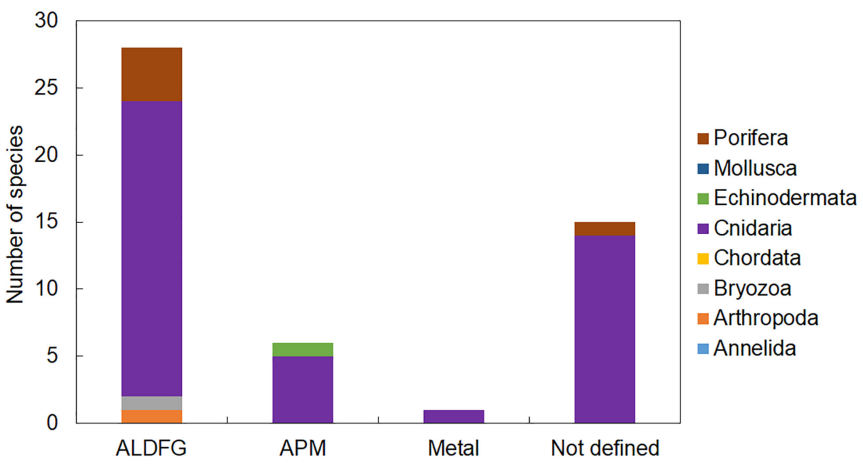

FIGURE 4 | The number of species by taxa found entangled in different typologies of marine litter on Mediterranean reefs. ALDFG, abandoned, lost, or otherwise discarded fishing gear; APM, artificial polymer materials.

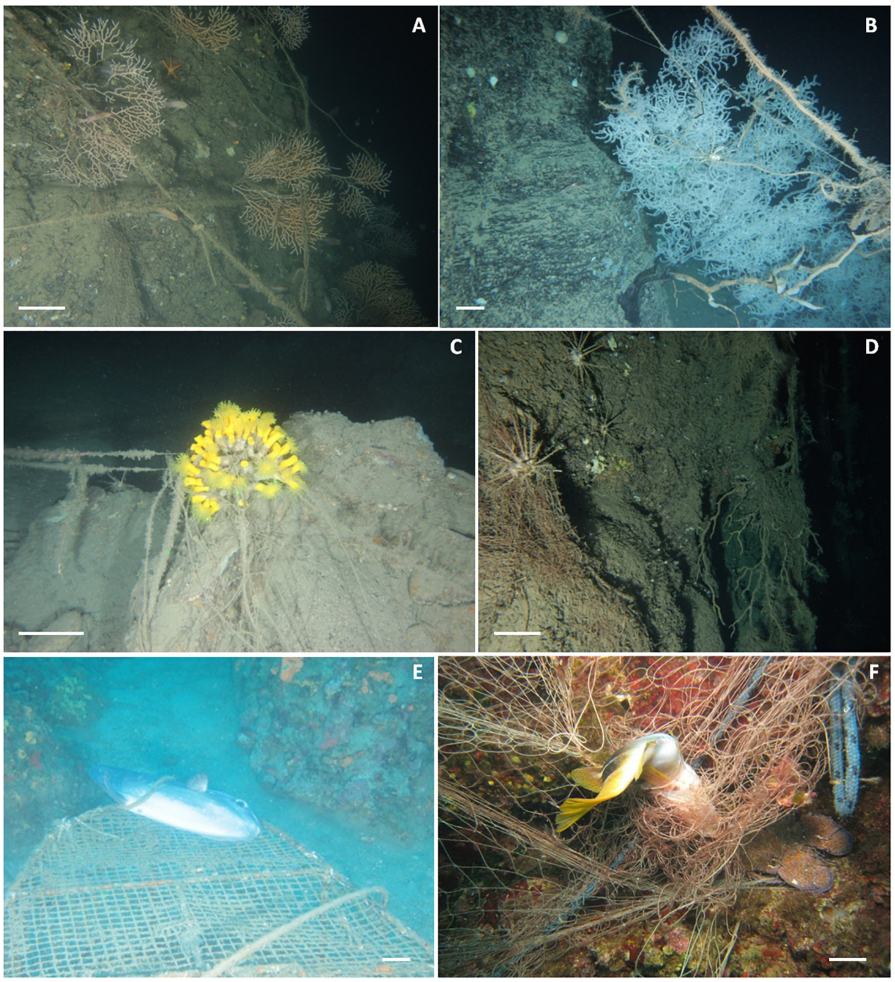

FIGURE 5 | Examples of marine litter impacts on biogenic reefs in the Mediterranean Sea. Scale bar: 10 cm. **(A)** lines and ropes entangling *Eunicella cavolini* colonies; **(B)** old long line and monofilaments entangled on a colony of *Leiopathes glaberrima*, peeling off part of its tissue (with evidence of necrosis); **(C)** *Dendrophyllia cornigera* colony completely entangled in a lost longline; **(D)** lost nets entrapping a specimen of Cidaridae and a dead gorgonian; **(E,F)** examples of ghost-fishing: a sunfish (*Mola mola*) entrapped in a fishing pot and a painted comber (*Serranus scriba*) entrapped in a lost net.

et al., 2017; Consoli et al., 2019) and even their death (Maldonado et al., 2013; Deidun et al., 2015; Consoli et al., 2018; Enrichetti et al., 2019; **Figure 5D**).

Coral skeletal characteristics, determining the rigidity and fragility of a colony, as well as the size and shape of individuals, determine the resistance to friction, which explains the different responses of the various species of coral to mechanical impacts (Bo et al., 2014; Fabri et al., 2014; Angiolillo and Canese, 2018). In this review, the most impacted species resulted in those that easily remain entangled due to their medium-large colony size, an arborescent morphology, and a flexible skeleton (e.g., *Antipathella subpinnata, Leiopathes glaberrima, Callogorgia verticillata, Dendrophyllia cornigera, Paramuricea clavata,* **Figures 5A–D**), as observed in other studies (Asoh et al., 2004; Bo et al., 2014; Valisano et al., 2019). Numerous examples from this review illustrate marine litter impacts on vulnerable (VU) and endangered (EN) species (IUCN criteria, **Table 1**) and sensitive habitats, such as CWCs (Orejas et al., 2009; Madurell et al., 2012), coral gardens (Bo et al., 2014, 2015; Fabri et al., 2014; Angiolillo et al., 2015) and coralligenous assemblages (Sbrescia et al., 2008; Valisano et al., 2019) that are more vulnerable because of slow growth rate and longevity of their coral species (MacDonald et al., 1996; Consoli et al., 2018).

The impact of the hook-and-line fishery on the seafloor is generally perceived as lower when compared with other fishing methodologies, such as bottom trawling (Macfadyen et al., 2009). However, monofilament fishing line is responsible for the largest part of entanglements observed on Mediterranean reefs and, more in general, represent the major impact in rocky areas, not suitable for trawling (Angiolillo, 2019). Kroodsma et al. (2018) estimated that globally longline fishing is the most widespread activity, detected in 45% of the ocean more than trawling (9.4%). However, longline incidence can strongly vary according to the region, and even if in many areas it may be mainly confined to artisanal fishing grounds, passive gears could drift for long distances driven by currents. Due to its extensive use, often

extremely long configuration, and low cost, its cumulative effects over time might be very detrimental (Macfadyen et al., 2009). Moreover, line and longline are now made of non-biodegradable synthetic fibers and, once lost, can persist in the environment for centuries (Carr, 1987; Thompson et al., 2004; Moore, 2008; Barnes et al., 2009; Watters et al., 2010; Bo et al., 2014).

The reduction in the coverage of habitat-forming species and the detrimental effect on the diversity and abundance of reef invertebrates and fishes resulting from human-induced pressure can cause substantial modifications to the structure and functioning of reef ecosystems (Bo et al., 2014; Clark et al., 2016; Valisano et al., 2019). The accumulation of fishing debris represents one of the major causes of habitat degradation of Mediterranean reefs. Thus, destructive practices (e.g., fishing and anchoring) that can threaten arborescent corals should be banned in the proximity of the coral forests (Chimienti et al., 2020).

Ghost-Fishing

Ghost-fishing represents another aspect of entanglement. Crabs, octopus, fishes, and many small invertebrates may be taken in traps, nets, gear, or other litter items that continue to "fish" if lost at sea. In Mediterranean reefs, according to this review, ghost-fishing was exclusively related to fishing gears (**Supplementary Table S1**) and was observed for four species belonging to the phylum Arthropoda (*Geryon trispinosus*, *Maja squinado*, *Munida rugosa,* and *Palinurus elephas*) and 10 Chordata (*Conger conger*, *Epinephelus aeneus*, *Mobula mobular*, *Mola mola*, *Scorpaena notata*, *S. porcus*, *S. scrofa*, *Serranus scriba*, *Scyliorhinus* spp., and *Symphodus roissali,* **Figures 5E,F**).

Water turbidity, making the litter and the gear less visible, as well as the presence of organisms in or near the nets, are factors that may contribute to organisms being entangled in, or strangled by, abandoned fishing gear, resulting in domino effects of damage. Benthic invertebrates, such as crabs and echinoderms, may become entangled in nets, traps, or other kinds of debris lying on the seafloor while scavenging animals that have already become entangled (Good et al., 2010). In this way, ghost fishing gear may continue to catch for a long time a large variety of organisms (Carr, 1987; Matsuoka et al., 2005; Brown and Macfadyen, 2007). The impossibility of moving and breathing, compromising the ability to acquire food and escaping from predators, might eventually lead to death for stress, starvation, or drowning (Ayaz et al., 2010; Butterworth et al., 2012; Enrichetti et al., 2020). Moreover, entanglement, abrasion, and restricted movements can lead to lesions at risk of infections and amputation (Laist, 1997; Chiappone et al., 2005; Criddle et al., 2009; Gregory, 2009; NOAA, 2014).

It was estimated that in some areas, ghost fishing might remove up to 30% of commercial species, with a significant economic impact on fisheries (Gilman et al., 2016). The time over which lost fishing gears continue to entangle organisms is highly variable, depending on the location and the gear typology (Erzini, 1997; Matsuoka et al., 2005; Erzini et al., 2008). Derelict gill nets and trammel nets, for instance, are estimated to continue catching marine biota for a period ranging between 30 and 568 days (Matsuoka et al., 2005). However, the impact of ghost-fishing on marine populations is difficult to quantify as an unknown number of marine animals die or are consumed by predators at sea and decompose without being recorded (Katsanevakis and Issaris, 2010). Hence, the effects on the population dynamics and the mortality rates of many affected species are probably underestimated (Katsanevakis and Issaris, 2010). No specific studies were carried out on this issue in the Mediterranean Sea reef systems, and only some descriptive observations are available. An experimental study exists only for shallow waters (i.e., Ayaz et al., 2006).

Coverage

Coverage was mainly linked to fishing gear (in particular nets, **Figure 6A**) and impacted four Cnidaria species (*Corallium rubrum*, *Eunicella cavolini*, *Madrepora oculata*, and *Paramuricea clavata*) and one Porifera (*Geodia cydonium*). The white coral (*M. oculata*) was also found covered by artificial polymer materials (plastic sheets, bags, and objects, **Figure 6B**) as well as chemicals (bauxite residues). Coverage can induce stress in sessile organisms (e.g., corals and sponges) by depriving them of light and oxygen. de Carvalho-Souza et al. (2018) reported many examples of reef sites that suffered significant losses of coral cover related to suffocation by macrolitter. Marine litter may cover large portions of the settled communities (Saldanha et al., 2003), impeding the recolonization of large organisms (Galgani et al., 2015), preventing gas exchange and oxygenation, and diminishing the feed capacity of the organisms (Kühn et al., 2015).

Behavioral

Marine litter can also cause behavioral changes in marine organisms and be used as shelter and refuge. We found evidence of 8 fish species using general waste and one species using fishing gears to hide from predators in Mediterranean reefs (**Supplementary Table S1**). Several authors observed the crab *Paromola cuvieri* (Angiolillo and Pisapia, 2015; Taviani et al., 2017; Mecho et al., 2018; Angiolillo, 2019; Pierdomenico et al., 2019) to use unusual camouflage shelters carrying on plastic on its exoskeleton, instead of usual sponges or gorgonians (**Figure 6C**). The high availability of marine litter may indeed result in its use by reef species instead of natural materials, with unknown ecological implications (de Carvalho-Souza et al., 2018). The squat lobster *Munida* spp. was found hidden in lost fishing gear (Pierdomenico et al., 2018), while some individuals of the shrimp *Plesionika* spp. were found aggregated on litter accumulations (Pierdomenico et al., 2019).

Some other types of litter such as tires, cans, glass bottles, and larger objects (e.g., washing machines, bins, etc.) can be adopted as shelters and refuge by vagile fauna (**Figure 6D**). Fishes, or other vagile invertebrates, can take advantage of artificial three-dimensional structures, especially in an otherwise soft-sediment environment (Angiolillo, 2019) or in a degraded environment where natural structuring species functioning as shelter are reduced. Even if these artificial substrata, used as a refuge by organisms, may enhance biodiversity, they interfere with life on the seabed and modify the spatial heterogeneity at different spatial scales, altering the natural environment, the community structure, and possibly ecosystem functioning

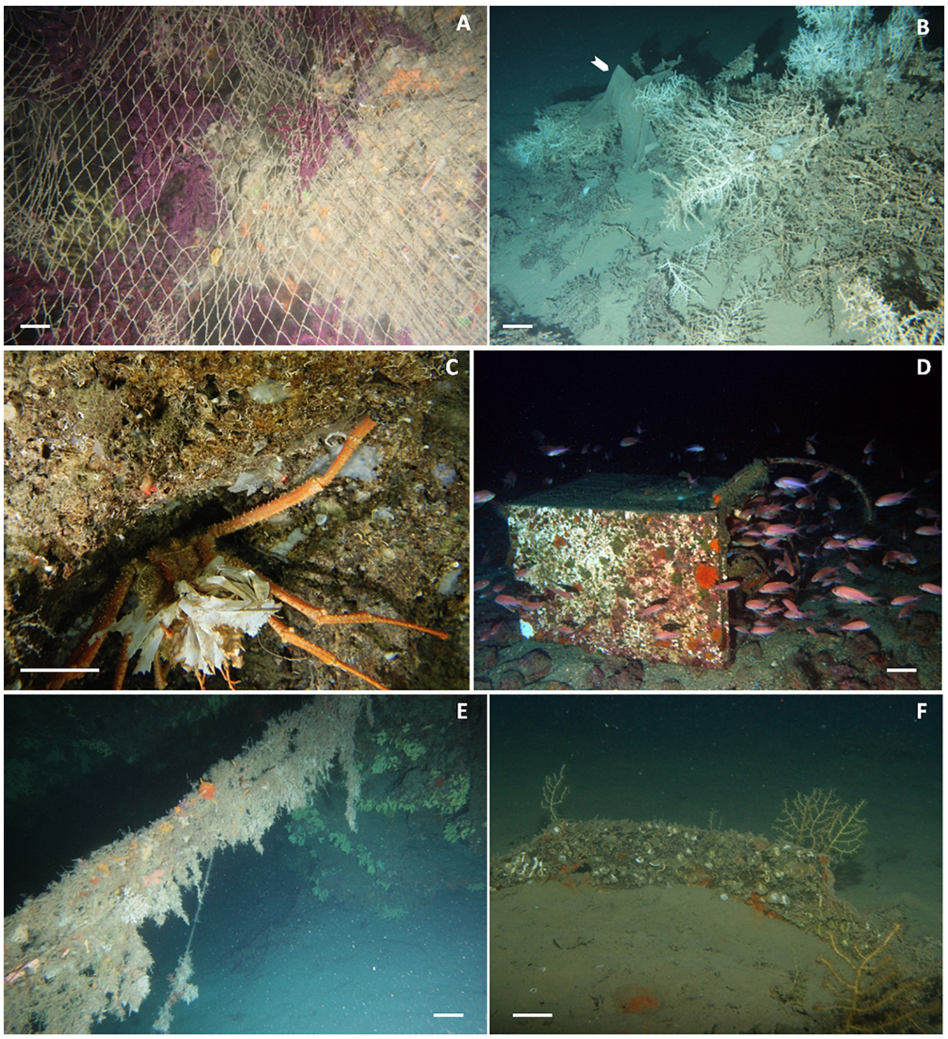

FIGURE 6 | (A) Abandoned or lost net completely covering the sea bottom, suffocating *Paramuricea clavata* colonies and other sessile organisms; **(B)** plastic sheet (white arrow) covering colonies of *Madrepora oculata*; **(C)** the crustacean *Paromola cuvieri* carrying plastic on the back, instead of sponges/gorgonians; **(D)** a washing machine completely covered by encrusting organisms and used by marine goldfish (*Anthias anthias*) as a refuge; **(E)** hanging fish net completely overgrown by encrusting and epibenthic organisms such as sponges, hydroids, bryozoans, and ascidians; **(F)** little gorgonians growing on human-made hard substrata.

(Saldanha et al., 2003; UNEP, 2009; Sánchez et al., 2013; de Carvalho-Souza et al., 2018; Angiolillo, 2019).

Other Interactions (Substratum and Incorporation)

Marine litter can also serve as an alternative substratum for sessile species on Mediterranean reefs (**Figures 6E,F**). Ten cnidarian species were found growing on fishing gears, as well as three Annelida, three Echinodermata, one Mollusca, and one Porifera species (**Supplementary Table S1**). Also general waste can provide a substratum for benthic reef species (four Cnidaria and one Echinodermata). Moreover, other examples of other interactions with marine litter came from Aymà et al. (2019). They recovered with an Agassiz trawl some fragments of a *Desmophyllum pertusum* colony growing on a nylon net cords at 752–864 m depth in the Blanes Canyon (Western Mediterranean Sea). Chimienti et al. (2020) observed a steel cable directly within a group of *Antipathella subpinnata* colonies in the Tremiti Islands MPA. Angiolillo and Canese (2018) observed fishing lines fully incorporated in the yellow scleractinian *Dendrophyllia cornigera* on the Mantice Shoal in the Ligurian Sea. Savini et al. (2014) found litter incorporated into the skeletons of living coral colonies in the Apulian ridge in the Ionian Sea. We named this interaction – the ability of gorgonians and corals to grow and/or include marine litter in their coral framework – "incorporation."

DISCUSSION

Globally, de Carvalho-Souza et al. (2018) reported marine litter driven ecological disruptions on 418 reef species belonging

to eight reef taxa. The authors found that entanglement and catches in ALDFG represent the most common impacts on marine biota in these environments. In the Mediterranean Sea, the present review reports evidence for 78 taxa impacted by marine litter on reefs (**Table 1** and **Supplementary Table S1**). The large majority belonged to the phylum Cnidaria, followed by Chordata, Arthropoda, Porifera, and Echinodermata. The remaining taxa represented less than 5%. This number is probably underestimated due to the scarcity of specific studies focusing on this topic and the difficulty of working on reefs. The majority of the studies focused on coralligenous and CWC (**Figure 7**) that are more vulnerable to these types of impacts. No information is available, regarding litter impact, in other reef systems, probably due to the greater sampling effort and increasing scientific interest for the first ones.

A wide diversity of interactions between marine litter and reef organisms was observed in the Mediterranean, including entanglement, coverage, and ghost-fishing. In most cases, impacts were due to ALDFG or other fishery-related waste. The effects of marine litter on animal forests and reef species could be manifold and can be direct (e.g., broken branches for corals and ghost-fishing for fish) or indirect. Parasitic colonization was, for instance, reported by several authors because of the abrasion induced by marine litter. On the other side, some species may take advantage of litter, using it as shelter and refuge.

However, at present, our knowledge of the deleterious effects of marine litter on Mediterranean reefs is limited and heterogeneous in space (**Figure 2**). Data from the Aegean-Levantine (**Figure 7A**) and the Adriatic Sea (**Figure 7D**) subregions are, for instance, very scarce, whereas data from the southern Mediterranean Sea are completely missing (**Figure 2**). The Aegean Sea is rich in reefs (Giakoumi et al., 2013; Freiwald et al., 2017; Di Camillo et al., 2018; Chimienti et al., 2019) but at the same time, poor in studies regarding marine litter in these habitats (**Figure 7A**). Now, there is not any routinely monitoring program for seafloor litter on hard substrata in Greece that can fill this gap. The only surveys with ROV are carried out within the frame of research projects (e.g., Ioakeimidis et al., 2015) but not specifically include litter impact on bioconstructions.

This heterogeneous distribution could be due to the greater sampling efforts and technological availability in the western part of the Mediterranean basin respect to the other areas. Only some countries can use non-invasive visual approaches, in particular for deep-sea areas, due to expensive costs. Even if several projects on marine litter have been financed in the last years in Europe (Maes et al., 2019), the major part assessed litter distribution and abundance and not the direct impact on the seafloor and marine organisms, in particular on reefs. In general, the most common approaches to evaluate seafloor litter make use of opportunistic sampling. Litter impact assessments are indeed usually coupled with surveys or programs whose main aim is the study of biodiversity in coral reef assemblages by diving in shallow areas and through ROV in the deep sea since methods for determining seafloor litter distributions can be similar to those used for benthic assessments. The absence of specific monitoring protocols and the different strategies of data collection (sampling methodologies, unit of measures, parameters, etc.) and elaboration have led to obtaining heterogeneous data, often not comparable in a robust way.

The major part of the studies analyzed in this review gives only descriptive information about litter interaction. Very few studies provide a quantification of litter and species abundance and the number of affected individuals (i.e., Angiolillo et al., 2015; Consoli et al., 2019; Enrichetti et al., 2019, 2020). Moreover, several studies have analyzed still images, sub-samples of video surveys, whereas others have analyzed a continuous video to collect quantitative data. Some papers evaluated the occurrence of the impact by considering the percentage of frames showing litter interacting with marine organisms (i.e., Bo et al., 2014, 2020). Thus, there is an increasing need to collect litter data regularly using common templates, harmonized procedures, and joint items categories and types of impacts. Standardization of monitoring approaches and existing datasets is under development across European countries to generate comparable information about the temporal and spatial distribution of marine litter and its impact (Molina Jack et al., 2019). Since the MSFD included marine litter as one of the eleven descriptors to define the GES of European seas (Galgani et al., 2013), seafloor litter data collection has significantly increased in the last years, mainly through trawl-surveys (Maes et al., 2018; Spedicato et al., 2019). Litter items in fishery catches are now regularly recorded in many European countries as part of other environmental monitoring activities (e.g., the MEDITS program; Spedicato et al., 2019). Instead, no uniform programs exist to collect litter data on reefs/hard substrata and to assess/quantify litter harms on marine biota (as requested by D10C4 of the MSFD and Indicator 24 of the EcAp). One of the reasons is due to the not mandatory status of these indicators. Only recently, the MSFD and the UN Environment/MAP Regional Plan on Marine Litter Management in the Mediterranean have begun to take into account the entanglement in their future monitoring. In May 2019, the MSFD TG Litter Working Group (TG-ML) proposed guidelines for the assessment of marine litter interaction and entanglement on benthic organisms using visual methods, applicable to the seafloor and reef systems. This protocol harmonizes the procedures for collecting and reporting marine litter data (distribution, occurrence, abundance, litter, and impact categories) that are gathered on the back of existing biodiversity surveys. The protocol is under review by the TG-ML to provide an accurate methodology applicable for MSFD monitoring to facilitate the identification of sources and trends, data analysis, comparison among countries, etc.

Some effort in this sense has already been made in Italy in the implementation of the first monitoring cycle of the MSFD, in the framework of Descriptor 1 on biodiversity. A unique monitoring protocol was developed to collect data on biodiversity and marine litter simultaneously. The status of populations (species richness, abundance, morphologies, epibiosis, necrosis), litter distribution, and its impact on organisms (focusing in particular on the most structuring species, i.e., corals and sponges), were assessed in coralligenous habitats. In this way, it will be possible to relate the number of entangled individuals/colonies for each structuring species to the total

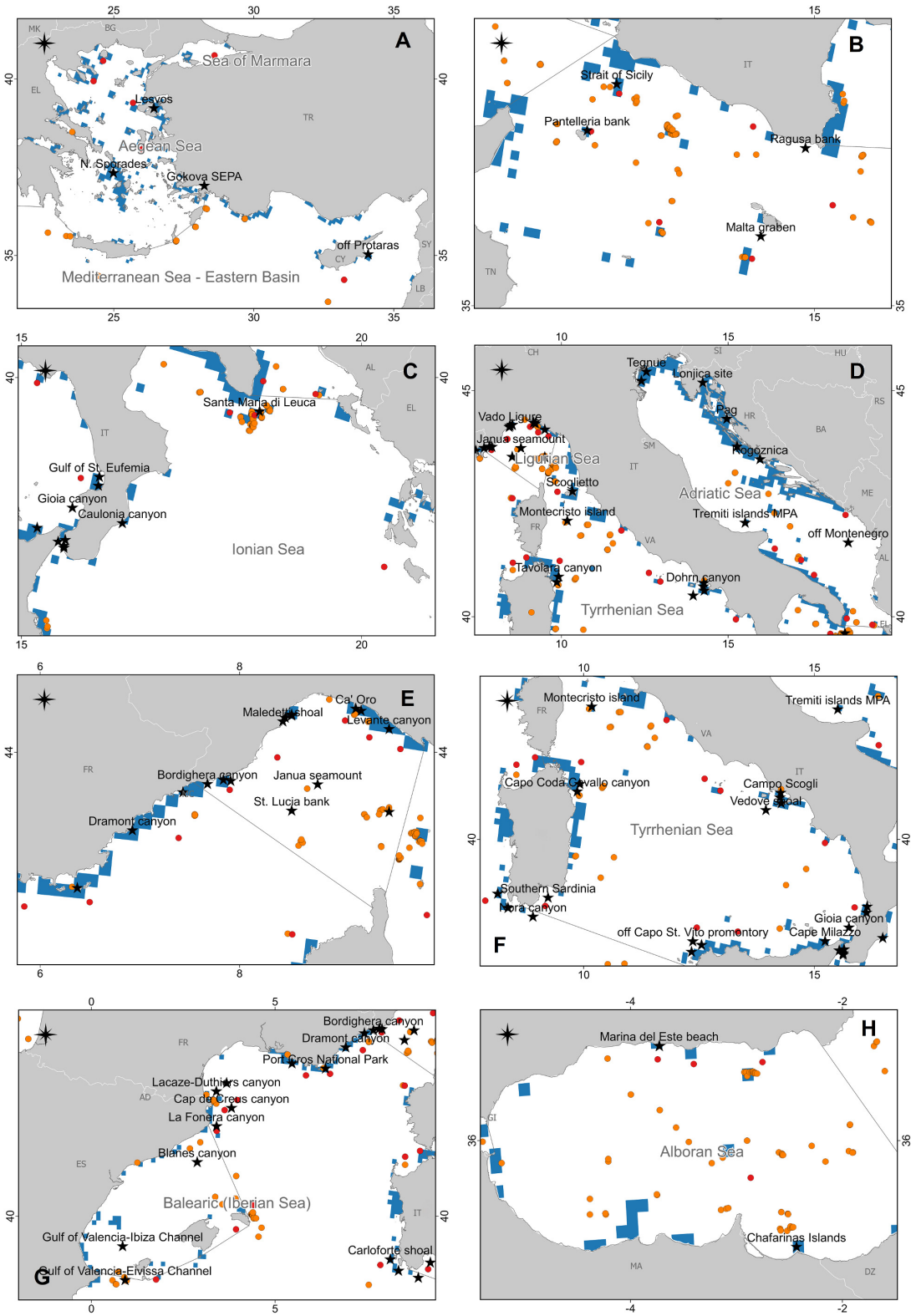

FIGURE 7 | The map reports the case studies collected in this review (black stars) together with the presence of coralligenous areas according to Giakoumi et al. (2013; light blue), and the presence of cold-water corals (CWCs) according to Chimienti et al. (2019; red circles) and Freiwald et al. (2017; orange circles). **(A)** Aegean and Eastern Mediterranean Seas; **(B)** Strait of Sicily; **(C)** Ionian Sea; **(D)** Adriatic Sea and North Tyrrhenian Sea; **(E)** Ligurian Sea and the northwestern Mediterranean Sea; **(F)** South Tyrrhenian Sea; **(G)** Iberian Sea and the northwestern Mediterranean Sea; **(H)** Alboran Sea.

number of individuals/colonies in a defined area. Data are available since 2016 and will represent the first baseline for future comparisons. The data mentioned above could also be used to populate the secondary criteria D10C4 of the MSFD and Candidate Indicator of the IMAP. Indeed, since reef coral communities have a strong potential to be entangled by marine litter, some structuring sessile suspension feeders have already been proposed as indicators. For instance, in 2018, SPA/RAC suggested an approach to study entanglement using benthic invertebrates as indicators of entanglement events, since they offer the possibility of monitoring this impact at a wide range of depths (UNEP/MAP and SPA/RAC, 2018).

Given the difficulties to differentiate entanglement by active fishing gears (by-catch) from entanglement due to ALDFG (ghost-fishing) or other kinds of marine litter for seabird, marine mammals, sea turtles, and fish (Anastasopoulou and Fortibuoni, 2019), Galgani et al. (2018) proposed animal forests as priority elements to monitor the spatio-temporal trends of entanglement in shallow and deep waters. Some previous reviews (de Carvalho-Souza et al., 2018; Anastasopoulou and Fortibuoni, 2019), as well as the present work, indicated cnidarian species as the taxa most affected by entanglement, caused mainly by fishing gear. The vulnerable habitat-forming cnidarian species, characterized by few dominant coral species and by an incredible variety of symbiotic associations, are slow-growing and long-living species (Sheehan et al., 2017) with an extensive distribution and high abundance. They are exposed to marine litter occurring in fishing areas, MPAs, and both coastal and remote areas. The massive and arborescent morphologies of these taxa and their sessile characteristic make them more susceptible to be entangled (Bo et al., 2014; de Carvalho-Souza et al., 2018) and at the same time, allow researchers to obtain an accurate location of the entanglement event, preventing from the misinterpretation in the case of interaction with active fishing gear (by-catch). However, at present, there is not enough data on the differences in entanglement rates among species and life stages, allowing to assess species vulnerability, the frequency of interactions with different marine litter types, and the possible implications in terms of populations. Bo et al. (2014) provided insight into the different responses of some structuring species to physical impacts, depending on the resistance of the coral skeleton, to its morphological and mechanical characteristics. Fragility, recovery ability, as well as reproductive and growth strategies, represent other factors that can determinate different responses to entanglement (MacDonald et al., 1996). The positive correlation between the number of dead colonies and the presence of ALDFG was showed by Angiolillo et al. (2015), indicating the detrimental effects of fisheries. Broken branches, damaged morphologies, and epibiosis can represent secondary consequences of the direct impact during fishing operations, such as the eradication of some specimens from their natural site. Therefore, the sensitivity of a benthic species should be an essential parameter to understand the capability of a species to cope with this impact. For instance, in the north-western Mediterranean Sea, visual surveys have provided evidence of the almost omnipresent incidence of marine litter in all investigated areas, highlighting as in reef systems fishery is a significant source and cause of impact.

Nevertheless, very few studies put in relationship the fishing effort, the rate of losing gear, and the by-catch to assess the entanglement rate (i.e., Enrichetti et al., 2019). Difficulties exist because no official data are available on the patterns of exploitation of artisanal and overall recreational fishing, which contribute in an important way to the impact on reef systems, also in offshore areas. Data on the fishing effort are thus needed to assess this source of impact (e.g., Enrichetti et al., 2019) and define mitigation measures (Bo et al., 2020). An appropriate database targeting fishing effort is needed for small fishery (artisanal and recreational), as suggested by some authors (Bo et al., 2020).

Gear can be lost or discarded due to several intentional and unintentional causes (Richardson et al., 2018), such as contact with other fishing gears, bad weather conditions, tracking systems malfunction, and catching or snagging on submerged features. Fishers can lose their gear also due to improper fishing methods or because of difficulty in retrieving it. On the other hand, gear can be deliberately abandoned when fishers are operating illegally or when the disposal onshore is not practical or economical, especially where reception facilities in the port are unavailable (Gilman, 2015; UNEP, 2015). In the Mediterranean Sea, it was estimated that 0.05% of gillnet and 3.2% of nets were lost per boat per year (Macfadyen et al., 2009). However, the amounts can be highly variable at small spatial scales (Macfadyen et al., 2009; Gilman, 2015).

The high persistence and widespread distribution of fishing gear at sea are due to the use of synthetic, durable, and buoyant materials (Erzini, 1997; Laist, 1997; Sampaio et al., 2012). Moreover, the increasing expansion of fishing effort and fishing grounds determined a wider ALDFG distribution (Macfadyen et al., 2009; Gilardi et al., 2010; Gilman, 2015; Kroodsma et al., 2018). The by-catch of a wide variety of reef species operated by longline and artisanal fishing gear is widely known in the Mediterranean Sea (Mastrototaro et al., 2010; Bo et al., 2014; D'Onghia et al., 2017) and can harm benthic communities (Erzini et al., 1997; Mytilineou et al., 2014; Enrichetti et al., 2019). The analysis of benthic organisms in fishery discards can provide information on reef species sensitivity to fisheries and their probability of being caught in a specific area (Enrichetti et al., 2019). The discard investigation, coupled with the visual approach to assess community structure and the extent of the impact, could represent a useful instrument to gain an overall view of the problem. The identification and mapping of areas where reef species are mostly exposed to the impact of fishing activities (i.e., co-existence of fishing grounds, presence of ALDFG, distribution of sensitive species, probability of encounters between sensitive species and marine litter, etc.) could represent a first step to rationalizing the sampling efforts.

Despite the prevalence of ALDFG, also other types of litter were recorded on biogenic reefs, mainly made of artificial polymer materials (i.e., plastic bottles, bags, and sheets). Oceanographic currents and wind can disperse plastic items over long distances, both vertically and horizontally, depending

on plastic lightness, buoyancy, and durability (Watters et al., 2010; Tubau et al., 2015; Vieira et al., 2015). Plastic degrades slowly, and its biological decomposition is negligible. On the seafloor, in particular below the photic zone where the light is absent, and the temperatures and oxygen concentrations are low, the decomposition process is further slowed down. A study carried out in the Saronikos Gulf (Greece) showed that PET bottles can remain intact for approximately 15 years and then began to deteriorate, with the consequent release of chemical compounds (Ioakeimidis et al., 2016). Physical degradation determinates the formation of abundant small plastic fragments, with the consequence of a high persistence of plastic litter, especially on the seafloor (Andrady, 2015; Galgani et al., 2015; Tubau et al., 2015). Another study observed coral polyps ingesting microplastic fragments with detrimental consequences for the colonies (Hall et al., 2015). Therefore, plastic and microplastics represent a significant environmental threat for the marine environment, including reef systems (Lamb et al., 2018).

The other forms of interaction described in this review (colonization, substrate, and behavioral) are under-studied, and they may represent a form of adaptation to a changing environment. The seafloor was considered for a long time an unlimited natural dump for the disposal of any kind of garbage (Ramirez-Llodra et al., 2011; Angiolillo, 2019). Anything that ends in the sea is in a short time colonized and reused. Iconic examples are represented by the wrecks, used as a suitable habitat for a variety of sessile organisms, and as a refuge for vagile fauna. Even if these interactions of organisms with anthropogenic artifacts are often considered neutral, the large evidence of the adaptive behavior of species, such as *Paromola cuvieri*, should make us reflect on the substantial and irreversible changes that humans are bringing to marine environments.

CONCLUSION

(1) This review provides evidence that marine litter and specifically ALDFG, threaten Mediterranean reefs. However, the information available is mainly qualitative and geographically unbalanced, and this knowledge gap prevents from quantitatively assessing the phenomenon in a way that could inform policy-makers in MSFD and IMAP implementation. Some areas resulted particularly poor in data and information, i.e., the southern Mediterranean (**Figure 2**), the Aegean-Levantine Sea (**Figure 7A**), and the Adriatic Sea subregions (**Figure 7D**). Thus, an effort should be made to fill these geographical gaps, in particular in the southern basins.

(2) Considering the widespread impact of ALDFG in biogenic reefs, the identification of high exposure risk areas (i.e., fishing grounds), the measure of the impact relating the abundance of litter with entangled target species, the probability of a species to be entangled (sensitivity), the fishing effort, the rates of lost fishing and by-catch are needed for the evaluation of the effects of marine litter on biota.

(3) On the seabed, some invertebrate taxa have a high risk of entanglement and may thus be good candidates for monitoring programs on the temporal and spatial variability of entanglements, giving the possibility to gain long-term data at all depths and significant observations *in situ*, in particular in areas of intense fishing activity, high density of litter, or high abundance of vulnerable species (Consoli et al., 2018; Galgani et al., 2018).

(4) To date, baseline litter abundance and the effects of marine litter on marine communities and its habitats remain poorly known (Maes et al., 2018) and probably underestimated (de Carvalho-Souza et al., 2018). Litter was present on the seafloor before specific scientific investigations started in the 1990s, and due to the persistence of some litter materials, the monitoring of litter should consider accumulation processes for past decades.

(5) The harmonization of methodologies and regular assessments through opportunistic approaches in long-term benthic biodiversity monitoring is essential to compare data and gain long-term support to the evaluation of accumulation and impacts. Moreover, the development of models on pathways for litter distribution and transfer could represent a useful instrument for tracking litter spread and impact (Galgani et al., 2019).

(6) Several actions are already set on to reduce litter impact, ranging from the removing of litter on the seafloor to the reduction of ALDFG through prevention and mitigation (FAO, 2016). However, to date, these initiatives are mainly limited to shallow waters. The high number of taxa and protected/vulnerable species impacted by marine litter in the Mediterranean Sea reefs, even in the deep sea, indicates that marine biodiversity is under threat. Thus, there is an urgency to implement effective management actions and enforce measures to reduce marine litter inputs.

(7) The impacted reef species are mainly vulnerable and slow-growing species, some of them protected at international levels. It is important to take into account their natural resilience, considering that they may need decades to recover (Clark et al., 2014). Moreover, more complete biodiversity inventories of their spatial distribution are essential to define conservation strategies (Clark et al., 2012; Bo et al., 2020). In particular, the establishment of a network of inshore and offshore protected areas (de Juan and Lleonart, 2010) and the identification of specific fishery restrictions (Bo et al., 2020) to preserve these hotspots of biodiversity and to improve the ecological status of the reef systems, is suggested. All these efforts should be strongly encouraged to develop prevention and mitigation approaches and increase awareness on this topic to preserve and conserve valuable and vulnerable marine ecosystems.

AUTHOR CONTRIBUTIONS

MA designed the study. MA and TF collected the data, wrote the manuscript, and gave the final approval for publication.

Both authors contributed to the article and approved the submitted version.

ACKNOWLEDGMENTS

We are very grateful to Aikaterini Anastasopoulou from the Hellenic Centre for Marine Research for helping in the bibliographic research and providing information and comments regarding the Aegean Sea. We would like to thank both reviewers for their insightful comments on the paper, as these comments led us to an improvement of the work.

SUPPLEMENTARY MATERIAL

The Supplementary Material for this article can be found online at: https://www.frontiersin.org/articles/10.3389/fmars.2020.581966/full#supplementary-material

REFERENCES

Anastasopoulou, A., and Fortibuoni, T. (2019). "Impact of plastic pollution on marine life in the Mediterranean Sea," in *Handbook of Environmental Chemistry*, eds F. Stock, G. Reifferscheid, N. Brennholt, and E. Kostianaia (Cham: Springer), 1–12. doi: 10.1007/698_2019_421

Andrady, A. L. (2015). "Persistence of plastic litter in the oceans," in *Marine Anthropogenic Litter*, eds M. Bergmann, M. Gutow, and L. Klages (Cham: Springer), 57–72. doi: 10.1007/978-3-319-16510-3

Angiolillo, M. (2019). "Debris in deep water," in *World Seas: an Environmental Evaluation*, 2nd Edn, ed. C. Sheppard (Cambridge, MA: Academic Press), 251–268. doi: 10.1016/B978-0-12-805052-1.00015-2

Angiolillo, M., and Canese, S. (2018). "Deep gorgonians and corals of the Mediterranean Sea," in *Corals in a Changing World*, eds C. Duque and E. T. Camacho (Rijeka: InTech). doi: 10.5772/intechopen.69686

Angiolillo, M., Lorenzo, B., Farcomeni, A., Bo, M., Bavestrello, G., Santangelo, G., et al. (2015). Distribution and assessment of marine debris in the deep Tyrrhenian Sea (NW Mediterranean Sea, Italy). *Mar. Pollut. Bull.* 92, 149–159. doi: 10.1016/j.marpolbul.2014.12.044

Angiolillo, M., and Pisapia, M. (2015). *Colori Profondi del Mediterraneo*. Roma: ISPRA.

Asoh, K., Yoshikawa, T., Kosaki, R., and Marschall, E. A. (2004). Damage to cauliflower coral by monofilament fishing lines in Hawaii. *Conserv. Biol.* 18, 1645–1650. doi: 10.1111/j.1523-1739.2004.00122.x

Avio, C. G., Gorbi, S., and Regoli, F. (2017). Plastics and microplastics in the oceans: from emerging pollutants to emerged threat. *Mar. Environ. Res.* 128, 2–11. doi: 10.1016/j.marenvres.2016.05.012

Ayaz, A., Acarli, D., Altinagac, U., Ozekinci, U., Kara, A., and Ozen, O. (2006). Ghost fishing by monofilament and multifilament gillnets in Izmir Bay, Turkey. *Fish. Res.* 79, 267–271. doi: 10.1016/j.fishres.2006.03.029

Ayaz, A., Ünal, V., Acarli, D., and Altinagac, U. (2010). Fishing gear losses in the Gökova Special Environmental Protection Area (SEPA), eastern Mediterranean, Turkey. *J. Appl. Ichthyol.* 26, 416–419. doi: 10.1111/j.1439-0426.2009.01386.x

Aymà, A., Aguzzi, J., Canals, M., Company, J. B., Lastras, G., Mecho, A., et al. (2019). "Occurrence of living cold-water corals at large depths within submarine canyons of the Northwestern Mediterranean Sea," in *Mediterranean Cold-Water Corals: Past, Present and Future*, ed. C. J. C. Orejas (Cham: Springer), 271–284. doi: 10.1007/978-3-319-91608-8_26

Ballesteros, E. (2006). Mediterranean coralligenous assemblages: a synthesis of present knowledge. *Oceanogr. Mar. Biol.* 44, 123–195.

Barnes, D. K. A., Galgani, F., Thompson, R. C., and Barlaz, M. (2009). Accumulation and fragmentation of plastic debris in global environments. *Philos. Trans. R. Soc. B* 364, 1985–1998. doi: 10.1098/rstb.2008.0205

Bavestrello, G., Cerrano, C., Zanzi, D., and Cattaneo-Vietti, R. (1997). Damage by fishing activities to the Gorgonian coral *Paramuricea clavata* in the Ligurian Sea. *Aquat. Conserv. Mar. Freshw. Ecosyst.* 7, 253–262.

Betti, F., Bavestrello, G., Bo, M., Ravanetti, G., Enrichetti, F., Coppari, M., et al. (2020). Evidences of fishing impact on the coastal gorgonian forests inside the Portofino MPA (NW Mediterranean Sea). *Ocean Coast. Manag.* 187:105105. doi: 10.1016/j.ocecoaman.2020.105105

Betti, F., Bavestrello, G., Fravega, L., Bo, M., Coppari, M., Enrichetti, F., et al. (2019). On the effects of recreational SCUBA diving on fragile benthic species: the Portofino MPA (NW Mediterranean Sea) case study. *Ocean Coast. Manag.* 182:104926. doi: 10.1016/j.ocecoaman.2019.104926

Bianchi, C. N. (1981). *Policheti Serpulidei. Guide per il Riconoscimento Delle specie Animali Delle Acque Lagunari e Costiere Italiane. AQ/1/96. 5*. Genova: Consiglio Nazionale delle Ricerche.

Bianchi, C. N., and Morri, C. (2000). Marine biodiversity of the Mediterranean Sea: situation, problems and prospects for future research. *Mar. Poll. Bull.* 40, 367–376. doi: 10.1016/S0025-326X(00)00027-8

Bo, M., Bava, S., Canese, S., Angiolillo, M., Cattaneo-Vietti, R., and Bavestrello, G. (2014). Fishing impact on deep Mediterranean rocky habitats as revealed by ROV investigation. *Biol. Conserv.* 171, 167–176. doi: 10.1016/j.biocon.2014.01.011

Bo, M., Bavestrello, G., Angiolillo, M., Calcagnile, L., Canese, S., Cannas, R., et al. (2015). Persistence of pristine deep-sea coral gardens in the Mediterranean Sea (SW Sardinia). *PLoS One* 10:e0119393. doi: 10.1371/journal.pone.0119393

Bo, M., Coppari, M., Betti, F., Massa, F., Gay, G., Cattaneo-Vietti, R., et al. (2020). Unveiling the deep biodiversity of the Janua Seamount (Ligurian Sea): first Mediterranean sighting of the rare Atlantic bamboo coral Chelidonisis aurantiaca Studer, 1890. *Deep Res. Part I Oceanogr. Res. Pap.* 156:103186. doi: 10.1016/j.dsr.2019.103186

Boudouresque, C. F. (2004). Marine biodiversity in the Mediterranean: status of species, populations and communities. *Sci. Rep. Port Cros Natl.* 20, 97–146.

Brown, J., and Macfadyen, G. (2007). Ghost fishing in European waters: impacts and management responses. *Mar. Policy* 31, 488–504. doi: 10.1016/j.marpol.2006.10.007

Butterworth, A., Clegg, I., and Bass, C. (2012). *Marine Debris: A Global Picture of the Impact on Animal Welfare and of Animal-Focused Solutions*. London: World Society for the Protection of Animals.

Carr, A. (1987). Impact of non degradable marine debris on the ecology and survival outlook of sea turtles. *Mar. Pollut. Bull.* 18, 352–356. doi: 10.1016/S0025-326X(87)80025-5

Cattaneo-Vietti, R., Bavestrello, G., Bo, M., Canese, S., Vigo, A., and Andaloro, F. (2017). Illegal ingegno fishery and conservation of deep red coral banks in the Sicily Channel (Mediterranean Sea). *Aquat. Conserv. Mar. Freshw. Ecosyst.* 27, 604–616. doi: 10.1002/aqc.2731

Chiappone, M., Dienes, H., Swanson, D. W., and Miller, S. L. (2005). Impacts of lost fishing gear on coral reef sessile invertebrates in the Florida Keys National Marine Sanctuary. *Biol. Conserv.* 121, 221–230. doi: 10.1016/j.biocon.2004.04.023

Chimienti, G., Bo, M., and Mastrototaro, F. (2018). Know the distribution to assess the changes: mediterranean cold-water coral bioconstructions. *Rend. Lincei Sci. Fis. Nat.* 29, 583–588. doi: 10.1007/s12210-018-0718-3

Chimienti, G., Bo, M., Taviani, M., and Mastrototaro, F. (2019). "Occurrence and biogeography of mediterranean cold-water corals," in *Mediterranean Cold-Water Corals: Past, Present and Future*, ed. C. J. C. Orejas (Springer International Publishing AG), 213–243. doi: 10.1007/978-3-319-91608-8_19

Chimienti, G., De Padova, D., Mossa, M., and Mastrototaro, F. (2020). A mesophotic black coral forest in the Adriatic Sea. *Sci. Rep.* 10:8504. doi: 10.1038/s41598-020-65266-9

Clark, M. R., Althaus, F., Schlacher, T. A., Williams, A., Bowden, D. A., and Rowden, A. A. (2016). The impacts of deep-sea fisheries on benthic communities: a review. *ICES J. Mar. Sci.* 73, i51–i69. doi: 10.1093/icesjms/fsv123

Clark, M. R., Rowden, A. A., Schlacher, T. A., Guinotte, J., Dunstan, P. K., Williams, A., et al. (2014). Identifying ecologically or biologically significant areas (EBSA): a systematic method and its application to seamounts in the south Pacific Ocean. *Ocean Coast Manag.* 91, 65–79. doi: 10.1016/j.ocecoaman.2014.01.016

Clark, M. R., Schlacher, T. A., Rowden, A. A., Stocks, K. I., and Consalvey, M. (2012). Science priorities for seamounts: research links to conservation and management. *PLoS One* 7:e29232. doi: 10.1371/journal.pone.0029232

Coll, M., Piroddi, C., Steenbeek, J., Kaschner, K., Ben Rais Lasram, F., Aguzzi, J., et al. (2010)). The Biodiversity of the Mediterranean Sea: estimates, Patterns, and Threats. *PLoS One* 5:e11842. doi: 10.1371/journal.pone.0011842

Consoli, P., Andaloro, F., Altobelli, C., Battaglia, P., Campagnuolo, S., Canese, S., et al. (2018). Marine litter in an EBSA (Ecologically or Biologically Significant Area) of the central Mediterranean Sea: abundance, composition, impact on benthic species and basis for monitoring entanglement. *Environ. Pollut.* 236, 405–415. doi: 10.1016/j.envpol.2018.01.097

Consoli, P., Scotti, G., Romeo, T., Cristina, M., Esposito, V., Alessandro, M. D., et al. (2019). Characterization of seafloor litter on Mediterranean shallow coastal waters: evidence from Dive Against Debris®, a citizen science monitoring approach. *Mar. Pollut. Bull.* 150:110763. doi: 10.1016/j.marpolbul.2019.110763

Corcoran, P. L., Moore, C. J., and Jazvac, K. (2014). An anthropogenic marker horizon in the future rock record. *GSA Today* 24, 4–8. doi: 10.1130/GSATG198A.1

Costello, M. J., Coll, M., Danovaro, R., Halpin, P., Ojaveer, H., and Miloslavich, P. (2010). A census of marine biodiversity knowledge, resources, and future challenges. *PLoS One* 5:e12110. doi: 10.1371/journal.pone.001211

Criddle, K. R., Amos, A. F., Carroll, P., Coe, J. M., Donohue, M. J., Harris, J. H., et al. (2009). *Tackling Marine Debris in the 21st Century*. Washington DC: The National Academies Press.

Davies, J. S., Guillaumont, B., Tempera, F., Vertino, A., Beuck, L., Ólafsdóttir, S. H., et al. (2017). A new classification scheme of European cold-water coral habitats: implications for ecosystem-based management of the deep sea. *Deep Sea Res. Part II Top. Stud. Oceanogr.* 145, 102–109. doi: 10.1016/j.dsr2.2017.04.014

de Carvalho-Souza, G. F., Llope, M., Tinôco, M. S., Medeiros, D. V., Maia-Nogueira, R., and Sampaio, C. L. S. (2018). Marine litter disrupts ecological processes in reef systems. *Mar. Pollut. Bull.* 133, 464–471. doi: 10.1016/j.marpolbul.2018.05.049

de Juan, S., and Lleonart, J. (2010). A conceptual framework for the protection of vulnerable habitats impacted by fishing activities in the Mediterranean high seas. *Ocean Coast Manag.* 53, 717–723. doi: 10.1016/j.ocecoaman.2010.10.005

Deidun, A., Andaloro, F., Bavestrello, G., Canese, S., Consoli, P., Micallef, A., et al. (2015). First characterisation of a *Leiopathes glaberrima* (Cnidaria: Anthozoa: Antipatharia) forest in Maltese exploited fishing grounds. *Ital. J. Zool.* 82, 271–280. doi: 10.1080/11250003.2014.986544

Deudero, S., and Alomar, C. (2015). Mediterranean marine biodiversity under threat: reviewing influence of marine litter on species. *Mar. Pollut. Bull.* 98, 58–68. doi: 10.1016/j.marpolbul.2015.07.012

Di Camillo, C. G., Ponti, M., Bavestrello, G., Krzelj, M., and Cerrano, C. (2018). Building a baseline for habitat-forming corals by a multi-source approach, including Web Ecological Knowledge. *Biodivers. Conserv.* 27, 1257–1276. doi: 10.1007/s10531-017-1492-8

D'Onghia, G., Calculli, C., Capezzuto, F., Carlucci, R., Carluccio, A., Grehan, A., et al. (2017). Anthropogenic impact in the Santa Maria di Leuca cold-water coral province (Mediterranean Sea): observations and conservation straits. *Deep Sea Res. Part II Top. Stud. Oceanogr.* 145, 87–101. doi: 10.1016/j.dsr2.2016.02.012

D'Onghia, G., Capezzuto, F., Cardone, F., Carlucci, R., Carluccio, A., Chimienti, G., et al. (2015). Macro- and megafauna recorded in the submarine Bari Canyon (southern Adriatic, Mediterranean Sea) using different tools. *Medit. Mar. Sci.* 16, 180–196. doi: 10.12681/mms.1082

D'Onghia, G., Maiorano, P., Sion, L., Giove, A., Capezzuto, F., Carlucci, R., et al. (2010). Effects of deep-water coral banks on the abundance and size structure of the megafauna in the Mediterranean Sea. *Deep Sea Res. II* 57, 397–411. doi: 10.1016/j.dsr2.2009.08.022

Enrichetti, F., Bava, S., Bavestrello, G., Betti, F., Lanteri, L., and Bo, M. (2019). Artisanal fishing impact on deep coralligenous animal forests: a Mediterranean case study of marine vulnerability. *Ocean Coast. Manag.* 177, 112–126. doi: 10.1016/j.ocecoaman.2019.04.021

Enrichetti, F., Dominguez-Carrió, C., Toma, M., Bavestrello, G., Canese, S., and Bo, M. (2020). Assessment and distribution of seafloor litter on the deep Ligurian continental shelf and shelf break (NW Mediterranean Sea). *Mar. Pollut. Bull.* 151:110872. doi: 10.1016/j.marpolbul.2019.110872

Erzini, K. (1997). An experimental study of gill net and trammel net "ghost fishing" off the Algarve (southern Portugal). *Mar. Ecol. Prog. Ser.* 158, 257–265. doi: 10.3354/meps158257

Erzini, K., Bentes, L., Coelho, R., Lino, P. G., Monteiro, P., Ribeiro, J., et al. (2008). Catches in ghost-fishing octopus and fish traps in the northeastern Atlantic Ocean (Algarve, Portugal). *Fish. Bull.* 106, 321–327.

Erzini, K., Monteiro, C. C., Ribeiro, J., Santos, M. N., Gaspar, M., Monteiro, P., et al. (1997). An experimental study of gill net and trammel net "ghost fishing" off the Algarve (southern Portugal). *Mar. Ecol. Prog. Ser.* 158, 257–265. doi: 10.3354/meps158257

Fabri, M. C., Pedel, L., Beuck, L., Galgani, F., Hebbeln, D., Freiwald, A., et al. (2014). Megafauna of vulnerable marine ecosystems in French Mediterranean submarine canyons: spatial distribution and anthropogenic impacts. *Deep Res. Part II Top. Stud. Oceanogr.* 104, 184–207. doi: 10.1016/j.dsr2.2013.06.016

Falace, A., Kaleb, S., Curiel, D., Miotti, C., Galli, G., Querin, S., et al. (2015). Calcareous bio-concretions in the Northern Adriatic Sea: habitat types, environmental factors that influence Habitat distributions, and predictive modeling. *PLoS One* 10:e0140931. doi: 10.1371/journal.pone.0140931

FAO (2016). *Abandoned, Lost and Discarded Gillnets and Trammel Nets: Methods to Estimate Ghost Fishing Mortality, and the Status of Regional Monitoring and Management, by Eric Gilman, Francis Chopin, Petri Suuronen and Blaise Kuemlangan. FAO Fisheries and Aquaculture Technical Paper No.* 600. Rome: FAO.

Fortibuoni, T., Ronchi, F., Mačić, V., Mandić, M., Mazziotti, C., Peterlin, M., et al. (2019). A harmonized and coordinated assessment of the abundance and composition of seafloor litter in the Adriatic-Ionian macroregion (Mediterranean Sea). *Mar. Pollut. Bull.* 139, 412–426. doi: 10.1016/j.marpolbul.2019.01.017

Fosså, J. H., Mortensen, P. B., and Furevik, D. M. (2002). The deep-water coral *Lophelia pertusa* in Norwegian waters: distribution and fishery impacts. *Hydrobiologia* 471, 1–12. doi: 10.1023/A:1016504430684

Freiwald, A., Beuck, L., Ruggeberg, A., Taviani, M., and Hebbeln, D. (2009). The white coral community in the central Mediterranean sea revealed by ROV surveys. *Oceanography* 22, 58–74.

Freiwald, A., Rogers, A., Hall-Spencer, J., Guinotte, J. M., Davies, A. J., et al. (2017). *Global Distribution of Cold-Water Corals (version 5.0). Fifth Update to the Dataset in Freiwald et al. (2004) by UNEP-WCMC, in Collaboration with Andre Freiwald and John Guinotte*. Cambridge: UN Environment World Conservation Monitoring Centre.

Galgani, F., Hanke, G., and Maes, T. (2015). "Global distribution, composition and abundance of marine litter," in *Marine anthropogenic Litter*, eds M. Bergmann, L. Gutow, and M. Klages (Berlin: Springer Open), 29–56.

Galgani, F., Hanke, G., Werner, S., and De Vrees, L. (2013). Marine litter within the European Marine Strategy Framework Directive. *ICES J. Mar. Sci.* 70, 1055–1064. doi: 10.1093/icesjms/fst122

Galgani, F., Leaute, J. P., Moguedet, P., Souplet, A., Verin, Y., Carpentier, A., et al. (2000). Litter on the sea floor along European coasts. *Mar. Pollut. Bull.* 40, 516–527. doi: 10.1016/S0025-326X(99)00234-9

Galgani, F., Pham, C. K., Claro, F., and Consoli, P. (2018). Marine animal forests as useful indicators of entanglement by marine litter. *Mar. Pollut. Bull.* 135, 735–738. doi: 10.1016/j.marpolbul.2018.08.004

Galgani, F., Souplet, A., and Cadiou, Y. (1996). Accumulation of debris on the deep sea floor off the French Mediterranean coast. *Mar. Ecol. Ser.* 142, 225–234. doi: 10.3354/meps142225

Galgani, L., Beiras, R., Galgani, F., Panti, C., and Borja, A. (2019). Editorial: "impacts of marine litter.". *Front. Mar. Sci.* 6:208. doi: 10.3389/fmars.2019.00208

Gall, S. C., and Thompson, R. C. (2015). The impact of debris on marine life. *Mar. Pollut. Bull.* 92, 170–179. doi: 10.1016/j.marpolbul.2014.12.041

Garrabou, J., and Ballesteros, E. (2000). Growth of Mesophyllum alternans and *Lithophyllum frondosum* (Corallinales, Rhodophyta) in the northwestern Mediterranean. *Eur. J. Phycol.* 35, 1–10. doi: 10.1080/09670260010001735571

Giakoumi, S., Sini, M., Gerovasileiou, V., Mazor, T., Beher, J., Possingham, H. P., et al. (2013). Ecoregion-based conservation planning in the mediterranean:

dealing with large-scale heterogeneity. *PLoS One* 8:e76449. doi: 10.1371/journal.pone.0076449

Gilardi, K. V. K., Carlson-Bremer, D., June, J. A., Antonelis, K., Broadhurst, G., and Cowan, T. (2010). Marine species mortality in derelict fishing nets in Puget Sound, WA and the cost/benefits of derelict net removal. *Mar. Pollut. Bull.* 60, 376–382. doi: 10.1016/j.marpolbul.2009.10.016

Gilman, E. (2015). Status of international monitoring and management of abandoned, lost and discarded fishing gear and ghost fishing. *Mar. Policy* 60, 225–239. doi: 10.1016/j.marpol.2015.06.016

Gilman, E., Chopin, F., Suuronen, P., and Kuemlangan, B. (2016). *Abandoned, Lost and Discarded Gillnets and Trammel Nets. Methods to Estimate Ghost Fishing Mortality, and Status of Regional Monitoring and Management. FAO Fisheries and Aquaculture Technical Paper 600*. Rome: Food and Agriculture Organization of the United Nations, 79.

Giusti, M., Canese, S., Fourt, M., Bo, M., Innocenti, C., Goujard, A., et al. (2019). Coral forests and Derelict Fishing Gears in submarine canyon systems of the Ligurian Sea. *Prog. Oceanogr.* 178:102186. doi: 10.1016/j.pocean.2019.102186

Goffredo, S., Caroselli, E., Gasparini, G., Marconi, G., Putignano, M. T., Pazzini, C., et al. (2011). Colony and polyp biometry and size structure in the orange coral *Astroides calycularis* (Scleractinia: Dendrophylliidae). *Mar. Biol. Res.* 7, 272–280. doi: 10.1080/17451000.2010.492222

Good, T. P., June, J. A., Etnier, M. A., and Broadhurst, G. (2010). Derelict fishing nets in Puget Sound and the Northwest Straits: patterns and threats to marine fauna. *Mar. Pollut. Bull.* 60, 39–50. doi: 10.1016/j.marpolbul.2009.09.005

Gregory, M. R. (2009). Environmental implications of plastic debris in marine settings—entanglement, ingestion, smothering, hangers-on, hitch-hiking and alien invasions. *Philos. Trans. R. Soc. B Biol. Sci.* 364, 2013–2025. doi: 10.1098/rstb.2008.0265

Hall, N. M., Berry, K. L. E., Rintoul, L., and Hoogenboom, M. O. (2015). Microplastic ingestion by scleractinian corals. *Mar. Biol.* 162, 725–732. doi: 10.1007/s00227-015-2619-7

Harmelin, J.-G., and Marinopoulos, J. (1994). Population structure and partial mortality of the gorgonian *Paramuricea clavata* (Risso) in the northwestern Mediterranean (France, Port-Cros Island). *Mar. Life* 4, 5–13.

Hess, N. A., Ribic, C. A., and Vining, I. (1999). Benthic marine debris, with an emphasis on fishery-related items, surrounding Kodiak Island, Alaska, 1994-1996. *Mar. Pollut. Bull.* 38, 885–890. doi: 10.1016/S0025-326X(99)00087-9

Houard, T., Boudouresque, C. F., Barcelo, A., Cottalorda, J., Formentin, J., Jullian, E., et al. (2012). Occurrence of a lost fishing net within the marine area of the Port-Cros National Park (Provence, northwestern Mediterranean Sea). *Sci. Rep. Port Cros Natl.* 118, 109–118.

Ingrosso, G., Abbiati, M., Badalamenti, F., Bavestrello, G., Belmonte, G., Cannas, R., et al. (2018). Mediterranean Bioconstructions along the Italian Coast. *Adv. Mar. Biol.* 79, 61–136. doi: 10.1016/bs.amb.2018.05.001

Ioakeimidis, C., Fotopoulou, K. N., Karapanagioti, H. K., Geraga, M., Zeri, C., Papathanassiou, E., et al. (2016). The degradation potential of PET bottles in the marine environment: an ATR-FTIR based approach. *Sci. Rep.* 6:23501. doi: 10.1038/srep23501

Ioakeimidis, C., Papatheodorou, G., Fermeli, G., Streftaris, N., and Papathanassiou, E. (2015). Use of ROV for assessing marine litter on the seafloor of Saronikos Gulf (Greece): a way to fill data gaps and deliver environmental education. *Springerplus* 4:463. doi: 10.1186/s40064-015-1248-4

Jambeck, J. R., Geyer, R., Wilcox, C., Siegler, T. R., Perryman, M., Andrady, A., et al. (2015). Plastic waste inputs from land into the ocean. *Science* 347, 768–771. doi: 10.1126/science.1260352

Katsanevakis, S., and Issaris, Y. (2010). Impact of marine litter on sea life: a review. *Rapp. Comm. Int. Mer. Médit.* 557.

Keller, A. A., Fruh, E. L., Johnson, M. M., Simon, V., and McGourty, C. (2010). Distribution and abundance of anthropogenic marine debris along the shelf and slope of the US West Coast. *Mar. Pollut. Bull.* 60, 692–700. doi: 10.1016/j.marpolbul.2009.12.006

Kipson, S., Linares, C., Čižmek, H., Cebrián, E., Ballesteros, E., Bakran-Petricioli, T., et al. (2015). Population structure and conservation status of the red gorgonian *Paramuricea clavata* (Risso, 1826) in the Eastern Adriatic Sea. *Mar. Ecol.* 36, 982–993. doi: 10.1111/maec.12195

Koutsodendris, A., Papatheodorou, G., Kougiourouki, O., and Georgiadis, M. (2008). Benthic marine litter in four Gulfs in Greece, Eastern Mediterranean; abundance, composition and source identification. *Estuar. Coast. Shelf Sci.* 77, 501–512. doi: 10.1016/j.ecss.2007.10.011

Kroodsma, D. A., Mayorga, J., Hochberg, T., Miller, N. A., Boerder, K., Ferretti, F., et al. (2018). Tracking the global footprint of fisheries. *Science* 359, 904–908. doi: 10.1126/science.aao5646

Kühn, S., Bravo Rebolledo, E. L., and van Franeker, J. A. (2015). "Deleterious effects of litter on marine life," in *Marine Anthropogenic Litter*, eds M. Bergmann, L. Gutow, and M. Klages (Cham: Springer), 75–116. doi: 10.1007/978-3-319-16510-3_4

Laist, D. W. (1997). "Impacts of marine debris: entanglement of marine life in marine debris including a comprehensive list of species with entanglement and ingestion records," in *Marine Debris Sources, Impacts and Solutions*, eds J. M. Coe and D. B. Rogers (New York, NY: Springer), 99–413. doi: 10.1007/978-1-4613-8486-1

Lamb, J. B., Willis, B. L., Fiorenza, E. A., Couch, C. S., Howard, R., Rader, D. N., et al. (2018). Plastic waste associated with disease on coral reefs. *Science* 359, 460–462. doi: 10.1126/science.aar3320

Lee, D. I., Cho, H. S., and Jeong, S. B. (2006). Distribution characteristics of marine litter on the sea bed of the East China Sea and the South Sea of Korea. *Estuar. Coast. Shelf Sci.* 70, 187–194. doi: 10.1016/j.ecss.2006.06.003

Li, W. C., Tse, H. F., and Fok, L. (2016). Plastic waste in the marine environment: a review of sources, occurrence and effects. *Sci. Total Environ.* 566–567, 333–349. doi: 10.1016/j.scitotenv.2016.05.084

Lo Iacono, C., Robert, K., Gonzalez-Villanueva, R., Gori, A., Gili, J. M., and Orejas, C. (2018). Predicting cold-water coral distribution in the Cap de Creus Canyon (NW Mediterranean): implications for marine conservation planning. *Prog. Oceanogr.* 169, 169–180. doi: 10.1016/j.pocean.2018.02.012

Ma, Y., Halsall, C. J., Crosse, J. D., Graf, C., Cai, M., He, J., et al. (2015). Persistent organic pollutants in ocean sediments from the North Pacific to the Arctic Ocean. *J. Geophys. Res. Oceans* 120, 2723–2735.

MacDonald, D. S., Little, M., Eno, N. C., and Hiscock, K. (1996). Disturbance of benthic species by fishing activities: a sensitivity index. *Aquat. Conserv. Mar. Freshw. Ecosyst.* 6, 257–268.

Macfadyen, G., Huntington, T., and Cappell, R. (2009). *Abandoned, Lost or Otherwise Discarded Fishing Gear. UNEP Regional Seas Reports and Studies No.185; FAO Fisheries and Aquaculture Technical Paper, No. 523*. Rome: FAO.

Madurell, T., Orejas, C., Requena, S., Gori, A., Purroy, A., Lo Iacono, C., et al. (2012). "The benthic communities of the Cap de Creus canyon," in *Mediterranean Submarine Canyons: Ecology and Governance*, eds M. Würtz, et al. (Gland: IUCN), 123–132.

Maes, T., Barry, J., Leslie, H. A., Vethaak, A. D., Nicolaus, E. E. M., Law, R. J., et al. (2018). Below the surface: twenty-five years of seafloor litter monitoring in coastal seas of North West Europe (1992–2017). *Sci. Total Environ.* 630, 790–798. doi: 10.1016/j.scitotenv.2018.02.245

Maes, T., Perry, J., Aliji, K., Clarke, C., and Birchenough, S. N. R. (2019). Shades of grey: marine litter research developments in Europe. *Mar. Pollut. Bull.* 146, 274–281. doi: 10.1016/j.marpolbul.2019.06.019

Maldonado, M., Aguilar, R., Blanco, J., García, S., Serrano, A., and Punzón, A. (2015). Aggregated clumps of lithistid sponges: A singular, reef-like bathyal habitat with relevant paleontological connections. *PLoS One* 10:e0125378. doi: 10.1371/journal.pone.0125378

Maldonado, M., López-Acosta, M., Sánchez-Tocino, L., and Sitjá, C. (2013). The rare, giant gorgonian *Ellisella paraplexauroides*: demographics and conservation concerns. *Mar. Ecol. Progr. Ser.* 479, 127–141. doi: 10.3354/meps10172

Mastrototaro, F., D'Onghia, G., Corriero, G., Matarrese, A., Maiorano, P., Panetta, P., et al. (2010). Biodiversity of the white coral bank off Cape Santa Maria di Leuca (*Mediterranean Sea*): An update. *Deep Sea Res. Part II Top. Stud. Oceanogr.* 57, 412–430. doi: 10.1016/j.dsr2.2009.08.021

Melli, V., Angiolillo, M., Ronchi, F., Canese, S., Giovanardi, O., Querin, S., et al. (2017). The first assessment of marine debris in a Site of Community Importance in the north-western Adriatic Sea (*Mediterranean Sea*). *Mar. Pollut. Bull.* 114, 821–830. doi: 10.1016/j.marpolbul.2016.11.012

Matsuoka, K., Nakashima, T., and Nagasawa, N. (2005). A review of ghost fishing: scientific approaches to evaluation and solutions. *Fish. Sci.* 71, 691–702. doi: 10.1111/j.1444-2906.2005.01019.x

Mecho, A., Aguzzi, J., De Mol, B., Lastras, G., Ramirez-Llodra, E., Bahamon, N., et al. (2018). Visual faunistic exploration of geomorphological human-impacted

deep-sea areas of the north-western Mediterranean Sea. *J. Mar. Biol. Assoc. U.K.* 98, 1241–1252. doi: 10.1017/S0025315417000431

Micheli, F., Halpern, B. S., Walbridge, S., Ciriaco, S., Ferretti, F., Fraschetti, S., et al. (2013). Cumulative human impacts on Mediterranean and Black Sea marine ecosystems: assessing current pressures and opportunities. *PLoS One* 8:e79889. doi: 10.1371/journal.pone.0079889

Miyake, H., Shibata, H., and Furushima, Y. (2011). "Deep-sea litter study using deep-sea observation tools," in *Interdisciplinary Studies on Environmental Chemistry-Marine Environmental Modeling & Analysis*, eds K. Omori, X. Guo, N. Yoshie, N. Fujii I, C. Handoh, A. Isobe, et al. (Setagaya-ku: TERRAPUB).

Moccia, D., Cau, A., Alvito, A., Canese, S., Cannas, R., Bo, M., et al. (2019). New sites expanding the "Sardinian cold-water coral province" extension: a new potential cold-water coral network? *Aquat. Conserv. Mar. Freshw. Ecosyst.* 29, 153–160. doi: 10.1002/aqc.2975

Molina Jack, M. E., Chaves Montero, M., del, M., Galgani, F., Giorgetti, A., Vinci, M., et al. (2019). EMODnet marine litter data management at pan-European scale. *Ocean Coast. Manag.* 181:104930. doi: 10.1016/j.ocecoaman.2019.104930

Moore, C. J. (2008). Synthetic polymers in the marine environment: a rapidly increasing, long-term threat. *Environ. Res.* 108, 131–139. doi: 10.1016/j.envres.2008.07.025

Moore, S. L., and Allen, M. J. (2000). Distribution of anthropogenic and natural debris on the mainland shelf of the Southern California Bight. *Mar. Pollut. Bull.* 40, 83–88. doi: 10.1016/S0025-326X(99)00175-7

Morand, S., and Lajaunie, C. (2018). "A brief history on the links between health and biodiversity," in *Biodiversity and Health*, 1st Edn, eds S. Morand and C. Lajaunie (London: Iste Press), 1–14. doi: 10.1016/b978-1-78548-115-4.50001-9

Moschino, V., Riccato, F., Fiorin, R., Nesto, N., Picone, M., Boldrin, A., et al. (2019). Is derelict fishing gear impacting the biodiversity of the Northern Adriatic Sea? An answer from unique biogenic reefs. *Sci. Total Environ.* 663, 387–399. doi: 10.1016/j.scitotenv.2019.01.363

Mytilineou, C., Smith, C. J., Anastasopoulou, A., Papadopoulou, K. N., Christidis, G., Bekas, P., et al. (2014). New cold-water coral occurrences in the Eastern Ionian Sea: results from experimental long line fishing. *Deep Sea Res. Part II Top. Stud. Oceanogr.* 99, 146–157. doi: 10.1016/j.dsr2.2013.07.007

Neves, D., Sobral, P., Ferreira, J. L., and Pereira, T. (2015). Ingestion of microplastics by commercial fish off the Portuguese coast. *Mar. Pollut. Bull.* 101, 119–126. doi: 10.1016/j.marpolbul.2015.11.008

NOAA (2014). *Report on the Entanglement of Marine Species in Marine Debris with an Emphasis on Species in the United States*. Available online at: www.MarineDebris.noaa.gov (accessed March 5, 2020).

Orejas, C., Gori, A., Lo Iacono, C., Puig, P., Gili, J. M., and Dale, M. R. T. (2009). Cold-water corals in the Cap de Creus canyon, northwestern Mediterranean: spatial distribution, density and anthropogenic impact. *Mar. Ecol. Prog. Ser.* 397, 37–51. doi: 10.3354/meps08314

Pasquini, G., Ronchi, F., Strafella, P., Scarcella, G., and Fortibuoni, T. (2016). Seabed litter composition, distribution and sources in the Northern and Central Adriatic Sea (Mediterranean). *Waste Manag.* 58, 41–51. doi: 10.1016/j.wasman.2016.08.038

Piazzi, L., Gennaro, P., and Balata, D. (2012). Threats to macroalgal coralligenous assemblages in the Mediterranean Sea. *Mar. Pollut. Bull.* 64, 2623–2629. doi: 10.1016/j.marpolbul.2012.07.027

Pierdomenico, M., Cardone, F., Carluccio, A., Casalbore, D., Chiocci, F., Maiorano, P., et al. (2019). Megafauna distribution along active submarine canyons of the central Mediterranean: relationships with environmental variables. *Prog. Oceanogr.* 171, 49–69. doi: 10.1016/j.pocean.2018.12.015

Pierdomenico, M., Russo, T., Ambroso, S., Gori, A., Martorelli, E., D'Andrea, L., et al. (2018). Effects of trawling activity on the bamboo-coral Isidella elongata and the sea pen Funiculina quadrangularis along the Gioia Canyon (Western Mediterranean, southern Tyrrhenian Sea). *Prog. Oceanogr.* 169, 214–226. doi: 10.1016/j.pocean.2018.02.019

Ramírez, F., Coll, M., Navarro, J., Bustamante, J., and Green, A. J. (2018). Spatial congruence between multiple stressors in the Mediterranean Sea may reduce its resilience to climate impacts. *Sci. Rep.* 8:14871. doi: 10.1038/s41598-018-33237-w

Ramirez-Llodra, E., De Mol, B., Company, J. B., Coll, M., and Sardà, F. (2013). Effects of natural and anthropogenic processes in the distribution of marine litter in the deep Mediterranean Sea. *Prog. Oceanogr.* 118, 273–287. doi: 10.1016/j.pocean.2013.07.027

Ramirez-Llodra, E., Tyler, P. A., Baker, M. C., Bergstad, O. A., Clark, M. R., Escobar, E., et al. (2011). Man and the Last Great Wilderness: human Impact on the Deep Sea. *PLoS One* 6:e22588. doi: 10.1371/journal.pone.0022588

Richardson, K., Asmutis-Silvia, R., Drinkwin, J., Gilardi, K. V. K., Giskes, I., Jones, G., et al. (2019). Building evidence around ghost gear: global trends and analysis for sustainable solutions at scale. *Mar. Pollut. Bull.* 138, 222–229. doi: 10.1016/j.marpolbul.2018.11.031

Richardson, K., Gunn, R., Wilcox, C., and Hardesty, B. D. (2018). Understanding causes of gear loss provides a sound basis for fisheries management. *Mar. Policy* 96, 278–284. doi: 10.1016/j.marpol.2018.02.021

Ronchi, F., Galgani, F., Binda, F., Mandić, M., Peterlin, M., Tutman, P., et al. (2019). Fishing for Litter in the Adriatic-Ionian macroregion (Mediterranean Sea): strengths, weaknesses, opportunities and threats. *Mar. Policy* 100, 226–237. doi: 10.1016/j.marpol.2018.11.041

Rossi, S. (2013). The destruction of the "animal forests" in the oceans: towards an over-simplification of the benthic ecosystems. *Ocean Coast. Manag.* 84, 77–85. doi: 10.1016/j.ocecoaman.2013.07.004

Rossi, S., Bramanti, L., Gori, A., and Orejas, C. (2017). "An overview of the animal forests of the world," in *Marine Animal Forests, The Ecology of Benthic Biodiversity Hotspots*, eds S. Rossi, L. Bramanti, A. Gori, and C. Orejas (Cham: Springer), 1–26. doi: 10.1007/978-3-319-17001-5_1-1

Rosso, A., Vertino, A., Di Geronimo, I., Sanfilippo, R., Sciuto, F., Di Geronimo, R., et al. (2010). Hard- and soft-bottom thanatofacies from the Santa Maria di Leuca deep-water coral province, Mediterranean. *Deep Sea Res.* 57, 360–379. doi: 10.1016/j.dsr2.2009.08.024

Saldanha, H. J., Sancho, G., Santos, M. N., Puente, E., Gaspar, M. B., Bilbao, A., et al. (2003). The use of biofouling for ageing lost nets: a case study. *Fish. Res.* 64, 141–150. doi: 10.1016/S0165-7836(03)00213-3

Salomidi, M., Smith, C., Katsanevakis, S., and Panayotidis, P. (2009). "Some observations on the structure and distribution of gorgonian assemblages in the Eastern Mediterranean Sea," in *Proceedings of the 1er Symposium sur la Conservation du Coralligène et autres bio concrétions de Méditerranée*, Tabarka, 16–17.

Sampaio, I., Braga-Henriques, A., Pham, C., Ocaña, O., De Matos, V., Morato, T., et al. (2012). Cold-water corals landed by bottom longline fisheries in the Azores (north-eastern Atlantic). *J. Mar. Biol. Assoc. U.K.* 92, 1547–1555. doi: 10.1017/S0025315412000045

Sánchez, P., Masó, M., Sáez, R., De Juan, S., Muntadas, A., and Demestre, M. (2013). Baseline study of the distribution of marine debris on soft-bottom habitats associated with trawling grounds in the northern Mediterranean. *Sci. Mar.* 77, 247–255. doi: 10.3989/scimar03702.10A

Savini, A., Vertino, A., Marchese, F., Beuck, L., and Freiwald, A. (2014). Mapping cold-water coral habitats at different scales within the Northern Ionian Sea (central Mediterranean): an assessment of coral coverage and associated vulnerability. *PLoS One* 9:e87108. doi: 10.1371/journal.pone.0087108

Sbrescia, L., Di Stefano, F., Russo, M., and Russo, G. F. (2008). Influence of sport fishing on gorgonians in MPA of Punta Campanella. *Biol. Mar. Mediterr.* 15, 172–173.

Sheehan, E., Rees, A., Bridger, D., Williams, T., and Hall-Spencer, J. M. (2017). Strandings of NE Atlantic gorgonians. *Biol. Conserv.* 209 482–487. doi: 10.1016/j.biocon.2017.03.020

Spedicato, M. T., Zupa, W., Carbonara, P., Fiorentino, F., Follesa, M. C., Galgani, F., et al. (2019). Spatial distribution of marine macro-litter on the seafloor in the northern Mediterranean Sea: the MEDITS initiative. *Sci. Mar.* 83, 257–270. doi: 10.3989/scimar.04987.14A

Spengler, A., and Costa, M. F. (2008). Methods applied in studies of benthic marine debris. *Mar. Pollut. Bull.* 56, 226–230. doi: 10.1016/j.marpolbul.2007.09.040

Stefatos, A., Charalampakis, M., Papatheodorou, G., and Ferentinos, G. (1999). Marine debris on the seafloor of the Mediterranean Sea: examples from two enclosed gulfs in Western Greece. *Mar. Pollut. Bull.* 38, 389–393. doi: 10.1016/S0025-326X(98)00141-6

Taviani, M., Angeletti, L., Canese, S., Cannas, R., Cardone, F., Cau, A. B., et al. (2017). The "Sardinian cold-water coral province" in the context of the Mediterranean coral ecosystems. *Deep Sea Res. Part II Top. Stud. Oceanogr.* 145, 61–78. doi: 10.1016/j.dsr2.2015.12.008

Terrón-Sigler, A. (2015). *Conservation Biology of the Endangered Orange Coral Astroides Calycularis*. [Ph.D. thesis]. Seville: The University of Seville.

Thompson, R. C., Olsen, Y., Mitchell, R. P., Davis, A., Rowland, S. J., John, A. W. G., et al. (2004). Lost at sea: Where is all the plastic? *Science* 304:838. doi: 10.1126/science.1094559

Tosi, L., Zecchin, M., Franchi, F., Bergamasco, A., Da Lio, C., Baradello, L., et al. (2017). Paleochannel and beach-bar palimpsest topography as initial substrate for coralligenous buildups offshore Venice, Italy. *Sci. Rep.* 7:1321. doi: 10.1038/s41598-017-01483-z

Tsounis, G., Martinez, L., Bramanti, L., Viladrich, N., Gili, J. M., Martinez, Á, et al. (2012). Anthropogenic effects on reproductive effort and allocation of energy reserves in the Mediterranean octocoral *Paramuricea clavata*. *Mar. Ecol. Prog. Ser.* 449, 161–172. doi: 10.3354/meps09521

Tubau, X., Canals, M., Lastras, G., Rayo, X., Rivera, J., and Amblas, D. (2015). Marine litter on the floor of deep submarine canyons of the Northwestern Mediterranean Sea: the role of hydrodynamic processes. *Prog. Oceanogr.* 134, 379–403. doi: 10.1016/j.pocean.2015.03.013

Tursi, A., Mastrototaro, F., Matarrese, A., Maiorano, P., and D'Onghia, G. (2004). Biodiversity of the white coral reefs in the Ionian Sea (Central Mediterranean). *Chem. Ecol.* 20(Suppl.), 107–116. doi: 10.1080/02757540310001629170

UNEP (2009). *Marine Litter: A Global Challenge*. Nairobi: UNEP.

UNEP (2015). *Marine Litter Assessment in the Mediterranean*. Athens: UNEP.

UNEP/MAP, and SPA/RAC (2018). *Defining the most representative species for IMAP Candidate Indicator 24*. Tunis: UNEP.

Valisano, L., Palma, M., Pantaleo, U., Calcinai, B., and Cerrano, C. (2019). Characterization of North-Western Mediterranean coralligenous assemblages by video surveys and evaluation of their structural complexity. *Mar. Pollut. Bull.* 148, 134–148. doi: 10.1016/j.marpolbul.2019.07.012

Vieira, R. P., Raposo, I. P., Sobral, P., Gonçalves, J. M. S., Bell, K. L. C., and Cunha, M. R. (2015). Lost fishing gear and litter at Gorringe Bank (NE Atlantic). *J. Sea Res.* 100, 91–98. doi: 10.1016/j.seares.2014.10.005

Watters, D. L., Yoklavich, M. M., Love, M. S., and Schrodeder, D. M. (2010). Assessing marine debris in deep seafloor habitats off California. *Mar. Pollut. Bull.* 60, 131–138. doi: 10.1016/j.marpolbul.2009.08.019

Worm, B., Lotze, H. K., Jubinville, I., Wilcox, C., and Jambeck, J. (2017). Plastic as a persistent marine pollutant. *Annu. Rev. Environ. Resour.* 42, 1–26. doi: 10.1146/annurev-environ-102016-060700

Yoshikawa, T., and Asoh, K. (2004). Entanglement of monofilament fishing lines and coral death. *Biol. Conserv.* 117, 557–560. doi: 10.1016/j.biocon.2003.09.025

Conflict of Interest: The authors declare that the research was conducted in the absence of any commercial or financial relationships that could be construed as a potential conflict of interest.

frontiers in Marine Science

ORIGINAL RESEARCH
published: 08 October 2020
doi: 10.3389/fmars.2020.575218

Hyperspectral and Lidar: Complementary Tools to Identify Benthic Features and Assess the Ecological Status of *Sabellaria alveolata* Reefs

Touria Bajjouk[1], Cecile Jauzein[2], Lucas Drumetz[3], Mauro Dalla Mura[4,5], Audrey Duval[6] and Stanislas F. Dubois[1]*

[1] Ifremer, Dynamiques des Ecosystèmes Côtiers (DYNECO), Laboratoire d'Ecologie Benthique Côtière (LEBCO), Plouzané, France, [2] Ifremer, Dynamiques des Ecosystèmes Côtiers (DYNECO), Laboratoire d'Ecologie Pélagique (PELAGOS), Plouzané, France, [3] Laboratoire des Sciences et Techniques de l'Information, de la Communication et de la Connaissance (Lab-STICC), IMT Atlantique, Université Bretagne Loire (UBL), Brest, France, [4] Gipsa Lab, Grenoble INP, Centre National de la Recherche Scientifique (CNRS), University of Grenoble Alpes, Grenoble, France, [5] Tokyo Tech World Research Hub Initiative (WRHI), School of Computing, Tokyo Institute of Technology, Tokyo, Japan, [6] Ifremer, LITTORAL, Laboratoire Environnement Ressources de Bretagne Occidentale (LERBO), Concarneau, France

OPEN ACCESS

Edited by:
Massimo Ponti, University of Bologna, Italy

Reviewed by:
Paolo Rossi, University of Modena and Reggio Emilia, Italy
Stefania Lisco, University of Bari Aldo Moro, Italy

***Correspondence:**
Touria Bajjouk
touria.bajjouk@ifremer.fr

Specialty section:
This article was submitted to Marine Ecosystem Ecology, a section of the journal Frontiers in Marine Science

Received: *22 June 2020*
Accepted: *02 September 2020*
Published: *08 October 2020*

Citation:
Bajjouk T, Jauzein C, Drumetz L, Dalla Mura M, Duval A and Dubois SF (2020) Hyperspectral and Lidar: Complementary Tools to Identify Benthic Features and Assess the Ecological Status of Sabellaria alveolata Reefs. Front. Mar. Sci. 7:575218. doi: 10.3389/fmars.2020.575218

Sabellaria alveolata is a sedentary gregarious tube-building species widely distributed from southwest Scotland to Morocco. This species builds what are currently considered the largest European biogenic reefs in the bay of Mont-Saint-Michel (France). As an ecosystem engineer, *S. alveolata* generates small to large scale topographic complexity, creating numerous spatial and trophic niches for other species to colonize. *Sabellaria* reefs are also under anthropogenic pressures, leading locally to massive degradation. However, stakeholders lack spatially explicit measures of reef ecological status, at adapted spatial resolution to provide key management information for this protected habitat. Traditional field surveys are extremely time-consuming and rely on expertise for visual ecological status assessment. The present study aims at using an automatic processing approach based on optical airborne data to (i) assess the potential of hyperspectral imagery to discriminate *Sabellaria* bioconstructions and its main ecosystem associated habitats, including different types of substrate as well as biological components and (ii) to use the combination of the hyperspectral and LiDAR signals to estimate the spatial structure of the different bioconstruction types (veneers vs. hummocks and platforms) and ecological phases (retrograding and prograding). A reef from Mont-Saint-Michel was used as a test site. We built a processing chain based on supervised classification using the Mahalanobis distance to generate an accurate distribution map (overall accuracy of 88% and a Kappa of 0.85) of 10 *Sabellaria*-related benthic features, including large reef developing on sand and smaller veneers encrusting rocky shore areas. Specific spectral indices were used to define the spatial distribution of the main primary producers, in particular the microphytobenthos. Joining the hyperspectral and LiDAR data led characterizing the distribution of *S. alvealata's* ecological status (prograding and retrograding phases) with an overall classification accuracy and Kappa coefficient that can respectively amount to up to 93 and 0.86.

In our study site, the *Sabellaria* reef area (between 5.52 and 6.76 ha) was dominated by retrograding phases (between 53 and 58%). Our results showed that this automatic processing chain could be relevant for the spatial characterization of other *Sabellaria* reef sites. Study perspectives tend toward a quantitative estimation of their ecological status index.

Keywords: benthic habitats, biogenic reefs, ecological status, hyperspectral, intertidal, lidar, mapping

INTRODUCTION

Biogenic reefs are not only limited to coral reefs but also include a wide variety of species capable of building biogenic structures (or bioconstructions), including the gregarious tube-building worms of the Sabellariidae family. Over the world coastlines, large bioconstructions are found on the coasts of South America, built by the species *Phragmatopoma lapidosa* (Kinberg, 1866) and *Sabellaria wilsoni* (Lana and Gruet, 1989). On European coasts, the largest intertidal bioconstructions are built by the species *Sabellaria alveolata* (Linnaeus, 1767), which is presented from the north of the English coast to the south of the Moroccan coast. *Sabellaria* growths mainly on rocky area (Muir et al., 2016), but can also be present on soft sediments. In France, the Sainte-Anne reef (Mont-Saint-Michel bay) is known as the largest European bioconstruction. *S. alveolata* is an engineer species that generates small to large scale topographic complexity and creates numerous spatial and trophic niches for other species to colonize (Dubois et al., 2002, 2006; Bonifazi et al., 2019). Moreover, by modifying local hydrodynamics, *S. alveolata* reef structures also impact the habitats of benthic assemblages located in the immediately surrounding sediments (Dubois et al., 2002; Jones et al., 2018).

S. alveolata reefs are also under direct mechanical disturbances (recreational fishing) and indirect anthropogenic pressures (shellfish cultures) that can lead to massive degradation of some reef areas. Current damages are characterized by irregular surface features with lower densities of *S. alveolata* tubes (Dubois et al., 2002). Gruet (1982) described an evolving *S. alveolata* morphotype, from "veneers," where the tubes adhere to the substratum, to "hummocks" where the tubes radiate out from the initial settlement point before reaching "platforms" formed of extensive areas of hummocks fused together. Any one of these types can display outward signs of being in a "progradation" or "retrogradation" phases (Curd et al., 2019), either partially or totally. At European level, these formations are targeted, under the designation of Special Areas of Conservation (SACs), as a part of marine habitat (type 1170 "Reef") to be protected by the European Union's Habitats Directive 92/43/EEC. The latter states that bioconstructions should currently be monitored in order to acquire the missing knowledge regarding their management and ultimately their preservation.

Several studies searched for indicators to characterize the ecological state of *S. alveolata* reefs. Desroy et al. (2011) developed a "Health Status Index" for the Mont-Saint-Michel bay bioconstructions, based on fragmentation, morphological types and epibiont coverage. However, this index is only applicable to areas where *S. alveolata* formations reach extensive bioconstructions, which strongly restricts its application potential. More recently, Curd et al. (2019) attempted to investigate the relationship between the structural appearance of the bioconstruction and physiological state of the tube-building polychete. In this study, physiological indicators (lipid markers and metabolic enzymes) were used as biochemical indicators of *S. alveolata* health status, and linked to bioconstructions types (veneers or hummocks). Biochemical analyses are useful tools to investigate worm's health status, but they are costly, time-consuming and not always connected to the reef status or phase (progradation vs. retrogradation). Other indicators were previously developed from *in situ* surveys. However, their use is limited to the surrounding extension of the evaluated area: analysis carried out on a larger scale (whole reef) leads to a simplification of the "landscape" and therefore potentially to wrong reef ecological assessments. Jones et al. (2018) analyzed the effects of a continuous and increasing disturbance on beta diversity indices. They also stressed the importance of spatial and temporal scales for evaluating the impact of disturbances on *S. alveoata* reefs. Indeed, there is a real need for effective management to develop alternative analytical tools that (i) allow for approaching metrics measured *in situ* to assess conservation status on a large scale and (ii) guarantee robust reproducibility of acquired information. Moreover, all these studies used destructive sampling techniques, which although still commonplace in benthic ecology, are not viable options in low-abundance habitats (Beisiegel et al., 2017).

Several studies of *S. alveolata* reefs have been achieved using remote sensing techniques. Acoustic tools were more specifically adopted as suitable method for *Sabellaria* reefs in subtidal areas (Griffin et al., 2020). The most the studies were mainly based on aerial photography (Bonnot-Courtois et al., 2005; Desroy et al., 2011) or satellite imagery (Marchand and Cazoulat, 2003; Jones, 2017) as well as UAVs (unmanned aerial vehicles) as an efficient and cost-effective tool for fine scale reef characterization (Ventura et al., 2018; Collin et al., 2019). Noernberg et al. (2010) have also exploited aerial photographs and LiDAR (Light Detection and RAnging) digital elevation model to quantify intertidal complex landform volume. A more recent work used artificial neural network modeling to map *S. alveolata* relative abundance (Collin et al., 2018). Such studies have been successful to investigate reef formations developing on soft-sediment, where bioconstructions sit on top of sediment are discrete objects relatively easy to identify. Yet, most of the reef formations in Europe develop over hard rocky substrata, and compete for space with other species and macroalgae (Firth et al., 2015). To the best of our knowledge, no study has tackled the problem

of automatically separating reef bioconstructions from other associated benthic features in a rocky reef environment, nor has any study tried to remotely and automatically assess *S. alveolata* reef ecological status.

To overcome limitations in large scale *S. alveolata* reef characterization, we propose an approach based on the combination of two complementary techniques: (i) LiDAR a widely used tool to depict the 3D habitat structural complexity (Wedding et al., 2008; Davies and Asner, 2014; D'Urban et al., 2020) and (ii) hyperspectral imagery that allows for the characterization of bio-optical properties variability in time and space (Fyfe, 2003; Schmidt and Skidmore, 2003; Chennu et al., 2013; Bajjouk et al., 2019b). Hyperspectral imagery has been used in coastal areas to study shallow tropical coral reefs, reef-forming species with symbiotic microalgae species with primary photosynthetic pigments (Petit et al., 2017; Bajjouk et al., 2019a). Characterizing reef-forming species such as *S. alveolata*, a species without photosynthetic pigments and obvious spectral reflectance is a challenging task. By using hyperspectral images coupled with field observations, we also aim at better estimating the microphytobenthos (hereafter MPB) spatial distribution in sediments surrounding the bioconstructions. MPB is a key information for understanding the role of engineered habitats and species biological activities (feces and pseudofaeces) (Echappé et al., 2018).

We address here three main questions: (1) Do the bioconstructions of *S. alveolata* have a specific spectral signature, so that one can discriminate reefs from other associated habitats, including MPB patches (2) Does the spectral signature of *S. alveolata* bioconstructions allow for the identification of reef constructions affixed to intertidal rocky substrate as well as soft-sediments? (3) Can we automatically and remotely estimate the ecological health status of these bioconstructions based on hyperspectral and LiDAR signal combination? Reefs located in the bay of Mont-Saint-Michel were used as a test site. Resulting spatial patterns are discussed regarding their ecological coherence. Future developments are finely formulated for *S. alveolata* conservation and management perspectives.

STUDY SITE DESCRIPTION

The Bay of Mont-Saint-Michel (France) is a coastal area of the Western part of the English Channel. The study site, named Champeaux (−1.53°, 48.73°), was located in the east part of this bay that hosts the largest *S. alveolata* reefs in Europe (**Figure 1**). The sedimentary environment of the bay is mainly controlled by tidal residual currents, typically characterized by an anticyclonic gyre (Noernberg et al., 2010). This site was chosen for its bioconstruction density and diversity of habitats: it includes both reefs developing on sand and bioconstructions developing on rocky shores (Lecornu et al., 2016) and stretches from the upper intertidal to the lower eulittoral zone.

In Champeaux, *S. alveolata* can build three-dimensional structures which present a variety of morphotypes (Gruet, 1972; Curd et al., 2019): elevated platforms, more or less coalescent ball-shaped structures (hummocks) or adhering to rocks (veneers). Each morphological structure can display different phases in

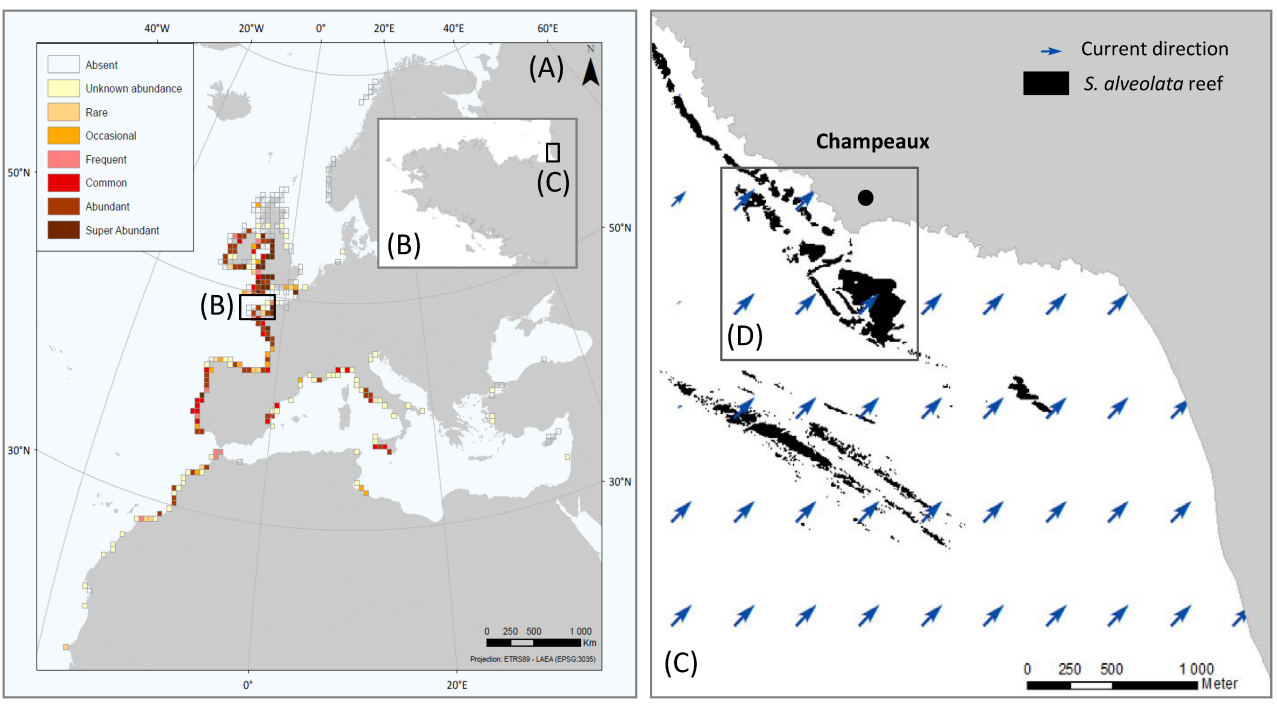

FIGURE 1 | Global distribution and abundance of *S. alveolata* (from Curd et al., 2020) **(A)**, Brittany region **(B)**, Eastern part of Mont-Saint-Michel bay **(C)** and study site showing *S. alveolata* existing map (from Basuyaux and Lecornu, 2015) **(D).**

the reef dynamics: progradation, where bioconstructions are expanding, with new surfaces colonized by the worms and retrogradation, where bioconstructions are eroding and reef surfaces are lost (Curd et al., 2019).

MATERIALS AND METHODS

Data Acquisition

Field and Laboratory Measurements

Several field surveys were carried out in 2019 across Champeaux site during the low spring tides:

(i) A field spectral library was acquired on the 22nd of April. Reflectance spectra were measured on 505 channels from 325 to 1075 nm using an Analytical Spectral Devices (ASD) field spectroradiometer that automatically averages 5 multiple records to provide a single output. The ASD was calibrated via a spectralon to provide reflectance standardized measurements. Reflectance recordings were carried out vertically, avoiding any shadow on the target and at a height allowing a homogeneous footprint. For each target, about three to five spectra were recorded to take into account intra-target variability. These measurements were taken on different homogeneous samples representing different types of benthic features: the spectral library is composed of 53 reflectance spectra of 10 different pure targets including three vegetation types (green and brown algae, MPB), *S. alveolata* bioconstructions developing on both rock and sediment area at different ecological phases, oyster reefs as well as substrate types (mud, sand, shells and rocks). Principal component analysis (PCA) was used as an exploratory tool to summarize and to visualize the information in the benthic features described by their spectral signatures. PCA was performed using R statistical software.

(ii) A total of 221 field control points (**Figure 2B**) were set on the 17th and 18th of June. Photography is associated with each spectroradiometric measurement. All the descriptive information of the target (substrates and epibionts) was also recorded for each measurement. Efforts were made to cover a wide range of ecologically diverse features of the reef providing an on-foot access.

(iii) During the same summer field survey, on June 17th, samples were collected for identification of the main genera or species present in MPB communities. MPB was harvested using pieces of artificial substrates, cut in a nylon net of 100 μm mesh. Substrates consisted in small squares of 2.5 cm^2. They were deployed in four stations located few meters apart from each other, in an area close to *S. alveolata* reefs and where MPB biofilms are recurrently observed at low tide. Pieces of artificial substrates were placed on wet

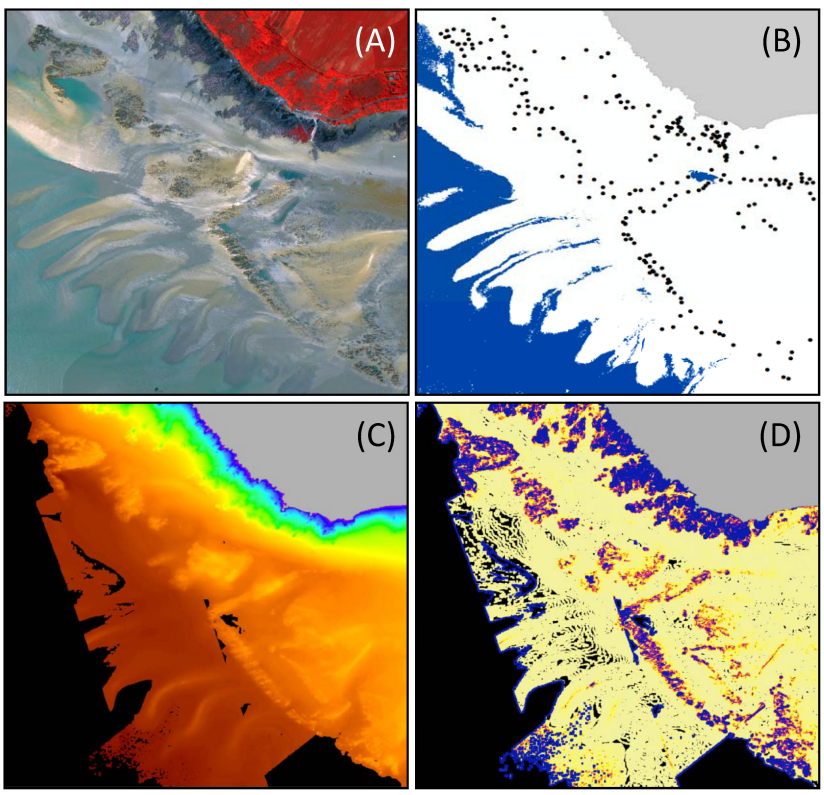

FIGURE 2 | Data acquired on Champeaux site. Hyperspectral **(A)** and field data **(B)** were specifically acquired for the present study. lidar bathymetry data **(C)** were provided by SHOM, the French hydrographic office and rugosity **(D)** was computed from bathymetry data.

sand 2 h before low tide. They were collected at low tide, when colonized by a biofilm of MPB cells, and immediately transferred to plastic tubes containing 4 ml of filtered seawater with a fixative (1% final concentration of Lugol's solution). Samples were brought back to the laboratory and kept at 4°C until analysis. Before microalgal cell identification and counting, tubes were agitated in order to help for detachment of MPB cells from the substrate. Then, a sub-sample was taken, diluated 100x in filtered seawater and settled for 12 h in a Utermhöl chamber (Utermöhl, 1958). Most of supernatant was replaced by bleach (0.1% diluted in milliQ water) during one night, in order to remove a large part of organic matter residues and preserve silice frustule. Bleach was then replaced by milliQ water and microalgal cells were settled again for 12 h. Identification and counting of cells were conducted under 400 magnification, using an inverted microscope (Zeiss Axio Observer).

All field position measurements were made using a GARMIN GPS with an uncertainty of 3 m. The position recording of ground control points was done by allowing the device to capture as many satellite signals as possible and thus increase the precision of the geolocalization. Positions have then been expressed in the same projection system as that of hyperspectral images (Lambert-93 associated with the RGF93 geodetic system). Locations of ground control points were matched to images and verified by visual inspection. This last operation was performed by experts who know well the surveyed area using the ArcGIS tool.

Airborne Optical Data Acquisition

An airborne survey was carried out on June 17, 2019 as part of the BIOHERM Project, using an hyperspectral imaging sensor of the Hyspex VNIR 1600 type deployed at an altitude of 1 200 m (**Figure 2A**). The sensor measured radiance between 400 nm and 1 000 nm with spectral and spatial resolutions of respectively 3.7 nm and 0.5 m, providing a total of 160 spectral bands.

LiDAR data (**Figure 2C**) were acquired in March 2019 as part of the Litto3D program (Litto3D, 2019). LiDAR topo-bathymetric data comes from a HawkEye III sensor used in dual configuration: Chiroptera (Topo- Shallow Channel) and Deep Channel. The point cloud density in topographic configuration (corresponding to the area of interest for our study) is 8 points/m^2 with a planimetric and vertical precision better than 20 cm. All data are expressed in the Lambert-93 projection system associated with the RGF93 geodetic system, and in the IGN69 altimeter system, compatible with the WGS84 world system at metric level. For the purpose of the analysis, the LiDAR point cloud was interpolated to a 1 m regular grid DEM (Digital Elevation Model). The DEM was also used to create layers describing seafloor topographic rugosity (**Figure 2D**) using Arc GIS Benthic Terrain Modeler tool (NOAA and Oregon State University).

Data Pre-processing

Geometric and atmospheric corrections were performed prior to image processing (**Figure 3**). Orthorectification allowed generating geolocated images in the Lambert 93 system. The relative geometric precision obtained was of the order of the pixel. Atmospheric corrections were subsequently applied using the ATCOR software on each flight line in order to obtain reflectance images above the water surface. The oxygen absorption band, around 760 nm, was linearly interpolated. A post empirical correction was thereafter applied. It was carried out in two steps: (i) a linear correction based on the overlap between the lines to correct the variation in lighting conditions, (ii) a second linear correction, for each spectral band, which allowed for the correction of local atmospheric effects not or poorly taken into account by the atmospheric model. Their correction was done using measurements on a calibrated reference target installed on site. Land and water area were masked using, respectively, coastal shoreline derived from LiDAR data and Infra-Red band thresholding.

Data Processing

The imagery data processing procedure consisted of several steps. They are illustrated in the workflow diagram (**Figure 3**) and are detailed below.

Vegetation Index Computation

At first, spectral vegetation indices were computed in order to specifically characterize vegetation present in the study site. The principle consists in linking together certain characteristics and the measurements acquired in at least two spectral bands. Two indices were calculated using ENVI image processing software: (i) the Normalized Difference Vegetation Index (hereafter NDVI, Tucker, 1979), widely used to analyze vegetation (Cracknell, 2001; Pu et al., 2008; Kushnir et al., 2011) and (ii) the Diatom index (Van der Wal et al., 2010; Launeau et al., 2018) as MPB sampling analysis revealed that this compartment was mainly dominated by diatoms in the study site (**Figure 4N**).

To enhance discrimination of benthic features that characterize the area, topographic and spectral indices layers were merged with hyperspectral masked image, as classification input, using layer stacking processing (**Figure 4**). Prior to their concatenation, the hyperspectral image and the LiDAR data were georeferenced to the same projection system with a precision of 0.5 and 0.2 m respectively. They were then merged together in the same file thanks to the "Layer stacking" function implemented in the ENVI image processing software using the "Nearest Neighbor" resampling method.

Classification

The Mahalanobis distance (Richards, 1999), found to be most suitable in a majority of applications (McLachlan, 1999; Chang et al., 2004; Xiang et al., 2008; Govender et al., 2008), was used as distance function in the classification algorithm. This distance also has the advantage of taking into account the correlations of the data set (De Maesschalck et al., 2000). Indeed, hyperspectral data are measured over a large number and continuous spectral bands, each band containing potential redundant information. In addition, a Mahalanobis distance metric is scale-invariant and can adjust the geometrical distribution of data so that the distance

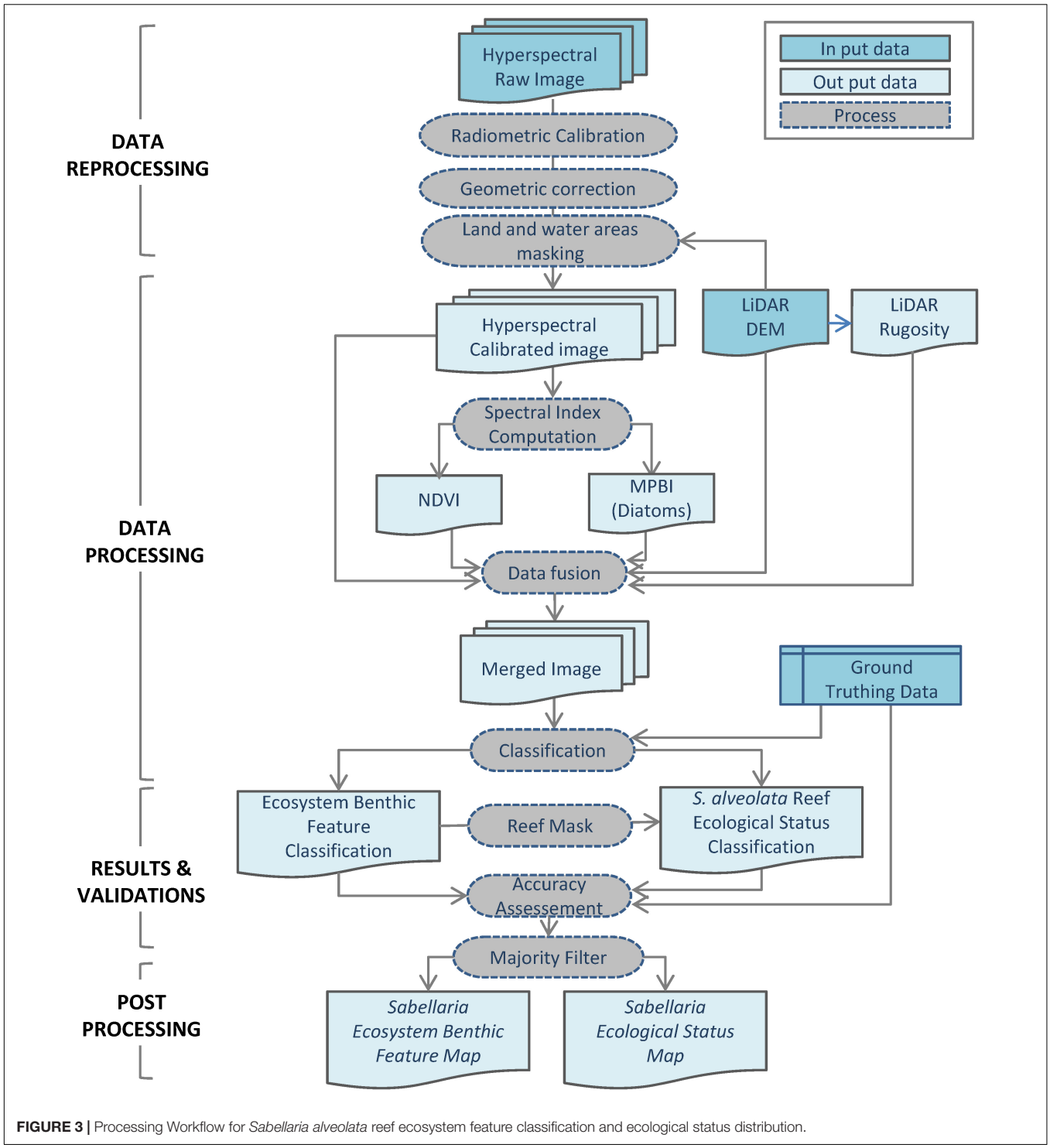

FIGURE 3 | Processing Workflow for *Sabellaria alveolata* reef ecosystem feature classification and ecological status distribution.

between similar data points is small (Xing et al., 2003). This is supposed to enhance the classification performance.

To perform image classification, regions of interest (ROIs, areas of image that contain pixels of the same spectral characteristics representing the same seabed feature according to field observations) were created interactively. Ten habitat classes were considered to produce associated *S. alveolata* benthic habitat maps. Supervised classification clustered pixels in a dataset into classes based on previously defined training data. All pixels were classified to the closest ROI class using the Mahalanobis classification function implemented in ENVI software. For *S. alveolata* ecological status estimation, classification was applied in the same way but only on areas where it was previously detected.

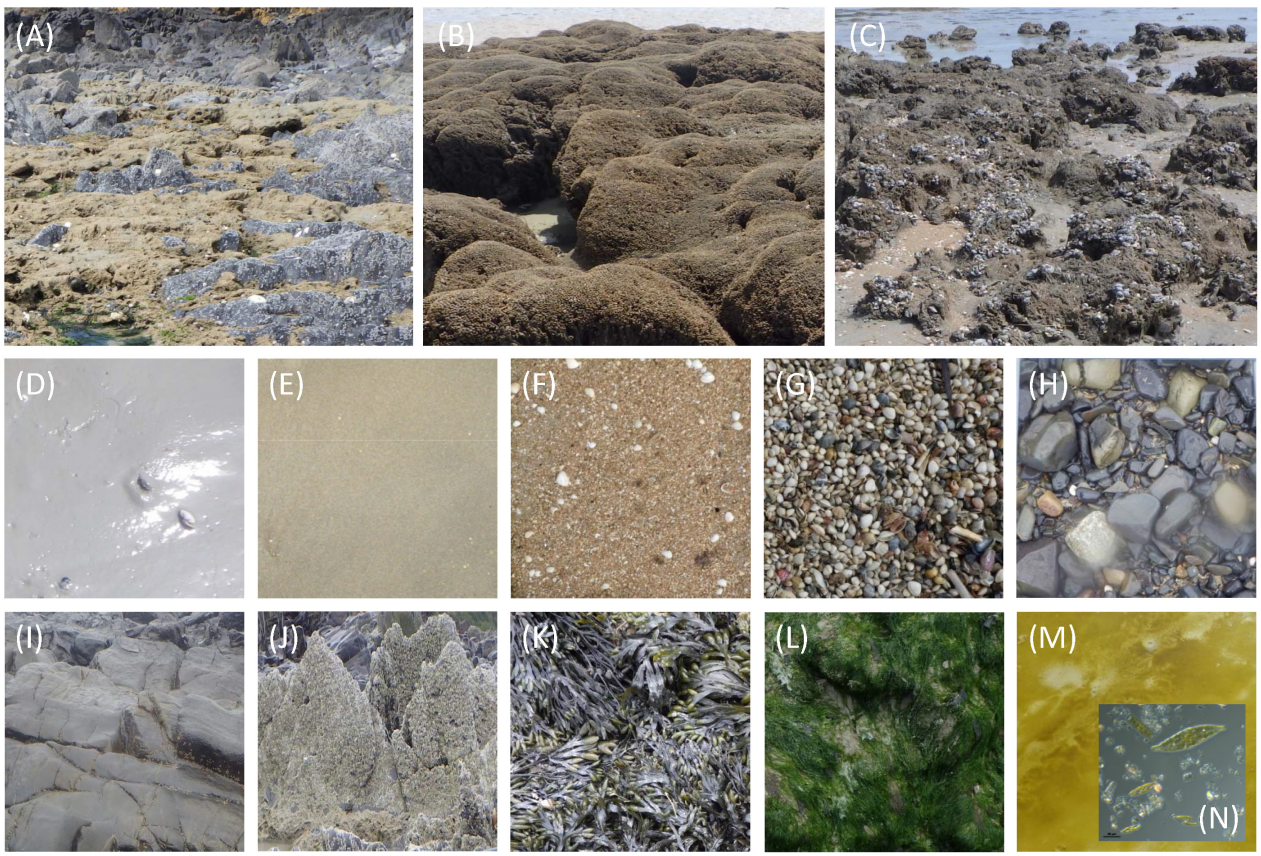

FIGURE 4 | *Sabellaria alveolata* reef ecosystem benthic features: *S. alveolata* on rock **(A)**, healthy *S. alveolata* on sand **(B)**, degraded *S. alveolata* on sand **(C)**, muddy sediments **(D)**, sand **(E)**, coarse sediments **(F),** shells **(G)**, pebble and cobble substrates **(H)**, bare rock **(I)**, rock with epifauna **(J)**, brown algae **(K)**, green algae **(L)**, microphytobenthos **(M)** mainly composed of diatoms **(N)** of the Naviculaceae family and Amphora, Pleurosigma or Gyrosigma genera.

Accuracy Assessment

The classification quality was assessed quantitatively using accuracy assessment based on comparison with field reference data none overlapping from the data used for training the classification algorithms. The kappa coefficient and the overall accuracy, the two statistics most prominently used (Foody and Mathur, 2006), were computed for classification accuracy assessment. Both the precision of localization of field data and the high spatial variability that exhibits the *S. alveolata* ecological status make the classification accuracy assessment of this latter very difficult to carry out. As it was stressed by Florén et al. (2015), low prediction accuracies could have several explanations but it is likely that most of them are driven by inaccurate positioning and/or the small-scale heterogeneity of the habitats as it is the case in the present study. Thus, many field data fell erroneously near the reefs when plotted on the image and thus could not be used. To overcome this issue, "hummocks" type observations were discarded because they do not constitute continuous formations and their localization lacks precision as they are occupying surfaces often lower than the image resolution (50 cm). For the *S. alveolata* reef status, data extraction from the classified image was done by searching the observed status within a radius of 2 m. This allowed to take into account the GPS accuracy (3 m) and thus to increase the number of kept samples for statistical evaluation. Overall accuracy and Kappa coefficient were thereafter calculated and compared for both datasets. For qualitative accuracy evaluation, we also plotted sample field data on ecological status classification map and made a comparison with the status estimated in the field.

Post-processing

As is often used in the post-processing of a thematic per-pixel classification map (e.g., Stuckens et al., 2000), a "Majority filter," that generalizes and reduces single pixel misclassification, was applied using ArcGIS tool. This filter considers a neighborhood of pixels and assigns to the central pixel the semantic class most occurring in all pixels in the neighborhood. The kernel of the filter was the eight nearest neighbors (a three-by-three window) to the processed cell.

RESULTS

Spectral Reflectance Signatures

Field spectra were acquired to examine if *S. alveolata* bioconstructions have a sufficiently specific spectral signature

leading to their identification and discrimination from the other benthic feature present in the study site. Recorded spectra are shown in **Figure 5**. Measures over 900 nm, less reliable due to the instrument sensitivity in this spectral region, have been dismissed.

Benthic features showed clear differences in their spectral reflectance shapes and/or their magnitudes (**Figure 5**). For vegetation types, reflectance values were low in the visible bands but showed a strong increase with wavelength above 673 nm reaching high levels in the entire infrared region

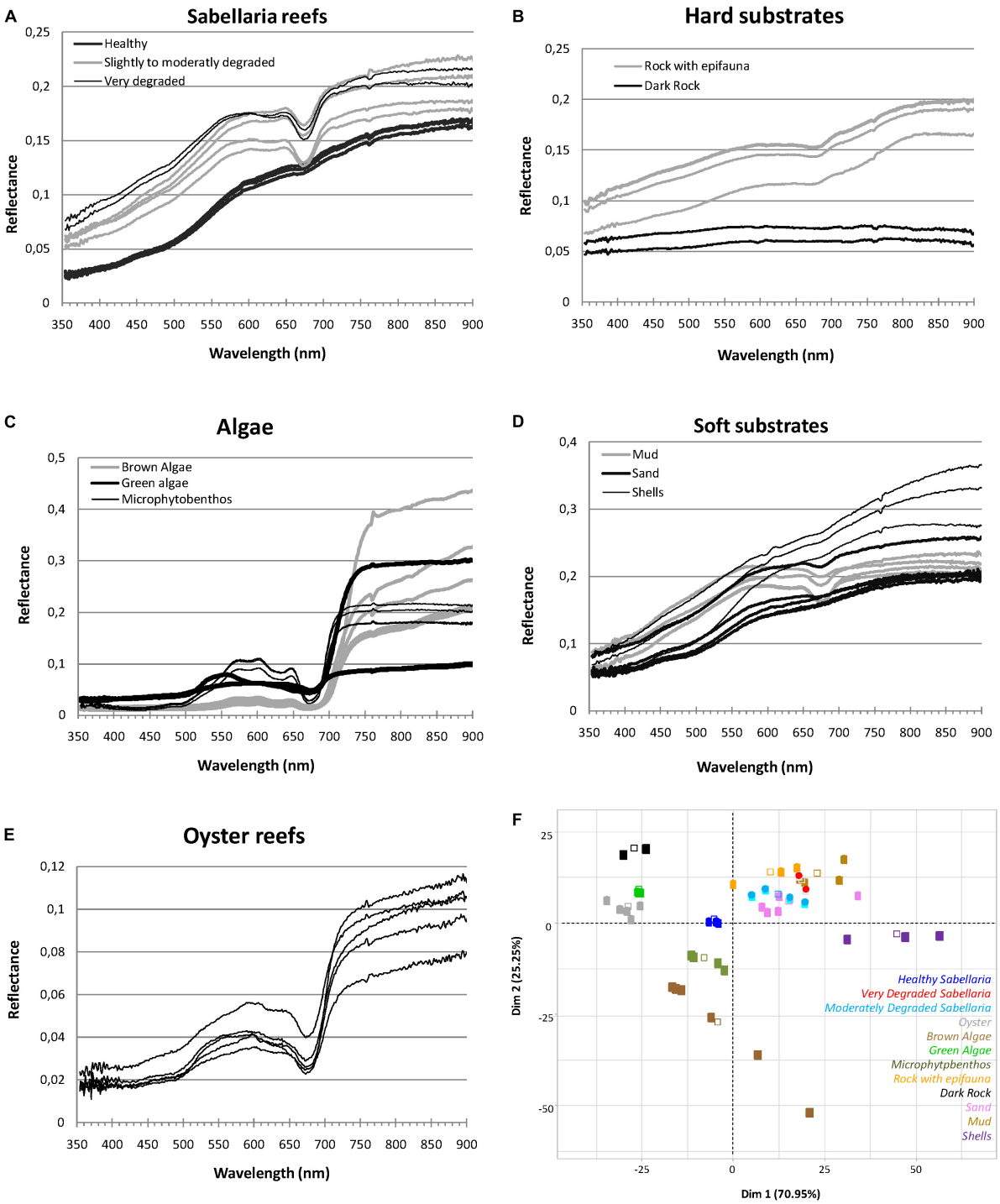

FIGURE 5 | Spectral signature of *Sabellaria alveolata* reef **(A)** and associated benthic features **(B–E)** with the corresponding PCA analysis biplot of the two first dimensions **(F)**.

(**Figure 5C**). The spectral signature presents a significant jump between the absorption at 673 nm and the reflection in the near infrared. This jump is generally less marked on the spectral signature of the MPB population. Conversely, the absorption peak at this wavelength is stronger in the latter. The MPB also present several peaks of reflectance in the visible around 570, 602, and 646 nm when smaller specific absorption features were observed in reflectance spectra at 581 nm and 632 nm compared to macroalgae (**Figure 5C**). Brown algae reflectance spectra displayed lower values in the green part of the spectrum than the other vegetation types. For substrate types, spectra showed increasing reflectance with increasing wavelength in both visible and near infrared ranges (**Figures 5B,D**). Soft sediments displayed overall higher reflectance values than hard substrata. The highest values were recorded for shelly sediment (shells) in the infrared region. The lowest values were recorded for dark rock with an almost flat spectrum all over the range of wavelengths analyzed, without any obvious absorption feature. The spectrum corresponding to mud showed an absorption band at 673 nm similar to that of microphytobenthos. Oyster reefs exhibited greater variability in their spectral amplitude than *S. alveolata* reefs, especially in the infrared region, with some peaks of reflectance in the visible that were not always well discriminated. Regarding *S. alveolata* reefs, the spectral signatures of prograding bioconstructions showed a shape similar to that of sand with, however, a lower amplitude (**Figure 5A**). With the state of degradation, their reflectance values increased and the shape of the spectrum was modified: degraded reef portions in retrograding reefs showed spectrum similar to muddy sediments, with an absorption peak at 673 nm.

According to statistical analysis, the first two dimensions of the PCA accounted for 71 and 25% of the total variation in the dataset, respectively, expressing together more than 96% of the data variability (**Figure 5F**). Correlation biplots showed that the specific spectral signature of some benthic features, such as dark rock, shells, macroalgae as well as prograding *S. alveolata* reefs, was probably sufficient for their discrimination. However, other benthic features seemed to be more difficult to distinguish solely on the basis of their spectral signature, as for rocky substrata (Rock) with epifauna, fine sand sediment and retrograding *S. alveolata* reefs.

Benthtic Feature Classification and Validation

Preprocessed airborne data were classified using statistical supervised classifier based on Mahalanobis distance. As a result, dominant habitat types were automatically grouped into classes representing the pattern of Champeaux site ecosystem (**Figure 6**). Among the 10 benthic feature classes obtained, three were identified as soft substrates (fine sand, mud and coarse sediments), and two of them as hard substrates (rocky reefs and "other hard substrates"). Microphytobenthos was differentiated from macroalgae and displayed patches with varying levels of biomass. The pattern of class distribution also revealed the distinction between the two types of *S. alveolata* formations, large reefs developing on sand and adhering to rocky reefs on high shore.

The performance of the obtained classification was assessed using the confusion matrix method (**Figure 7**). In this approach, classified benthic habitats were compared with field observed benthic features, resulting in an overall accuracy of 88% and a Kappa of 0.85. Khi^2 test ($p < 0.0001$, $\alpha = 5\%$) corroborated the high performance of the used classifier for *S. alveolata* formations and its associated benthic features. Few confusions were recorded, however, mainly between *S. alveolata* on sand and bare sand sediments or between *S. alveolata* on rocky substrata and coarse sediments, but in much lower proportions than correctly classified pixels.

Remote Estimation of S. *alveolatta* Reef Ecological Status

In order to continuously map ecological status, supervised Mahalanobis distance based classifier was applied to each pixel of merged hyperspectral and LiDAR data. Prograding and retrograding phases were provided with 0.5 m spatial resolution. The ecological status map obtained exhibited an heterogeneous distribution with a co-presence of prograding and retrograding phases whatever the location (**Figure 8**). Nevertheless, prograding phase seemed to be seaward dominant, where retrograding phase was mainly present in the southeast part of the study site and closed to the shoreline.

The calculated overall accuracy and Kappa coefficient varied with the number of pixels used in the evaluation. Values of 0.77 and 0.55 were obtained, respectively, when using 22 samples, but increased to 0.93 and 0.86, respectively, taking into account a larger field dataset (113 samples). The *S. alveolata* area in the Champeaux site was estimated at 5.52 and 6.76 ha, respectively with and without post-processing spatial filtering (**Table 1**). *Sabellaria* reefs in this site seemed to be slightly dominated by retrograded phase (58 and 53% respectively).

DISCUSSION

By using an automatic supervised classification algorithm, we demonstrated the ability of combining hyperspectral and LiDAR signals to (i) provide a high-resolution (0.5 m) map with 10 identified habitat classes describing *S. alveolata* reefs and their associated benthic features; (ii) accurately discriminate two *S. alveolata* reef forms, large reefs developing on sand and smaller veneers encrusting rocky shore areas, as well as its main ecosystem associated habitats, and (iii) reliably and remotely estimate the spatial structure of these bioconstructions ecological prograding vs. retrograding phase. Further details are presented in the following sections.

Seabed Type Spectral Discrimination

The visual inspection of field-measured spectra acquired in the Mont-Saint-Michel bay (France) shows that most of the spectral profiles are characterized by numerous absorption bands, mainly due to the presence of pigments. Previous studies showed that differences in pigment mixtures mostly

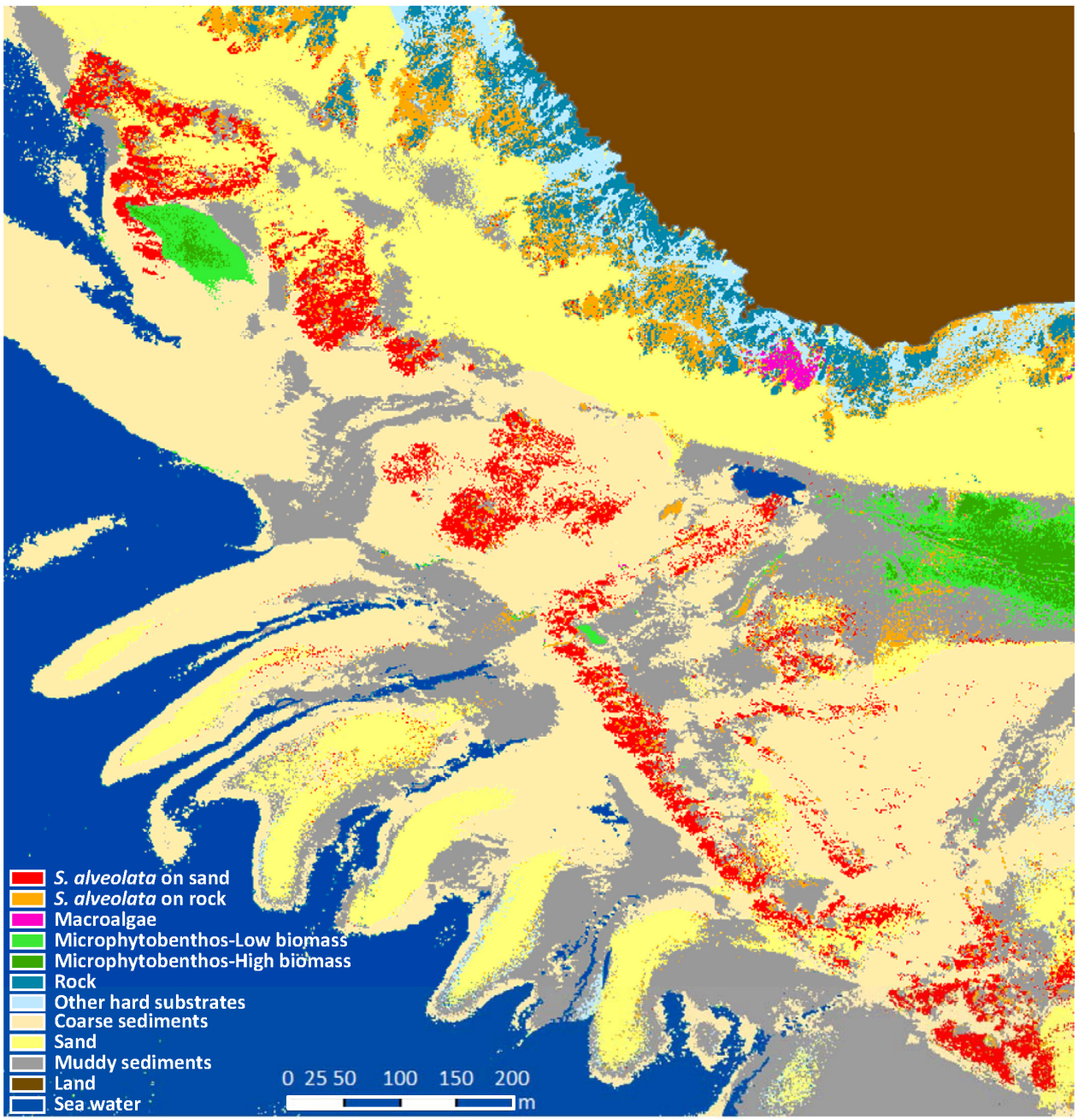

FIGURE 6 | Benthic habitat map of Champeaux site obtained from the hyperspectral airborne imagery using supervised classification based on Mahalanobis distance.

explain differences observed in specific spectral signatures (Guillaumont et al., 1997; Méléder et al., 2003; Jesus et al., 2014). The absorption band observed at 673 nm is characteristic of all plants due to the ubiquitous presence of chlorophyll a, while chlorophyll c is responsible for absorption bands at 581 and 632 nm (Kuczynska et al., 2015) as displayed by brown algae and microalgae spectra. Chlorophylls a and c are dominant pigments in diatoms, haptophytes (Haptophyta or Prymnesiophyta) and to a lesser extent in some dinoflagellates (Kuczynska et al., 2015; Coupel et al., 2015). These two pigments typify microphytobenthos assemblages dominated by diatoms (Méléder et al., 2003; Jesus et al., 2014). These observations are coherent with taxonomic analyses of biofilm samples that show communities highly dominated by diatoms. Apart from chlorophylls, diatoms contain carotenoids in their pigment profile that are mainly composed of carotene, fucoxanthin and diatoxanthin under light conditions (Kuczynska et al., 2015). Carotenoids exhibit an intense absorption between 400 and

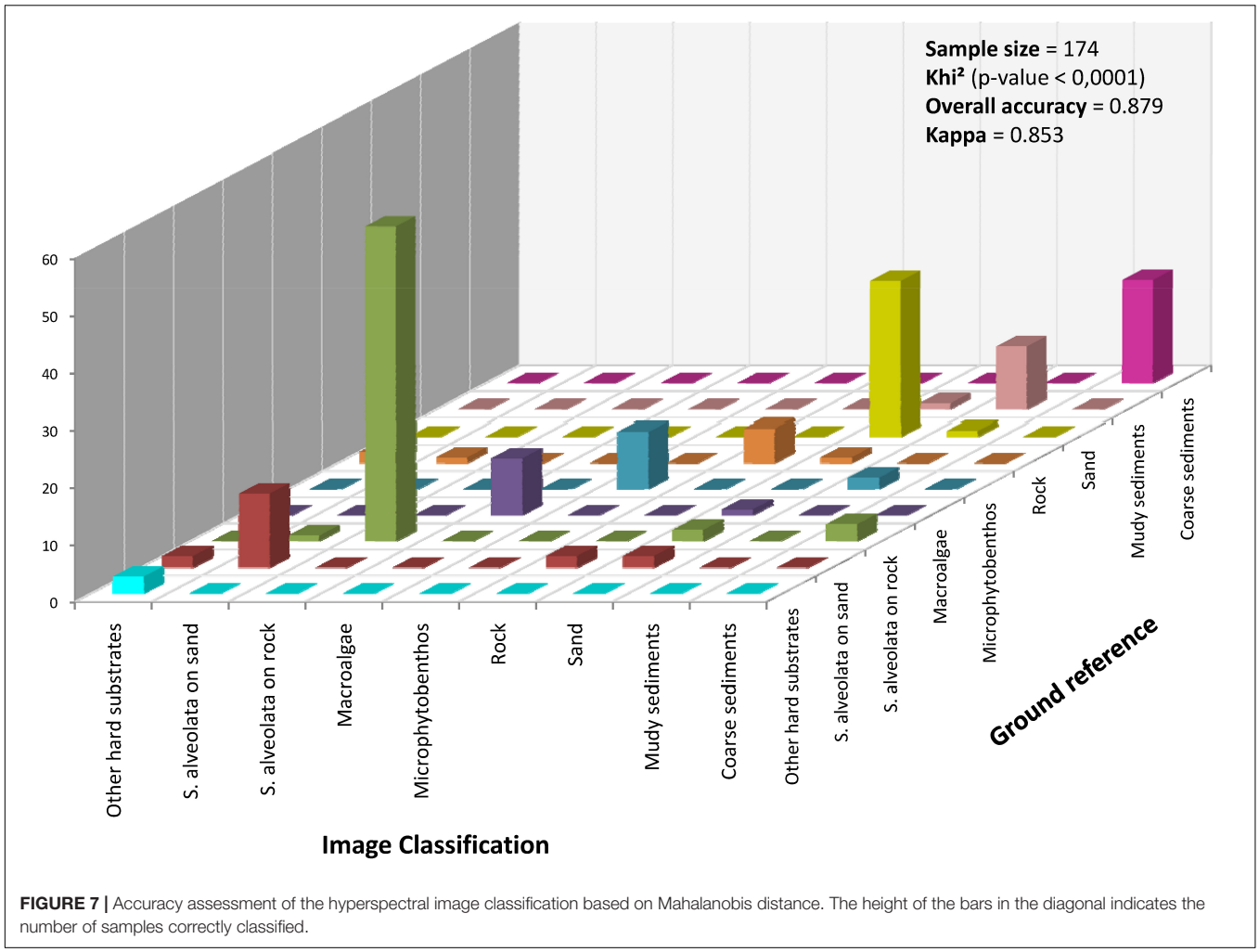

FIGURE 7 | Accuracy assessment of the hyperspectral image classification based on Mahalanobis distance. The height of the bars in the diagonal indicates the number of samples correctly classified.

500 nm, fucoxanthin having a slightly higher absorption band (460–570 nm) than the others (Kuczynska et al., 2015). The dominance of fucoxanthin in the pigment profile of brown algae (Kirk, 1977) can also explain the main specificity of the spectral signature of this group. Lower reflectance spectra were observed for brown algae compared to other vegetation types in the blue-green part of the spectrum. This mainly results from a high concentration of fucoxanthin per cell, exhibiting high absorption in the range 460–570 nm (Kuczynska et al., 2015).

Intertidal substrates have spectral characteristics that seem to be related to both their mineral and chemical composition, as well as their structural properties (grain size and sorting parameters). Typical reflectance spectra of substrates reveal spectral shapes characterized by increasing reflectance with increasing wavelength, similar to those recorded by previous studies (Guillaumont, 1991; Méléder et al., 2003; Bajjouk et al., 2019a). Dark rocks are however an exception. Their gray black color seems to explain the very weak reflectance on all the visible and infrared spectral range. The slight absorption that appears at 673 nm is characteristic of vegetation and is observed in muddy sediment spectra, due to adhering alga cells in poor physiological state and chlorophyll a degradation products that also participate in absorption at 673 nm (Méléder et al., 2003).

Coherence of Benthic Feature Distributions

Multivariate analysis showed that although spectral richness, confusions between certain features (e.g., retrograding *S. alveolata* reefs vs. sand sediments) are possible. The integration of LiDAR sensor information into the hyperspectral image provides an additional characteristic on the nature of the topographic complexity that can help for improving the discrimination between benthic features. As discussed by Chang et al. (2004), materials in real world imaging could occupy a full pixel or be either mixed with other targets such as background or embedded in a single pixel as a subpixel target. Unlike SAM (Spectral Angle Mapper) and Euclidean distance that are generally used for pure pixel-based classical image processing, Mahalanobis distance does not take into account the spectral correlation among pixels. This characteristic of Mahalanobis is very useful and brings crucial information in identification or discrimination of materials in real images. The *S. alveolata* reef

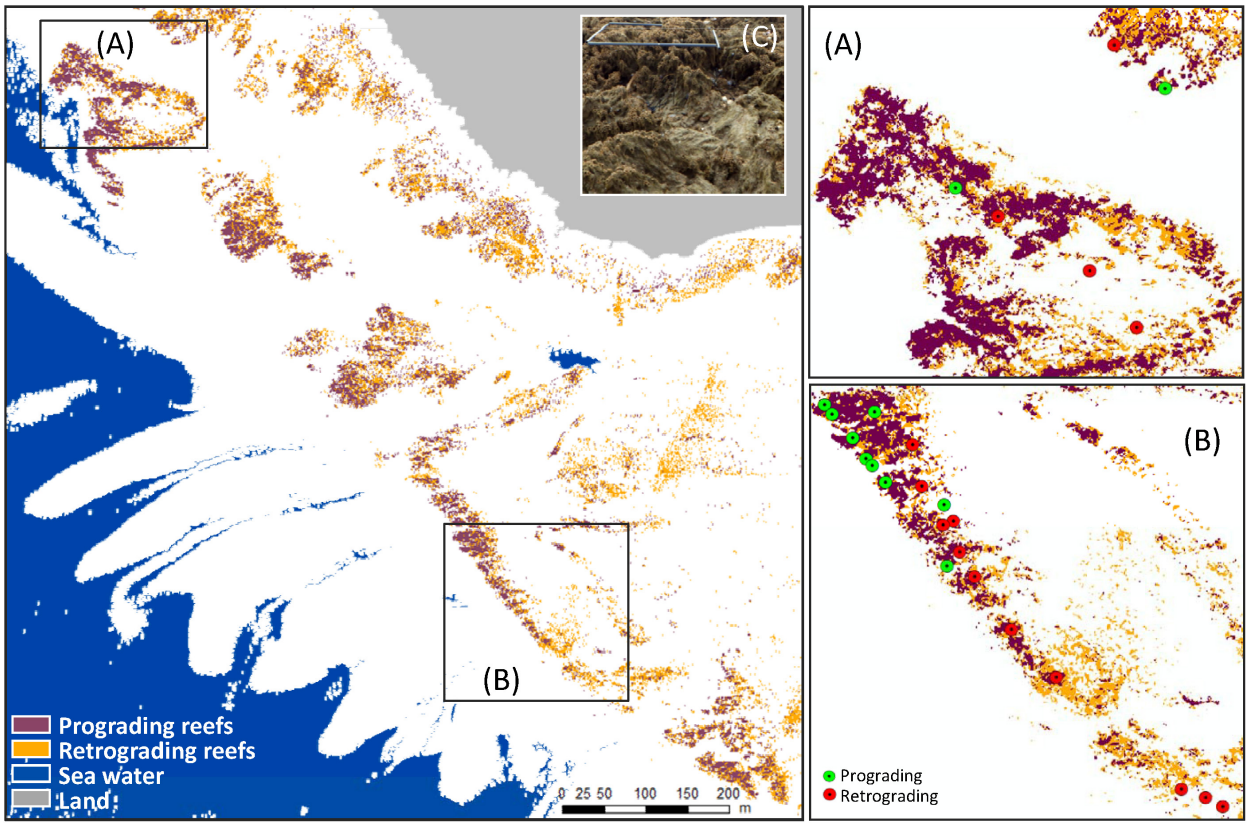

FIGURE 8 | *Sabellaria alveolata* reef ecological status distribution in Champeaux showing zones displaying plotted field samples on ecological status classification **(A,B)** and field photography with a quadrat of 0.5 × 0.5 cm on *S. alveolatta* reef exhibiting high spatial variability in ecological status **(C)**: prograding reef at the back of the image and retrograding reef in front of the image.

being spatially very heterogeneous in terms of abundance and structure, even at a high resolution, we therefore favor the use of Mahalanobis distance for image supervised classification.

The highly accurate overall accuracy (88% with a Kappa coefficient of 0.85) is consistent with the outputs of previous work that also successfully used this distance for image classification (Chang et al., 2004; Govender et al., 2008). Obtained results also reinforce the recommendations encouraging integration of direct observation field techniques with remotely sensed data to capture detailed habitat information at large scales, thus avoiding trade-offs between three types of scale: spatial, temporal and thematic (Lecours et al., 2015; Rhodes et al., 2015; D'Urban et al., 2020). The benthic habitat map of Champeaux obtained from the hyperspectral airborne imagery using Mahalanobis supervised classification allows the delineation of a higher number of discriminated habitats (ten) than what was identified using RGB (Red-Green-Blue) images and digital surface model, as shown for *S. alveolata* reefs growing atop of soft sediment exclusively (Collin et al., 2019). The most significant information that the pattern of class distribution reveals is the distinction between two types of *S. alveolata* formations; large reefs developing on sandy bottoms and smaller veneers encrusting rocky shore areas. This is the first time that the two types of intertidal *S. alveolata* reefs are automatically mapped and discriminated, revealing how relevant LiDAR information is. As stressed by Brown (2004), elevation data has the ability to enhance discrimination of intertidal species, since topographic metrics (e.g., elevation, rugosity or slope) can be computed and used as proxies for their position in relation to the tidal cycle. Visual inspection of the map shows, however, that pixels *a priori* automatically labeled "*S. alveolata* on rock" are actually located in an area (south-eastern part) without rocky substrata. This can be explained by the fact that bioconstructions in this specific area have a veneer shape but lack 3D structure, as is generally the case with *S. alveolata* reefs developing on sandy bottoms. Regarding reef ecological status distribution, the general orientation of the reef exhibits spatial pattern parallel to the coast. This is most likely due to the hydrodynamic conditions. Tidal currents at Champeaux are

TABLE 1 | *S. alveolata* area estimation based on combined LiDAR and hyperspectral data automatic classification.

	Area in ha (%)	
	Without spatial filter	**With spatial filter**
Progradation	2.820975 (0.42%)	2.61165 (0.47%)
Retrogradation	3.939875 (0.58%)	2.91138 (0.53%)
S. alveolata reef	6.76085	5.52303

often fast and opposite to near shore direction. As a resulting effect, sand transport and probably reef development extend perpendicularly to the main current direction (Gruet, 1986).

We also showed here the benefits of using specific spectral indices to improve discrimination between algal groups. By not being limited only to the commonly used NDVI—a generic index to detect vegetation—and by calculating a spectral index specific to diatoms, it was possible to separately map macroalgae and microphytobenthos populations. The presence of benthic microalgae in the sediments landward is consistent with previous works confirming the importance of *S. alveolata* bioconstructions in enhancing the local benthic primary production (Jones et al., 2018). Jones et al. (2018) have also demonstrated how the engineered sediment significantly affects the sedimentary characteristics of the associated reef sediment, specifically grain-size, organic matter content and ultimately microphytobenthos. 3-dimensional engineered structures act as a physical barrier: wave energy is reduced and tidal currents are slowed, increasing sedimentation between reef structures and coastline (Noernberg et al., 2010; Desroy et al., 2011; Jones et al., 2018).

Contribution of Hyperspectral and Lidar Combination to Reef Status Estimation

Estimating the ecological status of benthic habitats is a requirement of the European Union Habitat Directive, where reef-habitats are listed as priority (Council Directive 92/43/EEC). *Sabellaria alveolata* reefs of varying abundance are common on all European coasts and all developments toward automatic assessment of ecological status of this habitat would tremendously help large scale ecological assessments, while limiting time consuming and costly local surveys. Previous local investigation of reef ecological status based on reef types (veneer, hummock, platform) and phases (retrogradation and progradation) are costly in human resources and showed high inter-operator variability (Desroy et al., 2011). In this study, prograding and retrograding phases accurate map was provided with 0.5 m spatial resolution. An overall classification accuracy and Kappa coefficient of respectively 0.93 and 0.86 can be reached when using a validation against field data that takes into account a large sampling dataset. The sample field data plots on ecological status classification map also showed good coherence in terms of distribution pattern. This shows that the combination of LiDAR and hyperspectral reflectance variables had a robust explanatory capacity of the variability of *S. alveolata* reef ecological status. Indeed, LiDAR has also proven to be effective in characterizing health status of other ecosystems, namely shallow coral reefs. Using an artificial neural network classification, Collin et al. (2018) have shown that the dual combination of LiDAR surface and intensity variables had a robust explanatory power to predict the variability of coral reef states, with an overall accuracy of 0.75. We showed here that combined remote-sensing techniques can provide a high-confidence assessment of the prograding or retrograding phase of this habitat. This definitely calls for larger applications to other coastal areas.

The ecological status of *S. alveolata* reef was mapped continuously throughout Champeaux site. The 50 cm spatial resolution targeted in the present study outperformed the 75 m in Desroy et al. (2011). The latter authors used *in situ* expert-dependent estimation, while we based our method on an automatic objective processing for reef status estimation. Spatial patterns emerging from ecological status classification, also display a barrier reef on sand with a vigorous seaward front core, while the retrograded and sparse reefs are mainly located in the south-east part and next to shoreline. This seems to be consistent with previous work carried out by Collin et al. (2019) that have described a strong polarization of *S. alveolata* reefs with high abundance on forereef and low abundance on backreef. The forereef is subject to strong hydrodynamic and potentially higher coarse sediment resuspension, leading to increased tube-building activity, while the back reef mainly expands into more sheltered and muddier environments, less favorable to *S. alveolata* development (Bonnot-Courtois et al., 2008). Environmental impacts may also be exacerbated by human activities which shape the spatial pattern of reef status. Degraded reefs are mostly present in areas that are easily accessible to pedestrians. As it was observed for Mediterranean *S. alveolata* reef (Lisco et al., 2020), this degraded localization most likely drives the direct mechanical disturbances related to higher trampling and recreational fishing, leading to massive degradation of some reef areas (Dubois et al., 2002).

Perspectives for S. *alveolata* Reef Monitoring and Management

The trained classification yielded very accurate benthic feature identification. However, some pixels were wrongly classified. Processing improvements are thereby still needed to improve discrimination between mixed up classes. The strategy of field data acquisition can also be optimized to provide a sampling as balanced as possible between the different classes targeted. This can increase the efficiency of both calibration and validation steps. Another crucial criterion is the position accuracy, due to the high heterogeneity of the seafloor: an inaccuracy of only few meters often means a different substrate, a different species or a different ecological status (Florén et al., 2015). In future studies, field data should be collected and accurately positioned, by using for example DGPS (Differential Global Positioning System), to facilitate and make more robust accuracy assessment achievement. Placing benthic markers that can be identified in the imagery, as suggested by Mumby et al. (2004), is also a possibility to address this issue. Moreover, other classification algorithms, such as deep learning prediction (LeCun et al., 2015) should also be tested to examine their powerfulness compared to Mahalanobis distance based classification. This may allow for a better estimation of the areas occupied by benthic habitats, more particularly *S. alveolata* bioconstructions. Such a metric can be used in spatiotemporal dynamic monitoring or even integrated into ecological status indicators, as is the case for other habitats in European Directive framework (Duarte et al., 2017).

Regarding *S. alveolata r*eef status estimation, the work reported here represents a first step which illustrates a promising approach, based on the combination of hyperspectral and LiDAR data. The review of coral reef monitoring and assessment technologies carried out by Obura et al. (2019), emphasized that satellite data combined with airborne imagery and airborne LiDAR data are now routinely used in identifying and monitoring marine protected areas as a new ways to assess benthic habitat. Quantitative estimation of *S. alveolata* ecological status index is an attainable goal: further work, particularly a linear mixing model approach (Bioucas-Dias et al., 2012; Bajjouk et al., 2019b), may prove to be relevant to estimate *S. alveolata* epibiont abundance—a key element in reef dynamics—and possibly further develop a finer metric than the prograding vs. retrograding status qualitative estimation. Integrated applications of these remote sensing techniques are still lacking to target *S. alveolata* ecosystem spatial ecology. As wisely pointed out by D'Urban et al. (2020), there is a strong need for policymakers to have access to high-quality environmental information, in order to make objective conservation decisions leading to ecosystem service maintenance. In addition to helping gain a better understanding of ecological processes, 3D remote sensing approaches constitute an efficient tool for recording accurate environmental key information at both large scale and high spatial resolution. These characteristics are of great interest, especially for the study of rapidly changing environments such as those associated with *S. alveolata* reefs. We also highlight the relevance of such information in improving communication and targeted awareness-raising through their ability to provide virtual reality system overviews.

CONCLUSION

The present study is an initial step toward designing a new alternative operational approach targeting broad-scale, high-resolution, non-destructive monitoring of *S. alveolata* reefs. The main goal is to assess the potential of optical imagery, more specifically hyeperspectral and LiDAR data, for a high-resolution (0.5 m) spatial characterization of the *S. alveolata* reef ecosystem.

The main benthic features showed clear differences in their field spectral reflectance shapes and/or their magnitudes. However, statistical analysis revealed the difficulty to distinguish between some types solely on the basis of their spectral signatures. The joint analysis of the LiDAR sensor information with the hyperspectral imagery provides an additional characteristic on the nature of the topographic complexity, thus enhancing the discrimination capability.

By using an automatic supervised classification, we have shown for the first time the potential of hyperspectral and Lidar signal combination (i) to accurately discriminate the two *S. alveolata* reef forms, large reef developing on sand and smaller veneers encrusting rocky shore areas, as well as its main ecosystem associated habitats and (ii) to reliably and remotely estimate the spatial structure of these bioconstruction prograding and retrograding dynamic phases as a proxy of ecological status. This latter is commonly required by both scientists, for better understanding of ecosystem process, and managers, for better implementation of European directives.

The study also highlighted the importance of field positioning accuracy to perform a robust statistical validation, mainly in high spatial heterogeneity as displays the *S. alveolata* reefs. Further work has therefore been identified to improve obtained results and to provide quantitative information on *S. alveolata* reef ecological status. Such information, if is provided on a large scale and at a sufficient frequency, will allow (i) improved understanding of physical and biological structural changes of these complex bioconstructions, (ii) better prediction of their spatio-temporal evolution and (iii) elaboration of appropriate measures for their preservation and socio-economic management.

DATA AVAILABILITY STATEMENT

The online publication of data is planned at the end of the BIOHERM project in 2021. Requests to access the datasets should be directed to touria.bajjouk@ifremer.fr.

AUTHOR CONTRIBUTIONS

TB, LD, and MD designed the project strategy and performed funding acquisition. TB supervised and managed the project. TB, CJ, and SD collected field data. AD and CJ carried out the laboratory analysis. TB performed data processing and experimental validation and drafted the manuscript. SD validated the classification models. TB, CJ, SD, LD, and MD contributed to manuscript writing and editing. All authors shared the responsibility for contributing to the final version of the manuscript.

FUNDING

This work was funded by the CNES (French National Center for Space Studies) as part of the space scientific research TOSCA program to support the CHIMERE sensor and the Biodiversity mission. The study was carried out within the framework of the BIOHERM project (Ref. 4911/4500062124).

ACKNOWLEDGMENTS

We are very grateful to Yves Pastol from the SHOM (Hydrographic and Oceanographic Service of the Navy) for providing Lidar data acquired within the framework of Litto3D program. We also thank Pierre-Olivier Liabot and Simon Martin from Ifremer, for their help on field data acquisition, as well as Hytech Imaging for airborne data acquisition. We wish to warmly thank Amelia Curd, native English-speaker, for proofreading the manuscript. Finally, we would like to gratefully thank the two reviewers for their valuable comments and suggestions.

REFERENCES

Bajjouk, T., Mouquet, P., Ropert, M., Quod, J. P., Hoarau, L., Bigot, L., et al. (2019a). Detection of changes in shallow coral reefs status: towards a spatial approach using hyperspectral and multispectral data. *Ecol. Indic.* 96, 174–191. doi: 10.1016/j.ecolind.2018.08.052

Bajjouk, T., Zarati, I., Drumetz, L., and Dalla Mura, M. (2019b). "Spatial characterization of marine vegetation using semisupervised hyperspectral unmixing," in *Proceedings of the 2019 10th Workshop on Hyperspectral Imaging and Signal Processing: Evolution in Remote Sensing (WHISPERS)*, Piscataway, NJ.doi: 10.1109/WHISPERS.2019.8920949

Basuyaux, O., and Lecornu, B. (2015). *Cartographie des Hermelles sur la Façade ouest du Cotentin en 2014*. Durham: Produit SMEL.

Beisiegel, K., Darr, A., Gogina, M., and Zettler, M. L. (2017). Benefits and shortcomings of non-destructive benthic imagery for monitoring hard-bottom habitats. *Mar. Pollut. Bull.* 121, 5–15. doi: 10.1016/j.marpolbul.2017.04.009

Bioucas-Dias, J. M., Plaza, A., Dobigeon, N., Parente, M., Du, Q., Gader, P., et al. (2012). "Hyperspectral unmixing overview: geometrical, statistical, and sparse regression-based approaches," in *Proceedings of the IEEE Journal of Selected Topics in Applied Earth Observations and Remote Sensing*, Piscataway, NJ. doi: 10.1109/JSTARS.2012.2194696

Bonifazi, A., Lezzi, M., Ventura, D., Lisco, S., Cardone, F., and Gravina, M. F. (2019). Macrofaunal biodiversity associated with different developmental phases of a threatened Mediterranean *Sabellaria alveolata* (Linnaeus, 1767) reef. *Mar. Environ. Res.* 145, 97–111. doi: 10.1016/j.marenvres.2019.02.009

Bonnot-Courtois, C., Bassoulet, P., Tessier, B., Cayocca, F., Le Hir, P., and Baltzer, A. (2008). Remaniements sedimentaires superficiels sur l'estran occidental de la baie du Mont-Saint-Michel. *Eur. J. Environ. Civil Eng.* 12, 51–65. doi: 10.3166/ejece.12.51-65

Bonnot-Courtois, C., Fournier, J., Rollet, C., Populus, J., Guillaumont, B., and Loarer, R. (2005). Bio-morpho-sedimentary cartography of the tidal zones in the French Benthic Network context (complementary of coastal orthophotographs and Lidar data). *Photo Interprét.* 41, 13–27.

Brown, K. (2004). "Increasing classification accuracy of coastal habitats using integrated airborne remote sensing," in *Proceedings of the European Association of Remote Sensing Laboratories eProceedings, 3, SIG "Remote Sensing of the Coastal Zone*, Belgium.

Chang, C. I., Liu, W., and Chang, C. C. (2004). "Discrimination and identification for subpixel targets in hyperspectral imagery," in *Proceedings of the 2004 International Conference on Image Processing*, New York, NY.

Chennu, A., Färber, P., Volkenborn, N., Al-Najjar, M. A. A., Janssen, F., de Beer, D., et al. (2013). Hyperspectral imaging of the microscale distribution and dynamics of microphytobenthos in intertidal sediments. *Limnol. Oceanogr. Methods* 11, 511–528. doi: 10.4319/lom.2013.11.511

Collin, A., Dubois, S., James, D., and Houet, T. (2019). Improving intertidal reef mapping using UAV surface, red edge, and near-infrared data. *Drones* 3:67. doi: 10.3390/drones3030067

Collin, A., Dubois, S., Ramambason, C., and Etienne, S. (2018). Very high-resolution mapping of emerging biogenic reefs using airborne optical imagery and neural network: the honeycomb worm (*Sabellaria alveolata*) case study. *Int. J. Remote Sens.* 39, 5660–5675. doi: 10.1080/01431161.2018.1484964

Coupel, P., Matsuoka, A., Ruiz-Pino, D., Gosselin, M., Marie, D., Tremblay, J. E., et al. (2015). Pigment signatures of phytoplankton communities in the Beaufort Sea. *Biogeosciences* 12, 991–1006. doi: 10.5194/bg-12-991-2015

Cracknell, A. P. (2001). The exciting and totally unanticipated success of the AVHRR in applications for which it was never intended. *Adv. Space Res.* 28, 233–240. doi: 10.1016/s0273-1177(01)00349-0

Curd, A., Cordier, C., Firth, L. B., Bush, L., Gruet, Y., Le Mao, P., et al. (2020). A broad-scale long-term dataset of *Sabellaria alveolata* distribution and abundance curated through the REEHAB (REEf HABitat) Project. *SEANOE* doi: 10.17882/72164

Curd, A., Pernet, F., Corporeau, C., Delisle, L., Firth, L. B., Nunes, F. L., et al. (2019). Connecting organic to mineral: how the physiological state of an ecosystem-engineer is linked to its habitat structure. *Ecol. Indic.* 98, 49–60. doi: 10.1016/j.ecolind.2018.10.044

Davies, A. B., and Asner, G. P. (2014). Advances in animal ecology from 3D-LiDAR ecosystem mapping. *Trends Ecol. Evol.* 29, 681–691. doi: 10.1016/j.tree.2014.10.005

De Maesschalck, R., Jouan-Rimbaud, D., and Massart, D. L. (2000). The mahalanobis distance. *Chemometr. Intellig. Lab. Syst.* 50, 1–18. doi: 10.1016/S0169-7439(99)00047-7

Desroy, N., Dubois, S. F., Fournier, J., Ricquiers, L., Le Mao, P., Guerin, L., et al. (2011). The Conservation status of *Sabellaria alveolata* (L.) (*Polychaeta*: *Sabellariidae*) reefs in the Bay of Mont-Saint-Michel. *Aquat. Conserv. Mar. Freshw. Ecosyst.* 21, 462–471. doi: 10.1002/aqc.1206

Duarte, B., Neto, J. M., Marques, J. C., Adams, J. B., and Caçador, I. (2017). Marine angiosperm indices used to assess ecological status within the water framework directive and south african national water act: learning from differences and common issues. *Ecol. Indic.* 83, 192–200. doi: 10.1016/j.ecolind.2017.07.032

Dubois, S., Commito, J. A., Olivier, F., and Retiere, C. (2006). Effects of epibionts on *Sabellaria alveolata* (L.) biogenic reefs and their associated fauna in the Bay of Mont Saint-Michel. *Estuar. Coast. Shelf Sci.* 68, 635–646. doi: 10.1016/j.ecss.2006.03.010

Dubois, S., Retiere, C., and Olivier, F. (2002). Biodiversity associated with *Sabellaria alveolata* (*Polychaeta*: *Sabellariidae*) reefs: effects of human disturbances. *J. Mar. Biol. Assoc. U. K.* 82, 817-26. doi: 10.1017/S0025315402006185

D'Urban, J. T., Williams, G. J., Walker-Springett, G., and Davies, A. J. (2020). Three-dimensional digital mapping of ecosystems: a new era in spatial ecology. *Proc. R. Soc. B* 287:20192383. doi: 10.1098/rspb.2019.2383

Echappé, C., Gernez, P., Méléder, V., Jesus, B., Cognie, B., Decottignies, P., et al. (2018). Satellite remote sensing reveals a positive impact of living oyster reefs on microalgal biofilm development. *Biogeosciences* 15, 905–918. doi: 10.5194/bg-15-905-2018

Firth, L. B., Nova Mieszkowska, L. M., Grant, L. E., Bush, A. J., Davies, M. T., Frost, P. S., et al. (2015). Historical comparisons reveal multiple drivers of decadal change of an ecosystem engineer at the range edge. *Ecol. Evol.* 5, 3210-22. doi: 10.1002/ece3.1556

Florén, K., Tulldahl, M., and Wikström, S. (2015). "Using Lidar and satellite data to estimate cover of substrate and vegetation in the Baltic sea," in *Proceedings of the 35th EARSeL Symposium - European Remote Sensing: Progress, Challenges and Opportunities Stockholm*, Sweden.

Foody, G. M., and Mathur, A. (2006). The use of small training sets containing mixed pixels for accurate hard image classification: training on mixed spectral responses for classification by a SVM. *Remote Sens. Environ.* 103, 179–189. doi: 10.1016/j.rse.2006.04.001

Fyfe, S. K. (2003). Spatial and temporal variation in spectral reflectance: are seagrass species spectrally distinct? *Limnol. Oceanogr.* 48, 464–479. doi: 10.4319/lo.2003.48.1_part_2.0464

Govender, M., Chetty, K., Naiken, V., and Bulcock, H. (2008). A comparison of satellite hyperspectral and multispectral remote sensing imagery for improved classification and mapping of vegetation. *Water SA* 34, 147–154. doi: 10.4314/wsa.v34i2.183634

Griffin, R. A., Jones, R. E., Lough, N. E., Lindenbaum, C. P., Alvarez, M. C., Clark, K. A., et al. (2020). Effectiveness of acoustic cameras as tools for assessing biogenic structures formed by Sabellaria in highly turbid environments. *Aquat. Conserv. Mar. Freshw. Ecosyst.* 30, 1121–1136. doi: 10.1002/aqc.3313

Gruet, Y. (1972). Aspects morphologiques et dynamiques de constructions de l'annélide polychète *Sabellaria alveolata* (Linné). *Revue Travaux l'Institut. Pêches Mar.* 36, 131–161.

Gruet, Y. (1982). *Recherches sur L'écologie des "Récifs" D'hermelles Édifiés par l'Annélide Polychète Sabellaria alveolata Linné*. Ph. D thesis, Université de Nantes, Nantes.

Gruet, Y. (1986). Spatio-temporal changes of sabellarian reefs built by the sedentary polychaete *Sabellaria alveolata* (Linne). *Mar. Ecol.* 7, 303–319. doi: 10.1111/j.1439-0485.1986.tb00166.x

Guillaumont, B. (1991). "Utilisation de l'imagerie satellitaire pour les comparaisons spatiales et temporelles en zones intertidale," in *Proceedings of the Esturaries ans Coasts: Spatial and Temporal Intercomparisons - ECSA 19 Symposium*, Olsen.

Guillaumont, B., Bajjouk, T., and Talec, P. (1997). "Seaweed and remote sensing: a critical review of sensors and data processing," in *Progress in Phycological Research*, eds F. E. Round, and D. J. Chapman (London: Biopress Ltd), 213–282.

Jesus, B., Rosa, P., Mouget, J. L., Méléder, V., Launeau, P., and Barillé, L. (2014). Spectral-radiometric analysis of taxonomically mixed microphytobenthic biofilms. *Remote Sens. Environ.* 140, 196–205. doi: 10.1016/j.rse.2013.08.040

Jones, A. (2017). *Effect of an Engineer Species on the Diversity and Functioning of Benthic Communities: the Sabellaria Alveolata Reef Habitat*, Doctoral thesis, Université de Bretagne occidentale, Brest.

Jones, A., Dubois, S., Desroy, N., and Fournier, J. (2018). Interplay between abiotic factors and species assemblages mediated by the ecosystem engineer *Sabellaria alveolata* (Annelida: Polychaeta). *Estuar. Coast. Shelf Sci.* 200, 1–18. doi: 10.1016/j.ecss.2017.10.001

Kinberg, J. G. H. (1866). Annulata Nova. Öfversigt af Königlich vetenskapsakademiens förhandlingar. *Remote Sens.* 22, 239–258.

Kirk, J. T. O. (1977). Thermal dissociation of fucoxanthin-prothein binding in pigment complexes from chloroplasts of *Hormosira*(phaeophyta). *Plant Sci. Lett.* 9, 373–380. doi: 10.1016/0304-4211(77)90109-2

Kuczynska, P., Jemiola-Rzeminska, M., and Strzalka, K. (2015). Photosynthetic pigments in diatoms. *Mar. Drugs* 13, 5847–5881. doi: 10.3390/md13095847

Kushnir, V., Korotaev, G., Kogan, F., and Powel, A. M. (2011). "Consequences of Land and Marine Ecosystems Interaction for the Black Sea Coastal Zone," in *Use of Satellite and In-Situ Data to Improve Sustainability. NATO Science for Peace and Security Series C: Environmental Security*, eds F. Kogan, A. Powell, and O. Fedorov (Dordrecht: Springer), doi: 10.1007/978-90-481-9618-0_21

Lana, P. D., and Gruet, Y. (1989). *Sabellaria wilsoni* sp.n. (*Polychaeta*, *Sabellariidae*) from the southeast coast of Brazil. *Zool. Scripta* 18, 239–244. doi: 10.1111/j.1463-6409.1989.tb00449.x

Launeau, P., Méléder, V., Verpoorter, C., Barillé, L., Kazemipour-Ricci, F., Giraud, M., et al. (2018). Microphytobenthos biomass and diversity mapping at different spatial scales with a hyperspectral optical model. *Remote Sens.* 10:716. doi: 10.3390/rs10050716

Lecornu, B., Schlund, E., Basuyaux, O., Cantat, O., and Dauvin, J. C. (2016). Dynamics (from 2010-2011 to 2014) of *Sabellaria alveolata* reefs on the western coast of Cotentin (English Channel, France). *Reg. Stud. Mar. Sci.* 8, 157–169. doi: 10.1016/j.rsma.2016.07.004

Lecours, V., Devillers, R., Schneider, D. C., Lucieer, V. L., Brown, C. J., and Edinger, E. N. (2015). Spatial scale and geographic context in benthic habitat mapping: review and future directions. *Mar. Ecol. Prog. Ser.* 535, 259–284. doi: 10.3354/meps11378

LeCun, Y., Bengio, Y., and Hinton, G. (2015). Deep learning. *Nature* 521:436. doi: 10.1038/nature14539

Lisco, S. N., Acquafredda, P., Gallicchio, S., Sabato, L., Bonifazi, A., Cardone, F., et al. (2020). The sedimentary dynamics of *Sabellaria alveolata* bioconstructions (Ostia, Tyrrhenian Sea, central Italy). *J. Palaeogeogr.* 9, 1–18. doi: 10.1186/s42501-019-0050-6

Litto3D (2019). Litto3D Partie Maritime. Produit Réseau d'Observation du Littoral Normand et Picard (ROLNP), Service Hydrographique et Océanographique de la Marine (SHOM), l'Etat, Région Normandie, Région Hauts-de-France, Agence de l'eau Seine Normandie, Agence de l'eau Artois-Picardie, Parc Naturel Marin des Estuaires Picards et de la Mer d'Opale- V. 20190831.

Marchand, Y., and Cazoulat, R. (2003). Biological reef survey using spot satellite data classification by cellular automata method e bay of Mont Saint-Michel. *Comput. Geosci.* 29, 413–421. doi: 10.1016/s0098-3004(02)00116-4

McLachlan, G. J. (1999). Mahalanobis distance. *Resonance* 4, 20–26. doi: 10.1007/BF02834632

Méléder, V., Launeau, P., Barillé, L., and Rincé, Y. (2003). Cartographie des peuplements du microphytobenthos par télédétection spatiale visible-infrarouge dans un écosystème conchylicole. *C. R. Biol.* 326, 377–389. doi: 10.1016/s1631-0691(03)00125-2

Muir, A. P., Nunes, F. L., Dubois, S. F., and Pernet, F. (2016). Lipid remodelling in the reef-building honeycomb worm, *Sabellaria alveolata*, reflects acclimation and local adaptation to temperature. *Sci. Rep.* 6:35669. doi: 10.1038/srep35669

Mumby, P. J., Hedley, J. D., Chisholm, J. R. M., Clark, C. D., Ripley, H., and Jaubert, J. (2004). The cover of living and dead corals from airborne remote sensing. *Coral Reefs* 23, 171–183. doi: 10.1007/s00338-004-0382-1

Noernberg, M. A., Fournier, J., Dubois, S., and Populus, J. (2010). Using airborne laser altimetry to estimate *Sabellaria alveolata* (Polychaeta: Sabellariidae) reefs volume in tidal flat environments. *Estuar. Coast. Shelf Sci.* 90, 93–102. doi: 10.1016/j.ecss.2010.07.014

Obura, D. O., Appeltans, W., Amornthammarong, N., Aeby, G., Bax, N. J., Bishop, J., et al. (2019). Coral reef monitoring, reef assessment technologies, and ecosystem-based management. *Front. Mar. Sci.* 6:580. doi: 10.3389/fmars.2019.00580

Petit, T., Bajjouk, T., Mouquet, P., Rochette, S., Vozel, B., and Delacourt, C. (2017). Hyperspectral remote sensing of coral reefs by semi-analytical model inversion - Comparison of different inversion setups. *Remote Sens. Environ.* 190, 348–365. doi: 10.1016/j.rse.2017.01.004

Pu, R., Gong, P., Tian, Y., Miao, X., Carruthers, R. I., and Anderson, G. L. (2008). Using classification and NDVI differencing methods for monitoring sparse vegetation coverage: a case study of saltcedar in Nevada, USA. *Internat. J. Remote Sens.* 29, 3987–4011. doi: 10.1080/01431160801908095

Rhodes, C. J., Henrys, P., Siriwardena, G. M., Whittingham, M. J., and Norton, L. R. (2015). The relative value of field survey and remote sensing for biodiversity assessment. *Methods Ecol. Evol.* 6, 772–781. doi: 10.1111/2041-210x.12385

Richards, J. A. (1999). *Remote Sensing Digital Image Analysis*. Berlin: Springer-Verlag. doi: 10.1007/978-3-662-03978-6

Schmidt, K. S., and Skidmore, A. K. (2003). Spectral discrimination of vegetation types in a coastal wetland. *Remote Sens. Environ.* 85, 92–108. doi: 10.1016/s0034-4257(02)00196-7

Stuckens, J., Coppin, P. R., and Bauer, M. E. (2000). Integrating contextual information with per-pixel classification for improved land cover classification. *Remote Sens. Environ.* 71, 282–296. doi: 10.1016/s0034-4257(99)00083-8

Tucker, C. J. (1979). Red and photographic infrared linear combinations for monitoring vegetation. *Remote Sens. Environ.* 8, 127–150. doi: 10.1016/0034-4257(79)90013-0

Utermöhl, H. (1958). Zur Vervoll kommung der quantitativen phytoplankton-methodik. *Mitteilungen. Int. Ver. Theor. Angew. Limnol.* 9, 1–38. doi: 10.1080/05384680.1958.11904091

Van der Wal, D., Wielemaker-van den Dool, A., and Herman, P. M. (2010). Spatial synchrony in intertidal benthic algal biomass in temperate coastal and estuarine ecosystems. *Ecosystems* 2010, 338–351. doi: 10.1007/s10021-010-9322-9

Ventura, D., Bonifazi, A., Gravina, M. F., Belluscio, A., and Ardizzone, G. (2018). Mapping and classification of ecologically sensitive marine habitats using unmanned aerial vehicle (UAV) imagery and object-based image analysis (OBIA). *Remote Sens.* 10:1331. doi: 10.3390/rs10091331

Wedding, L. M., Friedlander, A. M., McGranaghan, M., Yost, R. S., and Monaco, M. E. (2008). Using bathymetric lidar to define nearshore benthic habitat complexity: implications for management of reef fish assemblages in Hawaii. *Remote Sens. Environ.* 112, 4159–4165. doi: 10.1016/J.RSE.2008.01.025

Xiang, S., Nie, F., and Zhang, C. (2008). Learning a Mahalanobis distance metric for data clustering and classification. *Pat. Recogn.* 41, 3600–3612. doi: 10.1016/j.patcog.2008.05.018

Xing, E. P., Jordan, M. I., Russell, S. J., and Ng, A. Y. (2003). "Distance metric learning with application to clustering with side-information," in *Proceedings of the Advances in Neural Information Processing Systems*, Boston.

Conflict of Interest: The authors declare that the research was conducted in the absence of any commercial or financial relationships that could be construed as a potential conflict of interest.

frontiers in Marine Science

ORIGINAL RESEARCH
published: 21 October 2020
doi: 10.3389/fmars.2020.571115

Local Human Impacts Disrupt Relationships Between Benthic Reef Assemblages and Environmental Predictors

Amanda K. Ford[1,2,3,4], Jean-Baptiste Jouffray[3,5], Albert V. Norström[3], Bradley R. Moore[6,7,8], Maggy M. Nugues[9,10], Gareth J. Williams[11], Sonia Bejarano[12], Franck Magron[6], Christian Wild[2] and Sebastian C. A. Ferse[1,2]*

[1] Department of Ecology, Leibniz Centre for Tropical Marine Research (ZMT), Bremen, Germany, [2] Department of Marine Ecology, Faculty of Biology and Chemistry (FB2), University of Bremen, Bremen, Germany, [3] Stockholm Resilience Centre, Stockholm University, Stockholm, Sweden, [4] School of Marine Studies, Faculty of Science, Technology and Environment, The University of the South Pacific, Suva, Fiji, [5] Global Economic Dynamics and the Biosphere Academy Programme, Royal Swedish Academy of Sciences, Stockholm, Sweden, [6] Pacific Community (SPC), Noumea, New Caledonia, [7] Institute for Marine and Antarctic Studies, University of Tasmania, Hobart, TAS, Australia, [8] National Institute of Water and Atmospheric Research, Nelson, New Zealand, [9] EPHE, PSL Research University, UPVD-CNRS, USR3278 CRIOBE, Paris, France, [10] Labex Corail, CRIOBE, Moorea, French Polynesia, [11] School of Ocean Sciences, Bangor University, Anglesey, United Kingdom, [12] Reef Systems Research Group, Leibniz Centre for Tropical Marine Research (ZMT), Bremen, Germany

OPEN ACCESS

Edited by:
Cristina Linares, University of Barcelona, Spain

Reviewed by:
Kirsten L. L. Oleson, University of Hawai'i at Mānoa, United States
Nadine Schubert, University of Algarve, Portugal

***Correspondence:**
Amanda K. Ford
amandakford@hotmail.com

Specialty section:
This article was submitted to Marine Ecosystem Ecology, a section of the journal Frontiers in Marine Science

Received: *09 June 2020*
Accepted: *31 August 2020*
Published: *21 October 2020*

Citation:
Ford AK, Jouffray J-B, Norström AV, Moore BR, Nugues MM, Williams GJ, Bejarano S, Magron F, Wild C and Ferse SCA (2020) Local Human Impacts Disrupt Relationships Between Benthic Reef Assemblages and Environmental Predictors. Front. Mar. Sci. 7:571115. doi: 10.3389/fmars.2020.571115

Human activities are changing ecosystems at an unprecedented rate, yet large-scale studies into how local human impacts alter natural systems and interact with other aspects of global change are still lacking. Here we provide empirical evidence that local human impacts fundamentally alter relationships between ecological communities and environmental drivers. Using tropical coral reefs as a study system, we investigated the influence of contrasting levels of local human impact using a spatially extensive dataset spanning 62 outer reefs around inhabited Pacific islands. We tested how local human impacts (low versus high determined using a threshold of 25 people km^{-2} reef) affected benthic community (i) structure, and (ii) relationships with environmental predictors using pre-defined models and model selection tools. Data on reef depth, benthic assemblages, and herbivorous fish communities were collected from field surveys. Additional data on thermal stress, storm exposure, and market gravity (a function of human population size and reef accessibility) were extracted from public repositories. Findings revealed that reefs subject to high local human impact were characterised by relatively more turf algae (>10% higher mean absolute coverage) and lower live coral cover (9% less mean absolute coverage) than reefs subject to low local human impact, but had similar macroalgal cover and coral morphological composition. Models based on spatio-physical predictors were significantly more accurate in explaining the variation of benthic assemblages at sites with low (mean adjusted-R^2 = 0.35) rather than high local human impact, where relationships became much weaker (mean adjusted-R^2 = 0.10). Model selection procedures also identified a distinct shift in the relative importance of different herbivorous fish functional groups in explaining benthic communities depending on the local human impact level. These

results demonstrate that local human impacts alter natural systems and indicate that projecting climate change impacts may be particularly challenging at reefs close to higher human populations, where dependency and pressure on ecosystem services are highest.

Keywords: climate change, reef degradation, ecological reorganisation, ecological homogenisation, generalised additive models, model selection

INTRODUCTION

Humans have become a dominant force of planetary change (Steffen et al., 2007). Ecosystems worldwide are being fundamentally altered by climate change impacts against a diverse backdrop of local anthropogenic stressors. Our ability to reliably predict the future configuration of affected ecosystems requires a thorough understanding of interactions between these different stressor types (Williams et al., 2019). Increasing evidence indicates that ecosystems are being reorganised or homogenised into stress-tolerant or opportunistic communities, leading to novel systems that differ from their previous state in terms of their dominant constituents (Graham et al., 2014; Morse et al., 2014). Quantifying ecological reorganisation over broad scales remains challenging due to coarse taxonomic resolution inherent to large datasets that are necessary to address this topic. Nonetheless, this phenomenon may significantly alter a system's relationship with various environmental and climate change-related drivers (Côté and Darling, 2010; Williams G.J. et al., 2015). Understanding what role local human impacts play in driving ecological reorganisation and changing a system's relationship with its biophysical environment is thus pivotal to improving predictive models and informing local management (Robinson et al., 2018; Jouffray et al., 2019; Henderson et al., 2020).

Inherent high biodiversity and the presence of multiple stressors acting at local and global scales make tropical coral reefs a unique system to examine how local human impacts drive ecological states (Hoegh-Guldberg et al., 2007; Ban et al., 2014; Norström et al., 2016; Darling et al., 2019). Locally, rapidly expanding coastal development, sewage input, and agricultural practices are reducing water quality, whilst the modernisation of fishing gear and expedited market access are facilitating overexploitation of coastal fisheries resources (Fabricius et al., 2005; Brewer et al., 2012; Hamilton et al., 2012). Globally, the intensity and frequency of thermal anomalies, unusual weather patterns, and destructive storm events are increasing (Gattuso et al., 2015; van Hooidonk et al., 2016; IPCC, 2019), and recovery windows between stress events are narrowing (Riegl et al., 2013; Hughes et al., 2018). The productivity and provision of ecosystem services (e.g., Woodhead et al., 2019) of coral reef benthic communities differ depending on their composition (Ferrario et al., 2014; Rogers et al., 2018), underlining the importance of quantifying how communities are affected by global change. The widespread negative effects of climate change-related stressors are relatively well-understood. However, despite more than half the world's coral reefs being located within 30 min travel time from human populations (Maire et al., 2016), the role of local stressors remains somewhat contested. These local stressors can range greatly in their intensity depending on inherent factors such as human population density and the level of exploitation of, or reliance on, marine resources.

Higher human population densities have been linked to reductions in reef fish biomass and coral cover, and to increases in fleshy (turf and macro-) algal cover (Sandin et al., 2008; Williams I.D. et al., 2015; Heenan et al., 2016; Smith et al., 2016). However, coarse taxonomic resolution (inherent to large-scale datasets) can lead to the conclusion that there is no link between local stressors and reef condition (e.g., Bruno and Valdivia, 2016). This may be a particular issue in regions such as the tropical Pacific where species diversity is exceptionally high and fleshy macroalgae, frequently stated as principal alternative organisms on degraded reefs, do not play such a dominant role in benthic dynamics compared, for instance, to the Caribbean region (Roff and Mumby, 2012). Furthermore, reefs are increasingly existing in a partially degraded condition between distinct regimes (Mumby, 2017), likely having undergone ecological homogenisation resulting from the non-random removal of species with particular traits in response to environmental factors (McWilliam et al., 2020). In this case, coral cover can remain moderate but comprises a less diverse community of stress-tolerant and opportunistic types (Côté and Darling, 2010; van Woesik et al., 2011; Riegl et al., 2013). Ecological homogenisation is visible across reef habitat types, with inshore reefs that are naturally exposed to a more challenging environment (e.g., in terms of light, temperature, and sediment input) favouring a smaller species pool of stress-resistant corals compared to nearby outer reef habitats (Rogers, 1990; Browne et al., 2013; Williams et al., 2013; Schoepf et al., 2015; Morgan et al., 2016).

A recent study demonstrated that whilst sea surface temperature (SST), chlorophyll concentration, and wave energy have strong power in predicting benthic assemblages at remote reefs, this predictive power is lost or the relationships fundamentally altered at reefs closer to human populations (Williams G.J. et al., 2015). Considering the dominant role of humans in shaping ecosystems, factors associated with local anthropogenic impacts may have overtaken biophysical drivers in structuring these altered reefs. It has also been postulated that reorganisation toward a stress-tolerant coral community could increase resilience to climate change, assuming co-tolerance between local and climate change-related stressors (Côté and Darling, 2010), in line with the concept of "intrinsic resistance" (Darling and Côté, 2018). Indeed, coral richness does not translate into higher resilience to disturbances (Zhang et al., 2014). Better understanding and accounting for the role that local human impacts play in shaping benthic

communities and their relationships with environmental drivers is important for developing theories, designing experiments, setting baselines, informing management, as well as optimising large-scale spatial predictive models for coral reef futures.

Here, we investigate how local human impacts affect coral reef benthic communities in the tropical Pacific. We start by classifying 62 island sites into two levels of local human impact (low versus high) using a set threshold of human population density informed by previous work (i.e., D'agata et al., 2014). We then ask whether the level of local human impact influences benthic community structure or the relationship between benthic community structure and spatio-physical explanatory drivers. Lastly, we examine the relative roles of ten biophysical parameters as drivers of benthic community structure under low versus high local human impact. We hypothesised that benthic community structure would be more related to spatio-physical drivers on reefs exposed to low local human impact compared to those with high local human impact, where we expect human-associated factors to have become more dominant. This approach allowed us to develop on the findings of Williams G.J. et al. (2015) by testing whether decoupling between reefs and biophysical drivers in the presence of humans was also detectable between different levels of local human impact.

MATERIALS AND METHODS

Study Area and Sampling Design

This study intended to build on work from Williams G.J. et al. (2015) by assessing in more detail how local population density, rather than human presence/absence, potentially decouples the relationship between reef benthos and larger-scale environmental drivers. To do so, we utilised a large-scale dataset that is unique in having both site-level ecological (fish and benthic) and socio-economic data (in particular human density per reef area at the site level), which is missing from other datasets that rely on global socioeconomic estimates for human population density, or in some cases district-level surveys. Fish and benthic communities at 62 reefs within 17 different Pacific Island countries and territories were surveyed once between 2003 and 2008 (see **Supplementary Figure 1** for map) as part of the Pacific Regional Oceanic and Coastal Fisheries Development Programme (PROCFish/C/CoFish) under the auspices of the Pacific Community (SPC). Importantly, all reefs were in close vicinity to, and used by, coastal human communities across a large range of intensities (e.g., relative human density ranged from 1.3 to 1705 humans km^{-2} reef). For site disturbance history, sampling dates and detailed sampling methodology, refer to **Supplementary Table 1** and Pinca et al. (2010). Though it is important to acknowledge that the sampling programme was not originally designed in a way to address macroecological questions or aggregate beyond the state/territory level, we did our best to account for the shortcomings in the design by including additional information such as observer bias (see section "Data Analyses" for details on environmental parameters included). Furthermore, while data may not be representative of the current-day scenario, it is the trends that are important for this study. Accordingly, we are confident that despite some inevitable compromising, this gave us the best possible dataset to look at the effects of site-specific human density.

Field Surveys

Underwater surveys covered outer (fore-) reefs, with on average nine (n = 3–47) joint fish-benthic 50 m transects measured at each site. Transect data were pooled within each site. Reef fish communities were measured using the variable distance-sampling underwater visual census method along transects (described in Labrosse et al., 2002). Data on abundance and size were recorded to species-level for herbivorous fish. Counts were converted to biomass (g m^{-2}) from established length-weight relationships (Kulbicki et al., 2005). Benthic cover data was obtained using the medium-scale approach described by Clua et al. (2006). This method is based on a semi-quantitative description of ten 25 m^2 (5 × 5 m) quadrats laid down on each side of the 50 m transect (i.e., 20 replicate quadrats/500 m^2 per transect). Surveyors first recorded abiotic and live coral substrates, i.e., sand, rubble, rocky slab, boulders, and hard coral − live, bleached, and long dead, with live coral divided into broad morphologies (e.g., branching, encrusting, massive). Each component was quickly estimated using a semi-quantitative scale ranging from 0 to 100% per quadrat, in units of 5%. Secondly, benthic groups (e.g., macroalgae–inclusive of calcified and fleshy types, turf algae, crustose coralline algae [CCA], sponges, cyanobacteria) growing over abiotic substrate such as long dead coral were recorded using the same semi-quantitative scale (**Table 1**).

Fishing grounds were initially delineated from information given by local fishers and quantified from satellite interpretations (similar to methods in Close and Hall, 2006; Léopold et al., 2014). Total reef area (km^2) within each fishing ground was then derived from reef areas quantified by the Millennium Coral Reef Mapping Project from satellite images (Andréfouët et al., 2006). Socioeconomic assessments determined total population within communities with access to the fishing ground, allowing subsequent calculation of human population relative to reef area (referred to as "relative human density"). Finfish landings for each site, determined from interviews with fishers, were extrapolated to total finfish catch per year per reef area ("relative fishing pressure") (see Pinca et al., 2010).

Data Analyses

Response Variables

As response variables, we selected the main benthic groups (i.e., those with a mean composition >10% of benthic community): dead coral (incorporating long dead coral, rubble, boulders, and pavement), live hard coral, and algal groups (differentiating turf algae, macroalgae, and CCA). We also assessed the proportional representation (within the live hard coral community) of the three most commonly observed morphological groups: branching, encrusting and massive morphologies. Pairwise relationship tests (*corvif* function–Zuur et al., 2009) established no collinearity among the response variables (correlation; $R^2 < 0.5$). **Table 1** provides an overview of the benthic variables and their ranges.

TABLE 1 | Benthic variables included in the models and their ranges.

Variable	Description	Range (%)
live hard coral	mean cover (%) of live hard coral	6.1–65.1
dead hard coral	mean cover (%) of dead hard coral; including rubble, boulders, and pavement. Dead hard coral may also include biotic groups (i.e., growing over the dead coral), which are further classified as additional categories below*	5.5–61.2
branching morphologies	proportion (%) of branching coral morphologies within live hard coral community	0.1–85.6
encrusting morphologies	proportion (%) of encrusting coral morphologies within live hard coral community	2.8–72.9
massive morphologies	proportion (%) of massive coral morphologies within live hard coral community	0.1–60.6
CCA	mean cover (%) of crustose coralline algae	0.2–43.5
macroalgae	mean cover (%) of macroalgae; inclusive of calcified and fleshy types	0.0–31.2
turf algae	mean cover (%) of turf algae	0.0–45.6

**not all categories are mutually exclusive–abiotic (e.g., dead coral, sand) and live coral substrates were recorded up to 100%, and biotic cover (e.g., algal groups) was recorded separately up to 100% (i.e., sum of substrate and biotic cover ≠100%).*

Model Predictors

We had to make a feasible choice of how to determine low versus high impact sites. Rather than choosing a completely arbitrary threshold, we selected one that was informed by previous findings by D'agata et al. (2014)–using boosted regression trees for the same dataset, the authors identified 25 people km^{-2} reef to be the threshold after which taxonomic diversity of parrotfishes significantly declined. We then ran a sensitivity analysis to demonstrate how robust our findings were (see section "Assumptions and Sensitivity Tests"). To compare reefs exposed to different disturbance regimes, we thus categorised all sites into those subject to low (i.e., <25 people km^{-2} reef; $n = 29$) and high (i.e., >25 people km^{-2} reef; $n = 33$) local human impact. Relative human density correlates with relative exploitation–i.e., relative human density was collinear ($R^2 = 0.8$) with fishing pressure (tonnes fish km^{-2} reef $year^{-1}$; **Table 2**). This threshold was also a median point and allowed similar sample sizes in each impact level (see **Supplementary Figure 2**). Relative human density also showed weak positive correlation with market gravity–an index combining the population size of nearby human settlements and their accessibility to reefs (Cinner and Maire, 2018; Cinner et al., 2018). However, we decided to base our study on relative human density as we had unique site-level data and we see this metric to be more directly linked to benthic communities in terms of human density-dependent sewage and agricultural run-off in addition to subsistence and artisanal fishing.

The selected biophysical predictors included a variety of factors that were either collected during field surveys or extracted from public data repositories (**Table 2**). Due to inherent differences in coral reefs across latitudinal scales (e.g., Hughes et al., 1999; Harriott and Banks, 2002), latitude was represented by degree distance from the equator without differentiating between north and south (0–23.9°). Degree heating weeks (DHW) data were extracted from the NOAA Coral Reef Thermal Anomaly Database (CoRTAD version 4 — Casey et al., 2012). Storm exposure was quantified from the NOAA IBTrACS-WMO data (Knapp et al., 2010a,b) within ArcMAP 10.4 (ESRI, 2011), where the number of storms (categories 1–5 on the Saffir-Simpson Hurricane Scale) passing within a 50 km radius of each site (Behrmann projection) was extracted. Storm exposure and DHW data were confined to 12 years prior to each respective site's survey date based on the premise that remote reefs can recover from acute disturbances within this timeframe (Sheppard et al., 2008; Gilmour et al., 2013). Reef depth, estimated during field surveys, was averaged over all transects at each site. Island relief refers to each site's geomorphology, and was classified into three categories: atoll, low-lying island, and high island based on available information (see **Supplementary Table 1** for references), and authors' knowledge. Island relief was included as a predictor due to its known influence on coral reef benthic and fish communities (Donaldson, 2002; Houk et al., 2015). Herbivorous fish from selected families (e.g., excluding herbivorous damselfish) encountered during visual surveys were classified into functional groups according to Heenan et al. (2016) (see **Supplementary Table 2**). Biomasses (g m^{-2}) of the following functional groups were then incorporated as predictors: browsers, grazers, detritivores, scrapers and small excavators, and large excavators and bioeroders. Market gravity (Cinner and Maire, 2018) was extracted for each site in QGIS (QGIS Development Team, 2019) and was incorporated as a continuous predictor.

Prior to model fitting, paired plots were assessed for collinearity between model terms. Strong collinearity ($R^2 > -0.9$) between latitude and DHW precluded their joint inclusion in subsequent models, and consequently latitude was selected because of its complete reef-specific dataset (DHW data limited to $n = 55$ sites). Multi-collinearity was also then tested using the generalised variance inflation factor (*GVIF*) function (*car* package—Fox and Weisberg, 2019) where values >3 suggest collinearity; as a result longitude was excluded from all models and the joint inclusion of browsers and scrapers was prohibited (i.e., individual best-fit models -see "Statistical Models" section- were constrained to contain only one or the other).

Statistical Models

All statistical analyses were performed in R version 3.6.1 (R Development Core Team, 2019). Differences in benthic community structure between reefs exposed to low versus high local human impact level were tested using *t*-tests with appropriate variance structures depending on homogeneity of variance test outcomes. Due to surveyor discrepancies in recording turf algal cover, we created a random effect (*bias_score*)

TABLE 2 | Predictor descriptions and ranges at outer reefs.

Predictor	Description	Range
reef depth[a,b]	mean depth (m) of transects	3.9–10.5
degree heating weeks (DHW)	measure of cumulative thermal stress–sum of previous 12 weeks where thermal stress anomaly ≥1°C; value averaged over 12 years preceding survey; negatively collinear (R^2 = −0.9) with latitude; only available for n = 55 sites	0.6–3.5
latitude[a,b]	degrees (°) distance from equator (absolute value). Negatively collinear (R^2 = −0.9) with DHW	0.0–23.9
longitude	degrees (°) longitude on continuous scale (i.e., −175 counted as 185), included to account for distance from the Coral Triangle biodiversity hotspot	134.3–214.2 (i.e., −145.8)
storm exposure[a,b]	total number of storms (cat. 1 to 5 on the Saffir-Simpson Hurricane Scale) passing within 50 km of site within previous 12 years	0–14
relief[a,b]	3 classifications: 1 = atoll; 2 = low-lying island; 3 = high island	
browser biomass[b]	biomass (g m^{-2}) of browsers	0.1–58.5
detritivore biomass[b]	biomass (g m^{-2}) of detritivores	0.5–62.8
excavator biomass[b]	biomass (g m^{-2}) of large excavators and bioeroders	0.0–369.1
grazer biomass[b]	biomass (g m^{-2}) of grazers	1.1–161.0
scraper biomass[b]	biomass (g m^{-2}) of scrapers and small excavators	1.9–134.3
relative human density	number of people within communities of the primary/customary resource users (living adjacent to/accessing fishing grounds within the reef area) related to total reef area (people km^{-2} reef), positively collinear (R^2 = 0.7) with relative fishing pressure. Used to determine local human impact level	1.3–1705
relative fishing pressure	annual reef finfish catch (tonnes) km^{-2} reef $year^{-1}$; positively collinear (R^2 = 0.8) with relative human density	0.1–78.2
market gravity[b]	index that combines human population size and reef accessibility	0–1140

[a]*predictor incorporated in spatio-physical models.* [b]*predictor used in model selection procedures. For sources of data, see main text.*

to be incorporated within turf algae models (see **Supplementary Figure 3** for details). No surveyor-related discrepancies were evident for other benthic groups (see **Supplementary Figure 3**). To test how turf algal cover differed across the two local human impact levels we thus used a linear mixed effects model incorporating *bias_score* as a random effect. All hereon described models were run separately for sites predetermined to be exposed to either low or high local human impacts to explicitly test for decoupling of abiotic and biotic predictors under different disturbance regimes.

To test whether the level of local human impact influenced the relationship between benthic community structure and spatio-physical explanatory drivers, we developed a spatio-physical model (i.e., focussing on spatial and physical predictors only) that included storm exposure, reef depth, latitude, and island relief. To account for non-linear relationships between response variables and predictors, we applied generalised additive mixed effects models (GAMM) using the *gamm4* (Wood and Scheipl, 2014) and *lme4* packages. To account for possible spatial autocorrelation, ten unique island clusters (*cluster*) were identified and incorporated into models as a random effect (for details see **Supplementary Figure 4**). For turf algae models, *bias_score* was additionally included as a random effect. To avoid overfitting, the number of knots within models was limited to four. We retained the adjusted-R^2 (Adj-R^2) values from the model output to quantify each model's explanatory power. Adj-R^2 values for each response variable were then compared (by paired *t*-tests) to test overall differences in model performance in explaining benthic community structure under the two local human impact levels.

Lastly, to examine the relative roles of ten biophysical parameters as predictors of benthic community structure under low versus high local human impacts, we applied model selection techniques using the *MuMIn* package (Barton, 2016). From an initial model containing ten biophysical predictors (i.e., those included in the spatio-physical model as well as biomass of herbivorous fish functional groups, and market gravity–see **Table 2**), the dredge function was used to run all possible predictor combinations and rank models from best to worst based on Akaike weight. The function also returns a value between 0 and 1 for each predictor that reflects its relative importance (RI), representing the total Akaike weight of all models containing that predictor (i.e., higher values correspond to greater RI). Output models were restricted to comprising a maximum of four predictors. One sample (Niue) was removed from the model selection procedure due to a lack of data for market gravity (i.e., n = 61). Model selection was run separately for sites with low and high levels of local human impact, and all models incorporated the *uGamm* wrapper function to allow the inclusion of random effects consistent with spatio-physical model constructions. To assess incongruities between benthic communities exposed to different local human impact levels, we retained the best-fit model structures (i.e., all predictors included in models with Akaike weight >0.05) for each benthic response variable, as well as the RI of individual predictors.

Assumptions and Sensitivity Tests

All response variables were logit-transformed (appropriate for percentage data — Warton and Hui, 2011) using the *car* package, following adjustment using each respective variable's minimum value >0. All model predictors were standardised (*z*-scores) to allow comparisons between predictors with largely varying effect sizes and numeric values (Zuur et al., 2009). Model residuals were checked for the violation of model assumptions using the

gam.check function (see **Supplementary Figure 5**). As part of a sensitivity analysis, spatio-physical models were additionally run using ±5 and ±10 humans km^{-2} reef as a threshold from which to categorise "low" and "high" impact sites, with consistent outcomes observed (see **Supplementary Table 3**). Furthermore, we repeated the same for a range of thresholds based on human density relative to outer reef area (as opposed to full reef area), again with consistent outcomes observed (see **Supplementary Table 4**).

RESULTS

Benthic Assemblages Under Contrasting Local Human Impacts

Benthic communities subject to high local human impact were associated with lower live hard coral cover (−9.2% mean absolute coverage; *t*-test: $p = 0.002$; **Figure 1A**). However, the relative contribution of different coral morphologies within the live hard coral community did not differ significantly with local human impact level (**Figure 1B**). The only algal group that differed significantly depending on the local impact level was turf algae, which was higher under high local human impact (+10.7% mean absolute coverage; linear mixed effects model: $p = 0.015$; **Figure 1C**).

Predictive Strength of Spatio-Physical Model

The pre-defined spatio-physical model exhibited relatively high power in explaining benthic assemblage variance at sites with low local human impacts (mean Adj-R^2 ± SE; 0.35 ± 0.09; **Figure 2**), but model performance was severely compromised when local human impacts were high (0.10 ± 0.04; paired *t*-test: $p = 0.01$). When considering only the substrate types and dominant morphological groups (i.e., without the algal groups) the mean adjusted-R^2 for sites with low local human impacts increases to 0.44 ± 0.06 but stays unchanged at sites with high local human impacts. When local human impacts were low, spatio-physical predictors explained a high proportion of the variance of live hard coral (Adj-$R^2 = 0.52$) and macroalgae (Adj-$R^2 = 0.59$) cover, and the relative contribution of branching (Adj-$R^2 = 0.64$) and massive (Adj-$R^2 = 0.50$) coral morphologies. Conversely, these variables were consistently poorly explained when local human impacts were high (Adj-R^2 = 0.00, 0.26, 0.17, 0.10, respectively). No variance in turf algae was explained by this model for reefs at either local human impact level. Significant differences in the power of the spatio-physical model in explaining benthic assemblage variance between "low" and "high" impact sites held constant when the threshold was moved ±5 and 10 humans km^{-2} reef (i.e., paired *t*-test: $p < 0.05$; **Supplementary Table 3**).

Relative Importance of Predictors

Best-fit models tailored for each individual benthic variable comprised distinctly different predictors depending on the level of local human impact (**Figure 3A**). Two of the predictors where discrepancies were most apparent were storm exposure and grazer biomass, which were only selected for best-fit models at sites with low and high local human impacts, respectively. Similarly, reef depth was selected as part of best-fit models for more response variables (live hard coral, branching morphologies, and macroalgae) at sites with low local human impacts. Further discrepancies under the two levels of local human impact were revealed by comparing the mean RI of each predictor (**Figures 3B,C**), as the RI trends for predictors almost reversed between low versus high local human impact sites. At sites with low local human impacts, the individual predictors with the highest RI in explaining benthic communities were storm exposure, scraper biomass, and island relief, followed by reef depth (**Figure 3B**). Contrastingly, apart from island relief which was on average the most important predictor, storm exposure, scraper biomass, and reef depth were among the least important predictors when local human impact was high (**Figure 3C**). For benthic communities exposed to high local human impact, biomass of grazers, detritivores, and browsers, as well as market gravity, ranked as the most important predictors of benthic community structure.

Individual relationships of best-fit predictors for each response variable further emphasised discrepancies between benthic communities and environmental predictors driven by local human impacts (for all plots see **Supplementary Figure 6**). A clear example of this discrepancy can be seen in coral compositional changes with increasing storm exposure. Whilst live hard coral cover remained unrelated to storm exposure under both local human impact levels (**Figure 4A**), the morphological composition was closely correlated with storm exposure at sites where local human impacts were low (**Figures 4B–D**). Specifically, with increasing storm exposure, the relative proportion of branching morphologies decreased significantly (**Figure 4B**), whereas encrusting (**Figure 4C**) and massive (**Figure 4D**) morphologies increased. No morphological changes with storm exposure were observed at sites with high local human impacts. Though these relationships appear primarily driven by few points at the higher end of storm exposure, they remained consistent when all reefs exposed to >10 storms were removed from the analysis–i.e., significant at "low" impact sites (branching coral $p = 0.02$; encrusting coral $p = 0.02$; massive coral $p = 0.03$), insignificant at "high" impact sites (all morphological growth forms $p > 0.05$), and no relationship for either impact level for total live hard coral cover ($p > 0.05$).

DISCUSSION

Under increasing climate change-associated stressors and local anthropogenic influence (Burke et al., 2011; Gattuso et al., 2015; IPCC, 2019), it is particularly important for researchers and planners to maximise the ability of models to predict ecosystem futures to allow appropriate mitigation strategies to be implemented. This study indicates that the role of local human impacts in changing coral reef ecological communities and their responses to environmental drivers should be accounted for. The results revealed that local human impacts influenced

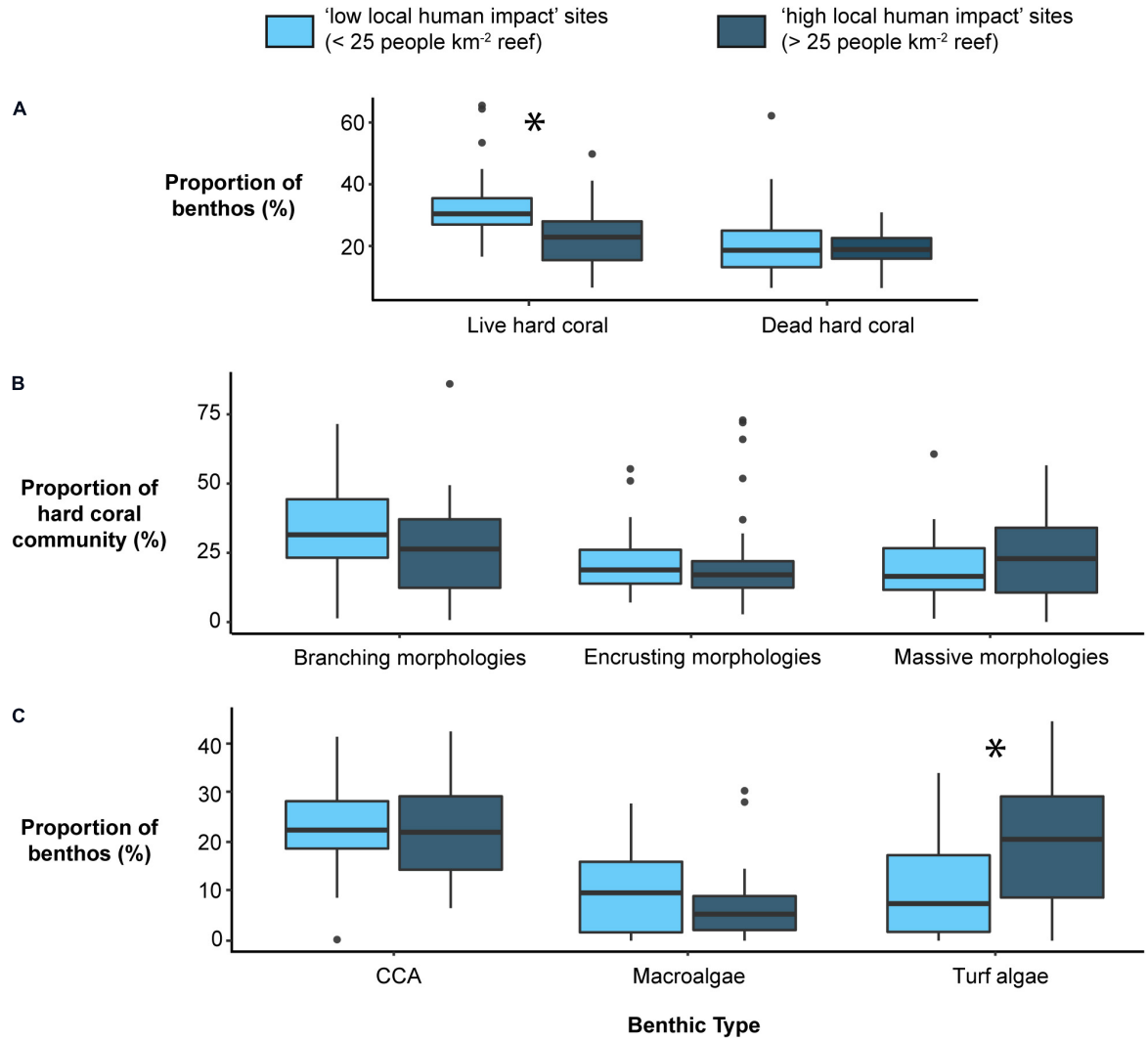

FIGURE 1 | Boxplots detailing **(A)** benthic cover (%) of substrate types (from left to right; live hard coral, dead hard coral), **(B)** the relative proportion (%) of the three most dominant morphologies in the live hard coral community (branching, encrusting, massive), and **(C)** benthic cover (%) of different algal groups (CCA, macroalgae, turf algae), at sites determined to have low or high local impacts. *Indicate significant differences ($p < 0.05$) in cover of the respective benthic variable between local impact levels according to two-sample *t*-tests, or for turf algae according to linear mixed effect models incorporating *bias_score* as a random effect (see section "Model Predictors").

both benthic community structure and relationships with biophysical predictors. Specifically, models based on spatio-physical predictors (i.e., reef depth, latitude, storm exposure, and relief) exhibited high power at explaining benthic assemblages under low local human impacts but were strongly compromised where local human impacts were high. Importantly, these outcomes remained similar when our threshold for human impacts, informed by previous work, was reduced or increased in the frame of a sensitivity analysis. Increasing sewage input, agricultural run-off, and sedimentation are potential changes associated with increasing human densities that reduce water quality and affect benthic communities (Fabricius, 2005; Fabricius et al., 2005; Ford et al., 2017). Furthermore, as fishing removes biomass of functionally important fish species, important top-down control of some benthic organisms is lost (Bellwood et al., 2004). These localised human impacts may homogenise benthic communities by driving ecological reorganisation that favours tolerant taxa (Darling et al., 2019). Our results indicate that this homogenisation may be occurring at Pacific Island reefs that are exposed to local human impacts, leading to novel systems that react fundamentally differently and unpredictably to environmental predictors compared to reefs less influenced by humans (Williams G.J. et al., 2015). In turn, we expect that local human impacts will influence responses of coral reefs to climate change-related stressors, and that reefs close to human populations will require context-specific management approaches to maximise their future sustainability and associated critical ecosystem services (Moberg and Folke, 1999).

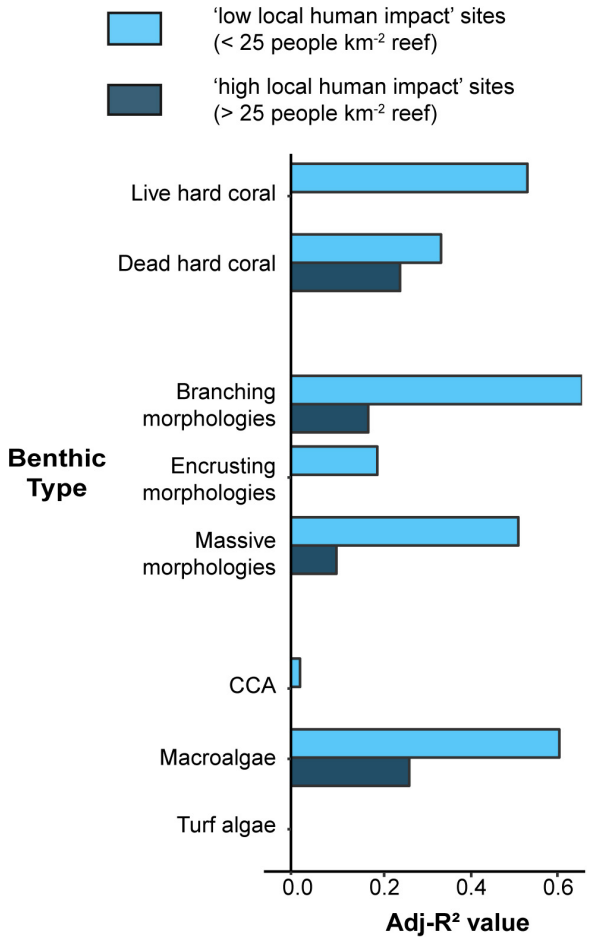

FIGURE 2 | Explanatory power (Adj-R^2) of the spatio-physical model (including the predictors storm exposure, reef depth, latitude, and island relief) in predicting individual benthic responses (live hard coral, dead hard coral, the proportion of branching, encrusting, and massive morphologies, and cover of algal groups CCA, macroalgae, and turf algae). Bars are absent where the Adj-R^2 value = 0.

The results emphasise the variation in benthic assemblages that exists among Pacific Island reefs exposed to different levels of local human impact. Benthic communities were not restricted to distinct regimes dominated by either hard corals or macroalgae, supporting previous studies from the Pacific (Bruno et al., 2009; Albert et al., 2012; Jouffray et al., 2015, 2019; Smith et al., 2016). In fact, macroalgae was the least common of all the algal groups, with turf algae and CCA more prominent on these outer reefs. Reefs at sites with higher local human impacts comprised significantly more turf algae and less live hard coral. Abundant and diverse outer reef coral communities (e.g., Ellis et al., 2017) have likely retained sensitive species, facilitating measurable differences (i.e., reductions in live hard coral cover) under higher local human impacts. Higher turf algae coverage at sites with more local human impacts provides further evidence that turf algae may become the dominant benthic group on degraded Pacific Island reefs (Jouffray et al., 2015; Smith et al., 2016; Tebbett and Bellwood, 2019). This may contrast with coral reef systems in the Caribbean, where macroalgae naturally play a more dominant role (Roff and Mumby, 2012). Furthermore, a signal of local human impact may have been detected if the data had distinguished macroalgae into fleshy/frondose and calcified types (e.g., Smith et al., 2016; Cannon et al., 2019). A similar link between human population size, hard coral cover, and turf algae has also recently been reported from sites in the Indian Ocean (Brown et al., 2017).

The spatio-physical models were weak in explaining the variance of benthic communities exposed to relatively more local human impacts. At these sites, model selection identified mostly local biotic controls or ecological features such as fish biomass and market gravity to be of highest RI. These results suggest that reefs altered by chronic local human impacts become decoupled from spatio-physical factors (Williams G.J. et al., 2015) and become more related to factors associated with human activities (e.g., market gravity) or local ecological features (e.g., biomass of functional groups of fish). Interestingly, this outcome contrasts to recent findings by Robinson et al. (2018) who did not detect decoupling at inhabited versus uninhabited reefs. Our different outcomes for decoupling could in part be explained by Robinson et al. (2018) combining (i) hard corals and CCA, and (ii) fleshy macroalgae and turf algae, each of which we found to exhibit different responses to local impacts (i.e., with higher local impacts hard coral cover decreased whereas CCA remained unchanged, turf algae increased whereas macroalgae remained unchanged). Model selection indicated that the specific spatio-physical predictors whose influence was most disrupted by local human impacts were storm exposure and reef depth. Storms can have mixed effects, benefitting reefs by alleviating thermal stress during warmer summer months but also causing physical destruction, particularly to delicate branching coral morphologies, leading to a higher proportion of more robust massive morphologies (Heron et al., 2005; Manzello et al., 2007). Accordingly, when local human impacts were low, coral communities comprised relatively less branching and more encrusting and massive morphologies at sites subject to more frequent storms. However, relationships between storm exposure and benthic assemblages were only observed at sites classified as having low local human impacts. Returning to the concept that local human impacts drive ecological reorganisation, we would expect reefs with less local human impacts to harbour a great diversity of species and morphologies, thus allowing for greater levels of ecological reorganisation in response to a stormier environment (i.e., favouring more robust morphologies). We anticipate that Pacific reefs would more likely display this phenomenon than Caribbean reefs due to a significantly larger initial species pool, with greater response diversity and functional redundancy affording a higher level of ecological insurance (Elmqvist et al., 2003; Bellwood et al., 2004; Nyström, 2006), and a loss of structurally complex coral species throughout most of the Caribbean over past decades (Alvarez-Filip et al., 2009). It would be interesting to test whether storm exposure results in more conspicuous negative impacts on coral cover (e.g., Gardner et al., 2005) in less diverse regions due to the limited capacity for ecological reorganisation to a tolerant community, even in

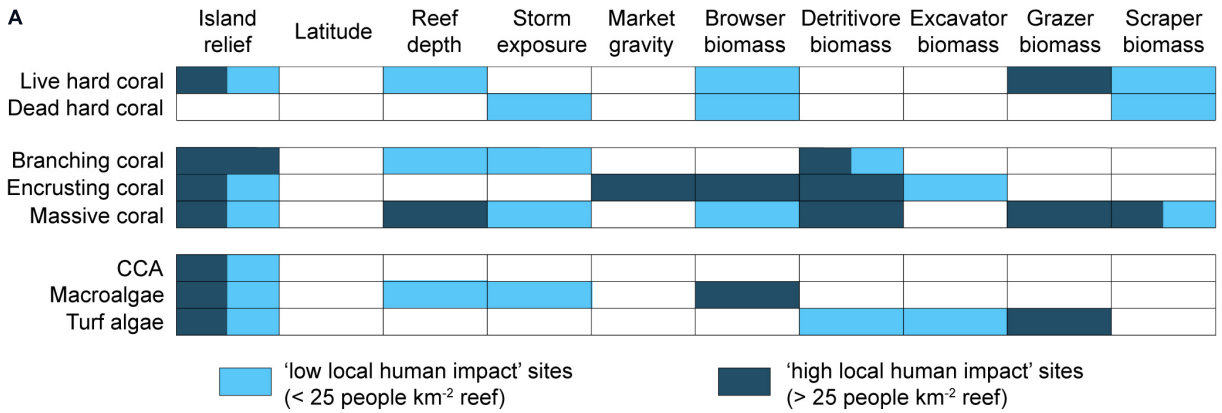

B

Predictor	RI
Storm exposure	0.288
Scraper biomass	0.250
Island relief	0.244
Reef depth	0.138
Browser biomass	0.086
Detritivore biomass	0.079
Excavator biomass	0.047
Latitude	0.040
Grazer biomass	0.031
Market gravity	0.023

C

Predictor	RI
Island relief	0.195
Browser biomass	0.096
Market gravity	0.084
Detritivore biomass	0.075
Grazer biomass	0.074
Latitude	0.044
Reef depth	0.042
Scraper biomass	0.041
Storm exposure	0.038
Excavator biomass	0.030

FIGURE 3 | (A) Outcome of model selection procedures: coloured boxes indicate that the predictor was selected for best-fit models (i.e., those with Akaike weight >0.05) at sites subject to low and/or high levels of local impacts. The overall mean relative importance of each predictor (RI–based on total Akaike weight of all models including that predictor) in explaining the benthic response variables is shown separately for sites subject to **(B)** low and **(C)** high local impacts. Note: though model selection was limited to four predictors per model, all predictors included in models with Akaike weight >0.05 are shown meaning there may be more than four predictors shown within one impact level for a response variable. Model outputs for best-fit models are available in **Supplementary Table 5**.

sites with minimal local human impact. In terms of reef depth, benthic communities at sites with low local human impacts also exhibited a higher level of depth-structuring (particularly in terms of coral cover and composition, consistent with Huston, 1985) compared to those with high local human impacts. Island relief was also identified as being a strong predictor of benthic community structure (despite being found to be a weak predictor on central-western Pacific reefs – Robinson et al., 2018), and interestingly this role was maintained regardless of local human impact level. Importantly, when considering latitude–collinear with DHW/cumulative thermal stress–as an individual predictor, our results neither contradict nor confirm previous observations that local impacts exacerbate the sensitivity of coral communities to thermal stress (Wiedenmann et al., 2013; Ellis et al., 2019), instead highlighting a large variance among sites.

Thermal stress and the intensity of storms are projected to increase under future climate change scenarios (IPCC, 2019), with profound implications for coral reefs and adjacent ecosystems. Our findings suggest that while the effects of factors associated with climate change (e.g., storm exposure) on Pacific reef benthic assemblages may be reasonably well-predicted where local impacts are low, system responses become less predictable as local human impacts increase. In both marine and terrestrial systems, structural changes caused by local impacts have profoundly changed how ecosystems respond to natural stressors: for example, local stressors have affected how parts of Australia's Great Barrier Reef have recovered from recent climate change impacts (MacNeil et al., 2019; Mellin et al., 2019) and habitat fragmentation and modification have exacerbated recent impacts of tropical and temperate forest fires (Brando et al., 2014; Alencar et al., 2015; Taylor et al., 2016). Because the effects of storms are strongly dependent not only on their intensity, but also the extent of the fetch, their frequency, and intrinsic reef properties such as topography (Lugo et al., 2000; Heron et al., 2005), this study incorporated all recorded storms (category 1–5 on the Saffir-Simpson Hurricane Scale) passing within 50 km of each site. We thus cannot deduce benthic community responses to increasing storm *intensity*, which is projected to occur (IPCC, 2019).

Functional groups of herbivorous fishes also emerged to be of contrasting RI depending on the level of local human impact, shifting from scrapers and small excavators at less impacted reefs to grazers at more impacted reefs. Browsers were of similar importance at reefs exposed to both local human impact levels, perhaps linked to the fact that their food source (macroalgae) remained constant regardless of local human impact level. Additional reasons for this could be that browsers have remained more resilient to fishing pressure than other herbivores, or

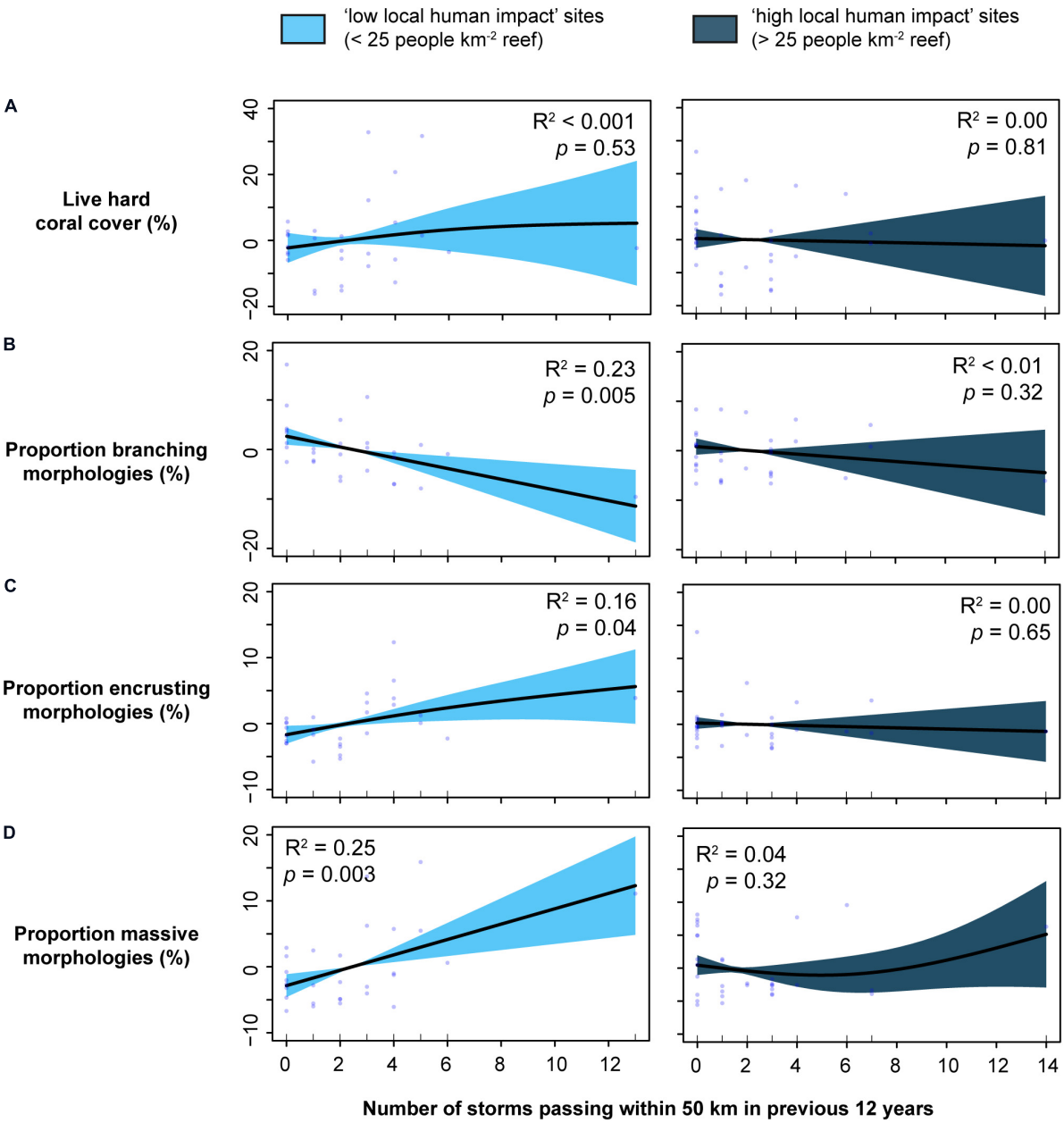

FIGURE 4 | Smoother plots of normalised residuals from generalised additive models with 95% confidence intervals (shaded areas) to exemplify discrepancies in response-predictor relationships between local impact levels, using storm exposure as an example. The plots represent the explanatory power of storm exposure in predicting **(A)** live hard coral cover, and the proportion of **(B)** branching, **(C)** encrusting, and **(D)** massive morphologies, separated for sites with low versus high local impacts. Refer to **Supplementary Figure 6** for all predictor-response plots from best-fit models.

that visual survey data does not accurately represent browser populations (for example some browser species are known to be particularly wary of divers–Kulbicki, 1998). Fish that act on turf algae and/or on surfaces available for coral settlement seem to be more sensitive to local human impacts, likely in response to benthic community shifts. Scrapers and small excavators clear substrate for calcifiers, justifying their higher RI in models focussed on less locally impacted reefs where live hard coral cover was higher and conditions for settlement and growth of juvenile corals were likely better (e.g., less nutrients, lower sedimentation). Contrastingly, grazers crop and maintain algal turfs, explaining their importance under higher local human impacts where turf algae were more dominant. These results align with findings in the Hawaiian Archipelago, where biomass of grazers and scrapers were the most important predictors of turf/macroalgal, and calcified regimes, respectively (Jouffray et al., 2015; see also Robinson et al., 2018). Though collinearity tests ruled out significant, potentially confounding relationships

between biomass of different functional groups with individual abiotic predictors, it is important to acknowledge that fish communities themselves can be affected by various physical predictors (Williams I.D. et al., 2015; Samoilys et al., 2019), which could in turn influence benthic structure.

Other factors not included in these analyses are known to structure benthic assemblages, including chlorophyll, SSTs, and wave exposure (Gove et al., 2013, 2015; Williams et al., 2013; Robinson et al., 2018; Darling et al., 2019). Remotely sensed chlorophyll data captures offshore productivity, but we expected land-based input to dominate many of these reefs which are close to land, while the survey design (sometimes around the periphery of small islands/atolls) made wave exposure challenging to quantify. Additionally, wave exposure, mean SSTs, and climatological ranges can be relatively well-captured by latitude in the Pacific (Gove et al., 2013). Also, although this study goes into more detail than many similar large-scale analyses by evaluating coral growth forms, it is still limited in its ability to quantify ecological reorganisation, which would require higher resolution data (at least family or genus). This limitation can be overcome by broad-scale surveys refining the level at which hard coral communities are recorded, which will become easier with improvements in automated software tools. These results do however emphasise that even broad morphological groupings (i.e., branching, massive, encrusting morphologies) provide pertinent information on ecological changes and can improve model performance compared to when overall hard coral cover is considered (Gove et al., 2015).

Importantly, the threshold used in this study for determining low and high human impact, while informed by a previous study, was set *a priori* and thus does not allow defining a "carrying capacity" of human density–this would require a different survey design and analytical approach, and should be pursued in future studies. We would however suggest that although this metric is most applicable to areas where customary resource use is common practice, we anticipate that this threshold (25 humans km^{-2} reef) is highly relevant across the tropical Pacific (i.e., given that it is a median point in this dataset for which sites were selected due to being regionally representative of fished areas). Furthermore, the study design was not originally meant to address macroecological questions but was nonetheless the best available to study the questions we were interested in (with incorporation of appropriate secondary data on local environmental context). Again, future studies should address this by appropriate designs that allow for large-scale comparability and collect both ecological and socio-economic local data. Our findings indicate that island relief is a factor that should be considered in designing regional sampling programmes with comparable sites. Finally, we should aim to obtain context-specific information on factors associated with human population density (e.g., sewage treatment presence, farming and associated fertiliser-usage) that strengthens our ability to predict benthic communities under various levels of human population density and improve its use as a proxy of local human impact.

Our findings contribute to a better understanding of the role of local human impacts on highly diverse ecosystems such as tropical coral reefs. The results provide empirical evidence that local human impacts drive conspicuous changes in benthic community relationships with environmental predictors, with indications of ecological reorganisation. Even if decisive steps are taken to reduce fossil fuel emissions, most reefs will suffer long-term degradation from the effects of climate change by 2050, and >75% of reefs will experience annual severe bleaching (Frieler et al., 2013; van Hooidonk et al., 2016). Our results show that local human impacts can lead to increasingly unpredictable relationships between benthic communities and their physical environment, and that overlooking their role could pave the way to significant errors in future projections, potentially compromising mitigation efforts.

DATA AVAILABILITY STATEMENT

The raw data supporting the conclusions of this article will be made available by the authors, without undue reservation.

AUTHOR CONTRIBUTIONS

AF developed the study idea with close support from J-BJ, AN, BM, and SF. AF led the statistical analyses together with input from J-BJ, GW, and SF. BM and FM provided expertise on the original data. All authors provided support throughout the interpretation of the results and development of the manuscript and approve this final version.

FUNDING

The COFish and PROCFish-C Programmes were funded by the European Union. AF, SB, and SF were funded by the (German) Federal Ministry of Education and Research (BMBF) through the "Nachwuchsgruppen Globaler Wandel 4 + 1" (REPICORE, grant number 01LN1303A).

ACKNOWLEDGMENTS

We would like to thank the Pacific Community survey team, in particular Samasoni Sauni, Pierre Boblin, Ribanataake Awira, Laurent Vigliola and Silvia Pinca, as well as the fisheries officers across the PICTs who assisted with logistics and data collection. Data collection was made possible by the support of in-country Fisheries Divisions, as well as the chiefs and people of all local communities at the surveyed sites. The research reported in this manuscript contributes to the Programme on Ecosystem Change and Society (www.pecs-science.org).

SUPPLEMENTARY MATERIAL

The Supplementary Material for this article can be found online at: https://www.frontiersin.org/articles/10.3389/fmars.2020.571115/full#supplementary-material

REFERENCES

Albert, S., Dunbabin, M., Skinner, M., Moore, B., and Grinham, A. (2012). "Benthic shift in a Solomon Islands' lagoon: corals to cyanobacteria," in *Proceedings of the 12th International Coral Reef Symposium, Cairns, Australia, 9-13 July 2012*, Cairns, 1–5.

Alencar, A. A., Brando, P. M., Asner, G. P., and Putz, F. E. (2015). Landscape fragmentation, severe drought, and the new Amazon forest fire regime. *Ecol. Appl.* 25, 1493–1505. doi: 10.1890/14-1528.1

Alvarez-Filip, L., Dulvy, N. K., Gill, J. A., Côté, I. M., and Watkinson, A. R. (2009). Flattening of Caribbean coral reefs: region-wide declines in architectural complexity. *Proc. R. Soc. B Biol. Sci.* 276, 3019–3025. doi: 10.1098/rspb.2009.0339

Andréfouët, S., Muller-Karger, F. E., Robinson, J. A., Kranenburg, C. J., Torres-Pulliza, D., Spraggins, S. A., et al. (2006). "Global assessment of modern coral reef extent and diversity for regional science and management applications: a view from space," in *Proceedings of 10th International Coral Reef Symposium*, Okinawa, 1732–1745.

Ban, S. S., Graham, N. A. J., and Connolly, S. R. (2014). Evidence for multiple stressor interactions and effects on coral reefs. *Glob. Change Biol.* 20, 681–697. doi: 10.1111/gcb.12453

Barton, K. (2016). *MuMIn: Multi-Model Inference. R Package Version 1.15.6*. Available online at: https://CRAN.R-project.org/package=MuMIn (accessed April 15, 2020).

Bellwood, D. R., Hughes, T. P., Folke, C., and Nyström, M. (2004). Confronting the coral reef crisis. *Nature* 429, 827–833. doi: 10.1038/nature02691

Brando, P. M., Balch, J. K., Nepstad, D. C., Morton, D. C., Putz, F. E., Coe, M. T., et al. (2014). Abrupt increases in Amazonian tree mortality due to drought–fire interactions. *Proc. Natl. Acad. Sci. U.S.A.* 111, 6347–6352. doi: 10.1073/pnas.1305499111

Brewer, T. D., Cinner, J. E., Fisher, R., Green, A., and Wilson, S. K. (2012). Market access, population density, and socioeconomic development explain diversity and functional group biomass of coral reef fish assemblages. *Glob. Environ. Change* 22, 399–406. doi: 10.1016/j.gloenvcha.2012.01.006

Brown, K. T., Bender-Champ, D., Bryant, D. E. P., Dove, S., and Hoegh-Guldberg, O. (2017). Human activities influence benthic community structure and the composition of the coral-algal interactions in the central Maldives. *J. Exp. Marine Biol. Ecol.* 497, 33–40. doi: 10.1016/j.jembe.2017.09.006

Browne, N. K., Smithers, S. G., and Perry, C. T. (2013). Spatial and temporal variations in turbidity on two inshore turbid reefs on the Great Barrier Reef, Australia. *Coral Reefs* 32, 195–210. doi: 10.1007/s00338-012-0965-1

Bruno, J. F., Sweatman, H., Precht, W. F., Selig, E. R., and Schutte, V. G. W. (2009). Assessing evidence of phase shifts from coral to macroalgal dominance on coral reefs. *Ecology* 90, 1478–1484. doi: 10.1890/08-1781.1

Bruno, J. F., and Valdivia, A. (2016). Coral reef degradation is not correlated with local human population density. *Sci. Rep.* 6:29778. doi: 10.1038/srep29778

Burke, L. M., Reytar, K., Spalding, M., and Perry, A. (2011). *Reefs at Risk Revisited*. Washington, DC: World Resources Institute.

Cannon, S. E., Donner, S. D., Fenner, D., and Beger, M. (2019). The relationship between macroalgae taxa and human disturbance on central Pacific coral reefs. *Marine Pollut. Bull.* 145, 161–173. doi: 10.1016/j.marpolbul.2019.05.024

Casey, K. S., Selig, E. R., and Foti, G. (2012). *The Coral Reef Temperature Anomaly Database (CoRTAD) Version 4 - Global, 4 km Sea Surface Temperature and Related Thermal Stress Metrics for 1981-10-31 to 2010-12-31 (NODC Accession 0087989). Version 2.2*. Silver Spring, MD: National Oceanographic Data Center, NOAA.

Cinner, J. E., Maire, E., Huchery, C., MacNeil, M. A., Graham, N. A. J., Mora, C., et al. (2018). Gravity of human impacts mediates coral reef conservation gains. *Proc. Natl. Acad. Sci. U.S.A.* 115, E6116–E6125. doi: 10.1073/pnas.1708001115

Cinner, J., and Maire, E. (2018). *Global Gravity of Coral Reefs Spatial Layer*. Queensland: James Cook University.

Close, C. H., and Hall, G. B. (2006). A GIS-based protocol for the collection and use of local knowledge in fisheries management planning. *J. Environ. Manage.* 78, 341–352. doi: 10.1016/j.jenvman.2005.04.027

Clua, E., Legendre, P., Vigliola, L., Magron, F., Kulbicki, M., Sarramegna, S., et al. (2006). Medium scale approach (MSA) for improved assessment of coral reef fish habitat. *J. Exp. Marine Biol. Ecol.* 333, 219–230. doi: 10.1016/j.jembe.2005.12.010

Côté, I. M., and Darling, E. S. (2010). Rethinking ecosystem resilience in the face of climate change. *PLoS Biol.* 8:e1000438. doi: 10.1371/journal.pbio.1000438

D'agata, S., Mouillot, D., Kulbicki, M., Andréfouët, S., Bellwood, D. R., Cinner, J. E., et al. (2014). Human-mediated loss of phylogenetic and functional diversity in coral reef fishes. *Curr. Biol.* 24, 555–560. doi: 10.1016/j.cub.2014.01.049

Darling, E. S., and Côté, I. M. (2018). Seeking resilience in marine ecosystems. *Science* 359, 986–987. doi: 10.1126/science.aas9852

Darling, E. S., McClanahan, T. R., Maina, J., Gurney, G. G., Graham, N. A. J., Januchowski-Hartley, F., et al. (2019). Social–environmental drivers inform strategic management of coral reefs in the Anthropocene. *Nat. Ecol. Evol.* 3, 1341–1350. doi: 10.1038/s41559-019-0953-8

Donaldson, T. J. (2002). High islands versus low islands: a comparison of fish faunal composition of the Palau islands. *Environ. Biol. Fishes* 65, 241–248. doi: 10.1023/A:1020067931910

Ellis, J., Anlauf, H., Kürten, S., Lozano-Cortés, D., Alsaffar, Z., Cúrdia, J., et al. (2017). Cross shelf benthic biodiversity patterns in the Southern Red Sea. *Sci. Rep.* 7:437. doi: 10.1038/s41598-017-00507-y

Ellis, J. I., Jamil, T., Anlauf, H., Coker, D. J., Curdia, J., Hewitt, J., et al. (2019). Multiple stressor effects on coral reef ecosystems. *Glob. Change Biol.* 25, 4131–4146. doi: 10.1111/gcb.14819

Elmqvist, T., Folke, C., Nyström, M., Peterson, G., Bengtsson, J., Walker, B., et al. (2003). Response diversity, ecosystem change, and resilience. *Front. Ecol. Environ.* 1:488–494. doi: 10.2307/3868116

ESRI (2011). *ArcGIS Desktop: Release 10*. Redlands, CA: Environmental Systems Research Institute.

Fabricius, K., De'ath, G., McCook, L., Turak, E., and Williams, D. (2005). Changes in algal, coral and fish assemblages along water quality gradients on the inshore Great Barrier Reef. *Marine Pollut. Bull.* 51, 384–398. doi: 10.1016/j.marpolbul.2004.10.041

Fabricius, K. E. (2005). Effects of terrestrial runoff on the ecology of corals and coral reefs: review and synthesis. *Marine Pollut. Bull.* 50, 125–146. doi: 10.1016/j.marpolbul.2004.11.028

Ferrario, F., Beck, M. W., Storlazzi, C. D., Micheli, F., Shepard, C. C., and Airoldi, L. (2014). The effectiveness of coral reefs for coastal hazard risk reduction and adaptation. *Nature Commun.* 5:3794. doi: 10.1038/ncomms4794

Ford, A. K., Hoytema, N. V., Moore, B. R., Pandihau, L., Wild, C., and Ferse, S. C. A. (2017). High sedimentary oxygen consumption indicates that sewage input from small islands drives benthic community shifts on overfished reefs. *Environ. Conserv.* 44, 405–411. doi: 10.1017/S0376892917000054

Fox, J., and Weisberg, S. (2019). *An R Companion to Applied Regression*, 3rd Edn. Thousand Oaks CA: Sage Publications.

Frieler, K., Meinshausen, M., Golly, A., Mengel, M., Lebek, K., Donner, S. D., et al. (2013). Limiting global warming to 2 °C is unlikely to save most coral reefs. *Nature Clim. Change* 3, 165–170. doi: 10.1038/nclimate1674

Gardner, T. A., Côté, I. M., Gill, J. A., Grant, A., and Watkinson, A. R. (2005). Hurricanes and caribbean coral reefs: impacts, recovery patterns, and role in long-term decline. *Ecology* 86, 174–184. doi: 10.1890/04-0141

Gattuso, J.-P., Magnan, A., Billé, R., Cheung, W. W. L., Howes, E. L., Joos, F., et al. (2015). Contrasting futures for ocean and society from different anthropogenic CO2 emissions scenarios. *Science* 349:aac4722. doi: 10.1126/science.aac4722

Gilmour, J. P., Smith, L. D., Heyward, A. J., Baird, A. H., and Pratchett, M. S. (2013). Recovery of an isolated coral reef system following severe disturbance. *Science* 340, 69–71. doi: 10.1126/science.1232310

Gove, J. M., Williams, G. J., McManus, M. A., Clark, S. J., Ehses, J. S., and Wedding, L. M. (2015). Coral reef benthic regimes exhibit non-linear threshold responses to natural physical drivers. *Marine Ecol. Prog. Series* 522, 33–48. doi: 10.3354/meps11118

Gove, J. M., Williams, G. J., McManus, M. A., Heron, S. F., Sandin, S. A., Vetter, O. J., et al. (2013). Quantifying climatological ranges and anomalies for pacific coral reef ecosystems. *PLoS One* 8:e61974. doi: 10.1371/journal.pone.0061974

Graham, N. A., Cinner, J. E., Norström, A. V., and Nyström, M. (2014). Coral reefs as novel ecosystems: embracing new futures. *Curr. Opin. Environ. Sustain.* 7, 9–14. doi: 10.1016/j.cosust.2013.11.023

Hamilton, R. J., Giningele, M., Aswani, S., and Ecochard, J. L. (2012). Fishing in the dark-local knowledge, night spearfishing and spawning aggregations in the Western Solomon Islands. *Biol. Conserv.* 145, 246–257. doi: 10.1016/j.biocon.2011.11.020

Harriott, V., and Banks, S. (2002). Latitudinal variation in coral communities in eastern Australia: a qualitative biophysical model of factors regulating coral reefs. *Coral Reefs* 21, 83–94. doi: 10.1007/s00338-001-0201-x

Heenan, A., Hoey, A. S., Williams, G. J., and Williams, I. D. (2016). Natural bounds on herbivorous coral reef fishes. *Proc. R. Soc. B Biol. Sci.* 283:20161716. doi: 10.1098/rspb.2016.1716

Henderson, C. J., Gilby, B. L., Schlacher, T. A., Connolly, R. M., Sheaves, M., Maxwell, P. S., et al. (2020). Landscape transformation alters functional diversity in coastal seascapes. *Ecography* 43, 138–148. doi: 10.1111/ecog.04504

Heron, S., Morgan, J., Eakin, M., and Skirving, W. (2005). "Hurricanes and their effects on coral reefs," in *Status of Caribbean Coral Reefs after Bleaching and Hurricanes in 2005*, eds C. Wilkinson and D. Souter (Townsville: Global Coral Reef Monitoring Network and Reef and Rainforest Research Centre), 31–36.

Hoegh-Guldberg, O., Mumby, P. J., Hooten, A. J., Steneck, R. S., Greenfield, P., Gomez, E., et al. (2007). Coral reefs under rapid climate change and ocean acidification. *Science* 318, 1737–1742. doi: 10.1126/science.1152509

Houk, P., Camacho, R., Johnson, S., McLean, M., Maxin, S., Anson, J., et al. (2015). The micronesia challenge: assessing the relative contribution of stressors on coral reefs to facilitate science-to-management feedback. *PLoS One* 10:e0130823. doi: 10.1371/journal.pone.0130823

Hughes, T. P., Anderson, K. D., Connolly, S. R., Heron, S. F., Kerry, J. T., Lough, J. M., et al. (2018). Spatial and temporal patterns of mass bleaching of corals in the Anthropocene. *Science* 359, 80–83. doi: 10.1126/science.aan8048

Hughes, T. P., Baird, A. H., Dinsdale, E. A., Moltschaniwskyj, N. A., Pratchett, M. S., Tanner, J. E., et al. (1999). Patterns of recruitment and abundance of corals along the Great Barrier Reef. *Nature* 397, 59–63. doi: 10.1038/16237

Huston, M. A. (1985). Patterns of species diversity on coral reefs. *Annu. Rev. Ecol. Syst.* 16, 149–177. doi: 10.1146/annurev.es.16.110185.001053

IPCC (2019). "Summary for policymakers," in *IPCC Special Report on the Ocean and Cryosphere in a Changing Climate*, eds H.-O. Pörtner, D. C. Roberts, V. Masson-Delmotte, P. Zhai, M. Tignor, E. Poloczanska, et al. (Geneva: IPCC).

Jouffray, J.-B., Nyström, M., Norström, A. V., Williams, I. D., Wedding, L. M., Kittinger, J. N., et al. (2015). Identifying multiple coral reef regimes and their drivers across the Hawaiian archipelago. *Philos. Trans. R. Soc. B Biol. Sci.* 370:20130268. doi: 10.1098/rstb.2013.0268

Jouffray, J.-B., Wedding, L. M., Norström, A. V., Donovan, M. K., Williams, G. J., Crowder, L. B., et al. (2019). Parsing human and biophysical drivers of coral reef regimes. *Philos. Trans. R. Soc. B Biol. Sci.* 286:20182544. doi: 10.1098/rspb.2018.2544

Knapp, K. R., Applequist, S., Howard, J. D., Kossin, J. P., Kruk, M., and Schreck, C. (2010a). *NCDC International Best Track Archive for Climate Stewardship (IBTrACS) Project, Version 3*. Silver Spring, MD: NOAA National Centers for Environmental Information. doi: 10.7289/V5NK3BZP

Knapp, K. R., Kruk, M. C., Levinson, D. H., Diamond, H. J., and Neumann, C. J. (2010b). The international best track archive for climate stewardship (IBTrACS). *Bull. Amer. Meteor. Soc.* 91, 363–376. doi: 10.1175/2009BAMS2755.1

Kulbicki, M. (1998). How the acquired behaviour of commercial reef fishes may influence the results obtained from visual censuses. *J. Exp. Marine Biol. Ecol.* 222, 11–30. doi: 10.1016/S0022-0981(97)00133-0

Kulbicki, M., Guillemot, N., and Amand, M. (2005). A general approach to length-weight relationships for New Caledonian lagoon fishes. *Cybium* 29, 235–252.

Labrosse, P., Kulbicki, M., and Ferraris, J. (2002). *). Underwater Visual Fish Census Surveys: Proper use and Implementation*. Noumea, New Caledonia: Secretariat of the Pacific Community (SPC).

Léopold, M., Guillemot, N., Rocklin, D., and Chen, C. (2014). A framework for mapping small-scale coastal fisheries using fishers' knowledge. *ICES J. Mar. Sci.* 71, 1781–1792. doi: 10.1093/icesjms/fst204

Lugo, A. E., Rogers, C. S., and Nixon, S. W. (2000). Hurricanes, coral reefs and rainforests: resistance, ruin and recovery in the caribbean. *AMBIO J. Hum. Environ.* 29, 106–114. doi: 10.1579/0044-7447-29.2.106

MacNeil, M. A., Mellin, C., Matthews, S., Wolff, N. H., McClanahan, T. R., Devlin, M., et al. (2019). Water quality mediates resilience on the Great Barrier Reef. *Nature Ecol. Evol.* 3, 620–627. doi: 10.1038/s41559-019-0832-3

Maire, E., Cinner, J., Velez, L., Huchery, C., Mora, C., D'agata, S., et al. (2016). How accessible are coral reefs to people? A global assessment based on travel time. *Ecol. Lett.* 19, 351–360. doi: 10.1111/ele.12577

Manzello, D. P., Brandt, M., Smith, T. B., Lirman, D., Hendee, J. C., and Nemeth, R. S. (2007). Hurricanes benefit bleached corals. *Proc. Natl. Acad. Sci. U.S.A.* 104, 12035–12039. doi: 10.1073/pnas.0701194104

McWilliam, M., Pratchett, M. S., Hoogenboom, M. O., and Hughes, T. P. (2020). Deficits in functional trait diversity following recovery on coral reefs. *Philos. Trans. R. Soc. B Biol. Sci.* 287:20192628. doi: 10.1098/rspb.2019.2628

Mellin, C., Matthews, S., Anthony, K. R. N., Brown, S. C., Caley, M. J., Johns, K. A., et al. (2019). Spatial resilience of the Great Barrier Reef under cumulative disturbance impacts. *Glob. Change Biol.* 25, 2431–2445. doi: 10.1111/gcb.14625

Moberg, F., and Folke, C. (1999). Ecological goods and services of coral reef ecosystems. *Ecol. Econ.* 29, 215–233. doi: 10.1016/S0921-8009(99)00009-9

Morgan, K. M., Perry, C. T., Smithers, S. G., Johnson, J. A., and Daniell, J. J. (2016). Evidence of extensive reef development and high coral cover in nearshore environments: implications for understanding coral adaptation in turbid settings. *Sci. Rep.* 6:29616. doi: 10.1038/srep29616

Morse, N., Pellissier, P., Cianciola, E., Brereton, R., Sullivan, M., Shonka, N., et al. (2014). Novel ecosystems in the Anthropocene: a revision of the novel ecosystem concept for pragmatic applications. *Ecol. Soc.* 19:12. doi: 10.5751/ES-06192-190212

Mumby, P. J. (2017). Embracing a world of subtlety and nuance on coral reefs. *Coral Reefs* 36, 1003–1011. doi: 10.1007/s00338-017-1591-8

Norström, A. V., Nyström, M., Jouffray, J.-B., Folke, C., Graham, N. A., Moberg, F., et al. (2016). Guiding coral reef futures in the Anthropocene. *Front. Ecol. Environ.* 14:490–498. doi: 10.1002/fee.1427

Nyström, M. (2006). Redundancy and response diversity of functional groups: implications for the resilience of coral reefs. *ambi* 35, 30–35. doi: 10.1579/0044-7447-35.1.30

Pinca, S., Kronen, M., Friedman, K., Magron, F., Chapman, L., Tardy, E., et al. (2010). *Regional Assessment Report: Profiles and Results from Survey Work at 63 Sites across 17 Pacific Island Countries and Territories*. Noumea: Pacific Regional Oceanic and Coastal Fisheries Development Programme (PROCFish/C/CoFish).

QGIS Development Team (2019). *QGIS Geographic Information System. Open Source Geospatial Foundation Project*. Available online at: http://qgis.osgeo.org (accessed August 21, 2020).

R Development Core Team (2019). *R: A Language and Environment for Statistical Computing*. Vienna: R Foundation for Statistical Computing.

Riegl, B., Berumen, M., and Bruckner, A. (2013). Coral population trajectories, increased disturbance and management intervention: a sensitivity analysis. *Ecol. Evol.* 3, 1050–1064. doi: 10.1002/ece3.519

Robinson, J. P. W., Williams, I. D., Yeager, L. A., McPherson, J. M., Clark, J., Oliver, T. A., et al. (2018). Environmental conditions and herbivore biomass determine coral reef benthic community composition: implications for quantitative baselines. *Coral Reefs* 37, 1157–1168. doi: 10.1007/s00338-018-01737-w

Roff, G., and Mumby, P. J. (2012). Global disparity in the resilience of coral reefs. *Trends Ecol. Evol.* 27, 404–413. doi: 10.1016/j.tree.2012.04.007

Rogers, A., Blanchard, J. L., and Mumby, P. J. (2018). Fisheries productivity under progressive coral reef degradation. *J. Appl. Ecol.* 55, 1041–1049. doi: 10.1111/1365-2664.13051

Rogers, C. (1990). Responses of coral reefs and reef organisms to sedimentation. *Mar. Ecol. Prog. Ser.* 62, 185–202. doi: 10.3354/meps062185

Samoilys, M. A., Halford, A., and Osuka, K. (2019). Disentangling drivers of the abundance of coral reef fishes in the Western Indian Ocean. *Ecol. Evol.* 9, 4149–4167. doi: 10.1002/ece3.5044

Sandin, S. A., Smith, J. E., DeMartini, E. E., Dinsdale, E. A., Donner, S. D., Friedlander, A. M., et al. (2008). Baselines and degradation of coral reefs in the Northern Line Islands. *PLoS One* 3:e1548. doi: 10.1371/journal.pone.0001548

Schoepf, V., Stat, M., Falter, J. L., and McCulloch, M. T. (2015). Limits to the thermal tolerance of corals adapted to a highly fluctuating, naturally extreme temperature environment. *Sci. Rep.* 5:17639. doi: 10.1038/srep17639

Sheppard, C., Harris, A., and Sheppard, A. L. S. (2008). Archipelago-wide coral recovery patterns since 1998 in the Chagos Archipelago, central Indian Ocean. *Mar. Ecol. Prog. Ser.* 362, 109–117. doi: 10.3354/meps07436

Smith, J. E., Brainard, R., Carter, A., Grillo, S., Edwards, C., Harris, J., et al. (2016). Re-evaluating the health of coral reef communities: baselines and evidence for human impacts across the central Pacific. *Proc. R. Soc. B* 283:20151985. doi: 10.1098/rspb.2015.1985

Steffen, W., Crutzen, P. J., and McNeill, J. R. (2007). The Anthropocene: are humans now overwhelming the great forces of nature? *Ambio* 36, 614–621. doi: 10.2307/25547826

Taylor, A. H., Trouet, V., Skinner, C. N., and Stephens, S. (2016). Socioecological transitions trigger fire regime shifts and modulate fire–climate interactions in the Sierra Nevada, USA, 1600–2015 CE. *Proc. Natl. Acad. Sci. U.S.A.* 113, 13684–13689. doi: 10.1073/pnas.1609775113

Tebbett, S. B., and Bellwood, D. R. (2019). Algal turf sediments on coral reefs: what's known and what's next. *Mar. Pollut. Bull.* 149:110542. doi: 10.1016/j.marpolbul.2019.110542

van Hooidonk, R., Maynard, J., Tamelander, J., Gove, J., Ahmadia, G., Raymundo, L., et al. (2016). Local-scale projections of coral reef futures and implications of the Paris Agreement. *Sci. Rep.* 6:39666. doi: 10.1038/srep39666

van Woesik, R., Sakai, K., Ganase, A., and Loya, Y. (2011). Revisiting the winners and the losers a decade after coral bleaching. *Mar. Ecol. Prog. Ser.* 434, 67–76. doi: 10.3354/meps09203

Warton, D. I., and Hui, F. K. C. (2011). The arcsine is asinine: the analysis of proportions in ecology. *Ecology* 92, 3–10. doi: 10.1890/10-0340.1

Wiedenmann, J., D'Angelo, C., Smith, E. G., Hunt, A. N., Legiret, F.-E., Postle, A. D., et al. (2013). Nutrient enrichment can increase the susceptibility of reef corals to bleaching. *Nature Clim. Change* 3, 160–164. doi: 10.1038/nclimate1661

Williams, G. J., Gove, J. M., Eynaud, Y., Zgliczynski, B. J., and Sandin, S. A. (2015). Local human impacts decouple natural biophysical relationships on Pacific coral reefs. *Ecography* 38, 751–761. doi: 10.1111/ecog.01353

Williams, G. J., Graham, N. A. J., Jouffray, J.-B., Norström, A. V., Nyström, M., Gove, J. M., et al. (2019). Coral reef ecology in the Anthropocene. *Funct. Ecol.* 33, 1014–1022. doi: 10.1111/1365-2435.13290

Williams, G. J., Smith, J. E., Conklin, E. J., Gove, J. M., Sala, E., and Sandin, S. A. (2013). Benthic communities at two remote Pacific coral reefs: effects of reef habitat, depth, and wave energy gradients on spatial patterns. *PeerJ* 1:e81. doi: 10.7717/peerj.81

Williams, I. D., Baum, J. K., Heenan, A., Hanson, K. M., Nadon, M. O., and Brainard, R. E. (2015). Human, oceanographic and habitat drivers of central and Western pacific coral reef fish assemblages. *PLoS One* 10:e0120516. doi: 10.1371/journal.pone.0120516

Wood, S., and Scheipl, F. (2014). *gamm4: Generalized Additive Mixed Models Using mgcv and lme4. R Package Version 0.2–3*. Available online at: https://cran.r-project.org/package=gamm4

Woodhead, A. J., Hicks, C. C., Norström, A. V., Williams, G. J., and Graham, N. A. J. (2019). Coral reef ecosystem services in the Anthropocene. *Funct. Ecol.* 33, 1023–1034. doi: 10.1111/1365-2435.13331

Zhang, S. Y., Speare, K. E., Long, Z. T., McKeever, K. A., Gyoerkoe, M., Ramus, A. P., et al. (2014). Is coral richness related to community resistance to and recovery from disturbance? *PeerJ* 2:e308. doi: 10.7717/peerj.308

Zuur, A., Ieno, E., Walker, N., Saveliev, A. A., and Smith, G. M. (2009). *Mixed Effects Models and Extensions in Ecology with R*. New York, NY: Springer Science+Business Media.

Conflict of Interest: The authors declare that the research was conducted in the absence of any commercial or financial relationships that could be construed as a potential conflict of interest.

The reviewer KO declared a past collaboration with several of the authors J-BJ, AN, GW, and SF to the handling editor.

frontiers in Marine Science

ORIGINAL RESEARCH
published: 12 November 2020
doi: 10.3389/fmars.2020.571451

A Diver-Portable Respirometry System for *in-situ* Short-Term Measurements of Coral Metabolic Health and Rates of Calcification

Walter Dellisanti[1,2,3], Ryan H. L. Tsang[4], Put Ang Jr.[4,5], Jiajun Wu[1,3], Mark L. Wells[6,7] and Leo L. Chan[1,2,3]**

[1] State Key Laboratory of Marine Pollution, City University of Hong Kong, Hong Kong, China, [2] Department of Biomedical Sciences, City University of Hong Kong, Hong Kong, China, [3] Shenzhen Key Laboratory for the Sustainable Use of Marine Biodiversity, Research Centre for the Oceans and Human Health, City University of Hong Kong, Shenzhen Research Institute, Shenzhen, China, [4] Marine Science Laboratory, Chinese University of Hong Kong, Hong Kong, China, [5] Institute of Space and Earth Information Science, The Chinese University of Hong Kong, Hong Kong, China, [6] School of Marine Sciences, University of Maine, Orono, ME, United States, [7] State Key Laboratory of Satellite Ocean Environment Dynamics, Second Institute of Oceanography, Ministry of Natural Resources, Hangzhou, China

OPEN ACCESS

Edited by:
Massimo Ponti, University of Bologna, Italy

Reviewed by:
Arjun Chennu, Leibniz Centre for Tropical Marine Research (LG), Germany
Christian Lott, HYDRA Marine Sciences, Germany

***Correspondence:**
Mark L. Wells
mlwells@maine.edu
Leo L. Chan
leochan@cityu.edu.hk

Specialty section:
This article was submitted to Marine Ecosystem Ecology, a section of the journal Frontiers in Marine Science

Received: *10 June 2020*
Accepted: *14 October 2020*
Published: *12 November 2020*

Citation:
Dellisanti W, Tsang RHL, Ang P Jr, Wu J, Wells ML and Chan LL (2020) A Diver-Portable Respirometry System for in-situ Short-Term Measurements of Coral Metabolic Health and Rates of Calcification. Front. Mar. Sci. 7:571451. doi: 10.3389/fmars.2020.571451

Underwater visual monitoring methods are used broadly to evaluate coral reef conditions in the natural environment, but quantitative measurements of the coral holobiont has been largely restricted to photophysiological assessment of the endosymbionts. An underwater respirometer has been designed to make routine, diver-operated, non-invasive measurements at coral surfaces, but the realistic *in situ* accuracy and precision capabilities of this device has not been critically assessed; an essential step if these measurements are to be useful for quantifying spatial and seasonal patterns of coral metabolism. We developed specific protocols for this system to survey shallow coral colonies and detect metabolic profiles (respiration, photosynthesis, and biocalcification), diel cycles (day and night), and photosynthesis-irradiance curves. Analysis of data from *in situ* and laboratory-controlled conditions showed good replication among coral colonies and high precision measurements of temperature, oxygen and pH fluxes over 15-min incubation times without noticeable detrimental effects on coral health. Moreover, marked differences were observed in coral calcification rates between estuarine-influenced and coastal marine conditions, despite the absence of significant differences in visual appearance or other health indicators, revealing the system's potential for early detection of marginally adverse conditions for coral metabolism. Its ease of operation and rapid quantification of the physiological status of the corals make this respirometer well suited for use by reef scientists, monitoring agencies, and stakeholders in biogenic reefs conservation efforts. Moreover, the high spatial and temporal resolution of these underwater respirometer data will have the potential to discriminate the effects of local stressors on coral health from those generated by broader changes associated with climate drivers.

Keywords: coral monitoring, coral physiology, underwater, non-invasive, holobiont

INTRODUCTION

Warm-water coral reef systems are critical marine resources, yet their health and capacity for growth are under increasing threats from climate stressors. Although many shallow marine ecosystems will be influenced by shifting climate, the risks to coral reef systems are of particular concern due to their demonstrated sensitivity to altered environmental conditions and their central role in broadly sustaining marine biodiversity. Rising seawater temperatures and ocean acidification (Gruber, 2011; Ciais et al., 2013; Kuffner et al., 2015) are identified as the primary climate drivers influencing coral metabolic status, oxidative stress (Coles and Brown, 2003), bleaching events (Fitt et al., 2001) and reduced rates of biocalcification (Hoegh-Guldberg et al., 2007; Hughes et al., 2017). Environmental changes that lead to decreased coral food supply can exacerbate these impacts (Borell and Bischof, 2008). The scale and duration of mass bleaching events have increased significantly over the past three decades, leading to widespread coral death (Pandolfi et al., 2011; Donner et al., 2017). In addition to the accumulating impacts from global change, many nearshore corals, and particularly the urban reefs (Heery et al., 2018), are subjected to changing local stressors, including increased turbidity, nutrient loading, and as a consequence, greater dissolved oxygen fluctuations (Wong et al., 2018). Higher environmental variability in these areas has led to the selection of more stress-tolerant species (Darling et al., 2012) but less diverse reefs (Duprey et al., 2017). It is becoming increasingly important to discriminate between local and climate derived coral stress when developing coral reef mitigation and preservation strategies. Quantifying the status of coral health in present-day ocean conditions along with the early indicators of changing stress is key to understanding, forecasting, and responding to manifest effects of climate and regional anthropogenic stressors on future coral reef ecosystems (Hoegh-Guldberg et al., 2017).

Identifying sensitive indicators of coral physiology to assess chronic and acute stress has thus become a keen objective over the past few decades, and different tools and strategies have been developed for both laboratory and field studies (Rinkevich, 1995; Weber et al., 2007; van Oppen et al., 2017). Coral metabolism has been a focus of study since the development of techniques to precisely assess the carbonate system-O_2 relationships in seawater (Gattuso et al., 1999). Laboratory experiments historically have relied on the destructive sampling of whole corals or fragments of coral colonies for shore-based study under artificial settings that do not fully reflect the natural or fluctuating conditions that corals experience *in situ*. Field assessments, in turn, have depended largely on measuring proxies for benthic metabolism as a whole and lack the needed resolution to evaluate the physiological status of individual coral taxa (Bates et al., 2010; Courtney et al., 2018). More recently, the net autotrophic/heterotrophic coral metabolism within the three-dimensional structure of reef systems has been investigated non-invasively using eddy correlation techniques with acoustic Doppler velocimeters coupled with oxygen microsensors (Long et al., 2013). However, to be effective this approach requires quantitative measures of water flow dynamics over the reef and the temporal and spatial distributions of dissolved oxygen in surrounding waters; information lacking for most reef systems. The net photosynthesis or respiration of groups or large individual coral colonies can be estimated in benthic chambers through the study of the dissolved oxygen dynamics (Kuhl et al., 1995; Yates and Halley, 2003; Camp et al., 2015), and although short-term incubations show no visual signs of coral stress, these methods still may not adequately reproduce the water flow characteristics necessary for representative coral health (Camp et al., 2015). But even with suitable care, the apparatus for these studies is cumbersome, making the approach poorly suited for the wider observation of reef systems.

Investigation of oxygen and pH dynamics at the scale of individual coral polyps now is possible using diver-operated microelectrodes on motorized platforms (Weber et al., 2007; Jimenez et al., 2011; Schrameyer et al., 2014). Oxygen dynamics near the coral-water interface shift from supersaturation during the daytime, as a consequence of photosynthesis by the dinoflagellate endosymbionts, to hypoxia at night from respiration of the holobiont and surface-associated bacteria (Shashar et al., 1993; Kuhl et al., 1995; Gardella and Edmunds, 1999). Measurements of similar micro-gradients and diel fluctuations in pH gradients, as well as dissolved inorganic carbon (DIC), can indirectly inform on carbonate availability for coral biocalcification under natural *in situ* regimes of dissolved oxygen, seawater pH and irradiance (Weber et al., 2007; Wangpraseurt et al., 2014). The collective application of these non-destructive tools has revolutionized the study of *in situ* coral physiological status, but they are labor-intensive and impractical for the broader surveys needed to assess the health of coral systems in the context of ecosystem stress.

Despite these remarkable advances, using endosymbiotic O_2 production and holobiont respiration as indicator of coral health still has significant limitations. This dynamic balance results from a composite of metabolic processes; for example, increased respiration can result from both enhanced coral feeding or oxidative stress. A key coral-centric gauge is the rate of calcification. Scleractinian corals build their $CaCO_3$ skeletons through the uptake of calcium and carbonate ions from seawater. Biomineralization occurs within the few nanometers of space between the basal calicoblastic epithelium and the skeleton surface (Falini et al., 2015; Reggi et al., 2016), and $CaCO_3$ deposition rates are energy dependent due in part to the metabolic control of pH within the interstitial layer (Cohen and Holcomb, 2009; Venn et al., 2011). Ocean acidification, resulting from coastal processes or elevated atmospheric pCO_2, increase the energy requirements for calcification, and thereby can decrease calcification rates when coral energy reserves are low (McCulloch et al., 2012). Acidification or other environmental stressors also may affect the interaction between the endosymbionts and corals, thereby limiting the net productivity of the symbiosis (Anthony et al., 2008), and thus energy supply. With the forecast of decreased plankton (food) productivity with global warming (Brierley and Kingsford, 2009), and its likely negative effect

on coral energy reserves, synergies between ocean acidification and increased temperatures may exacerbate effects on coral biocalcification rates, making it a key indicator of coral physiological status.

A diver-operated instrument has been developed—the Community *In situ* Metabolism (CISME) device (CISME Instruments, LLC)—to assess coral health *in situ* through quantifying the rates of coral gross photosynthesis (P_g) and respiration (R), the associated changes in pH, and coral calcification rates (CA) (Murphy et al., 2012). As with any field-based instrument, exploring the analytical reproducibility is of paramount concern, particularly when applied in complex reef systems. We tested this device under well-controlled conditions in laboratory aquaria, and in the field on coral communities in Hong Kong waters with the aim to provide an independent assessment for its practical use as a tool for studying and observing corals *in situ*, and to quantify the effective precision, stability, and repeatability of these physiological measurements. Our findings show that the device had no negative impact on corals, and the measured physiological rates can be combined with water column environmental data to quantify daily variations in coral metabolism. Sensitive measures of R, P_g, and CA at high spatial and temporal resolutions across reef systems not only will provide early indications of stress onset or altered levels, but also will aid reef conservation efforts by helping to resolve those effects attributable to local stressors versus broader climate-driven change.

MATERIALS AND METHODS

Instrumentation

The diver-operated instrument (**Figure 1**) is commercially available as the Community *In situ* Metabolism device (CISME Instruments LLC, www.cisme-instruments.com). The analysis principle is the comparison of net oxygen production rates measured under controlled irradiance to net oxygen utilization rates under dark conditions. Simultaneously, the change in pH can be used to estimate the DIC flux within the chamber during incubations (**Figure 2**). The magnitude of oxygen and pH changes under light and dark conditions is interpreted as a proxy for health of the coral holobiont.

The system comprises three interconnected components: the electronic control module and tablet, contained in transparent sealed housings, and the incubation chamber head (**Figure 1**). Control of the device, sensor output data, instrument status, and all menu options are displayed on the tablet (iDive Housing) using the instrument mobile App v1.20 (Mera). The incubation chamber head contains O_2, pH and temperature sensors, a water circulation pump, and the light-emitting diode (LED) illumination array (**Figure 1c**). On deployment, a neoprene ring on the exterior of the head is pressed gently against the coral surface to provide a sealed attachment, creating a small fluidic chamber (5.5 cm diameter, ∼70 mL volume). The upper surface holds an array of LEDs behind a glass plate the intensity of which can be controlled by the user. The water flow is regulated to ∼0.9 L min^{-1} (pump at 5000 rpm) but it can be adjusted up to ∼1.3 L min^{-1} (7000 rpm, **Supplementary Figure S1** online). Sensor data (O_2 and pH) are live-streamed on the tablet so that the diver can monitor for anomalies, in which case the deployment settings then can be adjusted through the underwater interface, or conditions altered according to the experimental design (**Figure 2C**). The chamber water is circulated through a sample loop (∼18 mL volume) attached to the upper side of the incubation head with sealing, quick-disconnect fittings, enabling multiple samples to be collected on a single deployment or dive. The disconnected sample loops remained sealed for transport to the surface, where the water was collected for total alkalinity (A_t) measurements to quantify coral calcification rates. No special cleaning steps were used after deployments, with the system simply being rinsed well after each dive with freshwater and placed in a shaded place until the transportation to the laboratory.

Sensor Calibrations

Dissolved oxygen was measured within the chamber using an O_2 sensitive fluorescent indicator (PreSens Precision Sensing GmbH) on a fiber-optical cable. The reference dye and O_2 probe were excited by a green LED and the overall luminescence measured (Murphy et al., 2012). Sensors were calibrated at the beginning of the study under laboratory-controlled conditions. The dissolved oxygen measurements were calibrated using the 2-point calibration method, measuring the O_2 concentration at 0% (N_2-gas bubbling) and 100% (air-saturated water) (**Supplementary Figure S2a** online). The ion-selective field effect transistor pH sensor (Durafet, Honeywell Inc.) is highly precise and stable in seawater (Martz et al., 2010), in contrast with standard glass electrodes. The sensor was calibrated first with National Bureau of Standards (NBS) buffers (pH 4.01, 7.00, 10.06) at 25°C (**Supplementary Figure S2b** online) and then corrected for accuracy (± 0.003; n = 5) using the average offset from Tris buffer #T32 certified seawater reference material (CRM) provided by the A. Dickson Laboratory, Scripps Institution of Oceanography. The ISFET^{TM} Temperature sensor was calibrated in a temperature-controlled water bath and compared to Onset HOBO^{TM} light/temperature data logger (**Supplementary Figure S2c** online). The LED light intensity is adjustable (0–100%) by varying its voltage supply through the instrument's application. The light output (0–2500 mmol m^{-2} s^{-1}; **Figure 3A**) was measured with a LiCor^{TM} light-meter and compared to *in situ* irradiance recorded with the Onset HOBO light/temperature data logger.

Instrument Operating Protocols

The incubation protocols were optimized to avoid visually detectable stress on the corals (**Figure 4**; **Supplementary Table S2** online) and to reduce the necessary dive durations. The measurements were initiated by measuring the decrease in oxygen concentrations over 5 min in the dark to quantify respiration. LEDs on the chamber ceiling were then turned on

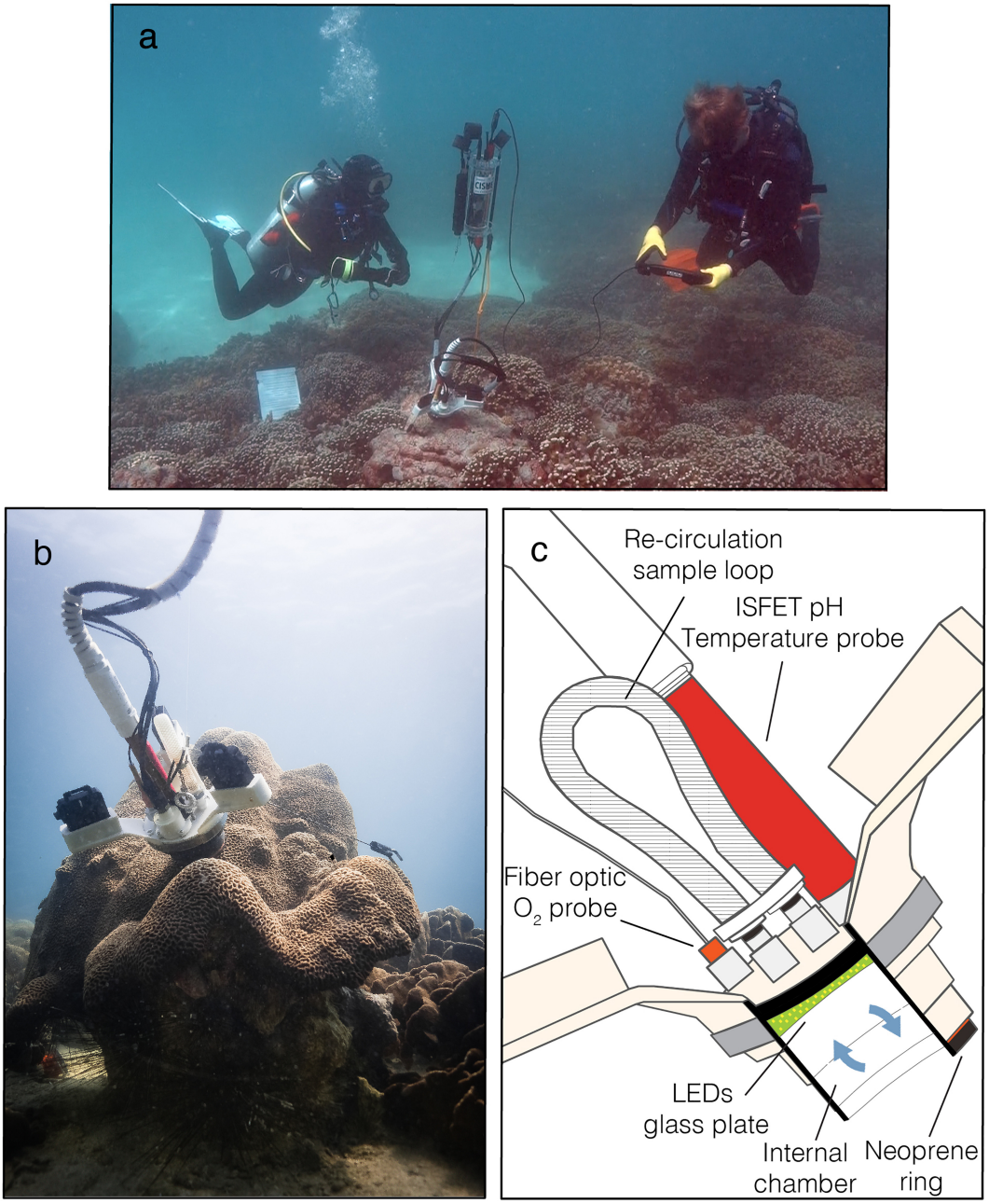

FIGURE 1 | The CISME system operated by SCUBA divers to survey shallow coral colonies. The system simultaneously measures temperature and changes in dissolved oxygen and pH on flat surfaces of stony corals under regulated light and dark conditions. **(a)** The whole system includes the electronic housing, the incubation head and the tablet. The housing is slightly positive while the incubation head is deployed on surveyed coral. The divers can control the system and adjust the settings using the tablet according to the experimental investigation. Underwater photo credits: Dr. Alina Szmant. **(b)** Close-up of CISME deployment: the incubation head is attached to the coral surface with retractile anchors that allows the sealing during the incubation. **(c)** The technical detail (perspective section) of incubation head shows sensors and the LEDs illumination array. The seawater is being recirculated within the chamber and a discrete water sample can be collected through the removal of sample loop.

at 460 mmol m^{-2} s^{-1}, simulating the average *in situ* light levels, and the increase in oxygen concentrations due to net photosynthesis (P_n) measured over 10 min. Here, identical settings were used to measure *i)* differences in the metabolic rates of corals *in situ* and in the laboratory experiments, *ii)* metabolic changes in the morning, afternoon and night metabolism, *iii)* the reproducibility of measurements from the same or different spots on a single coral colony, *iv)* the response of metabolic indicators among different colonies of the same genus measured on the same dive, and *v)*

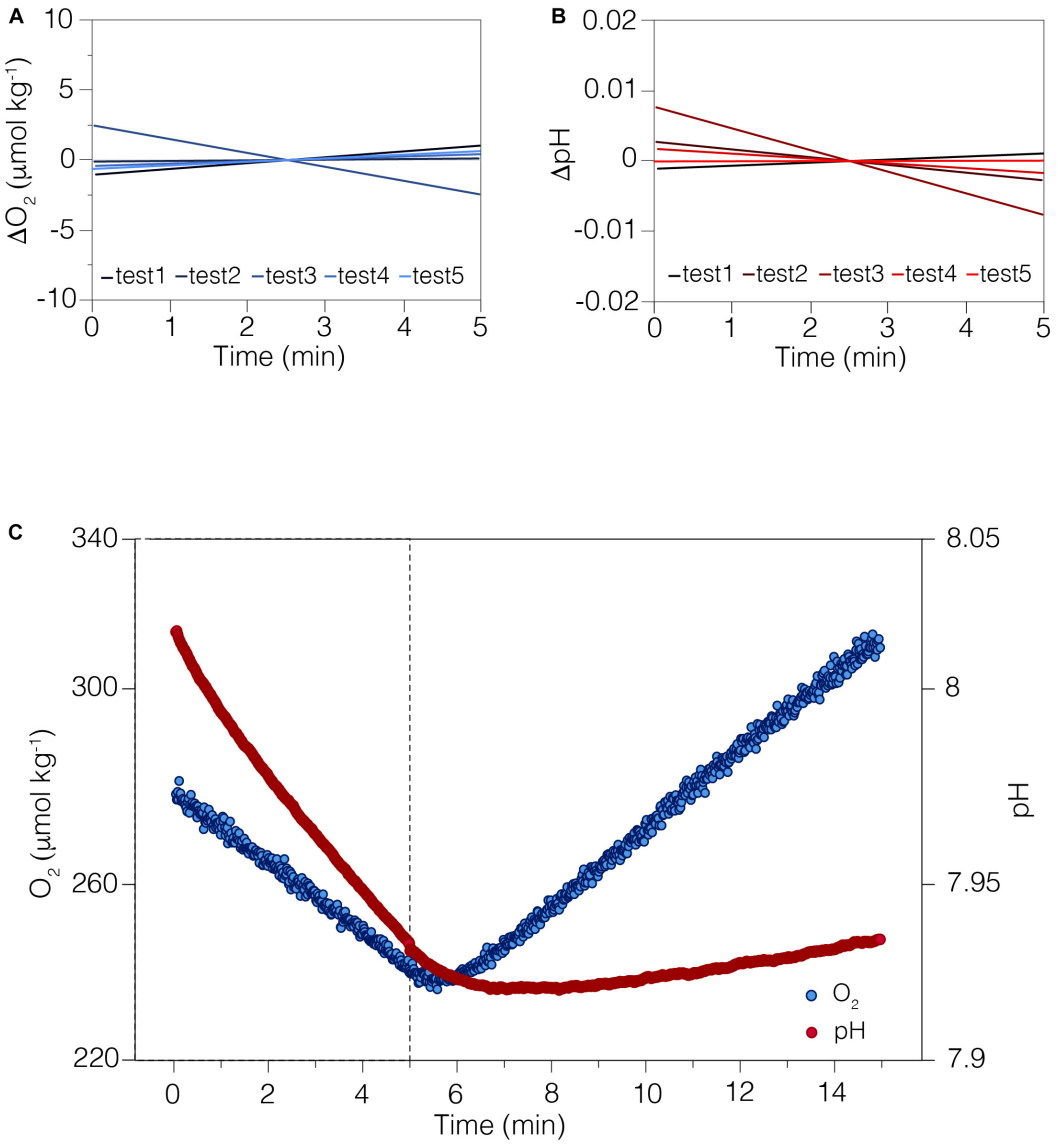

FIGURE 2 | The sensors performance during CISME deployments. **(A)** The stability of the O_2 sensor measured in filtered seawater over the 5-min in an open container in laboratory-controlled conditions. Trend lines of five independent test show anomalies from the mean. **(B)** The stability of the pH sensor over the 5-min in an open container in laboratory-controlled conditions. Trend lines of five independent test show anomalies from the mean. The slight trend in both sensors is likely due to small changes in temperature during the test. **(C)** Real-time O_2 and pH data stream and status of analysis displayed on the tablet during typical 15-min incubation on coral surface, 5-min in the dark followed by 10-min in regulated light conditions. The analytical precision, defined as one standard deviation over time, for O_2 was ±2.33 mmol kg^{-1} and ± 0.02 pH.

the replication of photosynthesis – irradiance curves from a single colony.

Quantification of Metabolic Rates

Dissolved oxygen and pH data were recorded every 1–2 s and displayed in real-time on the tablet. After downloading these data, R and P_n were calculated by regressing the change in oxygen concentrations against time during 5-min dark (R) and 10-min light incubations (P_n) on the coral surfaces (**Figure 2C**). P_g was calculated by adding the absolute value of R to P_n. P_g:R ratios were then calculated as measure of energetic daily productivity of corals. The respiratory (RQ) and photosynthetic (PQ) quotients were estimated from calculation of DIC fluxes during incubations with CO2Sys program (Pierrot et al., 2006; see section "Coral Energetics").

Measurement of A_t and pH enabled full characterization of the seawater carbonate system (CO_2, HCO_3^-, CO_3^{2-}, H^+, and OH^-), and thereby informed on the availability of carbon substrates for calcification (Pierrot et al., 2006). The parameters of the seawater carbonate system (DIC, pCO_2, Ωa) were calculated from measurements of temperature, salinity, pH and total alkalinity using the CO2Sys v2.3 program (Pierrot et al., 2006)

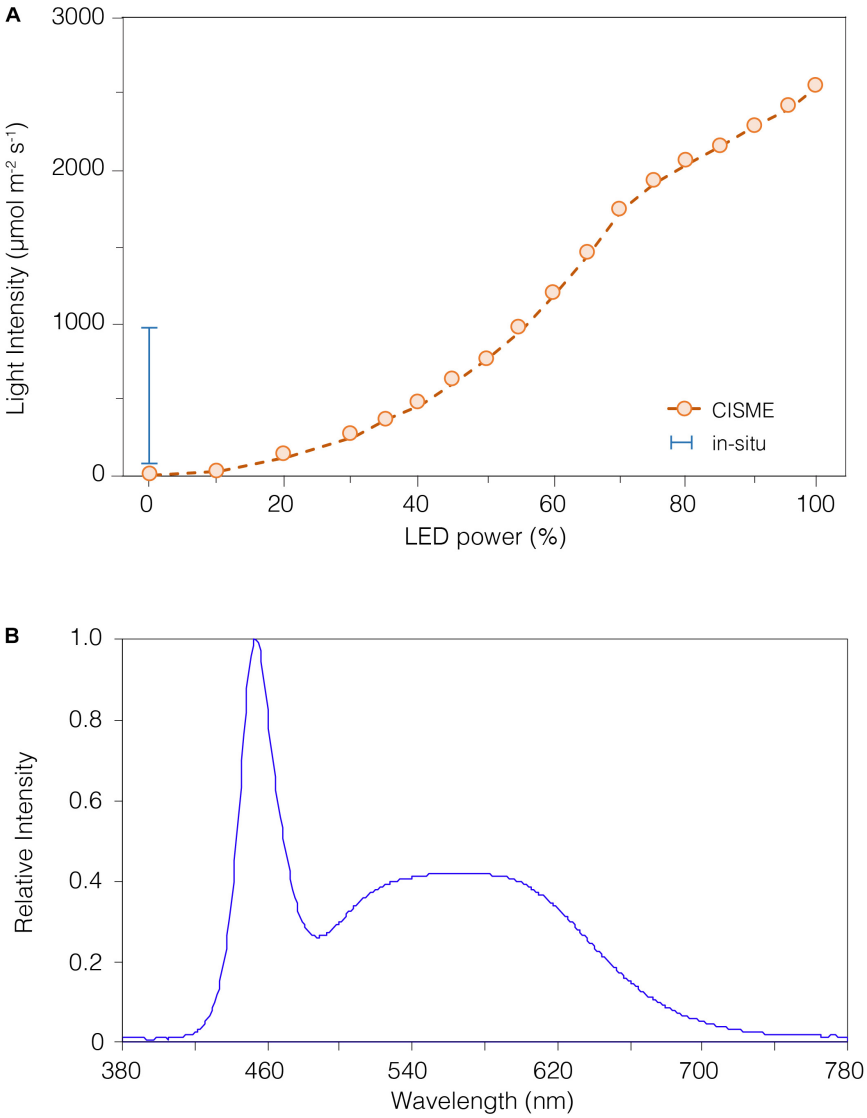

FIGURE 3 | The light intensity of the LED array can be regulated by altering the input power. **(A)** The non-linear relationship between LED power and light intensity (open circles), as measured using a LiCor light-meter. The light intensity can be adjusted up to ~2500 µmol m^{-2} s^{-1}, or near maximal levels of natural light at sea level. Daily *in situ* light levels measured with a HOBO logger are depicted by the range bar for reference. The *in situ* light was measured by the HOBO logger during an 18-month survey and showed a median of ~410 µmol m^{-2} s^{-1}, which was the level selected for our study. **(B)** The LED array emitted a light at 380–780 nm, as measured in sub-aerial conditions with a UPRTrek LED-meter. The highest peak was recorded at 450 nm (violet-blue light), and the color temperature recorded was 7000°K (Luxeon warm white). While the shape of this spectrum differs from natural sunlight, it encompasses the range of photosynthetically active radiation (PAR) and has very limited contribution from damaging UV (<400) wavelengths.

using the carbonic acid dissociation constants K_1, K_2 from Leuker et al. (2000), K_{HSO4} concentration from Dickson (1990) and K_{HF} from Perez and Fraga (1987).

The sample loop containing chamber water was removed after the light incubations, and the sealed loop returned to the surface (within 30 min) where it was transferred into 20 mL glass vials containing 15 mL of saturated solution of $HgCl_2$ (0.08% final concentration). Samples were stored in the dark at 4°C until analysis for A_t using a calibrated, open-cell potentiometric acid-titration with a G20s Mettler-Toledo automatic titrator equipped with a DGi115-SC electrode (Dickson et al., 2007). Analytical precision was ±1.1 mmol kg^{-1} and the accuracy was ±8.2 (n = 14) µmol kg^{-1} (2209.12 mmol kg^{-1} measured), as calculated from the average (±1 std) offset from CRM values (batch #168 for CO_2 and #A11 for titrant, 2207.62 mmol kg^{-1}). CA rates were then determined with the alkalinity anomaly technique (Schoepf et al., 2017) using the following formula:

$$Calcification = \frac{\Delta At \cdot V \cdot \rho}{2 \cdot t \cdot S}$$

where DA_t (mmol kg^{-1}) is the difference in A_t between standard seawater and sample loop water, V (L) is the total volume of the

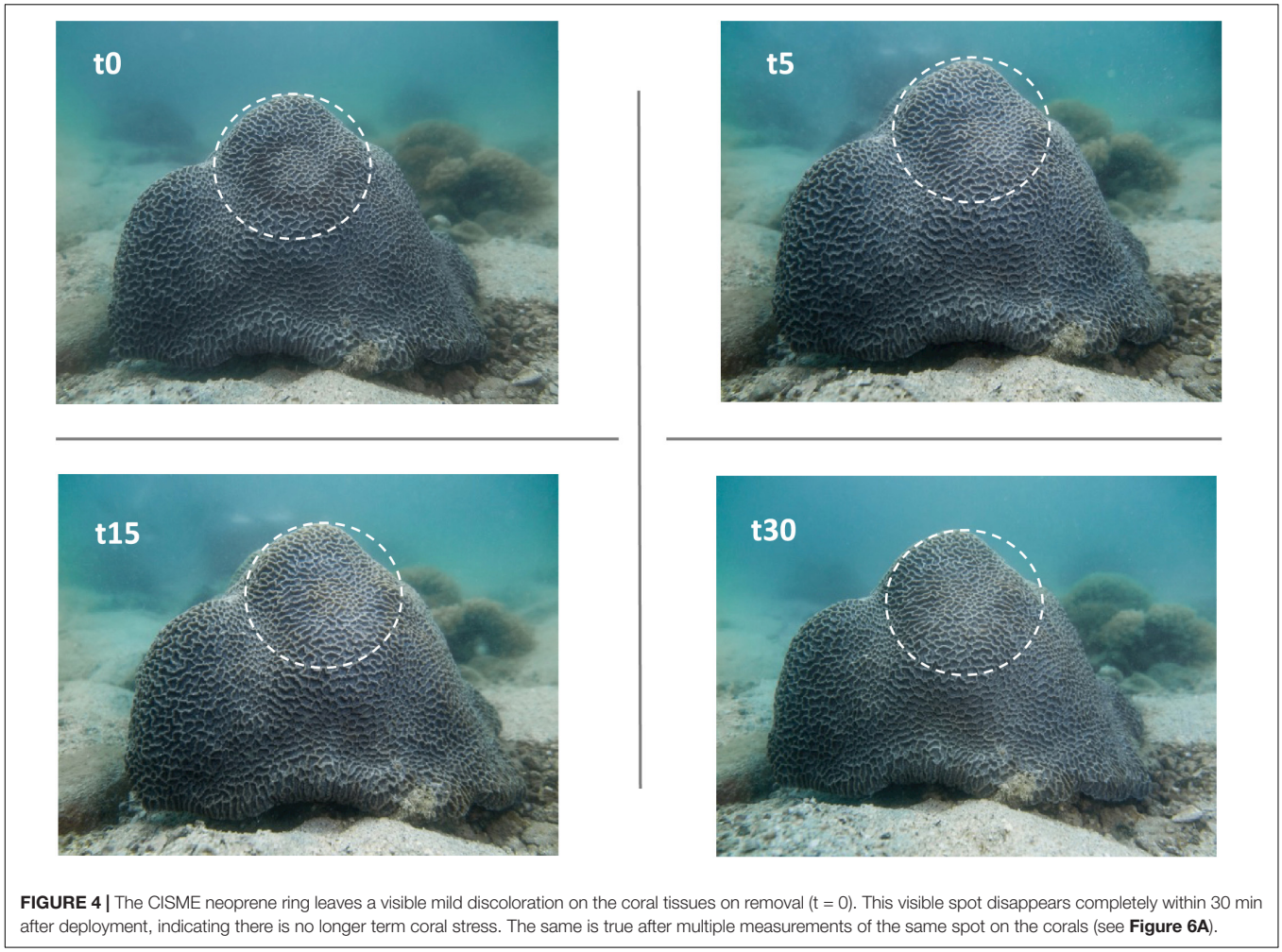

FIGURE 4 | The CISME neoprene ring leaves a visible mild discoloration on the coral tissues on removal (t = 0). This visible spot disappears completely within 30 min after deployment, indicating there is no longer term coral stress. The same is true after multiple measurements of the same spot on the corals (see **Figure 6A**).

chamber (0.088 L), r is the seawater density (~1.023 g cm^{-3}), t (h) is the incubation time (15 min) and S is the coral surface area investigated (24.5 cm^2).

All data were normalized to the two-dimensional coral surface area within the chamber. In cases where the coral surface had irregularities (e.g., bioerosion, disease, attached particles), corrected coral tissue surface areas were calculated using digital photographic techniques. Briefly, an 18 × 13 cm stainless steel frame (Nikonos^{TM} Close Up Unit) was mounted with a digital camera in a diving housing, and the frame positioned surrounding the coral target region for photographs. The digital photographs were analyzed with the computer image program GIMP (Version 2.8, www.gimp.org). The lens distortion was corrected with the image software. The temporary ring left after removal of the incubation chamber was selected and the number of pixels representing coral tissue then calculated:

$$Coral\ Surface = \frac{(pixels\ final\ \cdot 24\ cm2)}{pixels\ start}$$

where pixels start is the original number of pixels in the photograph, and pixels final is the number of pixels of corrected surface area (with non-coral parts removed).

Survey and Collection of Coral Fragments

The *in situ* measurements and collection of coral fragments for the laboratory experiments were carried out in a shallow area (2–4 m depth) region of Mirs Bay at Chek Chau, Port Island (Hong Kong, 22.502° N –114.356° E). This site contains abundant and easily accessible massive coral colonies of Hong Kong's flagship coral species, *Platygyra* spp., which has a boulder-like shape that is well suited for deployments of this instrument. Here, twelve apparently healthy colonies of *Platygyra* spp. were randomly selected and fragments (surface area 30–45 cm^2) were collected with a hammer and chisel. Six of these fragments were analyzed immediately *in situ*, and then all twelve fragments were transported within two hours to the laboratory in transparent zip-lock bags. Further underwater surveys were performed to investigate the difference of metabolic rates on six independent *Platygyra* spp. colonies (**Figure 6B**), while measures at stepped increasing irradiance levels were taken on a single independent colony of *Platygyra* sp. (**Figure 6C**) located at the same study site.

We also used the instrument to investigate *Cyphastrea* sp. at East Dam, Sai Kung (Hong Kong, 22.360° N – 114.376° E). Here,

we conducted *in situ* measurements on the same spot (n = 5) and different spots (n = 4) of an independent colony of *Cyphastrea* sp. (**Figure 6A**).

Both East Dam and Mirs Bay are well known diving sites located in sheltered areas and are largely free from direct runoff or anthropogenic pressures. The underwater instrument surveys were conducted following the established practices of coral monitoring programs in Hong Kong waters, which include the collection of water column parameters, sunlight intensities and rainfall amounts. These sites were chosen so that CISME findings would augment the existing long-term monitoring datasets (Wong et al., 2018).

A further assessment of coral health was carried out to compare the metabolic rates of *Platygyra* spp. in two nearby sites; A Ye Wan (n = 3), Tung Ping Chau Marine Park (22.546° N – 114.431° E), and Gruff Head (n = 3), Hoi Ha Wan Marine Park (22.475° N – 114.324° E). Both sites are located in Marine Parks but have different temporal trends in coral coverage (Wong et al., 2018) and are subjected to different hydrodynamics and freshwater discharge conditions.

All underwater surveys using the instrument presented in this study were conducted from November 2017 to July 2018 (with exception for Marine Parks' survey conducted during the summer 2019), usually between 1000 h and 1300 h, excluding the afternoon and diel cycles experiments. Environmental conditions at both the survey site and in the laboratory aquaria (**Table 1**) were measured with a YSI multiparameter sonde (YSI Exo2 Water Sonde) calibrated prior to each sampling day with standard materials (Xylem Ltd). The pH was measured on the total hydrogen ion scales and calibrated with a Tris buffer (CRM #T32). Discrete water samples (500 mL) were collected in both sites for the determination of total alkalinity (A_t). **Supplementary Information** about water quality parameters and climatological data were drawn from the Environmental Protection Department (www.epd.gov.hk) and Hong Kong Observatory of the Government of Hong Kong S.A.R., China (www.hko.gov.hk).

TABLE 1 | Environmental conditions of seawater at different locations (*in situ* vs. laboratory) on 13th April 2018.

Parameter	*In situ*	Laboratory
Chlorophyll (mg L^{-1})	1.40 ± 0.3	1.05 ± 0.05
Conductivity (mS cm^{-1})	47376.2 ± 86.28	45722.9 ± 19.12
Dissolved Oxygen (mg L^{-1})	6.51 ± 0.2	7.21 ± 0.01
Salinity (psu)	32.75 ± 0.06	31.48 ± 0.01
Dissolved solids (mg L^{-1})	32465.49 ± 52.84	31338.65 ± 8.23
Blue-Green Algae (mg L^{-1})	0.62 ± 0.35	0.84 ± 0.07
Turbidity	0.00 ± 0.08	0.00 ± 0.03
pH (total)	7.91 ± 0.01	7.82 ± 0.03
Temperature (°C)	22.31 ± 0.17	22.3 ± 0.03
GPS	22.502° N - 114.356° E	22.422° N - 114.214° E

Values are means (±SD).

Laboratory Conditions

Laboratory experiments were conducted to evaluate the reproducibility of metabolic indicator measurements under well-regulated conditions in flowing seawater aquaria. We studied the precision of metabolic responses using repeated measurements from the same point on the coral surface, among coral fragments under the same environmental conditions, and on different coral fragments at different times of the day and night. The findings were compared to coral metabolic indicators of corals *in situ* under similar temperature and salinity conditions as in the laboratory aquaria.

Coral incubations were conducted in flowing seawater aquaria at the Simon F.S. Li Marine Science Laboratory, the Chinese University of Hong Kong (22.422° N – 114.214° E). The coral fragments were allowed to recover for three weeks in an outdoor tank (300 L) equipped with natural flow-through seawater (1 L min^{-1}). The outdoor tank was under a plastic rooftop with natural light filtered to 25% intensity (**Supplementary Table S1** online). Besides sensor calibrations, all the laboratory experiments were carried out in the same outdoor setup between April to August 2018 as previously described by Dellisanti et al. (2020). The metabolic rates were measured in laboratory conditions during three weeks acclimation (**Figures 5A,B**); morning and afternoon conditions (**Figures 5C,D**) and during the diel cycle (**Figures 5E,F**). In this way, the coral fragments experienced the same light and flow conditions, but were subject to the natural fluctuations in source water conditions near the mouth of Shing Mun river, Tolo Harbor. This region can be subjected to variable water quality from terrestrial runoff events and limited anthropogenic discharges (EPD, 2017).

Statistical Analysis

All metabolic rates data (respiration, photosynthesis and calcification) were processed by the Dixon's Q test to identify and reject a single outlier (two-sided test) prior to further statistical analysis. A paired t-test ($p < 0.05$) was used to compare metabolic variables during each incubation (*in situ* vs. laboratory; morning vs. afternoon; diel cycle; coral spots and light intensities). The coefficient of variation (CV%) was used to compare the variability of measurements and calculated as ratio of standard deviation to the mean values of measurements. Results were considered significant with $p < 0.05$. Statistical analysis was performed with IBM SPSS Statistics v26.0 (IBM Corp., Armonk, United States).

RESULTS

Instrument Performance

Both the O_2 and pH sensors were tested under temperature-controlled (±0.01°C) indoor conditions in the laboratory, and achieved good precision and accuracy; the O_2 sensor (PreSens) precision was ±2.33 mmol kg^{-1} (±1.04% saturation) in filtered (0.22 mm) seawater, and the ion-selective field effect transistor pH sensor (ISFET Durafet, Honeywell Inc.) precision was ±0.02 pH (measured pH 8.07) in Tris buffered seawater (calculated pH 8.09 from batch #T32 CRM, A. Dickson Laboratory, Scripps

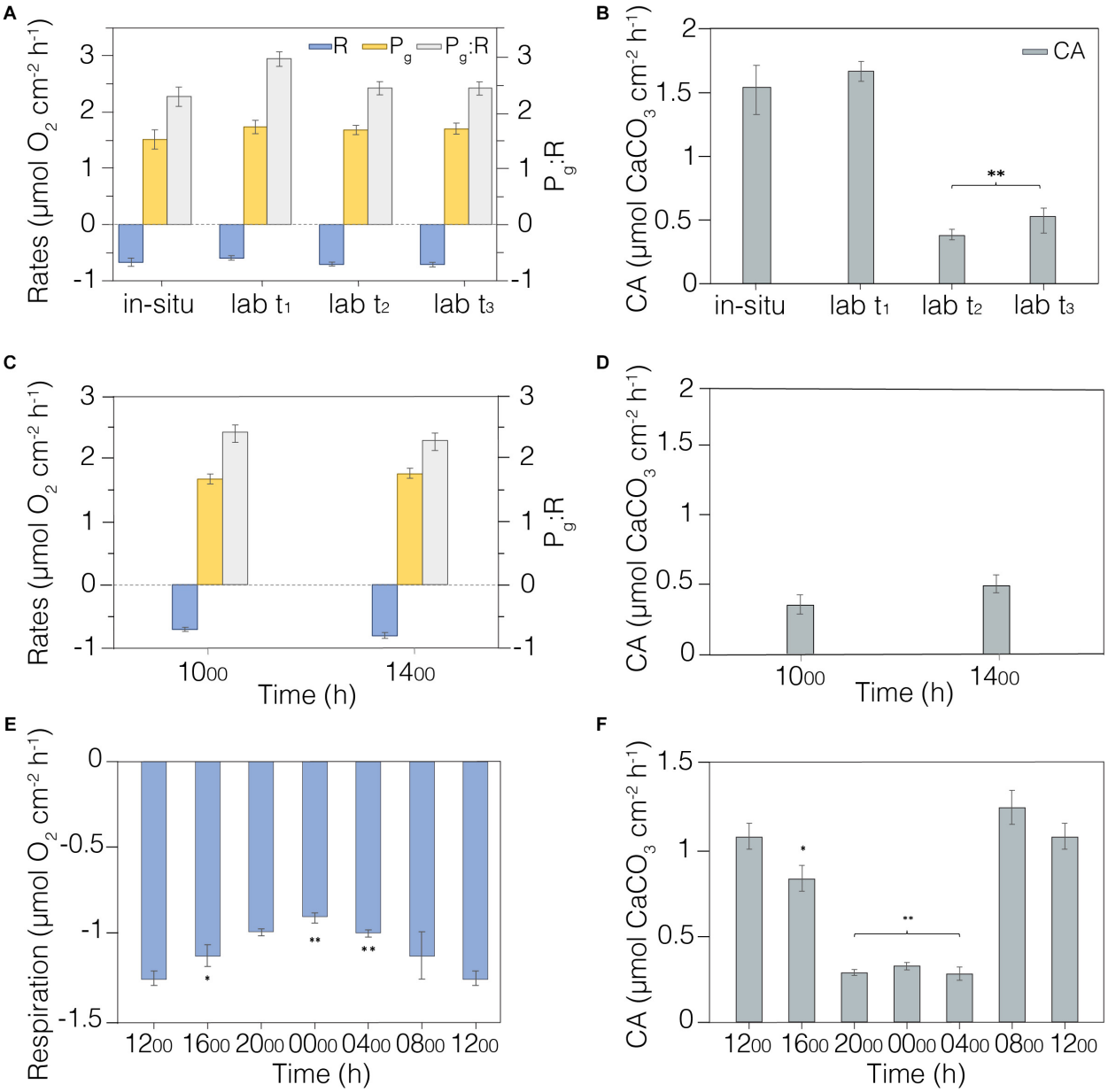

FIGURE 5 | Metabolic rates measured in laboratory conditions. **(A)** Field and laboratory comparison of metabolic rates (R, P_g, and P_g:R) measured *in situ* (n = 6) and in laboratory-controlled conditions during the acclimation period (n = 12). **(B)** Calcification rates measured *in situ* (n = 6) and in laboratory acclimation tank (n = 12). **(C)** Morning and afternoon metabolisms (R, P_g, and P_g:R) were verified during measurements at two time period ranges (1000–1300 h and 1400–1700 h; n = 12). **(D)** Calcification rates measured in morning (1000–1300 h) and afternoon (1400–1700 h); n = 12. **(E)** Diel coral respiration was investigated using measurements taken every four hours (n = 4); values at 1200 h are the same. **(F)** Calcification rates measured every four hours (n = 4); values at 1200 h are the same. Average and standard error shown. **Indicates significative differences $p < 0.01$; *indicates significative differences $p < 0.05$. The legend is shown in the first panel.

Institution of Oceanography) (**Figures 2A,B**). An example of the real-time O_2 and pH data stream acquired during a typical deployment on corals -5 min dark incubation followed by 10 min incubation - is shown in **Figure 2C**. The LED color temperature and light spectrum, measured using a UPRTrek LED-meter, was warm white and 380–780 nm, **Figure 3B**). The LEDs intensity chosen for all light incubations was ∼460 mmol m^{-2} s^{-1} (equivalent to 40% setting) as close as possible to the median irradiance over 18 months of *in situ* measurements (∼410 mmol m^{-2} s^{-1}; Onset HOBO data logger).

Instrument Deployments

The instrument and coupled devices were easily handled underwater and could be transported by a single diver. Even so, good scientific diving expertise and an understanding of the ecological purpose of respirometry measurements is necessary

to maintain diver safety and protect the surrounding corals. On the bottom, release of the carabiners connecting the components together enabled straightforward deployment of the incubation chamber, with the slightly positive buoyant control module floating free of the coral surface (**Figure 1a**). The incubation chamber could be optimally positioned with information from the sensor feedback on the user interface and secured to the coral with retractile anchors (**Figure 1b**). Working in pairs in good marine conditions, divers were able to survey 5 to 6 colonies in less than 120 min; i.e., within the no-decompression time limits for shallow depths (<4 m depth).

Close attachment of the incubation chamber to the coral surface was essential to enable measurements of short-term changes in oxygen, pH and alkalinity. Although a visible ring spot initially was left on the coral surface after the attachment, it faded quickly after removal of the incubation chamber and vanished completely within 15–30 min (**Figure 4**). Longer-term studies in laboratory aquaria confirmed that there were no negative visible effects or mortality caused by even repeated attachment of the instrument's chamber to the same general spot on the corals.

Laboratory Experiments

We first scrutinized the coral fragments for signs of longer-term stress associated with collection and transportation to the laboratory aquaria. Incubation measurements were recorded on six *Platygyra* spp. colonies *in situ* on 13th April 2018, while fragments (n = 12) were collected from other *Platygyra* spp. colonies in the vicinity. Coral metabolic indicators were measured on the fragments after 3 days (t_1) of acclimation and weekly over the next 2 weeks (t_2 and t_3). There were no significant changes in respiration (R; $p = 0.438$) or gross photosynthesis (P_g; $p = 0.179$) measured as the group mean over this 2-week interval (R = 0.67 ± 0.03 mmol O_2 cm^{-2} h^{-1}; P_g = 1.66 ± 0.05 mmol O_2 cm^{-2} h^{-1}; n = 6), and R and P_g were equivalent to those measured *in situ* (**Figure 5A**, **Table 2**). However, P_g:R ratios were 23% higher in the laboratory after 3-days acclimation ($p < 0.01$) than *in situ*, but then stabilized during the second week of acclimation to levels similar to those measured *in situ* ($p = 0.403$; P_g:R = 2.38 ± 0.05; ure 5a). Calcification rates (CA) in the laboratory aquaria were similar to *in situ* values at t_1 ($p = 0.573$; 1.68 ± 0.09 mmol $CaCO_3$ cm^{-2} h^{-1}) but by t_2 the rates had dropped significantly to 0.38 ± 0.05 mmol $CaCO_3$ cm^{-2} h^{-1} ($p < 0.01$) and remained unchanged at t_3 (**Figure 5B**, **Table 2**).

Changes in irradiance have the potential to affect net photosynthetic rates, and so there was concern that metabolic status estimates could change over the course of the day. Indeed, the irradiance in laboratory aquaria was higher in the morning (46.24 ± 21.84 μmol m^{-2} s^{-1}) compared to afternoon (7.57 ± 3.32 μmol m^{-2} s^{-1}) due to shading by the adjacent building (**Supplementary Table S1**). Measurements were taken every 20 min on the *Platygyra* spp. fragments (n = 12) during

TABLE 2 | Metabolic rates measured in different conditions in this study.

	R (O_2) mmol cm^{-2} h^{-1}	P_g (O_2) mmol cm^{-2} h^{-1}	P_g:R	CA ($CaCO_3$) mmol cm^{-2} h^{-1}
In situ	−0.67 (0.07)	1.51 (0.17)	2.27 (0.17)	1.26 (0.12)
Lab t_1	−0.59 (0.04)	1.73 (0.12)	2.94 (0.13)**	1.68 (0.09)
Lab t_2	−0.70 (0.03)	1.68 (0.08)	2.42 (0.12)*	0.38 (0.05)**
Lab t_3	−0.71 (0.04)	1.71 (0.10)	2.43 (0.16)	0.53 (0.10)
Morning	−0.70 (0.03)	1.68 (0.08)	2.42 (0.12)	0.38 (0.05)
Afternoon	−0.80 (0.05)	1.77 (0.06)	2.30 (0.16)	0.29 (0.05)
1200 h	−1.24 (0.04)	2.92 (0.26)	2.34 (0.14)	1.08 (0.08)
1600 h	−1.11 (0.06)*	2.81 (0.07)	2.55 (0.12)	0.84 (0.08)*
2000 h	−0.97 (0.02)	*na*	*na*	0.29 (0.02)**
0000 h	−0.89 (0.03)**	*na*	*na*	0.32 (0.02)
0400 h	−0.98 (0.02)**	*na*	*na*	0.28 (0.04)
0800 h	−1.11 (0.14)	2.86 (0.24)	2.64 (0.17)	1.25 (0.10)**
1200 h	−1.24 (0.04)	2.92 (0.26)	2.34 (0.14)	1.08 (0.08)
Same spot	−0.52 (0.03)	1.04 (0.03)	2.04 (0.16)	*na*
Different spots	−0.16 (0.02)**	0.88 (0.02)**	5.78 (0.74)**	*na*
Different colonies	−1.06 (0.05)	2.51 (0.09)	2.42 (0.20)	2.20 (0.19)
0 mmol m^{-2} s^{-1}	−0.64 (0.08)	*na*	*na*	*na*
190 mmol m^{-2} s^{-1}	*na*	1.38 (0.09)	2.24 (0.28)	*na*
360 mmol m^{-2} s^{-1}	*na*	2.11 (0.07)**	3.44 (0.41)**	*na*
750 mmol m^{-2} s^{-1}	*na*	2.52 (0.07)**	4.12 (0.52)*	*na*
1900 mmol m^{-2} s^{-1}	*na*	2.66 (0.11)	4.33 (0.50)	*na*
2500 mmol m^{-2} s^{-1}	*na*	2.42 (0.11)**	3.95 (0.43)*	*na*
CV in situ	16.63 (5.71)	12.62 (6.60)	14.92 (4.37)	20.80 (12.56)
CV lab	16.76 (7.11)	12.23 (6.34)	18.37 (6.12)	33.94 (14.15)*

*R = respiration; Pg = gross photosynthesis; P_g:R = gross photosynthesis to respiration ratio; CA = calcification. Values are means (±standard error), except CV values which are expressed as means (±SD). **indicates significative differences $p < 0.01$; *indicates significative differences $p < 0.05$.*

morning (1000-1300 h) and afternoon (1400–1700 h). There were no significant differences between morning and afternoon in R (p = 0.199), P_g (p = 0.573), P_g:R (p = 0.403) (**Figure 5C**), or CA (p = 0.18) (**Figure 5D**). The coefficient of variation (CV) of replicate measurements of R and P_g in the morning or afternoon was better than 20%, while the afternoon P_g:R ratios were slightly more variable (±23.1%, **Figure 5C**). CA rates estimated from changes in A_t in had a greater CV in the morning (37.6%) and afternoon (53.9%), indicating a greater fluctuation in DIC uptake rate among the fragments. Even so, grouping measurements from the morning and afternoon yielded precisions of <7% for R, P_g and P_g:R and 15% for CA: R = 0.75 ± 0.05 mmol O_2 cm^{-2} h^{-1}, P_g = 1.73 ± 0.05 mmol O_2 cm^{-2} h^{-1}, P_g:R = 2.36 ± 0.06, and CA = 0.34 ± 0.05 mmol $CaCO_3$ cm^{-2} h^{-1}. Although these results showed that the metrics of analyses were uniform from late morning to early afternoon under natural sunlight conditions, we conservatively restricted all subsequent laboratory and *in situ* sampling to between 1000–1300 h.

We quantified coral R and CA over a diel cycle to gain better insight into the natural metabolic transitions. Oxygen consumption and changes in alkalinity were measured every four hours on *Platygyra* spp. fragments (n = 4) in the laboratory aquaria (**Figures 5E,F**). R decreased steadily by about 2% per hour from noon to midnight, with midnight values being ∼30% lower than that at noon (1.24 ± 0.04 vs. 0.89 ± 0.03 mmol O_2 cm^{-2} h^{-1}; **Table 2**). This decrease became significant (p < 0.01) after 2000 h. A similar diel trend was observed in rates of CA, whereby maximum rates of 1.25 ± 0.10 mmol $CaCO_3$ cm^{-2} h^{-1} occurred during the morning and mid-day but decreased sharply by ∼27% to a minimum of 0.30 ± 0.01 mmol $CaCO_3$ cm^{-2} h^{-1} during the dark hours.

In situ Experiments

Assessing the functional, or effective measurement precision of these analyses among coral fragments within a controlled uniform environment is an important step, but it also is necessary to assess this measurement precision in natural reef environments. We measured this precision *in situ* on a single colony of *Cyphastrea* sp. using repeated short-term deployments (15 min) on a single dive at the same position on the colony (n = 5), and then among different spots (n = 4) on the colony (**Figure 6A**). The CV for repeated measures of R, P_g and P_g:R on the same spot were 12.0%, 5.4%, and 17.3%, respectively, while the variation measured across different positions on the same colony was greater for R and P_g:R (> 25%), but lower for P_g (<5%). Measurements of *in situ* metabolism on different colonies of *Platygyra* spp. in the same dive site also showed good replication (**Figure 6B**), with the CV in R and P_g being 12.02% and 8.8%, respectively, while P_g:R and CA being somewhat higher (20.48% and 21.13%) (n = 6). These metabolic rates were similar to those measured in the laboratory aquaria (P_g = 2.51 ± 0.09 mmol O_2 cm^{-2} h^{-1}; R = 1.06 ± 0.05 mmol O_2 cm^{-2} h^{-1}; P_g:R = 2.42 ± 0.20; CA = 2.20 ± 0.19 mmol $CaCO_3$ cm^{-2} h^{-1}; **Table 2**).

The photosynthetic production of the coral holobiont changes with irradiance (Sawall and Hochberg, 2018), and so we used repeated measurements to evaluate the precision of net photosynthesis (P_n) and R as a function of PAR intensity. Measurements were taken at five irradiance levels from 0–2500 mmol m^{-2} s^{-1} on a single *Platygyra* sp. colony (**Figure 6C**). The maximum P_g and P_g:R ratios were detected at ∼1980 mmol m^{-2} s^{-1} (2.66 ± 0.11 mmol O_2 cm^{-2} h^{-1} and 4.33 ± 0.50,

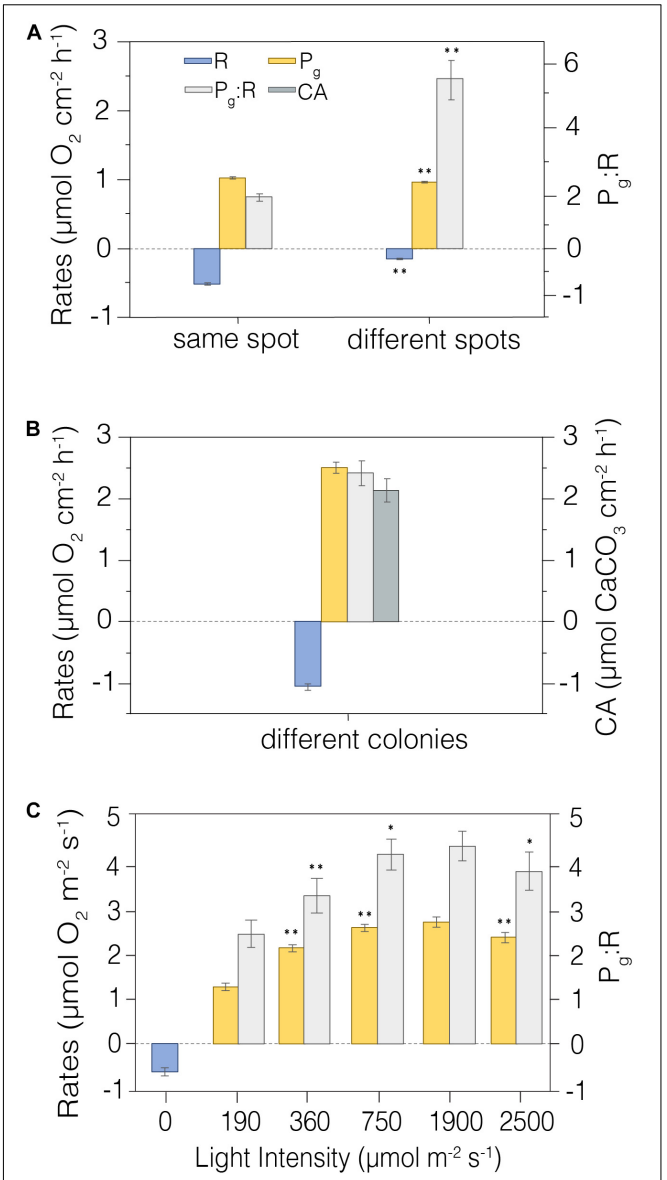

FIGURE 6 | Metabolic rates measured *in situ*. **(A)** Repeated CISME measurements taken from the same precise location on a coral surface relative to repeated measurements taken from independent locations on a single *Cyphastrea* sp. colony (n = 4). **(B)** CISME measurements from *Platygyra* spp. colonies in the same dive site (n = 6). **(C)** Photosynthesis and respiration rates as a function of stepped increasing simulated PAR in the CISME chamber (n = 5); the measurements were made on a colony experiencing *in situ* incident radiation of ∼400 µmol m^{-2} s^{-1}. Average and standard error shown. Average and standard error shown. **indicates significative differences p < 0.01; *Indicates significative differences p < 0.05. Legend is shown in the first panel.

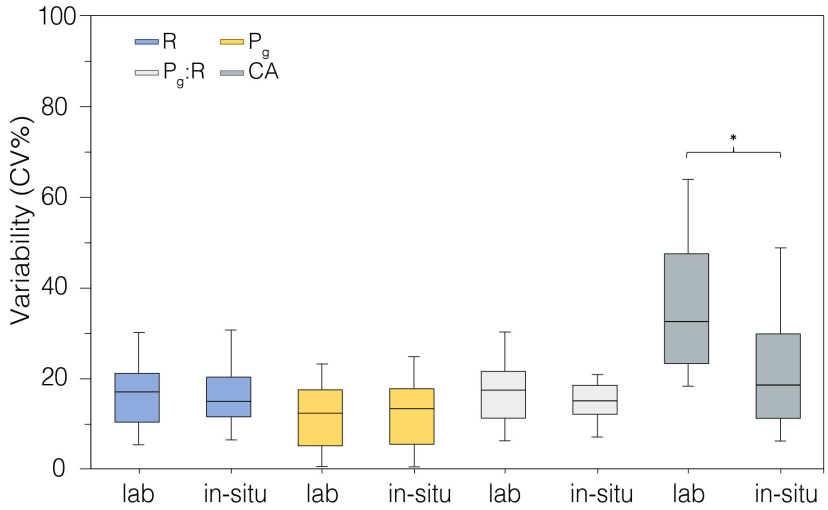

FIGURE 7 | Coefficient of variability (CV%) calculated from metabolic rates measured in laboratory-controlled conditions (n = 18) and *in situ* (n = 18). *indicates statistical difference $p < 0.05$.

respectively), but these values were very similar to those observed at ∼750 mmol m^{-2} s^{-1} ($p > 0.05$; **Table 2**). As with the earlier laboratory and field measurements, the variation in P_g was generally <10%, although the variation in R and P_g:R was greater (>20%) (**Figure 6C**).

The precision of measurements for each parameter taken in the laboratory-controlled conditions and *in situ* was compared (**Figure 7**). The variability among replicate measurements was similar between laboratory and field data, with higher variability observed in CA rates in the laboratory aquaria relative to field rates ($p < 0.05$, **Figure 7**, **Table 2**).

We compared the *in situ* metabolic data (O_2 vs. $CaCO_3$ production) of corals from Mirs Bay with those in laboratory conditions. Data collected *in situ* showed a weak positive relationship between measured O_2 production (from gross photosynthesis) and daily calcification (1.18 ± 0.40, R^2 = 0.27), but no discernable relationship was observed in the laboratory aquaria (5.35 ± 4.11, R^2 = 0.01; **Figure 8**).

Finally, we conducted a preliminary assessment of how well the instrument could discriminate the metabolic status (R, Pg, Pg/R, and CA) of coral at different geographic locations in the Hong Kong region (**Figure 9**). Colonies of *Platygyra* spp. were sampled in A Ye Wan (n = 3), Tung Ping Chau Marine Park, and Gruff Head (n = 3), Hoi Ha Wan Marine Park. Measured levels of R, Pg and Pg/R were similar across both sites, but calcification rates were essentially zero in corals at Gruff Head (-0.18 ± 0.16 μmol CaCO3 cm^{-2} h^{-1}) relative to that measured in A Ye Wan (1.57 ± 0.13 μmol $CaCO_3$ cm^{-2} h^{-1}) (**Figure 9**).

DISCUSSION

The purpose of this study was to evaluate the precision and accuracy of a novel underwater respirometry system for the measurement of sensitive indicators of stress on coral health. Assessing the metabolic status of corals and reef systems has relied on a variety of approaches and quantitative indicators. Microsensor O_2 profiles at the coral diffusive boundary layer yield insights at the single polyp, or multiple polyp scales (Kuhl et al., 1995; Larkum et al., 2003; Yates and Halley, 2003; Camp et al., 2015; Nelson and Altieri, 2019), but these technologies are not logistically suited for surveying. Pulse amplitude modulated (PAM) fluorimetry can rapidly provide indications of coral health by quantifying the photophysiology of endosymbionts (Beer et al., 1998; Ralph et al., 1999), but cannot yield information on coral growth. At the other end of the spectrum, reef-scale net ecosystem production and calcification can be estimated through measuring a combination of seawater pH, DIC, A_t, or pCO_2 to constrain the seawater carbonate system (Anthony et al., 2011; McMahon et al., 2018), however, they require substantial observational infrastructures. The underwater respirometry system tested here (CISME) can bridge small-scale to reef system approaches by providing quantitative metabolic data at colony scales with an easily portable, self-contained unit that can be used effectively without expert training or elaborate observational networks.

The preliminary work investigating the functionality of the instrument was promising (Murphy et al., 2012; Dellisanti et al., 2020), but significant questions remained about its effective reproducibility in coral studies. That is, do these metabolic measures yield sufficient accuracy and precision to enable meaningful quantitative comparisons among laboratory and field studies, across reef systems, and over the time scales needed to establish the effect of climate drivers? Our study investigated this question.

Instrument Performance

The instrument design combines the detection of *in situ* metabolic indicators with comparative ease of use by scientific divers. The instrument is reasonably compact, can be operated

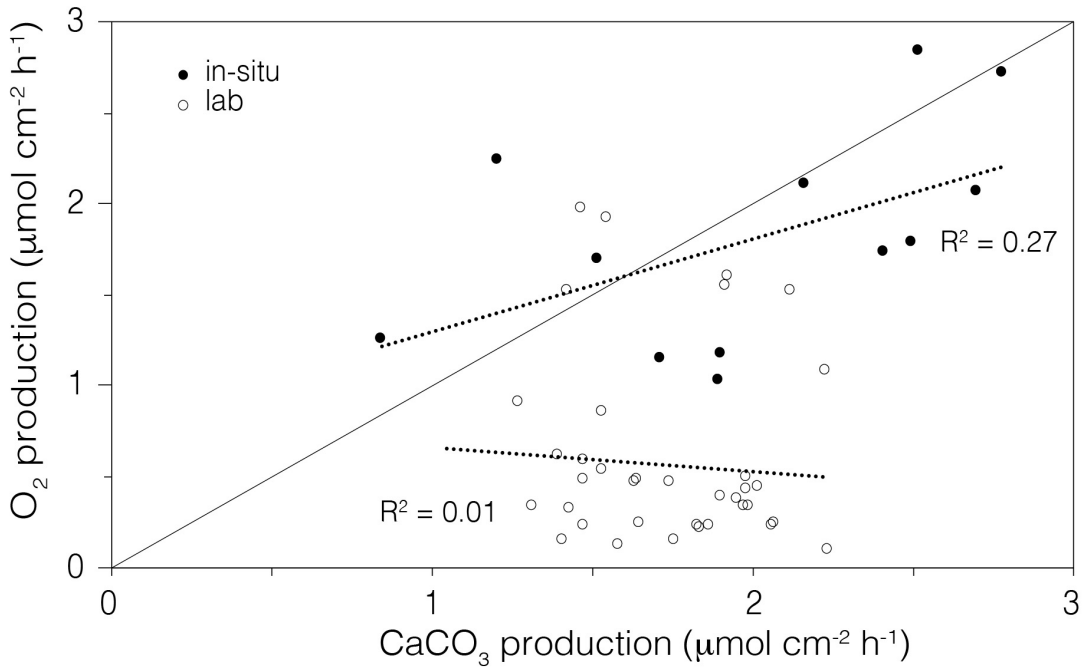

FIGURE 8 | Comparison of the average rate of O_2 production (gross photosynthesis) to the average rate of calcium carbonate production (daily calcification) in the laboratory aquaria (open circle) and *in situ* (closed circle) corals. The line shows the 1:1 relationship between the moles of O_2 produced and moles of $CaCO_3$ precipitated.

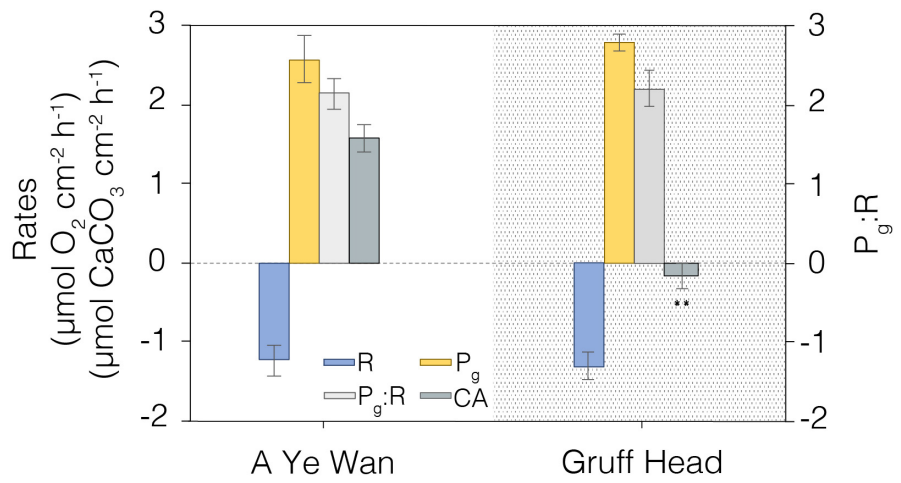

FIGURE 9 | A comparison of coral metabolic rates measured in summer, 2019 at A Ye Wan (n = 3), Tung Ping Chau Marine Park, and Gruff Head (n = 3), Hoi Ha Wan Marine Park. Average and standard error shown. **Indicates significative differences $p < 0.01$.

in both deep and reasonably turbulent waters, and the output data can be processed using basic statistics and commonly available free software. To our knowledge it is the first system that enables practical measurements of underwater respirometry sufficiently rapidly to survey several coral colonies in shallow marine areas on a single dive, while simultaneously enabling the collection of other standard coral monitoring data. Measurements of dissolved O_2 and pH fluxes are considered to be drivers and indicators of coral energetic dynamics, including respiration, photosynthesis and calcification (Falkowski et al., 1984; Cohen et al., 2016), and the non-invasive sampling of these parameters with this instrument enables the *in situ* analysis of coral metabolic processes. This innovative underwater respirometer, used in conjunction with standard coral and environmental monitoring practices (e.g., spatial surveys, water quality indicators, etc.), represents a significant advance in the capacity to study and evaluate the status of reef ecosystems.

Our findings show that the instrument provided highly precise and accurate measurements of coral-induced changes in dissolved O_2 and seawater pH compared to other studies using benthic chambers (Yates and Halley, 2003; Camp et al., 2015). The alkalinity anomaly method for determining short-term calcification rates, using open-cell potentiometric acid-titration (Dickson et al., 2007), is more accurate than the buoyant weight methods (Schoepf et al., 2017). Moreover, combining pH measurements and alkalinity enables characterization of the seawater carbonate system, providing estimates of the DIC composition and aragonite saturation (**Ωa**) state. We recognize that alkalinity and total dissolved inorganic carbon (vs. pH) yields more precise calculations of the carbonate system (Riebesell et al., 2011) but higher levels of precision generally are not required for the study of biological systems (e.g., the Global Ocean Acidification Observation Network; www.goa-on.org).

Corals are delicate, slow-growing organisms that can easily be damaged by physical disturbance, so an overriding concern of any *in situ* methods is whether corals are negatively impacted by the measurement process itself. In this case, a soft neoprene ring is pressed against the coral surface using stabilizing harnesses to create a small chamber (**Figure 1c**). Most deployments lasted 15 min in duration, the minimum time to ensure significant changes in A_t could be detected, but shorter times could be used if calcification rates were not measured. On removal of the chamber, a mucoid "ring" was routinely observed where the neoprene was in contact with the coral, but this feature was short-lived (**Figure 4**). While coral polyps on the periphery of the chamber (i.e., under the neoprene seal) exhibited signs of short term stress (mucus production), there were no negative effects observed on coral morphology or energetics with repeated discrete measurements at different times on the same region of coral fragments in laboratory aquaria or *in situ* (**Figures 5**, **6**). This independence between peripheral and within-chamber polyps is consistent with indications of semi-autonomy among neighboring polyps (Nothdurft and Webb, 2009). The implication then is that the chamber measurement over these 15-min deployments adequately reflects the ambient metabolic state of the sampled coral surface.

The benefit of short-term incubations is the potential for replicate measurement to capture the variability in metabolic status *in situ* over the same coral structure, among colonies having varying proximity to local point-source stressors (e.g., anthropogenically influenced discharges), or the cumulative local and global impacts on corals over time or latitudinal ranges. However, our findings show that the choice of the deployment spot is crucial and based on the morphology of the coral colony. For instance, the variability of measurements taken on a single *Cyphastrea* spp. coral colony was much higher when measured on different spots (**Figure 6A**), likely due to its encrusting-irregular surface. On the other hand, the boulder morphology of *Platygyra* spp. was more practical and precise when the energetics were compared between five colonies (**Figure 6B**). We were able to examine the metabolic status of 6 coral colonies on a single dive in shallow waters, lowering incubation times from hours (e.g., Camp et al., 2015) to minutes. Single measurements of oxygen fluxes (R or P_g) could be processed within 5 min on the underwater tablet, allowing replication at both temporal and spatial scales. Four to six replicates were used in field studies here to assess this variability; more than would be practical for general reef survey protocols.

Coral Metabolic Rates

Corals experience natural day-to-night variations in the gradient of dissolved oxygen and DIC between coral tissue and the surrounding waters (Allemand et al., 2011; Schoepf et al., 2017). Under sunlight, the photosynthetic production by the endosymbionts yields O_2, energy as ATP, and carbohydrates to the coral tissue (Falkowski et al., 1984). Most of the photo-produced O_2 (78–90%) is consumed by respiration (Kuhl et al., 1995; Al-Horani et al., 2003b; Levy et al., 2004) while the excess is released to the surrounding water (Al-Horani et al., 2003a, 2007). Many coral species, such as *Platygyra* spp., shift to heterotrophic feeding at night extending their polyps on planktonic prey, when they become dependent on O_2 flux from the external environment for respiration (Al-Horani et al., 2003a). The night-time decrease in available O_2 can limit coral respiration, and thereby the needed adenosine triphosphate (ATP) supply to fuel dark calcification (Al-Horani et al., 2007); a significant problem for reefs exposed to low night-time dissolved O_2 concentrations. Indeed, night-time respiration under our laboratory setting was $\sim$ 29% lower than the daytime measured rates (**Figure 5C**), in general agreement with other findings (Schneider et al., 2009). Even though the flowing seawater in our aquaria was well oxygenated, night-time calcification rates were $\sim$73% lower than daytime rates (**Figure 5C**), consistent with earlier findings that daily photosynthesis has a major role in enhancing the calcification process (Falkowski et al., 1984; Cohen et al., 2016).

Measurements of R were highly replicable in laboratory-controlled conditions and similar to that measured *in situ* (**Figure 5**). The endosymbiont contribution to the O_2 consumption/CO_2 production in dark conditions (Kuhl et al., 1995; Hawkins et al., 2016) was not considered here; it was assumed that short incubation times (5 min) were insufficient for any flux from the symbionts to significantly alter the seawater chemistry in the benthic chamber. However, cellular respiration of the coral holobiont produces CO_2, causing pH to decrease, so care must be taken during respirometry measurements to ensure that the resultant shift in **Ωa** does not substantially affect calcification rates (Andersson et al., 2011). Our data showed a reduction of 0.1 **Ωa** per minute of dark incubation, which with our local seawater would lead to carbonate dissolution conditions (**Ωa** $\leq$ 1) in the chamber after 20 min of dark incubation. In the protocols proposed here, we selected 5 min dark incubations, resulting in an overall reduction of about 0.5 to 2.5 **Ωa** (**Supplementary Table S2** online), even shorter dark incubations would be necessary in reef systems having lower initial **Ωa** levels.

The ratio of oxygen produced through photosynthesis and oxygen consumed by dark respiration provides an energetic measure of coral capacity for self-maintenance and growth. P_g:R ratios measured on *Platygyra* spp. and *Cyphastrea* spp. did not differ among different experimental treatments and always

remained above the minimum level for functional autotrophy (e.g., =2, Coles and Jokiel, 1977), although the ratios were lower than measured for other species in Hong Kong waters (McIlroy et al., 2019). Moreover, differences in P_g:R values largely resulted from variations in R rather than P_g. These findings would suggest that these corals were near their physiological limits (i.e., maximum P_g) when we measured these metabolic rates; i.e., during the wet season between April to August 2018. However, a more detailed survey on seasonal and spatial pattern of coral metabolism would be needed to confirm this tentative conclusion.

We compared the precision of measurements for each parameter taken in the laboratory-controlled conditions and *in situ* (**Figure 7**). The variability among replicate measurements was very similar between laboratory and field data. Our R, P_g, and P_g:R data (n = 18) suggest that the natural variation of metabolic parameters between fragments or colonies belonging to the same species is about ± 20%, and it might depend on polyp vs endosymbionts symbiotic status of single colonies. The higher variability of CA in the laboratory aquaria over time relative to that *in situ* ($p < 0.05$, **Figure 7**) likely was related to both lower, and more variable alkalinity in the Tolo Harbor source waters compared to the more stable, and higher alkalinity in Mirs Bay (2042.76 ± 158.27 mmol kg^{-1} vs. 2270.84 ± 88.74 mmol kg^{-1}, respectively; n = 18; **Table 1**). The outer-estuarine seawater source for the outdoor tanks is more directly influenced by freshwater discharge than the field site, and thus would be more susceptible to natural fluctuations of seawater chemistry. Moreover, the significant reduction of natural light intensities in laboratory versus *in situ* conditions, from 395.48 ± 168.5 to 20.73 ± 23.43 mmol m^{-2} s^{-1} (**Supplementary Table S1**, online) may also have contributed to lower CA (**Figures 5B,D**).

Conducting reef surveys logistically requires sampling at different times of the day (i.e., light levels), so how much variability occurs between the morning and afternoon sampling of coral metabolic indicators? We found there was no difference in the rates of R, P_g, or CA in multiple measures during the morning (1000–1300 h) and afternoon (1400–1700 h) in the natural light exposed aquaria (**Figure 5C**), although discrete measurements showed a slight trend consistent with light levels decreasing from 46.24 ± 21.84 (morning) to 7.57 ± 3.32 mmol m^{-2} s^{-1} (afternoon; **Supplementary Table S1**, online). However, R and CA rates were slightly reduced in the afternoon (1600 h) by 11 and 23%, respectively, when we quantified the rates over the diel cycle (**Figures 5E,F**; $p < 0.05$), likely reflecting the greater variation in day-time light levels during this experiment (from 126.9 ± 37.28 in the morning to 27.18 ± 3.89 mmol m^{-2} s^{-1} in the afternoon; **Supplementary Table S1**, online). Nevertheless, these results demonstrate the flexibility in the practical application of the instrument as a reef survey tool.

Coral Energetics

The instrument also fills an important methodological gap by quantifying the energetic costs of individual *in situ* corals under present day conditions, thereby informing on the potential impacts under future scenarios. In their overall energetics, corals consume oxygen during aerobic respiration to break down glucose and create ATP, while simultaneously, under sunlight conditions, endosymbiont-mediated photosynthesis produces glucose, releasing O_2 as a by-product. This positive feedback loop (Gardella and Edmunds, 1999) fuels the metabolically demanding process of calcification (Cohen and Holcomb, 2009), where a plasma membrane Ca^{2+} - ATPase regulates the exchange of Ca^{2+} and H^+ from the calicoblastic cells into the calcifying space (Murphy and Richmond, 2016). In this framework, 1 ATP is consumed by coral respiration per mmol of $CaCO_3$ produced, with the overall energetic expenditure for calcification being ∼30% of the total energy budget (Cohen and McConnaughey, 2003). The *in situ* metabolic data for corals from Mirs Bay showed a weak positive relationship between measured gross photosynthesis and daily calcification, indicating that the environmental conditions (e.g., alkalinity, sunlight irradiance) supported a more sustainable coral growth compared to corals maintained in the laboratory aquaria (**Figure 8**). Although the P_g of the laboratory-housed coral fragments were sufficient to maintain healthy colonies, consistent with their robust visual appearance, their rates of calcification (i.e., growth) were substantially lower than that of *in situ* corals having equally robust visual appearance and equivalent P_g (**Figure 5B**). These findings illustrate the potential deeper insights that would stem from use of this respirometry instrument in spatial and temporal assessments of the health status of reef systems.

As a further example of this point we conducted a preliminary assessment of the potential effects of local stressors by comparing coral metabolic indicators between two Hong Kong marine parks. Tung Ping Chau Marine Park hosts visually robust corals and the A Ye Wan shore has the highest coral coverage in Hong Kong (>50%); a low stress endmember for the Hong Kong region. In contrast, the Gruff Head area in Hoi Ha Wan Marine Park, situated ∼10 km across Mirs Bay, has a much lower coverage of corals (∼20%) that is in a state of decline (Wong et al., 2018). Gruff Head experiences higher freshwater and anthropogenic inputs from both Tolo Harbor and Channel and the local river in Hoi Ha, especially during the summer (wet season). Both sites had similar hardy rates of P_g, R, and P_g:R, suggestive of healthy corals, but dramatically different levels of CA, with rates equivalent to zero for Gruff Head (**Figure 9**). That is, unlike corals at A Ye Wan, corals at Gruff Head were maintaining their physiology but not growing during the summer sampling period. Although the relative status of corals in these two marine parks cannot be adequately assessed from this single point sampling, these data illustrate the strength of this combination of metabolic indicators for investigating spatial distributions of local stressor effects.

The change in O_2 and pH during our deployments can provide information about individual coral metabolic quotients (Q) (Gattuso and Jaubert, 1990), whereby the photosynthetic quotient (PQ) is the ratio of oxygen production and carbon sequestration through photosynthesis and the respiratory quotient (RQ) is the ratio of carbon release and oxygen consumption during dark respiration. Estimates of these values for reef systems are generally assumed on the order of ∼1 (Muscatine et al.,

1981; Atkinson and Falter, 2003; Taddei et al., 2008; Falter et al., 2012; Takeshita et al., 2016, 2018; Bednarz et al., 2018), but few data sets are available on coral reefs, and we are unaware of any calculated from single coral colonies *in situ*. The positive (production) and negative (respiration) change in pH measured during our deployments (e.g., **Figure 2C**) enables direct estimation of these coral metabolic quotients (Gattuso and Jaubert, 1990) through the calculation of DIC with the CO2Sys program (Pierrot et al., 2006). However, O_2 and DIC fluxes are dependent on many factors, and metabolic quotients can be variable. Indeed, the PQ calculated from our measurements was 1.22 ± 0.33 mol O_2:mol C in laboratory but was substantially lower *in situ*, at 0.66 ± 0.38 mol O_2:mol C, spanning the reported range for whole reef systems. Low PQ could occur due to super saturation of oxygen in seawater or hydrodynamics at the surface of corals as observed in previous studies (Atkinson and Grigg, 1984; Taddei et al., 2008; Bolden et al., 2019) coupled with the DIC bioavailability. Conversely, our estimated single colony RQ was substantially higher than the reported community estimates in the laboratory (1.47 ± 0.42 mol C:mol O_2) and particularly *in situ* (1.83 ± 0.44 mol C:mol O_2; **Supplementary Table S3**, online), suggesting a deeper investigation on the stoichiometry of metabolic quotients should be implemented in future coral reef ecology studies (Takeshita et al., 2016). Moreover, it has been suggested that large variability of Q could be due to environmental factors, diel cycle and sampling bias (Bolden et al., 2019). The carbon fluxes estimated from metabolic rates detected by this respirometry system could allow a further investigation about coral health under different conditions. Taken together with seawater carbonate system, a more general information on the coral health status can be extrapolated into the metabolic "pulse" of coral communities (Cyronak et al., 2018, Bolden et al., 2019).

The present study focused on massive and encrusting coral colonies, and though the respirometry system can be applied to other benthic organisms (Murphy et al., 2012) there are limitations to its use. The chamber head area (24.5 cm^2) can be too large when there is no clear flat surface, or with coral colonies in early growth stages. A smaller chamber head is available, but the lower volume might necessitate shorter incubations, with potentially less reliable R and P_g determinations, and likely prevent the analytical resolution of calcification rates (at least without more sophisticated alkalinity methods). The study of branching corals still would require fragmentation to introduce coral pieces to the chamber, obviating the benefits of non-destructive sampling of coral metabolic rates. There also are some concerns that corals with rough polyps (e.g., *Lithopyllon* spp., *Goniopora* spp., *Fungia* spp.) may prevent adequate seal formation between the neoprene ring and coral surface, and thus they may not be suitable for these measurements. In its present form then, the best approach for using this system for coral monitoring likely would require selecting morphologically suitable "sentinel" coral colonies that could be revisited on regular time intervals.

A major ethical issue in coral research is balancing the needs for collection of coral fragments to study in the laboratory against the necessary goal of protecting reef systems. The underwater respirometry system evaluated here also is capable of non-destructive *in situ* experimentation. For example, the effect of changing irradiance on R, P_g, and CA can be studied through programming of the LED array. The detachable chamber recirculation loop (**Figure 1**) can be used to introduce alternate chemical or biological conditions to evaluate their effects on coral metabolism; e.g., changes in A_t, turbidity, or plankton abundance. These studies could focus on short-term effects during single deployments, but also could evaluate longer-term outcomes by resampling the exposed coral spot over days or weeks. Our point is that this respirometry system has strong potential not only for *in situ* assessment of the health of individual corals in reef systems, but also for investigating aspects of coral metabolism without the need of the destructive collection of corals. There also are potential useful applications for studying non-coral calcifying incrusting organisms, such as microbial mats and crustose coralline algae.

Accurate and precise assessment of coral metabolic processes is key to improving our knowledge of the reef building species, and how their ecosystems are influenced to varying degrees by the combination of local and global anthropogenic disturbance. The Community *In situ* Metabolism (CISME) respirometry system enables comparatively rapid, non-destructive measurement of coral physiological indicators, with a level of precision and accuracy that enables the detection of small differences in coral metabolism among corals and over their natural diel cycles. The system is better suited for high spatial and temporal resolution sampling than other methods (Weber et al., 2007; Long et al., 2013, Camp et al., 2015). It can be an important tool then for studying the effects of local stressors (point and regional scale). Its practicality and low cost of use also would help support the continuous collection of observations needed to detect effects associated with interannual and decadal scale ocean-atmosphere climate variability (e.g., El Niño Southern Oscillation, Pacific Decadal Oscillation, North Atlantic Oscillation), as well as the evolution of climate-driven changes in marine systems. Further development and application of this instrument and similar methodologies will improve our ability to generate rich and timely information about the energetic status of corals, which is urgently needed for coral reef management and conservation efforts.

DATA AVAILABILITY STATEMENT

The original contributions presented in the study are publicly available. This data can be found here: PANGAEA accession number PDI-25286.

AUTHOR CONTRIBUTIONS

WD, RT, PA, and MW conceived and conducted the experiments. WD, RT, and MW analyzed the results. All authors reviewed the manuscript.

FUNDING

This study was supported by the Collaborative Research Fund (C7013-19G) of the Hong Kong Research Grants Council; the National Natural Science Foundation of China (41641047); the Internal Research Project of State Key Laboratory of Satellite Ocean Environment Dynamics, Second Institute of Oceanography, State Oceanic Administration (No. SOEDZZ1702), and the SKLMP Seed Collaborative Research Fund (SCRF/0027).

ACKNOWLEDGMENTS

We thank all the persons involved who provided support for the experiments, in particular Mr. Oliver Petterson Stubbs for helping to collect coral fragments, Mr. Kelvin So, Ms. Zoe Wong, Mr. Jeffrey Chung, and Dr. Alan Lin for the assistance during the laboratory work, Ms. Mirna Zordan for the technical artwork, and Prof. John Hodgkiss for the proof-reading. We thank the Marine Parks Division, Agriculture Fisheries and Conservation Department, HKSARG, for the permission to use data collected within Marine Parks. We are particularly grateful to the two reviewers, whose detailed and thoughtful comments greatly improved the manuscript.

SUPPLEMENTARY MATERIAL

The Supplementary Material for this article can be found online at: https://www.frontiersin.org/articles/10.3389/fmars.2020.571451/full#supplementary-material

REFERENCES

Al-Horani, F. A., Al-Moghrabi, S. M., and de Beer, D. (2003a). Microsensor study of photosynthesis and calcification in the scleractinian coral, *Galaxea fascicularis*: active internal carbon cycle. *J. Exp. Mar. Bio. Ecol.* 142, 419–426. doi: 10.1007/s00227-002-0981-8

Al-Horani, F. A., Al-Moghrabi, S. M., and de Beer, D. (2003b). The mechanism of calcification and its relation to photosynthesis and respiration in the scleractinian coral *Galaxea fascicularis*. *Mar. Biol.* 142, 419–426.

Al-Horani, F. A., Tambutté, E., and Allemand, D. (2007). Dark calcification and the daily rhythm of calcification in the scleractinian coral, *Galaxea fascicularis*. *Coral Reefs* 26, 531–538. doi: 10.1007/s00338-007-0250-x

Allemand, D., Tambutté, E., Zoccola, D., and Tambutté, S. (2011). "Coral calcification, cells to reefs," in *Coral Reefs: An Ecosystem in Transition*, eds Z. Dubinsky and N. Stambler (Cham: Springer), 119–150. doi: 10.1007/978-94-007-0114-4_9

Andersson, A. J., Mackenzie, F. T., and Gattuso, J.-P. (2011). "Effects of Ocean acidification on benthic processes, organisms and ecosystems," in *Ocean Acidification*, eds J.-P. Gattuso and L. Hansson (Oxford: OUP), 122–153.

Anthony, K., Kleypas, A., and Gattuso, J.-P. (2011). Coral reefs modify their seawater carbon chemistry–implications for impacts of ocean acidification. *Glob. Change Biol.* 17, 3655–3666. doi: 10.1111/j.1365-2486.2011.02510.x

Anthony, K. N., Kline, D. I., Diaz-Pulido, G., Dove, S., and Hoegh-Guldberg, O. (2008). Ocean acidification causes bleaching and productivity loss in coral reef builders. *Proc. Natl. Acad. Sci. U.S.A.* 105, 17442–17446. doi: 10.1073/pnas.0804478105

Atkinson, M. J., and Falter, J. L. (2003). "Coral reefs," in *Biogeochemistry of Marine Systems*, eds K. Black and G. Shimmield (Boca Raton, FL: CRC Press), 44–64.

Atkinson, M. J., and Grigg, R. W. (1984). Model of a coral reef ecosystem. *Coral Reefs* 3, 13–22. doi: 10.1007/BF00306136

Bates, N. R., Amat, A., and Andersson, A. J. (2010). Feedbacks and responses of coral calcification on the Bermuda reef system to seasonal changes in biological processes and ocean acidification. *Biogeosciences* 7, 2509–2530. doi: 10.5194/bg-7-2509-2010

Bednarz, V. N., Naumann, M. S., Cardini, U., van Hoytema, N., Rix, L., Al-Rshaidat, M. M. D., et al. (2018). Contrasting seasonal responses in dinitrogen fixation between shallow and deep-water colonies of the model coral Stylophora pistillata in the northern Red Sea. *PLoS One* 13:e0199022. doi: 10.1371/journal.pone.0199022

Beer, S., Ilan, M., Eshel, A., Weil, A., and Brickner, I. (1998). Use of pulse amplitude modulated (PAM) fluorometry for in situ measurements of photosynthesis in two Red Sea faviid corals. *Mar. Biol.* 131, 607–612. doi: 10.1007/s002270050352

Bolden, I. W., Sachs, J. P., and Gagnon, A. C. (2019). Temporally-variable productivity quotients on a coral atoll: implications for estimates of reef metabolism. *Mar. Chem.* 217:103707. doi: 10.1016/j.marchem.2019.103707

Borell, E. M., and Bischof, K. (2008). Feeding sustains photosynthetic quantum yield of a Scleractinian coral during thermal stress. *Oecologia* 157, 593–601. doi: 10.1007/s00442-008-1102-2

Brierley, A. S., and Kingsford, M. J. (2009). Impacts of climate change on marine organisms and ecosystems. *Curr. Biol.* 19, 602–614. doi: 10.1016/j.cub.2009.05.046

Camp, E. F., Krause, S.-L., Santos, L. M. F., Naumann, M. S., Kikuchi, R. K. P., Smith, D. J., et al. (2015). The "Flexi-Chamber": a novel cost-effective in situ respirometry chamber for coral physiological measurements. *PLoS One* 10:e0138800. doi: 10.1371/journal.pone.0138800

Ciais, P., Sabine, C., Bala, G., Bopp, L., Brovkin, V., Canadell, J., et al. (2013). "Carbon and other biogeochemical cycles," in *Climate Change: The Physical Science Basis. Contribution of Working Group I to the Fifth Assessment Report of the Intergovernmental Panel on Climate Change*, eds T. F. Stocker, D. Qin, G.-K. Plattner, M. Tignor, S. K. Allen, J. Boschung, et al. (Cambridge, MA: Cambridge University Press), 106.

Cohen, A. L., and Holcomb, M. (2009). Why corals care about ocean acidification: uncovering the mechanism. *Oceanography* 22, 118–127. doi: 10.5670/oceanog.2009.102

Cohen, A. L., and McConnaughey, T. A. (2003). "Geochemical perspectives on coral mineralization," in *Biomineralization*, eds P. M. Dove, S. Weiner, S. Weiner, and J. J. deYoreo (Chantilly: The Mineralogical Society of America), 151–187. doi: 10.1515/9781501509346-011

Cohen, I., Dubinsky, Z., and Erez, J. (2016). Light enhanced calcification in hermatypic corals: new insights from light spectral responses. *Front. Mar. Sci.* 2:122. doi: 10.3389/fmars.2015.00122

Coles, S. L., and Brown, B. E. (2003). Coral bleaching – capacity for acclimatization and adaptation. *Adv. Mar. Biol.* 46, 183–223. doi: 10.1016/S0065-2881(03)46004-5

Coles, S. L., and Jokiel, P. L. (1977). Effects of temperature on photosynthesis and respiration in hermatypic corals. *Mar. Biol.* 43, 209–2016. doi: 10.1007/BF00402313

Courtney, T. A., De Carlo, E. H., Page, H. N., Bahr, K. D., Barro, A., Howins, N., et al. (2018). Recovery of reef-scale calcification following a bleaching event in Kâne'ohe Bay. *Hawai'i. Limnol. Oceanogr.* 3, 1–9. doi: 10.1002/lol2.10056

Cyronak, T., Andersson, A. J., Langdon, C., Albright, R., Bates, N. R., Caldeira, K., et al. (2018). Taking the metabolic pulse of the world's coral reefs. *PLoS ONE* 13:e0190872. doi: 10.1371/journal.pone.0190872

Darling, E. S., Alvarez-Filip, L., Oliver, T. A., McClanahan, T. R., and Coté, I. M. (2012). Evaluating life history strategies of reef corals from species traits. *Ecol. Lett.* 15, 1378–1386. doi: 10.1111/j.1461-0248.2012.01861.x

Dellisanti, W., Tsang, R. H. L., Ang, P. Jr., Wu, J., Wells, M. L., and Chan, L. L. (2020). Metabolic performance and thermal and salinity tolerance of the coral Platygyra carnosa in Hong Kong waters. *Mar. Poll. Bull.* 153:111005. doi: 10.1016/j.marpolbul.2020.111005

Dickson, A. G. (1990). Standard potential of the reaction: AgCl(s) + 12H2(g) = Ag(s) + HCl(aq), and and the standard acidity constant of the ion HSO4- in

synthetic sea water from 273.15 to 318.15 K. *J. Chem. Thermodyn.* 22, 113–127. doi: 10.1016/0021-9614(90)90074-Z

Dickson, A. G., Sabine, C. L., and Christian, J. R. (2007). *Guide to Best Practices for Ocean CO2 Measurement*. Sidney: North Pacific Marine Science Organization.

Donner, S. D., Rickbeil, G. J. M., and Heron, S. F. (2017). A new, high-resolution global mass coral bleaching database. *PLoS One* 12:e0175490. doi: 10.1371/journal.pone.0175490

Duprey, N. N., McIlroy, S. E., Ng, T. P. T., Thompson, P. D., Kim, T., Wong, J. C. Y., et al. (2017). Facing a wicked problem with optimism: issues and priorities for coral conservation in Hong Kong. *Biodivers. Conserv.* 26, 2521–2545. doi: 10.1007/s10531-017-1383-z

Falini, G., Fermani, S., and Goffredo, S. (2015). Coral biomineralization: a focus on intra-skeletal organic matrix and calcification. *Semin. Cell. Dev. Biol.* 46, 17–26. doi: 10.1016/j.semcdb.2015.09.005

Falkowski, P. G., Dubinsky, Z., Muscatine, L., and Porter, J. W. (1984). Light and the bioenergetics of a symbiotic coral. *Bioscience* 34, 705–709. doi: 10.2307/1309663

Falter, J. L., Lowe, R. J., Atkinson, M. J., and Cuet, P. (2012). Seasonal coupling and de-coupling of net calcification rates from coral reef metabolism and carbonate chemistry at Ningaloo Reef, Western Australia. *J. Geophys. Res.* 117:C05003. doi: 10.1029/2011JC007268

Fitt, W. K., Brown, B. E., Warner, M. E., and Dunne, R. P. (2001). Coral bleaching: interpretation of thermal tolerance limits and thermal thresholds in tropical corals. *Coral Reefs* 20, 51–65. doi: 10.1007/s003380100146

Gardella, D. J., and Edmunds, P. J. (1999). The oxygen microenvironment adjacent to the tissue of the scleractinian Dichocoenia stokesii and its effects on symbiont metabolism. *Mar. Biol.* 135, 289–295. doi: 10.1007/s002270050626

Gattuso, J.-P., and Jaubert, J. (1990). Effect of light on oxygen and carbon dioxide fluxes and on metabolic quotients measured in situ in a zooxanthellate coral. *Limnol. Oceanogr.* 35, 1796–1804. doi: 10.4319/lo.1990.35.8.1796

Gattuso, J.-P., Frankignoulle, M., and Smith, S. V. (1999). Measurement of community metabolism and significance in the coral reef CO2 source-sink debate. *PNAS* 96, 1317–1322. doi: 10.1073/pnas.96.23.13017

Gruber, N. (2011). Warming up, turning sour, losing breath: ocean biogeochemistry under global change. *Philos. T. R. Soc. A* 369, 1980–1996. doi: 10.1098/rsta.2011.0003

Hawkins, T. D., Hagemeyer, J. C. G., Hoadley, K. D., Marsh, A. G., and Warner, M. E. (2016). Partitioning of respiration in an animal-algal symbiosis: implication for different aerobic capacity between *Symbiodinium* spp. *Front. Physiol.* 7:128. doi: 10.3389/fphys.2016.00128

Heery, E. C., Hoeksema, B. W., Browne, N. K., Reimer, J. D., Ang, P. O., Huang, D., et al. (2018). Urban coral reefs: degradation and resilience of hard coral assemblages in coastal cities of East and Southeast Asia. *Mar. Poll. Bull.* 135, 654–681. doi: 10.1016/j.marpolbul.2018.07.041

Hoegh-Guldberg, O., Mumby, P. J., Hooten, A. J., Steneck, R. S., Greenfield, P., Gomez, E., et al. (2007). Coral reefs under rapid climate change and ocean acidification. *Science* 318, 1737–1742. doi: 10.1126/science.1152509

Hoegh-Guldberg, O., Poloczanska, E. S., Skirving, W., and Dove, S. (2017). Coral reef ecosystems under climate change and ocean acidification. *Front. Mar. Sci.* 4:158. doi: 10.3389/fmars.2017.00158

Hughes, T. P., Kerry, J., Alvarez-Noriega, M., Álvarez-Romero, J. G., Anderson, K. D., Baird, A. H., et al. (2017). Global warming and recurrent mass bleaching of corals. *Nature* 543, 373–377. doi: 10.1038/nature21707

Jimenez, I. M., Kuhl, M., Larkum, A. W. D., and Ralph, P. J. (2011). Effects of flow and colony morphology on the thermal boundary layer of corals. *J. R. Soc. Interface* 8, 1785–1795. doi: 10.1098/rsif.2011.0144

Kuffner, L. B., Lidz, B. H., Hudson, J. H., and Anderson, J. S. (2015). A century of ocean warming on Florida Keys coral reefs: historic in situ observation. *Estuar. Coasts* 38, 1085–1096. doi: 10.1007/s12237-014-9875-5

Kuhl, M., Cohen, Y., Dalsgaard, T., Jorgensen, B. B., and Revsbech, N. P. (1995). Microenvironment and photosynthesis of zooxanthellae in scleractinian corals studied with microsensors for O2, pH and light. *Mar. Ecol. Prog. Ser.* 117, 159–172. doi: 10.3354/meps117159

Larkum, A. W. D., Koch, E. M., and Kuhl, M. (2003). Diffusive boundary layers and photosynthesis of the epilithic algal community of coral reefs. *Mar. Biol.* 142, 1073–1082. doi: 10.1007/s00227-003-1022-y

Leuker, T. J., Dickson, A. G., and Keeling, C. D. (2000). Ocean pCO2 calculated from dissolved inorganic carbon, alkalinity, and equations for K1 and K2: validation based on laboratory measurements of CO2 in gas and seawater at equilibrium. *Mar. Chem.* 70, 105–119. doi: 10.1016/S0304-4203(00)00022-0

Levy, O., Dubinsky, Z., Schneider, K., Achituv, Y., Zakai, D., and Gorbunov, M. Y. (2004). Diurnal hysteresis in coral photosynthesis. *Mar. Ecol. Prog. Ser.* 268, 105–117. doi: 10.3354/meps268105

Long, M. H., Berg, P., de Beer, D., and Zieman, J. (2013). In situ coral reef oxygen metabolism: an eddy correlation study. *PLoS One* 8:e0058581. doi: 10.1371/journal.pone.0058581

Martz, T. R., Connery, J. R., and Johnson, K. S. (2010). Testing the Honeywell Durafet for seawater pH applications. *Limnol. Oceanogr.* 8, 172–184. doi: 10.4319/lom.2010.8.172

McCulloch, M., Falter, J., Trotter, J., and Montagna, P. (2012). Coral resilience to ocean acidification and global warming through pH up-regulation. *Nat. Clim. Change* 2:1473. doi: 10.1038/nclimate1473

McIlroy, S. E., Thompson, P. D., Yuan, F. L., Bonebrake, T. C., and Baker, D. M. (2019). Subtropical thermal variation supports persistence of corals but limits productivity of coral reefs. *Proc. R. Soc. B Biol. Sci.* 286:20190882. doi: 10.1098/rspb.2019.0882

McMahon, A., Santos, I. R., Schulz, K. G., Cyronak, T., and Maher, D. T. (2018). Determining coral reef calcification and primary production using automated alkalinity, pH and pCO2 measurements at high temporal resolution. *Estuar. Coast. Mar. Sci.* 209, 80–88. doi: 10.1016/j.ecss.2018.04.041

Murphy, B. A., Mazel, C. H., Whitehead, R., and Szmant, A. M. (2012). "CISME: a self-contained diver portable metabolism and energetics system," in *Proceedings of the Oceans*, Hampton Roads, VA, 1–7. doi: 10.1109/OCEANS.2012.6405075

Murphy, J. W. A., and Richmond, R. H. (2016). Changes to coral health and metabolic activity under oxygen deprivation. *PeerJ* 4:e1956. doi: 10.7717/peerj.1956

Muscatine, L., McCloskey, L. R., and Marian, R. E. (1981). Estimating the daily contribution of carbon from zooxanthellae to coral animal respiration. *Limnol. Oceanogr.* 26, 601–611. doi: 10.4319/lo.1981.26.4.0601

Nelson, H. R., and Altieri, A. H. (2019). Oxygen: the universal currency on coral reefs. *Coral Reefs* 38, 177–198. doi: 10.1007/s00338-019-01765-0

Nothdurft, L. D., and Webb, G. E. (2009). Clypeotheca, a new skeletal structure in scleractinian corals: a potential stress indicator. *Coral Reefs* 28, 143–153. doi: 10.1007/s00338-008-0439-7

Pandolfi, J. M., Connolly, S. R., Marshall, D. J., and Cohen, A. (2011). Projecting coral reef futures under global warming and ocean acidification. *Science* 333, 418–422. doi: 10.1126/science.1204794

Perez, F. F., and Fraga, F. (1987). Association constant of fluoride and hydrogen ions in seawater. *Mar. Chem.* 21, 161–168. doi: 10.1016/0304-4203(87)90036-3

Pierrot, D., Lewis, E., and Wallace, D. W. R. (2006). *MS Excel Program Developed for CO2 System Calculations*. ORNL/CDIAC-105a. Oak Ridge: Carbon Dioxide Information Analysis Center.

Ralph, P., Gademann, R., Larkum, A. W. D., and Schreiber, U. (1999). In situ underwater measurement of photosynthetic activity of coral zooxanthellae and other reef-dwelling dinoflagellate endosymbionts. *Mar. Ecol. Prog. Ser.* 180, 139–147. doi: 10.3354/meps180139

Reggi, M., Fermani, S., Levy, O., Dubinsky, Z., Goffredo, S., and Falini, G. (2016). "Influences of coral intra-skeletal organic matrix on calcium carbonate precipitation," in *The Cnidaria, Past, Present and Future*, eds S. Goffredo and Z. Dubinsky (Cham: Springer), 207–222. doi: 10.1007/978-3-319-31305-4_13

Riebesell, U., Fabry, V. J., Hansson, L., and Gattuso, J.-P. (2011). *Guide to Best Practices for Ocean Acidification Research and Data Reporting*. Brussels: Publications Office of the European Union.

Rinkevich, B. (1995). Restoration strategies for coral reefs damaged by recreational activities: the use of sexual and asexual recruits. *Restor. Ecol.* 3, 241–251. doi: 10.1111/j.1526-100X.1995.tb00091.x

Sawall, Y., and Hochberg, E. J. (2018). Diel versus time-integrated (daily) photosynthesis and irradiance relationship of coral reef organisms and communities. *PLoS One* 13:e0208607. doi: 10.137/journal.pone.0208607

Schneider, K., Levy, O., Dubinsky, Z., and Erez, J. (2009). In situ diel cycles of photosynthesis and calcification in hermatypic corals. *Limnol. Oceanogr.* 54, 1995–2002. doi: 10.4319/lo.2009.54.6.1995

Schoepf, V., Hu, X., Holcomb, M., Cai, W.-J., Li, Q., Wang, Y., et al. (2017). Coral calcification under environmental change: a direct comparison of the alkalinity anomaly and buoyant weight techniques. *Coral Reefs* 36, 13–25. doi: 10.1007/s00338-016-1507-z

Schrameyer, V., Wangpraseurt, D., Hill, R., Kuhl, M., Larkum, A. W. D., and Ralph, P. J. (2014). Light respiratory processes and gross photosynthesis in two scleractinian corals. *PLoS One* 9:e110814. doi: 10.1371/journal.pone.0110814

Shashar, N., Cohen, Y., and Loya, Y. (1993). Extreme diel fluctuations of oxygen in diffusive boundary layers surrounding stony corals. *Biol. Bull.* 185, 455–461. doi: 10.2307/1542485

Taddei, D., Cuet, P., Frouin, P., Esbelin, C., and Clavier, J. (2008). Low community photosynthetic quotient in coral reef sediments. *Comptes Rendus Biol.* 331, 668–677. doi: 10.1016/j.crvi.2008.06.006

Takeshita, Y., Cyronak, T., Martz, T. R., Kindeberg, T., and Andersson, A. J. (2018). Coral reef carbonate chemistry variability at different functional scales. *Front. Mar. Sci.* 5:175. doi: 10.3389/fmars.2018.00175

Takeshita, Y., McGillis, W., Briggs, E. M., Carter, A. L., Donham, E. M., Martz, T. R., et al. (2016). Assessment of net community production and calcification of a coral reef using a boundary layer approach. *J. Geophys. Res. Oceans* 121, 5655–5671. doi: 10.1002/2016JC011886

van Oppen, M. J. H., Gates, R. D., Blackall, L. L., Cantin, N., Chakravarti, L. K., Chan, W. Y., et al. (2017). Shifting paradigms in restoration of the world's coral reefs. *Glob. Change Biol.* 23, 3437–3448. doi: 10.1111/gcb.13647

Venn, A., Tambutté, E., Holcomb, M., Allemand, D., and Tambutté, S. (2011). Live tissue imaging shows reef corals elevate pH under their calcifying tissue relative to seawater. *PLoS One* 6:e20013. doi: 10.1371/journal.pone.0020013

Wangpraseurt, D., Polerecky, L., Larkum, A. W. D., Ralph, P. J., Nielsen, D. A., Pernice, M., et al. (2014). The in-situ light microenvironment of corals. *Limnol. Oceanol.* 59, 917–926. doi: 10.4319/lo.2014.59.3.0917

Weber, M., Faerber, P., Meyer, V., Lott, C., and Eickert, G. (2007). In situ applications of a new diver-operated motorized microsensor profiler. *Environ. Sci. Technol.* 41, 6210–6215. doi: 10.1021/es070200b

Wong, K. T., Chui, A. P. Y., Lam, E. K. Y., and Ang, P. Jr. (2018). A 30-year monitoring of changes in coral community structure following anthropogenic disturbances in Tolo Harbour and Channel, Hong Kong. *Mar. Poll. Bull.* 133, 900–910. doi: 10.1016/j.marpolbul.2018.06.049

Yates, K. K., and Halley, R. B. (2003). Measuring coral reef community metabolism using new benthic chamber technology. *Coral Reefs* 22, 247–255. doi: 10.1007/s00338-003-0314-315

Conflict of Interest: The authors declare that the research was conducted in the absence of any commercial or financial relationships that could be construed as a potential conflict of interest.

frontiers in Marine Science

ORIGINAL RESEARCH
published: 13 November 2020
doi: 10.3389/fmars.2020.603438

High Coral Bycatch in Bottom-Set Gillnet Coastal Fisheries Reveals Rich Coral Habitats in Southern Portugal

*Vítor Dias[1], Frederico Oliveira[1], Joana Boavida[2], Ester A. Serrão[1], Jorge M. S. Gonçalves[1] and Márcio A. G. Coelho[1]**

[1] CCMAR-Centro de Cieñcias do Mar, Faculty of Sciences and Technology, Universidade do Algarve, Campus de Gambelas, Faro, Portugal, [2] University of Aix-Marseille, University of Toulon, CNRS, IRD, Mediterranean Institute of Oceanography (MIO) UTM 110, Marseilles, France

OPEN ACCESS

Edited by:
Carlo Cerrano,
Marche Polytechnic University, Italy

Reviewed by:
Alessandro Cau,
University of Cagliari, Italy
Laura Schejter,
CONICET Mar del Plata, Argentina

***Correspondence:**
Márcio A. G. Coelho
macoelho@ualg.pt

Specialty section:
This article was submitted to Marine Ecosystem Ecology, a section of the journal Frontiers in Marine Science

Received: 06 September 2020
Accepted: 27 October 2020
Published: 13 November 2020

Citation:
Dias V, Oliveira F, Boavida J, Serrão EA, Gonçalves JMS and Coelho MAG (2020) High Coral Bycatch in Bottom-Set Gillnet Coastal Fisheries Reveals Rich Coral Habitats in Southern Portugal. Front. Mar. Sci. 7:603438. doi: 10.3389/fmars.2020.603438

Bottom-contact fisheries are unquestionably one of the main threats to the ecological integrity and functioning of deep-sea and circalittoral ecosystems, notably cold-water corals (CWC) and coral gardens. Lessons from the destructive impact of bottom trawling highlight the urgent need to understand how fisheries affect these vulnerable marine ecosystems. At the same time, the impact of other fishing gear and small-scale fisheries remains sparsely known despite anecdotal evidence suggesting their impact may be significant. This study aims to provide baseline information on coral bycatch by bottom-set gillnets used by artisanal fisheries in Sagres (Algarve, southwestern Portugal), thereby contributing to understand the impact of the activity but also the diversity and abundance of corals in this region. Coral bycatch frequency and species composition were quantified over two fishing seasons (summer-autumn and spring) for 42 days. The relationship with fishing effort was characterized according to métiers (n = 6). The results showed that 85% of the gillnet deployments caught corals. The maximum number of coral specimens per net was observed in a deployment targeting *Lophius budegassa* (n = 144). In total, 4,326 coral fragments and colonies of 22 different species were captured (fishing depth range of 57–510 m, mean 139 ± 8 m). The most affected species were *Eunicella verrucosa* (32%), *Paramuricea grayi* (29%), *Dendrophyllia cornigera* (12%), and *Dendrophyllia ramea* (6%). The variables found to significantly influence the amount of corals caught were the target species, net length, depth, and mesh size. The 22 species of corals caught as bycatch belong to Orders Alcyonacea (80%), Scleractinia (18%), Zoantharia (1%), and Antipatharia (1%), corresponding to around 13% of the coral species known for the Portuguese mainland coast. These results show that the impact of artisanal fisheries on circalittoral coral gardens and CWC is potentially greater than previously appreciated, which underscores the need for new conservation measures and alternative fishing practices. Measures

such as closure of fishing areas, frequent monitoring onboard of fishing vessels, or the development of encounter protocols in national waters are a good course of action. This study highlights the rich coral gardens of Sagres and how artisanal fisheries can pose significant threat to corals habitats in certain areas.

Keywords: coral gardens, marine animal forests, biodiversity conservation and management, vulnerable marine ecosystems, cold-water corals, benthic invertebrate bycatch, bottom fisheries impact

INTRODUCTION

The impact of human activities on marine life is a global crisis that has left virtually no area of the ocean unaffected, with benthic habitats like coral-dominated ecosystems among those most strongly impacted (Halpern et al., 2008). There are many stressors threatening the ecological integrity and functioning of coral ecosystems, including pollution (Ragnarsson et al., 2017; Consoli et al., 2020), overfishing (Hughes, 1994; Jackson, 2001), oil and gas extraction (Glover and Smith, 2003; Purser and Thomsen, 2012; Cordes et al., 2016), ocean acidification (Bramanti et al., 2013; Movilla et al., 2014; Albright et al., 2018), and global warming (Hughes et al., 2017, 2018). However, the direct impact of fisheries using bottom-contact gear remains the primary cause of habitat destruction and biomass removal (Hall–Spencer et al., 2002; Glover and Smith, 2003; Hourigan, 2009). This is of special concern for circalittoral and deep coral communities (i.e., those below 50 m depth, henceforth referred to as "deep") such as coral gardens and cold-water corals (CWC), which have life-history traits (e.g., slow growth rates and late age at maturity) that make recovery from physical damage especially difficult, if even possible.

Coral gardens and CWC reefs are key ecosystems in the marine realm. The tridimensional complex species that build these habitats, known as engineers, create high structural complexity that provides shelter, feeding, and nursery grounds for many organisms, including many species of commercial value (Buhl-Mortensen et al., 2010; Ashford et al., 2019), supporting levels of biodiversity comparable to those found in tropical coral reefs and terrestrial forests (Rossi, 2013; Rossi et al., 2017). These habitats include coral species from several taxonomical groups (Orders Scleractinia, Zoantharia, Antipatharia, Corallimorpharia, Alcyonacea, and Pennatulacea), representing nearly 65% of all known coral species (Roberts, 2006; Cairns, 2007). In 2004, the United Nations General Assembly (UNGA) drew attention to the susceptibility of deep coral communities and other habitats to the impacts of deep-sea fisheries, designating them as vulnerable marine ecosystems (VMEs) that required urgent conservation and protection actions (UNGA, 2004; Fuller, 2008). As a result of several resolutions of the UNGA, Regional Fisheries Management Organizations (RFMO) and local governments adopted several measures to protect VMEs (UNGA, 2019), including the reduction of the frequency of significant adverse impacts by bottom-contact fisheries like trawling (e.g., encounter or "move-on" rule triggered by a bycatch threshold) (Parker et al., 2009; Aguilar et al., 2017; Davies et al., 2017) and the creation of Marine Protected Areas (MPA) in areas where VMEs occur (Armstrong and van den Hove, 2008; Huvenne et al., 2016).

Among the various types of gears used by deep-sea fisheries, bottom trawling is notorious for being the most destructive and has received increasing pressure for legislation banning its use worldwide. Indeed, in 2018 the European Parliament instituted a ban on trawling below 800 m depth in European waters (Clark et al., 2016; European Parliament and the Council of the European Union, 2016; Victorero et al., 2018). Other fishing techniques used in the deep-sea, such as longline, have been shown to have a much smaller impact on coral communities (Pham et al., 2015). However, some studies suggest that the extensive use and often considerable long configuration of this gear may also pose a threat to complex deep-sea benthic habitats, including coral communities. For instance, Mytilineou et al. (2014) have found that during experimental longline fishing in the Ionian Sea, 72% of the longline sets used in hake and blackspot seabream fisheries captured corals. In the Azores, Sampaio et al. (2012) reported that 15.2% (n = 45 out of 297) of the fishing trips of the longline fleet surveyed landed corals, with at least 205 specimens caught.

Although there are several studies on the impact of fishing gear on deep-sea ecosystems, most studies focused on large scale industrial fisheries, which represent a very small fraction of the fishing work force (Shester and Micheli, 2011). Worldwide, artisanal fisheries employ over 20 million workers, both directly and indirectly through processing, marketing, and distributing (McGoodwin, 2001; Teh and Sumaila, 2013). In the EU, artisanal fisheries represent 84% of the fishing fleet and employ around 100,000 workers (Garcia et al., 2008; Guyader et al., 2013; Lloret et al., 2018). Yet, studies documenting the impact of artisanal fisheries on deep coral communities and other benthic ecosystems are still scarce when compared to large-scale fisheries (Guyader et al., 2013; Lloret et al., 2018). Generally, artisanal fisheries are considered to have a lower impact on benthic communities. The actual effect, however, may be largely obscured and much greater than assumed due to the lack of reliable data for this sector and because some of the gears used are not selective (Lloret et al., 2018). For example, Shester and Micheli (2011) demonstrated experimentally that for bottom-set gillnets deployed over rocky reefs, ca. 77% of the interactions between nets and corals caused the removal or partial damage of the colonies. While that study focused on shallow-water communities, the results suggest that bottom-set gillnets represent a critical conservation concern that extends to deep coral communities as artisanal fisheries also operate over deep habitats.

This study investigates the impact of bottom-set gillnets used by artisanal fisheries on deep coral communities in Sagres, Algarve, southern Portugal. The aims of the study are to (1) better understand the biodiversity of corals in the area; (2) provide a baseline quantitative assessment of coral bycatch frequency and of the species affected by different types of bottom-set gillnets used in local fisheries; and (3) identify coral bycatch and diversity "hotspots" that could constitute priority management areas.

MATERIALS AND METHODS

Study Area and Data Collection

To assess the impact of bottom-set gillnets on circalittoral and deep coral habitats, the coral bycatch of a fishing vessel operating in Sagres, southern Portugal (**Figure 1**), was documented over 42 workdays during the summer-autumn of 2019 (1 September to 16 October) and spring of 2020 (11 May to 5 June). Coastal fisheries in Portugal are predominantly small-scale operations (∼91% of the fleet has <12 m hull length; DGRM, 2018) that can be categorized into different métiers, i.e., a group of fishing activities that targets a specific assemblage of species, using one kind of fishing gear, in a particular period of the year within the same area (EC, 2008; Deporte et al., 2012). In Sagres, the fishing fleet is mostly composed of small vessels (<12 m hull length) that operate locally and use multiple artisanal gear such as traps, pots, bottom longlines, trotlines, jigs, trammel nets, and small bottom-set gillnets. A few larger coastal multigear vessels (12–15 m hull length) use trammel nets and bottom-set gillnets to fish demersal and benthic species. We documented coral bycatch in a vessel belonging to the latter group, which mainly operates using bottom-set gillnets with different mesh sizes to fish several target species year-round (**Table 1**). The vessel mainly targets Black-bellied angler (*Lophius budegassa*) and John dory (*Zeus faber*). Several secondary species, including European spiny lobster (*Palinurus elephas*), pink spiny lobster (*Palinurus mauritanicus*), Atlantic wreckfish (*Polyprion americanus*), and blonde ray (*Raja brachyura*), are also targeted for their high commercial value. In this study, the métiers were defined according to the hierarchy presented in decision 2008/949/EC from the European Commission (EC, 2008), all of which are part of the category "set of gillnets," differing at the levels of target assemblage (i.e., target species) and mesh size used (**Table 1**). For target species in which more than one mesh size was used (i.e., European spiny lobster and pink spiny lobster), we defined one métier per target species as few deployments used a smaller mesh size (one out of two in *P. mauritanicus* and three out of nine in *P. elephas*).

To simplify the results, our treatments were divided according to métier and the periods over which coral bycatch was monitored (i.e., "seasons"). These were chosen as a function of regulatory fishery closures for the target species and weather conditions, as some of the rocky-bottom-dwelling targeted species are not fished during winter to prevent damage or loss of the nets (**Table 1**). Coral bycatch and the amount of target species caught were quantified individually for each set of gillnets deployed. The geographic positions and depth at the start and endpoints of the nets, as well as the soaking time (in days) were also recorded. The average depth of each net set was calculated using the start and endpoint depths for deployments that followed a straight line, and the depth of each vertex point for deployments following a zigzag course (see **Figure 1**). Collected corals were preserved and identified to the maximum taxonomical level using available guides (e.g., Carpine and Grasshoff, 1975; Grasshoff, 1992; Cairns and Kitahara, 2012) and expert opinion. For the purpose of this study, the coral fauna assessed included members of the subclasses Octocorallia and Hexacorallia (orders Antipatharia, Zoantharia, and Scleractinia). For specimens in which species could not be identified based on visual inspection of colony alone, the morphology of skeletal sclerites (octocorals) and corallites (scleractinians) was analyzed. The maximum height and width of each specimen (orientation inferred from the presence of a holdfast or from the branching pattern characteristic to each species; **Supplementary Figure S1**) were measured in the lab. The specimens were classified as fragments or whole colony depending on the presence of holdfast (e.g., Octocorallia) or presence of substrate attached to the colony (Scleractinia). Additionally, the dry weight of *Dendrophyllia* spp. was also measured in order to estimate bycatch biomass.

Data Analysis

In order to understand the relationship between target species landings and coral bycatch, the fishing and bycatch data were standardized as catch per unit of effort (CPUE). CPUE represents the number of specimens caught (N of fish or lobster *vs.* coral) as a function of the product of the soaking time (T in days) and the net length per 100 m deployed (L) (**Equation 1**). The analysis of the spatial distribution of the CPUEs did not include four of the 139 nets documented for which only one GPS coordinate was available, or the soaking time was not determined.

The effect of different métiers on bycatch was tested with a general addictive model (GAM) using a Poisson distribution and a log-link function. We modeled the number of corals caught per net (response variable) as a function of target species, mesh size, depth, net length, and soaking time (fixed factors). Model selection was based on generalized cross-validation (GCV) criterion and adjusted R^2. Because overdispersion was detected, the standard errors were corrected using a quasi-GAM model with the variance given by 2.06 × 1.04, where 2.06 represents the mean and 1.04 the dispersion parameter (ϕ). Backward selection and *F*-test were used to determine statistical significance of the variables and interaction terms. Model validation was performed through

$$CPUE = \frac{N}{L \times T}$$

EQUATION 1 | Fishing effort calculated as catch per unit of effort (CPUE) for each bottom-set gillnet in Sagres (Portugal) during the two sampling seasons documented. CPUE represents the number of specimens (fish/lobster or coral) caught (*N*) as a function of the product of the soaking time (T in days) and the net length per 100 m deployed (*L*).

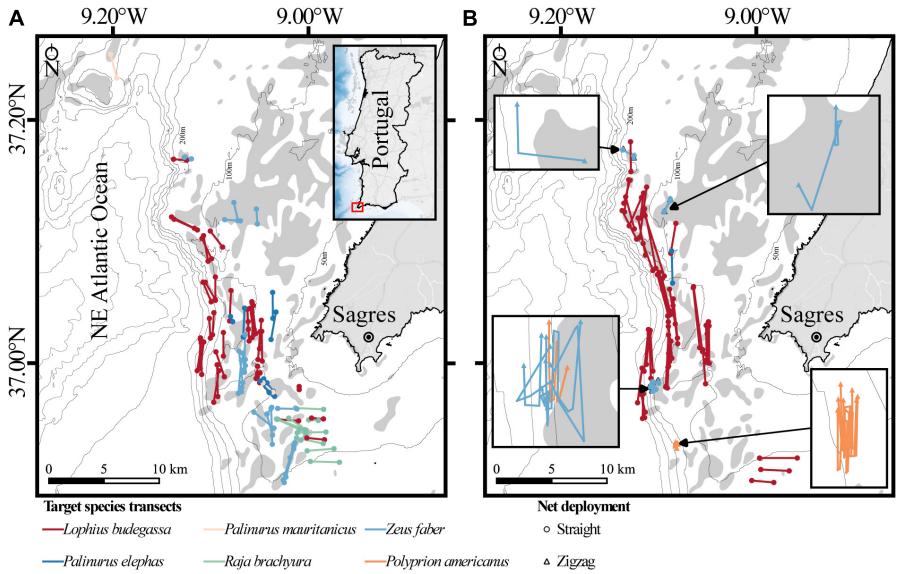

FIGURE 1 | Map of the study area off the coast of Sagres (southern Portugal) showing the transects of bottom-set gillnets used to document coral bycatch in circalittoral and deep-sea habitats. **(A)** Summer-autumn sampling season (1 September to 31 October) with inset showing the location of the study area in Portugal. **(B)** Spring sampling season (11 May to 5 June) with insets zooming on nets deployed following a zigzag course. Sets of gillnets are shown by target species (colors). Bathymetric isobaths are as follows: 50 m, 100–500 m (increments of 100 m), and >500 m (increment of 200 m).

TABLE 1 | Features of the target species métier (average ± standard error) of the bottom-set gillnets deployed during the documentation of coral bycatch in Sagres (southern Portugal) during the two seasons studied.

Season	Target species	Closure of fisheries (months)	Net length (km)	Depth (m)	Soaking time (days)	Mesh size (mm)	Number of nets deployed
Summer-autumn	*Lophius budegassa*	01–02 (>3%)	2.07 ± 0.11	148 ± 15	4.6 ± 0.3	240	38
	Palinurus elephas	10–12	1.70 ± 0.26	83 ± 4	8.4 ± 1.3	110/200	8
	Palinurus mauritanicus	10–12	1.75 ± 0.51	225 ± 67	10.0 ± 4.0	200/240	2
	Raja brachyura	05–06 (>5%)	2.11 ± 0.23	97 ± 2	2.8 ± 0.3	240	10
	Zeus faber	NA	1.94 ± 0.24	101 ± 5	1.0 ± 0.0	200	20
Spring	*Lophius budegassa*	01–02 (>3%)	3.25 ± 0.13	157 ± 14	4.1 ± 0.3	240	47
	Palinurus elephas	10–12	2.91 ± 0.00	96 ± 0	7.0 ± 0.0	200	1
	Polyprion americanus	NA	3.24 ± 0.07	135 ± 6	0.9 ± 0.4	200	7
	Zeus faber	NA	3.12 ± 0.63	124 ± 14	1.0 ± 0.0	200	6

visual inspection of the residuals (quantile–quantile plot, histogram of residuals, residuals *vs*. predictors plot, and observed *vs*. fitted values plot) to detect any violation of the assumptions (**Supplementary Figure S2**). The analyses were performed using the MGCV package (Wood, 2017) in R version 3.6.2 (R Core Team, 2019).

The resemblance of the coral communities (species composition and abundance) caught by the different métiers was evaluated using principal coordinates analysis (PCoA). Because the GAM analysis did not show any relationship between coral bycatch and sampling season, the data were pooled. Coral species data for each net was used to calculate a dissimilarity matrix using Hellinger distance (Kindt and Coe, 2005). The resulting dissimilarity matrix was then used as input for the PCoA. Important contributions to the overall ordination along the first two PCoA axes were evaluated using Pearson correlation between the descriptors (coral species) and PCoA1 and PCoA2. To further analyze the results of the PCoA, the influence of depth on differences in species composition between métiers was evaluated with a distance-based redundancy analysis (db-RDA). In this technique, the ordination is constrained by the environmental variable. The species matrix was transformed using the Hellinger transformation (Kindt and Coe, 2005), which together with the environmental matrix (i.e., depth matrix) was used as input for the db-RDA. The significance of the constraint imposed by depth was tested with an ANOVA like permutation test (9999 permutations). Furthermore, scaling method 2 was used to represent db-RDA with the position of the species vectors representing the correlation between species. The PCoA and db-RDA analyses were performed using the BiodiversityR package (Kindt and Coe, 2005) in R version 3.6.2.

RESULTS

Coral bycatch was documented for a total of 139 net deployments: 78 in the summer-autumn and 61 in the spring sampling seasons. Coral specimens were caught in 118 of the nets (85%), covering a total length of 300.32 km. A total of 4326 specimens were collected (45% of which entire colonies) over the 42-day survey period: 2404 specimens over 22 days in the summer-autumn season and 1922 specimens over 20 days in the spring season. On average (±SE), we recovered 31.1 (±2.7) corals from each net, with a maximum of 144 corals caught in a single net (target species: Black-bellied angler). The maximum number of coral species found in a single net was 10 species, with an average (±SE) of 4.31 (±0.2) coral species per net.

Coral Bycatch Biodiversity and Bathymetric Distribution

The diversity of coral species captured as bycatch in the study area was high. A total of 22 different taxa were identified: 17 from the Order Alcyonacea (*Acanthogorgia armata*, *Acanthogorgia hirsuta*, *Callogorgia verticillata*, *Corallium rubrum*, *Ellisella paraplexauroides*, *Eunicella verrucosa*, *Eunicella labiata*, *Eunicella gazella*, *Isidella elongata*, *Leptogorgia sarmentosa*, *Paramuricea clavata*, *Paramuricea grayi*, *Spinimuricea atlantica*, *Viminella flagellum*, (Octocorallia) sp.1, (Octocorallia) sp.2, and (Octocorallia) sp.3), three from the Order Scleractinia (*Dendrophyllia cornigera*, *Dendrophyllia Ramea*, and *Pourtalosmilia anthophyllites*), one from the Order Zoantharia (*Savalia savaglia*), and 1 from the Order Antipatharia (*Antipathella subpinnata*). The gorgonians *E. verrucosa* (1380 specimens), *P. grayi* (1271 specimens), and *C. verticillata* (247), and the scleractinians *D. cornigera* (522 specimens) and *D. ramea* (249 specimens) were the most frequent species, making up 85% of the total amount of coral bycatch (**Figure 2**). It is worth noting that most *C. verticillata* specimens were caught in the spring sampling season in 12 net sets targeting *Z. faber* (four nets) and *P. americanus* (eight nets) deployed at 99–170 m depth. Overall, the diversity found in both sampling seasons was similar in terms of species composition and abundance. Exceptions include the species *A. armata*, *I. elongata*, (Octocorallia) sp.3, *V. flagellum*, and *P. anthophyllites*, which were only caught during the spring sampling season, and species (Octocorallia) sp.1 and (Octocorallia) sp.2 during the summer-autumn.

The size of the specimens collected varied considerably reflecting species-specific differences in growth form and size (**Table 2**). For instance, colonies of *E. verrucosa* had an average height and width of 22.9 cm (±0.3) and 15.5 cm (±0.2), respectively (**Supplementary Figure S3A**), whereas *P. grayi* colonies were on average 17.6 cm (±0.3) long and 11.9 cm (±0.2) wide (**Supplementary Figure S3B**). *C. verticillata* was the species with the largest fan area (**Table 2**). The giant gorgonian *E. paraplexauroides* with candelabrum-shaped colonies was the tallest coral species collected (**Table 2**). From the three scleractinian species caught as bycatch, *D. ramea* was the largest species (**Table 2**) with an average colony weight of 331.4 g (±95.1) and 38.1 (±8.9) polyps per colony.

The majority of specimens and species were caught at locations shallower than 120 m depth (90 and 68%, respectively), where most fishing effort occurred (**Figures 3**, **4**). Notable exceptions include the deep-water species *I. elongata* (296–510 m), *A. subpinnata* (85–510 m), and *C. verticillata* (99–293 m), which were caught at average depths of 417, 169, and 141 m, respectively. The octocorals *P. grayi* (85–97 m), *L. sarmentosa* (57–124 m), and *C. rubrum* (73–134 m) were the species collected at shallower areas, with average depths of 89, 92, and 97 m, respectively (**Figure 3**). Interestingly, several specimens of *E. labiata* and *E. gazella* were caught deeper than the bathymetric ranges reported in the literature (**Figure 3**).

Spatial Patterns of Fishing Effort and Bycatch

Consistent with the expectations, total coral bycatch was generally higher when the nets were deployed on or nearby areas where rocky substrate is known to occur (**Figure 4**). When examining the CPUEs for the pooled dataset (i.e., irrespective of coral or target species), the mismatch between the amounts of coral and target species caught is evident, particularly in the summer-autumn for which the nets captured substantially more coral than fish or lobster (**Figure 4A**). For instance, six of the nets deployed in the summer-autumn sampling season had a CPUE for coral specimens higher than 3.40 (n/day.100 m; **Figure 4A**), which had an average net length of 1.99 km, thus corresponding to more than 60 corals per net. In contrast, for the spring survey season there is a better correspondence between the amount of coral and fish caught, with areas where coral bycatch was high, generally matching those with high fish or lobster catches (**Figure 4B**). Only three of the 61 nets deployed in the spring sampling season had a coral CPUE higher than 3.40 (n/day.100 m; **Figure 4B**).

The preferred Poisson GAM model (**Supplementary Table S1**) for the amount of coral caught as bycatch, supported by both the GCV and adjusted R^2, included four significant factors: target species, depth, net length, and mesh size without any interaction term. The total deviance explained by the model was 40.3%. Overall, all variables have a strong effect on the amount of incidental coral catches (GCV = 21.53; R^2 = 0.379): target species (df = 5, F = 6.049, $p < 0.01$), mesh size (df = 2, F = 4.910, $p < 0.01$), net length (df = 1, F = 15.820, $p < 0.01$), and depth (df = 1, F = 15.198, $p < 0.01$). The coral CPUE (n/day.100 m) was generally higher than that of the target species for the métiers documented, except for fishing activities targeting pink spiny lobster (*P. mauritanicus*) and blonde ray (*R. brachyura*; **Supplementary Figure S4** and **Figure 5**). The spatial analysis of CPUEs by target species shows that the métiers targeting John dory and Atlantic wreckfish have the highest CPUEs, but also the highest removal rates of corals (**Figure 5** and **Supplementary Figure S4**). In the case of the John dory fishery, the pattern is only evident at a few locations during the summer-autumn sampling season, with most net deployments capturing comparatively few fish (**Figure 5C**). Conversely, and despite being the dominant fishery of the vessel that we followed in this study, the métier used to fish black-bellied angler showed

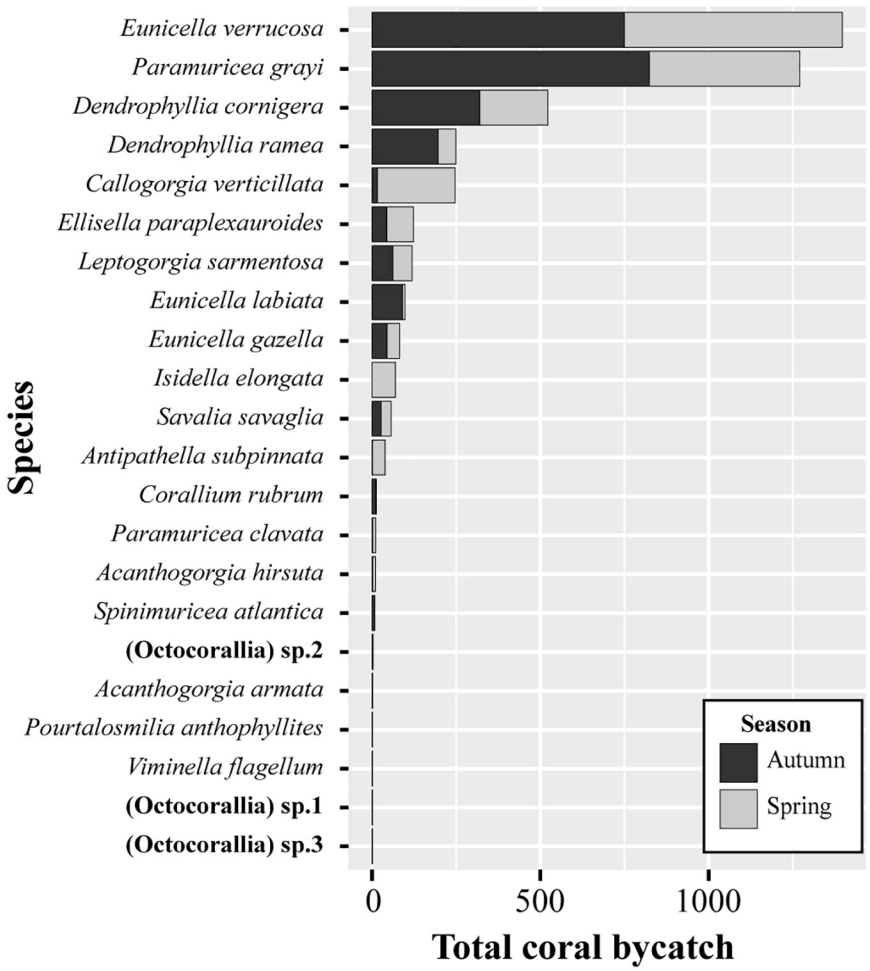

FIGURE 2 | Species composition and total amount of the corals caught as bycatch in bottom-set gillnets during the two sampling seasons in Sagres (southern Portugal). In total, 4326 specimens (branch fragments or entire colonies) were collected from 118 gillnet deployments.

the lowest overall coral removal rates, with the exception of a single set that removed 144 coral specimens (**Figures 5A,B**).

For the five coral species most often caught as bycatch, the spatial segregation of fishing effort across the two sampling seasons is evident, with most incidental captures during the spring season occurring further offshore (**Figure 6**). Additionally, for *P. grayi* (**Figure 6A**), *E. verrucosa* (**Figure 6B**), and the two *Dendrophyllia* species (**Figures 6C,D**), more specimens were caught in the nets deployed in the summer-autumn sampling season (i.e., higher CPUEs). In contrast, *C. verticillata* (**Figure 6E**) was mainly caught during the spring sampling season with CPUE values being higher for this season.

Coral Bycatch Community Structure and Biodiversity Hotspots

The variation in coral community structure per gillnet set is illustrated in the PCoA analysis for the entire dataset, with the two axes capturing 43.59% of the variation in the ecological distances. The analysis shows weak separation in species composition and abundance between the majority of the métiers documented, with the exception of the métier for *P. americanus*, which is clearly segregated from the remaining métiers (**Figure 7**). This separation is strongly correlated with the coral species *C. verticillata* for which a high number of colonies was caught during the spring sampling season (the only season in which the métier was used; **Figure 7**).

As expected, the depth at which the nets were deployed was found to significantly affect coral bycatch species composition and abundance (df = 1, $F = 11.861$, $p < 0.01$). The variation in coral community structure per net set could be partially explained by differences in the depth of deployment, with the constrained ordination axis (i.e., that defined by depth) accounting for 9.42% of the total variation in the distance matrix. Overall, the constrained ordination axis and the first residual axis of the db-RDA contributed to explain 33.29% of the variation found in the distance matrix (**Figure 8**). The depth vector in the db-RDA indicates the direction in the graph for which net sets were deployed at deeper depths (right-hand side of **Figure 8**). This shows that deeper deployments contained more *C. verticillata*,

TABLE 2 | Species composition and description of the variability between colonies and fragments of the number of specimens (No) and sizes (height and width) of all specimens collected as bycatch in bottom-set gillnets during the two sampling seasons in Sagres (southern Portugal).

Species	Colony			Fragment		
	No.	Average height (cm) (min–max)	Average width (cm) (min–max)	No.	Average height (cm) (min–max)	Average width (cm) (min–max)
Eunicella verrucosa	746	22.9 (6.3 – 41.5)	15.5 (2.5 – 41.5)	634	15.3 (3.5 – 38.9)	11.9 (2.0 – 32.7)
Paramuricea grayi	667	17.6 (3.0 – 40.5)	11.6 (2.2 – 36.5)	604	12.3 (3.2 – 42.4)	8.2 (1.7 – 10.2)
Dendrophyllia cornigera	241	8.4 (4.2 – 20.0)	8.6 (2.2 – 90.5)	281	7.8 (2.7 – 19.7)	7.5 (1.0 – 23.0)
Dendrophyllia ramea	36	14.7 (5.0 – 38.8)	11.9 (2.9 – 39.5)	213	10.8 (3.2 – 88.0)	8.2 (1.3 – 32.5)
Callogorgia verticillata	8	34.3 (20.5 – 49.8)	32.6 (8.8 – 57.1)	239	29.4 (8.7 – 63.4)	23.2 (2.8 – 109.3)
Ellisella paraplexauroides	17	70.4 (35.0 – 107.7)	15.1 (6.6 – 33.0)	106	55.7 (15.9 – 104.1)	11.0 (1.4 – 50.0)
Leptogorgia sarmentosa	32	28.9 (6.2 – 64.3)	26.7 (5.0 – 61.9)	87	23.6 (9.2 – 53.7)	19.8 (5.7 – 62.1)
Eunicella labiata	56	23.7 (13.1 – 41.5)	15.7 (4.2 – 33.5)	59	14.9 (6.0 – 34.8)	11.3 (3.0 – 26.0)
Eunicella gazella	39	14.1 (7.4 – 25.3)	11.7 (4.8 – 20.7)	43	13.4 (6.4 – 30.5)	10.6 (3.5 – 19.7)
Isidella elongata	49	13.2 (4.5 – 22.4)	8.3 (3.0 – 23.0)	21	11.1 (7.8 – 16.8)	6.9 (3.1 – 10.4)
Savalia savaglia	4	39.0 (26.2 – 68.0)	19.5 (12.9 – 31.3	53	22.5 (3.9 – 80.4)	14.2 (2.3 – 48.0)
Antipathella subpinnata	19	35.1 (16.0 – 67.5)	24.8 (8.0 – 44.3)	20	22.0 (8.7 – 57.9)	19.3 (5.8 – 49.3)
Corallium rubrum	1	5.0	7.3	12	6.8 (4.8 – 10.2)	4.2 (1.5 – 8.5)
Paramuricea clavata	4	12.6 (9.1 – 18.3)	9.1 (1.8 – 13.0)	7	11.0 (5.7 – 17.2)	8.2 (5.8 – 12.3)
Acanthogorgia hirsuta	7	18.0 (8.3 – 28.0)	18.2 (10.4 – 21.7)	3	9.1 (7.7 – 11.2)	8.0 (5.7 – 11.0)
Spinimuricea atlantica	6	27.8 (21.7 – 37.5)		2	20.25 (15.5 – 25.0)	
(Octocorallia) sp. 2	2	21.5 (20.7 – 22.2)	6.7 (2.1 – 11.3)	1	23.6	3.5
Acanthogorgia armata	1	17.4	17.2	1	11.9	12.2
Pourtalosmilia anthophyllites	1	4.0	4.0	0		
Viminella flagellum	0			1	72.7	13.0
(Octocorallia) sp. 1	0			1	26.0	
(Octocorallia) sp. 3	1	8.7	4.3	0		

I. elongata, *A. subpinnata*, and *S. savaglia*, whereas shallow deployments contained more *P. grayi*, *E. verrucosa*, *D. ramea*, *D. cornigera*, and *L. sarmentosa* (**Figure 8**). Additionally, the db-RDA analyses show that the species *D. cornigera*, *D. ramea*, and *P. grayi* are more correlated with each other, as their vector directions create small angles between them, implying that these species tend to appear in the same nets. The same pattern occurs for the pair of species *C. verticillata* with *S. savaglia* and *I. elongata* with *A. subpinnata*. Conversely, species like *P. grayi* and *I. elongata* or *E. verrucosa* and *S. savaglia* are negatively correlated (i.e., with opposite vector directions) and are not generally recovered in the same net.

The spatial abundance and alpha diversity found in each net allowed us to identify four main areas where the diversity and abundance are highest, which we classified as coral *hotspots* (**Figure 9**). In the hotspot areas, coral diversity was up to 22 species and 144 specimens. Other areas displayed lower but still relatively high diversity (11–16 species) and abundance (72–108 specimens) (**Figure 9**).

DISCUSSION

This study confirms anecdotal evidence suggesting that the impact of bottom-set gillnets on deep-sea coral communities in Portugal, and on marine animal forests in general, is greater than previously appreciated. The coral removal rates reported here, while far lower than those reported for bottom trawling (Clark et al., 2016; Victorero et al., 2018), are substantially higher than what has been described for other fishing gears such as longlines and traps (Mytilineou et al., 2014; Pham et al., 2015). Overall, our findings highlight the urgent need to better understand the large-scale impacts of artisanal and other coastal multifleet and multispecific fisheries, as well as the urgent need for appropriate management policies to conserve and protect existing coral gardens and CWCs.

Impact of Bottom-Set Gillnets on Coral Communities

Similar to previous studies conducted in other regions, bottom-set gillnets had a substantial impact on coral gardens and CWC reefs in Sagres with high levels of coral removal (Shester and Micheli, 2011). In total, 4326 coral specimens, a large proportion of which entire colonies (45%), were caught as bycatch in the 118 nets deployed over the 42-day period of our survey, corresponding to an average (±SE) of 31.1 (±2.7) corals per net. When considering each net's length and soaking time, the removal rates become less pronounced (average coral CPUE of 0.92/day.100 m), although in some areas, particularly those for which the nets were deployed over rocky-bottom habitat, the CPUE was as high as 13.02/day.100 m (top 5% of 4.14–13.02/day.100 m). Based on the average of coral bycatch per net and daily number of nets recovered, a single fishing vessel

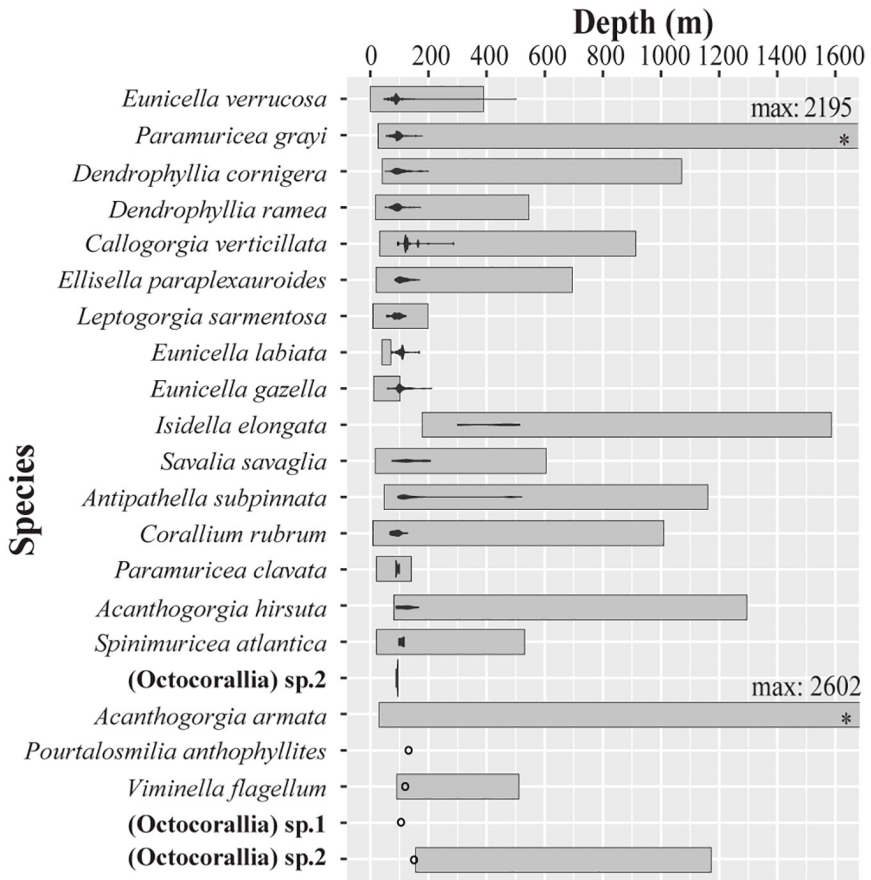

FIGURE 3 | Collection depth ranges of the coral species caught as coral bycatch by bottom-set gillnets in Sages (southern Portugal) during the two seasons studied. The bathymetric distribution recorded in the literature for each species is shown as gray band. The abundance of each species at each depth is also shown with a violin plot.

using bottom-set gillnet can catch between 26,421–27,902 corals as bycatch per year (extrapolated to 214–226 fishing days to discount 27–39 days of bad weather). Such high levels of coral bycatch, although based on a different metric, are in line with the findings of Shester and Micheli (2011) for small-scale fisheries (SSF) in Baja California (Mexico), where gillnet sets had the highest removal rate (0.37 gorgonians per m^2) when compared with fish and lobster traps. In that study, the authors report that only 21.7% of the gillnet sets interacted with gorgonians, which is much lower than what we observed here (85%), though it is possible this disparity reflects site-specific differences in coral density.

While not unexpected, our analysis indicates that the type of substrate over which the nets are deployed strongly influences coral bycatch, as the amount of coral caught in rocky-bottom areas was generally higher than in areas where hard seabed does not occur. Most coral species are found on hard substrate where they can form dense aggregations with complex architecture, which substantially increases the probability of corals becoming snagged or entangled in the nets, thus causing damage or detachment of the colonies. This association is well correlated with the ecology of the target species, which is particularly evident in the amount of coral caught when fisherman deploy sets for John Dory, a species that typically is associated with rocky habitats. In contrast, the fishery of Black-bellied angler, a species which lives on sandy or gravel-covered sea bottom (Maravelias and Papaconstantinou, 2003), had lower impact, except for deployments that crossed (or were very close to) rocky substrate. Unsurprisingly, our study also showed that coral community composition and species abundance vary significantly with depth. For instance, *P. grayi* and *Dendrophyllia* spp. are distributed in shallower habitats, while *I. elongata*, *S. savaglia*, *C. verticillata*, and *A. subpinnata* occur at greater depths. Different depths are normally associated with different environmental factors (i.e., sea bottom temperature, bottom current velocity, and chlorophyll-a concentration), which contribute to differences in community stratification as different species can have different optimal environments (Stone, 2006).

The magnitude of disturbance observed here is still considerably lower than that documented for trawlers. For example, in seamounts off the coast of Australia, it has been estimated that only 10 deep-sea trawlers passes would be required to completely decimate an area with 15–20% coral cover (Pitcher, 2000; Burridge et al., 2003; Clark et al., 2010). Although we

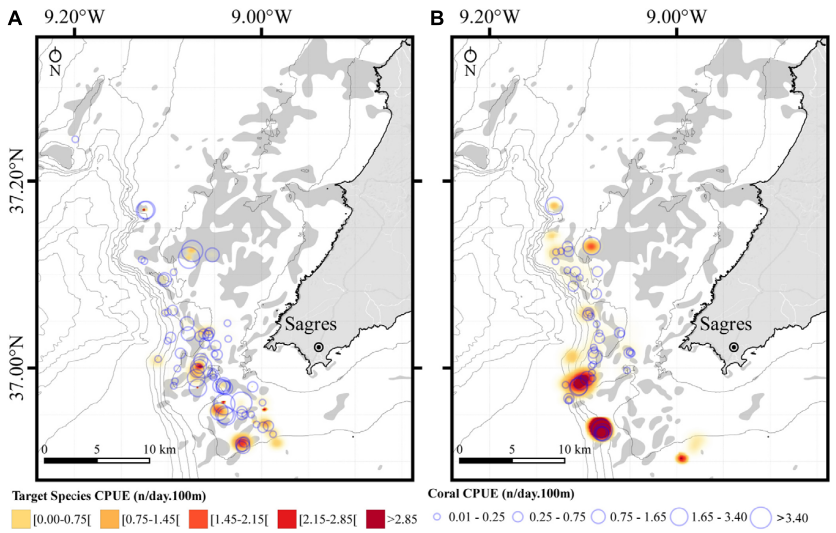

FIGURE 4 | Spatial distribution of the total fishing effort for target species and coral bycatch in bottom-set gillnets off the coast of Sagres (southern Portugal). Fishing effort was calculated as the catch per unit effort (CPUE) and represents the number of specimens (fish/lobster or coral) as a function of the product of the net soaking time (days) and 100 m of net length deployed. **(A)** Summer-autumn sampling season (1 September to 16 October 2019). **(B)** Spring sampling season (11 May to 5 June 2020). CPUEs for the target species are displayed as heatmaps generated using triweight kernel density and corals displayed as bubbles. Bathymetric isobaths are as follows: 50 m, 100–500 m (increments of 100 m), and >500 m (increment of 200 m). Rocky substrate is represented as gray shadow.

did not attempt to quantify actual removal rates (i.e., amount removed according to the abundance *in situ*), our results suggest that it is likely that the community structure (i.e., size of colonies and species diversity) in the study area was different in the past. Deep-water coral species have slow growth rates and as such population recovery and reestablishment (Bavestrello et al., 1997) in the face of constant partial and total damage can be very slow (if possible at all), especially after decades of fishing. For instance, the recovery time of *E. verrucosa* has been estimated to range between 17 and 20 years, which can lead to the replacement of *E. verrucosa* colonies by shorter-lived species with quicker recovery rates (e.g., *Alcyonium digitatum*; Kaiser et al., 2018). These recovery times may be substantially longer for scleractinian and anthipatharian species that grow much slower.

Other fishing gears for which data are available like longlines and traps appear to have a much lower impact on coral communities compared to that caused by bottom-set gillnets. For instance, Pham et al. (2015) reported removal rates of 0.32 corals per 1000 hooks (1.15 corals per set) for deep-sea longline fishing in the Azores. For the vessel we followed in Sagres, the average coral CPUE for bottom-set gillnets was 0.92 per day.100 m (31.1 corals per set). These observations indicate that bottom-set gillnets have a higher removal rate, as we report 27 times the average coral removal per set of fishing gear. Additionally, Shester and Micheli (2011) did not report any coral bycatch from fish and lobster traps, suggesting that traps have the lowest overall impact on benthic communities.

In addition to complete removal of benthic habitat-formers, set gillnets can cause other types of physical damage, including abrasion, breakage, and partial mortality (Shester and Micheli, 2011; Bo et al., 2014). In the particular case of corals, the colonies are expected to survive and recover from partial mortality, as natural breakage is part of their population dynamics and evolutionary ecology (Hughes and Jackson, 1980; Hughes et al., 1992). However, partial colony mortality is known to have profound effects on fitness by reducing fecundity and resource availability (Wahle, 1985; Page and Lasker, 2012). Moreover, the damage caused by abrasion and breakage can promote the development of disease and necrosis points, which can further increase mortality (Bavestrello et al., 1997). While we did not evaluate the effect of these processes (beyond the biomass of fragments removed) on surviving colonies, it is expected that the extent of coral mortality caused by gillnets in Sagres, and globally, is an underestimation of the real impact (Sampaio et al., 2012). More broadly, decades of unchecked damage to these habitats, as is likely the case in Sagres, can result in long-term (potentially permanent) changes in community composition and structure, which can reduce local biodiversity and the associated fishing catches (Cryer et al., 2002; Clark and Rowden, 2009; Atkinson et al., 2011; Clark et al., 2016).

Overall, the gorgonians *E. verrucosa* (the pink sea fan) and *P. grayi* and the scleractinians *Dendrophyllia* spp. were the most severely impacted species, making up nearly 80% of the total bycatch. *E. verrucosa*, in particular, is listed as a species of principal importance in the United Kingdom and vulnerable in the IUCN Red List and may warrant protection (IUCN, 1996). For instance, our results indicate that the colonies of *E. verrucosa* caught as bycatch in Sagres were generally small (average height: 22.9 ± 0.3 cm; average width 15.5 ± 0.2 cm) considering the species can reach 25–50 cm in height and a similar width (Grasshoff, 1992). Similarly, the scleractinian *D. cornigera* (12% of total bycatch) can reach a height of 60 cm, yet the maximum height of the colonies collected in this study was 20 cm (Brito and Ocaña, 2004). These observations suggest that decades of

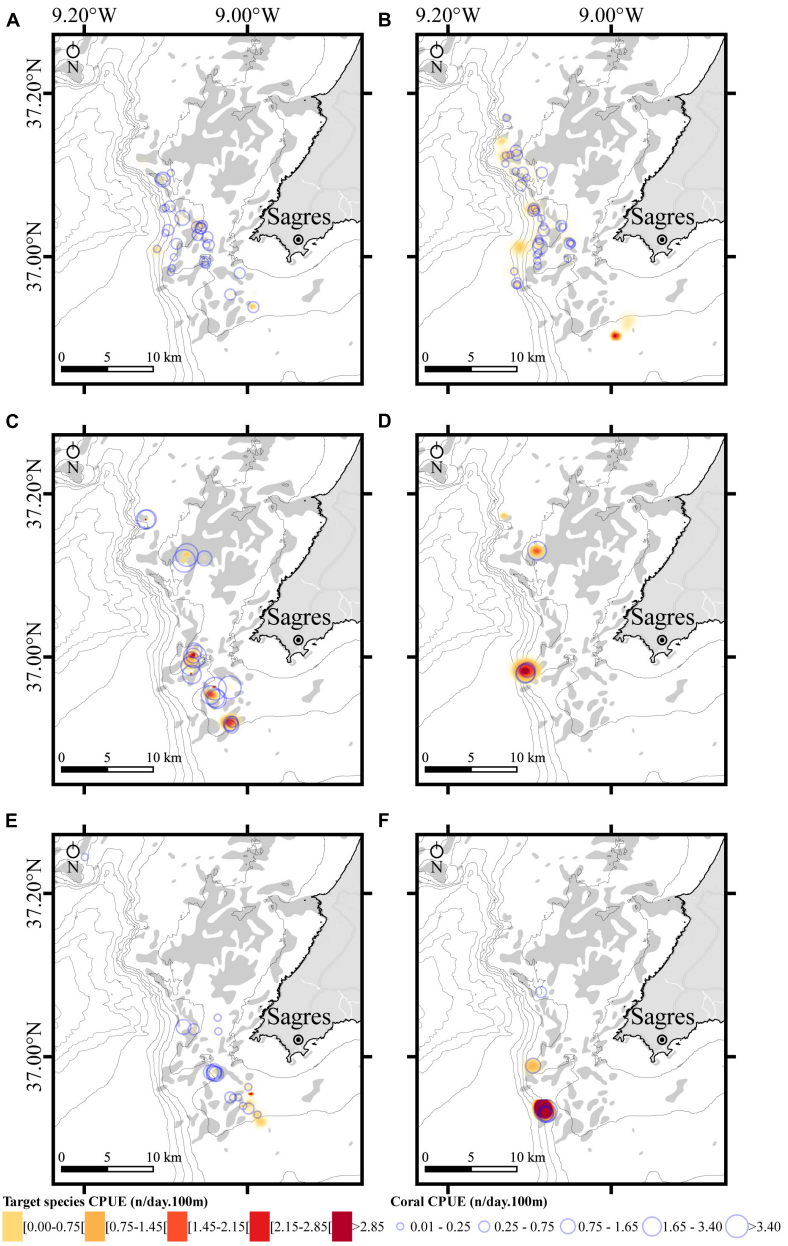

FIGURE 5 | Spatial distribution of the fishing effort for target species and coral bycatch in bottom-set gillnets off the coast of Sagres (Portugal) during the summer-autumn (left panels) and spring (right panels) sampling seasons. Fishing effort was calculated as the catch per unit of effort (CPUE) and represents the number of specimens (fish/lobster or coral) as a function of the product of the net soaking time (days) and 100 m of net length deployed. **(A,B)** Lophius budegassa; **(C,D)** Zeus faber; **(E)** Raja brachyura, Palinurus elephas, Palinurus mauritanicus pooled; and **(F)** Palinurus elephas and Polyprion americanus pooled. The maps in E and F show seasonally deployed nets for species that are targeted over specific periods of the year. CPUEs for the target species are displayed as heatmaps generated using triweight kernel density and corals displayed as bubbles. Bathymetric isobaths are as follows: 50 m, 100–500 m (increments of 100 m), and >500 m (increment of 200 m). Rocky substrate is represented as gray shadow.

accidental captures of these coral species by artisanal fisheries are taking a toll on the populations, as their recovery is too slow (Kaiser et al., 2018) to recover from such fishing pressures.

Coral Biodiversity

The diversity of coral species recovered as bycatch from bottom-set gillnets in Sagres was surprisingly high given the relatively small-scale and geographic coverage of our study. Previous assessments of deep-sea (<200 m depth) coral diversity for the Northeast Atlantic listed 173 species of corals, including antipatharians, gorgonians, and scleractinians (Hall-Spencer et al., 2007; Oliveira et al., 2015; Boavida et al., 2016a,b), with a total of 174 species known to occur in the exclusive economic zone (EEZ) of mainland Portugal (i.e., excluding Madeira and

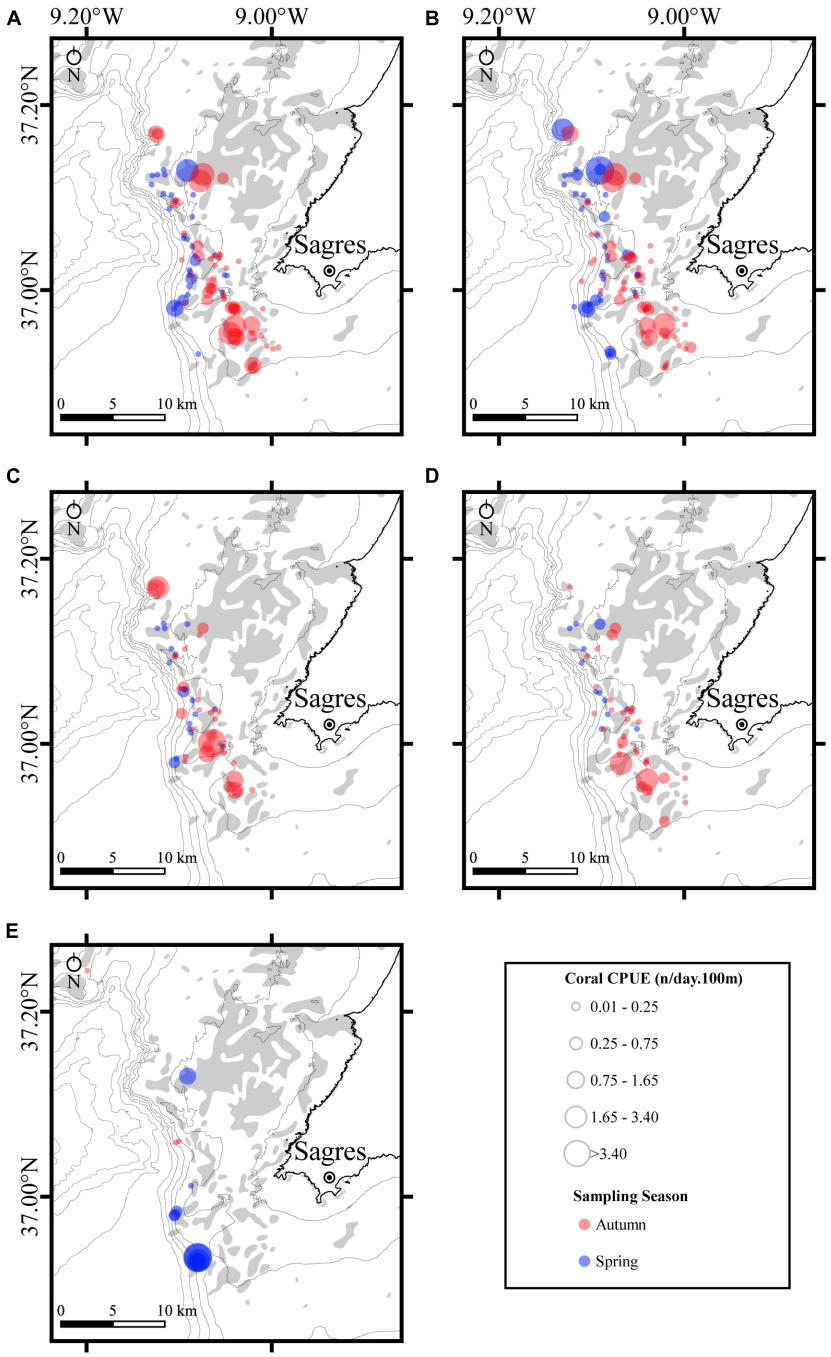

FIGURE 6 | Spatial distribution of the fishing effort for the five specimens of coral caught as bycatch in bottom-set-gillnets off the coast of Sagres (Portugal) during summer-autumn (blue color) and spring (red color) sampling seasons. Fishing effort was calculated as the catch per unit of effort (CPUE) and represents the number of specimens (coral) as a function of the product of the net soaking time (days) and 100 m of net length deployed. **(A)** *Paramuricea grayi*; **(B)** *Eunicella verrucosa*; **(C)** *Dendrophyllia cornigera*; **(D)** *Dendrophyllia ramea*; and **(E)** *Callogorgia verticillata*. CPUEs for the corals are displayed as bubbles. Bathymetric isobaths are as follows: 50 m, 100–500 m (increments of 100 m), and >500 m (increment of 200 m). Rocky substrate is represented as gray shadow.

the Azores; Horton et al., 2020). We found a total of 22 species of corals belonging to the anthozoan Subclasses Octocorallia (n = 17) and Hexacorallia (n = 5), which corresponds to 13% of the species known to occur in mainland Portugal and more than previous recorded in the OCEANA/MeshAtlantic ROV campaign for circalittoral off Sagres (Monteiro et al., 2013; Nestorowicz, 2020). Despite the high number of species identified, this is likely an underestimation of the diversity of coral garden and CWC reef forming species in Sagres as our survey was limited to a 57–510 m depth range, and mostly to the

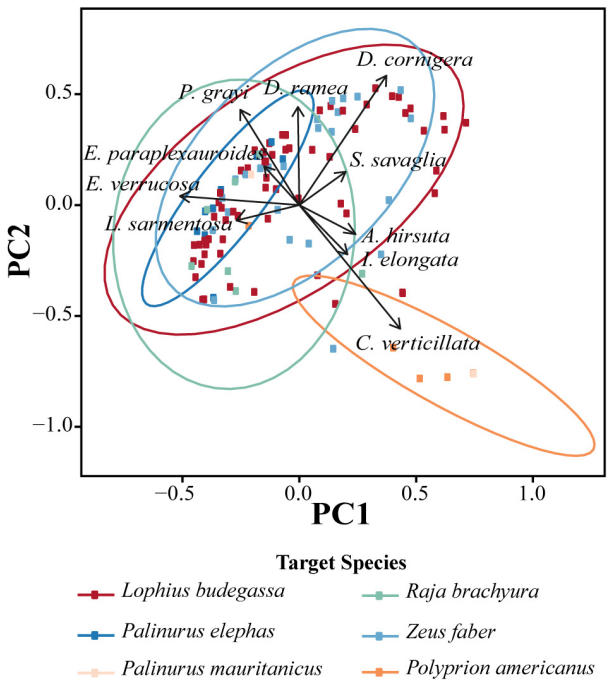

FIGURE 7 | Principal coordinate analysis (PCoA) showing the variation in the coral species community structure from bycatch using bottom-set gillnets during two sampling seasons off the coast of Sagres (Portugal). PCoA plot based on species composition per net deployed and métier. The species matrix describing the ecological resemblance per net was calculated using the Hellinger distance. The vectors display the Pearson correlations (p-value < 0.05) between the descriptors (i.e., coral species captures per net) and the PCoA1 and PCoA2. PCoA biplot of the métier documented in both sampling seasons. Significant groupings defined by métier are shown in color. For more information concerning the PCoA, refer to Section "Materials and Methods."

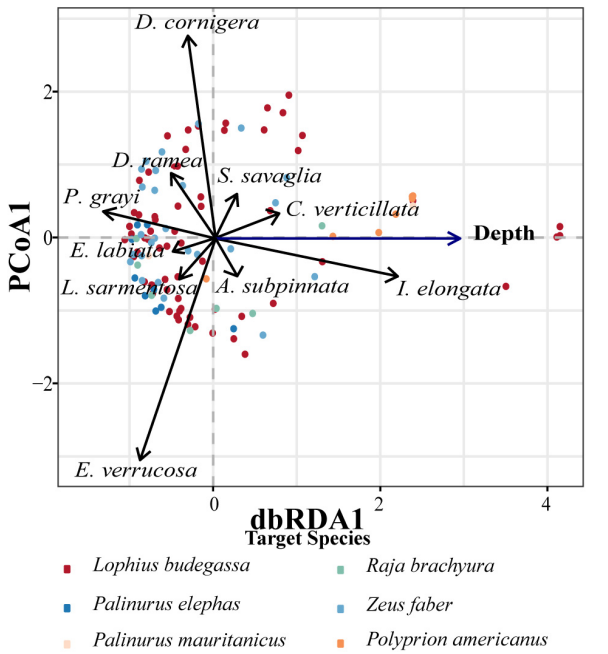

FIGURE 8 | Variation of the coral community according to the depth (db-RDA), from the assessment of coral bycatch using bottom-set gillnets during two sampling seasons off the coast of Sagres (Portugal). Species composition per net was converted to a resemblance matrix using Hellinger distance and the variable depth described as constrained ordination axis. The vectors display the Pearson correlations (p-value < 0.05) between the descriptors (i.e., coral species captures per net) and the dbRDA1 and PCoA1. Db-RDA biplot shows the variation of the coral community according to the depth at which nets were deployed. The depth vector indicates the trend from shallow (left) to deep (right). Significant groupings defined by métier are shown in color. For more information concerning the db-RDA refer to Section "Materials and Methods."

upper 120 m (67% of the nets). Interestingly, the collection depths of the three species of *Eunicella* were higher than the bathymetric range documented in the literature.

Our analysis of the spatial distribution of coral bycatch alpha diversity and captures identified four main biodiversity hotspots in the study area with up to 22 species and 144 specimens. These findings are in accordance with recent recommendations put forward by OCEANA, which urged Portugal to expand the Natura 2000 Network to incorporate seamounts and other coral garden areas around Cape St. Vincent (Oceana., 2005, 2011). The unique richness of this area warrants a special status of protection, especially given the high direct impact of fisheries through coral removal (as documented here), as well as by lost and discarded fishing gear, a secondary effect of commercial fishing activities on benthic communities that has also been documented (Oliveira et al., 2015; Vieira et al., 2015).

Conservation and Management Implications

This study shows that the impact of bottom-set gillnets on coral gardens and CWC reefs seems to be significant, underlining the conservation concern that fishing operations using this type of gear creates. Reducing the impact of gillnets on these habitats requires active measures that fall within one of several categories (not mutually exclusive), including measures of spatial management (i.e., MPAs), environmental legislation (i.e., list habitats as VMEs or Essential Fish Habitat-EFH), and fisheries management (i.e., temporary closures and other restrictions, and the use of alternative fishing gear). The creation of MPAs, eventually associated with VMEs and/or EFH, can be an effective measure to protect slow-growing benthic communities (and the biodiversity associated) such as coral gardens and CWCs. Only a few studies have attempted to assess the impact of deep water MPAs, as MPA placement in deep waters is still in its infancy (Markantonatou et al., 2014; Huvenne et al., 2016). Additionally, closure of certain areas to bottom trawling has been modeled and found to be potentially effective in the protection of coral gardens and CWCs, with negligible losses for bottom trawlers (Lagasse et al., 2015).

With regard to fisheries management, some of the strategies that have been adopted include frequent monitoring onboard of fishing vessels (i.e., in order to reinforce bycatch and landing

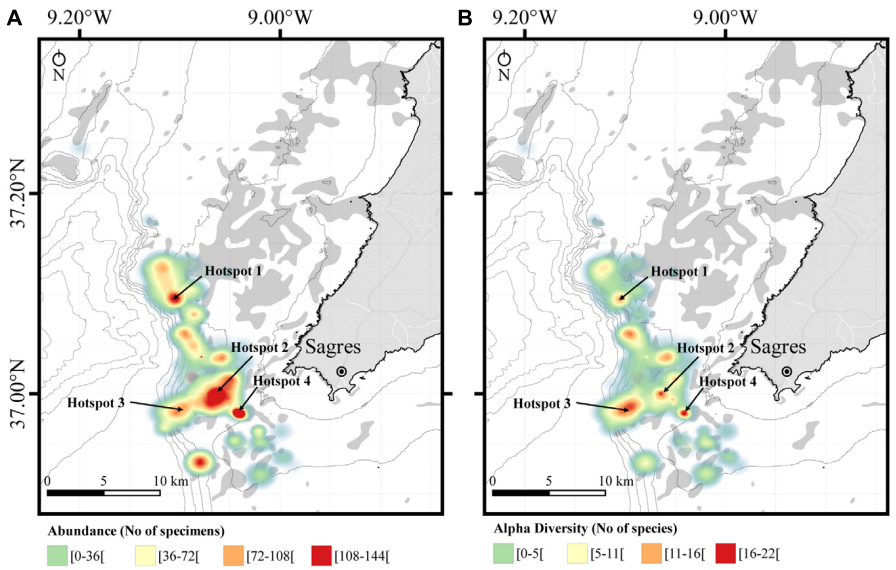

FIGURE 9 | Spatial distribution of coral bycatch and biodiversity (no. of species) caught as incidental catches in bottom-set gillnets in Sagres (southern Portugal). Identification of possible hotspots of coral gardens that should be protected from significant adverse impacts. Hotspots coordinates as the center point of the hotspots in WGS84 (GPS). Hotspot 1: N37.0952 W-9.1058; Hotspot 2: N36.99565 W-9.06177; Hotspot 3: N36.98156 W-9.10291; Hotspot 4: N36.98032 W-9.04086. **(A)** Density map of corals showing the hotspots based on the number of corals collected in each net deployed. **(B)** Diversity map of corals showing hotspots based on the diversity of corals collected in each net deployed. Coral diversity and abundance are displayed as heatmaps generated using triangular kernel density. Bathymetric isobaths are as follows: 50 m, 100–500 m (increments of 100 m), and >500 m (increment of 200 m).

laws), temporary closure of certain areas where the fishing effort is very low and coral bycatch very high (e.g., Hattonand Rockall Banks; Wright et al., 2015), and development of protocols for encounters such as move-on rules in national waters (UNGA, 2009). The move-on protocol, in particular, currently applies solely to areas beyond national jurisdiction and it mandates that when the catch of a fishing vessel (i.e., single trawl tow or set of static fishing gear) reaches a bycatch threshold of a VME indicator species, the vessel has to stop its fishing activity and move two nautical miles (NM) away from the site (Rogers and Gianni, 2010). In the Northwest Atlantic Fisheries Organization area, the thresholds were defined by weight and largely without scientific basis despite widespread advice of the scientific community for lower thresholds (Aguilar et al., 2017). In the North East Atlantic Fisheries Commission (NEAFC) area, the protocol defines that a temporary closure with 2NM on each side of the trawler track or a 2NM-radius from the most likely position of the encounters should be applied when encounters surpass a threshold of 30 kg of live coral or 400 kg of live sponges for trawler tows and other gear like gillnets, and 10 specimens per 1000 hooks or 1200 m of longline gear (FAO, 2016). If the NEAFC VME threshold for gillnets (30 kg of coral) was to be applied to the métiers studied, at least 10,345 colonies of *E. verrucosa* (average dry weight of colonies 2.901 ± 0.078 g, n = 988) or 350 colonies of *Dendrophyllia* spp. (average dry weight of colonies 85.49 ± 7.45 g, n = 819) would have to be caught in a single set to trigger the move-on rule, a value 67 and two times higher than the highest bycatch value documented in this study for a single set, respectively. Even though this estimates are based on weight data for entire colonies only (i.e., excluding fragments) and dry weight (as opposed to wet weight), a capture of more than 10,000 colonies to trigger the move-on rule would constitute a profound impact on the coral communities studied here.

Such protocols can be improved by lowering or adapting (i.e., account for the life-history traits of the dominant VME species) the thresholds based on bycatch data (as provided in this study), and by increasing the move-on and closure distances (Rogers and Gianni, 2010; Aguilar et al., 2017). These measures could also be adopted in waters of national jurisdiction, since many VME indicator species are found throughout these areas and have long been impacted by fisheries. For instance, in national waters, it may be advisable that each gear type have its own threshold and move-on distance. As an example for fishing activities using similar métiers to those documented in Sagres, the vessels could move at least 1.0NM from the middle point of the most likely position of encounters (e.g., biodiversity hotspots identified in **Figure 9**) because the average length of each net was 1.99 km for our study. Caution should be taken in setting distance that could be used as move-on as information about coral gardens distribution is scarce. In areas where gorgonians are common, fisheries regulators may consider instituting a threshold based on the number and size of specimens instead of weight, as it is easy to overlook the scale of the impact on the ecosystem when simply measuring the weight of a gorgonian colony (just a few grams for potentially quite old individuals). Counting specimens in these métiers is also simpler to implement.

Frequent monitoring onboard of fishing vessels, although expensive, can be a valuable management tool as well given that it can contribute to effectively implement and enforce fishing regulations (both proposed and existing), thereby reducing coral

bycatch (Boenish et al., 2020). An alternative approach that has been used in a Portofino MPA (Ligurian Sea, Italy) and which could be adopted in other areas is to assess the spatial allocation of fisheries using bottom-contact gear to identify vulnerable areas (Markantonatou et al., 2014). Using different fishing gear that cause substantially lower impacts, while not a panacea, can also help reducing the impacts on coral gardens and CWC reefs. In that regard, a potential alternative is the use of bottom longlines or traps, as these gear cause substantially lower impacts to benthic ecosystems (Shester and Micheli, 2011).

Final Remarks

This study is a pioneer assessment of the interaction between artisanal fisheries using bottom-set static gear and coral communities in mainland Portugal. Additional research will be required to fully understand the extent of the damage caused by these activities. SSF constitute more than 90% of the Portuguese fishing fleet and our findings may only show the "tip of the iceberg" of the potentially irreversible crippling of deep-sea coral habitats. Studies of this type provide essential contributions to the knowledge of the distribution and abundance of corals in southwestern Portugal, and worldwide in general. We have identified a number of important biodiversity hotspots for which habitat mapping using newer technologies like ROVs will prove essential to confirm the presence of VMEs and evaluate the scale of fishing impacts. Our findings also highlight the importance of stricter control measures onboard of fishing vessels and draws attention to the fact that artisanal fisheries as a whole pose a serious threat to the ecological functioning and integrity of coral gardens and CWC reefs in certain areas. Nevertheless, this study highlights the importance of collaborating with fishermen in order to better understand deep-sea coral biodiversity, as well as of how scientists and fishermen can work together to protect such vulnerable species. In that regard, recent efforts, including work led by our team (in prep), have shown that the tremendous amount of coral biomass generated in fishing vessels using bottom-contact gear constitutes a major resource for restoration ecology (Montseny et al., 2019, 2020).

DATA AVAILABILITY STATEMENT

The datasets presented in this study can be found in online repositories. The names of the repository/repositories and accession number(s) can be found below: https://doi.org/10.6084/m9.figshare.13142774.v2.

AUTHOR CONTRIBUTIONS

MC, JB, and ES conceived the study. VD conducted field work. VD, FO, and MC conducted data analyses and wrote the manuscript. JB, ES, and JG critically reviewed the manuscript. All authors gave the approval for the publication of the manuscript.

FUNDING

This research was funded by projects HABMAR (Grant No. MAR-01.04.02-FEAMP-0018) co-financed by the European Maritime and Fisheries Fund of the Operational Program MAR 2020 for Portugal (Portugal 2020), TECPESCA (Grant No. MAR2020 16-01-04-FMP-0010), and MARSW (Grant No. POSEUR/ICNF/LPN). Furthermore, this study received Portuguese national funds from FCT—Foundation for Science and Technology through project UIDB/04326/2020 and fellowship SFRH/BSAB/150485/2019. ES thanks a Pew Marine Fellowship.

ACKNOWLEDGMENTS

We would like to thank DOCAPESCA Baleeira-Sagres for providing facilities to process the coral specimens. We are grateful to the captain Casimiro and his fishing crew for the collaboration and help onboard of the fishing vessel. In addition, we would like to thank the students Ana Carneiro, Sandra Costa, and Candice Parkes together with the volunteer Ana Gheorghiu for the help in measuring, tagging, and photographing the specimens collected.

SUPPLEMENTARY MATERIAL

The Supplementary Material for this article can be found online at: https://www.frontiersin.org/articles/10.3389/fmars.2020.603438/full#supplementary-material

REFERENCES

Aguilar, R., Perry, A. L., and López, J. (2017). "Conservation and Management of Vulnerable Marine Benthic Ecosystems," in *Marine Animal Forests*, eds S. Rossi, L. Bramanti, A. Gori, and C. Orejas (Cham: Springer International Publishing), 1–43. doi: 10.1007/978-3-319-17001-5_34-1

Albright, R., Takeshita, Y., Koweek, D. A., Ninokawa, A., Wolfe, K., Rivlin, T., et al. (2018). Carbon dioxide addition to coral reef waters suppresses net community calcification. *Nature* 555, 516–519. doi: 10.1038/nature25968

Armstrong, C. W., and van den Hove, S. (2008). The formation of policy for protection of cold-water coral off the coast of Norway. *Mar. Policy* 32, 66–73. doi: 10.1016/j.marpol.2007.04.007

Ashford, O. S., Kenny, A. J., Barrio Froján, C. R. S., Downie, A.-L., Horton, T., and Rogers, A. D. (2019). On the influence of vulnerable marine ecosystem habitats on peracarid crustacean assemblages in the northwest atlantic fisheries organization regulatory area. *Front. Mar. Sci.* 6:401. doi: 10.3389/fmars.2019.00401

Atkinson, L., Field, J., and Hutchings, L. (2011). Effects of demersal trawling along the west coast of southern Africa: multivariate analysis of benthic assemblages. *Mar. Ecol. Prog. Ser.* 430, 241–255. doi: 10.3354/meps08956

Bavestrello, G., Cerrano, C., Zanzi, D., and Cattaneo-Vietti, R. (1997). Damage by fishing activities to the Gorgonian coral Paramuricea clavata in the Ligurian Sea. *Aquat. Conserv.* 7, 253-262.

Bo, M., Bava, S., Canese, S., Angiolillo, M., Cattaneo-Vietti, R., and Bavestrello, G. (2014). Fishing impact on deep Mediterranean rocky habitats as revealed by ROV investigation. *Biol. Conserv.* 171, 167–176. doi: 10.1016/j.biocon.2014.01.011

Boavida, J., Assis, J., Reed, J., Serrão, E. A., and Gonçalves, J. M. S. (2016a). Comparison of small remotely operated vehicles and diver-operated video

of circalittoral benthos. *Hydrobiology* 766, 247–260. doi: 10.1007/s10750-015-2459-y

Boavida, J., Paulo, D., Aurelle, D., Arnaud-Haond, S., Marschal, C., Reed, J., et al. (2016b). A well-kept treasure at depth: precious red coral rediscovered in atlantic deep coral gardens (SW Portugal) after 300 Years. *PLoS One* 11:e0147228. doi: 10.1371/journal.pone.0147228

Boenish, R., Willard, D., Kritzer, J. P., and Reardon, K. (2020). Fisheries monitoring: perspectives from the United States. *Aquac. Fish.* 5, 131–138. doi: 10.1016/j.aaf.2019.10.002

Bramanti, L., Movilla, J., Guron, M., Calvo, E., Gori, A., Dominguez-Carrió, C., et al. (2013). Detrimental effects of ocean acidification on the economically important Mediterranean red coral (*Corallium rubrum*). *Glob. Change Biol.* 19, 1897–1908. doi: 10.1111/gcb.12171

Brito, A., and Ocaña, O. (2004). *Corals of the Canary Islands: skeleton anthozoa of the littoral and deep bottoms*. La Laguna: Francisco Lemus.

Buhl-Mortensen, L., Vanreusel, A., Gooday, A. J., Levin, L. A., Priede, I. G., Buhl-Mortensen, P., et al. (2010). Biological structures as a source of habitat heterogeneity and biodiversity on the deep ocean margins: biological structures and biodiversity. *Mar. Ecol* 31, 21–50. doi: 10.1111/j.1439-0485.2010.00359.x

Burridge, C. Y., Pitcher, C., Wassenberg, T. J., Poiner, I., and Hill, B. J. (2003). Measurement of the rate of depletion of benthic fauna by prawn (shrimp) otter trawls: an experiment in the Great Barrier Reef. *Australia. Fish. Res.* 60, 237–253. doi: 10.1016/S0165-7836(02)00179-0

Cairns, S., and Kitahara, M. (2012). An illustrated key to the genera and subgenera of the Recent azooxanthellate Scleractinia (Cnidaria. Anthozoa), with an attached glossary. *ZooKeys* 227, 1–47. doi: 10.3897/zookeys.227.3612

Cairns, S. D. (2007). Deep-water corals: an overview with special reference to diversity and distribution of deep-water scleractinian corals. *Bull. Mar. Sci.* 81:12.

Carpine, C., and Grasshoff, M. (1975). *Les Gorgonaires de la Méditerranée*. Monaco: Institut océanographique.

Clark, M. R., Althaus, F., Schlacher, T. A., Williams, A., Bowden, D. A., and Rowden, A. A. (2016). The impacts of deep-sea fisheries on benthic communities: a review. *ICES J. Mar. Sci.* 73, i51–i69. doi: 10.1093/icesjms/fsv123

Clark, M. R., Bowden, D. A., Baird, S. J., and Stewart, R. (2010). Effects of fishing on the benthic biodiversity of seamounts of the "Graveyard" complex, northern Chatham Rise. *N.Z. Aquat. Environ. Biodiv. Rep.* 46, 1–40. doi: 10.1007/978-3-319-17001-5_37-1

Clark, M. R., and Rowden, A. A. (2009). Effect of deepwater trawling on the macro-invertebrate assemblages of seamounts on the Chatham Rise, New Zealand. *Deep Sea Res. Part Oceanogr. Res. Pap.* 56, 1540–1554. doi: 10.1016/j.dsr.2009.04.015

Consoli, P., Sinopoli, M., Deidun, A., Canese, S., Berti, C., Andaloro, F., et al. (2020). The impact of marine litter from fish aggregation devices on vulnerable marine benthic habitats of the central Mediterranean Sea. *Mar. Pollut. Bull.* 152:110928. doi: 10.1016/j.marpolbul.2020.110928

Cordes, E. E., Jones, D. O. B., Schlacher, T. A., Amon, D. J., Bernardino, A. F., Brooke, S., et al. (2016). Environmental impacts of the deep-water oil and gas industry: a review to guide management strategies. *Front. Environ. Sci.* 4:58. doi: 10.3389/fenvs.2016.00058

Cryer, M., Hartill, B., and O'Shea, S. (2002). Modification of marine benthos by trawling: toward a generalization for the deep ocean. *Ecol. Appl.* 12, 1824–1839. doi: 10.1890/1051-0761(2002)012[1824:mombbt]2.0.co;2

Davies, J. S., Guillaumont, B., Tempera, F., Vertino, A., Beuck, L., Ólafsdóttir, S. H., et al. (2017). A new classification scheme of European cold-water coral habitats: implications for ecosystem-based management of the deep sea. *Deep Sea Res. Part II Top. Stud. Oceanogr.* 145, 102–109. doi: 10.1016/j.dsr2.2017.04.014

Deporte, N., Ulrich, C., Mahévas, S., Demanèche, S., and Bastardie, F. (2012). Regional métier definition: a comparative investigation of statistical methods using a workflow applied to international otter trawl fisheries in the North Sea. *ICES J. Mar. Sci.* 69, 331–342. doi: 10.1093/icesjms/fsr197

DGRM (2018). *RELATÓRIO ANUAL-FROTA DE PESCA PORTUGUESA -Ű 2018. Direção Geral de Recursos Naturais, Segurança e Serviços Marítimos*. Available online at: https://www.ine.pt/xurl/pub/358627638 (accessed May 7, 2020).

EC (2008). Adopting a multiannual Community programme pursuant to Council Regulation (EC) No 199/2008 establishing a Community framework for the collection, management and use of data in the fisheries sector and support for scientific advice regarding the common fisheries policy. *Off. J. Eur. Union L* 346/37, 1–22.

European Parliament and the Council of the European Union (2016). *REGULATION (EU) 2016/ 2336 of the European Parliament and of the Council - of 14 December 2016 - establishing specific conditions for fishing for deep-sea stocks in the north-east Atlantic and provisions for fishing in international waters of the north-east Atlantic and repealing Council Regulation (EC) No 2347 / 2002*. Brussels: European Parliament and the Council of the European Union.

FAO (2016). Vulnerable marine ecosystems - Processes and practices in the high seas. *FAO Fish. Aquac. Tech. Pap.* 595, 1–30. doi: 10.1163/9789004248601_002

Fuller, S. D. (2008). *Vulnerable Marine Ecosystems Dominated by Deep-Water Corals and Sponges in the NAFO Convention Area*. Dartmouth: NAFO, 25.

Garcia, S. M., Allison, E. H., Andrew, N., Béné, C., Bianchi, G., de Graaf, G., et al. (2008). *Towards Integrated Assessment and Advice in Small-Scale Fisheries: Principles and Processes*. Rome: Food and Agriculture Organization of the United Nations.

Glover, A. G., and Smith, C. R. (2003). The deep-sea floor ecosystem: current status and prospects of anthropogenic change by the year 2025. *Environ. Conserv.* 30, 219–241. doi: 10.1017/S0376892903000225 doi: 10.1017/s0376892903000225

Grasshoff, M. (1992). *Die Flachwasser-Gorgonarien von Europa und Westafrika: Cnidaria, Anthozoa*. Frankfurt am Main: Senckenbergische Naturforschende Ges.

Guyader, O., Berthou, P., Koutsikopoulos, C., Alban, F., Demanèche, S., Gaspar, M. B., et al. (2013). Small scale fisheries in Europe: a comparative analysis based on a selection of case studies. *Fish. Res.* 140, 1–13. doi: 10.1016/j.fishres.2012.11.008

Hall-Spencer, J., Rogers, A., Davies, J., and Foggo, A. (2007). Deep-sea coral distribution on seamounts, oceanic islands, and continental slopes in the Northeast Atlantic. *Bull. Mar. Sci.* 81, 135-146.

Hall–Spencer, J., Allain, V., and Fosså, J. H. (2002). Trawling damage to Northeast Atlantic ancient coral reefs. *Proc. R. Soc. Lond. B Biol. Sci.* 269, 507–511. doi: 10.1098/rspb.2001.1910

Halpern, B. S., Walbridge, S., Selkoe, K. A., Kappel, C. V., Micheli, F., D'Agrosa, C., et al. (2008). A global map of human impact on marine ecosystems. *Science* 319, 948–952. doi: 10.1126/science.1149345

Horton, T., Kroh, A., Ahyong, S., Bailly, N., Boyko, C. B., Brandão, S. N., et al. (2020). *World Register of Marine Species (WoRMS)*. WoRMS Editorial Board. Available online at: https://www.marinespecies.org [accessed August 14, 2020).

Hourigan, T. (2009). Managing fishery impacts on deep-water coral ecosystems of the USA: emerging best practices. *Mar. Ecol. Prog. Ser.* 397, 333–340. doi: 10.3354/meps08278

Hughes, T. P. (1994). Catastrophes, phase shifts, and large-scale degradation of a caribbean coral reef. *Science* 265, 1547-1551.

Hughes, T. P., Ayre, D., and Connell, J. H. (1992). The evolutionary ecology of corals. *Trends Ecol. Evol.* 7, 292–295. doi: 10.1016/0169-5347(92)90225-Z

Hughes, T. P., and Jackson, J. B. C. (1980). Do corals lie about their age? some demographic consequences of partial mortality, fission, and fusion. *Science* 209:713. doi: 10.1126/science.209.4457.713

Hughes, T. P., Kerry, J. T., Álvarez-Noriega, M., Álvarez-Romero, J. G., Anderson, K. D., Baird, A. H., et al. (2017). Global warming and recurrent mass bleaching of corals. *Nature* 543, 373–377. doi: 10.1038/nature21707

Hughes, T. P., Kerry, J. T., Baird, A. H., Connolly, S. R., Dietzel, A., Eakin, C. M., et al. (2018). Global warming transforms coral reef assemblages. *Nature* 556, 492–496. doi: 10.1038/s41586-018-0041-2

Huvenne, V. A. I., Bett, B. J., Masson, D. G., Le Bas, T. P., and Wheeler, A. J. (2016). Effectiveness of a deep-sea cold-water coral marine protected area, following eight years of fisheries closure. *Biol. Conserv.* 200, 60–69. doi: 10.1016/j.biocon.2016.05.030

IUCN (1996). Eunicella verrucosa: World Conservation Monitoring Centre: The IUCN Red List of Threatened Species 1996: e.T8262A12903486. Gland: IUCN, doi: 10.2305/IUCN.UK.1996.RLTS.T8262A12903486.en

Jackson, J. B. C. (2001). Historical Overfishing and the Recent Collapse of Coastal Ecosystems. *Science* 293, 629–637. doi: 10.1126/science.1059199

Kaiser, M. J., Hormbrey, S., Booth, J. R., Hinz, H., and Hiddink, J. G. (2018). Recovery linked to life history of sessile epifauna following exclusion of towed mobile fishing gear. *J. Appl. Ecol.* 55, 1060–1070. doi: 10.1111/1365-2664.13087

Kindt, R., and Coe, R. (2005). *Tree Diversity Analysis. A Manual and Software for Common Statistical Methods for Ecological*

and Biodiversity Studies. Nairobi: World Agroforestry Centre (ICRAF).

Lagasse, C., Knudby, A., Curtis, J., Finney, J., and Cox, S. (2015). Spatial analyses reveal conservation benefits for cold-water corals and sponges from small changes in a trawl fishery footprint. *Mar. Ecol. Prog. Ser.* 528, 161–172. doi: 10.3354/meps11271

Lloret, J., Cowx, I. G., Cabral, H., Castro, M., Font, T., Gonçalves, J. M. S., et al. (2018). Small-scale coastal fisheries in European Seas are not what they were: ecological, social and economic changes. *Mar. Policy* 98, 176–186. doi: 10.1016/j.marpol.2016.11.007

Maravelias, C., and Papaconstantinou, C. (2003). Size-related habitat use, aggregation patterns and abundance of angler fish (*Lophius budegassa*) in the Mediterranean Sea determined by generalized additive modelling. *J. Mar. Biol. Assoc.* 83, 1171-1178.

Markantonatou, V., Marconi, M., Cappanera, V., Campodonico, P., Bavestrello, A., Cattaneo-Vietti, R., et al. (2014). "Spatial Allocation of Fishing Activity on Coralligenous Habitats in Portofino MPA (Liguria, Italy)," in *Proceedings of the 2nd Mediterranean Symposium on the Conservation of Coralligenous and Other Calcareous Bio-Concretions*, Portoroz, 118–123.

McGoodwin, J. R. (2001). *Understanding the Cultures of Fishing Communities: A Key to Fisheries Management and Food Security*. Rome: FAO.

Monteiro, P., Bentes, L., Oliveira, F., Afonso, C., Rangel, M., Alonso, C., et al. (2013). *Atlantic Area Eunis Habitats. Adding New Habitat Types From European Atlantic Coast to the EUNIS Habitat Classification*. Faro: CCMAR-Universidade do Algarve.

Montseny, M., Linares, C., Viladrich, N., Capdevila, P., Ambroso, S., Díaz, D., et al. (2020). A new large-scale and cost-effective restoration method for cold-water coral gardens. *Aquat. Conserv. Mar. Freshw. Ecosyst* 30, 977-987. doi: 10.1002/aqc.3303

Montseny, M., Linares, C., Viladrich, N., Olariaga, A., Carreras, M., Palomeras, N., et al. (2019). First attempts towards the restoration of gorgonian populations on the Mediterranean continental shelf. *Aquat. Conserv. Mar. Freshw. Ecosyst*. 29, 1278–1284. doi: 10.1002/aqc.3118

Movilla, J., Orejas, C., Calvo, E., Gori, A., López-Sanz, À, Grinyó, J., et al. (2014). Differential response of two Mediterranean cold-water coral species to ocean acidification. *Coral Reefs* 33, 675–686. doi: 10.1007/s00338-014-1159-9

Mytilineou, C., Smith, C. J., Anastasopoulou, A., Papadopoulou, K. N., Christidis, G., Bekas, P., et al. (2014). New cold-water coral occurrences in the Eastern Ionian Sea: results from experimental long line finishing. *Deep Sea Res. Part II Top. Stud. Oceanogr.* 99, 146-157. doi: 10.1016/j.dsr2.2013.07.007

Nestorowicz, I.-M. (2020). Identifying Priority Habitats in the upper São Vicente Submarine Canyon (Portugal). Dissertation/master's thesis. Belgium: University of Algarve/CCMAR/Ghent University.

Oceana. (2005). *The Seamounts of the Gorringe Bank*. Bergen: OCEANA.

Oceana. (2011). *Workshop on the Improvement of the Definitions of Habitats on the OSPAR List*. Bergen: OCEANA.

Oliveira, F., Monteiro, P., Bentes, L., Henriques, N. S., Aguilar, R., and Gonçalves, J. M. S. (2015). Marine litter in the upper São Vicente submarine canyon (SW Portugal): abundance, distribution, composition and fauna interactions. *Mar. Pollut. Bull.* 97, 401–407. doi: 10.1016/j.marpolbul.2015.05.060

Page, C. A., and Lasker, H. R. (2012). Effects of tissue loss, age and size on fecundity in the octocoral *Pseudopterogorgia elisabethae*. *J. Exp. Mar. Biol. Ecol.* 434, 47–52. doi: 10.1016/j.jembe.2012.07.022

Parker, S., Penney, A., and Clark, M. (2009). Detection criteria for managing trawl impacts on vulnerable marine ecosystems in high seas fisheries of the South Pacific Ocean. *Mar. Ecol. Prog. Ser.* 397, 309–317. doi: 10.3354/meps08115

Pham, C. K., Diogo, H., Menezes, G., Porteiro, F., Braga-Henriques, A., Vandeperre, F., et al. (2015). Deep-water longline fishing has reduced impact on Vulnerable Marine Ecosystems. *Sci. Rep.* 4:4837. doi: 10.1038/srep04837

Pitcher, C. (2000). Implications of the effects of trawling on sessile megazoobenthos on a tropical shelf in northeastern Australia. *ICES J. Mar. Sci.* 57, 1359–1368. doi: 10.1006/jmsc.2000.0911

Purser, A., and Thomsen, L. (2012). Monitoring strategies for drill cutting discharge in the vicinity of cold-water coral ecosystems. *Mar. Pollut. Bull.* 64, 2309–2316. doi: 10.1016/j.marpolbul.2012.08.003

R Core Team (2019). *R: A Language and Environment for Statistical Computing*. Vienna: R Foundation for Statistical Computing.

Ragnarsson, S. Á, Burgos, J. M., Kutti, T., van den Beld, I., Egilsdóttir, H., Arnaud-Haond, S., et al. (2017). "The Impact of Anthropogenic Activity on Cold-Water Corals," in *Marine Animal Forests*, eds S. Rossi, L. Bramanti, A. Gori, and C. Orejas (Cham: Springer International Publishing), 989–1023. doi: 10.1007/978-3-319-21012-4_27

Roberts, J. M. (2006). Reefs of the deep: the biology and geology of cold-water coral ecosystems. *Science* 312, 543–547. doi: 10.1126/science.1119861

Rogers, D. A. D., and Gianni, M. (2010). *The Implementation of UNGA Resolutions 61/105 and 64/72 in the Management of Deep-Sea Fisheries on the High Seas*. London: International Programme on the State of the Ocean.

Rossi, S. (2013). The destruction of the 'animal forests' in the oceans: towards an over-simplification of the benthic ecosystems. *Ocean Coast. Manag.* 84, 77–85. doi: 10.1016/j.ocecoaman.2013.07.004

Rossi, S., Bramanti, L., Gori, A., and Orejas, C. (2017). "*Animal Forests of the World: An Overview*," *in Marine Animal Forests: The Ecology of Benthic Biodiversity Hotspots*. Cham: Springer International Publishing, 3–23. doi: 10.1007/978-3-319-17001-5

Sampaio, Í, Braga-Henriques, A., Pham, C., Ocaña, O., de Matos, V., Morato, T., et al. (2012). Cold-water corals landed by bottom longline fisheries in the Azores (north-eastern Atlantic). *J. Mar. Biol. Assoc. U.K.* 92, 1547–1555. doi: 10.1017/S0025315412000045

Shester, G. G., and Micheli, F. (2011). Conservation challenges for small-scale fisheries: bycatch and habitat impacts of traps and gillnets. *Biol. Conserv.* 144, 1673–1681. doi: 10.1016/j.biocon.2011.02.023

Stone, R. P. (2006). Coral habitat in the Aleutian Islands of Alaska: depth distribution, fine-scale species associations, and fisheries interactions. *Coral Reefs* 25, 229–238. doi: 10.1007/s00338-006-0091-z

Teh, L. C. L., and Sumaila, U. R. (2013). Contribution of marine fisheries to worldwide employment: global marine fisheries employment. *Fish Fish.* 14, 77–88. doi: 10.1111/j.1467-2979.2011.00450.x

UNGA (2004). *Resolution 59/25 Sustainable fisheries, including through the 1995 Agreement for the Implementation of the Provisions of the United Nations Convention on the Law of the Sea of 10 December 1982 relating to the Conservation and Management of Straddling Fish Stocks and Highly Migratory Fish Stocks, and related instruments. A/RES/*59/25. New York, NY: UNGA.

UNGA (2009). *Resolution 64/72 Sustainable fisheries, including through the 1995 Agreement for the Implementation of the Provisions of the United Nations Convention on the Law of the Sea of 10 December 1982 relating to the Conservation and Management of Straddling Fish Stocks and Highly Migratory Fish Stocks, and related instruments A/RES/64/72*. New York, NY: UNGA.

UNGA (2019). *74/18. Sustainable fisheries, including through the* 1995 Agreement for the Implementation of the Provisions of the United Nations Convention on the Law of the Sea of 10 December 1982 relating to the Conservation and Management of Straddling Fish Stocks and Highly Migratory Fish Stocks, and related instruments. A/RES/74/18. New York, NY: UNGA.

Victorero, L., Watling, L., Deng Palomares, M. L., and Nouvian, C. (2018). Out of sight. but within reach: a global history of bottom-trawled deep-sea fisheries from >400 m depth. *Front. Mar. Sci.* 5:98. doi: 10.3389/fmars.2018.00098

Vieira, R. P., Raposo, I. P., Sobral, P., Gonçalves, J. M. S., Bell, K. L. C., and Cunha, M. R. (2015). Lost fishing gear and litter at Gorringe Bank (NE Atlantic). *J. Sea Res.* 100, 91–98. doi: 10.1016/j.seares.2014.10.005

Wahle, C. M. (1985). Habitat-related patterns of injury and mortality among Jamaican gorgonians. *Bull. Mar. Sci.* 37, 23.

Wood, S. N. (2017). *Generalized Additive Models: An Introduction with R*, 2nd Edn. London: Chapman and Hall.

Wright, G., Ardron, J., Gjerde, K., Currie, D., and Rochette, J. (2015). Advancing marine biodiversity protection through regional fisheries management: a review of bottom fisheries closures in areas beyond national jurisdiction. *Mar. Policy* 61, 134–148. doi: 10.1016/j.marpol.2015.06.030

Conflict of Interest: The authors declare that the research was conducted in the absence of any commercial or financial relationships that could be construed as a potential conflict of interest.

frontiers in Marine Science

ORIGINAL RESEARCH
published: 20 November 2020
doi: 10.3389/fmars.2020.571256

Light Limitation and Depth-Variable Sedimentation Drives Vertical Reef Compression on Turbid Coral Reefs

Kyle M. Morgan[1], Molly A. Moynihan[1,2], Nivedita Sanwlani[1] and Adam D. Switzer[1,3]*

[1] Asian School of the Environment, Nanyang Technological University, Singapore, Singapore, [2] Earth Observatory of Singapore, Interdisciplinary Graduate School, Nanyang Technological University, Singapore, Singapore, [3] Earth Observatory of Singapore, Nanyang Technological University, Singapore, Singapore

Turbid coral reefs experience high suspended sediment loads and low-light conditions that vertically compress the maximum depth of reef growth. Although vertical reef compression is hypothesized to further decrease available coral habitat as environmental conditions on reefs change, its causative processes have not been fully quantified. Here, we present a high-resolution time series of environmental parameters known to influence coral depth distribution (light, turbidity, sedimentation, currents) within reef crest (2–3 m) and reef slope (7 m) habitats on two turbid reefs in Singapore. Light levels on reef crests were low [mean daily light integral (DLI): 13.9 ± 5.6 and 6.4 ± 3.0 mol photons m^{-2} day^{-1} at Kusu and Hantu, respectively], and light differences between reefs were driven by a 2-fold increase in turbidity at Hantu (typically 10–50 mg l^{-1}), despite its similar distance offshore. Light attenuation was rapid (Kd_{PAR}: 0.49–0.57 m^{-1}) resulting in a shallow euphotic depth of <11 m, and daily fluctuations of up to 8 m. Remote sensing indicates a regional west-to-east gradient in light availability and turbidity across southern Singapore attributed to spatial variability in suspended sediment, chlorophyll-*a* and colored dissolved organic matter. Net sediment accumulation rates were ∼5% of gross rates on reefs (9.8–22.9 mg cm^{-2} day^{-1}) due to the resuspension of sediment by tidal currents, which contribute to the ecological stability of reef crest coral communities. Lower current velocities on the reef slope deposit ∼4 kg m^2 more silt annually, and result in high soft-sediment benthic cover. Our findings confirm that vertical reef compression is driven from the bottom-up, as the photic zone contracts and fine silt accumulates at depth, reducing available habitat for coral growth. Assuming no further declines in water quality, future sea level rise could decrease the depth distribution of these turbid reefs by a further 8–12%. This highlights the vulnerability of deeper coral communities on turbid reefs to the combined effects of both local anthropogenic inputs and climate-related impacts.

Keywords: vertical reef compression, light attenuation, turbidity, sedimentation, Anthropocene, Southeast Asia

OPEN ACCESS

Edited by:
Bert W. Hoeksema, Naturalis Biodiversity Center, Netherlands

Reviewed by:
Ross Jones, Australian Institute of Marine Science (AIMS), Australia
Tom Bridge, Museum of Tropical Queensland, Australia

****Correspondence:***
Kyle M. Morgan
kmorgan@ntu.edu.sg

Specialty section:
This article was submitted to Marine Ecosystem Ecology, a section of the journal Frontiers in Marine Science

Received: *10 June 2020*
Accepted: *14 October 2020*
Published: *20 November 2020*

Citation:
Morgan KM, Moynihan MA, Sanwlani N and Switzer AD (2020) Light Limitation and Depth-Variable Sedimentation Drives Vertical Reef Compression on Turbid Coral Reefs. Front. Mar. Sci. 7:571256. doi: 10.3389/fmars.2020.571256

INTRODUCTION

Coral reefs in Southeast (SE) Asia have suffered significant ecological declines (Heery et al., 2018). Widespread reductions in coral cover, species diversity, and reef structural complexity from climate-related disturbances (Guest et al., 2012; Perry and Morgan, 2017; Hughes et al., 2018) are compounded by localized threats to coral reefs, including land-derived siltation and nutrient

loading (Kamp-Nielsen et al., 2002; Baum et al., 2015; Duprey et al., 2020). Declining water quality in the region has been attributed to poorly regulated land-use change, rapid human population growth, and the urbanization of coastal watersheds (Kamp-Nielsen et al., 2002; Syvitski et al., 2005). These anthropogenic stressors can significantly elevate background seawater turbidity and sedimentation, creating low-light conditions, and threaten up to 95% of coastal reefs within SE Asia (Burke et al., 2011). Specifically, the deleterious impacts of elevated turbidity and chronic sedimentation on corals include: (1) reduced coral growth and calcification; (2) smothering of benthic communities and recruitment substrates; and (3) excessive particle loading on coral surfaces (Fabricius, 2005; Erftemeijer et al., 2012; Risk, 2014; Jones et al., 2016; Bainbridge et al., 2018). As a result, coral community compositions on human-impacted reefs have shifted to favor slow-growing and stress-tolerant taxa (Cleary et al., 2016), influencing rates of reef calcification and bioconstruction (Perry and Alvarez-Filip, 2018; Januchowski-Hartley et al., 2020). Localized environmental change is therefore a major present and future issue for SE Asian coral reefs, because the region supports high marine biodiversity (Bellwood and Hughes, 2001) and a very populous coastal zone (Hinrichsen, 2016).

Turbid coral reefs are well-adapted to inhabit areas of naturally high turbidity and low light (e.g., Morgan et al., 2016), and exhibit a tolerance and morphological plasticity to fluctuating abiotic conditions, such as sedimentation, eutrophication, temperature, and light (Anthony et al., 2005; Goodkin et al., 2011; Guest et al., 2012; Morgan et al., 2017). These marginal conditions for coral growth may afford turbid reefs a degree of protection from global climate-related disturbance events (e.g., prolonged ocean warming), as the shading effect of the overlying seawater turbidity can reduce the additive stress of solar irradiance on corals (Morgan et al., 2017; Burt et al., 2020). However, turbid coral reefs remain susceptible to increasing localized inputs from human activities (e.g., seafloor dredging) that may push environmental conditions beyond the threshold for coral growth (Erftemeijer et al., 2012; de Soares, 2020). For example, vertical reef compression, defined here as the shrinking of the total depth range over which photosynthetic corals can grow and reef bioconstruction occurs (e.g., Morgan et al., 2016; Heery et al., 2018), restricts reef-building in turbid waters to between 6–12 m (Goodkin et al., 2011; Heery et al., 2018; Chow et al., 2019). The maximum depth limit of coral growth is primarily dependent on the euphotic depth [i.e., the depth where photosynthetic available radiation (PAR) is 1% of its surface value], below which net photosynthesis occurs. Even minor local increases in suspended sediment load (e.g., 1–10 mg l^{-1}), which may have limited direct physiological impacts on the corals themselves, can disproportionately influence coral distribution by attenuating more light and further shallowing the photic floor on these already light-limited reefs (Jones et al., 2015; Storlazzi et al., 2015; Morgan et al., 2020). While a conceptual understanding of vertical reef compression currently exists, the physical environments of turbid reef settings are not well quantified, and greater knowledge of the cause-effect pathways that limit the depth range of coral reef development is needed.

In Singapore, an island megacity that has experienced intense urban development over the past 50 years, long-term monitoring of offshore coral reefs shows divergent trajectories in reef communities associated with depth. Shallow reef crest habitats (2–3 m depth) exhibit stable coral cover and diversity over time, whereas, deeper reef slope corals (7 m depth) have seriously declined, and a transition to soft-sediment benthic substrates has occurred (Guest et al., 2016). These temporal trends in vertical reef compression have been attributed to increasing suspended sediment in offshore waters and accompanying reductions in light (e.g., Lai et al., 2015), but rarely have these parameters been examined together. Furthermore, turbidity regimes on reefs are not yet quantified, and little attention has been given to the physical properties of the suspended sediment themselves, despite the insights they may provide. Here, we present a high-resolution time series of the physical environment for reef crest and reef slope habitats on two turbid reefs in Singapore, where a 27-year record of benthic cover is available, to establish the causative processes driving vertical reef compression. Our field measurements provide an assessment of light, turbidity, sedimentation and currents over a 30-day period and are accompanied by regional remote sensing analysis of ocean optical properties to address the following questions: (1) what are the processes limiting the depth distribution of corals on turbid reefs? (2) how do the physical environments differ between reefs in Singapore? and (3) how will turbid reefs respond to future anthropogenic and climate-related stressors? Given that coastal reefs in SE Asia play a key role in maintaining biodiversity, and that anthropogenic activities in the region continue to intensify, it is crucial to understand the factors that influence habitat availability within turbid settings.

MATERIALS AND METHODS

Field Setting

This study was conducted on two fringing coral reefs (Pulau Hantu and Kusu Island) located off the southern coast of Singapore, within the Singapore Strait (**Figure 1**). Pulau Hantu (1.226247°N, 103.747049°E) is sheltered by adjacent islands and reefs at the western side of the Southern Islands group in an area of intense industrialization and ship traffic. Kusu Island (1.225354°N, 103.860104°E), on the eastern side of the Southern Islands group, experiences comparatively higher exposure and lower anthropogenic impacts. The reef platforms are relatively comparable in size (16–30 ha), and cross-reef morphology is characterized by a shallow sand flat (∼2–3 m depth), an outer reef crest that supports low-profile sediment-tolerant coral taxa and macroalgae (∼2–3 m depth), and a steep fore-reef slope where coral cover is low and soft-sediment dominates at depth (Hilton and Ming, 1999; **Supplementary Figure 1**). The depth of the surrounding seafloor in southern Singapore is relatively consistent (10–15 m), with no major onshore-offshore increase in water depth. High-velocity tidal flows occur throughout the wider Singapore Strait (Chen et al., 2005), and suspended particulate matter in the water column drives episodically chronic sedimentation on reefs (Low and Chou, 1994; Browne et al.,

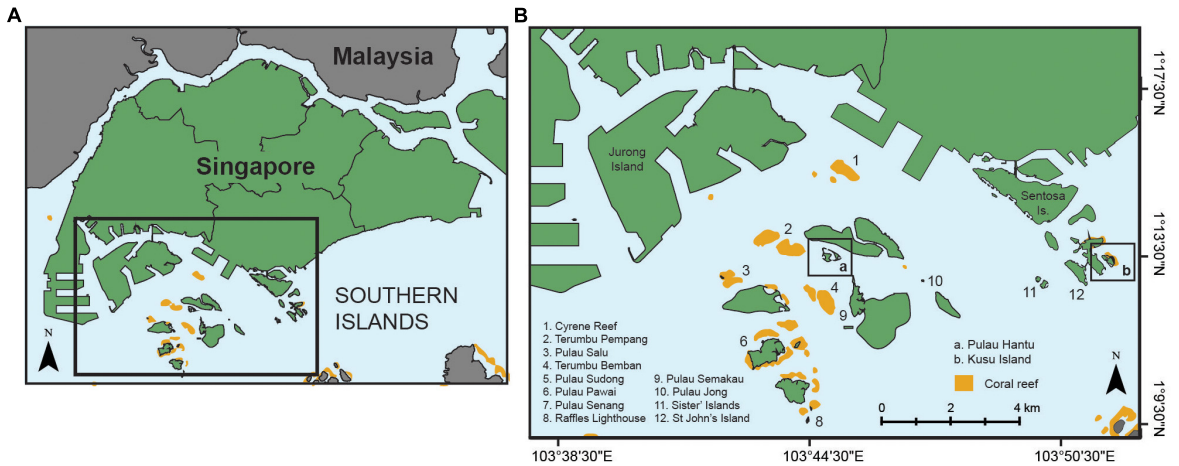

FIGURE 1 | Location of **(A)** Pulau Hantu and **(B)** Kusu Island within the Southern Islands group positioned off the south coast of Singapore Island.

2015). Changes in benthic community structure at Hantu and Kusu reefs over a 27-year time series (see Guest et al., 2016; **Supplementary Figure 2**) suggest that reef crest coral cover at Hantu, following an initial decline in 1997–1998, has remained relatively consistent (24% cover). Coral cover on the reef crest of Kusu demonstrated relatively high cover in 2004–2005 (48% cover). On the reef slope, declines in coral cover to <10% have occurred at both sites alongside a 20% increase in fine sediment cover (Guest et al., 2016).

Environmental Data Collection

Environmental parameters (light, turbidity, temperature, currents) known to influence coral growth were measured over a 30-day field deployment during the southwest monsoon (August 2018) at Kusu and Hantu reefs. Data was collected using instruments deployed within reef crest (2–3 m depth) and reef slope (7 m depth) habitats comparable to those in long-term benthic monitoring assessments (Guest et al., 2016). Irradiance (PAR) was recorded at each fixed depth every 10 min using pre-calibrated Odyssey® submersible light recorders (Shaffer and Beaulieu, 2012). Instantaneous light measurements (μmol photons m^{-2} s^{-1}) were recorded during daylight hours (700–1900 h) and used to calculate a DLI (mol photons m^{-2} day^{-1}) by summing the 12 h of continuous light at instantaneous levels (per second quantum flux measurements) for every second across the daylight period. For example, instantaneous measurements were multiplied by 600, as there are 600 s in every 10 min sampling period (Jones et al., 2015). Near-bed turbidity (i.e., the degree to which water loses its transparency due to the presence of suspended particulates) was also recorded every 10 min (30 s bursts at 12 Hz) using a horizontal-mounted optical backscatter nephelometer (AQUA*logger*® 310TY) with in-build pressure sensor deployed 0.3 m from the bed on the reef crest. Values were recorded as Formazin Turbidity Units (FTU) and then converted to suspended sediment concentration (SSC as mg l^{-1}). The conversion factor between FTU and SSC was calculated using the SSC Converter within AQUA*talk* software using a linear relationship (R^2 = 0.67) derived from the gravimetric analysis of 26 field water samples filtered through pre-weighed Whatman GF/F filter papers (SSC = FTU × 2). Optical sensors (PAR and turbidity) were cleaned weekly during the deployment period to remove biofouling. However, to ensure data quality, only data recorded 3 days after cleaning at Hantu (12 days total) and 4 days after cleaning at Kusu (16 days total) were used for analysis. Reef currents were measured using tilt-current meters (TCM-1: Lowell Instruments) deployed at each site to record current speed (cm s^{-1}), direction (bearing) and water temperature every 10 min (30 s bursts at 4 Hz).

Time-Series (Running Means Percentile) Analysis

Raw light, turbidity and current time-series data were plotted and all erroneous data values were removed. Mean values for the depth zones across the 30-day period at Kusu and Hantu were calculated and tested for statistical significance using t-tests. However, because environmental conditions on reefs are highly variable, long-term averages may not sufficiently capture short periods of environmental extremes (Jones et al., 2015). To examine the range of likely environmental conditions across the time-scales from hours to weeks, a running means percentile approach was applied to the time-series data to create percentile plots (Jones et al., 2015). We calculated the running means for each environmental parameter over different time periods (30 min, 1 h, 6 h, 12 h, 1-12/16 days, for turbidity and current data; 1-12/16 days for DLI data) and then summarized the results as an average with associated percentile values (100th, 99th, 95th, and 80th for turbidity and current data; 50th, 20th, and 5th for DLI data).

Reef Sedimentation and Grain Properties

Gross and net sediment accumulation rates were measured within the depth zones at both reefs. To measure gross sediment accumulation (i.e., the downward flux of particles suspended within the water column), three cylindrical tube traps (7 cm

diameter × 30 cm length) were attached to a stake 0.3 m off the seabed. Net accumulation was measured using SedPods (Field et al., 2013), a flat cylindrical concrete unit (15 cm height × 15 cm diameter) that replicates a coral/reef surface and allows for resuspension of particles by tidal currents (**Supplementary Figure 1**). Following the 30-day deployment, all traps were capped and retrieved, washed with deionised water to remove salts, dried and weighed to determine sediment mass. Sediment accumulation rates (mg cm^{-2} day^{-1}) were calculated by dividing the total amount of dry sediment retained over the deployment period (mg day^{-1}) by the trap surface area (cm^{-2}). To establish physical comparisons between trap material and sediments deposited on corals, sediment was collected directly from the surface of five massive (*Dipsastraea* sp.) and five foliose corals (*Pachyseris* sp.) on the reef slope of Hantu (4–7 m depth) using Pasteur pipettes. Benthic seafloor sediment samples (∼100 g) were also collected for comparison at both sites.

The grain size properties of tube trap, SedPod and coral surface sediments (<1 mm) were measured using laser diffraction analysis (Malvern Mastersizer 3000). Benthic samples, which comprised both fine (<1 mm) and coarse (>1 mm) material, were first dry sieved at 0.5 phi intervals, weighed and the proportion of material relative to the total sediment mass was calculated. The separated fine fraction (<63 μm) was analyzed using laser diffraction and the data were combined with the results from sieve analysis to estimate bulk sediment grain statistics using GRADISTAT (Blott and Pye, 2001; Morgan and Kench, 2016). The relative proportions of non-reef derived particles (i.e., clastic), total organic carbon (TOC) and total inorganic carbon (TIC) in the bulk sediment mass were estimated using the loss-on-ignition (LOI) method (Heiri et al., 2001).

Sediment Deposition and Resuspension Potential

To estimate sediment deposition potential on reefs, the hydrodynamic properties of suspended sediment particles were first established by converting the grain size data to an equivalent settling velocity (*ws*) using the equations of Gibbs et al. (1971). Sediment deposition potential was then modeled by dividing the average settling velocity of tube trap particles by the current velocities (*cv*) recorded by TCM-1 current meters every 10 min. The percent of time where current velocities fell below the threshold required to keep particles in suspension was then calculated ($ws/cv \geq 1.25$; Cheng and Chiew, 1999). Resuspension rates were calculated as the difference in sediment accumulation rate (mg cm^{-2} day^{-1}) between gross (tube traps) and net sediment accumulation (SedPods). Based on comparisons of the grain size distributions between trap methods deployed at the same location, we estimate the size classes of resuspended sediment by their relative absence on SedPods when compared to tube traps.

Light Diffuse Attenuation Coefficient (Kd_{PAR}) and Euphotic Depth (Zd)

The diffuse attenuation coefficient of PAR (Kd_{PAR}) was calculated using daily (at 1200 h) field irradiance data collected from fixed PAR loggers at reef crest (2–3 m depth) and reef slope sites (7 m depth) (Eq. 1), which were depth-adjusted for daily changes in water level (tidal range: 3.35 m).

$$\mathrm{KdPAR\,(z)} = -\frac{\ln\left(\mathrm{PAR\left(z+dz\right)}\right) - \ln\left(\mathrm{PAR\,(z)}\right)}{\mathrm{dz}} \quad (1)$$

The euphotic depth (Zd) is defined as the depth at which 1% of the surface irradiance remains (Saulquin et al., 2013; Macdonald, 2015), and was calculated as in Eq. 2.

$$\mathrm{PAR\,(Z)} = \mathrm{PAR}\ \left(0^{-}\right) \times \exp[-\mathrm{Kd\,(PAR)} \times \mathrm{Z}] \quad (2)$$

Remote Sensing Analysis

To examine the spatial distribution of ocean optical properties in southern Singapore, the Level-2 (L2) products of Sentinel-3 Ocean and Land Color Instrument with a 300 m spatial resolution were used. We extracted the following bio-optical constituents from the L2 suite based on the neural network atmospheric correction (Doerffer and Schiller, 2007; Brockmann et al., 2016): (1) algal pigment concentration (chlorophyll-*a* in mg m^{-3}), (2) total suspended matter concentrations (TSM in mg l^{-1}), (3) diffuse attenuation coefficient (Kd_{490} in m^{-1}), (4) water-inherent optical properties of colored dissolved organic matter (CDOM) absorption (adg at 443 nm in m^{-1}), (5) PAR (μmol quanta m^{-2} s^{-1}), and (6) euphotic depth (m) derived from Kd_{490}. These parameters were displayed as either actual concentrations of optically active substances, or as their inherent optical properties (IOP). The main neural network derived water-leaving reflectance after atmospheric correction. Subsequently, the IOP module retrieved the absorption and scattering coefficients from the water-leaving reflectance and the concentrations of optically active constituents.

RESULTS

Environmental Conditions on Reefs

Temperature was consistent (mean: 29.5°C) between reefs, as well as with depth between habitats ($p > 0.05$, *t*-test). Mean turbidity (SSC) across the 30-day deployment period was significantly higher at Hantu (42 ± 40 mg l^{-1}) than Kusu (16 ± 19 mg l^{-1}) ($p < 0.05$, *t*-test), with Hantu experiencing a wider range of turbidity values (Hantu: 0.4–230 mg l^{-1}; Kusu: 0.06–118 mg l^{-1}) (**Figure 2A**). The time-series data show a substantial peak in SSC (August 17–19) at both sites midway during the study (**Figure 3A**). Running means analysis across multiple time frames (from minutes to weeks) was used to characterize temporal trends across the time-series data. These show that upper percentiles values of SSC (100th, 99th, and 95th) at both sites, which represent periodic pulses in turbidity on reefs, decline with increasing temporal scale (**Figure 3A** and **Supplementary Table 1**). A faster decline in these values was observed at Kusu, indicating lower background SSC once short-term turbidity peaks were smoothed. In comparison, the 80th and 50th (median) percentiles were relatively consistent at both reefs and were substantially lower at Kusu compared to Hantu. Mean turbidity values

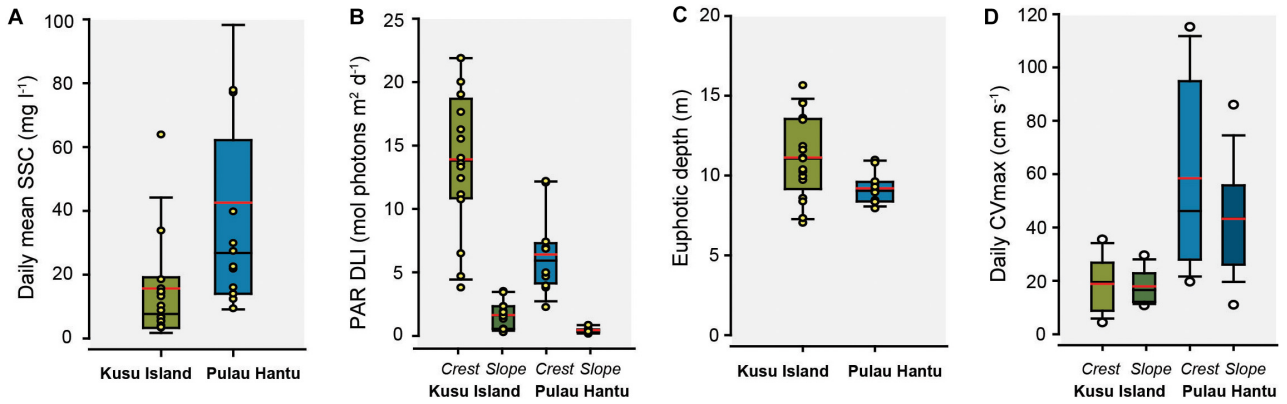

FIGURE 2 | Boxplots of **(A)** daily mean suspended sediment concentration (SSC: mg l^{-1}), **(B)** PAR daily light integral (DLI: mol photons m^{-2} day^{-1}), **(C)** euphotic depth (Zd: m), and **(D)** daily maximum current velocity (CV_{max}: cm s^{-1}) at reef crest and reef slope sites on Kusu Island (green) and Pulau Hantu (blue). Red lines show mean values. Circles represent the daily values recorded of each parameter.

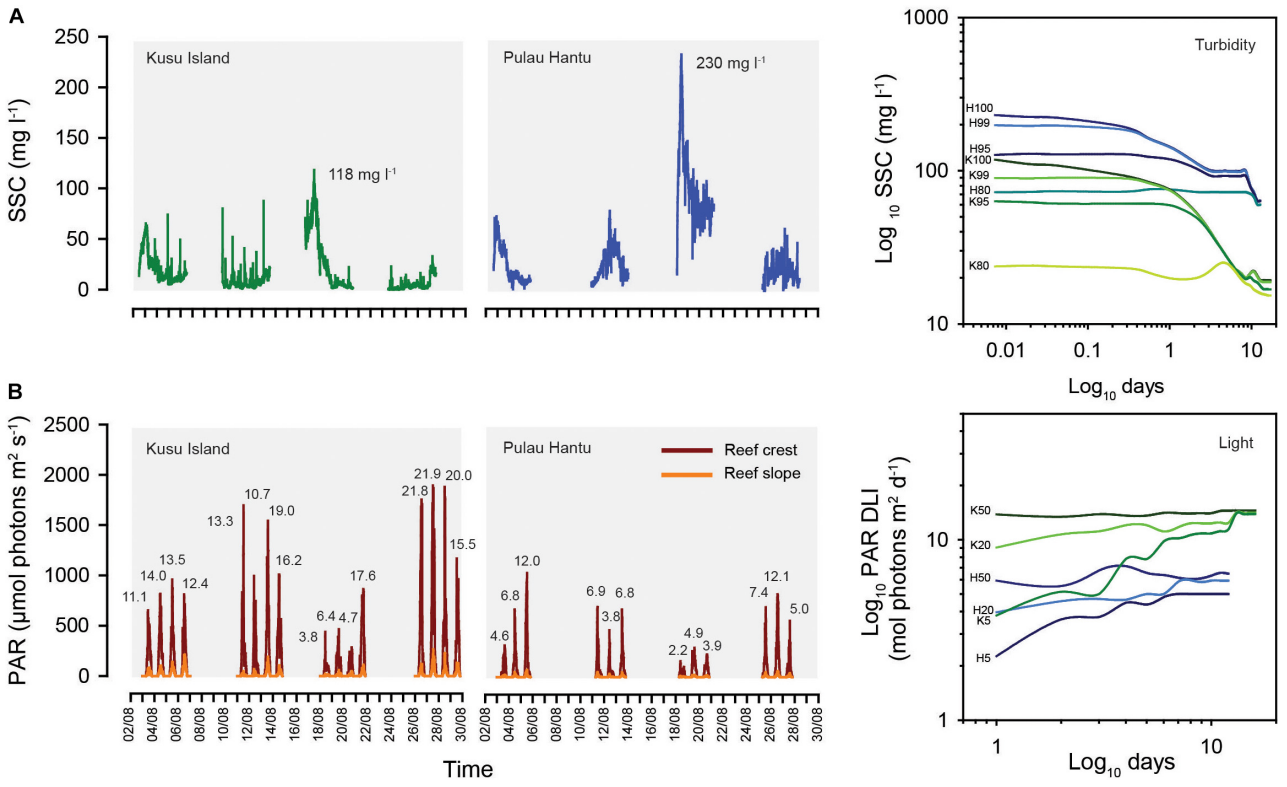

FIGURE 3 | Time-series data over the 30-day deployment for **(A)** suspended sediment concentration (SSC; mg l^{-1}) and **(B)** instantaneous PAR measurements (µmol photons m^{-2} s^{-1}) at Kusu Island (K/green) and Pulau Hantu (H/blue). Daily light integrals (DLI: mol photons m^{-2} day^{-1}) for reef crest sites are shown above each light profile. Panels on the right show percentile plots of the running means percentile analysis for suspended sediment concentration and light at both reefs. The 100th (maximum), 99th and 95th and 80th percentiles (for turbidity) and 50th, 20th, 5th (for light) of the running means are displayed.

derived from running means across the full range of time-scales were 2-fold lower at Kusu (11.5–15.6 mg l^{-1}) than at Hantu (40–42.5 mg l^{-1}). Collectively, running means percentile analysis shows pronounced separation in turbidity regimes between the reefs.

Both reefs experienced 12 h of daylight (0700–1900 h). The daily maximum irradiance (instantaneous PAR) on the reef crest peaked at approximately solar noon, reaching 1024 and 2196 µmol photons m^{-2} s^{-1} at Hantu and Kusu, respectively (**Figure 3B**). Mean daily maximum irradiance exhibited high

variability across the deployment period, and was significantly higher at Kusu (1052 ± 591 μmol photons m^{-2} s^{-1}) than at Hantu (542 ± 265 μmol photons m^{-2} s^{-1}) ($p < 0.05$, *t*-test). This translated into substantially higher mean DLI values at the reef crest of Kusu (13.9 ± 5.6 mol photons m^{-2} day^{-1}) compared to Hantu (6.4 ± 3.0 mol photons m^{-2} day^{-1}) (**Figure 2B**). Within reefs, both reef slope sites recorded low mean daily maximum instantaneous PAR (Kusu: 113 ± 72 μmol photons m^{-2} s^{-1}; Hantu: 37 ± 18 μmol photons m^{-2} s^{-1}) and low mean DLI values (Kusu: 1.6 ± 1.0 μmol m^{-2} s^{-1}; Hantu: 0.44 ± 0.2 μmol m^{-2} s^{-1}). Over the deployment period, reef slope sites experienced very low-light conditions (≤0.8 DLI) on 5 of the 16 days at Kusu and 11 of the 12 days at Hantu. These values corresponded with periodic increases in SSC (>50 mg l^{-1}), which also reduced reef crest DLI values (**Figure 3B**). Running means analysis (days to weeks) of DLI values show that the 50th percentile (median) is relatively consistent over varying temporal resolutions (**Figure 3B** and **Supplementary Table 2**). Whereas the 20th and 5th percentile present an upward trend in agreement with the upper percentile turbidity values at these same sites. There are clear differences in light conditions between reefs, with Kusu characterized by higher light levels and less temporal variability.

Daily Kd_{PAR} (taken at 1200 h) shows rapid light attenuation across the deployment period with average Kd_{PAR} values ranging between 0.49 ± 0.13 m^{-1} and 0.57 ± 0.10 m^{-1} at Kusu and Hantu, respectively. We also observed daily shifts in the euphotic depth (**Figure 4**). There were differences in the amount of light attenuation variability between sites, where light penetration on Hantu fluctuated within a substantially narrower envelope than at Kusu. When PAR is reduced to 1% of the surface irradiance (Zd), the euphotic depth ranged between 7.0 and 15.6 m depth (mean: 11.1 ± 2.5 m) at Kusu, and 7.94 and 10.99 m (mean: 9.2 ± 0.9 m) at Hantu (**Figures 2C**, **4**).

Maximum daily current velocities (daily CV_{max}) at Hantu were higher than those recorded at Kusu, at both the reef crest and reef slope (**Figure 2D**). Maximum current conditions have a greater influence on reef sediment dynamics than "normal" (mean) conditions. At Hantu, daily CV_{max} on the reef crest reached a peak velocity of 119 cm^{-1} s^{-1} following low tide, and recorded crest velocities were more variable than those on the reef slope (reef crest: 17.6–119 cm^{-1} s^{-1}; reef slope: 6–91 cm^{-1} s^{-1}) (**Figure 2D**). However, averaged daily CV_{max} at Hantu were similar between the crest (58 ± 34 cm^{-1} s^{-1}) and slope (43 ± 20 cm^{-1} s^{-1}). In comparison, daily CV_{max} at Kusu varied over a smaller range (reef crest: 10–30.5 cm^{-1} s^{-1}; reef slope: 3.5–35 cm^{-1} s^{-1}) and did not align to individual tidal phases, but was higher during periods of increased tidal range (**Figure 5A**). Averaged daily CV_{max} velocities at Kusu were the same between the crest and slope (18 cm^{-1} s^{-1}). Running means percentile analysis (100th, 99th, and 95th) show declines in current velocity with increasing temporal resolution, and higher current velocities at Hantu compared to Kusu (**Figure 5** and **Supplementary Table 3**). Within reefs, upper percentiles exhibited separation in current velocities between depth zones, particularly at Kusu, where velocities were higher at the reef crest than on the reef slope. At Hantu, the separation between depth zones is not as clear, because although reef crest sites generally experience higher velocities over finer time-scales, they become similar when coarser running average time-scales are applied (**Figure 5B**).

Sediment Accumulation Rates and Grain Properties

Gross sediment accumulation rates were high at all sites (≥9.8 mg cm^{-2} day^{-1}) and significantly greater than net sediment accumulation rates ($p < 0.05$, *t*-test; **Figures 6A,B**). Highest gross sediment accumulation was recorded at Kusu. At both reefs, gross sediment accumulation was higher on the reef slope (Kusu: 22.9 ± 0.3 mg cm^{-2} day^{-1}; Hantu: 17.1 ± 0.8 mg cm^{-2} day^{-1}) than the reef crest (Kusu: 18.2 ± 4.2 mg cm^{-2} day^{-1}; Hantu: 9.8 ± 0.9 mg cm^{-2} day^{-1}). Net sediment accumulation rates showed similar spatial trends between reefs and depth zones, but were ∼5% of gross sediment accumulation for the same location (0.1–1.2 mg cm^{-2} day^{-1}; **Figure 6B**).

Grain size analysis showed that tube trap and SedPods sediment was dominated by silt-sized particles (<63 μm; tube traps: 86–96%; SedPods: 80–83%), with mean grain sizes of between 6.2–8.8 μm (average: 8.17 ± 1.2 μm) and 9.51–15.5 μm (average: 13.2 ± 2.5 μm), respectively (**Supplementary Table 4**). Grain size distributions differed between trapping methods (**Figure 6C**). Tube traps sediments were unimodal with a dominant peak at 7 μm (fine silt), whereas SedPods were typically bimodal, exhibiting a lower peak at 7 μm (fine silt) and a secondary peak at 250 μm (fine sand). Sediments were primarily non-reef derived particles (tube traps: 80–84%; SedPods: 77–79%), with a relatively high TOC content (tube traps: 13–15%; SedPods: 13%), and a small proportion of TIC (i.e., reef-derived carbonate) (tube traps: 2–6%; SedPods: 7–9%). Coral surface sediment showed close similarities in mean grain sizes between replicate corals within the same genera (**Figure 6D**), but grain sizes were distinct between foliose *Pachyseris* sp. (10.78 μm) and massive *Dipsastraea* sp. (28.3 μm). Interestingly, foliose *Pachyseris* sp. had a very similar grain size distribution to tube trap sediments, which were dominated by fine silt particles, whereas massive *Dipsastraea* sp. had a coarser silt-to-sand grain size distribution that aligned closely with sediments deposited on SedPods (**Figure 6**).

In contrast, reef crest benthic sediments were dominated by allochthonous gravels (>1000 μm; coral, molluscan and octocoral grains) and fine-to-coarse (125–750 μm) sand (**Figure 6C**). Mean grain sizes of benthic sediment differed between reefs and depth zones (**Supplementary Table 4**). Benthic reef crest sediments were coarser at Kusu compared to Hantu (1093 and 524 μm, respectively), and reef crest sediments at both reefs were coarser than those on the reef slope (314 and 183 μm, respectively). Differences in mean grain size between depth zones were driven by the relative absence in silt particles on the reef crests, which only accounted for 1–7% of the total sediment, compared to the reef slope sediment, which comprised 29% (Kusu) and 48% (Hantu) of the total benthic sediment (**Supplementary Table 4**).

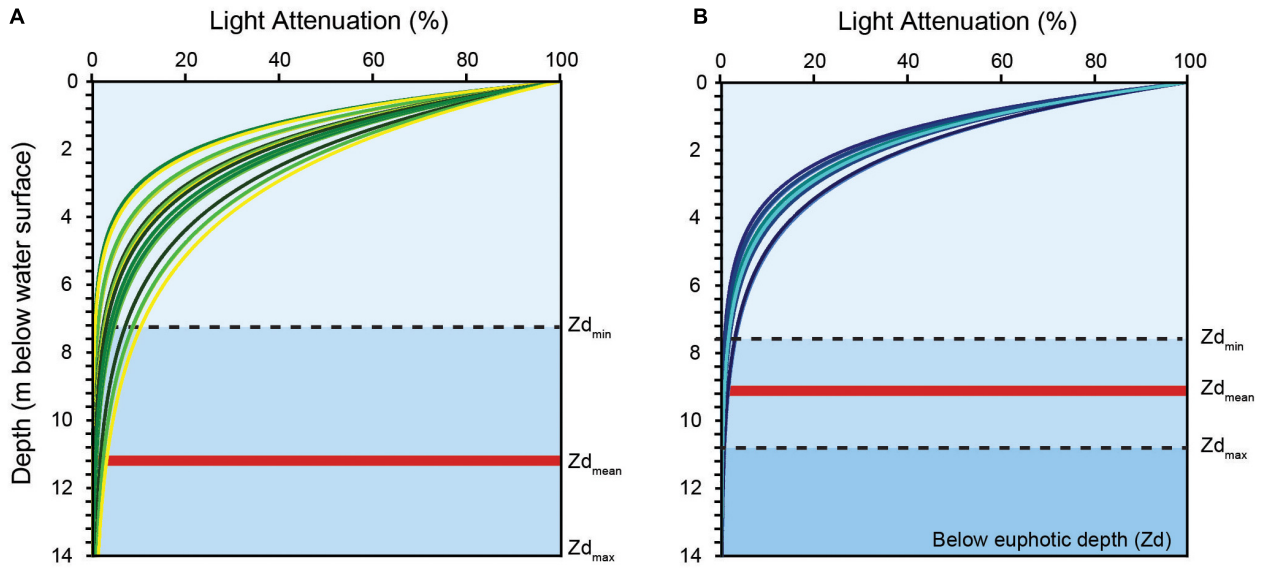

FIGURE 4 | Light attenuation (%) with depth (m) at **(A)** Kusu Island (green) and **(B)** Pulau Hantu (blue). Kd_{PAR} values were derived from daily (at 1200 h) field measurements of Photosynthetic Active Radiation (PAR). Minimum, maximum and average euphotic depths (Zd) as 1% of surface PAR are shown.

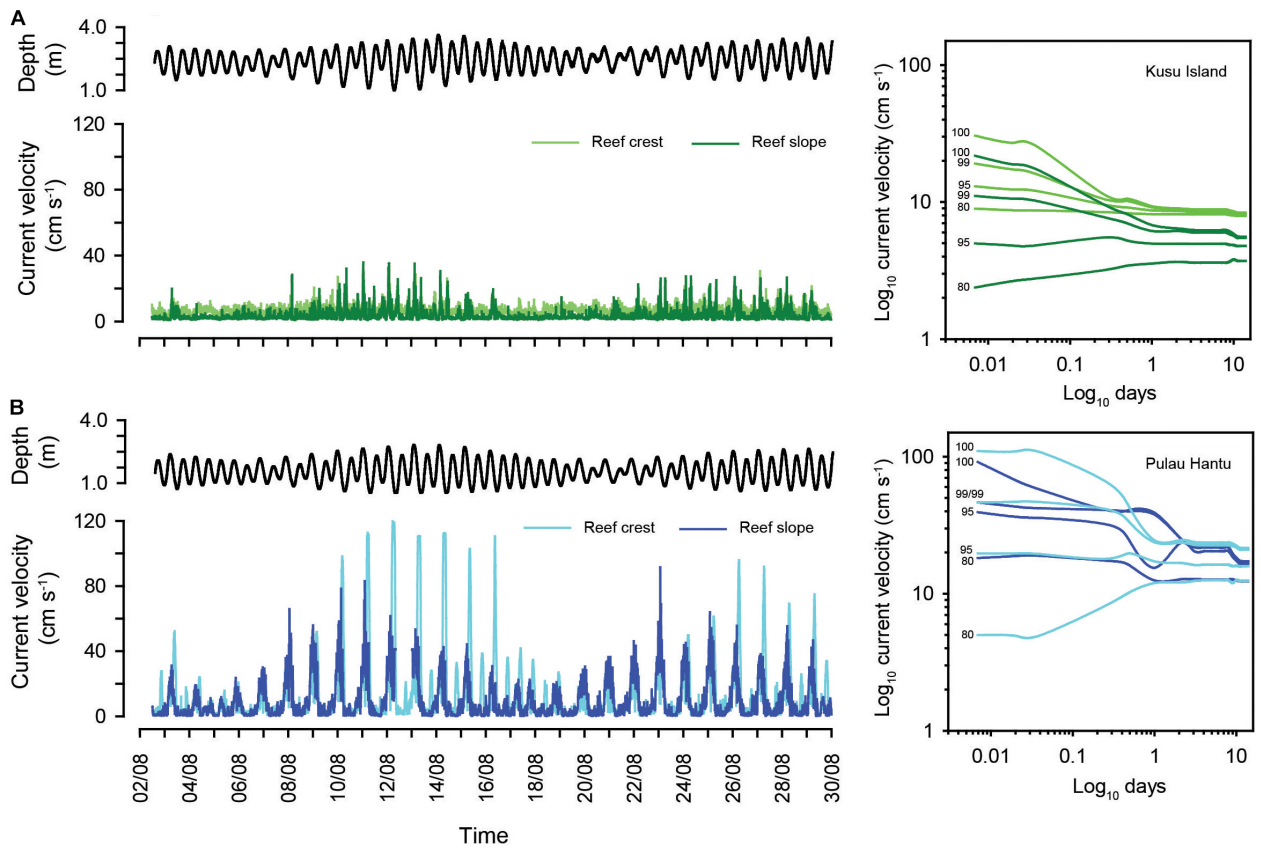

FIGURE 5 | Time series of current velocities (cm s^{-1}) for reef crest and reef slope sites at **(A)** Kusu Island (green) and **(B)** Pulau Hantu (blue). Water depth (m) across the 30-day deployment is shown for each site (black). Panels on the right show percentile plots of the running means percentile analysis for each depth zone. The 100th (maximum), 99th and 95th and 80th percentiles of the running means are displayed.

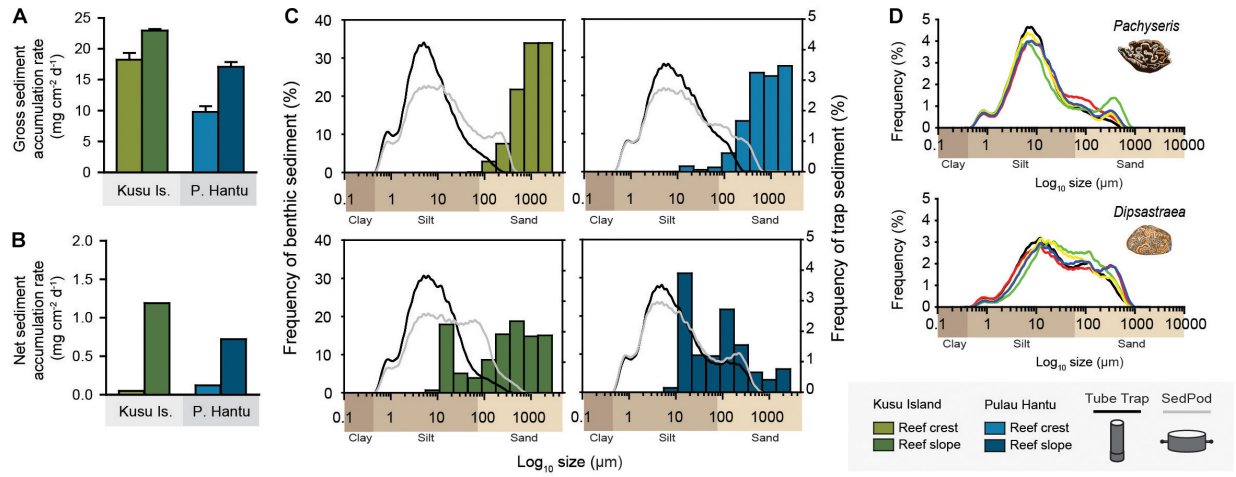

FIGURE 6 | (A,B) Gross and net sediment accumulation rates (mg cm^{-2} day^{-1}) derived from traps deployed within reef crest (2–3 m depth) and reef slope habitats (7 m depth) at Kusu Island (green) and Pulau Hantu (blue) reefs over a 30-day period (August 2018). **(C)** Log of particle size distribution (%) of sediments (µm) collected in tube traps (black line), SedPods (gray line) and benthic sediments (bars). **(D)** Log of particle size distribution (%) of coral surface sediment of foliose *Pachyseris* sp. and massive *Dipsastraea* sp. corals.

Reef Sediment Dynamics

Silt particles within reef crest and reef slope benthic sediments were larger in size (medium to coarse silt) than those collected in/on traps (very fine to fine silt; **Figure 6C**). Resuspension rates were higher at the reef crest (Kusu: 21.7 mg day^{-1}; Hantu: 18.1 mg day^{-1}) than the reef slope (Kusu: 16.3 mg day^{-1}; Hantu: 9.6 mg day^{-1}), matching differences in maximum current velocities (CV_{max}) between these sites. A wider grain size range was resuspended at reef crest sites (up to 22.4 and 39.9 µm at Kusu and Hantu, respectively), whereas on the reef slope, particle size ranges were restricted to finer particles (up to 12.6 and 14.2 µm at Kusu and Hantu reefs, respectively). Importantly, maximum CV_{max} was observed only 0.2–5.4% of the total time during the 30-day deployment period for both crest and slope environments (**Supplementary Table 5**).

Spatial Distribution of Light and Turbidity Across Southern Singapore

Monthly averaged (August 2018) seawater optical properties across southern Singapore are consistent with field measurements at Kusu and Hantu. Spatial maps of Kd_{490}, a proxy for turbidity, show high light attenuation (~0.5 m^{-1}) and a shallow euphotic depth (Zd) of <7 m across southern Singapore (**Figure 7**). Spatial patterns in PAR align with Kd_{490}, as higher PAR was observed in waters surrounding Kusu (~1500 µmol quanta m^{-2} s^{-1}) than Hantu (~800 µmol quanta m^{-2} s^{-1}). Overall, remote sensing analysis demonstrates that Hantu received lower light intensity and had a shallower euphotic depth compared to Kusu because of the higher rate of light attenuation. Remote sensing analysis across the wider Singapore region indicated that spatial differences in Kd_{490} and PAR corresponded with higher concentrations of total suspended matter (TSM) surrounding Hantu and its nearby reefs (as evident in **Figure 7**) and that TSM declines eastward towards Kusu. Turbidity is therefore modulated in part by chlorophyll-*a* and CDOM, which exhibit similar spatial patterns to TSM. However, chlorophyll-*a* concentrations are relatively low compared to CDOM, and thus, light attenuation is controlled by a combination of CDOM and suspended sediment, particularly at western locations during this time period.

DISCUSSION

We provide a high-resolution times series of light and turbidity for Singapore's coral reefs, and present a process-based interpretation of the factors contributing to vertical reef compression on turbid reefs using additional physical parameters. We show that rapid light attenuation through seawater, as a function of high turbidity (10–50 mg l^{-1}), is a critical control restricting the maximum depth of coral growth and bioconstruction. Light conditions on Singapore's reefs were low and had high temporal variability over the 30-day deployment period in the absence of seasonality. Reductions in instantaneous PAR and DLI aligned with periods of increased turbidity (lasting 1–3 days) that reached up to 118 and 230 mg l^{-1} at Kusu and Hantu, respectively. Deeper reef slope sites experienced very low light or "twilight" conditions (≤0.8 DLI) (Jones et al., 2015) on 31% of days at Kusu and 91% of days at Hantu. These data highlight the marginal, and fluctuating, conditions on turbid reefs that are distinct from clear-water reefs (Burt et al., 2020), as well as the complexities of establishing relevant baseline environmental data to characterize these systems. Light levels were consistent with other turbid reef environments, where data is available (Macdonald, 2015; Morgan et al., 2017; Chow et al., 2019; Loiola et al., 2019), but we found substantial differences in irradiance levels between reefs of close proximity (~12 km) and a similar distance offshore (~5 km). These differences can be attributed to higher

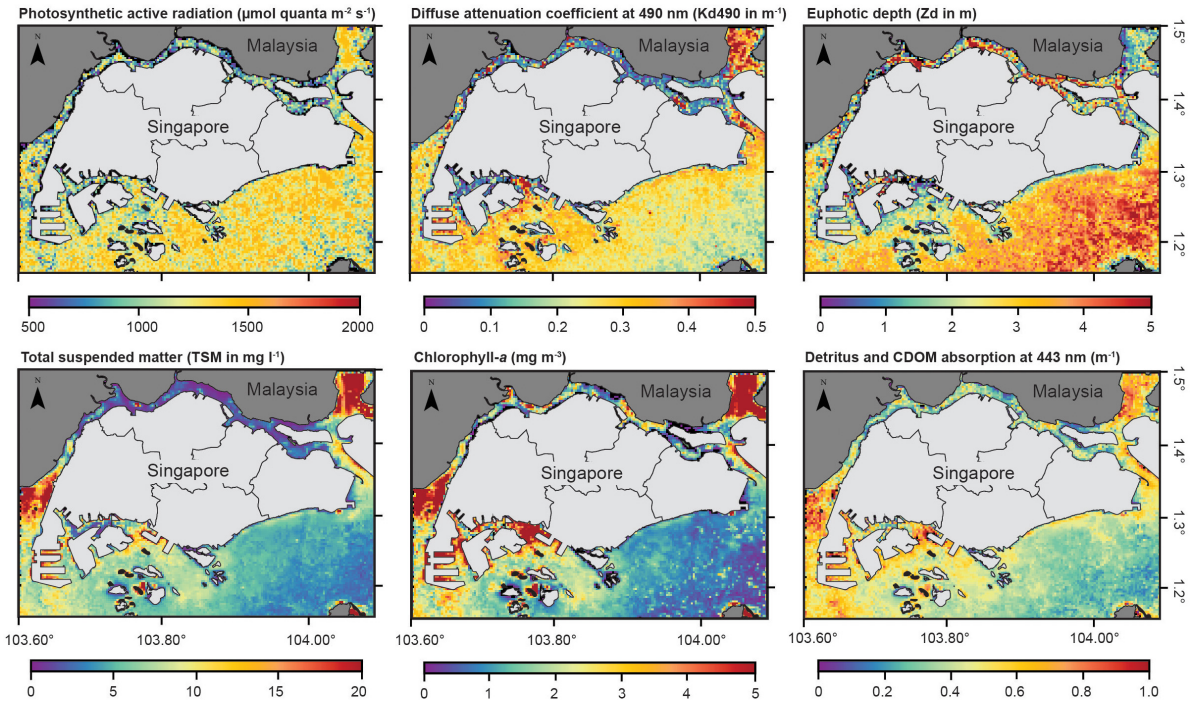

FIGURE 7 | Monthly (August 2018) averaged satellite-derived (Sentinel-3) maps of seawater optical properties across southern Singapore. Maps show spatial patterns in light: photosynthetic active radiation (PAR in µmol quanta m^{-2} s^{-1}), light attenuation coefficient (Kd_{490} in m^{-1}), euphotic depth (m); and the constituents of seawater turbidity: chlorophyll-*a* (mg m^{-3}), total suspended matter concentration (TSM in mg l^{-1}), colored dissolved organic matter (CDOM) absorption at 443 nm (m^{-1}).

background seawater turbidity at Hantu compared to Kusu, and to a lesser degree, may reflect differences in reef elevation. Spatial patterns in turbidity and light regimes contrast more well-established inshore-offshore water quality gradients that occur over larger spatial scales (e.g., Great Barrier Reef, Fabricius et al., 2016; Jakarta Bay, Cleary et al., 2016), and may give insight into the source of turbidity on reefs in Singapore.

Monthly-averaged remote sensing analysis supports a regional west-to-east gradient in ocean optical properties within southern Singapore (**Figure 7**), consistent with field measurements. Although this data provides a coarser measure of light and turbidity on reefs, it allows for interpretations to be made over greater spatial scales. Western islands that experience stronger tidal flows, caused by the funneling of water through adjacent reef structures (e.g., Pulau Hantu, Semakau and Terumbu Pempang), exhibited higher turbidity and lower light (Chen et al., 2005). In contrast, more exposed eastern reefs (e.g., Kusu, Sister's and St John's Islands) were subject to lower turbidity and higher light conditions. As different suspended particles can have varying effects on light attenuation (Storlazzi et al., 2015), and for coral health (Fabricius et al., 2003; Weber et al., 2006; Bainbridge et al., 2012; Duckworth et al., 2017), it is critical to characterize the water column components that limit light on reefs. Both optical analysis and field data showed that siliciclastic sediment particles are the main component of seawater turbidity. However, the spatial distribution of TSM also coincides with elevated concentrations of chlorophyll-*a* and CDOM, indicating that although recent coastal development in Singapore (e.g., land reclamation, seafloor dredging) may have contributed to vertical reef compression by increasing suspended sediment (Low and Chou, 1994; Erftemeijer et al., 2012), total light attenuation on reefs is also driven by other background constituents which operate over greater spatial scales. For example, satellite remote sensing has demonstrated that high CDOM around Sumatra reaches the Malacca Straits (Siegel et al., 2018), and influences the Singapore Straits waters (Liew and Kwoh, 2003). The relatively low chlorophyll-*a* concentration around Singapore (**Figure 7**) confirms that light attenuation was dominated by a combination of CDOM absorption, probably from terrestrial sources, and sediment scattering that both likely vary with monsoon seasonality.

Light attenuation curves demonstrated that downwelling irradiance was rapid at both sites (Kd_{PAR}: 0.49–0.57 m^{-1}), but also highly responsive to localized conditions on reefs (**Figure 4**). The values of Kd_{PAR} we observed on Singapore's reefs far exceeded global values from a wide geographic range of clear-water reef settings (0.045–0.071 m^{-1}; see Laverick et al., 2020), as well as those from other turbid reef environments (0.08–0.11 m^{-1} at the Abrolhos complex, Brazil; Freitas et al., 2019). These values were primarily attributed to high suspended sediment in the water, which was compounded by the dominance of dark-colored siliciclastic particles that absorb light more effectively than lighter (in color) carbonate sediments (Storlazzi et al., 2015). As a result, the euphotic depth (Zd) on Singapore's

reefs is very shallow, but migrates daily as much as 3–8 m (±11% average change). The depth distribution of coral species on Singapore's reefs are well documented and show declining live coral, species richness and diversity over a short vertical range, with a maximum depth of 10 m (Chow et al., 2019). Long-term survey data also suggest low and declining coral cover at the photic floor (Guest et al., 2016). These data are consistent with our own observations of reef slope communities (∼5 m at Hantu and ∼7 m at Kusu), which align with the minimum euphotic depth (Zd_{min}) rather than the maximum values (Zd_{max}) we recorded (**Figure 4**). Below Zd_{min}, hard coral assemblages transition to non-phototrophic sponge and gorgonian communities with limited reef-building potential (**Supplementary Figure 1**). For comparison, a recent global analysis showed that transitions to mesophotic coral ecosystems typically occurred between 36.1 ± 5.6 m (shallow-upper mesophotic) and 61.9 ± 9.6 m (upper-lower mesophotic) (Laverick et al., 2020). Our time series of light analysis provides additional support for the classification of turbid reefs as "shallow-water mesophotic reefs" (*sensu* Morgan et al., 2016), because despite their shallow depth (<10 m) these reefs share key characteristics in both light conditions and ecological communities, where light limitation is the major driver structuring benthic assemblages.

Light effects on benthic communities are compounded by depth-related differences in sedimentation rates (**Figure 6**). Our combined datasets suggest vertical reef compression in turbid settings is also a consequence of sediment dynamics. High velocity tidal currents winnow fine particles from the reef crest, defined here as "tidal sweeping", and greater silt deposition occurs on reef slopes. This process is also likely an important driver of localized turbidity at the reef-scale that often differs from off-reef conditions. Given the high background suspended sediment concentrations, tidal sweeping helps maintain the ecological stability of shallow-water corals (2–3 m) in Singapore, as strong diurnal tidal flows keep fine sediments in suspension (Maxwell, 1968; Cacciapaglia and van Woesik, 2015). Evidence of this winnowing effect on Singapore's reefs include: (1) higher measured resuspension rates and current velocities on the reef crest, (2) relatively low silt in reef crest benthic sediment (< 7%) and a high relative abundance of silt on the reef slope (29–48%), typical of a depositional fore-reef slope setting (e.g., Morgan and Kench, 2014), (3) a coarser silt mean grain size in benthic and SedPod sediment within the reef crest, and (4) a 20% increase in soft sediment benthic cover on reef slopes (Guest et al., 2016). We also found large differences between net and gross sedimentation rates on reefs (**Figure 6**), and emphasize that net sedimentation derived from SedPods (Field et al., 2013) provide a more realistic estimate of sediment deposition and retention. Here, net sedimentation values from SedPods were ∼5% of gross rates derived from tube traps, and deposit an additional 4 kg m^2 of silt-sized sediment to reef slopes annually. If gross sedimentation rates at Kusu were applied, this would equate to an overestimation of 66 kg m^{-2} $year^{-1}$ (66.4 kg m^{-2} $year^{-1}$ versus 0.36 kg m^{-2} $year^{-1}$) on the reef crest and 80 kg m^{-2} $year^{-1}$ on the slope (83.5 kg m^{-2} $year^{-1}$ versus 4.38 kg m^{-2} $year^{-1}$).

Our data suggests that vertical reef compression is being driven from the bottom-up, as the photic zone contracts and fine silts accumulate at depth (**Figure 8**), reducing both habitat availability and coral diversity (e.g., Morgan et al., 2020). Sediment deposited on reef slope corals had distinct size distributions, which replicated those exhibited by gross and net sedimentation trapping methods (**Figure 6**). Morphology-specific grain size ranges were likely a result of colony-level differences in water flow (Hench and Rosman, 2013; Duckworth et al., 2017), whereby foliose taxa (*Pachyseris* sp.) trap fine silt particles and massive growth forms (*Dipsastraea* sp.) trap silt and fine sand. Smothering of corals by sediment has been shown to preferentially occur on encrusting and foliose (but not branching) growth forms under periods of chronic sedimentation (Jones et al., 2020). Singapore's coral communities are dominated by encrusting, massive and foliose forms, whereas branching species (e.g., *Acropora* spp.) are largely devoid on reefs. This may make reef slope coral communities more vulnerable to sedimentation effects, as corals shift to flatter horizontal morphologies with depth to increase light capture. Although certain colony-level mechanisms (e.g., sacrificial zones, surface inclination) can help mitigate the effects of sediment smothering on corals (Jones et al., 2019), field observations indicate sediment loading occurs on reef slope colonies. Therefore, the ability of reef currents to sort sediment particles deposited on coral surfaces has important implications, because sediment impacts are strongly influenced by sediment type (Te, 1992; Duckworth et al., 2017). While the physical properties of the suspended sediment in Singapore may pose a greater threat to complex coral morphologies, the ultimate influence of coral-sediment interactions depends on the total magnitude of reef sedimentation.

Our process-based assessment of vertical reef compression on turbid coral reefs is critical for understanding the response of benthic communities to future local and global environmental change (**Figure 8**). Under naturally turbid conditions, light propagates deeper to extend the depth range of coral growth, with diverse benthic communities and complex reef framework on the slope (**Figure 8A**). Localized increases in suspended particles reduce light penetration to shoal the euphotic zone, and coral communities transition to stress-tolerant and low-profile taxa (Morgan et al., 2016; Perry and Alvarez-Filip, 2018). Tidal sweeping can maintain reef crest communities by limiting sedimentation, but high sedimentation on reef slopes reduces available coral habitat (**Figure 8B**). Further declines in water quality can dramatically compress the zone of active reef growth (**Figure 8C**), as suspended particles adsorb light and greater sediment accumulation on reef slopes convert more benthic surfaces to soft-sediment. Under higher future sea levels associated with global climate change (**Figure 8D**), estimated deficits between vertical reef accretion by living coral communities (1.29 ± 0.20 mm $year^{-1}$) and projected sea level rise (3.0 ± 1.3 mm $year^{-1}$) in Singapore suggest water depths could increase by 20–60 cm in the next 80 years (Tkalich et al., 2013; Januchowski-Hartley et al., 2020). Raising of the euphotic depth by this amount will compress available reef habitat by 8–12% assuming no additional declines in water quality. A higher sea level may also affect reef crest sediment dynamics, including

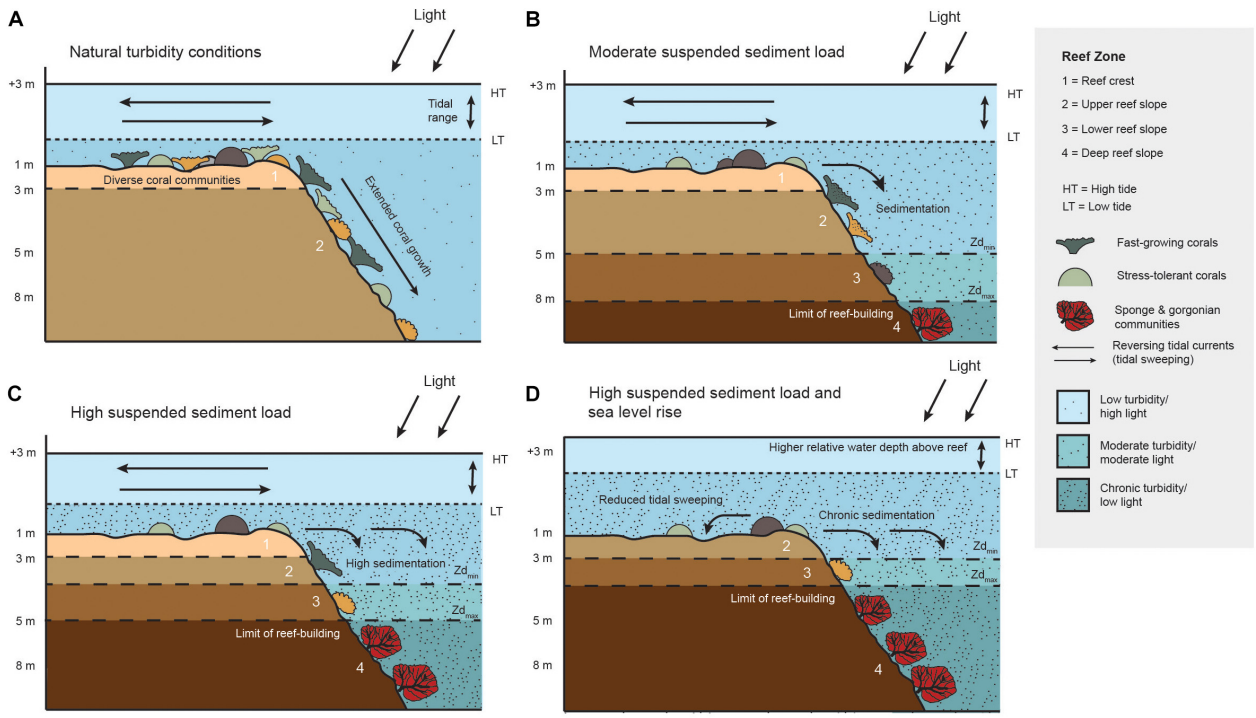

FIGURE 8 | Schematic diagram demonstrating vertical reef compression on turbid coral reefs caused by a shoaling euphotic depth (Zd) and higher net sedimentation on the reef slope. Panels show how the photic zone and benthic communities respond to local and climate-related impacts: **(A)** natural turbidity conditions, **(B)** moderate suspended sediment load, **(C)** high suspended sediment load, and **(D)** combined high suspended sediment load and sea level rise.

tidal sweeping, to further elevate turbidity. For example, an observation-based study predicted a doubling in the average daily maximum suspended sediment concentration (11–20 mg l^{-1}) with a 20 cm sea level rise (Ogston and Field, 2010). If projected relative water level changes occur in synergy with intensified local stressors, reef communities may become highly fragmented and ecologically redundant due to an increasing lack of light and a greater abundance of soft-sediment benthic cover.

CONCLUSION

Current understanding of vertical reef compression on turbid reefs remains largely speculative, or overly simplified, because of insufficient field data. Here, we find that on turbid coral reefs in Singapore, the depth range available for coral growth is shallow (<11 m) and determined by: (1) rapid attenuation of PAR over short depth ranges and (2) depth-related differences in reef hydrodynamics and sedimentation. Light attenuation is driven by suspended particulate matter in the water column, comprised of sediment, chlorophyll-*a* and CDOM, which dramatically shoals the euphotic depth. Reef slopes experience high net sedimentation of siliciclastic silt particles, which smother consolidated substrates and reduce available coral habitat. Critically, coral morphology influences the type and particle size of sediment deposited on coral surfaces. Our findings support reported ecological patterns for Singapore's reefs over the past 27 years, where reef crest corals have retained relative ecological stability as tidal sweeping removes excess silt particles, and slope communities have converted to soft-sediment benthic cover. This suggests that turbid coral communities, in particular deeper corals at the photic floor, are highly vulnerable to the synergistic effects of local anthropogenic stressors and future sea level rise.

DATA AVAILABILITY STATEMENT

The raw data supporting the conclusions of this article will be made available by the authors, without undue reservation.

AUTHOR CONTRIBUTIONS

KM conceived and designed the project and conducted the sediment analysis. KM and MM carried out the fieldwork. KM and NS undertook the data analysis. NS performed the remote sensing. KM prepared the manuscript, with contributions by MM, NS, and AS. All authors gave their final approval for publication.

FUNDING

This research was supported by Singapore's National Research Foundation (NRF) under the Marine Science Research and Development Programme (MSRDP-P11). KM is a beneficiary

of an AXA Research Fund Postdoctoral Grant and a Nanyang Presidential Postdoctoral Research Fellowship.

ACKNOWLEDGMENTS

We would like to acknowledge the crew of Dolphin Explorer for their assistance during fieldwork. Research was carried out under Singapore National Park Board permit (NP/RP17-044a). We would like to thank the reviewers for their thoughtful and constructive comments.

SUPPLEMENTARY MATERIAL

The Supplementary Material for this article can be found online at: https://www.frontiersin.org/articles/10.3389/fmars.2020.571256/full#supplementary-material

REFERENCES

Anthony, K. R., Hoogenboom, M. O., and Connolly, S. R. (2005). Adaptive Variation in Coral geometry and the optimization of internal colony light climates. *Funct. Ecol.* 19, 17–26. doi: 10.1111/j.0269-8463.2005.00925.x

Bainbridge, Z. T., Wolanski, E., Álvarez-Romero, J. G., Lewis, S. E., and Brodie, J. E. (2012). Fine sediment and nutrient dynamics related to particle size and floc formation in a Burdekin River flood plume. *Austr. Mar. Pollut. Bull.* 65, 236–248. doi: 10.1016/j.marpolbul.2012.01.043

Bainbridge, Z., Lewis, S., Bartley, R., Fabricius, K., Collier, C., Waterhouse, J., et al. (2018). Fine sediment and particulate organic matter: A review and case study on ridge-to-reef transport, transformations, fates, and impacts on marine ecosystems. *Mar. Pollut. Bull.* 135, 1205–1220. doi: 10.1016/j.marpolbul.2018.08.002

Baum, G., Januar, H. I., Ferse, S. C. A., and Kunzmann, A. (2015). Local and regional impacts of pollution on coral reefs along the thousand islands north of the megacity Jakarta. *Indonesia. PLoS One* 10:e0138271. doi: 10.1371/journal.pone.0138271

Bellwood, D. R., and Hughes, T. P. (2001). Regional-scale assembly rules and biodiversity of coral reefs. *Science* 292, 1532–1534. doi: 10.1126/science.1058635

Blott, S., and Pye, K. (2001). GRADISTAT: a grain size distribution and statistics package for the analysis of unconsolidated sediments. *Earth Surf. Process. Landforms*. 26, 1237–1248.

Brockmann, C., Doerffer, R., Peters, M., Stelzer, K., Embacher, S., and Ruescas, A. (2016). Evolution of the C2RCC neural network for Sentinel 2 and 3 for the retrieval of ocean colour products in normal and extreme optically complex waters. *Eur. Space Agency*. 740:54.

Browne, N. K., Tay, J. K. L., Low, J., Larson, O., and Todd, P. A. (2015). Fluctuations in coral health of four common inshore reef corals in response to seasonal and anthropogenic changes in water quality. *Mar. Environ. Res.* 105, 39–52. doi: 10.1016/j.marenvres.2015.02.002

Burke, L., Reytar, K., Spalding, M., and Perry, A. (2011). *Reefs at Risk Revisited*. Washington, D C: World Resources Institute.

Burt, J. A., Camp, E. F., Enochs, I. C., Johansen, J. L., Morgan, K. M., Riegl, B., et al. (2020). Insights from extreme coral reefs in a changing world. *Coral Reefs*. 39, 495–507. doi: 10.1007/s00338-020-01966-y

Cacciapaglia, C., and van Woesik, R. (2015). Reef-coral refugia in a rapidly changing ocean. *Glob. Chang. Biol.* 21, 2272–2282. doi: 10.1111/gcb.12851

Chen, M., Murali, K., Khoo, B.-C., Lou, J., and Kumar, K. (2005). Circulation Modelling in the Strait of Singapore. *J. Coast. Res.* 215, 960–972. doi: 10.2112/04-0412.1

Cheng, N.-S. S., and Chiew, Y.-M. M. (1999). Analysis of initiation of sediment suspension from bed load. *J. Hydraul. Eng.* 125, 855–861. doi: 10.1061/(ASCE)0733-94291999125:8(855)

Chow, G. S. E., Chan, Y. K. S., Jain, S. S., and Huang, D. (2019). Light limitation selects for depth generalists in urbanised reef coral communities. *Mar. Environ. Res.* 147, 101–112. doi: 10.1016/j.marenvres.2019.04.010

Cleary, D. F. R., Polónia, A. R. M., Renema, W., Hoeksema, B. W., Rachello-Dolmen, P. G., Moolenbeek, R. G., et al. (2016). Variation in the composition of corals, fishes, sponges, echinoderms, ascidians, molluscs, foraminifera and macroalgae across a pronounced in-to-offshore environmental gradient in the Jakarta Bay–Thousand Islands coral reef complex. *Mar. Pollut. Bull.* 110, 701–717. doi: 10.1016/j.marpolbul.2016.04.042

de Soares, M. O. (2020). Marginal reef paradox: A possible refuge from environmental changes? *Ocean Coast. Manag.* 185:105063. doi: 10.1016/j.ocecoaman.2019.105063

Doerffer, R., and Schiller, H. (2007). The MERIS case 2 water algorithm. *Int. J. Remote Sens.* 28, 517–535. doi: 10.1080/01431160600821127

Duckworth, A., Giofre, N., and Jones, R. (2017). Coral morphology and sedimentation. *Mar. Pollut. Bull.* 125, 289–300. doi: 10.1016/j.marpolbul.2017.08.036

Duprey, N. N., Wang, T. X., Kim, T., Cybulski, J. D., Vonhof, H. B., Crutzen, P. J., et al. (2020). Megacity development and the demise of coastal coral communities: Evidence from coral skeleton δ15N records in the Pearl River estuary. *Glob. Chang. Biol.* 26, 1338–1353. doi: 10.1111/gcb.14923

Erftemeijer, P. L. A., Riegl, B., Hoeksema, B. W., and Todd, P. A. (2012). Environmental impacts of dredging and other sediment disturbances on corals: A review. *Mar. Pollut. Bull.* 64, 1737–1765. doi: 10.1016/j.marpolbul.2012.05.008

Fabricius, K. E. (2005). Effects of terrestrial runoff on the ecology of corals and coral reefs: review and synthesis. *Mar. Pollut. Bull.* 50, 125–146. doi: 10.1016/j.marpolbul.2004.11.028

Fabricius, K. E., Logan, M., Weeks, S. J., Lewis, S. E., and Brodie, J. (2016). Changes in water clarity in response to river discharges on the Great Barrier Reef continental shelf: 2002–2013. *Estuar. Coast. Shelf Sci.* 173, A1–A15. doi: 10.1016/j.ecss.2016.03.001

Fabricius, K. E., Wild, C., Wolanski, E., and Abele, D. (2003). Effects of transparent exopolymer particles and muddy terrigenous sediments on the survival of hard coral recruits. *Estuar. Coast. Shelf Sci.* 57, 613–621. doi: 10.1016/S0272-7714(02)00400-6

Field, M. E., Chezar, H., and Storlazzi, C. D. (2013). SedPods: A low-cost coral proxy for measuring net sedimentation. *Coral Reefs* 32, 155–159. doi: 10.1007/s00338-012-0953-5

Freitas, L. M., Oliveira, M., de, D. M., Leão, Z. M. A. N., and Kikuchi, R. K. P. (2019). Effects of turbidity and depth on the bioconstruction of the Abrolhos reefs. *Coral Reefs* 38, 241–253. doi: 10.1007/s00338-019-01770-3

Gibbs, R. J., Matthews, M. D., and Link, D. A. (1971). The Relationship Between Sphere Size And Settling Velocity. *SEPM J. Sediment. Res.* 41, 7–18. doi: 10.1306/74D721D0-2B21-11D7-8648000102C1865D

Goodkin, N. F., Switzer, A. D., McCorry, D., DeVantier, L., True, J. D., Hughen, K. A., et al. (2011). Coral communities of Hong Kong: Long-lived corals in a marginal reef environment. *Mar. Ecol. Prog. Ser.* 426, 185–196. doi: 10.3354/meps09019

Guest, J. R., Baird, A. H., Maynard, J. A., Muttaqin, E., Edwards, A. J., Campbell, S. J., et al. (2012). Contrasting patterns of coral bleaching susceptibility in 2010 suggest an adaptive response to thermal stress. *PLoS One* 7:e33353. doi: 10.1371/journal.pone.0033353

Guest, J. R., Tun, K., Low, J., Vergés, A., Marzinelli, E. M., Campbell, A. H., et al. (2016). 27 years of benthic and coral community dynamics on turbid, highly urbanised reefs off Singapore. *Sci. Rep.* 6:36260. doi: 10.1038/srep36260

Heery, E. C., Hoeksema, B. W., Browne, N. K., Reimer, J. D., Ang, P. O., Huang, D., et al. (2018). Urban coral reefs: Degradation and resilience of hard coral assemblages in coastal cities of East and Southeast Asia. *Mar. Pollut. Bull.* 135, 654–681. doi: 10.1016/j.marpolbul.2018.07.041

Heiri, O., Lotter, A. F., and Lemcke, G. (2001). Loss on ignition as a method for estimating organic and carbonate content in sediments: Reproducibility

and comparability of results. *J. Paleolimnol.* 25, 101–110. doi: 10.1023/A:1008119611481

Hench, J. L., and Rosman, J. H. (2013). Observations of spatial flow patterns at the coral colony scale on a shallow reef flat. *J. Geophys. Res. Ocean.* 118, 1142–1156. doi: 10.1002/jgrc.20105

Hilton, M. J., and Ming, C. L. (1999). Sediment facies of a low-energy, meso-tidal, fringing reef. *Singap. J. Trop. Geogr.* 20, 111–130. doi: 10.1111/1467-9493.00049

Hinrichsen, D. (2016). *Our common seas: Coasts in crisis*. London: Routledge.

Hughes, T. P., Anderson, K. D., Connolly, S. R., Heron, S. F., Kerry, J. T., Lough, J. M., et al. (2018). Spatial and temporal patterns of mass bleaching of corals in the Anthropocene. *Science* 359, 80–83. doi: 10.1126/science.aan8048

Januchowski-Hartley, F. A., Bauman, A. G., Morgan, K. M., Seah, J. C. L., Huang, D., and Todd, P. A. (2020). Accreting coral reefs in a highly urbanized environment. *Coral Reefs* 39, 717–731. doi: 10.1007/s00338-020-01953-3

Jones, R., Bessell-Browne, P., Fisher, R., Klonowski, W., and Slivkoff, M. (2016). Assessing the impacts of sediments from dredging on corals. *Mar. Pollut. Bull.* 102, 9–29. doi: 10.1016/j.marpolbul.2015.10.049

Jones, R., Fisher, R., and Bessell-Browne, P. (2019). Sediment deposition and coral smothering. *PLoS One* 14, 1–24. doi: 10.1371/journal.pone.0216248

Jones, R., Fisher, R., Stark, C., and Ridd, P. (2015). Temporal patterns in seawater quality from dredging in tropical environments. *PLoS One* 10, 1–25. doi: 10.1371/journal.pone.0137112

Jones, R., Giofre, N., Luter, H. M., Neoh, T. L., Fisher, R., and Duckworth, A. (2020). Responses of corals to chronic turbidity. *Sci. Rep.* 10, 1–13. doi: 10.1038/s41598-020-61712-w

Kamp-Nielsen, L., Vermaat, J. E., Wesseling, I., Borum, J., and Geertz-Hansen, O. (2002). Sediment properties along gradients of siltation in south-east Asia. *Estuar. Coast. Shelf Sci.* 54, 127–137. doi: 10.1006/ecss.2001.0822

Lai, S., Loke, L. H. L., Hilton, M. J., Bouma, T. J., and Todd, P. A. (2015). The effects of urbanisation on coastal habitats and the potential for ecological engineering: A Singapore case study. *Ocean Coast. Manag.* 103, 78–85. doi: 10.1016/j.ocecoaman.2014.11.006

Laverick, J. H., Tamir, R., Eyal, G., and Loya, Y. (2020). A generalized light−driven model of community transitions along coral reef depth gradients. *Glob. Ecol. Biogeogr.* 29, 1554–1564. doi: 10.1111/geb.13140

Liew, S. C., and Kwoh, L. K. (2003). *Mapping Optical Parameters of Coastal Sea Waters using the Hyperion Imaging Spectrometer: Intercomparison with MODIS Ocean Color Products*. New Jersey, NJ: IEEE.

Loiola, M., Cruz, I. C. S., Lisboa, D. S., Mariano-Neto, E., Leão, Z. M. A. N., Oliveira, M. D. M., et al. (2019). Structure of marginal coral reef assemblages under different turbidity regime. *Mar. Environ. Res.* 147, 138–148. doi: 10.1016/j.marenvres.2019.03.013

Low, J. K. Y., and Chou, L. M. (1994). "Sedimentation rates in Singapore waters," in *Proceedings, Third ASEAN-Australia Symposium on Living Coastal Resources.* (Bangkok: Chulalongkorn University), 697–701.

Macdonald, R. K. (2015). *Turbidity and light attenuation in coastal waters of the Great Barrier Reef*. Thesis, Mackay: James Cook University, 232.

Maxwell, W. (1968). *Atlas of the Great Barrier Reef*. Available online at: http://agris.fao.org/agris-search/search.do?recordID=XF2017003063 (accessed June 7, 2020).

Morgan, K. M. M., and Kench, P. S. S. (2014). A detrital sediment budget of a Maldivian reef platform. *Geomorphology* 222, 122–131. doi: 10.1016/j.geomorph.2014.02.013

Morgan, K. M., and Kench, P. S. (2016). Reef to island sediment connections on a Maldivian carbonate platform: using benthic ecology and biosedimentary depositional facies to examine island-building potential. *Earth Surf. Process. Landform.* 41, 1815–1825. doi: 10.1002/esp.3946

Morgan, K. M., Perry, C. T., Arthur, R., Williams, H. T. P., and Smithers, S. G. (2020). Projections of coral cover and habitat change on turbid reefs under future sea-level rise. *Proc. Biol. Sci.* 287:20200541. doi: 10.1098/rspb.2020.0541

Morgan, K. M., Perry, C. T., Johnson, J. A., and Smithers, S. G. (2017). Nearshore Turbid-Zone Corals Exhibit High Bleaching Tolerance on the Great Barrier Reef Following the 2016 Ocean Warming Event. *Front. Mar. Sci.* 4:224. doi: 10.3389/fmars.2017.00224

Morgan, K. M., Perry, C. T., Smithers, S. G., Johnson, J. A., and Daniell, J. J. (2016). Evidence of extensive reef development and high coral cover in nearshore environments: implications for understanding coral adaptation in turbid settings. *Sci. Rep.* 6:29616. doi: 10.1038/srep29616

Ogston, A. S., and Field, M. E. (2010). Predictions of Turbidity Due to Enhanced Sediment Resuspension Resulting from Sea-Level Rise on a Fringing Coral Reef: Evidence from Molokai. *Hawaii. J. Coast. Res.* 26, 1027–1037. doi: 10.2112/jcoastres-d-09-00064.1

Perry, C. T., and Alvarez-Filip, L. (2018). Changing geo-ecological functions of coral reefs in the Anthropocene. *Funct. Ecol.* 33, 976–988. doi: 10.1111/1365-2435.13247

Perry, C. T., and Morgan, K. M. (2017). Bleaching drives collapse in reef carbonate budgets and reef growth potential on southern Maldives reefs. *Sci. Rep.* 7, 1–9. doi: 10.1038/srep40581

Risk, M. J. (2014). Assessing the effects of sediments and nutrients on coral reefs. *Curr. Opin. Environ. Sustain.* 7, 108–117. doi: 10.1016/j.cosust.2014.01.003

Saulquin, B., Hamdi, A., Gohin, F., Populus, J., Mangin, A., and D'Andon, O. F. (2013). Estimation of the diffuse attenuation coefficient KdPAR using MERIS and application to seabed habitat mapping. *Remote Sens. Environ.* 128, 224–233. doi: 10.1016/j.rse.2012.10.002

Shaffer, J. M., and Beaulieu, J. J. (2012). Calibration of the OdysseyTM Photosynthetic Irradiance RecorderTM for absolute irradiance measures. *J. Freshw. Ecol.* 27, 599–605. doi: 10.1080/02705060.2012.711259

Siegel, H., Gerth, M., Stottmeister, I., Baum, A., and Samiaji, J. (2018). "Remote sensing of coastal discharge of SE Sumatra (Indonesia)," in *Remote Sensing of the Asian Seas*, eds V. Barale and M. Gade (Berlin: Springer), 359–379.

Storlazzi, C. D., Norris, B. K., and Rosenberger, K. J. (2015). The influence of grain size, grain color, and suspended-sediment concentration on light attenuation: Why fine-grained terrestrial sediment is bad for coral reef ecosystems. *Coral Reefs* 34, 967–975. doi: 10.1007/s00338-015-1268-0

Syvitski, J. P. M., Vo, C. J., Kettner, A. J., and Green, P. (2005). Impact of humans on the flux of terrestrial sediment to the global coastal ocean. *Science* 308, 376–380.

Te, F. T. (1992). Response to higher sediment loads by Pocillopora damicornis planulae. *Coral Reefs* 11, 131–134. doi: 10.1007/BF00255466

Tkalich, P., Vethamony, P., Luu, Q. H., and Babu, M. T. (2013). Sea level trend and variability in the Singapore Strait. *Ocean Sci.* 9, 293–300. doi: 10.5194/os-9-293-2013

Weber, M., Lott, C., and Fabricius, K. E. (2006). Sedimentation stress in a scleractinian coral exposed to terrestrial and marine sediments with contrasting physical, organic and geochemical properties. *J. Exp. Mar. Bio. Ecol.* 336, 18–32. doi: 10.1016/j.jembe.2006.04.007

Conflict of Interest: The authors declare that the research was conducted in the absence of any commercial or financial relationships that could be construed as a potential conflict of interest.

frontiers in Marine Science

ORIGINAL RESEARCH
published: 20 January 2021
doi: 10.3389/fmars.2020.594537

Bottom Trawling Threatens Future Climate Refugia of Rhodoliths Globally

Eliza Fragkopoulou[1], Ester A. Serrão[1], Paulo A. Horta[2], Gabrielle Koerich[2] and Jorge Assis[1]*

[1] Center of Marine Sciences, University of Algarve, Faro, Portugal, [2] Phycology Laboratory, Department of Botany, Biological Sciences Center, Federal University of Santa Catarina, Florianopolis, Brazil

Climate driven range shifts are driving the redistribution of marine species and threatening the functioning and stability of marine ecosystems. For species that are the structural basis of marine ecosystems, such effects can be magnified into drastic loss of ecosystem functioning and resilience. Rhodoliths are unattached calcareous red algae that provide key complex three-dimensional habitats for highly diverse biological communities. These globally distributed biodiversity hotspots are increasingly threatened by ongoing environmental changes, mainly ocean acidification and warming, with wide negative impacts anticipated in the years to come. These are superimposed upon major local stressors caused by direct destructive impacts, such as bottom trawling, which act synergistically in the deterioration of the rhodolith ecosystem health and function. Anticipating the potential impacts of future environmental changes on the rhodolith biome may inform timely mitigation strategies integrating local effects of bottom trawling over vulnerable areas at global scales. This study aimed to identify future climate refugia, as regions where persistence is predicted under contrasting climate scenarios, and to analyze their trawling threat levels. This was approached by developing species distribution models with ecologically relevant environmental predictors, combined with the development of a global bottom trawling intensity index to identify heavily fished regions overlaying rhodoliths. Our results revealed the importance of light, thermal stress and pH driving the global distribution of rhodoliths. Future projections showed poleward expansions and contractions of suitable habitats at lower latitudes, structuring cryptic depth refugia, particularly evident under the more severe warming scenario RCP 8.5. Our results suggest that if management and conservation measures are not taken, bottom trawling may directly threaten the persistence of key rhodolith refugia. Since rhodoliths have slow growth rates, high sensitivity and ecological importance, understanding how their current and future distribution might be susceptible to bottom trawling pressure, may contribute to determine the fate of both the species and their associated communities.

Keywords: climate change, distribution shifts, coralligenous reefs, ecosystem structuring species, coralline algae, species distribution modeling, maerl

OPEN ACCESS

Edited by:
Massimo Ponti, University of Bologna, Italy

Reviewed by:
Fabio Rindi, Polytechnic University of Marche, Italy
Sebastian Teichert, Friedrich-Alexander Universität Erlangen-Nürnberg, Germany

****Correspondence:***
Eliza Fragkopoulou
eli_frag@hotmail.com

Specialty section:
This article was submitted to Marine Ecosystem Ecology, a section of the journal Frontiers in Marine Science

Received: *13 August 2020*
Accepted: *28 December 2020*
Published: *20 January 2021*

Citation:
Fragkopoulou E, Serrão EA, Horta PA, Koerich G and Assis J (2021) Bottom Trawling Threatens Future Climate Refugia of Rhodoliths Globally. Front. Mar. Sci. 7:594537. doi: 10.3389/fmars.2020.594537

INTRODUCTION

In a world where climate is changing rapidly affecting the distribution of marine species (Cheung et al., 2009; Leadley et al., 2010; Poloczanska et al., 2013; Pecl et al., 2017), climate refugia, i.e., regions with stable habitat conditions through variable time intervals, may play a fundamental role in enabling population persistence, preserving local ecosystem functioning and serving as sources for the replenishment of impacted regions (Hewitt, 2004; Provan and Bennett, 2008; Keppel et al., 2012). This is particularly relevant for low dispersive species whose limited ability to track climate change by migration to new suitable regions may result in regional extinctions (Assis et al., 2017b). Climate change impacts may be greater when affecting ecosystem structuring species that support rich and diverse communities (Hoegh-Guldberg and Bruno, 2010). A collapse of such species, already observed for coral reefs (Carpenter et al., 2008; Hudges et al., 2018), kelp forests (Wernberg et al., 2015; Assis et al., 2017a) and seagrass meadows (Marbà and Duarte, 2010; Arias-Ortiz et al., 2018), has produced cascading effects reducing local biodiversity levels and disrupting ecosystem services (García Molinos et al., 2015; Pecl et al., 2017). In this scope, climate refugia function as regions of climate stability providing effective conservation of global biodiversity (inter and intra-specific) under climate change (Keppel et al., 2012; Morelli et al., 2016, 2020).

Despite the potential role of climate refugia, additional localized stressors may still compromise the future fate of ecosystems (Halpern et al., 2008; O'Leary et al., 2017). Cumulative effects of localized disturbances can act in synergy, accelerating or exacerbating the outcomes of climate change alone, and decreasing overall ecosystem resilience (Carilli et al., 2010; Costello et al., 2010; Halpern et al., 2015). For instance, bottom trawling has particularly destructive effects on benthic communities, decreasing biomass and eroding biogenic structures on the sea bottom (de Groot, 1984; Thrush and Dayton, 2002; Tillin et al., 2006; Olsgard et al., 2008). Conversely, reducing disturbance can have direct short or middle term impacts on ecosystems, in contrast to global climate change mitigation that can only be achieved in the long-term (Gurney et al., 2013; Strain et al., 2015). Nonetheless, analyses show that there are almost no pristine or unaffected ecosystems left globally, with overfishing and pollution being the primary threats to biodiversity (Costello et al., 2010; Halpern et al., 2015).

Under such serious threats to the future of marine biodiversity, maintenance of ecosystem functions will be very dependent on the persistence of ecosystem structuring species, such as seagrass, kelp, mangroves, corals (Hoegh-Guldberg and Bruno, 2010; Sasaki et al., 2015; O'Leary et al., 2017). Among such structural species, free-living calcareous algae commonly designated rhodoliths (of the orders Corallines, Hapalidiales and Sporolithales), are globally distributed, from the intertidal down to 270 m depth (Abella et al., 1998; Amado-Filho et al., 2012a; Riosmena-Rodriguez et al., 2017). Their three-dimensional structure provides habitat complexity creating biodiversity hotspots of highly diverse assemblages, while acting as shelters for invertebrates and other organisms, and as seed banks for algae (Abella et al., 1998; Amado-Filho, 2010; Fredericq et al., 2019; Veras et al., 2020). Additionally, they are important carbonate factories, contributing to the global carbon cycling (Amado-Filho et al., 2012a; van der Heijden and Kamenos, 2015). Although their ecological value has been acknowledged since the 19th century (Gran, 1893; Pruvot, 1897), rhodolith habitats are globally decreasing, mostly as a result of bottom fishing disturbance, and are expected to continue to decrease under the upcoming environmental changes, especially ocean warming and acidification (Hall-Spencer and Moore, 2000; Noisette et al., 2013; Martin and Hall-Spencer, 2017; Bernard et al., 2019). Anticipating and reducing the cumulative impacts on these rich and important ecosystems could improve their resilience, and in turn, promote and guide well-informed conservation and management of marine biodiversity.

This study aims to investigate the global future distributional shifts of the rhodolith biome under different climate change scenarios, using species distribution models, to identify crucial refugial regions providing persistent suitable habitat in the long-term. The major goal is to compare such persistent refugial habitat locations with their primary local threat, bottom trawling. This is done by quantifying global intensity of bottom trawling and overlaying it on predicted rhodolith distributions and their future climate refugia, in order to identify key regions of high conservation priority.

MATERIALS AND METHODS

Environmental and Occurrence Data

In order to examine the potential consequences of future climate change on the rhodolith biome, a set of environmental predictors were selected based on their biological relevance to the rhodolith physiology (Carvalho et al., 2020). Benthic predictors for the annual average values of temperature (minimum and maximum), pH, light, nitrate, phosphate, salinity and currents, were downloaded from Bio-ORACLE (Tyberghein et al., 2012; Assis et al., 2017b) for the present and for two contrasting best and worst future scenarios: the Representative Concentration Pathway (RCP) 2.6 characterized by a large reduction of greenhouse emissions over time and RCP 8.5, where emissions are predicted to continue to increase over time (Moss et al., 2010). Additionally, to account for sediment and pollutant load that may negatively influence the presence of rhodoliths (Wilson et al., 2004; Villas-Bôas et al., 2014), we developed environmental predictors accounting for the distance from major coastal cities (population >75th percentile of the distribution of population)[1] and the distance from river deltas (Global Estuaries Database; UNEP + Sea Around Us, 2003) as a proxy. Distances were produced as raster layers matching the resolution of Bio-ORACLE.

Rhodolith data were compiled by selecting species that primarily form rhodoliths (**Supplementary Material 1**). This conservative approach was preferred to a more extensive selection of species, as information about the form of records

[1]https://simplemaps.com/data/world-cities

(e.g., rhodoliths or crustose) is not available in the major online repositories and/or because of major taxonomic issues resulting to erratic records (e.g., the case of *Lithophyllum stictiforme*, where numerous species are passing under that name; Pezzolesi et al., 2019). Detailed georeferenced occurrence records of the selected species were compiled from OBIS (2020) and GBIF.org (2020). Additional records were extracted from a systematic search of the literature on the Web of Knowledge using each species name as a searching criterion (**Supplementary Material 2**). The compiled dataset was subjected to pruning by removing records on land, and outside known geographical and depth distributions (max 270 m; Riosmena-Rodriguez et al., 2017). Further, potential spatial autocorrelation was reduced by estimating the minimum correlated distance of the environmental predictors and leaving only one occurrence record within such distance.

As the biogeographical affinities and distributions of the selected species differed greatly (e.g., from polar to tropical species) with likely differences in physiological responses, the data were divided into two separate datasets for species distribution modeling: (1) polar-cold temperate and (2) tropical-warm temperate affiliated species (**Supplementary Material 1**).

Species Distribution Modeling

Species distribution models were developed using two machine learning algorithms: boosted regression trees (BRT; De'ath, 2007) and Adaptive Boosting (AdaBoost; Hothorn et al., 2010). Because these models use both presence and absence data (not available), a number of pseudo-absences equal to the number of presences were generated and chosen randomly from a kernel probability surface developed with the occurrence records (e.g., Assis et al., 2018). Cross-validation interactions (CV) were developed to optimize model parameters and assess for potential transferability by partitioning the occurrence records (presences and pseudo-absences) into independent random blocks (Valavi et al., 2019). Models were fitted with all combinations of model parameters for BRT (tree complexity: 1–6; learning rate: 0.01, 0.005, and 0.001; number of trees: 50–1,000, step 50) and AdaBoost (shrinkage: 0.25–1, step 0.25; number of interactions: 50–250, step 50; degrees of freedom: 1–12) and their predictive performance was evaluated by one withheld block at a time. For each model, a predictive map was developed and reclassified into a binary presence-absence surface, based on a threshold maximizing true skill statistics (Allouche et al., 2006). Model performance was assessed by AUC (Area Under Curve; Fielding and Bell, 1997) and sensitivity (true positive rate). Overfitting of final predictive models was reduced by using the parameters retrieving higher performance in CV and by forcing monotonic responses (e.g., negative for maximum temperatures and positive for all other environmental variables; Elith et al., 2008; Boavida et al., 2016; Assis et al., 2018).

In order to determine the relative contribution of each environmental predictor to the model, the mean increase in deviance (i.e., goodness of fit) was computed by adding a given predictor at a time to all alternative models (e.g., Assis et al., 2018). The significance of the models was estimated as the relative contribution of each environmental predictor to the model performance (Elith et al., 2008). Limiting thresholds were extracted from the individual fitting function of each predictor alone while averaging the effect of all alternative predictors, and were then compared with available literature for physiological limits (Assis et al., 2018). Reduced models with less predictors and higher potential for transferability were built by interactively removing one predictor at a time from the full model (i.e., all predictors), starting from the least to the highest contributing variable, until the difference in deviance between full and reduced model was higher than zero (Elith et al., 2008; Boavida et al., 2016; Assis et al., 2018). Final distribution maps for polar—cold temperate and tropical—warm temperate species were produced from the respective reduced models, averaging the BRT and AdaBoost with the highest predictive performance (Araújo and New, 2007). Forecasts for future refugia, contraction and expansion regions were inferred by comparing present and future predictions. In order to address conclusions at the biome level, these regions were aggregated into a unique map describing refugia, contraction and expansion areas for both polar—cold temperate and tropical—warm temperate species.

Bottom Trawling Overlay Estimation

Global data for bottom trawling reported for 2012–2016 (in days of activity per year) were downloaded from the Global Fishing Watch (Kroodsma et al., 2018). This information was used to generate a layer of "mean bottom trawling activity per year" matching the resolution and extent of Bio-ORACLE. This was used to infer the potential trawling impacts on rhodoliths globally, along the present and future distributions (local impacts on regions of refugia, contraction, and expansion). Areas were estimated per marine biogeographic realm (Spalding et al., 2007) after aggregating final distribution maps of polar—cold temperate and tropical—warm temperate species.

Species distribution modeling, trawling overlay area calculations and final maps were produced in R (R Development Core Team, 2018) using the packages blockCV, dismo, EMNeval, gbm, gdata, gstat, leaflet, mboost, parallel, raster, rgeos, rgdal, SDMTools, ggplot, and sp.

RESULTS

The initial 19,477 georeferenced occurrence records compiled for the rhodolith biome resulted into a final pruned dataset of 802 occurrences (**Supplementary Figure 1**). The models developed to predict the occurrence of rhodoliths retrieved a good performance for both warm and cold affiliated species (AUC: 0.87 and 0.92; sensitivity: 0.73 and 0.87, respectively) and showed distributions mostly determined by light availability (relative contribution: 33.35 ± 9.29), maximum ($18.81\% \pm 5.11$) and minimum temperature ($19.45\% \pm 9.67$) and pH (6.32 ± 4.78; **Figure 1**). The partial dependency plots showed suitable conditions for the warm affiliated species where light was above $\sim 2 \times 10^{-4}$ E * m^2 * yr^{-1}, temperature range 4–34°C and pH above 7.7 (**Supplementary Figure 2**); and for cold affiliated species where light was $\sim 2 \times 10^{-4}$ E * m^2 * yr^{-1}, temperature range −1.7–31°C and pH 7.9, respectively (**Supplementary Figure 3**). Global suitable rhodolith area for present-day

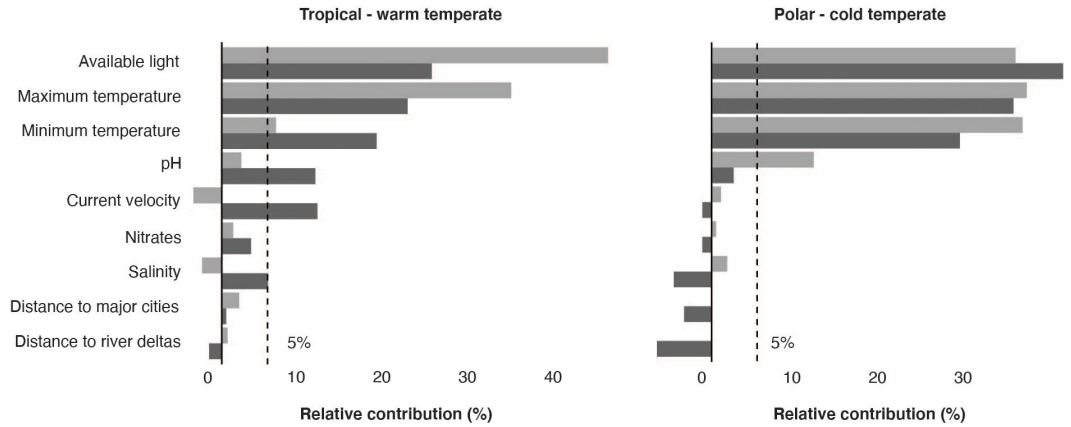

FIGURE 1 | Benthic environmental predictors used in adaptive boosting (light gray) and boosted regression trees (dark gray) and their relative contribution to the models' predictions for tropical—warm temperate and polar—cold temperate affiliated species.

conditions was estimated to ∼4.1 million km^2, distributed between 1 and 300 m depth (**Figure 2** and **Supplementary Figure 4**). The largest suitable areas were predicted in the temperate northern Atlantic (∼46% of the total distribution), followed by the Temperate Australasia (∼15%) and Temperate South America realms (∼15%; **Supplementary Table 1**).

Future projections varied depending on the climatic scenarios used, with RCP 8.5 causing the most profound distributional changes (**Figures 3**, **4**). Shifts to boreal and deeper areas were estimated to cause ∼19–50% range expansion, mostly in regions of the Temperate Northern Pacific (e.g., Japan, Okhotsk and Bering Seas) and the Artic (e.g., Labrador, Greenland and Norwegian Seas; **Supplementary Table 1**). At the same time, approximately 26–44% range contraction was estimated, particularly affecting shallower and tropical regions. Specifically, the tropical regions of the Eastern and Western Indo-Pacific were predicted to lose most of their rhodolith suitable habitats (67–80% and 62–81%, respectively; **Supplementary Table 1**). Taken together, these projections allowed to locate climatic refugia, i.e., regions providing suitable conditions for the present and the future (**Figures 3**, **4**). These represented 56–74% of the present distribution and were mostly located in the temperate regions of Northern Atlantic (∼1.1–1.4 million km^2), South America (∼346–353 thousands km^2) and Australasia (∼219–496 thousands km^2; **Supplementary Table 1**).

Bottom Trawling and Rhodolith Distribution

Overlaying global bottom trawling data with the distribution predicted for the present, revealed that ∼684 thousand km^2 of rhodolith suitable habitats are currently being trawled (**Figure 2** and **Supplementary Table 2**). The majority of trawling takes place on refugia (60–78%) located mostly in the Temperate Northern Atlantic (∼629 thousand km^2; **Supplementary Table 2**), with an overall estimated intensity of ∼140,000 days per year (**Supplementary Table 3**). Projected boreal expansions show an increase of suitable habitats in areas of current intensive bottom trawling activity, especially for the Temperate Northern Pacific, where suitable conditions in intensively trawled regions are estimated to increase by 900–1.750% depending on the RCP scenario (**Supplementary Table 2**).

DISCUSSION

Our analyses showed that rhodolith potential suitable area is ∼4.1 million km^2, widely distributed around the world's coastal regions. Future distribution areas are projected to undergo poleward and depth range shifts, coupled with a 26–44% range contraction in the shallower and tropical regions, a pattern highly dependent on the climate scenario considered. Projected refugia are mostly situated in temperate regions, with broader areas in the Northern Atlantic. Despite their ecological, conservational and evolutionary importance, refugia are currently under great local stress by intense bottom trawling, reaching up to ∼140,000 days, annually. Such localized and intense disturbances, acting in synergy with ongoing and projected climate changes, are likely to compromise the fate of the whole biome and its associated communities, since long lasting or irreversible impacts have already been observed in previously dredged regions, on the scale of years post-dredging (Hall-Spencer and Moore, 2000; Bernard et al., 2019).

Models showed that the distribution of rhodoliths is mainly shaped by light availability (above a minimum threshold), maximum and minimum temperature and pH (above a minimum threshold); environmental predictors that are directly linked with the physiology of photosynthetic calcifying organisms (Carvalho et al., 2020). While at the species level, limiting thresholds differ between rhodolith species (Martin and Hall-Spencer, 2017), our aim was a model-based inference of suitable habitats for the warm and cold rhodolith biomes (e.g., Jayathilake and Costello, 2018). The use of the newly developed pH benthic layers (Assis et al., 2017b) allowed to account for the potential role of ocean acidification, a well-described threat for rhodoliths (Kroeker

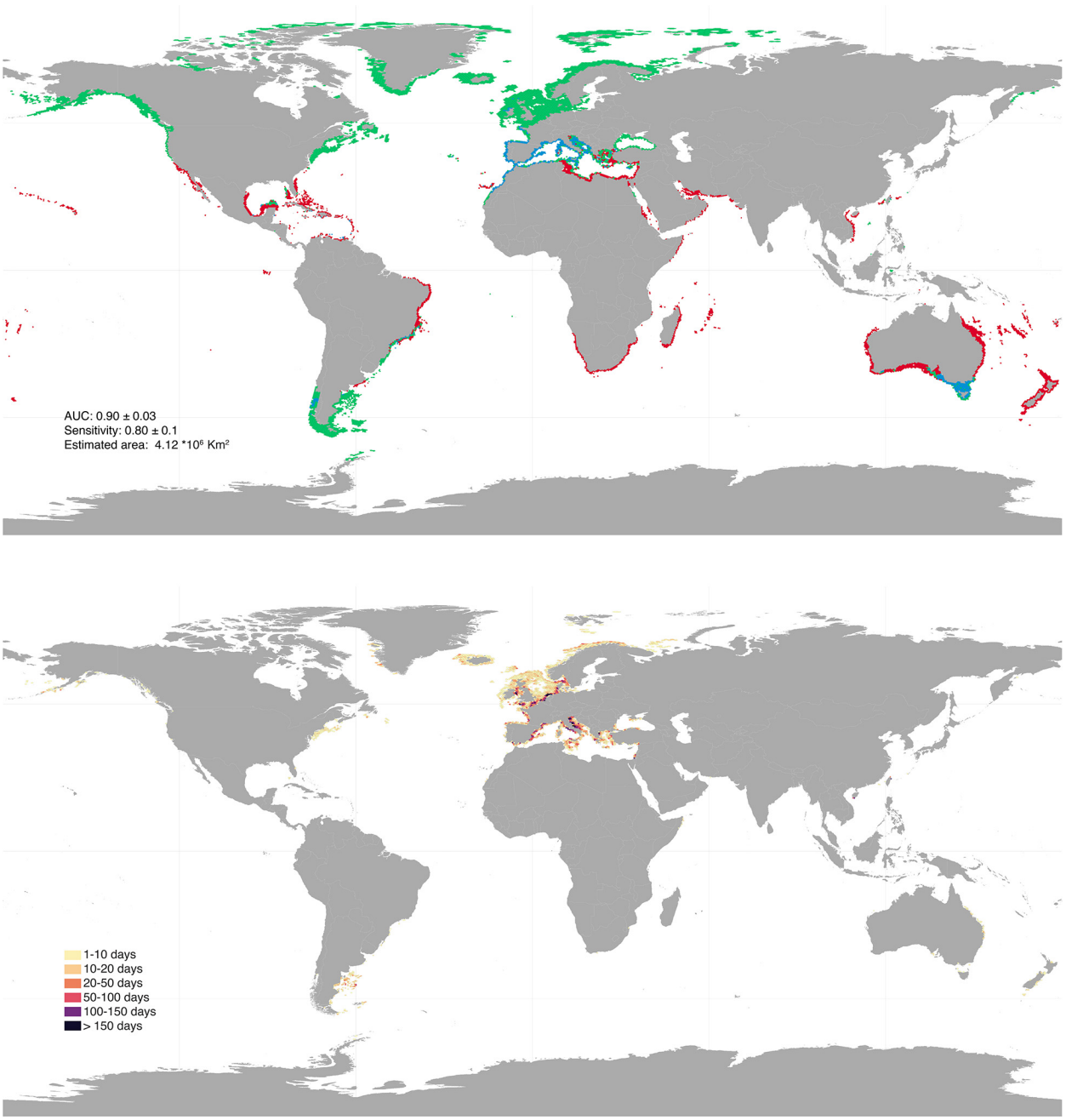

FIGURE 2 | Upper panel: global present-day rhodolith distribution as inferred for polar—cold temperate (green) and tropical—warm temperate affiliated species (red). Regions of overlap are depicted in blue. Bottom panel: bottom trawling intensity (days per year) overlaying rhodolith suitable habitats for present day distribution. Results were aggregated for better visualization. High resolution maps can be found in **Supplementary Material**.

et al., 2010; Noisette et al., 2013; Qui-Minet et al., 2019). Models inferred limiting thresholds (pH 7.7–7.9) closely corroborated ecophysiological experiments performed on rhodolith species, such as *Lithothamnion glaciale* (Büdenbender et al., 2011) and *Lithothamnion corallioides* (Noisette et al., 2013). However, contrasting responses between and within rhodolith species have been reported due to many complex and occasionally site-specific conditions (Sañé et al., 2016; Qui-Minet et al., 2019). Such conditions cannot be fully incorporated into large-scale modeling due to lack of regional data, resulting in frequent interpolation of presence data into regions of suitable habitat, where species do not occur or are not known to occur. In this scope, models' predicted suitable habitats can overestimate the potentially realized coverage. In pursuit of reducing potential overestimation, a selection of the most relevant, meaningful and available

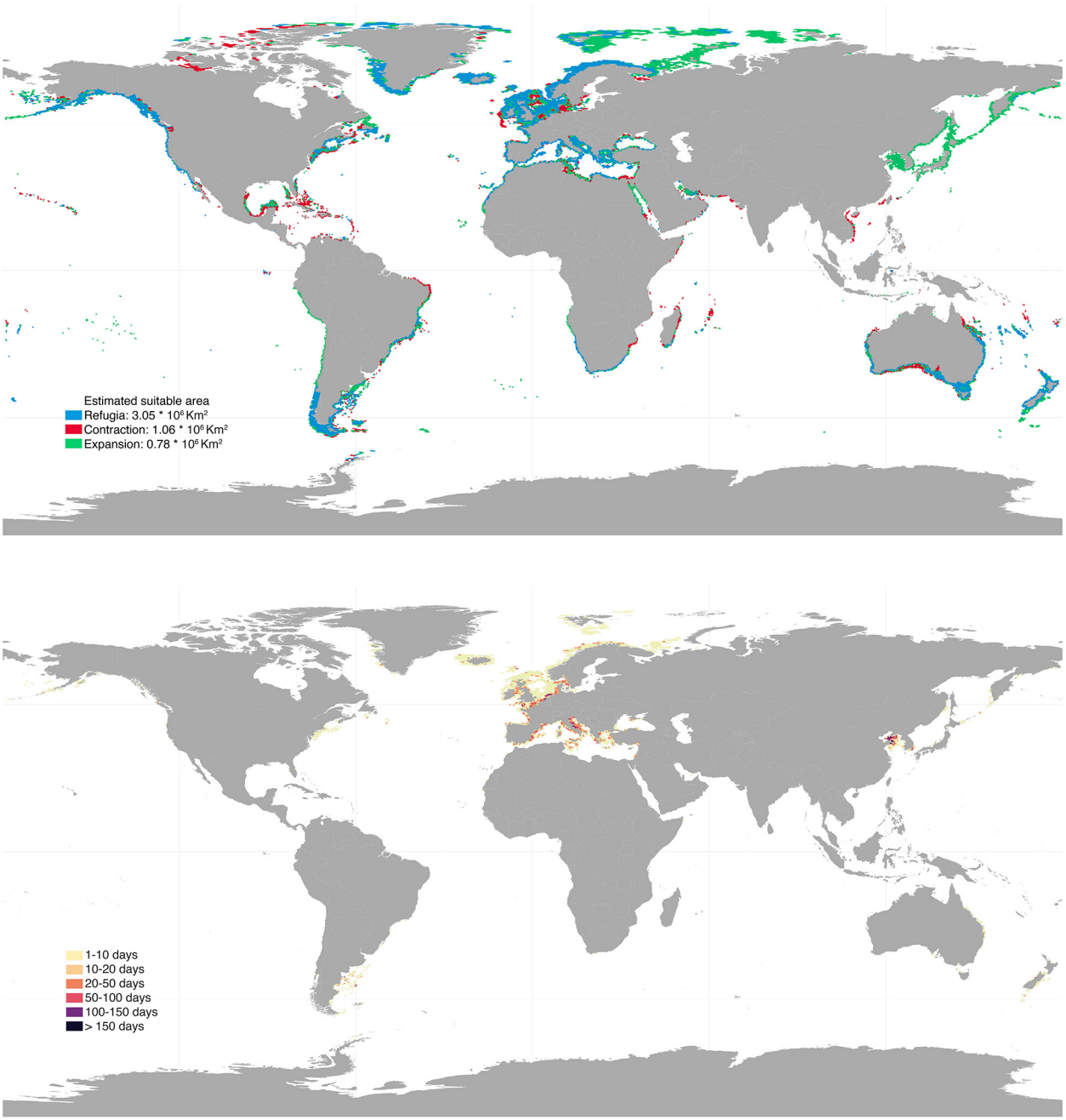

FIGURE 3 | Upper panel: global projected future distribution for rhodoliths under RCP 2.6 scenario. Blue, red, and green colors depict regions of refugia, range contraction and range expansion, respectively. Bottom panel: bottom trawling intensity (days per year) overlaying rhodolith suitable habitats under RCP 2.6. Results were aggregated for better visualization. High resolution maps can be found in **Supplementary Material**.

benthic predictors was used to achieve the best possible predictions at global scales (Carvalho et al., 2020). Our approach successfully identified well-known rhodolith banks, such as those in the northern Atlantic, Mediterranean, Caribbean, Australia and Brazil (Steller et al., 2003; Hall-Spencer et al., 2010; Amado-Filho et al., 2012a; Basso et al., 2016; Harvey et al., 2017), as well as recently discovered ones (e.g., South Africa; Adams et al., 2020). Additionally, by modeling the whole biome, we provide a first-order estimate of the potentially suitable rhodolith habitat globally, matching in scale that of macroalgae and exceeding by 10-fold the seagrass area (Short et al., 2007; Krause-Jensen and Duarte, 2016; Unsworth et al., 2019).

Our results further anticipate how future climate change might substantially affect the extent and geographical distribution of rhodoliths, particularly drastically under RCP 8.5. In line

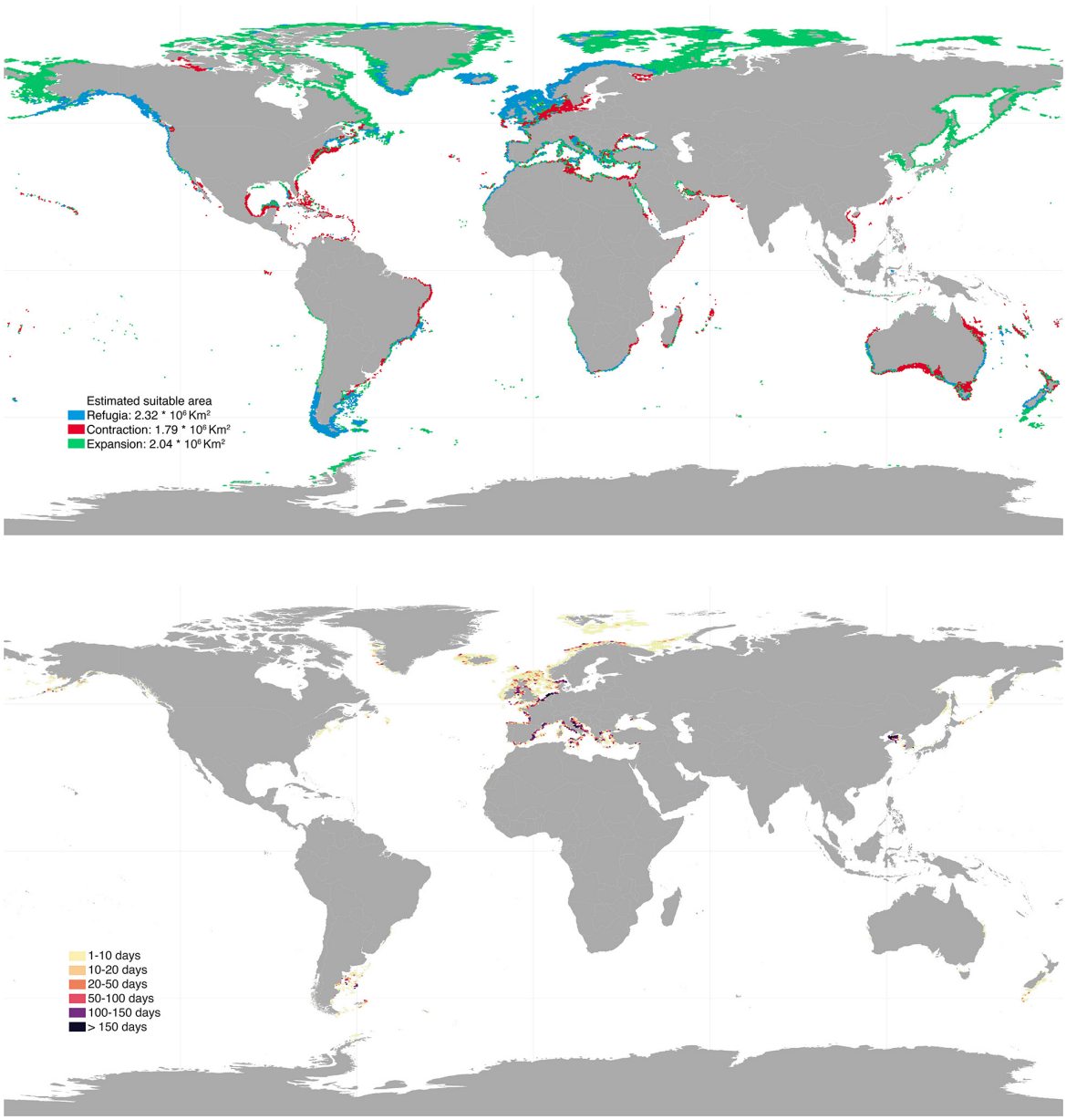

FIGURE 4 | Upper panel: global projected future distribution for rhodoliths under RCP 8.5 scenario. Blue, red, and green colors depict regions of refugia, range contraction and range expansion, respectively. Bottom panel: bottom trawling intensity (days per year) overlaying rhodolith suitable habitats under RCP 8.5. Results were aggregated for better visualization. High resolution maps can be found in **Supplementary Material**.

with global trends for marine biodiversity (e.g., Poloczanska et al., 2013; Beaugrand et al., 2015), the rhodolith biome is expected to undergo boreal and depth range shifts, coupled with habitat contractions at lower latitudes. Broader expansions are predicted along the Northern Pacific and Atlantic coasts (both east and west) and the Arctic, followed by smaller expansions in the southern hemisphere, constrained around the limited coastline of the few available islands. However, predicted expansions may be held back by the rhodolith limited dispersal and very slow growth rate (Blake and Maggs, 2003; Bosence and Wilson, 2003; Amado-Filho et al., 2012b; Pardo et al., 2019). Even if establishment is achieved, rhodoliths may affect the ecological balance and structure of the native communities (Ehrenfeld, 2010). Whereas, at the lower latitudes, depth range shifts might partially safeguard habitat suitability, extensive range contractions are predicted for many tropical and shallow regions.

Our models suggest that range contractions will intensify under the combination of high temperatures and ocean acidification (e.g., in the Gulf of Mexico and the Caribbean

Sea), corroborating previous experimental evidence with temperate (Noisette et al., 2013; Qui-Minet et al., 2019; Sordo et al., 2020) and tropical populations (Steller et al., 2007). Even in colder regions, such as the North Sea, the anticipated increase in acidification and temperature regimes is expected to result in range contraction (**Supplementary Figure 5**). The extensive projected losses may threaten regions of higher conservation value, with rich genetic and species diversity (Bittner et al., 2011; Basso et al., 2015; Gabrielson et al., 2018). Additionally, as rhodolith genetic and species diversity are still greatly underestimated (Twist et al., 2019; Caragnano et al., 2020), putative diversity losses may occur undetected, leading to potentially misperceived assessments of the rhodolith biome diversity and phylogeography, and gene pool conservation status (i.e., shifting genetic baselines; Assis et al., 2014). The exact ramifications of climate change on rhodolith ecosystems are hard to predict, as new insights on their role as bio-engineers and their complex relationships with associated species are only starting to be discovered (Steller et al., 2003; Horta et al., 2016; Gabara et al., 2018; Fredericq et al., 2019; Carvalho et al., 2020). For example, recent insights indicate that rhodoliths may be functioning as banks of microscopic stages (equivalent to seedbanks) for marine biodiversity, safeguarding species after local environmental stress incidents, as in the case of the 2010 Deepwater Horizon Oil Spill (Fredericq et al., 2019). As climate change is threatening the ecological balance of the complex and dynamic relationships shaped within the rhodolith ecosystems, potential cascading effects caused by species turnover (e.g., predominance of competitive fleshy algae) may lead to substantial biodiversity and biomass reduction of their entire ecosystem (Horta et al., 2016; Legrand et al., 2017; Gabara et al., 2018).

Combining distributional predictions through time yielded an estimate of climate refugia, i.e., key regions presenting suitable conditions for rhodoliths to thrive in both the present and future (Morelli et al., 2020). As rhodoliths support and promote high levels of biodiversity (Teichert, 2014; Gabara et al., 2018; Fredericq et al., 2019), their refugia may become important biodiversity hotspots and, therefore, high-priority conservation regions (Hoegh-Guldberg and Bruno, 2010; Groves et al., 2012). Such refugia were mainly predicted to persist in cold—temperate regions of the world, namely northern Mediterranean, northeast Atlantic and Pacific and south America (**Figures 3**, **4**). In the tropical regions, limited rhodolith suitable habitats may still be safeguarded by depth, particularly under the RCP 8.5 scenario, but, the mitigation of climate change impacts may not ensure persistence, if other, more localized disturbances (such as trawling) are acting in synergy with climate change (Halpern et al., 2008; O'Leary et al., 2017).

Rhodolith refugia are under great local threat from intensive bottom trawling (∼79,000–114,000 days annually), requiring urgent conservation management measures and regulation of this activity. Bottom trawling causes massive mortality of rhodoliths and their associated organisms, as it crushes, buries and eliminates any natural bottom features, while the plume of sediments lifted by trawling reduces light availability, blocks photosynthesis and contributes to additional losses of nearby, non-trawled rhodoliths (Hall-Spencer and Moore, 2000; Thrush and Dayton, 2002; Steller et al., 2003; Wilson et al., 2004; Gabara et al., 2018; Bernard et al., 2019). Such profound impacts are mostly irreversible and damages can still be observed for years post-trawling (Hall-Spencer and Moore, 2000; but see Barberá et al., 2017; Ordines et al., 2017). The limited rhodolith growth rate confers them an almost non-renewable resource status over human-relevant timescales (Blake and Maggs, 2003; Bosence and Wilson, 2003; Wilson et al., 2004).

Although rhodoliths are listed as an endangered landscape and trawling is prohibited over two of the most common species in Europe (*Lithothamnion coralliodes* and *Phymatolithon calcareum*; Barbera et al., 2003), we show that globally, the rhodolith biome may be lacking efficient protection. All the more, our findings might be underestimating the extent of trawled rhodoliths, since not all countries have or report fishing data and because the available trawling data were just a snapshot of the global fishing activity between 2012 and 2015 (Anticamara et al., 2011; Kroodsma et al., 2018). In fact, bottom trawling has been going on for centuries and especially around Europe (de Groot, 1984; Thurstan et al., 2014), where most of the long-term suitable rhodolith habitats are predicted. Such evidence indicates that trawling could have already caused broad-scale habitat disturbance on the European rhodolith ecosystems.

To our knowledge, our findings provide the first global estimate of the (present and future) rhodolith biome distribution, while discussing the potential combined effects of local stressors and future climate change. The identification of key climate refugia areas can guide future conservation management strategies and help prioritize areas for conservation in which populations will persist under climate change (Groves et al., 2012; Morelli et al., 2016). Extensive range shifts are already being observed, but more aggressive changes are expected. Considering the uncertainty of climate scenarios and the difficulty of ensuring international cooperation to meet the goals of the Paris agreement to reduce the rate of emissions (UN Framework Convention on Climate Change), reducing stressors in the local scale is an effective way to successfully mitigate some of the major impacts these ecosystems face. This can be achieved in the short/mid-term by governmental regulations to change fishing grounds or replace highly destructive fishing gears. Such actions may contribute to a rapid reduction of the direct destruction of these ecosystems, determining the fate of important biomes to sustain marine biodiversity in general.

DATA AVAILABILITY STATEMENT

The original contributions presented in the study are included in the article/**Supplementary Material**. Original rasters with model predictions and the modeling scripts can be found in figshare: https://doi.org/10.6084/m9.figshare.13295786.v2. Any further inquiries can be directed to the corresponding author/s.

AUTHOR CONTRIBUTIONS

ES, JA, and EF conceived the study. JA produced and provided the scripts for the analyses. EF compiled the data and conducted the analyses and drafted the manuscript with the support of JA, ES, PH, and GK. All authors edited the manuscript before submission.

FUNDING

This study was supported by the Foundation for Science and Technology (FCT) of Portugal through the project UIDB/ 04326/2020, PTDC/BIA-CBI/6515/2020, fellowships SFRH/BD/ 144878/2019, SFRH/BSAB/150485/2019, the transitional norm—DL57/2016/CP1361/CT0035, and by a Pew Marine Fellowship.

ACKNOWLEDGMENTS

We thank the two reviewers for their very constructive suggestions that help substantially to the improvement of our manuscript.

SUPPLEMENTARY MATERIAL

The Supplementary Material for this article can be found online at: https://www.frontiersin.org/articles/10.3389/fmars.2020.594537/full#supplementary-material

REFERENCES

Abella, E., Barberá, C., Borg, J. A., Glemarec, M., Grall, J., Hall-Spencer, J. M., et al. (1998). "Maërl grounds: habitats of high biodiversity in European seas," in *Proceedings of the Third European Marine Science and Technology Conference*, Lisbon, 170–179.

Adams, L. A., Maneveldt, G. W., Green, A., Karenyi, N., Parker, D., Samaai, T., et al. (2020). Rhodolith bed discovered off the South African coast. *Diversity* 12:125. doi: 10.3390/d12040125

Allouche, O., Tsoar, A., and Kadmon, R. (2006). Assessing the accuracy of species distribution models: prevalence, kappa and the true skill statistic (TSS). *J. Appl. Ecol.* 43, 1223–1232. doi: 10.1111/j.1365-2664.2006.01214.x

Amado-Filho, G. (2010). Seaweed diversity associated with a Brazilian tropical rhodolith bed. *Ciencias Mar.* 36, 371–391. doi: 10.7773/cm.v36i4.1782

Amado-Filho, G. M., Moura, R. L., Bastos, A. C., Salgado, L. T., Sumida, P. Y., Guth, A. Z., et al. (2012a). Rhodolith beds are major CaCO 3 BIO-factories in the tropical south West Atlantic. *PLoS One* 7:e0035171. doi: 10.1371/journal.pone.0035171

Amado-Filho, G. M., Pereira-Filho, G. H., Bahia, R. G., Abrantes, D. P., Veras, P. C., and Matheus, Z. (2012b). Occurrence and distribution of rhodolith beds on the Fernando de Noronha Archipelago of Brazil. *Aquat. Bot.* 101, 41–45. doi: 10.1016/j.aquabot.2012.03.016

Anticamara, J. A., Watson, R., Gelchu, A., and Pauly, D. (2011). Global fishing effort (1950-2010): trends, gaps, and implications. *Fish. Res.* 107, 131–136. doi: 10.1016/j.fishres.2010.10.016

Araújo, M. B., and New, M. (2007). Ensemble forecasting of species distributions. *Trends Ecol. Evol.* 22, 42–47. doi: 10.1016/j.tree.2006.09.010

Arias-Ortiz, A., Serrano, O., Masqué, P., Lavery, P. S., Mueller, U., Kendrick, G. A., et al. (2018). A marine heatwave drives massive losses from the world's largest seagrass carbon stocks. *Nat. Clim. Chang.* 8, 1–7. doi: 10.1038/s41558-018-0096-y

Assis, J., Araújo, M. B., and Serrão, E. A. (2018). Projected climate changes threaten ancient refugia of kelp forests in the North Atlantic. *Glob. Chang. Biol.* 24, e55–e66. doi: 10.1111/gcb.13818

Assis, J., Berecibar, E., Claro, B., Alberto, F., Reed, D., Raimondi, P., et al. (2017a). Major shifts at the range edge of marine forests: the combined effects of climate changes and limited dispersal. *Sci. Rep.* 7, 1–10. doi: 10.1038/srep44348

Assis, J., Serrão, E. A., Claro, B., Perrin, C., and Pearson, G. A. (2014). Climate-driven range shifts explain the distribution of extant gene pools and predict future loss of unique lineages in a marine brown alga. *Mol. Ecol.* 23, 2797–2810. doi: 10.1111/mec.12772

Assis, J., Tyberghein, L., Bosch, S., Verbruggen, H., Serrão, E. A., and De Clerck, O. (2017b). Bio-ORACLE v2.0: extending marine data layers for bioclimatic modelling. *Glob. Ecol. Biogeogr.* 27, 277–284. doi: 10.1111/geb.12693

Barbera, C., Bordehore, C., Borg, J. A., Glémarec, M., Grall, J., Hall-Spencer, J. M., et al. (2003). Conservation and management of northeast Atlantic and Mediterranean maerl beds. *Aquat. Conserv. Mar. Freshw. Ecosyst.* 13, 65–76. doi: 10.1002/aqc.569

Barberá, C., Mallol, S., Vergés, A., Cabanellas-Reboredo, M., Díaz, D., and Goñi, R. (2017). Maerl beds inside and outside a 25-year-old no-take area. *Mar. Ecol. Prog. Ser.* 572, 77–90. doi: 10.3354/meps12110

Basso, D., Babbini, L., Kaleb, S., Bracchi, V. A., and Falace, A. (2016). Monitoring deep Mediterranean rhodolith beds. *Aquat. Conserv. Mar. Freshw. Ecosyst.* 26, 549–561. doi: 10.1002/aqc.2586

Basso, D., Caragnano, A., Le Gall, L., and Rodondi, G. (2015). The genus Lithophyllum in the north-western Indian Ocean, with description of *L. yemenense* sp. nov., *L. socotraense* sp. nov., *L. subplicatum* comb. et stat. nov., and the resumed *L. affine*, *L. kaiseri*, and *L. subreduncum* (Rhodophyta, Corallinales). *Phytotaxa* 208, 183–200. doi: 10.11646/phytotaxa.208.3.1

Beaugrand, G., Edwards, M., Raybaud, V., Goberville, E., and Kirby, R. R. (2015). Future vulnerability of marine biodiversity compared with contemporary and past changes. *Nat. Clim. Chang.* 5, 695–701. doi: 10.1038/nclimate2650

Bernard, G., Romero-Ramirez, A., Tauran, A., Pantalos, M., Deflandre, B., Grall, J., et al. (2019). Declining maerl vitality and habitat complexity across a dredging gradient: insights from in situ sediment profile imagery (SPI). *Sci. Rep.* 9, 1–12. doi: 10.1038/s41598-019-52586-8

Bittner, L., Payri, C. E., Maneveldt, G. W., Couloux, A., Cruaud, C., de Reviers, B., et al. (2011). Evolutionary history of the Corallinales (Corallinophycidae, Rhodophyta) inferred from nuclear, plastidial and mitochondrial genomes. *Mol. Phylogenet. Evol.* 61, 697–713. doi: 10.1016/j.ympev.2011.07.019

Blake, C., and Maggs, C. A. (2003). Comparative growth rates and internal banding periodicity of maerl species (Corallinales, Rhodophyta) from northern Europe. *Phycologia* 42, 606–612. doi: 10.2216/i0031-8884-42-6-606.1

Boavida, J., Assis, J., Silva, I., and Serrão, E. A. (2016). Overlooked habitat of a vulnerable gorgonian revealed in the Mediterranean and Eastern Atlantic by ecological niche modelling. *Sci. Rep.* 6:36460. doi: 10.1038/srep36460

Bosence, D., and Wilson, J. (2003). Maerl growth, carbonate production rates and accumulation rates in the northeast Atlantic. *Aquat. Conserv. Mar. Freshw. Ecosyst.* 13, S21–S31. doi: 10.1002/aqc.565

Büdenbender, J., Riebesell, U., and Form, A. (2011). Calcification of the Arctic coralline red algae *Lithothamnion glaciale* in response to elevated CO 2. *Mar. Ecol. Prog. Series* 441, 79–87. doi: 10.3354/meps09405

Caragnano, A., Rodondi, G., Basso, D., Peña, V., le Gall, L., and Rindi, F. (2020). Circumscription of *Lithophyllum racemus* (Corallinales, Rhodophyta) from the western Mediterranean Sea reveals the species *Lithophyllum pseudoracemus* sp. nov. *Phycologia* [Epub ahead of print]. doi: 10.1080/00318884.2020.1829348

Carilli, J. E., Norris, R. D., Black, B., Walsh, S. M., and Mcfield, M. (2010). Century-scale records of coral growth rates indicate that local stressors reduce coral thermal tolerance threshold. *Glob. Chang. Biol.* 16, 1247–1257. doi: 10.1111/j.1365-2486.2009.02043.x

Carpenter, K. E., Abrar, M., Aeby, G., Aronson, R. B., Banks, S., Bruckner, A., et al. (2008). One-Third of Reef-Building Corals Face Elevated Extinction Risk from

Climate Change and Local Impacts. *Science* 321, 560–563. doi: 10.1126/science.1159196

Carvalho, V. F., Assis, J., Serrão, E. A., Nunes, J. M., Anderson, A. B., Batista, M. B., et al. (2020). Environmental drivers of rhodolith beds and epiphytes community along the South Western Atlantic coast. *Mar. Environ. Res.* 154:104827. doi: 10.1016/j.marenvres.2019.104827

Cheung, W. W. L., Lam, V. W. Y., Sarmiento, J. L., Kearney, K., Watson, R., and Pauly, D. (2009). Projecting global marine biodiversity impacts under climate change scenarios. *Fish Fish.* 10, 235–251. doi: 10.1111/j.1467-2979.2008.00315.x

Costello, M. J., Coll, M., Danovaro, R., Halpin, P., Ojaveer, H., and Miloslavich, P. (2010). A census of marine biodiversity knowledge, resources, and future challenges. *PLoS One* 5:e0012110. doi: 10.1371/journal.pone.0012110

de Groot, S. J. (1984). The impact of bottom trawling on benthic fauna of the North Sea. *Ocean Manag.* 9, 177–190. doi: 10.1016/0302-184X(84)90002-7

De'ath, G. (2007). Boosted trees for ecological modeling and prediction. *Ecology* 88, 243–251.

Ehrenfeld, J. G. (2010). Ecosystem consequences of biological invasions. *Annu. Rev. Ecol. Evol. Syst.* 41, 59–80. doi: 10.1146/annurev-ecolsys-102209-144650

Elith, J., Leathwick, J. R., and Hastie, T. (2008). A working guide to boosted regression trees. *J. Anim. Ecol.* 77, 802–813. doi: 10.1111/j.1365-2656.2008.01390.x

Fielding, A. H., and Bell, J. F. (1997). A review of methods for the assessment of prediction errors in conservation presence/absence models. *Environ. Conserv.* 24, 38–49. doi: 10.1017/S0376892997000088

Fredericq, S., Krayesky-Self, S., Sauvage, T., Richards, J., Kittle, R., Arakaki, N., et al. (2019). The critical importance of rhodoliths in the life cycle completion of both macro- and microalgae, and as holobionts for the establishment and maintenance of marine biodiversity. *Front. Mar. Sci.* 5:502. doi: 10.3389/fmars.2018.00502

Gabara, S. S., Hamilton, S. L., Edwards, M. S., and Steller, D. L. (2018). Rhodolith structural loss decreases abundance, diversity, and stability of benthic communities at santa catalina island. *CA Mar. Ecol. Prog. Ser.* 595, 71–88. doi: 10.3354/meps12528

Gabrielson, P. W., Hughey, J. R., and Diaz-Pulido, G. (2018). Genomics reveals abundant speciation in the coral reef building alga *Porolithon onkodes* (Corallinales, Rhodophyta). *J. Phycol.* 54, 429–434. doi: 10.1111/jpy.12761

García Molinos, J., Halpern, B. S. S., Schoeman, D. S. S., Brown, C. J. J., Kiessling, W., Moore, P. J. J., et al. (2015). Climate velocity and the future global redistribution of marine biodiversity. *Nat. Clim. Chang.* 6, 4–11. doi: 10.1038/nclimate2769

GBIF.org (2020). *GBIF Home Page*. Available online at: https://www.gbif.org (accessed October 20, 2020).

Gran, H. H. (1893). Algevegetationen i Tønsbergfjorden. Skrifter udgivne af Videnskabsselskabet i Christiania. I. *Math. Naturvidenskabelig Klasse* 1893, 1–38.

Groves, C. R., Game, E. T., Anderson, M. G., Cross, M., Enquist, C., Ferdaña, Z., et al. (2012). Incorporating climate change into systematic conservation planning. *Biodivers. Conserv.* 21, 1651–1671. doi: 10.1007/s10531-012-0269-3

Gurney, G. G., Melbourne-Thomas, J., Geronimo, R. C., Aliño, P. M., and Johnson, C. R. (2013). Modelling coral reef futures to inform management: can reducing local-scale stressors conserve reefs under climate change? *PLoS One* 8:e0080137. doi: 10.1371/journal.pone.0080137

Hall-Spencer, J. M., Kelly, J., and Maggs, C. A. (2010). *Background Document for Maërl beds Biodiversity Series*. London: OSPAR.

Hall-Spencer, J. M., and Moore, P. G. (2000). Scallop dredging has profound, long-term impacts on maerl habitats. *ICES J. Mar. Sci.* 57, 1407–1415. doi: 10.1006/jmsc.2000.0918

Halpern, B. S., Frazier, M., Potapenko, J., Casey, K. S., Koenig, K., Longo, C., et al. (2015). Spatial and temporal changes in cumulative human impacts on the world's ocean. *Nat. Commun.* 6:7615. doi: 10.1038/ncomms8615

Halpern, B. S., Walbridge, S., Selkoe, K. A., Kappel, C. V., Micheli, F., D'Agrosa, C., et al. (2008). A global map of human impact on marine ecosystems. *Science* 319, 948–952. doi: 10.1126/science.1149345

Harvey, A. S., Harvey, R. M., and Merton, E. (2017). The distribution, significance and vulnerability of Australian rhodolith beds: a review. *Mar. Freshw. Res.* 68, 411–428. doi: 10.1071/MF15434

Hewitt, G. M. (2004). Genetic consequences of climatic oscillations in the Quaternary. *Philos. Trans. R. Soc. B Biol. Sci.* 359, 183–195. doi: 10.1098/rstb.2003.1388

Hoegh-Guldberg, O., and Bruno, J. F. (2010). The impact of climate change on the World's marine ecosystems. *Science* 328, 1523–1528. doi: 10.1126/science.1189930

Horta, P. A., Riul, P., Amado Filho, G. M., Gurgel, C. F. D., Berchez, F., Nunes, J. M., et al. (2016). Rhodoliths in Brazil: current knowledge and potential impacts of climate change. *Braz. J. Oceanogr.* 64, 117–136. doi: 10.1590/S1679-875920160870064sp2

Hothorn, T., Bühlmann, P., Kneib, T., Schmid, M., and Hofner, B. (2010). Model-based boosting 2.0. *J. Mach. Learn. Res.* 11, 2109–2113.

Hudges, T. P., Kerry, J. T., Baird, A. H., Connolly, S. R., Dietzel, A., Eakin, C. M., et al. (2018). Global warming transforms coral reef assemblages. *Nature* 556, 492–496.

Jayathilake, D. R. M., and Costello, M. J. (2018). A modelled global distribution of the seagrass biome. *Biol. Conserv.* 226, 120–126. doi: 10.1016/j.biocon.2018.07.009

Keppel, G., Van Niel, K. P., Wardell-Johnson, G. W., Yates, C. J., Byrne, M., Mucina, L., et al. (2012). Refugia: identifying and understanding safe havens for biodiversity under climate change. *Glob. Ecol. Biogeogr.* 21, 393–404. doi: 10.1111/j.1466-8238.2011.00686.x

Krause-Jensen, D., and Duarte, C. M. (2016). Substantial role of macroalgae in marine carbon sequestration. *Nat. Geosci.* 9, 737–742. doi: 10.1038/ngeo2790

Kroeker, K. J., Kordas, R. L., Crim, R. N., and Singh, G. G. (2010). Meta-analysis reveals negative yet variable effects of ocean acidification on marine organisms. *Ecol. Lett.* 13, 1419–1434. doi: 10.1111/j.1461-0248.2010.01518.x

Kroodsma, D. A., Mayorga, J., Hochberg, T., Miller, N. A., Boerder, K., Ferretti, F., et al. (2018). Tracking the global footprint of fisheries. *Science* 359, 904–908. doi: 10.1126/science.aao5646

Leadley, P., Pereira, H., Alkemade, R., Fernandez, J. F., Scharlemann, J. P. W., Proenca, V., et al. (2010). *Biodiversity Scenarios: Projections of 21st century change in biodiversity and Associated Ecosystem Services*. Technical Series no. 50. Cambridge, MA: WCMC.

Legrand, E., Riera, P., Lutier, M., Grall, J., and Martin, S. (2017). Species interactions can shift the response of a maerl bed community to ocean acidification and warming. *Biogeosciences* 14, 5359–5376. doi: 10.5194/bg-14-5359-2017

Marbà, N., and Duarte, C. M. (2010). Mediterranean warming triggers seagrass (Posidonia oceanica) shoot mortality. *Glob. Chang. Biol.* 16, 2366–2375. doi: 10.1111/j.1365-2486.2009.02130.x

Martin, S., and Hall-Spencer, J. M. (2017). "Effects of ocean warming and acidification on rhodolith/maërl beds," in *Rhodolith/Maërl Beds: A Global Perspective*, eds W. Nelson, J. Aguirre, and R. Riosmena-Rodríguez (Cham: Springer), 55–85.

Morelli, T. L., Barrows, C. W., Ramirez, A. R., Cartwright, J. M., Ackerly, D. D., Eaves, T. D., et al. (2020). Climate change refugia: biodiversity change in the slow lane. *Front. Ecol. Environ.* 18, 228–234. doi: 10.1002/fee.2189

Morelli, T. L., Daly, C., Dobrowski, S. Z., Dulen, D. M., Ebersole, J. L., Jackson, S. T., et al. (2016). Managing climate change refugia for climate adaptation. *PLoS One* 11:e0159909. doi: 10.1371/journal.pone.0159909

Moss, R. H., Edmonds, J. A., Hibbard, K. A., Manning, M. R., Rose, S. K., Van Vuuren, D. P., et al. (2010). The next generation of scenarios for climate change research and assessment. *Nature* 463, 747–756. doi: 10.1038/nature08823

Noisette, F., Duong, G., Six, C., Davoult, D., and Martin, S. (2013). Effects of elevated pCO2 on the metabolism of a temperate rhodolith Lithothamnion corallioides grown under different temperatures. *J. Phycol.* 49, 746–757. doi: 10.1111/jpy.12085

OBIS (2020). *Ocean Biodiversity Information System. Intergov. Oceanogr. Comm.* Paris: UNESCO.

O'Leary, J. K., Micheli, F., Airoldi, L., Boch, C., De Leo, G., Elahi, R., et al. (2017). The resilience of marine ecosystems to climatic disturbances. *Bioscience* 67, 208–220. doi: 10.1093/biosci/biw161

Olsgard, F., Schaanning, M. T., Widdicombe, S., Kendall, M. A., and Austen, M. C. (2008). Effects of bottom trawling on ecosystem functioning. *J. Exp. Mar. Bio. Ecol.* 366, 123–133. doi: 10.1016/j.jembe.2008.07.036

Ordines, F., Ramón, M., Rivera, J., Rodríguez-Prieto, C., Farriols, M. T., Guijarro, B., et al. (2017). Why long term trawled red algae beds off Balearic Islands

(western Mediterranean) still persist? *Reg. Stud. Mar. Sci.* 15, 39–49. doi: 10.1016/j.rsma.2017.07.005

Pardo, C., Guillemin, M. L., Peña, V., Bárbara, I., Valero, M., and Barreiro, R. (2019). Local coastal configuration rather than latitudinal gradient shape clonal diversity and genetic structure of *Phymatolithon calcareum* maerl beds in North European Atlantic. *Front. Mar. Sci.* 6:149. doi: 10.3389/fmars.2019.00149

Pecl, G. T., Araújo, M. B., Bell, J. D., Blanchard, J., Bonebrake, T. C., Chen, I. C., et al. (2017). Biodiversity redistribution under climate change: impacts on ecosystems and human well-being. *Science* 355:eaai9214. doi: 10.1126/science.aai9214

Pezzolesi, L., Peña, V., Le Gall, L., Gabrielson, P. W., Kaleb, S., Hughey, J. R., et al. (2019). Mediterranean *Lithophyllum stictiforme* (Corallinales, Rhodophyta) is a genetically diverse species complex: implications for species circumscription, biogeography and conservation of coralligenous habitats. *J. Phycol.* 55, 473–492. doi: 10.1111/jpy.12837

Poloczanska, E. S., Brown, C. J., Sydeman, W. J., Kiessling, W., Schoeman, D. S., Moore, P. J., et al. (2013). Global imprint of climate change on marine life. *Nat. Clim. Chang.* 3, 919–925. doi: 10.1038/Nclimate1958

Provan, J., and Bennett, K. D. (2008). Phylogeographic insights into cryptic glacial refugia. *Trends Ecol. Evol.* 23, 564–571. doi: 10.1016/j.tree.2008.06.010

Pruvot, G. (1897). Essai sur les fonds et la faune de la Manche occidentale comparés à ceux du Golfe du Lion. *Irch. Zooz. Exp. Gén.* 5, 511–617.

Qui-Minet, Z. N., Coudret, J., Davoult, D., Grall, J., Mendez-Sandin, M., Cariou, T., et al. (2019). Combined effects of global climate change and nutrient enrichment on the physiology of three temperate maerl species. *Ecol. Evol.* 9, 13787–13807. doi: 10.1002/ece3.5802

R Development Core Team (2018). *A Language and Environment for Statistical Computing*. Vienna: R Found. Stat. Comput.

Riosmena-Rodriguez, R., Wendy, N., and Aguirre, J. (2017). *Rhodolith/Maërl Beds: A Global Perspective*. Cham: Springer International Publishing.

Sañé, E., Chiocci, F. L., Basso, D., and Martorelli, E. (2016). Environmental factors controlling the distribution of rhodoliths: an integrated study based on seafloor sampling, ROV and side scan sonar data, offshore the W-Pontine Archipelago. *Cont. Shelf Res.* 129, 10–22. doi: 10.1016/j.csr.2016.09.003

Sasaki, T., Furukawa, T., Iwasaki, Y., Seto, M., and Mori, A. S. (2015). Perspectives for ecosystem management based on ecosystem resilience and ecological thresholds against multiple and stochastic disturbances. *Ecol. Indic.* 57, 395–408. doi: 10.1016/j.ecolind.2015.05.019

Short, F., Carruthers, T., Dennison, W., and Waycott, M. (2007). Global seagrass distribution and diversity: a bioregional model. *J. Exp. Mar. Bio. Ecol.* 350, 3–20. doi: 10.1016/j.jembe.2007.06.012

Sordo, L., Santos, R., Barrote, I., Freitas, C., and Silva, J. (2020). Seasonal photosynthesis, respiration, and calcification of a temperate maërl bed in Southern Portugal. *Front. Mar. Sci.* 7:136. doi: 10.3389/fmars.2020.00136

Spalding, M. D., Fox, H. E., Allen, G. R., Davidson, N., Ferdaña, Z. A., Finlayson, M., et al. (2007). Marine ecoregions of the world: a bioregionalization of coastal and shelf areas. *Bioscience* 57:573. doi: 10.1641/B570707

Steller, D. L., Riosmena-Rodríguez, R., Foster, M. S., and Roberts, C. A. (2003). Rhodolith bed diversity in the Gulf of California: the importance of rhodolith structure and consequences of disturbance. *Aquat. Conserv. Mar. Freshw. Ecosyst.* 13, 5–20. doi: 10.1002/aqc.564

Steller, D. L., Hernández-Ayon, J., Riosmena-Rodríguez, R., and Cabello-Pasini, A. (2007). Effect of temperature on photosynthesis, growth and calcification rates of the free-living coralline alga Lithophyllum margaritae. *Cienc. Mar.* 33, 441–456. doi: 10.7773/cm.v33i4.1255

Strain, E. M. A., Van Belzen, J., Van Dalen, J., Bouma, T. J., and Airoldi, L. (2015). Management of local stressors can improve the resilience of marine canopy algae to global stressors. *PLoS One* 10:e0120837. doi: 10.1371/journal.pone.0120837

Teichert, S. (2014). Hollow rhodoliths increase Svalbard's shelf biodiversity. *Sci. Rep.* 4:6972. doi: 10.1038/srep06972

Thrush, S. F., and Dayton, P. K. (2002). Disturbance to marine benthic habitats by trawling and dredging: implications for marine biodiversity. *Annu. Rev. Ecol. Syst.* 33, 449–473. doi: 10.1146/annurev.ecolsys.33.010802.150515

Thurstan, R. H., Hawkins, J. P., and Roberts, C. M. (2014). Origins of the bottom trawling controversy in the British Isles: 19th century witness testimonies reveal evidence of early fishery declines. *Fish Fish.* 15, 506–522. doi: 10.1111/faf.12034

Tillin, H. M., Hiddink, J. G., Jennings, S., and Kaiser, M. J. (2006). Chronic bottom trawling alters the functional composition of benthic invertebrate communities on a sea-basin scale. *Mar. Ecol. Prog. Ser.* 318, 31–45. doi: 10.3354/meps318031

Twist, B. A., Neill, K. F., Bilewitch, J., Jeong, S. Y., Sutherland, J. E., and Nelson, W. A. (2019). High diversity of coralline algae in New Zealand revealed: knowledge gaps and implications for future research. *PLoS One* 14:e0225645. doi: 10.1371/journal.pone.0225645

Tyberghein, L., Verbruggen, H., Pauly, K., Troupin, C., Mineur, F., and De Clerck, O. (2012). Bio-ORACLE: a global environmental dataset for marine species distribution modelling. *Glob. Ecol. Biogeogr.* 21, 272–281. doi: 10.1111/j.1466-8238.2011.00656.x

Unsworth, R. K. F., McKenzie, L. J., Collier, C. J., Cullen-Unsworth, L. C., Duarte, C. M., Eklöf, J. S., et al. (2019). Global challenges for seagrass conservation. *Ambio* 48, 801–815. doi: 10.1007/s13280-018-1115-y

Valavi, R., Elith, J., Lahoz-Monfort, J. J., and Guillera-Arroita, G. (2019). Block CV: an R package for generating spatially or environmentally separated folds for k-fold cross-validation of species distribution models. *Methods Ecol. Evol.* 10, 225–232. doi: 10.1111/2041-210X.13107

van der Heijden, L. H., and Kamenos, N. A. (2015). Calculating the global contribution of coralline algae to carbon burial. *Biogeosci. Discuss.* 12, 7845–7877. doi: 10.5194/bgd-12-7845-2015

Veras, P., de, C., Pierozzi, I. Jr., Lino, J. B., Amado-Filho, G. M., Senna, A. R., et al. (2020). Drivers of biodiversity associated with rhodolith beds from euphotic and mesophotic zones: insights for management and conservation. *Perspect. Ecol. Conserv.* 18, 37–43. doi: 10.1016/j.pecon.2019.12.003

Villas-Bôas, A. B., de Sousa Tâmega, F. T., Andrade, M., Coutinho, R., and de Oliveira Figueiredo, M. A. (2014). Experimental effects of sediment burrial and light attenuation on two coralline algae of a deep water rhodolith bed in Rio de Janeiro, Brazil. *Cryptogamie Algologie* 35, 67–76. doi: 10.7872/crya.v35.iss1.2014.67

Wernberg, T., Bennett, S., Babcock, R. C., Bettignies, T., De Cure, K., Depczynski, M., et al. (2015). Climate-driven regime shift of a temperate marine ecosystem. *Science* 353, 169–172. doi: 10.1126/science.aad8745

Wilson, S., Blake, C., Berges, J. A., and Maggs, C. A. (2004). Environmental tolerances of free-living coralline algae (maerl): implications for European marine conservation. *Biol. Conserv.* 120, 279–289. doi: 10.1016/j.biocon.2004.03.001

Conflict of Interest: The authors declare that the research was conducted in the absence of any commercial or financial relationships that could be construed as a potential conflict of interest.

frontiers in Marine Science

PERSPECTIVE
published: 05 March 2021
doi: 10.3389/fmars.2021.591292

Needs and Gaps in Optical Underwater Technologies and Methods for the Investigation of Marine Animal Forest 3D-Structural Complexity

Paolo Rossi[1,2], Massimo Ponti[2,3,4], Sara Righi[2,5], Cristina Castagnetti[1,2], Roberto Simonini[2,5], Francesco Mancini[1,2], Panagiotis Agrafiotis[6], Leonardo Bassani[7], Fabio Bruno[2,8], Carlo Cerrano[2,9,10], Paolo Cignoni[11], Massimiliano Corsini[11], Pierre Drap[12], Marco Dubbini[7], Joaquim Garrabou[11,12], Andrea Gori[13], Nuno Gracias[14], Jean-Baptiste Ledoux[15,16], Cristina Linares[13], Torcuato Pulido Mantas[9], Fabio Menna[17], Erica Nocerino[12], Marco Palma[18,19], Gaia Pavoni[11], Alessandro Ridolfi[2,20,21], Sergio Rossi[2,22,23], Dimitrios Skarlatos[24], Tali Treibitz[25], Eva Turicchia[2,4,26], Matan Yuval[25] and Alessandro Capra[1,2]*

[1] Department of Engineering "Enzo Ferrari", University of Modena and Reggio Emilia, Modena, Italy, [2] Consorzio Nazionale Interuniversitario per le Scienze del Mare (CoNISMa), Rome, Italy, [3] Biological, Geological and Environmental Sciences Department, University of Bologna, Bologna, Italy, [4] Centro Interdipartimentale di Ricerca Industriale Fonti Rinnovabili, Ambiente, Mare ed Energia, University of Bologna, Ravenna, Italy, [5] Life Sciences Department, University of Modena and Reggio Emilia, Modena, Italy, [6] Department of Topography, School of Rural and Surveying Engineering, National Technical University of Athens, Athens, Greece, [7] Department of History, Cultures and Civilizations, University of Bologna, Bologna, Italy, [8] Department of Mechanical, Energy and Management Engineering, University of Calabria, Rende, Italy, [9] Department of Life and Environmental Sciences, Polytechnic University of Marche, Ancona, Italy, [10] Stazione Zoologica Anton Dohrn, Naples, Italy, [11] Istituto di Scienza e Tecnologie dell'Informazione – Consiglio Nazionale delle Ricerche (ISTI-CNR), Pisa, Italy, [12] LIS UMR 7020, Aix-Marseille Université, Centre national de la recherche scientifique – École nationale Supérieure d'Architecture de Montpellier (CNRS-ENSAM), Université De Toulon, Domaine Universitaire de Saint-Jérôme, Marseille, France, [13] Department of Evolutionary Biology, Ecology and Environmental Sciences, Institut de Recerca de la Biodiversitat (IRBio), University of Barcelona, Barcelona, Spain, [14] Computer Vision and Robotics Institute, University of Girona, Girona, Spain, [15] Institute of Marine Sciences Consejo Superior de Investigaciones Científicas (CSIC), Barcelona, Spain, [16] Centro Interdisciplinar de Investigação Marinha e Ambiental (CIIMAR), Porto, Portugal, [17] 3DOM – 3D Optical Metrology Unit, Fondazione Bruno Kessler (FBK) – Bruno Kessler Foundation, Trento, Italy, [18] Underwater Bio-Cartography (UBICA) srl, Genova, Italy, [19] Habitats Edge Ltd., Norwich, United Kingdom, [20] Department of Industrial Engineering, University of Florence, Florence, Italy, [21] Interuniversity Center of Integrated Systems for the Marine Environment (ISME), Genova, Italy, [22] Department of Biological and Environmental Sciences and Technologies, University of Salento, Lecce, Italy, [23] Labomar, Universidade Federal do Ceará, Fortaleza, Brazil, [24] Civil Engineering and Geomatics Department, Cyprus University of Technology, Limassol, Cyprus, [25] School of Marine Sciences, University of Haifa, Haifa, Israel, [26] Department of Cultural Heritage, University of Bologna, Ravenna, Italy

Marine animal forests are benthic communities dominated by sessile suspension feeders (such as sponges, corals, and bivalves) able to generate three-dimensional (3D) frameworks with high structural complexity. The biodiversity and functioning of marine animal forests are strictly related to their 3D complexity. The present paper aims at providing new perspectives in underwater optical surveys. Starting from the current gaps in data collection and analysis that critically limit the study and conservation of marine animal forests, we discuss the main technological and methodological needs

OPEN ACCESS

Edited by:
Christos Dimitrios Arvanitidis, Hellenic Centre for Marine Research, Greece

Reviewed by:
Thanos Dailianis, Hellenic Centre for Marine Research, Greece
Julie Bremner, Centre for Environment, Fisheries and Aquaculture Science (CEFAS), United Kingdom

***Correspondence:**
Paolo Rossi
paolo.rossi@unimore.it

Specialty section:
This article was submitted to Marine Ecosystem Ecology, a section of the journal Frontiers in Marine Science

Received: *04 August 2020*
Accepted: *10 February 2021*
Published: *05 March 2021*

Citation:
Rossi P, Ponti M, Righi S, Castagnetti C, Simonini R, Mancini F, Agrafiotis P, Bassani L, Bruno F, Cerrano C, Cignoni P, Corsini M, Drap P, Dubbini M, Garrabou J, Gori A, Gracias N, Ledoux J-B, Linares C, Mantas TP, Menna F, Nocerino E, Palma M, Pavoni G, Ridolfi A, Rossi S, Skarlatos D, Treibitz T, Turicchia E, Yuval M and Capra A (2021) Needs and Gaps in Optical Underwater Technologies and Methods for the Investigation of Marine Animal Forest 3D-Structural Complexity. Front. Mar. Sci. 8:591292. doi: 10.3389/fmars.2021.591292

for the investigation of their 3D structural complexity at different spatial and temporal scales. Despite recent technological advances, it seems that several issues in data acquisition and processing need to be solved, to properly map the different benthic habitats in which marine animal forests are present, their health status and to measure structural complexity. Proper precision and accuracy should be chosen and assured in relation to the biological and ecological processes investigated. Besides, standardized methods and protocols are strictly necessary to meet the FAIR (findability, accessibility, interoperability, and reusability) data principles for the stewardship of habitat mapping and biodiversity, biomass, and growth data.

Keywords: biodiversity, 3D monitoring, semantic segmentation, underwater photogrammetry, biogenic reefs conservation

INTRODUCTION

Precise maps are nowadays easily available on the land surface, providing location, extent, and topography of terrestrial ecosystems. Interestingly, it is roughly calculated that only 5% of the oceans floor is accurately mapped at the ecological community level (Rossi and Orejas, 2019). Thus, a complete 3D and semantically enriched description of benthic habitats is required through a technologically improved and methodologically robust approach.

Marine animal forests are benthic communities dominated by sessile suspension feeders (such as sponges, gorgonians, scleractinian corals, and bivalves) able to generate 3D frameworks with high structural complexity (Rossi et al., 2017). These organisms act as habitat-forming species, since they "modulate the availability of resources (other than themselves) to other species by causing physical state changes in biotic or abiotic materials" (Jones et al., 1994). The complex structures resulting from their growth significantly enhance the heterogeneity in most environmental factors (such as light, current, food availability, or sediment suspension), providing habitats for other species, enhancing species diversity, and directly or indirectly participating in or promoting building of biogenic reefs (Rossi et al., 2017).

The overall bioconstruction rate of the biogenic reefs made or promoted by animal forests varies according to different prevailing species, but has often low values: for example, growth in height is estimated to range from less than a millimeter to few centimeters per year, depending on species and environmental conditions (Coma et al., 1998; Kružić and Benković, 2012; Ordoñez et al., 2019). Higher rates are typical of healthy tropical coral reefs dominated by branching corals, while lower rates occur in temperate and cold seas dominated by sponges, gorgonians or bivalves. Negative growth rates of biogenic structures may arise when biological and chemical-physical erosion processes dominate over the bioconstruction ones (Davidson et al., 2018). For example, in the Mediterranean biogenic reefs, the integrity of gorgonian populations is threatened by: (i) mechanical damage due to fishing lines and nets, anchorages, and recreational divers; (ii) suffocation by mucilaginous benthic aggregates; (iii) increased water turbidity and sedimentation rates as a result from poor land management (Ponti et al., 2018 and references therein); (iv) the invasion from non-indigenous and/or predator species (Maldonado et al., 2013; Righi et al., 2020). Moreover, climate change is one of the most concern threat since seawater warming, and higher frequency and severity of marine heatwaves have increased the mass mortalities of animal forests in both tropical and temperate seas (Garrabou et al., 2019). The vast decline of erect sponges and gorgonians in the Mediterranean Sea (Cerrano et al., 2000; Turicchia et al., 2018) is reducing considerably the structural complexity of these ecosystems, with important consequences for ecosystem biodiversity, functioning, and the services they provide (Verdura et al., 2019).

The study of marine animal forests down to the mesophotic zone is usually performed by scuba-diving surveys (Cerrano et al., 2019), using visual estimations, photo-sampling, and direct assessments of variables (e.g., colony size, percent cover, presence of necrosis/bleaching). Yet, accuracy of measurements and spatial replication are often not taken into consideration and some direct measures (e.g., annual growth rates) may still be based on destructive sampling (Peirano et al., 2001; Marschal et al., 2004). Since many invertebrates and their symbiotic algae contain fluorescent pigments, fluorometry and photographic image analysis are increasingly employed as a non-invasive proxy for organism health state and pathogenesis patterns (see Caldwell et al., 2017 for references), and to analyze their population dynamic; however, these studies are labor-intensive and require manual interpretation (Zweifler et al., 2017; Montero-Serra et al., 2019).

Technological developments have made optical and acoustic techniques practical to provide non-destructive measurement estimates of large sections of tropical coral reefs in 3D (House et al., 2018; Rossi et al., 2020), but their application in cold and temperate animal marine forests is still limited (Palma et al., 2018). Moreover additional efforts are still needed to obtain high definition reconstructions that range from aggregations to single organisms as well as subsequent reconstructions to allow tracing of a possible structural shift over time. Indeed, ranging from small to broad spatial scale of marine animal forests (**Figure 1**), the use of photogrammetry for georeferencing the samples and for spatial data acquisition is a promising tool to study many aspects of these communities and evaluate ecological key parameters, from organism health to the species interactions

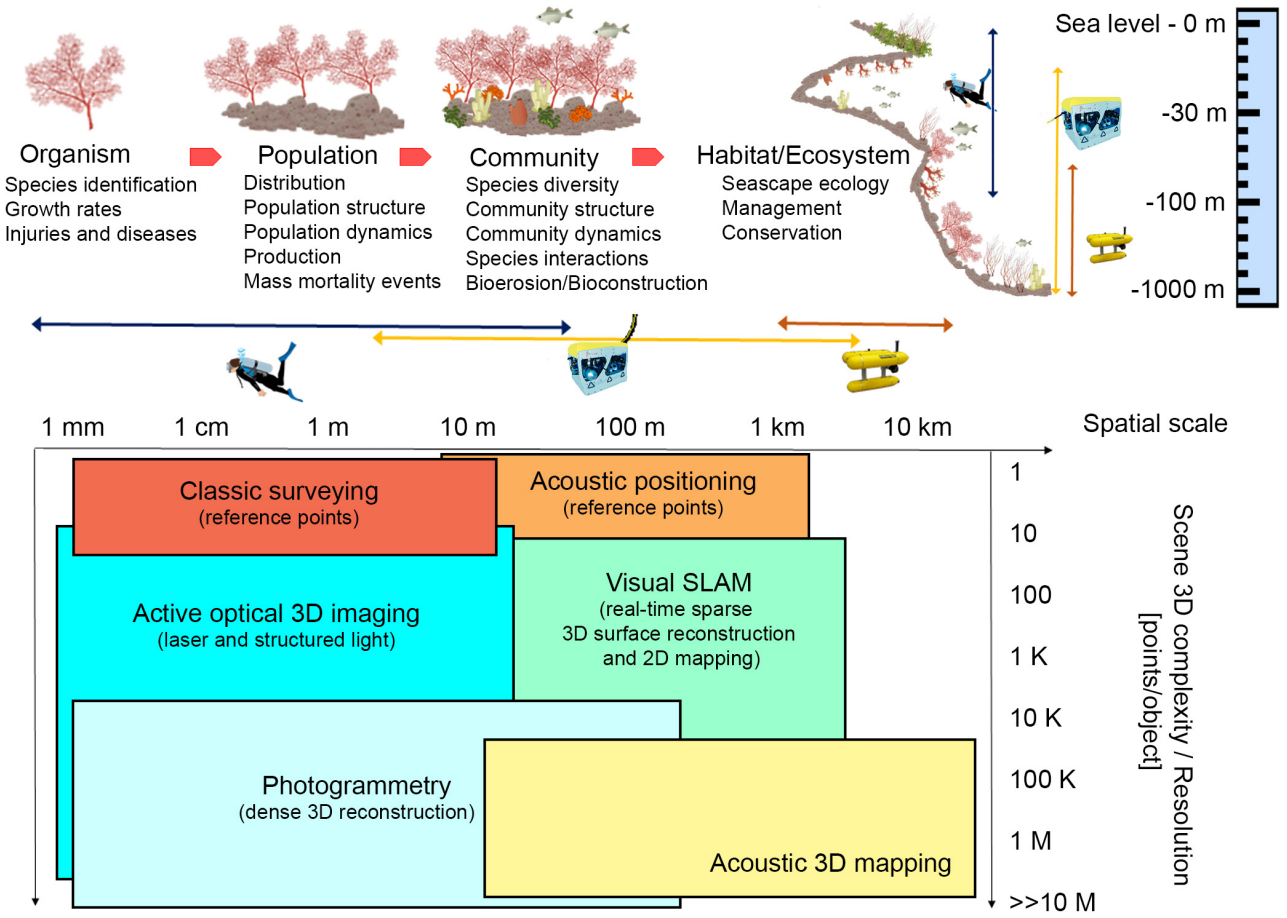

FIGURE 1 | Ecological key aspects of marine animal forests and different technological approaches that can be applied at different spatial scales, depth, and 3D complexity of investigated area. In the table at the bottom, SLAM stands for Simultaneous Localization And Mapping. Illustrations modified from Montero-Serra (2018), and NOAA. Source: IAN Symbols Library, University of Maryland.

at the basis of bioconstruction and bioerosion processes. Within this viewpoint paper we mainly focus on optical techniques, in particular photogrammetry. Acoustic techniques are effective and widely used, but at present they do not guarantee to reach the same accuracy and resolution as photogrammetry (Czechowska et al., 2020). At the scale of single organisms, accurate reconstructions of 3D individual morphology may considerably enhance the capability for species recognition, as well as the accurate quantification of survival and growth rates under variable environmental conditions (Olinger et al., 2019). At the population level, morphological information about organisms may allow for a precise description of the population size structure, its dynamic variation through time (Montero-Serra et al., 2019) and its functioning (Ledoux et al., 2010). At the community level, the careful reconstruction of the framework built up by the structural and the associated species may allow to precisely describe the community structure in terms of species composition, abundance, and evenness. Finally, at the large scale of habitat or ecosystems, 3D georeferenced reconstructions may allow for the application of landscape indexes and descriptors to the analysis of benthic communities.

Animal forests represent a perfect natural lab to develop complex new methodologies, aiming at understanding long-term dynamics and evolutionary processes (Ledoux et al., 2020) shaping these high-biodiversity and structurally complex systems, and eventually the existence of recovery mechanisms that can enhance their resilience to increasing threats (Kersting and Linares, 2019).

TECHNOLOGIES AND METHODOLOGIES

Data Acquisition

The underwater environment poses multiple challenges to 3D reconstruction-oriented explorations based on optical methodologies, such as low visibility, turbidity, light attenuation, and low data transfer rates. It is still challenging to acquire spatial data through photogrammetric methods at a wide area (wider than few square meters) at a few centimeters level of accuracy, which could be limiting for the study of large benthic species. New technologies and automation are required

both in data acquisition and analysis to quantify the structural complexity of animal forests. Besides, survey planning and adaptation strategies that are tailored for optical and acoustic 2D/3D maps reconstruction, dynamically adapted to local conditions, and oriented toward the optimal coverage of a site, need to be explored.

Scuba divers are still widely employed for surveying tasks at accessible diving depths, in clear warm and turbid/cold waters complying with safety limitations (Piazza et al., 2018; Nocerino et al., 2019). However, remotely operated vehicles (ROVs) and autonomous underwater vehicles (AUVs) have become increasingly reliable tools and have led to inspections at depths and across spatio-temporal scales hostile both to divers and crewed vehicles (**Figure 1**; Gori et al., 2011; Shihavuddin et al., 2013; Montseny et al., 2019). In both cases, reference information is required to support spatial continuous methodologies and produce a georeferenced 3D model. The position of stable reference points, installed on the sea floor, or the position of sensors can be performed through classic survey technique or acoustic positioning, depending on the dimension and depth of the investigated site (Bruno et al., 2019; Rossi et al., 2020; **Figure 1**). Moreover, acoustic positioning systems, combined with underwater tablet, may allow divers to plan specific paths to be followed during the survey (Scaradozzi et al., 2018), thus optimizing the acquisition phase and guaranteeing repeatable and complete data. For deeper surveys, acoustic positioning and ROV/AUV navigation data may only provide approximate georeferencing information that may be too coarse for adequately scaling the 3D models when these are created from a single camera. In such cases, the use of laser calipers can solve this problem (Istenič et al., 2020).

Undoubtedly, automatic optical and acoustic imagery classification, as well as 2D mapping (Franchi et al., 2018), would speed up and enhance animal forests investigation allowing non-destructive visual surveys, measuring morphological variables, and paving the way to more specific 3D reconstruction-oriented explorations. Acoustic based techniques are well-suited in large areas of interest (from 10 m to 10 km), and acoustic 3D mapping is successfully employed to map a wide portion of the sea floor at various depths, but in case of organism biometry, higher accuracy and resolution techniques are required. These systems operate in the long-range acquisition and do not suffer from turbidity, but the resulting 3D reconstructions have low resolution and accuracy compared to the optical ones (Lagudi et al., 2016; **Figure 1**).

On the other hand, optical systems are well-suited for close-range acquisition (a few centimeters to tenths of meters). Active optical 3D imaging techniques project different patterns on the investigated area. The triangulation is computed by intersecting the laser beam that passes through a pixel lit up by the pattern, and the projected pattern itself (Palomer et al., 2019). These tools allow to obtain accurate and high-resolution 3D reconstructions, but results are influenced by visibility conditions and acquisition distance (**Figure 1**). Passive techniques (photogrammetry) are based on multiple views of a scene and take advantage of structure from motion (SfM) and Multi View Stereo (MVS) algorithms (Burns et al., 2015). Natural or artificial light can be used to illuminate the scene. The triangulation is done by intersecting the optic rays that pass through a pixel in each image where the same feature is automatically identified and allows the generation of an accurate, dense 3D reconstruction (Westoby et al., 2012). Underwater photogrammetry has long been used because of its flexibility and low cost, potentially providing high-resolution imagery in the underwater context under well-planned protocols of data collection (Nocerino et al., 2019). RGB sensors are the most used in underwater applications because they allow achieving measurable and photorealistic products. Other sensors may offer new opportunities to visualize the internal and external morphology of bioconstructions, such as multispectral acquisitions (Nocerino et al., 2017) and high-resolution x-ray computed tomography, which can be applied to collected samples (Farber et al., 2016). For shallow water applications, surface autonomous vehicles equipped with acoustic and optical sensors (Stanghellini et al., 2020), and low altitude Unmanned Aerial Vehicle (UAV)-based photogrammetry (Casella et al., 2017; Agrafiotis et al., 2020) can provide important information outlining bathymetric profile, filling the gap between satellite and underwater imagery. In the latter case, compensation for water refraction is required (Agrafiotis et al., 2020). In addition, underwater multispectral and hyperspectral imagery is an emerging technique for applications in shallow and deep-sea environments. It is a passive technique in shallow waters; instead, at high depth, when solar illumination is not available, an active light source is necessary. Anyway, this technique works properly at an acquisition distance of 1–5 m, because of the strong absorption caused by the water column (Liu et al., 2020).

Simultaneous localization and mapping (SLAM) methodologies have proved to be effective for underwater explorations and subsea metrology applications. SLAM relies on data integration from navigation sensors (e.g., global positioning system—GPS, inertial measurements unit—IMU) and remote sensing or perception (e.g., camera, lidar, sonar) systems; it comprises a wide range of algorithms designed to provide an autonomous vehicle with the ability to move in an uncharted environment while producing a map (or model) of the scene (Menna et al., 2019).

3D animal forest formations can occur in flat and gently sloping seabeds, or even in vertical slopes, often with crevices, terraces and overhangs. This poses major difficulties in surveying from the surface and requires complex acquisition paths from ROVs/AUVs/divers to collect images for proper 3D reconstruction. When utilizing underwater photogrammetry (or other optical methodologies) to survey marine animal forests, there is an important trade-off, as well as specific drawbacks and limitations that need to be considered. The spatial resolution of final maps depends on the quality of input images: underwater images suffer from wavelength-specific attenuation and scattering, which cause image degradation to increase significantly with distance. Thus, the distance to the object has a strong effect on the quality of the obtained images and consequently the 3D reconstruction. Additionally, in very shallow waters, rippling caustic are adversely affecting SfM and MVS methods, leading to less

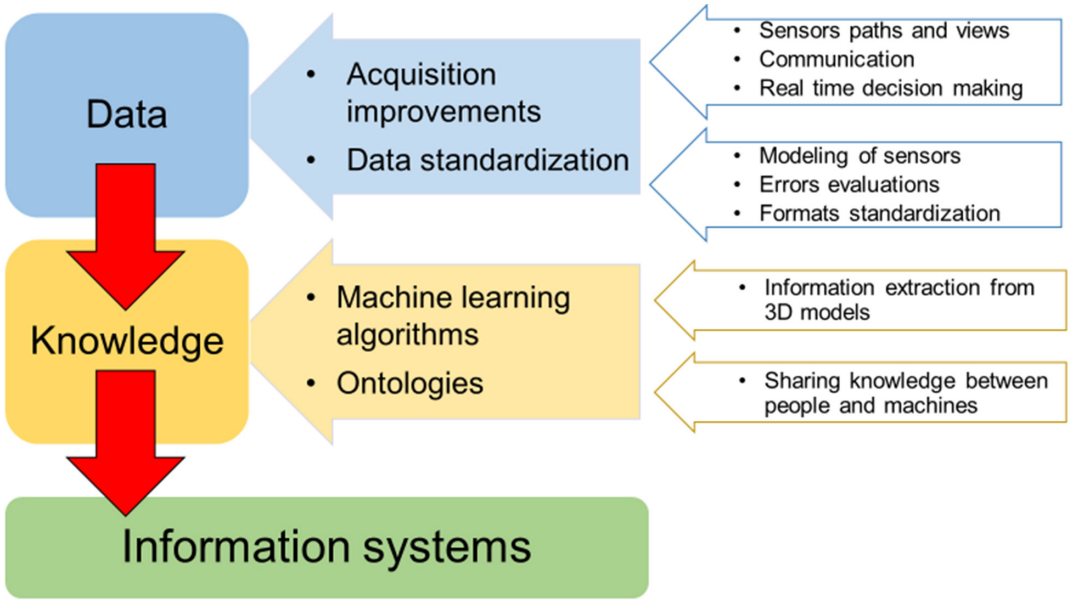

FIGURE 2 | Main needs and gaps for 3D complexity investigations of underwater marine animal forests. The generation of exchangeable knowledge (information system) starts from standardized data.

accurate matches (Agrafiotis et al., 2018) and causing issues in the SLAM based navigation of the ROVs and AUVs (Trabes and Jordan, 2017). A full reconstruction of the 3D complexity of underwater animal forests is challenging, occlusions can occur, and different view angles must be designed. Additionally, high data redundancy is required. Accurately designed acquisition paths (Vidal et al., 2020) and/or omnidirectional cameras (Bosch et al., 2019) could be used as well as forward-looking cameras and modular survey designs, adaptable in real-time. This requires serious navigation abilities from the AUV and is substantially unenforceable with human divers. New navigation technologies are needed, including visibility enhancement (Berman et al., 2020) for visual SLAM and obstacle avoidance to enable close-range photogrammetry of specific features. Neural networks might offer a solution to improve the AUV capabilities in terms of obstacle avoidance and real time decision-making. Computer simulations may help in training the neural networks and achieve such improvement. The photogrammetric approach has been successfully applied to hard corals, while gorgonians, soft corals and erect sponges pose important challenges due to their passive movement with water flow. However, a SfM technique has recently been tested on images from a gorgonian forest (Palma et al., 2018).

Image and Data Analysis

The collection of underwater imagery for the monitoring of marine animal forests became a widespread resource, leading to the accumulation of millions of images each year. However, the rate of image acquisition and the amount of the produced 2D orthophotos dramatically outpaces the human ability to extract information from them (Beijbom et al., 2015). The most commonly required data are the organisms' size and abundance, the spatial distribution of populations on a broader landscape, and their evolution in relation to the changes of the underwater environment. Detailed information about 2D statistical methods for assessing these parameters, but also to evaluate growth and mortalities using ortho-mosaics are summarized in Edwards et al. (2017), Pedersen et al. (2019), and Sandin et al. (2020). These large data collections consisting of images can also be coupled with previous experimental or field work observations and quantifications in single species or communities, enabling a validation of *ex situ* analysis and a large scale investigation. For example: crossing the numbers of carbon input and output of a single organism together with its distribution, density, population structure and biomass in large spatial approaches, may be the key to understand the role of the organism as a carbon immobilizer. Terrestrial tools (used to study land communities acting as carbon immobilizers for example) in marine systems are in implementation thanks to the advances in 3D-image analysis and quantification. Acquired digital data (images and 3D models) are also perfectly suited for the sharing within the scientific community and the public. This could enhance a multidisciplinary and shared research, in accordance with FAIR principles.

Regardless of the biological purpose, spatial analysis, such as detecting changes in organisms, implies the need to segment target species with a high degree of accuracy. Manual 2D segmentation, e.g., a per-pixel classification, is an extremely time-consuming process that can be accelerated using deep learning-based methodologies (Pavoni et al., 2020).

The information on the depth axis is fundamental to evaluate the volumetric change caused by the structural growth or erosion.

Additionally, many of the sessile organisms that constitute marine animal forests are hardly recognizable from a simple orthographic top-down view. The main prospect is to extend the semantic segmentation from images to height fields (2.5D) or 3D models. Open source segmentation software specifically targeted to marine species that handling 2.5D data have been already developed and distributed.

For example, TagLab[1] enables assisted and automatic annotation, leveraging a human-in-the-loop approach to improve the accuracy of automatic predictions. Besides, it supports the comparison of multi-temporal surveys, automatically extracting useful historical information from segmented regions.

3D automatic semantic segmentation is the open challenge yet to face. As highlighted by a comprehensive survey paper (Han et al., 2019), available deep learning architectures might fail in producing segmentation that meets the standards of ecological analysis. Moreover, the limits of architectures working on point clouds, such as the PointNet++ (Qi et al., 2017) and the one by Çiçek et al. (2016), that is a variant of the U-Net architecture originally developed for biomedical data analysis, are not clearly assessed in this application field due to lack of benchmark dataset. Multi-modal learning approaches, combining oriented images, RGB and depth information, might help to fill this gap and solve the task (Dai and Nießner, 2018).

DISCUSSION

In the context of animal forests mapping and 3D structural complexity analysis, the integration of different technologies could support multi-resolution and multi-scale surveying and monitoring. AUVs have the potential to efficiently investigate vast unexplored underwater regions, while ROVs allow for a higher resolution and more detailed mapping of smaller areas of interest that exceed the scuba-diving depth range.

Even if the scientific community is developing new approaches for improving "low" cost surveying and monitoring of the marine environment, their adoption is still not widespread since further testing and optimization of methodologies are needed. In addition, the limited funding for research, and the low interest of the general public in the seabed, slow these developments. Broad scale 3D reconstructions could improve the communication about the importance and diversity of marine environment and increase the public interest.

The main needs and gaps regarding the study of the 3D complexity of underwater animal forests are related to data collection and analysis (**Figure 2**), with concern to the improvement of diver-based or mobile robots (ROV/AUVs) methods in terms of positioning, guidance, and communication toward the surface. Adequate surveying performances of data collection platforms should be improved, depending on the level of robotic and further developments on real time decision capabilities (e.g., real time evaluation of the quality of the data gathered). Likewise, rigorous modeling of sensors, evaluation of metric accuracies and other methodological errors along with the standardization of data formats and analysis tools will be crucial focuses.

The efficiency and quality of collected data, including multiple sensors, data acquisition at multiple scales, and data fusion from multiple platforms and times, need to be supported by the development of machine learning algorithms and methods for biodiversity classification/segmentation and 3D models definition of underwater changing objects. Indeed, benthic populations display 3D behaviors in time whose accurate analysis on the high-resolution 3D representation of these habitats is still beyond modern solutions based either on geometry processing or on deep learning. Fully automated solutions dramatically reduce the human effort in 2D/3D analysis; however, the accuracy of deep learning-based methodologies in the recognition/segmentation of benthic organisms is still lower than human experts, and the dense marine animal forests with a large 3D development pose even more difficulties in the discrimination of organisms. An efficient analysis tool must consider a human in the loop approach, leaving the experts the chance to edit the automatic results thus improving the overall accuracy. In addition, the analysis of large image sets can directly or indirectly benefit from public engagement, through citizen science programs, as was the case with plankton (Robinson et al., 2017). Citizen science data need to be carefully pre-analyzed in terms of accuracy and reliability to evaluate their effective use for mapping and 3D reconstruction applications.

Finally, the development of an information system to better retrieve and manage information on 3D complexity from collected data through time should be addressed. The integration of data belonging to various expeditions, methodologies and purposes is an important need too. The integration of all the existing habitat mapping data in a common and open information system could provide a more accurate, spatially representative assessment of habitat degradation and a proper design and management of restoration actions (Gerovasileiou et al., 2019). Ecological data are highly heterogeneous and complex to manage, therefore providing a shared and common understanding of data and processes will improve data accessibility and analysis. Ontologies (a knowledge graph-based Web tool, see Guarino et al., 2009) have a meaningful role in supporting knowledge sharing expectations. A common understanding facilitates communication between people and information systems (machines) and enhances the ability to search for information across different knowledge repositories, in light of meeting the FAIR (i.e., findability, accessibility, interoperability, and reusability) data principles (Wilkinson et al., 2016).

DATA AVAILABILITY STATEMENT

All datasets generated for this study are included in the article/supplementary material, further inquiries can be directed to the corresponding author/s.

[1] https://github.com/cnr-isti-vclab/TagLab

AUTHOR CONTRIBUTIONS

AC, CCa, MPo, and PR contributed to the conception of the study. PR wrote the first draft of the manuscript and collected contributions and experiences of all the authors. AC, CCa, FMa, MPo, PR, RS, and SRi contributed to the revision of the first draft. All authors contributed to manuscript revision, read, and approved the submitted version.

FUNDING

This perspective manuscript is the result of the 3DSeaFor online workshop funded by EUROMARINE Call 2019 Foresight Workshops. This work was partially supported by an Italian Research Projects of National Interest (PRIN), funded by the Italian Ministry of University and Research: "Reef ReseArcH – Resistance and resilience of Adriatic mesophotic biogenic habitats to human and climate change threats" (Call 205; Prot. 2015J922E; 2017-2020) and by the TAO (Tecnologie per il monitorAggio cOstiero) project in the frame of the program POR-FESR (European Regional Development Fund, ERDF) 2014-2020 of the Emilia-Romagna Region. This work was partially supported by the U.S. National Science Foundation under Grant No. OCE 16-37396 (and earlier awards) as well as a generous gift from the Gordon and Betty Moore Foundation.

ACKNOWLEDGMENTS

We are grateful to the reviewers for their valuable comments and suggestions.

REFERENCES

Agrafiotis, P., Karantzalos, K., Georgopoulos, A., and Skarlatos, D. (2020). Correcting image refraction: towards accurate aerial image-based bathymetry mapping in shallow waters. *Remote Sens.* 12:322. doi: 10.3390/rs12020322

Agrafiotis, P., Skarlatos, D., Forbes, T., Poullis, C., Skamantzari, M., and Georgopoulos, A. (2018). Underwater photogrammetry in very shallow waters: main challenges and caustics effect removal. *Int. Arch. Photogramm. Remote Sens. Spatial Inf. Sci.* XLII-2, 15–22. doi: 10.5194/isprs-archives-XLII-2-15-2018

Beijbom, O., Edmunds, P. J., Roelfsema, C., Smith, J., Kline, D. I., Neal, B. P., et al. (2015). Towards automated annotation of benthic survey images: variability of human experts and operational modes of automation. *PLoS One* 10:e0130312. doi: 10.1371/journal.pone.0130312

Berman, D., Levy, D., Avidan, S., and Treibitz, T. (2020). Underwater single image color restoration using haze-lines and a new quantitative dataset. *IEEE Trans. Pattern Anal. Mach. Intell.* doi: 10.1109/tpami.2020.2977624

Bosch, J., Isteniè, K., Gracias, N., Garcia, R., and Ridao, P. (2019). Omnidirectional multi-camera video stitching using depth maps. *IEEE J. Oceanic Eng.* 99, 1–16. doi: 10.1109/JOE.2019.2924276

Bruno, F., Barbieri, L., Muzzupappa, M., Tusa, S., Fresina, A., Oliveri, F., et al. (2019). Enhancing learning and access to underwater cultural heritage through digital technologies: the case study of the "Cala Minnola" shipwreck site. *Digit. Appl. Archaeol. Cult. Herit* 13:e00103. doi: 10.1016/j.daach.2019.e00103

Burns, J. H. R., Delparte, D., Gates, R. D., and Takabayashi, M. (2015). Integrating structure-from-motion photogrammetry with geospatial software as a novel technique for quantifying 3D ecological characteristics of coral reefs. *PeerJ* 3:e1077. doi: 10.7717/peerj.1077

Caldwell, J. M., Ushijima, B., Couch, C. S., and Gates, R. D. (2017). Intra-colony disease progression induces fragmentation of coral fluorescent pigments. *Sci. Rep.* 7:14596. doi: 10.1038/s41598-017-15084-3

Casella, E., Collin, A., Harris, D., Ferse, S., Bejarano, S., Parravicini, V., et al. (2017). Mapping coral reefs using consumer-grade drones and structure from motion photogrammetry techniques. *Coral Reefs* 36, 269–275. doi: 10.1007/s00338-016-1522-0

Cerrano, C., Bastari, A., Calcinai, B., Di Camillo, C., Pica, D., Puce, S., et al. (2019). Temperate mesophotic ecosystems: gaps and perspectives of an emerging conservation challenge for the Mediterranean Sea. *Eur. Zool. J.* 86, 370–388. doi: 10.1080/24750263.2019.1677790

Cerrano, C., Bavestrello, G., Bianchi, C. N., Cattaneo-Vietti, R., Bava, S., Morganti, C., et al. (2000). A catastrophic mass-mortality episode of gorgonians and other organisms in the Ligurian Sea (North-western Mediterranean), summer 1999. *Ecol. Lett.* 3, 284–293. doi: 10.1046/j.1461-0248.2000.00152.x

Çiçek, Ö, Abdulkadir, A., Lienkamp, S. S., Brox, T., and Ronneberger, O. (2016). "3D U-Net: learning dense volumetric segmentation from sparse annotation," in *MICCAI Medical. Image Computing and Computer-Assisted Intervention*, Vol. 424–432, eds S. Ourselin, W. S. Wells, M. R. Sabuncu, G. Unal, and L. Joskowicz (New York, NY: Springer). doi: 10.1007/978-3-319-46723-8_49

Coma, R., Ribes, M., Zabala, M., and Gili, J. M. (1998). Growth in a modular colonial marine invertebrate. *Estuar. Coast. Shelf Sci.* 47, 459–470. doi: 10.1006/ecss.1998.0375

Czechowska, K., Feldens, P., Tuya, F., de Esteban, M. C., Espino, F., Haroun, R., et al. (2020). Testing side-scan sonar and multibeam echosounder to study black coral gardens: a case study from Macaronesia. *Remote Sens.* 12:3244. doi: 10.3390/rs12193244

Dai, A., and Nießner, M. (2018). "3dmv: joint 3d-multi-view prediction for 3d semantic scene segmentation," in *Proceedings of the 15th European Conference, Munich, Germany, September 8–14, 2018*, Munich, 452–468.

Davidson, T. M., Altieri, A. H., Ruiz, G. M., and Torchin, M. E. (2018). Bioerosion in a changing world: a conceptual framework. *Ecol. Lett.* 21, 422–438. doi: 10.1111/ele.12899

Edwards, C., Eynaud, Y., Williams, G. J., Pedersen, N. E., Zgliczyn-ski, B. J., Gleason, A. C. R., et al. (2017). Large-area imaging reveals biologically driven non-random spatial patterns of corals at a remote reef. *Coral Reefs* 36, 1291–1305. doi: 10.1007/s00338-017-1624-3

Farber, C., Titschack, J., Schonberg, C., Ehrig, K., Boos, K., Illerhaus, B., et al. (2016). Long-term macrobioerosion in the Mediterranean Sea assessed by micro-computed tomography. *Biogeoscience* 13, 3461–3474. doi: 10.5194/bg-13-3461-2016

Franchi, M., Ridolfi, A., and Zacchini, L. (2018). "A forward-looking sonar-based system for underwater mosaicing and acoustic odometry," in *Proceedings of the IEEE/OES Autonomous Underwater Vehicle Workshop (AUV)*, Porto. doi: 10.1109/auv.2018.8729795

Garrabou, J., Gómez-Gras, D., Ledoux, J. B., Linares, C., Bensoussan, N., López-Sendino, P., et al. (2019). Collaborative database to track mass mortality events in the Mediterranean Sea. *Front. Mar. Sci.* 6:707. doi: 10.3389/fmars.2019.00707

Gerovasileiou, V., Smith, C. J., Sevastou, K., Papadopoulou, N., Dailianis, T., Bekkby, T., et al. (2019). Habitat mapping in the European Seas-is it fit for purpose in the marine restoration agenda? *Mar. Policy* 106:103521. doi: 10.1016/j.marpol.2019.103521

Gori, A., Rossi, S., Berganzo, E., Pretus, J. L., Dale, M. R. T., and Gili, J. M. (2011). Spatial distribution patterns of the gorgonians *Eunicella singularis*, *Paramuricea clavata*, and *Leptogorgia sarmentosa* (Cap de Creus, northwestern Mediterranean Sea). *Mar. Biol.* 158, 143–158. doi: 10.1007/s00227-010-1548-8

Guarino, N., Oberle, D., and Staab, S. (2009). *What is an Ontology? Handbook on Ontologies*. Heidelberg: Springer, 1–17.

Han, X. F., Laga, H., and Bennamoun, M. (2019). Image-based 3d object reconstruction: state-of-the-art and trends in the deep learning era. *IEEE Trans. Pattern. Anal. Mach. Intell*, 1. doi: 10.1109/tpami.2019.2954885

House, J. E., Brambilla, V., Bidaut, L. M., Christie, A. P., Pizarro, O., Madin, J. S., et al. (2018). Moving to 3D: relationships between coral planar area, surface area and volume. *PeerJ* 6:e4280. doi: 10.7717/peerj.4280

Istenič, K., Gracias, N., Arnaubec, A., Escartín, J., and Garcia, R. (2020). Automatic scale estimation of structure from motion based 3D models using laser scalers in underwater scenarios. *ISPRS J. Photogramm. Remote Sens.* 159, 13–25. doi: 10.1016/j.isprsjprs.2019.10.007

Jones, C. G., Lawton, J. H., and Shachak, M. (1994). Organisms as ecosystem engineers. *Oikos* 69, 373–386. doi: 10.2307/3545850

Kersting, D. K., and Linares, C. (2019). Living evidence of a fossil survival strategy raises hope for warming-affected corals. *Sci. Adv.* 5:eaax2950. doi: 10.1126/sciadv.aax2950

Kružić, P. S., and Benković, L. (2012). The impact of seawater temperature on coral growth parameters of the colonial coral *Cladocora caespitosa* (Anthozoa, Scleractinia) in the eastern Adriatic Sea. *Facies* 58, 477–491. doi: 10.1007/s10347-012-0306-4

Lagudi, A., Bianco, G., Muzzupappa, M., and Bruno, F. (2016). An alignment method for the integration of underwater 3D data captured by a stereovision system and an acoustic camera. *Sensors* 16:536. doi: 10.3390/s16040536

Ledoux, J. B., Frias-Vidal, S., Montero-Serra, I., Antunes, A., Casado, B. C., Civit, S., et al. (2020). Assessing the impact of population decline on mating system in the overexploited mediterranean red coral. *Aquatic Conserv. Mar. Freshw. Ecosyst.* 30, 1149–1159. doi: 10.1002/aqc.3327

Ledoux, J. B., Garrabou, J., Bianchimani, O., Drap, P., Féral, J. P., and Aurelle, D. (2010). Fine-scale genetic structure and inferences on population biology in the threatened mediterranean red coral, *Corallium rubrum*. *Mol. Ecol.* 19, 4204–4216. doi: 10.1111/j.1365-294X.2010.04814.x

Liu, B., Liu, Z., Men, S., Li, Y., Ding, Z., He, J., et al. (2020). Underwater hyperspectral imaging technology and its applications for detecting and mapping the seafloor: a review. *Sensors* 20:4962. doi: 10.3390/s20174962

Maldonado, M., López-Acosta, M., Sánchez-Tocino, L., and Sitjà, C. (2013). The rare, giant gorgonian *Ellisella paraplexauroides*: demographics and conservation concerns. *Mar. Ecol. Prog. Ser.* 479, 127–141. doi: 10.3354/meps10172

Marschal, C., Garrabou, J., Harmelin, J. G., and Pichon, M. (2004). A new method for measuring growth and age in the precious mediterranean red coral *Corallium rubrum* (L.). *Coral Reefs* 23, 423–432. doi: 10.1007/s00338-004-0398-6

Menna, F., Nocerino, E., Nawaf, M. M., Seinturier, J., Torresani, A., Drap, P., et al. (2019). "Towards real-time underwater photogrammetry for subsea metrology applications," in *Proceedings of the OCEANS 2019*, Marseille, 1–10. doi: 10.1109/OCEANSE.2019.8867285

Montero-Serra, I. (2018). *Resilience of Long-Lived Mediterranean Gorgonians in a Changing World: Insights From Life History Theory and Quantitative Ecology*. Ph.D. thesis, University of Barcelona, Barcelona.

Montero-Serra, I., Garrabou, J., Doak, D. F., Ledoux, J. B., and Linares, C. (2019). Marine protected areas enhance structural complexity but do not buffer the consequences of ocean warming for an overexploited precious coral. *J. Appl. Ecol* 56, 1063–1074. doi: 10.1111/1365-2664.13321

Montseny, M., Linares, C., Viladrich, N., Olariaga, A., Carreras, M., Palomeras, N., et al. (2019). First attempts towards the restoration of gorgonian populations on the Mediterranean continental shelf. *Aquat. Conserv. Mar. Freshwater Ecosyst.* 29, 1278–1284. doi: 10.1002/aqc.3118

Nocerino, E., Dubbini, M., Menna, F., Remondino, F., Gattelli, M., and Covi, D. (2017). Geometric calibration and radiometric correction of the MAIA multispectral camera. *Int. Arch. Photogramm. Remote Sens. Spat. Inf. Sci.* 42, 149–156. doi: 10.5194/isprs-archives-xlii-3-w3-149-2017

Nocerino, E., Neyer, F., Grün, A., Troyer, M., Menna, F., Brooks, A. J., et al. (2019). Comparison of diver-operated underwater photogrammetric systems for coral reef monitoring. *Int. Arch. Photogramm. Remote Sens. Spat. Inf. Sci.* 42, 143–150. doi: 10.5194/isprs-archives-xlii-2-w10-143-2019

Olinger, L. K., Scott, A. R., McMurray, S. E., and Pawlik, J. R. (2019). Growth estimates of Caribbean reef sponges on a shipwreck using 3D photogrammetry. *Sci. Rep.* 9:18398. doi: 10.1038/s41598-019-54681-2

Ordoñez, A., Wangpraseurt, D., Lyndby, N. H., Kühl, M., and Diaz-Pulido, G. (2019). Elevated CO2 leads to enhanced photosynthesis but decreased growth in early life stages of reef building coralline algae. *Front. Mar.Sci.* 5:495. doi: 10.3389/fmars.2018.00495

Palma, M., Casado, M., Pantaleo, U., Pavoni, G., Pica, D., and Cerrano, C. (2018). SfM-based method to assess gorgonian forests (*Paramuricea clavata* (Cnidaria. Octocorallia). *Remote Sens.* 10:1154. doi: 10.3390/rs10071154

Palomer, A., Ridao, P., Forest, J., and Ribas, D. (2019). Underwater laser scanner: Ray-based model and calibration. *IEEE/ASME Trans. Mechatron.* 24, 1986–1997. doi: 10.1109/tmech.2019.2929652

Pavoni, G., Corsini, M., Fiameni, G., Callieri, M., Edwards, C., and Cignoni, P. (2020). On improving the training of models for the semantic segmentation of benthic communities from orthographic imagery. *Remote Sens.* 12:3106. doi: 10.3390/rs12183106

Pedersen, N. E., Edwards, C. B., Eynaud, Y., Gleason, A. C. R., Smith, J. E., and Sandin, S. A. (2019). The influence of habitat and adults on the spatial distribution of juvenile corals. *Ecography* 42, 1703–1713. doi: 10.1111/ecog.04520

Peirano, A., Morri, C., Bianchi, C. N., and Rodolfo-Metalpa, R. (2001). Biomass, carbonate standing stock and production of the mediterranean coral *Cladocora caespitosa* (L.). *Facies* 44, 75–80. doi: 10.1007/bf02668168

Piazza, P., Cummings, V. J., Lohrer, D. M., Marini, S., Marriott, P., Menna, F., et al. (2018). Divers-operated underwater photogrammetry: applications in the study of antarctic benthos. *Int. Arch. Photogramm. Remote Sens. Spat. Inf. Sci.* 42, 885–892. doi: 10.5194/isprs-archives-XLII-2-885-2018

Ponti, M., Turicchia, E., Ferro, F., Cerrano, C., and Abbiati, M. (2018). The understorey of gorgonian forests in mesophotic temperate reefs. *Aquat. Conserv.* 28, 1153–1166. doi: 10.1002/aqc.2928

Qi, C. R., Yi, L., Su, H., and Guibas, L. J. (2017). "Pointnet++: deep hierarchical feature learning on point sets in a metric space," in *Proceedings of the 31st International Conference on Neural Information Processing Systems*, 5099–5108.

Righi, S., Prevedelli, D., and Simonini, R. (2020). Ecology, distribution and expansion of a mediterranean native invader, the fireworm *Hermodice carunculata* (Annelida). *Mediterr. Mar. Sci.* 21, 575–591. doi: 10.12681/mms.23117

Robinson, K. L., Luo, J. Y., Sponaugle, S., Guigand, C., and Cowen, R. K. (2017). A tale of two crowds: public engagement in plankton classification. *Front. Mar. Sci.* 4:7. doi: 10.3389/fmars.2017.00082

Rossi, P., Castagnetti, C., Capra, A., Brooks, A. J., and Mancini, F. (2020). Detecting change in coral reef 3D structure using underwater photogrammetry: critical issues and performance metrics. *Appl. Geomatics* 12, 1–15. doi: 10.1007/s12518-019-00263-w

Rossi, S., Bramanti, L., Gori, A., and Orejas, C. (2017). *Marine Animal Forests. The Ecology of Benthic Biodiversity Hotspots*. Cham: Springer International Publishing.

Rossi, S., and Orejas, C. (2019). "Approaching cold-water corals to the society: novel ways to transfer knowledge," in *Proceding of the Mediterranean Cold-Water Corals: Past, Present and Future*, (Cham: Springer), 473–480. doi: 10.1007/978-3-319-91608-8_39

Sandin, S. A., Edwards, C. B., Pedersen, N. E., Vid, P., Gaia, P., Esmeralda, A., et al. (2020). Considering the rates of growth in two taxa of coral across Pacific islands. *Adv. Mar. Biol.* 87, 167–191. doi: 10.1016/bs.amb.2020.08.006

Scaradozzi, D., Zingaretti, S., Ciuccoli, N., Costa, D., Palmieri, G., Bruno, F., et al. (2018). Lab4Dive mobile smart lab for augmented archaeological dives. *IOP Conf. Ser. Mater. Sci. Eng.* 364:012054. doi: 10.1088/1757-899x/364/1/012054

Shihavuddin, A. S. M., Gracias, N., Garcia, R., Gleason, A., and Ginter, B. (2013). Image-based coral reef classification and thematic mapping. *Remote Sens.* 5, 1809–1841. doi: 10.3390/rs5041809

Stanghellini, G., Del Bianco, F., and Gasperini, L. (2020). OpenSWAP, an open architecture, low cost class of autonomous surface vehicles for geophysical surveys in the shallow water environment. *Remote Sens.* 12:2575. doi: 10.3390/rs12162575

Trabes, E., and Jordan, M. A. (2017). A node-based method for SLAM navigation in self-similar underwater environments: a case study. *Robotics* 6:29. doi: 10.3390/robotics6040029

Turicchia, E., Abbiati, M., Sweet, M., and Ponti, M. (2018). Mass mortality hits gorgonian forests at montecristo island. *Dis. Aquat. Org.* 131, 79–85. doi: 10.3354/dao03284

Verdura, J., Linares, C., Ballesteros, E., Coma, R., Uriz, M. J., Bensoussan, N., et al. (2019). Biodiversity loss in a mediterranean ecosystem due to an extreme

warming event unveil the role of an engineering gorgonian species. *Sci. Rep.* 9:5911. doi: 10.1038/s41598-019-41929-0

Vidal, E., Palomeras, N., Istenič, K., Gracias, N., and Carreras, M. (2020). Multisensor online 3D view planning for autonomous underwater exploration. *J. Field Rob.* 37, 1–25. doi: 10.1002/rob.21951

Westoby, M. J., Brasington, J., Glasser, N. F., Hambrey, M. J., and Reynolds, J. M. (2012). Structure-from-motion' photogrammetry: a low-cost, effective tool for geoscience applications. *Geomorphology* 179, 300–314. doi: 10.1016/j.geomorph.2012.08.021

Wilkinson, M. D., Dumontier, M., Aalbersberg, I. J., Appleton, G., Axton, M., Baak, A., et al. (2016). The FAIR guiding principles for scientific data management and stewardship. *Sci. Data* 3:160018. doi: 10.1038/sdata.2016.18

Zweifler, A., Akkaynak, D., Mass, T., and Treibitz, T. (2017). In situ analysis of coral recruits using fluorescence imaging. *Front. Mar. Sci.* 4:273. doi: 10.3389/fmars.2017.00273

Conflict of Interest: MPa owns and was employed by Habitats Edge Ltd and UBICA srl.

The remaining authors declare that the research was conducted in the absence of any commercial or financial relationships that could be construed as a potential conflict of interest.

frontiers in Marine Science

ORIGINAL RESEARCH
published: 17 June 2021
doi: 10.3389/fmars.2021.633057

Demo-Genetic Approach for the Conservation and Restoration of a Habitat-Forming Octocoral: The Case of Red Coral, *Corallium rubrum*, in the Réserve Naturelle de Scandola

OPEN ACCESS

Edited by:
Stelios Katsanevakis, University of the Aegean, Greece

Reviewed by:
Panagiotis Kasapidis, Hellenic Centre for Marine Research, Greece
Georgios Tsounis, California State University, Northridge, United States

***Correspondence:**
Joaquim Garrabou
garrabou@icm.csic.es
Jean-Baptiste Ledoux
jbaptiste.ledoux@gmail.com

Specialty section:
This article was submitted to Marine Ecosystem Ecology, a section of the journal Frontiers in Marine Science

Received: *24 November 2020*
Accepted: *10 May 2021*
Published: *17 June 2021*

Citation:
Gazulla CR, López-Sendino P, Antunes A, Aurelle D, Montero-Serra I, Dominici J-M, Linares C, Garrabou J and Ledoux J-B (2021) Demo-Genetic Approach for the Conservation and Restoration of a Habitat-Forming Octocoral: The Case of Red Coral, Corallium rubrum, in the Réserve Naturelle de Scandola. Front. Mar. Sci. 8:633057. doi: 10.3389/fmars.2021.633057

Carlota R. Gazulla[1,2], Paula López-Sendino[1], Agostinho Antunes[3,4], Didier Aurelle[5,6], Ignasi Montero-Serra[7], Jean-Marie Dominici[8], Cristina Linares[7], Joaquim Garrabou[1,5]* and Jean-Baptiste Ledoux[1,3]

[1] Institut de Ciències del Mar, Consejo Superior de Investigaciones Científicas, Barcelona, Spain, [2] Departament de Genètica i Microbiologia, Universitat Autònoma de Barcelona, Barcelona, Spain, [3] CIIMAR/CIMAR, Centro Interdisciplinar de Investigação Marinha e Ambiental, Universidade do Porto, Porto, Portugal, [4] Department of Biology, Faculty of Sciences, University of Porto, Porto, Portugal, [5] Aix Marseille Univ, Université de Toulon, CNRS, IRD, MIO, Marseille, France, [6] CNRS, EPHE, Institut de Systématique, Evolution, Biodiversité, Muséum National d'Histoire Naturelle, Sorbonne Université, Paris, France, [7] Departament de Biologia Evolutiva, Ecologia i Ciències Ambientals, Institut de Recerca de la Biodiversitat, Universitat de Barcelona, Barcelona, Spain, [8] Réserve Naturelle de Scandola, Parc Régional de Corse, Galeria, France

Marine protected areas (MPAs) are one of the most efficient conservation tools to buffer marine biodiversity loss induced by human activities. Beside effective enforcement, an accurate understanding of the eco-evolutionary processes underlying the patterns of biodiversity is needed to reap the benefits of management policies. In this context, integrating population genetics with demographic data, the demo-genetic approach, is particularly relevant to shift from a "species-based pattern" toward an "eco-evolutionary-based processes" conservation. Here, targeting a key species in the Mediterranean coralligenous, the red coral, *Corallium rubrum*, in an emblematic Mediterranean MPA, the "Réserve Naturelle de Scandola" (France), we applied demo-genetic approaches at two contrasted spatial scales, among populations and within one population, to (i) infer the demographic connectivity among populations in the metapopulation network and (ii) shed new light on the genetic connectivity and on the demographic transitions underlying the dynamics of a near-pristine population. Integrating different spatial and temporal scales, we demonstrated (i) an apparent temporal stability in the pattern of genetic diversity and structure in the MPA in spite of a dramatic demographic decline and (ii) contrasted levels of genetic isolation but substantial demographic connectivity among populations. Focusing on the near-pristine population, we complemented the characterization of red coral demographic connectivity suggesting (iii) temporal variability and (iv) the occurrence of collective dispersal. In addition, we demonstrated (v) contrasted patterns of spatial genetic structure (SGS), depending on the considered

stage-class (adults vs. juveniles), in the near-pristine population. This last result points out that the overall SGS resulted from a restricted dispersal of locally produced juveniles (SGS among adults and juveniles) combined to mortality during early life stages (decrease of SGS from juveniles to adults). Demonstrating the occurrence of two management units and the importance of two populations (CAVB and ALE) for the network of connectivity, we made recommendations for the management of the Réserve Naturelle de Scandola. Besides, we contributed to the implementation of scientifically driven restoration protocols in red coral by providing estimates for the size, density, and distances among patches of transplanted colonies.

Keywords: *Corallium rubrum*, temperate habitat-forming octocoral, marine protected area, demo-genetics, connectivity, spatial genetic structure, demographic transition, marine restoration

INTRODUCTION

Global change is drastically modifying the networks of interactions among the different levels of marine biodiversity, from genes to ecosystems, impacting ecosystem functioning and related socioeconomic services. Marine protected areas (MPAs) are one of the most efficient tools to buffer this anthropogenic biodiversity loss. Besides an effective enforcement (Edgar et al., 2014; Costello and Ballantine, 2015), the benefits of MPAs rely on an accurate understanding of the eco-evolutionary processes shaping and maintaining the patterns of biodiversity (Sale et al., 2005). Connectivity, defined as the exchange of individuals among populations (demographic connectivity) and their successful reproduction (genetic connectivity) (Lowe and Allendorf, 2010), is of critical importance in the functioning of MPAs. It underlies the dynamics and genetics of populations (Palumbi, 2004; Gagnaire et al., 2015). However, to date, design and management of MPAs usually rely on "species-based pattern" rather than "eco-evolutionary-based processes" considerations, restraining potentially their benefits.

One way to achieve the required shift, from a pattern- to a process-focused management, relies on the integration of population genetics into conservation strategies. While this is acknowledged since the beginning of conservation biology (Soulé, 1985), population genetics and genetic diversity remain overlooked by biodiversity managers (Cook and Sgrò, 2018; Laikre et al., 2020). This is particularly detrimental considering the recent developments in demo-genetic approaches that, combining demographic information with population genetics, allow the inference of eco-evolutionary processes acting over contemporary timescale. At large spatial scale (i.e., among populations), demo-genetic approaches allow, for instance, for the estimation of contemporary connectivity (see Waples and Gaggiotti, 2006; Broquet and Petit, 2009). Populations can thus be classified in terms of their role in the functioning of the network (e.g., source vs. sink) helping, accordingly, to prioritize conservation efforts. Beside their inputs in conservation, demo-genetic approaches can be used to improve restoration practices, especially when applied at fine spatial scale (i.e., among individuals within population). In marine sessile invertebrates, the combination between the dispersive larval phase and complex reproductive strategies (Bierne et al., 2016) can limit our understanding of ecological processes driving the population dynamics. Characterizing the fine-scale SGS within population, the non-random spatial distribution of genotypes through the formation of local pedigree structure (Vekemans and Hardy, 2004) allows to infer demographic parameters such as the "neighborhood size" (*Nb*) and the "mean parent-offspring distance" (σ_g) (see Rousset, 1997, Rousset, 2000). These two parameters provide insight into the distance range at which genetic interactions occurred among individuals within population (Vekemans and Hardy, 2004). Interestingly, SGS is a dynamic pattern, which can increase (e.g., Pardini and Hamrick, 2008) or decrease (e.g., Hampe et al., 2010) from juveniles to adults. Demographic processes such as density-dependent or -independent mortality during early-life stages may decrease the strength of SGS from propagule to recruit to adult-stage classes (e.g., Chung et al., 2003, 2007). Accordingly, the decomposition of SGS among stage classes can shed new light on the population dynamics of the targeted species by characterizing the interactions between the demographic and evolutionary processes shaping the pool of reproductive adults (Kalisz et al., 2001; Jacquemyn et al., 2006; Hampe et al., 2010). The characterization of the dynamics of the SGS within population and the estimation of related demographic parameters (*Nb* and σ_g) are thus of primary importance to support the definition of scientifically driven transplantation protocols (e.g., size and density of restored patches) and to set the size of restoration actions (e.g., distance among restored patches).

The Mediterranean Sea is a striking example of the challenges induced by global change on marine biodiversity. This biodiversity hotspot is submitted to direct anthropogenic pressures from overfishing to pollution and was recently recognized as a hotspot of climate change (Diffenbaugh et al., 2007; Cramer et al., 2018). In the last decades, mass mortality events (MMEs) linked to marine heat waves have been observed along thousands of kilometers of coastal habitats, impacting more than 90 species (Garrabou et al., 2019). Coralligenous biogenic reefs, which are among the richest Mediterranean communities (Ballesteros, 2006) and were recognized as priority habitats by the UNEP-MAP, have been particularly sensitive to MMEs (Garrabou et al., 2009, 2019). Populations of long-lived and habitat-forming macrobenthic species such as sponges, octocorals, or bryozoans were dramatically impacted by MMEs, with up to 80% of

impacted individuals in some locations (Cerrano et al., 2000; Garrabou et al., 2001, 2009, 2019). The reported high incidence and mortality rates in these key species may induce cascading effects at the ecosystem level, questioning the future of coralligenous communities (Gómez-Gras et al., 2021).

Here, focusing on red coral, *Corallium rubrum*, a key species of the Mediterranean coralligenous, in an emblematic Mediterranean MPA, the "Réserve Naturelle de Scandola" (Parc Naturel Regional de Corse, France), our main objective is to provide insight into red coral connectivity among and within populations in order to refine the management of the MPA and to contribute to the definition of scientifically driven restoration protocols. The relevance of this case study relies on two main issues. First, the Scandola Marine Reserve is one of the most emblematic MPAs in the Mediterranean. Characterized by a well-conserved biodiversity, including coralligenous habitats, and a unique and near-pristine population of red coral (Cave-b; Garrabou et al., 2017), the MPA is a reference for managers and scientists. However, little is known regarding the eco-evolutionary processes underlying the functioning of the MPA, and particularly the pattern of connectivity among populations. Then, following almost three decades of multidisciplinary studies (Abbiati et al., 1993; Santangelo et al., 1993), red coral has been established as a model species in conservation biology. This habitat-forming octocoral, with low population dynamics and late sexual maturity (Garrabou and Harmelin, 2002; Marschal et al., 2004; Torrents et al., 2005), is found in contrasted habitats mainly in the Western Mediterranean and neighboring Atlantic (Zibrowius et al., 1984; Boavida et al., 2016), from 5- to more than 1000-m depth (Knittweis et al., 2016). Warming-induced mortalities (Garrabou et al., 2001) and overharvesting for its use in jewelry (Bruckner, 2009) induced a dramatic shift in the demographic structure of shallow populations, questioning the evolutionary trajectory of the species (Montero-Serra et al., 2019). Patterns of genetic structure and diversity in shallow red coral populations have been characterized from global, to regional (including the Scandola Marine Reserve; see below), to local scales. Overall, the species shows a significant genetic structure among populations at a scale of tens of meters (Costantini et al., 2007a), which increases with geographic distance (i.e., isolation by distance pattern, IBD; Ledoux et al., 2010a; Aurelle et al., 2011; Aurelle and Ledoux, 2013). While the IBD suggests a limited gene flow occurring mainly among close-by populations, it is noteworthy that the connectivity of the species remains poorly characterized. At regional scale, some heterogeneity in the patterns of structure has been revealed (Ledoux et al., 2010a). Analyzing populations from the Scandola Marine Reserve, Ledoux et al. (2010a) revealed a lack of IBD combined to a relatively low level of genetic diversity compared to other regions. At local scale, the significant SGSs reported among individuals within an unprotected population (Ledoux et al., 2010b) suggest that red coral populations may be considered as complex networks of genetically related individuals interacting locally (few centimeters). While these data improved our abilities to restore declining populations, the eco-evolutionary processes, such as genetic connectivity and density-dependent or -independent mortality underlying the establishment of the reproductive pool in red coral populations (Montero-Serra et al., 2015, 2018), remain to be characterized in order to provide scientifically driven restoration protocols.

Based on a sampling at the population and individual levels, we applied complementary demo-genetic approaches at two contrasting spatial scales: among populations and among individuals within one population. In a first step, we characterized the patterns of genetic diversity and structure among six red coral populations (i) to infer the demographic connectivity among these populations. In a second step, we used a geo-referenced sampling considering two stage-classes, adults vs. juveniles, (ii) to decompose the SGS in the Cave-b population, and (iii) to further characterize the potential impact of genetic connectivity and early life-stage mortality on the population dynamics of this near-pristine population. Our results suggested the occurrence of collective dispersal, improving our current knowledge regarding the ecology of *C. rubrum*. Besides, we used the genetic structure and demographic connectivity patterns to prioritize management efforts in the Scandola Marine Reserve. We translated the SGS results into restoration advices. In particular, we provided estimates for the size, density, and distance among patches to restore red coral populations.

MATERIALS AND METHODS

Sampling and Spatial Data

Established in 1975 and listed as a world heritage site in 1983 by UNESCO, the Scandola Marine Reserve (Parc Naturel Regional de Corse, France) is particularly well enforced, belonging to the 0.23% of effectively protected Mediterranean surface (Claudet et al., 2020). In this MPA, individuals of *C. rubrum* from six populations were collected by SCUBA diving at depths from 15 to 25 m between 2015 and 2017 (**Figure 1A**). In five populations separated by distance ranging from 20 m to less than 2 km (DHM, ALI, ALE, PPL, and PLU), apical fragments (∼5 mm) from 30 to 51 mature individuals (i.e., colonies higher than 30 mm; Torrents et al., 2005) were randomly sampled. In Cave-b (CAVB), sampling was conducted following a 6.25-m-length horizontal transect at a depth of 23 m. Based on its demographic structure showing the highest biomass reported to date in the Mediterranean Sea (more than 100-fold) and the coexistence of a high number of juveniles, low size, and large centennial colonies in high density (201 colonies*m^{-2}), the Cave-b population is a unique and near-pristine population of red coral (Garrabou et al., 2017). The high density of this population combined to the morphological characteristics of the habitat prevents a georeferenced sampling at the individual level. Accordingly, 11 quadrats (25 × 25 cm) were sampled. The size of the quadrat was of the same order as the mean square parent–offspring distance (σ_g) estimated by Ledoux et al. (2010b). Nine quadrats were sampled every 50 cm along the transect. Two quadrats at the center of the transect were duplicated 25 cm above the transect. Within each quadrat, 15–20 adult colonies and a similar number of juvenile colonies were randomly collected (see **Figure 1B** and **Table 1**). In the red coral, sexual maturity was reported in colonies higher than 30 mm (Torrents et al., 2005). To

avoid potential mis-assignment in the reproductive status of the samples, we considered adult and juvenile colonies as colonies higher than 100 mm and between 5 and 10 mm, respectively. For the adult colonies, small fragments (<10 mm) were sampled while, for the juveniles, the whole colonies were sampled.

The resulting 634 apical fragments were conserved in 95% ethanol and stored at −20°C prior to DNA extraction.

DNA Extraction, Microsatellite Genotyping, and Quality Control

DNA extraction, microsatellite genotyping, and quality control are described in **Supplementary Material**. Briefly, all the individuals were genotyped using eight microsatellite loci amplified in three multiplexes: Multiplex 1 (Mic13/Mic20/Mic26), Multiplex 2 (Mic24/Mic25/Mic27), and Multiplex 3 (Mic22/Mic23) (Ledoux et al., 2010a). Following the quality control, statistical analyses were conducted with a dataset including 580 colonies, corresponding to the same number of unique multilocus genotypes, including 201 adults (CAVB-AD) and 166 juveniles (CAVB-JUV) from Cave-b and 213 individuals from five populations (**Table 1**).

Hardy–Weinberg Equilibrium and Genetic Diversity

Probability of identity (*Pi*; the average probability that two samples will share the same genotype), Hardy–Weinberg equilibrium, and genetic diversity analyses for each population, including total number of alleles, observed (H_o) and unbiased heterozygosity (H_e; Nei, 1973), f estimator of F_{IS}, and rarefied allelic richness ($Ar_{(56)}$; Petit et al., 1998), are described in **Supplementary Material**.

SGS Among Populations

A clustering analysis using STRUCTURE 2.2 (Pritchard et al., 2000) was conducted to evaluate the number of genetic clusters (K) from the individuals' genotypes without assumptions on population boundaries and considering the whole dataset. Because of the unbalanced sampling, we considered the admixture model with correlated allele frequencies (Falush et al., 2003, 2007) and population-specific ancestry prior (α) with an $\alpha = 0.17$ (=1/number of assumed populations; Wang, 2017). Ten independent runs were performed for each K with a burn-in period of 500,000 followed by 250,000 iterations. The K-value corresponding to "upper most hierarchical level of structure" was determined using Ln Pr(X| K) (Pritchard et al., 2000), the ΔK method (Evanno et al., 2005), and the MedMedK, MedMeaK, MaxMedK, and MaxMeaK statistics with three different thresholds (0.6, 0.7, and 0.8; Puechmaille, 2016), CLUMPP 1.1 (Jakobsson and Rosenberg, 2007), and DISTRUCT 1.1 (Rosenberg, 2003) were used for graphical outputs.

We conducted a discriminant analysis of principal components (DAPC, Jombart et al., 2010) in ADEGENET (Jombart, 2008). Contrary to STRUCTURE, DAPC describes patterns of diversity without assumption about the underlying population genetic model (Jombart et al., 2010). Data were transformed into principal components, and discriminant analyses were used to maximize variation among groups while minimizing variations within the group. We used the seven population locations (discriminating here among adults and juveniles from CAVB) as group prior. Based on the *a-score* method, the number of principal components was set to 46, while we retained three discriminant functions.

Global and pairwise differentiations were quantified using Weir and Cockerham's (1984) estimators of F_{ST} in GENEPOP (Rousset, 2008). Genotypic differentiation was tested using an exact test based on the MC algorithm (Guo and Thompson, 1992) with default parameters in GENEPOP.

Isolation by distance among populations was tested using a linear regression of genetic distances computed as $F_{ST}/(1 - F_{ST})$ over logarithms of the geographic distances ($ln(d)$) (Rousset, 1997). The significance of the correlation between the genetic distances ($F_{ST}/(1 - F_{ST})$) and the logarithms of geographic distances (Ln(d)) was tested by the Mantel test with 10,000 permutations in GENEPOP.

We used GESTE (Foll and Gaggiotti, 2006) to compute the population-specific F_{ST}. Measuring the genetic differentiation of each population, this method gives insight into the relative impact of genetic drift on the differentiation of the considered population (Gaggiotti and Foll, 2010).

Assignment Tests

Two sets of assignment tests in GeneClass2 (Piry et al., 2004) were conducted in order to (i) estimate the demographic connectivity among the six populations (not considering juveniles from CAVB) and (ii) detect migrants within the juveniles sampled in CAVB. First, we conducted a filtered assignment analysis following Lukoschek et al. (2016). We identified first-generation migrants (FGMs) in each population using the Bayesian criteria of Rannala and Mountain (1997) with 100,000 simulated genotypes and an alpha of 0.005. FGMs were removed from the dataset and reassigned to the reference dataset (i.e., dataset without FGMs). Migrants were assigned to a population if their assignment probability was >0.01. We allowed for multiple assignments (i.e., one individual originating potentially from different populations). When the assignment probability of an FGM was lower than 0.01 for all populations, we considered this FGM to come from an unsampled population.

Then, focusing on CAVB, we assigned CAVB-JUV considering the remaining samples (i.e., five populations + CAVB-AD) as reference. We used the Bayesian assignment method of Rannala and Mountain (1997) simulating 100,000 individuals and an alpha of 0.005. Following this analysis, CAVB-JUV was divided in two samples, CAVB-JUV-L and CAVB-JUV-M, distinguishing the juveniles originating from CAVB (locally produced) from the immigrant juveniles, respectively.

Fine-Scale SGS and Neighborhood Size

Focusing on CAVB, we analyzed the SGS by regressing the Nason's kinship coefficients (F_{ij}; Loiselle et al., 1995) among pairs of individuals on the logarithms of pairwise geographic distances, in SPAGEDI (Hardy and Vekemans, 2002). We first conducted this analysis considering a "global dataset" including CAVB-AD and CAVB-JUV-L. Then, we decomposed the SGS

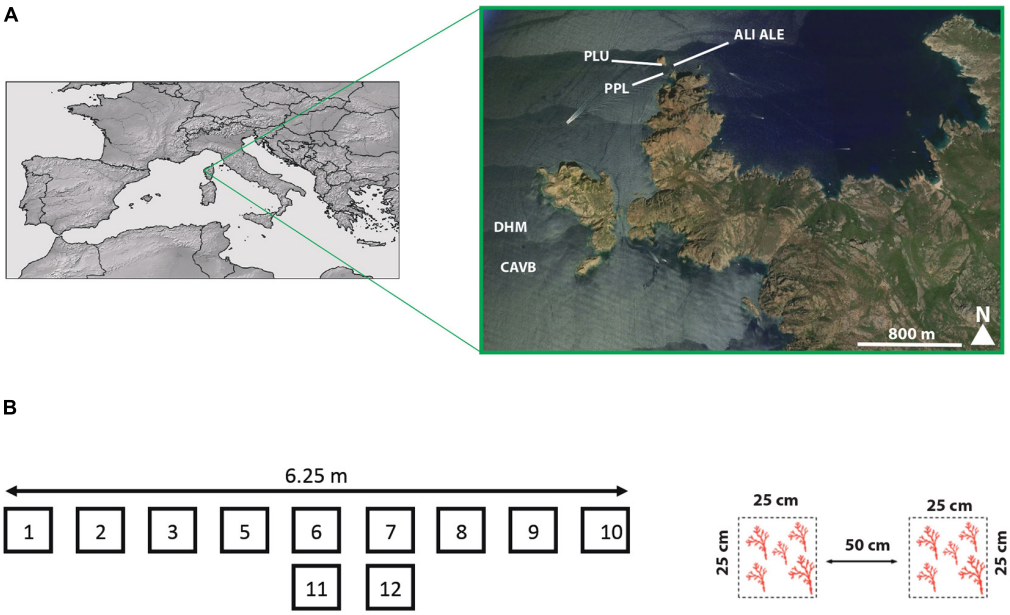

FIGURE 1 | (A) The « Réserve marine de Scandola » (Parc Naturel Régional de Corse, France) is located in the western coast of Corsica. Locations of the different populations sampled in the MPA are shown. The exact locations of CAVB and DHM are not shown on purpose. **(B)** Individual sampling conducted within the CAVB population. Adult and juvenile colonies were sampled within nine quadrats (25*25 cm) separated by 50 cm along a 6.25-m transect. Two quadrats were duplicated at the center of the transect, 25 cm under the main transect, resulting in 11 quadrats in total.

TABLE 1 | Location and genetic diversity estimators of the *Corallium rubrum* populations.

Population	Label	N	Latitude	Longitude	*r*	H_o	H_e	F_{IS}	$Ar_{(56)}$	Population-specific F_{ST} [95% CI]
Cave b	CAVB-AD	201	42°22′50″N	8°32′48″E	0.11	0.50	0.69	**0.25**	10.77	0.055 [0.044–0.067]
	CAVB-JUV	166				0.53	0.68	**0.22**	10.57	
Droite Harmelin	DHM	41	42°22′50″N	8°32′48″E	0.11	0.50	0.67	**0.24**	11.36	0.057 [0.041–0.075]
Corail Albinos extérieur	ALE	44	42°22′48″N	8°32′51.324″E	0.09	0.58	0.73	**0.22**	11.3	0.050 [0.036–0.067]
Corail Albinos intérieur	ALI	30	42°22′48″N	8°32′51.324″E	0.13	0.51	0.72	**0.30**	10.91	0.053 [0.035–0.072]
Grotte Palazzu	PLU	49	42°22′48.72″N	8°32′46.86″E	0.09	0.59	0.73	**0.20**	9.71	0.097 [0.070–0.123]
Passe Palazzu	PPL	49	42°22′47.64″N	8°32′51.288″E	0.09	0.57	0.72	**0.19**	9.81	0.079 [0.058–0.102]

N, number of individuals; r, frequency of null alleles estimated with FreeNa; H_o, observed heterozygosity; H_e, gene diversity (Nei, 1973); F_{IS}, following Weir and Cockerham (1984); $Ar_{(56)}$, rarefied allelic richness considering 56 genes. Population-specific F_{ST} and 95% CI. For Cave b (CAVB) and Droite Harmelin (DHM) samples, we only provided approximate coordinates. For Cave b, H_o, H_e F_{IS}, and $Ar_{(56)}$ are given for adults and juveniles. Bold values for F_{IS} correspond to populations where significant heterozygote deficiencies were observed (p-Values < 0.001). No significant difference was observed among adults and juveniles when comparing H_o, H_e F_{IS}, and $Ar_{(56)}$ (all p-Values > 0.05).

by conducting the same analyses considering three categories: CAVB-AD, CAVB-JUV-L, and a "between-generation" (i.e., each pair is composed by one juvenile and one adult), referring to allele frequencies within each group. In each case, significance of the slope of the linear regression (b) was tested using 10,000 permutations. The pattern of SGS was represented with a correlogram using eight distance classes ([0–25]; [25–75]; [75–150]; [150–231]; [231–300]; [300–376]; [376–451]; [451–625]). Approximate confidence intervals (95%) for average kinship values for each spatial distance were obtained by permuting individual locations 10,000 times. Differences in SGS among the different categories were assessed using the Sp statistics with $Sp = -b/(1 - \hat{F}_{(1)})$, with $\hat{F}_{(1)}$ being the mean F_{ij} among individuals belonging to the first distance interval (Vekemans and Hardy, 2004).

For the global dataset (CAVB-AD and CAVB-JUV-L), we computed the neighborhood size (N_b) as $N_b = 1/Sp$ and we deduced the moment estimate of the mean parent–offspring distance, σ_g, from $N_b = 4{*}\pi{*}D_e{*}\sigma_g{}^2$ (see Rousset, 1997) with the effective density, $D_e = 201$ ind*m^{-2} (all adult colonies take part in reproductive events; Garrabou et al., 2017) and $D_e = 100$ ind*m^{-2} (half of the adult colonies take part in reproductive events).

Sibship and Parentage Analysis

We characterized the pattern of relationships combining three different methods and considering two sets of individuals: (i) CAVB-JUV-L and CAVB-AD and (ii) CAVB-JUV-M.

First, we used the F_{ij} Nason's kinship coefficients. Theoretically, F_{ij} discriminates among different types of relationships: $F_{ij} = 0.25$ or $F_{ij} = 0.125$ is expected for full-sibs and half-sibs, respectively. However, depending on allele frequencies, F_{ij} is influenced by the polymorphism of the molecular markers. We conducted simulations based on the allele frequencies accounting for the six populations to estimate F_{ij} values linked to four levels of relationships: unrelated (UN), half-sibs (HS), full-sibs (FS), and parent-offspring (PO). RELATED R-package (Pew et al., 2015) was used to simulate 1,000 pairs of genotypes for each of the four categories. This allowed us to define threshold values for the different categories of relationships (see section "Results"). We then computed pairwise F_{ij}s within CAVB-JUV-L, within CAVB-JUV-M, and between CAVB-JUV-L and CAVB-AD, referring to the allele frequencies of the whole dataset, and we used the threshold values to characterize the pattern of relationships.

The maximum-likelihood method implemented in COLONY 2.0.6.1 (Jones and Wang, 2010) was used to reconstruct the parental relationships among individuals based on their multilocus genotypes. COLONY reconstructs sibship and assigns paternity jointly considering the likelihood over the entire pedigree. Analyses were conducted considering two sets of individuals (i.e., CAVB-JUV-L/CAVB-AD and CAVB-JUV-M). For each set, we conducted three runs with different seed numbers considering females and males as polygamous and using the full-likelihood method with very high likelihood precision and very long length of run. For the first set, individuals from CAVB-AD were considered as potential fathers or mothers, while the second set was conducted without potential parents.

The two methods showed contrasted results with a low number of concordant relationships, which may be explained by different factors such as the presence of null alleles. Accordingly, we contrasted the results obtained with the two methods in a third step, using the statistical approach implemented in ML-Relate (Kalinowski et al., 2006). The analysis based on F_{ij} involving a high number of pairs (>60,000), we thus focused on juveniles and, more particularly, on juveniles with $F_{ij} > 0.2625$ and on adult/juvenile pairs with $F_{ij} > 0.4228$ (see section "Results"). Regarding COLONY, we accounted for all the inferred HS, FS, and PO relationships. Overall, the first two methods identified 28 PO, 193 HS, and 16 FS relationships (see section "Results"). For each of the relationships identified with one method but not with the other, we considered the identified relationship as the putative relationship and the UN relationship as the alternative relationship in ML-Relate. The putative relationship was tested based on the sampling distribution of a test statistic obtained after simulations of 1,000 genotypes under the alternative hypothesis (see Kalinowski et al., 2006 for details).

RESULTS

Hardy–Weinberg Equilibrium and Genetic Diversity Estimators

Significant linkage disequilibrium after FDR correction was observed between *Mic13* and *Mic25* when considering all populations. However, no significant disequilibrium was observed when considering each population separately. The estimated frequency of null alleles was between 0.09 for PPL and 0.13 for ALI (mean over populations ± SE = 0.10 ± 0.01). The probability of identity (*Pi*) was $2.6 * 10^{-11}$, supporting the validity of the set of microsatellites to infer relationships among individuals. Observed heterozygosity values were between 0.50 for DHM and 0.59 for PLU (mean over populations ± SE = 0.54 ± 0.04). The gene diversity H_e ranged between 0.67 (DHM) and 0.74 (ALE) (mean over populations ± SE = 0.71 ± 0.02). The f estimator of F_{IS} varied between 0.19 (PPL) and 0.23 (CAVB-AD) (mean over populations ± SE = 0.23 ± 0.04). Significant departure from panmixia was observed in all populations (significant p-Value after FDR correction). The lowest and highest values of $Ar_{(56)}$ were observed for PLU (9.71) and DHM (11.36) (mean $Ar_{(56)}$ over populations ± SE = 10.63 ± 0.65) (see **Table 1**). None of the genetic diversity estimators was significantly different among CAVB-AD vs. CAVB-JUV (all p-Values > 0.05).

SGS Among Populations

L*nP(D)* increased slightly for the whole range of considered K-values (i.e., no plateau) with the strongest increases observed for $K = 2$ and $K = 3$. Evanno's method (Evanno et al., 2005) identified two different genetic clusters, while Peuchmaille statistics supported $K = 2$ (median/mean with threshold 0.7 and 0.8) and $K = 3$ (remaining statistics) (**Figure 2A**; **Supplementary Material**). For $K = 2$, the first cluster encompassed all the individuals from CAVB and DHM (mean membership coefficient = 0.93). The remaining individuals were grouped in a second cluster with a relatively high mean membership coefficient (0.87). When considering $K = 3$, this second cluster was divided in two clusters segregating the individuals from PLU (mean membership coefficient = 0.91). Those results were consistent considering null alleles as recessive alleles or missing data (data not shown).

In the DAPC analyses, individuals from CAVB and DHM were separated from the remaining individuals along the first axis, while the second axis separated the individuals from PLU from the individuals from ALI, ALE, and PPL. Those two axes represented 79.4% of the total variation in the data (**Figure 2B**).

The global F_{ST} was 0.069. The pairwise F_{ST}s ranged from 0.022 for ALI vs. ALE to 0.124 for CAVB vs. PLU. The genetic distance ($F_{ST}/(1 - F_{ST})$) and the geographic distance ($Ln(d)$) were not correlated rejecting the IBD among the six populations (p-Value = 0.22). The exact tests for genotypic differentiation were significant at the global level and for all pairwise comparisons except between ALI and ALE, separated by 20 m (see **Supplementary Material**). Regarding the temporal differentiation, the pairwise F_{ST} between CAVB-AD and CAVB-JUV was low (0.001), but the genotypic differentiation was significant (p-Value < 0.01).

The lowest population-specific F_{ST} was observed for ALE (0.050; 95% CI: 0.036–0.067) whereas the highest value was observed for PLU (0.097; 95% CI: 0.070–0.123). Based on 95%

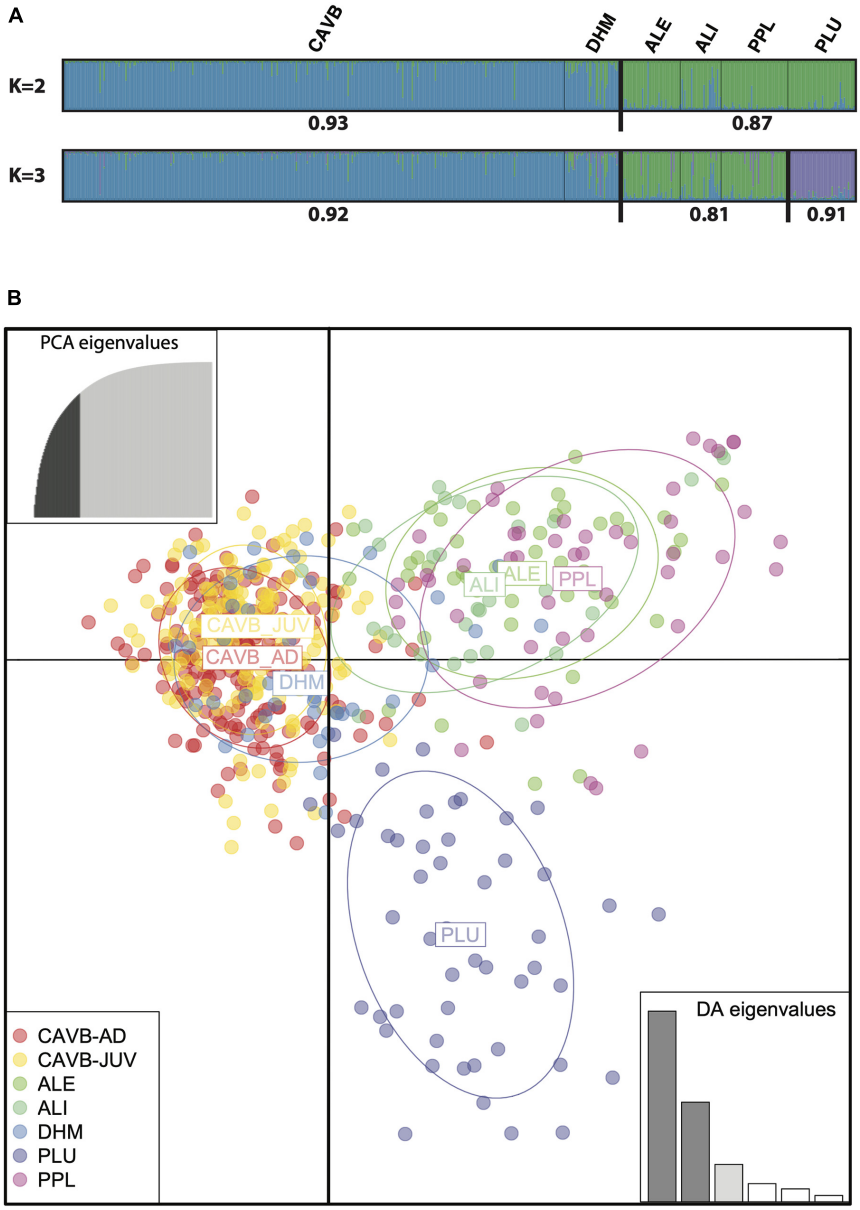

FIGURE 2 | Result of the clustering analysis of *Corallium rubrum* from the Scandola Marine Reserve conducted with STRUCTURE considering two and three clusters (*K*). **(A)** Each individual is represented by a vertical line partitioned in *K*–colored segments, which represent the individual membership fraction in *K* clusters. Thin and thick black vertical lines delineate the different populations and the different clusters, respectively. Sample names are shown above the assignment plots, while the mean membership coefficients for each cluster are shown below the assignment plots. **(B)** Scatter plot of the discriminant analysis of principal components (DAPC) based on a *a–score* of 46. Each dot corresponds to one individual ($n = 580$) from the seven populations (here CAVB-AD and CAVB-JUV were considered separately), which are represented by different colors. Inertia ellipses center on the mean for each population and include 67% of the individuals. The two axes of the scatter plot explained 52.1% and 27.3% of the total genetic variation in the dataset.

CI, significantly different population-specific F_{ST}s were observed for PLU vs. CAVB and PLU vs. ALE (**Table 1**).

Assignment Tests

Considering the whole dataset, 69 of the 419 individuals (16.4%) were identified as FGM, with eight (PPL) to 15 (DHM) FGMs per population. Considering assignment probability > 0.01 and allowing for multiple assignments, we assigned seven FGMs (10.1%) to three populations (CAVB, ALE, and PPL) indicating that 89.9% of the FGMs came from unsampled populations. Three populations (DHM, ALI, and PLU) did not produce any FGM. From the assigned FGMs, 50% came from CAVB.

When focusing on CAVB, 17 juveniles were not assigned to CAVB-AD (i.e., assignment probability < 0.005), while 10 juveniles were assigned to one of five other populations, with a probability higher than the assignment probability to CAVB-AD.

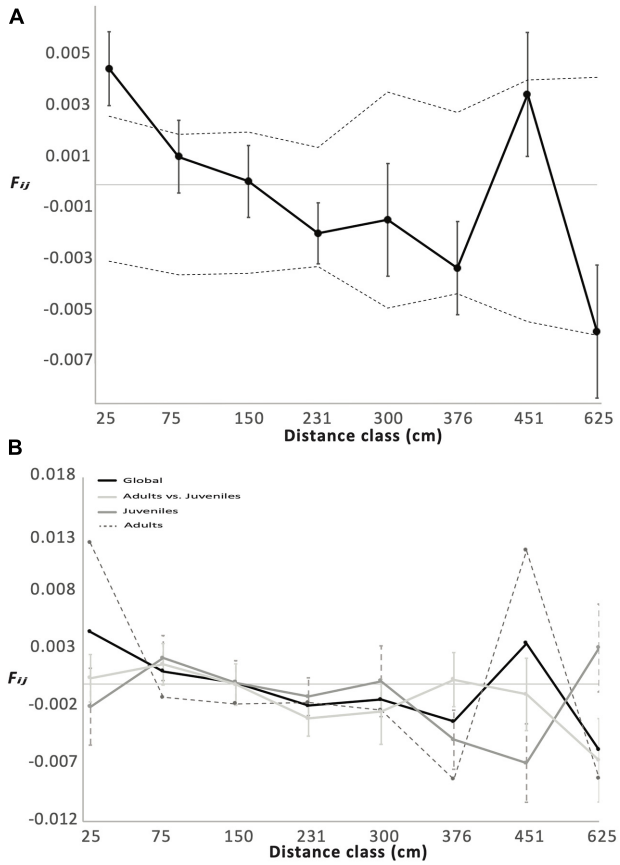

FIGURE 3 | Decomposing the spatial genetic structure among red coral colonies within the CAVB population. **(A)** Mean kinship coefficient (*Fij*) considering all the individuals (adults and juveniles) for each of distance class (*d*). Vertical lines correspond to standard errors. Dashed lines correspond to 95% confidence interval computed after 10,000 permutations of individual locations. The correlation among the genetic (F_{ij}) and geographic (ln(*d*)) distances among individuals was significant (*p*-Value = 0.04). **(B)** The global spatial genetic structure considering all the individuals (black line) is decomposed considering (i) only the pairs of adults (dotted line); (ii) only the pairs of juveniles (dark gray line); and (iii) only the pairs involving one adult and one juvenile (light gray line). The correlation among genetic (F_{ij}) and geographic (*ln(d)*) distances among individuals was significant when considering the juvenile pairs (*p*-Value = 0.04) and the adult–juvenile pairs (*p*-Value = 0.03) but not the adult pairs.

Accordingly, those 27 juveniles were considered as migrants. Considering only assignment probability higher than 0.01, nine of these 27 (33.3%) migrants were assigned to DHM. The 18 remaining migrants were considered as coming from unsampled population(s) (assignment probability < 0.01 in all populations).

Fine-Scale SGS

We demonstrated an overall SGS based on the marginally significant and negative correlation between Nason's kinship coefficients (F_{ij}) and *ln(d)* observed when considering the "global dataset" ($b = -1.7 * 10^{-3}$; *p*-Value = 0.04). From the neighborhood size (Nb = 575.3 individuals), we estimated the mean parent–offspring distance σ_g = 15.09 cm and 21.39 cm for D_e = 201 individuals*m^{-2} and D_e = 100 individuals*m^{-2}, respectively. The decrease in kinship with geographic distance remained significant considering the CAVB-JUV-L dataset ($b = -2.4*10^{-3}$; *p*-Value = 0.03) and the CAVB-AD/CAVB-JUV-L dataset ($b = -2.2*10^{-3}$; *p*-Value = 0.04). No significant correlation was observed ($b = -8.2*10^{-4}$; *p*-Value = 0.29) when considering CAVB-AD. In spite of a trend toward stronger SGS for CAVB-JUV-L and CAVB-AD/CAVB-JUV-L (Sp = 0.0024 and 0.0022, respectively) compared to the whole dataset (Sp = 0.0017), no significant difference in Sp was observed (**Figure 3** and **Table 2**).

Sibship and Parentage Analysis

The pairwise F_{ij} values for simulated unrelated (UN), halfsibs (HS), fullsibs (FS), and parent–offspring (PO) ranged from −0.1984 to 0.2625 (mean ± SD = −0.001 ± 0.071), −0.1160 to 0.4228 (0.126 ± 0.087), −0.0246 to 0.6393 (0.248 ± 0.106), and 0.0622 to 0.6556 (0.252 ± 0.077), respectively. Considering the overlaps of simulated F_{ij} distributions for the four categories of relationships (see **Supplementary Material 4**), we distinguished UN ($F_{ij} < -0.1160$) from related (HS, FS, and PO) pairs ($F_{ij} > 0.2625$). Within the related pairs, juvenile pairs with $0.2625 < F_{ij} < 0.4228$ were considered as HS or FS. Finally, pairs with $F_{ij} > 0.4228$ were assigned to PO or FS depending on whether they involved one adult/one juvenile or two juveniles, respectively. Note that some pairs (e.g., all the pairs with $-0.1160 < F_{ij} < 0.2625$) were not further considered since we were unable to assign a relationship category.

For the 351 pairs involving the 27 migrant juveniles (CAVB-JUV-M), the mean F_{ij} (±SD) was 0.0084 (0.1124). We identified eight related pairs ($F_{ij} > 0.2625$; 2.2%), from which seven were considered as HS or FS ($0.2625 < F_{ij} < 0.4228$; 1.9%) and one as FS ($F_{ij} > 0.4228$; 0.3%). Forty pairs were considered as UN ($F_{ij} < -0.1159$; 11.4%). UN and HS pairs occurred among juveniles belonging to the same or to different quadrats, while the FS involved individuals sampled within the same quadrat.

When considering 139 local juveniles (CAVB-JUV-L), the mean F_{ij} (±SD) was 0.0166 (0.0981). Among the 9,591 pairs, 689 (7.18%) were considered as UN ($F_{ij} < -0.1159$), while 153 HS or FS ($0.2625 < F_{ij} < 0.4228$; 1.6%) and six FS ($F_{ij} > 0.4228$; 0.06%) pairs were revealed. Two FS pairs involved juveniles sampled at the two extremes of the transect while 66 UN pairs involved juveniles sampled in the same quadrat.

The mean F_{ij} (±SD) among adults (CAVB-AD) was 0.0086 (0.1007). Among the 20,100 pairs, we identified 1761 (8.76%) UN ($F_{ij} < -0.1159$) and 329 (1.63%) related ($F_{ij} > 0.2625$) pairs. From the related pairs and considering the CAVB-AD samples involving different generations, 306 (1.52%) were considered as HS or similar second-degree relatives (e.g., grand-parent/grand-offspring, avunculate) ($0.2625 < F_{ij} < 0.4228$), while 23 (0.01%) were considered as FS or first-degree relatives ($F_{ij} > 0.4228$).

The mean F_{ij} (±SD) for CAVB-AD vs. CAVB-JUV-L was 0.0104 (0.0990). Among the 30,351 pairs, we identified 2,629 (8.66%) UN ($F_{ij} < -0.1159$) and 412 (1.35%) related ($F_{ij} > 0.2625$) pairs. From the related pairs, 387 (1.52%) were considered as HS or similar degree relationships

TABLE 2 | Decomposing the spatial genetic structure among individuals within Cave-b population: Summary statistics of the regression analyses between the geographic (*ln(d)*) and genetic (F_{ij}) distances among pairs of individuals.

	Global		Adults vs. juveniles		Adults		Juveniles	
	Moment estimate	**95% CI**	**Moment estimate**	**95% CI**	**Moment estimate**	**95% CI**	**Moment estimate**	**95% CI**
b	**-0.0017**	−0.0020; 0.0016	**-0.0023**	−0.0025; 0.0029	−0.0009	−0.0050; 0.0033	**-0.0023**	−0.0026; 0.0023
F_1	0.0045	−0.0030; 0.0027	0.0005	−0.0050; 0.0031	0.0123	−0.0054; 0.0048	−0.0019	−0.0069; 0.0061
Sp	0.0017	−0.0016; 0.0020	0.0023	−0.0029; 0.0025	0.0009	−0.0034; 0.0049	0.0023	−0.0023; 0.0025
Nb (individuals)	575.28							
σ^2_g (cm) $D_e = 201$ individus*m^{-2}	15.09							
σ^2_g (cm) $D_e = 100$ individus*m^{-2}	21.39							

We considered alternatively (i) all the individual pairs (Global); (ii) only individual pairs involving one adult and one juvenile (Adults vs. Juveniles); (iii) only individual pairs involving two adults (Adults); and (iv) individual pairs involving two juveniles (Juveniles). b: slope of the linear regression (in bold significant value at 0.05); $F_{(1)}$ the mean F_{ij} between individuals belonging to the first distance interval; Sp statistics with $Sp = -b/(1 - F_{(1)})$ (see Vekemans and Hardy, 2004). For the regression involving all the individuals (Global), we computed the neighborhood size (Nb) and the mean parent–offspring distance (σ^2_g) considering two different values of effective density (D_e).

(0.2625 < F_{ij} < 0.4228), while 25 (0.08%) were considered as PO ($F_{ij} > 0.4228$).

Regarding COLONY analyses, no HS and two (0.6%) FS pairs ($p > 0.6$) were observed in migrant juveniles (CAVB-JUV-M). Considering local juveniles (CAVB-JUV-L) and adults (CAVB-AD), 10 (0.1%) FS and 40 (0.4%) HS pairs were identified ($p > 0.6$) in addition to three PO pairs. All the PO pairs involved the same parent.

Filtering these results using the statistical test implemented in ML-Relate, we retained 114 HS, 7 FS among the local juveniles (CAVB-JUV-L), and 11 PO pairs when considering the adults. Within the migrant juveniles (CAVB-JUV-M), two HS and one FS pairs were retained.

DISCUSSION

Genetic Diversity and Structure in the Scandola Marine Reserve: Apparent Stability of the Diversity Pattern in Spite of a Dramatic Demographic Decline

We used complementary approaches to characterize the SGS among six red coral populations in the Scandola Marine Reserve. When considering the clustering approach, the first level of structure ($K = 2$) supports the occurrence of a geographic break among the northern (PLU, PPL, ALI, and ALE) and southern (CAVB and DHM) populations with high membership coefficients (0.87 and 0.93, respectively). For $K = 3$, individuals from PLU were segregated from the individuals from PPL, ALI, and ALE forming two subclusters, also characterized by high membership coefficients (0.91 and 0.81, respectively). This pattern was fully supported by the DAPC analyses, which discriminated among northern and southern populations along the first axis (52.1%), while individuals from PLU were separated from PPL, ALI, and ALE along the second axis (27.3%). When shifting at the population level, we found significant genotypic differentiation among all population pairs, with the exception of ALE vs. ALI, which belong to the same location (only apart by 15 m). Worthy of note is that the genetic distances between populations were not correlated with the geographic distances, rejecting the isolation-by-distance pattern (IBD). Computations of the population-specific F_{ST}s identified PLU as genetically isolated, compared to the remaining populations, which showed relatively homogenous values. Accordingly, a geographic imprint explains part of the global pattern (i.e., northern vs. southern clusters). Yet, the differentiation of PLU points out the importance of local genetic drift effects in the survey area, which may potentially explain the lack of IBD usually reported in this species (e.g., Ledoux et al., 2010a; Aurelle et al., 2011). Non-exclusive hypotheses can explain this genetic differentiation of PLU. Located in a cave, PLU can be isolated from neighboring populations due to hydrodynamic factors (e.g., Costantini et al., 2018). PLU is also impacted by a dramatic demographic decline with more than 90% of biomass lost during the last 15 years due to warming-induced MMEs (Gómez-Gras et al., 2021). This decline can potentially increase the effect of genetic drift in this particular population.

Overall, the pattern reported here, combining different genetic clusters with a lack of IBD, matches the pattern previously reported in the same region almost 10 years ago (Ledoux et al., 2010a). The same happens for the genetic diversity estimators, with values estimated here similar to previously reported values (Ledoux et al., 2010a). Changes in heterozygosity values are difficult to detect (Riquet et al., 2017), and a delay in the detection of genetic erosion is expected in long-lived species with overlapping generations such as red coral (e.g., Hailer et al., 2006). However, this apparent stability in the pattern of genetic structure and diversity remains surprising considering the dramatic demographic decline reported in red coral in this area (Gómez-Gras et al., 2021). While deserving cautious interpretation, this result highlights the need to consider complementary metrics such

as effective population sizes to characterize temporal trend in genetic diversity.

Integrating "Among Populations" and "Within Population" Demo-Genetic Approaches: Demographic Connectivity of Red Coral in the Scandola Marine Reserve

Our analyses suggested substantial demographic connectivity among the studied populations. Indeed, 16.4% of the mature individuals were identified as FGMs, in the six populations, including the drifting population of PLU. This result may appear counterintuitive in the context of the significant genetic structure observed even between populations separated by tens of meters (e.g., PPL vs. ALE). However, it is supported by recent studies in other Mediterranean octocorals reporting some levels of contemporary connectivity at least during recolonization steps (e.g., Arizmendi-Mejía et al., 2015; Padrón et al., 2018; Aurelle et al., 2020). Conciliating these, *a priori*, contradictory results imply further studies such as a detailed characterization of the balance between genetic drift and gene flow, during the course of population succession (i.e., from colonization to senescence). We hypothesize that the genetic imprint of migrants on a population will decrease from colonization to population maturation due to an increase of the genetic imprint of locally produced recruits. Our current understanding of the colonization processes (see below) combined to a potential underestimation of the influence of genetic drift on the patterns of spatial structure in *Corallium rubrum*, and other octocorals (Ledoux et al., 2015; Crisci et al., 2017; Pratlong et al., 2018) are in line with this hypothesis. Low reproductive success of migrants (i.e., limited genetic connectivity), due for instance to microenvironmental conditions favoring locally produced genotypes (e.g., Gorospe and Karl, 2013), may be another hypothesis to explore to solve this apparent paradox.

Following the filtering assignment, most of the FGMs identified (89.9%) came from unsampled populations. When considering the assigned migrants, two populations (CAVB and ALE) were identified as the main sources in the population network. In spite of a lack of isolation by distance, most of these assigned migrants came from neighboring populations separated by tens of meters (e.g., from CAVB to DHM), suggesting a low level of demographic connectivity among the Northern and Southern main genetic clusters. These analyses also support that the pool of migrants identified in each population came from (at least two) different sources. Accordingly, the multiple origins of migrants demonstrated in recently colonized and mature populations of other Mediterranean octocorals (*Paramuricea clavata and Eunicella cavolini*; see Mokhtar-Jamaï et al., 2011; Arizmendi-Mejía et al., 2015; Ledoux et al., 2018; Padrón et al., 2018; Aurelle et al., 2020) can be expanded to *C. rubrum*.

Focusing on the CAVB population, we refined the spatial features of the red coral demographic connectivity. Over the 166 juveniles analyzed here, 27 (16.2%) were considered as migrants, suggesting that, in spite of a substantial demographic connectivity, the vast majority of the juveniles was locally produced. A high level of self-recruitment was previously suggested as a central process in red coral population dynamics (Costantini et al., 2007b; Ledoux et al., 2010b). Considering the migrant juveniles sampled in CAVB (CAVB-JUV-M), the sibship analyses revealed the occurrence sibship aggregation. We identified two pairs of halfsibs and one pair of fullsibs in these juveniles, the two individuals of the three pairs being sampled in the same quadrat. Accordingly, collective dispersal, the dispersal of at least two sibs originating from the same reproductive event in a distant population (Broquet et al., 2013), may occur in red coral. The factors driving these events are still largely unknown (but see Ottmann et al., 2016). Beside abiotic factors (e.g., no mixing of mass water), biotic factors both at the larval (behavior) and adult (synchronous larval release) levels, combined to species reproductive strategies, have been called on to explain collective dispersal. In particular, most of the collective dispersals involving marine invertebrate larvae were reported in brooding or partially brooding species (e.g., Riquet et al., 2017, but see Dubé et al., 2020). The internal fertilization (Santangelo et al., 2003), brooding period (Bramanti et al., 2005), and larvae active swimming behavior (Martínez-Quintana et al., 2015) may drive collective dispersal in red coral.

Finally, we gained a first insight into the temporal features of red coral demographic connectivity. The assignment analyses suggest a lack of constant pattern, at least for the CAVB population. In the juveniles sampled in CAVB (CAVB-JUV), most of the migrants came from DHM. This DHM to CAVB migration was not reported when considering the pool of mature colonies. Temporal variability in the genetic make-up of larvae and juveniles has been previously reported in various marine species from fishes (e.g., Salles et al., 2016) to invertebrates (e.g., David et al., 1997; Riquet et al., 2017). This result is also in line with the recruitment variability reported in red coral (Garrabou and Harmelin, 2002). Considering the overlapping generations in this species, identifying the origin of migrants in different cohorts is a challenging task that was recently successfully achieved by analyzing different recruitment events, using settlement plates (Costantini et al., 2018). In this experimental framework, genetic heterogeneity among juveniles coming from two consecutive reproductive events was revealed (Costantini et al., 2018), consistently with the temporal variations reported here.

While the link between demographic and genetic connectivity remained to be fully characterized (but see below), the characterization of red coral demographic connectivity opens new perspectives for the management of the Scandola Marine Reserve.

Spatiotemporal Genetic Structure Among Individuals in a Near-Pristine Population: Complementing the Eco-Evolutionary Feedbacks Underlying Red Coral Population Dynamics

We demonstrated a statistically significant SGS when considering the adults and the local juvenile-stage classes in CAVB, a

population with a near-pristine demographic structure (high size colonies at high density = 201 colonies*m^{-2}; Garrabou et al., 2017). A statistically significant SGS within population has been previously demonstrated in red coral (Ledoux et al., 2010b), albeit in a declining population characterized by different demographic features (high density of small size colonies; 160 colonies*m^{-2}). This shared pattern in such contrasted demographic situations suggests that SGS among colonies may be a common feature of red coral populations. Interestingly, the moment estimator of the neighborhood size (*Nb*) estimated in CAVB was one order of magnitude higher than the *Nb* previously reported in the declining population (575.3 vs. 75 individuals), resulting in a slightly lower effective dispersal (σ_g; from 15.1 to 21.4 cm vs. from 22.6 to 32.1 cm). While this comparison should be taken with caution owing to the different sampling strategies (quadrats vs. individual sampling), a decrease of σ_g with a higher effective density is expected (see Vekemans and Hardy, 2004). This feedback between effective density and dispersal (i.e., higher dispersal in low-density population) was proposed as a process buffering, to some point, the increase of genetic drift expected in declining populations and may be critical for the maintenance of red coral populations (Ledoux et al., 2020).

Such restricted σ_g seems conflicting with the pattern of demographic connectivity previously drawn based on assignment method. One should keep in mind the different dispersal components (demographic vs. genetic) estimated by the two methods (Broquet and Petit, 2009). Moreover, estimation of σ_g based on SGS among individuals may underestimate long-distance dispersal (Leblois et al., 2004). Consistent with a potential underestimation of effective dispersal, the sibship analyses revealed for instance one parent–offspring pair separated by 300 cm, suggesting that longer-distance dispersal may happen.

We then decomposed the SGS accounting for the stage class of the individuals (i.e., adults and juveniles). We first revealed a significant SGS among adults and juveniles and showed that the significant SGS was retained in the juveniles but not in the adults. The significant SGS among stage classes corroborates the central role of restricted dispersal in the structure and in the dynamics of red coral populations. In spite of the demographic connectivity among populations previously discussed and of the occurrence of long-distance dispersal events, larvae recruit preferentially in the close vicinity of their parents (Ledoux et al., 2010b, this article). This restricted dispersal builds up the SGS within local juveniles. While potential methodological limitations (i.e., overlapping generations in the adult sample; see Berens et al., 2014) may take part in the random pattern observed among adult colonies, the decrease in SGS from juveniles to adults can be linked to an imprint of mortality during the early life stage (e.g., Chung et al., 2003; Hampe et al., 2010), corroborating the high mortality rates in the juveniles compared to adults reported by demographic surveys (Garrabou and Harmelin, 2002; Bramanti et al., 2007; Santangelo et al., 2012). The process underlying this demographic transition (e.g., self-thinning vs. density-independent mortality) remains a matter of discussion in red coral (Cau et al., 2016; Garrabou et al., 2017).

Shifting From Patterns to Processes to Improve the Conservation of Red Coral in the Scandola Marine Reserve and the Restoration of Declining Populations

Implemented more than 40 years ago, the Scandola Marine Reserve belongs to the 0.23% of the Mediterranean that is fully protected (Claudet et al., 2020). Beside harboring a unique and near-pristine shallow population of red coral (Garrabou et al., 2017), the benefits of the management conducted in this MPA on red coral are noteworthy (Linares et al., 2010, 2012). We revealed here contrasted connectivity among populations forming the red coral network. We highlighted the restricted connectivity, at least on a contemporary timescale, among the Northern and Southern parts of the MPA and, accordingly, the need to consider these localities as distinct management units. The potential for genetic isolation at local scale, as observed for PLU, is also of management interest. Indeed, isolated populations may be targeted by restoration to increase their effective population size and to buffer potential drift and related negative effects (e.g., expression of deleterious alleles and decrease population fitness; see Frankham, 2005; Garner et al., 2020). Still on the management prioritization, we identified two particular populations, namely, CAVB and ALE, as the main sources of migrants within the network. Additional populations must be sampled to refine this connectivity pattern. Moreover, while our results suggested relatively homogeneous levels of genetic diversity among the different populations, this pattern does not account for adaptive genetic variations (i.e., variations that produce advantages in fitness), which may be limited in this particular area (Ledoux et al., 2015). This is a crucial knowledge gap for an effective management of the MPA, which should be filled using available genomic resources (Pratlong et al., 2015, 2018).

Restoration actions are a promising tool in red coral at local scale (Montero-Serra et al., 2017). Restoration protocols usually rely on different components including the number of individuals to transplant, the transplanting design, and the choice of source populations (Weeks et al., 2011; Mijangos et al., 2015; Breed et al., 2019). Ledoux et al. (2010b) suggest to create small size and dense patches (tens to a hundred of colonies over half square meter) of reproductive colonies to mimic the patterns of structure characterizing red coral populations. Our results support this preliminary statement. We confirmed here the importance of restricted dispersal and of interactions among genetically and spatially related individuals in the dynamics of red coral populations. The size of a functional restored patch, i.e., promoting genetic interactions among colonies, depends on the density of transplanted colonies. Interestingly, in the two contrasted density situations analyzed so far (i.e., a declining population vs. near-pristine population), the mean effective dispersal remains within the order of tens of cm, with occasional more distant dispersal events. This restricted range of dispersal distances sets the scale for restoration actions (i.e., tens of cm). Yet, the parentage analyses revealed the potential for long-distance effective dispersal within population, beyond the mean parent–offspring distance (σ_g). Accordingly, it may be more efficient to

restore a particular location creating small and dense patches of colonies (tens to a hundred of colonies in 0.5 to 1 m^2 area), separated by 2 to 3 m, in order to "capture" these long-distance dispersers, rather than a low-density and continuous patch. Finally, sourcing is a critical aspect of restoration. The identification of FGMs from different origins supports the need to consider different populations for sourcing. However, one important gap here relies on the ability of red coral colonies to deal with the ongoing warming (Garrabou et al., 2019). In this context, the identification of the genomic factors and eco-evolutionary processes driving the response to thermal stress in red coral (Pratlong et al., 2015, 2018) is the next critical step to improve restoration actions in the warming context.

Overall, the spatially integrated demo-genetic approach presented here revealed poorly known aspects of red coral eco-evolution, with strong implications for the species conservation and restoration. While targeting this species is particularly relevant considering its key ecological role in the coralligenous community, we call for the development of comparative studies among species to increase the robustness of the management inputs coming from eco-evolution studies.

DATA AVAILABILITY STATEMENT

The original contributions presented in the study are included in the article/**Supplementary Material**, further inquiries can be directed to the corresponding author/s.

AUTHOR CONTRIBUTIONS

J-BL, J-MD, and JG designed the study. J-BL, IM-S, J-MD, CL, and JG collected the samples. CG, PL-S, and J-BL performed the molecular analyses. CG and J-BL conducted the statistical analyses and led the writing of the manuscript. All authors contributed critically to the drafts and gave the final approval for publication.

FUNDING

This research was supported by the Strategic Funding UIDB/04423/2020 and UIDP/04423/2020 through national funds provided by the FCT – Foundation for Science and Technology and European Regional Development Fund (ERDF), in the framework of the program PT2020, the Spanish MINECO (CGL2012-32194), the TOTAL Foundation PERFECT project, the MIMOSA project funded by the foundation Prince Albert II de Monaco, and the European Union's Horizon 2020 Research and Innovation Program under grant agreement N° 689518 (MERCES). This output reflects only the authors' view, and the European Union cannot be held responsible for any use that may be made of the information contained therein. J-BL was funded by an assistant researcher contract framework of the RD Unit—UID/Multi/04423/2019 – Interdisciplinary Centre of Marine and Environmental Research—financed by the European Regional Development Fund (ERDF) through COMPETE2020 – Operational Program for Competitiveness and Internationalization (POCI) and national funds through FCT/MCTES (PIDDAC). Genotyping was performed at the Genome Transcriptome Facility of Bordeaux (grants from the Conseil Régional d'Aquitaine n 20030304002FA and 20040305003FA, from the European Union FEDER n 2003227 and from Investissements d'Avenir ANR-10-EQPX-16-01). This work acknowledges the "Severo Ochoa Centre of Excellence" accreditation (CEX2019-000928-S). We acknowledge support of the publication fee by the CSIC Open Access Publication Support Initiative through its Unit of Information Resources for Research (URICI).

SUPPLEMENTARY MATERIAL

The Supplementary Material for this article can be found online at: https://www.frontiersin.org/articles/10.3389/fmars.2021.633057/full#supplementary-material

REFERENCES

Abbiati, M., Santangelo, G., and Novelli, S. (1993). Genetic variation within and between two Tyrrhenian populations of the Mediterranean alcyonarian *Corallium rubrum*. *Mar. Ecol. Prog. Ser.* 95, 245–250. doi: 10.3354/meps095245

Arizmendi-Mejía, R., Linares, C., Garrabou, J., Antunes, A., Ballesteros, E., Cebrian, E., et al. (2015). Combining genetic and demographic data for the conservation of a Mediterranean marine habitat-forming species. *PLoS One* 10:e0119585. doi: 10.1371/journal.pone.0119585

Aurelle, D., and Ledoux, J.-B. (2013). Interplay between isolation by distance and genetic clusters in the red coral *Corallium rubrum*: insights from simulated and empirical data. *Conserv. Genet.* 14, 705–716. doi: 10.1007/s10592-013-0464-0

Aurelle, D., Ledoux, J.-B., Rocher, C., Borsa, P., Chenuil, A., and Féral, J.-P. (2011). Phylogeography of the red coral (*Corallium rubrum*): inferences on the evolutionary history of a temperate gorgonian. *Genetica* 139, 855–869. doi: 10.1007/s10709-011-9589-6

Aurelle, D., Tariel, J., Zuberer, F., Haguenauer, A., Ribout, C., Masmoudi, M., et al. (2020). Genetic insights into recolonization processes of Mediterranean octocorals. *Mar. Biol.* 167:73. doi: 10.1007/s00227-020-03684-z

Ballesteros, E. (2006). Mediterranean coralligenous assemblages: a synthesis of present knowledge. *Oceanogr. Mar. Biol. An Annu. Rev.* 44, 123–195.

Berens, D. G., Braun, C., González-Martínez, S. C., Griebeler, E. M., Nathan, R., and Böhning-Gaese, K. (2014). Fine-scale spatial genetic dynamics over the life cycle of the tropical tree Prunus africana. *Heredity (Edinb)* 113, 401–407. doi: 10.1038/hdy.2014.40

Bierne, N., Bonhomme, F., and Arnaud-Haond, S. (2016). Editorial dedicated population genomics for the silent world: the specific questions of marine population genetics. *Curr. Zool.* 62, 545–550. doi: 10.1093/cz/zow107

Boavida, J., Paulo, D., Aurelle, D., Arnaud-Haond, S., Marschal, C., Reed, J., et al. (2016). A well-kept treasure at depth: precious red coral rediscovered in atlantic deep coral gardens (SW Portugal) after 300 Years. *PLoS One* 11:e0147228. doi: 10.1371/journal.pone.0147228

Bramanti, L., Magagnini, G., De Maio, L., and Santangelo, G. (2005). Recruitment, early survival and growth of the Mediterranean red coral *Corallium rubrum* (L 1758), a 4-year study. *J. Exp. Mar. Bio. Ecol.* 314, 69–78. doi: 10.1016/j.jembe.2004.08.029

Bramanti, L., Rossi, S., Tsounis, G., Gili, J. M., and Santangelo, G. (2007). Settlement and early survival of red coral on artificial substrates in different geographic

areas: some clues for demography and restoration. *Hydrobiologia* 580, 219–224. doi: 10.1007/s10750-006-0452-1

Breed, M. F., Harrison, P. A., Blyth, C., Byrne, M., Gaget, V., Gellie, N. J. C., et al. (2019). The potential of genomics for restoring ecosystems and biodiversity. *Nat. Rev. Genet.* 20, 615–628. doi: 10.1038/s41576-019-0152-0

Broquet, T., and Petit, E. J. (2009). Molecular estimation of dispersal for ecology and population genetics. *Annu. Rev. Ecol. Evol. Syst.* 40, 193–216. doi: 10.1146/annurev.ecolsys.110308.120324

Broquet, T., Viard, F., and Yearsley, J. M. (2013). Genetic drift and collective dispersal can result in chaotic genetic patchiness. *Evolution (N. Y)* 67, 1660–1675. doi: 10.1111/j.1558-5646.2012.01826.x

Bruckner, A. W. (2009). Rate and extent of decline in Corallium (pink and red coral) populations: existing data meet the requirements for a CITES Appendix II listing. *Mar. Ecol. Prog. Ser.* 397, 319–332. doi: 10.3354/meps08110

Cau, A., Bramanti, L., Cannas, R., Follesa, M. C., Angiolillo, M., Canese, S., et al. (2016). Habitat constraints and self-thinning shape Mediterranean red coral deep population structure: implications for conservation practice. *Sci. Rep.* 6:23322. doi: 10.1038/srep23322

Cerrano, C., Bavestrello, G., Bianchi, C. N., Cattaneo-vietti, R., Bava, S., Morganti, C., et al. (2000). A catastrophic mass-mortality episode of gorgonians and other organisms in the Ligurian Sea (North-western Mediterranean), summer 1999. *Ecol. Lett.* 3, 284–293. doi: 10.1046/j.1461-0248.2000.00152.x

Chung, M. Y., Epperson, B. K., and Chung, M. (2003). Genetic structure of age classes in *Camellia japonica* (Theaceae). *Evolution* 57, 62–73. doi: 10.1111/j.0014-3820.2003.tb00216.x

Chung, M., Nason, J., Nason, J., Nason, J., Nason, J., and Nason, J. (2007). Spatial demographic and genetic consequences of harvesting within populations of the terrestrial orchid *Cymbidium goeringii*. *Biol. Conserv.* 137, 125–137.

Claudet, J., Loiseau, C., Sostres, M., and Correspondence, M. Z. (2020). Underprotected marine protected areas in a global biodiversity hotspot. *One Earth* 2, 380–384. doi: 10.1016/j.oneear.2020.03.008

Cook, C. N., and Sgrò, C. M. (2018). Understanding managers' and scientists' perspectives on opportunities to achieve more evolutionarily enlightened management in conservation. *Evol. Appl.* 11, 1371–1388. doi: 10.1111/eva.12631

Costantini, F., Fauvelot, C., and Abbiati, M. (2007a). Genetic structuring of the temperate gorgonian coral (*Corallium rubrum*) across the western Mediterranean Sea revealed by microsatellites and nuclear sequences. *Mol. Ecol.* 16, 5168–5182.

Costantini, F., Fauvelot, C., and Abbiati, M. (2007b). Fine-scale genetic structuring in *Corallium rubrum*: evidence of inbreeding and limited effective larval dispersal. *Mar. Ecol. Prog. Ser.* 340, 109–119.

Costantini, F., Rugiu, L., Cerrano, C., and Abbiati, M. (2018). Living upside down: patterns of red coral settlement in a cave. *PeerJ* 6:e4649. doi: 10.7717/peerj.4649

Costello, M. J., and Ballantine, B. (2015). Biodiversity conservation should focus on no-take marine reserves: 94% of marine protected areas allow fishing. *Trends Ecol. Evol.* 30, 507–509. doi: 10.1016/j.tree.2015.06.011

Cramer, W., Guiot, J., Fader, M., Garrabou, J., Gattuso, J.-P., Iglesias, A., et al. (2018). Climate change and interconnected risks to sustainable development in the Mediterranean. *Nat. Clim. Chang.* 8, 972–980. doi: 10.1038/s41558-018-0299-2

Crisci, C., Ledoux, J.-B., Mokhtar-Jamaï, K., Bally, M., Bensoussan, N., Aurelle, D., et al. (2017). Regional and local environmental conditions do not shape the response to warming of a marine habitat-forming species /631/158 /631/208/457 /45/23 /45 /141 article. *Sci. Rep.* 7:5069. doi: 10.1038/s41598-017-05220-4

David, P., Perdieu, M.-A., Pernot, A.-F., and Jarne, P. (1997). Fine-Grained spatial and temporal population genetic structure in the marine bivalve *Spisula ovalis*. *Evolution* 51:1318. doi: 10.2307/2411061

Diffenbaugh, N. S., Pal, J. S., Giorgi, F., and Gao, X. (2007). Heat stress intensification in the Mediterranean climate change hotspot. *Geophys. Res. Lett.* 34, L11706. doi: 10.1029/2007GL030000

Dubé, C. E., Boissin, E., Mercière, A., and Planes, S. (2020). Parentage analyses identify local dispersal events and sibling aggregations in a natural population of *Millepora* hydrocorals, a free-spawning marine invertebrate. *Mol. Ecol.* 29, 1508–1522. doi: 10.1111/mec.15418

Edgar, G. J., Stuart-Smith, R. D., Willis, T. J., Kininmonth, S., Baker, S. C., Banks, S., et al. (2014). Global conservation outcomes depend on marine protected areas with five key features. *Nature* 506, 216–220. doi: 10.1038/nature13022

Evanno, G., Regnaut, S., and Goudet, J. (2005). Detecting the number of clusters of individuals using the software STRUCTURE: a simulation study. *Mol. Ecol.* 14, 2611–2620. doi: 10.1111/j.1365-294X.2005.02553.x

Falush, D., Stephens, M., and Pritchard, J. (2003). Inference of population structure using multilocus genotype data: linked loci and correlated allele frequencies. *Genetics* 164, 1567–1587.

Falush, D., Stephens, M., and Pritchard, J. K. (2007). Inference of population structure using multilocus genotype data: dominant markers and null alleles. *Mol. Ecol. Notes* 7, 574–578. doi: 10.1111/j.1471-8286.2007.01758.x

Foll, M., and Gaggiotti, O. (2006). Identifying the environmental factors that determine the genetic structure of populations. *Genetics* 174, 875–891. doi: 10.1534/genetics.106.059451

Frankham, R. (2005). Genetics and extinction. *Biol. Conserv.* 126, 131–140. doi: 10.1016/j.biocon.2005.05.002

Gaggiotti, O. E., and Foll, M. (2010). Quantifying population structure using the F-model. *Mol. Ecol. Resour.* 10, 821–830. doi: 10.1111/j.1755-0998.2010.02873.x

Gagnaire, P., Broquet, T., Aurelle, D., Viard, F., Souissi, A., Bonhomme, F., et al. (2015). Using neutral, selected, and hitchhiker loci to assess connectivity of marine populations in the genomic era. *Evol. Appl.* 8, 769–786. doi: 10.1111/eva.12288

Garner, B. A., Hoban, S., and Luikart, G. (2020). IUCN Red List and the value of integrating genetics. *Conserv. Genet.* 21, 795–801. doi: 10.1007/s10592-020-01301-6

Garrabou, J., and Harmelin, J. G. (2002). A 20-year study on life-history traits of a harvested long-lived temperate coral in the NW Mediterranean: insights into conservation and management needs. *J. Anim. Ecol.* 71, 966–978. doi: 10.1046/j.1365-2656.2002.00661.x

Garrabou, J., Coma, R., Bensoussan, N., Bally, M., Chevaldonné, P., Cigliano, M., et al. (2009). Mass mortality in Northwestern Mediterranean rocky benthic communities: effects of the 2003 heat wave. *Glob. Chang. Biol.* 15, 1090–1103. doi: 10.1111/j.1365-2486.2008.01823.x

Garrabou, J., Gómez-Gras, D., Ledoux, J.-B., Linares, C., Bensoussan, N., López-Sendino, P., et al. (2019). Collaborative database to track mass mortality events in the Mediterranean Sea. *Front. Mar. Sci.* 6:707. doi: 10.3389/fmars.2019.00707

Garrabou, J., Perez, T., Sartoretto, S., and Harmelin, J. G. (2001). Mass mortality event in red coral *Corallium rubrum* populations in the Provence region (France, NW Mediterranean). *Mar. Ecol. Prog. Ser.* 217, 263–272. doi: 10.3354/meps217263

Garrabou, J., Sala, E., Linares, C., Ledoux, J. B., Montero-Serra, I., Dominici, J. M., et al. (2017). Re-shifting the ecological baseline for the overexploited Mediterranean red coral. *Sci. Rep.* 7:42404. doi: 10.1038/srep42404

Gómez-Gras, D., Linares, C., Dornelas, M., Madin, J. S., Brambilla, V., Ledoux, J.-B., et al. (2021). Climate change transforms the functional identity of Mediterranean coralligenous assemblages. *Ecol. Lett.* 24, 1038–1051. doi: 10.1111/ele.13718

Gorospe, K. D., and Karl, S. A. (2013). Genetic relatedness does not retain spatial pattern across multiple spatial scales: dispersal and colonization in the coral, Pocillopora damicornis. *Mol. Ecol.* 22, 3721–3736. doi: 10.1111/mec.12335

Guo, S. W., and Thompson, E. A. (1992). Performing the exact test of hardy-weinberg proportion for multiple alleles. *Biometrics* 48:361. doi: 10.2307/2532296

Hailer, F., Helander, B., Folkestad, A. O., Ganusevich, S. A., Garstad, S., Hauff, P., et al. (2006). Bottlenecked but long-lived: high genetic diversity retained in white-tailed eagles upon recovery from population decline. *Biol. Lett.* 2, 316–319. doi: 10.1098/rsbl.2006.0453

Hampe, A., El Masri, L., and Petit, R. J. (2010). Origin of spatial genetic structure in an expanding oak population. *Mol. Ecol.* 19, 459–471. doi: 10.1111/j.1365-294X.2009.04492.x

Hardy, O. J., and Vekemans, X. (2002). spagedi: a versatile computer program to analyse spatial genetic structure at the individual or population levels. *Mol. Ecol. Notes* 2, 618–620. doi: 10.1046/j.1471-8286.2002.00305.x

Jacquemyn, H., Brys, R., Vandepitte, K., Honnay, O., and Roldán-Ruiz, I. (2006). Fine-scale genetic structure of life history stages in the food-deceptive orchid *Orchis purpurea*. *Mol. Ecol.* 15, 2801–2808. doi: 10.1111/j.1365-294X.2006.02978.x

Jakobsson, M., and Rosenberg, N. A. (2007). CLUMPP: a cluster matching and permutation program for dealing with label switching and multimodality in analysis of population structure. *Bioinformatics* 23, 1801–1806. doi: 10.1093/bioinformatics/btm233

Jombart, T. (2008). adegenet: a R package for the multivariate analysis of genetic markers. *Bioinformatics* 24, 1403–1405. doi: 10.1093/bioinformatics/btn129

Jombart, T., Devillard, S., and Balloux, F. (2010). Discriminant analysis of principal components: a new method for the analysis of genetically structured populations. *BMC Genet.* 11:94. doi: 10.1186/1471-2156-11-94

Jones, O. R., and Wang, J. (2010). COLONY: a program for parentage and sibship inference from multilocus genotype data. *Mol. Ecol. Resour.* 10, 551–555. doi: 10.1111/j.1755-0998.2009.02787.x

Kalinowski, S. T., Wagner, A. P., and Taper, M. L. (2006). ml-relate: a computer program for maximum likelihood estimation of relatedness and relationship. *Mol. Ecol. Notes* 6, 576–579. doi: 10.1111/j.1471-8286.2006.01256.x

Kalisz, S., Nason, J. D., Hanzawa, F. M., and Tonsor, S. J. (2001). Spatial population genetic structure in *Trillium grandiflorum*: the roles of dispersal, mating, history and selection. *Evolution* 55, 1560–1568. doi: 10.1111/j.0014-3820.2001.tb00675.x

Knittweis, L., Aguilar, R., Alvarez, H., Borg, J. A., Evans, J., Garcia, S., et al. (2016). "New depth record of the precious red coral *Corallium rubrum*," in *Proceedings of the CIESM (Commission Internationale pour l'Exploration Scientifique de la Mer Méditerranée)*, Vol. 41, Monaco, 467.

Laikre, L., Hoban, S., Bruford, M. W., Segelbacher, G., Allendorf, F. W., Gajardo, G., et al. (2020). Post-2020 goals overlook genetic diversity. *Science* 367, 1083–1085. doi: 10.1126/science.abb2748

Leblois, R., Rousset, F., and Estoup, A. (2004). Influence of spatial and temporal heterogeneities on the estimation of demographic parameters in a continuous population using individual microsatellite data. *Genetics* 166, 1081–1092. doi: 10.1534/genetics.166.2.1081

Ledoux, J., Aurelle, D., Bensoussan, N., Marschal, C., Feral, J., and Garrabou, J. (2015). Potential for adaptive evolution at species range margins: contrasting interactions between red coral populations and their environment in a changing ocean. *Ecol. Evol* 5, 1178–1192. doi: 10.1002/ece3.1324

Ledoux, J., Frias-Vidal, S., Montero-Serra, I., Antunes, A., Casado Bueno, C., Civit, S., et al. (2020). Assessing the impact of population decline on mating system in the overexploited Mediterranean red coral. *Aquat. Conserv. Mar. Freshw. Ecosyst.* 30, 1149–1159. doi: 10.1002/aqc.3327

Ledoux, J.-B., Frleta-Valić, M., Kipson, S., Antunes, A., Cebrian, E., Linares, C., et al. (2018). Postglacial range expansion shaped the spatial genetic structure in a marine habitat-forming species: implications for conservation plans in the Eastern Adriatic Sea. *J. Biogeogr.* 45, 2645–2657. doi: 10.1111/jbi.13461

Ledoux, J.-B., Garrabou, J., Bianchimani, O., Drap, P., Féral, J.-P., and Aurelle, D. (2010a). Fine-scale genetic structure and inferences on population biology in the threatened Mediterranean red coral, *Corallium rubrum*. *Mol. Ecol.* 19, 4204–4216. doi: 10.1111/j.1365-294X.2010.04814.x

Ledoux, J.-B., Mokhtar-Jamaï, K., Roby, C., Féral, J.-P., Garrabou, J., and Aurelle, D. (2010b). Genetic survey of shallow populations of the Mediterranean red coral [*Corallium rubrum* (Linnaeus, 1758)]: new insights into evolutionary processes shaping nuclear diversity and implications for conservation. *Mol. Ecol.* 19, 675–690. doi: 10.1111/j.1365-294X.2009.04516.x

Linares, C., Bianchimani, O., Torrents, O., Marschal, C., Drap, P., and Garrabou, J. (2010). Marine protected areas and the conservation of long-lived marine invertebrates: the Mediterranean red coral. *Mar. Ecol. Prog. Ser.* 402, 69–79. doi: 10.3354/meps08436

Linares, C., Garrabou, J., Hereu, B., Diaz, D., Marschal, C., Sala, E., et al. (2012). Assessing the effectiveness of marine reserves on unsustainably harvested long-lived sessile invertebrates. *Conserv. Biol.* 26, 88–96. doi: 10.1111/j.1523-1739.2011.01795.x

Loiselle, B. A., Sork, V. L., Nason, J., and Graham, C. (1995). Spatial genetic structure of a tropical understory shrub, *Psychotria officinalis* (Rubiaceae). *Am. J. Bot.* 82:1420. doi: 10.2307/2445869

Lowe, W. H., and Allendorf, F. W. (2010). What can genetics tell us about population connectivity? *Mol. Ecol.* 19, 3038–3051. doi: 10.1111/j.1365-294X.2010.04688.x

Lukoschek, V., Riginos, C., and van Oppen, M. J. H. (2016). Congruent patterns of connectivity can inform management for broadcast spawning corals on the Great Barrier Reef. *Mol. Ecol.* 25, 3065–3080. doi: 10.1111/mec.13649

Marschal, C., Garrabou, J., Harmelin, J. G., and Pichon, M. (2004). A new method for measuring growth and age in the precious red coral Corallium rubrum (L.). *Coral Reefs* 23, 423–432. doi: 10.1007/s00338-004-0398-6

Martínez-Quintana, A., Bramanti, L., Viladrich, N., Rossi, S., and Guizien, K. (2015). Quantification of larval traits driving connectivity: the case of *Corallium rubrum* (L. 1758). *Mar. Biol.* 162, 309–318. doi: 10.1007/s00227-014-2599-z

Mijangos, J. L., Pacioni, C., Spencer, P. B. S., and Craig, M. D. (2015). Contribution of genetics to ecological restoration. *Mol. Ecol.* 24, 22–37. doi: 10.1111/mec.12995

Mokhtar-Jamaï, K., Pascual, M., Ledoux, J.-B., Coma, R., Féral, J.-P., Garrabou, J., et al. (2011). From global to local genetic structuring in the red gorgonian *Paramuricea clavata*: the interplay between oceanographic conditions and limited larval dispersal. *Mol. Ecol.* 20, 3291–3305. doi: 10.1111/j.1365-294X.2011.05176.x

Montero-Serra, I., Garrabou, J., Doak, D. F., Figuerola, L., Hereu, B., Ledoux, J.-B., et al. (2017). Accounting for life-history strategies and timescales in marine restoration. *Conserv. Lett.* 11:e12341. doi: 10.1111/conl.12341

Montero-Serra, I., Garrabou, J., Doak, D. F., Ledoux, J., and Linares, C. (2019). Marine protected areas enhance structural complexity but do not buffer the consequences of ocean warming for an overexploited precious coral. *J. Appl. Ecol.* 56, 1063–1074. doi: 10.1111/1365-2664.13321

Montero-Serra, I., Linares, C., Doak, D. F., Ledoux, J. B., and Garrabou, J. (2018). Strong linkages between depth, longevity and demographic stability across marine sessile species. *Proc. R. Soc. Lond. B Biol. Sci.* 285:20172688. doi: 10.1098/rspb.2017.2688

Montero-Serra, I., Linares, C., García, M., Pancaldi, F., Frleta-Valić, M., Ledoux, J.-B., et al. (2015). Harvesting effects, recovery mechanisms, and management strategies for a long-lived and structural precious coral. *PLoS One* 10:e0117250. doi: 10.1371/journal.pone.0117250

Nei, M. (1973). Analysis of gene diversity in subdivided populations. *Proc. Natl. Acad. Sci. U.S.A.* 70, 3321–3323. doi: 10.1073/pnas.70.12.3321

Ottmann, D., Grorud-Colvert, K., Sard, N. M., Huntington, B. E., Banks, M. A., and Sponaugle, S. (2016). Long-term aggregation of larval fish siblings during dispersal along an open coast. *Proc. Natl. Acad. Sci. U.S.A.* 113, 14067–14072. doi: 10.1073/pnas.1613440113

Padrón, M., Costantini, F., Bramanti, L., Guizien, K., and Abbiati, M. (2018). Genetic connectivity supports recovery of gorgonian populations affected by climate change. *Aquat. Conserv. Mar. Freshw. Ecosyst.* 28, 776–787. doi: 10.1002/aqc.2912

Palumbi, S. R. (2004). Marine reserves and ocean neighborhodds: the spatial scale of marine populations and their management. *Annu. Rev. Environ. Resour.* 29, 31–68. doi: 10.1146/annurev.energy.29.062403.102254

Pardini, E. A., and Hamrick, J. L. (2008). Inferring recruitment history from spatial genetic structure within populations of the colonizing tree *Albizia julibrissin* (Fabaceae). *Mol. Ecol.* 17, 2865–2879. doi: 10.1111/j.1365-294X.2008.03807.x

Petit, R. J., El Mousadik, A., and Pons, O. (1998). Identifying populations for conservation on the basis of genetic markers. *Conserv. Biol.* 12, 844–855. doi: 10.1046/j.1523-1739.1998.96489.x

Pew, J., Muir, P. H., Wang, J., and Frasier, T. R. (2015). Related: an R package for analysing pairwise relatedness from codominant molecular markers. *Mol. Ecol. Resour.* 15, 557–561. doi: 10.1111/1755-0998.12323

Piry, S., Alapetite, A., Cornuet, J.-M., Paetkau, D., Baudouin, L., and Estoup, A. (2004). GENECLASS2: a software for genetic assignment and first-generation migrant detection. *J. Hered.* 95, 536–539. doi: 10.1093/jhered/esh074

Pratlong, M., Haguenauer, A., Brener, K., Mitta, G., Toulza, E., Garrabou, J., et al. (2018). Separate the wheat from the chaff: genomic scan for local adaptation in the red coral *Corallium rubrum*. *Peer Community Evol. Biol* Available online at: https://hal.archives-ouvertes.fr/hal-01974422 (accessed November 15, 2020).

Pratlong, M., Haguenauer, A., Chabrol, O., Klopp, C., Pontarotti, P., and Aurelle, D. (2015). The red coral (*Corallium rubrum*) transcriptome: a new resource for population genetics and local adaptation studies. *Mol. Ecol. Resour.* 15, 1205–1215. doi: 10.1111/1755-0998.12383

Pritchard, J., Stephens, M., and Donnelly, P. (2000). Inference of population structure using multilocus genotype data. *Genetics* 155, 945–959.

Puechmaille, S. J. (2016). The program structure does not reliably recover the correct population structure when sampling is uneven: subsampling and new estimators alleviate the problem. *Mol. Ecol. Resour.* 16, 608–627. doi: 10.1111/1755-0998.12512

Rannala, B., and Mountain, J. L. (1997). Detecting immigration by using multilocus genotypes. *Proc. Natl. Acad. Sci. U.S.A.* 94, 9197–9201.

Riquet, F., Comtet, T., Broquet, T., and Viard, F. (2017). Unexpected collective larval dispersal but little support for sweepstakes reproductive success in the highly dispersive brooding mollusc *Crepidula fornicata*. *Mol. Ecol.* 26, 5467–5483. doi: 10.1111/mec.14328

Rosenberg, N. A. (2003). Distruct: a program for the graphical display of population structure. *Mol. Ecol. Notes* 4, 137–138. doi: 10.1046/j.1471-8286.2003.00566.x

Rousset, F. (1997). Genetic differentiation and estimation of gene flow from F-statistics under isolation by distance. *Genetics* 145, 1219–1228.

Rousset, F. (2008). genepop'007: a complete re-implementation of the genepop software for Windows and Linux. *Mol. Ecol. Resour.* 8, 103–106. doi: 10.1111/j.1471-8286.2007.01931.x

Rousset (2000). Genetic differentiation between individuals. *J. Evol. Biol.* 13, 58–62. doi: 10.1046/j.1420-9101.2000.00137.x

Santangelo, G., Abbiati, M., Giannini, F., and Cicogna, F. (1993). Red coral fishing trends in the western Mediterranean Sea. *Sci. Mar.* 57, 139–143.

Sale, P. F., Cowen, R. K., Danilowicz, B. S., Jones, G. P., Kritzer, J. P., Lindeman, K. C., et al. (2005). Critical science gaps impede use of no-take fishery reserves. *Trends Ecol. Evol.* 20, 74–80. doi: 10.1016/j.tree.2004.11.007

Salles, O. C., Pujol, B., Maynard, J. A., Almany, G. R., Berumen, M. L., Jones, G. P., et al. (2016). First genealogy for a wild marine fish population reveals multigenerational philopatry. *Proc. Natl. Acad. Sci. U.S.A.* 113, 13245–13250. doi: 10.1073/pnas.1611797113

Santangelo, G., Bramanti, L., Rossi, S., Tsounis, G., Vielmini, I., Lott, C., et al. (2012). Patterns of variation in recruitment and post-recruitment processes of the Mediterranean precious gorgonian coral *Corallium rubrum*. *J. Exp. Mar. Biol. Ecol* 411, 7–13. doi: 10.1016/J.JEMBE.2011.10.030

Santangelo, G., Carletti, E., Maggi, E., and Bramanti, L. (2003). Reproduction and population sexual structure of the overexploited Mediterranean red coral *Corallium rubrum*. *Mar. Ecol. Prog. Ser.* 248, 99–108. doi: 10.3354/meps248099

Soulé, M. (1985). What is conservation biology? *Bioscience* 35, 727–734.

Torrents, O., Garrabou, J., Marschal, C., and Harmelin, J. G. (2005). Age and size at first reproduction in the commercially exploited red coral *Corallium rubrum* (L.) in the Marseilles area (France, NW Mediterranean). *Biol. Conserv.* 121, 391–397. doi: 10.1016/j.biocon.2004.05.010

Vekemans, X., and Hardy, O. J. (2004). New insights from fine-scale spatial genetic structure analyses in plant populations. *Mol. Ecol.* 13, 921–935. doi: 10.1046/j.1365-294x.2004.02076.x

Wang, J. (2017). The computer program structure for assigning individuals to populations: easy to use but easier to misuse. *Mol. Ecol. Resour.* 17, 981–990. doi: 10.1111/1755-0998.12650

Waples, R. S., and Gaggiotti, O. (2006). What is a population? An empirical evaluation of some genetic methods for identifying the number of gene pools and their degree of connectivity. *Mol. Ecol.* 15, 1419–1439. doi: 10.1111/j.1365-294X.2006.02890.x

Weeks, A. R., Sgro, C. M., Young, A. G., Frankham, R., Mitchell, N. J., Miller, K. A., et al. (2011). Assessing the benefits and risks of translocations in changing environments: a genetic perspective. *Evol. Appl.* 4, 709–725. doi: 10.1111/j.1752-4571.2011.00192.x

Weir, B. S., and Cockerham, C. C. (1984). Estimating F-statistics for the analysis of population structure. *Evolution (N. Y)* 38:1358. doi: 10.2307/2408641

Zibrowius, H., Monteiro-Marques, V., and Grasshoff, M. (1984). La répartition du *Corallium rubrum* dans l'Atlantique (Cnidaria: Anthozoa: Gorgonaria). *Téthys* 11, 163–170.

Conflict of Interest: The authors declare that the research was conducted in the absence of any commercial or financial relationships that could be construed as a potential conflict of interest.

Advantages of publishing in Frontiers

OPEN ACCESS
Articles are free to read for greatest visibility and readership

FAST PUBLICATION
Around 90 days from submission to decision

HIGH QUALITY PEER-REVIEW
Rigorous, collaborative, and constructive peer-review

TRANSPARENT PEER-REVIEW
Editors and reviewers acknowledged by name on published articles

Frontiers
Avenue du Tribunal-Fédéral 34
1005 Lausanne | Switzerland

Visit us: www.frontiersin.org
Contact us: frontiersin.org/about/contact

REPRODUCIBILITY OF RESEARCH
Support open data and methods to enhance research reproducibility

DIGITAL PUBLISHING
Articles designed for optimal readership across devices

FOLLOW US
@frontiersin

IMPACT METRICS
Advanced article metrics track visibility across digital media

EXTENSIVE PROMOTION
Marketing and promotion of impactful research

LOOP RESEARCH NETWORK
Our network increases your article's readership